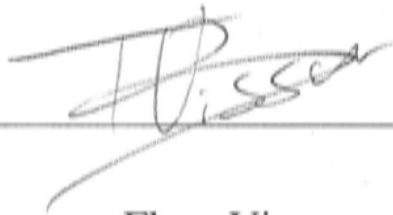


Sediment budget for cane land on the  
Lower Herbert River floodplain,  
North Queensland, Australia

Fleur Visser

A thesis submitted for the degree of Doctor of Philosophy of  
The Australian National University  
January 2003

This thesis is my own work except where otherwise acknowledged

A handwritten signature in black ink, appearing to read 'Fleur Visser', is positioned above a horizontal line. The signature is written in a cursive style with some overlapping strokes.

Fleur Visser

## Acknowledgments

Even after several years in the tropics, it kept surprising me that it was warmer outside than inside, despite thick grey rain clouds, from my Dutch point of view, suggesting otherwise. I extremely appreciate having had the opportunity to do my research for the experience it has given me to be in such a different environment. First of all, I would like to thank Dr. Christian Roth for his supervision and for making it all possible and securing the funding for this project. Also, without the help of my principal supervisor Professor Bob Wasson I would certainly still be stuck in the clay up in Ingham and this thesis would not have been written. The help of my third supervisor, Dr. Ian Prosser and that of Dr. David Post is honoured by having a drain and a creek named after them in this thesis.

Also it is important to thank the funders of this project: the Sugarcane Research and Development Corporation (SRDC), Bureau of Sugar Experimental Stations (BSES), and the Commonwealth Scientific Industrial Research Organization (CSIRO), and the Centre for Resource and Environmental studies (CRES) at the Australian National University (ANU), for their financial support.

This thesis could not have been completed without the support of many other people. Very important was John Regenzani from the BSES; the permission given by Tony and Mark Palmas to perform so much work on their properties (I believe pulling our Land Rover out of the drain has given Tony much enjoyment in return). Many thanks for that same reason also must go to Steve Fortini in the Upper Stone and to Henry Benton, John Biasi and Fred Leonardi who let me 'plant' erosion pins on their headlands and forgave me for driving around their properties in extremely wet conditions.

Invaluable was the support I got from CSIRO technicians and the BSES, most of all from Aaron Hawdon for helping out in the field during ever too frequent flood conditions which provided us with those important opportunities for swimming practise; David Fanning for getting me more erosion pins and profile supports at short notice, and also Peter Fitch, Terry Fitzgerald, David Mitchell, Roger Penny and Glen Park for their help in the field and for making sure everything worked as smoothly as possible.

Thanks to Malcolm Hodgen, who managed to deal with my requests over the telephone and still remain patient whilst creating great maps. Also to Anne Henderson for earlier maps used in the field. Thanks to Mike Hutchinson and other people who provided advise on data analysis. Not to be forgotten are Delia Muller and Glenda Stanton at CSIRO, Townsville, for logistical support and booking planes and Margo Davies at CRES for assuring contact with Bob and for printing out this thesis (without her this thesis would certainly not have appeared!). Thanks to Shelly Far and Leah for lab help.

How can someone work on such a project without the support of many friends? Most of all thanks to Erin Porter, Marlies van Zetten, Penny Hancock, and Susan van Kooij, but also to Mike, Ian, Christina, and all the other people at Davies Lab in Townsville, which is a great place to work. Talking of which, so is CRES: Adrian and Michelle, Ioan, Rosie and Wendy. Furthermore Ken and David, Rohan, and the people at ReefHQ - Thanks!

Finally, many thanks to my parents for letting me go without complaining and showing support all the way through, Lieutske, whilst she was doing her own thing in England, Kenny the Killer Whale for REALLY being there, and Triple-J for providing the great soundtrack. Oh... and Matt provided his own special telephone soundtrack (and the name 'Ripple Corner Catchment', as replacement in this thesis for the locally used 'Visser Catchment').

## Abstract

Land use in the river catchments of tropical North Queensland appears to have increased the export of sediment and nutrients to the coast. Although evidence of harmful effect of sediment on coastal and riverine ecosystems is limited, there is a growing concern about its possible negative impacts. Sugarcane cultivation on the floodplains of the tropical North Queensland river catchments is thought to be an important source of excess sediment in the river drainage systems.

Minimum-tillage, trash blanket harvesting has been shown to reduce erosion from sloping sugarcane fields, but in the strongly modified floodplain landscape other elements (e.g. drains, water furrows and headlands) could still be important sediment sources. The main objectives of this thesis are to quantify the amount of sediment coming from low-lying cane land and identify the important sediment sources in the landscape. The results of this thesis enable sugarcane farmers to take targeted measures for further reduction of the export of sediment and nutrients.

Sediment budgets provide a useful approach to identify and quantify potential sediment sources. For this study a sediment budget is calculated for a part of the Ripple Creek catchment, which is a sub-catchment of the Lower Herbert River. The input of sediment from all potential sources in cane land and the storage of sediment within the catchment have been quantified and compared with the output of sediment from the catchment. Input from, and storage on headlands, main drains, minor drains and water furrows, was estimated from erosion pin and surface profile measurements. Input from forested upland, input from fields and the output at the outlet of the catchment was estimated with discharge data from gauged streams and flumes. Data for the sediment budget were collected during two 'wet'-seasons: 1999-2000 and 2000-2001.

The results of the sediment budget indicate that this tropical floodplain area is a net source of sediment. Plant cane fields, which do not have a protective trash cover, were the largest net source of sediment during the 1999-2000 season. Sediment input from water furrows was higher, but there was also considerable storage of sediment in this landscape element. Headlands tend to act as sinks. The source or sink function of drains is less clear, but seems to depend on their shape and vegetation cover.

An important problem in this study is the high uncertainty in the estimates of the sediment budget components and is, for example, likely to be the cause of the imbalance in the sediment budget. High uncertainties have particularly affected the results from the 2000-2001 season. The main source of uncertainty is spatial variation in the erosion and deposition

processes. Uncertainty has to be taken into consideration when interpreting the budget results.

The observation of a floodplain as sediment source contradicts the general understanding that floodplains are areas of sediment storage within river catchments. A second objective of this thesis was therefore to provide an answer to the question: how can floodplains in the tropical North Queensland catchments can be a source of sediment?

In geomorphic literature various factors have been pointed out, that could control floodplain erosion processes. However, their importance is not 'uniquely identified'. Among the most apparent factors are the stream power of the floodwater and the resistance of the floodplain surface both through its sedimentary composition and the vegetation cover.

If the cultivated floodplains of the North Queensland catchments are considered in the light of these factors, there is a justified reason to expect them to be a sediment source. Cultivation has lowered the resistance of their surface; increased drainage has increased the drainage velocity and flood control structures have altered flooding patterns.

For the Ripple Creek floodplain four qualitative scenarios have been developed that describe erosion and deposition under different flow conditions. Two of these scenarios were experienced during the budget study, involving runoff from local hillslopes and heavy rainfall, which caused floodplain erosion. In the longer term larger flood events, involving floodwater from the Herbert River, may lead to different erosion and deposition processes.

The present study has shown that the tropical floodplain of the Herbert River catchment can be a source of sediment under particular flow conditions. It has also shown which elements in the sugarcane landscape are the most important sediment sources under these conditions. This understanding will enable sugarcane farmers to further reduce sediment export from cane land and prevent the negative impact this may have on the North Queensland coastal ecosystems

# Contents

Acknowledgments	iii
Abstract	v
Contents	vii
List of Tables	xiv
List of Figures	xvii

## PART I

Introductory Chapters	1
-----------------------	---

### Chapter 1

Introduction	2
1.1 Humid tropics and sugarcane cultivation	2
1.2 Increase in soil erosion since European settlement: the off-site effects	4
1.3 Effects of sediments and nutrients on the Great Barrier Reef World Heritage Area and riverine ecosystems	6
1.3.1 Increased sediment and nutrient inputs	6
1.3.2 Effects of sediment on coral reef systems	6
<i>Effects of sediment related chemicals</i>	7
1.3.3 Effects of sediment on other marine ecosystems	8
1.3.4 Effects of sediments on freshwater ecosystems	8
1.3.5 Conclusion	9
1.4 Soil erosion in low-lying sugarcane land	10
1.4.1 Sources of sediment: the first thesis objective	11
1.4.2 Soil erosion on floodplains: a second thesis objective	13
1.5 Thesis outline	13

### Chapter 2

<b>The Herbert River Catchment: a site description</b>	<b>14</b>
2.1 Introduction	14
2.2 General catchment description	16
2.3 Geology	16
2.4 Geomorphology	17
<i>The Herbert River delta</i>	19
2.5 Climate	20
2.6 Hydrology of the Herbert River	21
<i>Discharge patterns in the Herbert River Catchment</i>	21
<i>Sediment and nutrient runoff</i>	23
2.7 The Ripple Creek Sub-catchment	24
<i>The Ripple Creek drainage system</i>	25
<i>Land use</i>	25
<i>Soils</i>	27
<i>Palmas' site</i>	30

<b>PART II</b>	
<b>Composition of a sediment budget for low-lying sugarcane land</b>	<b>31</b>
<i>Outline</i>	31
<b>Chapter 3</b>	
<b>The sediment budget approach</b>	<b>32</b>
3.1 Erosion and storage	32
3.2 The sediment budget approach	33
3.2.1 Analysing catchment systems	33
3.2.2 Sediment budget applications	33
3.2.3 Sediment budget presentation	34
3.3 Sediment budget limitations	34
3.3.1 Variation in time and space	34
3.3.2 Budget balance and uncertainty	35
3.3.3 Summary	37
3.4 Considerations for a sediment budget in low-lying cane land	37
<i>Balancing the budget equation</i>	38
<i>Spatial variation</i>	39
<i>Temporal variation</i>	39
<i>Budget uncertainty</i>	40
<b>Chapter 4</b>	
<b>Development of the sediment budget and methods for quantification of the budget components</b>	<b>41</b>
4.1 Introduction	41
4.2 Budget Area	41
4.3 Budget output and upland input components	42
4.4 Quantification of the sediment sources and sinks	44
4.4.1 Introduction	44
4.4.2 Caesium-137 tracer	45
4.4.3 Other indirect erosion measurement methods	46
4.4.4 Modelling	47
4.4.5 Plot studies	48
4.5 Budget composition	48
4.6 Particle size problems	49
<b>Chapter 5</b>	
<b>Output from the Ripple Corner Catchment</b>	<b>51</b>
5.1 Introduction	51
5.2 Water discharge estimation	51
5.3 Sediment concentration estimation	52
5.3.1 SSC – turbidity relationship for the Ripple Corner Catchment	53
5.4 Location and equipment	54
5.5 Raw data availability	55
5.5.1 Ripple Drain 99-00	56
5.5.2 Ripple Drain 00-01	57
5.5.3 Prosser Drain 99-00	58
5.5.4 Prosser Drain 00-01	58
5.6 Water depth and drain cross-sectional areas	58



5.6.1	Depth adjustments Ripple Drain 99-00	59
5.6.2	Depth adjustments Ripple Drain 00-01	60
5.6.3	Depth adjustments Prosser Drain 99-00 and 00-01	60
5.7	Water flow velocity	62
5.7.1	Velocity calibration	63
5.7.2	Velocity distribution	63
5.7.3	Flood events	66
5.8	Suspended sediment concentrations	67
5.8.1	Ripple Drain 99-00	68
5.8.2	Ripple Drain 00-01	69
5.8.3	Prosser Drain 99-00	70
5.8.4	Prosser Drain 00-01	71
5.9	Further data improvement	72
5.9.1	Depth-discharge rating curve Ripple Drain 99-00	73
5.9.2	Depth-discharge rating curve Ripple Drain 00-01	74
5.9.3	Depth-discharge rating curve Prosser Drain 99-00	75
5.9.4	Depth-discharge rating curve Prosser Drain 00-01	76
5.9.5	Comparison of Ripple and Prosser Drain data	77
5.9.6	Missing turbidity data	80
5.10	Load calculations	81
5.10.1	Ripple Drain load calculations	81
5.10.2	Prosser Drain load calculations	83
5.10.3	Summary of the load calculations and implications for the sediment budget	85

## Chapter 6

<b>Upland input</b>	<b>87</b>	
6.1	Introduction	87
6.2	Gauging location and equipment	87
6.3	Raw data Post Creek	88
6.3.1	1999-2000 data	89
6.3.2	Gap filling 1999-2000 data	89
6.3.3	2000-2001 data	90
6.3.4	Raw data appearance	90
6.4	Depth data adjustment	90
6.5	Discharge estimation	91
6.5.1	Depth – Discharge rating curve	91
6.5.2	Missing discharge data substitution	93
6.6	Sediment concentration estimation	94
6.6.1	SSC estimation	94
6.6.2	Turbidity meter calibration	95
6.6.3	Missing turbidity data	97
6.7	Load calculations	98

## Chapter 7

<b>Fields</b>	<b>102</b>	
7.1	Introduction	102
7.2	Ratoon data	103
7.2.1	Set up	103
7.2.2	Raw data	104

7.2.3	Flume hydrographs and backwatering	105
7.2.4	Rating curves	106
7.2.5	Sediment export	108
7.2.6	Ratoon fields load calculation	109
7.3	Plant cane data	111
7.3.1	Introduction	111
7.3.2	Set up	112
7.3.3	Raw data	113
7.3.4	Reverse flow	113
7.3.5	Comparing hydrographs	114
7.3.6	Rating curves	115
7.3.7	Sediment export	116
7.3.8	Plant flume load estimation for the 00-01 season	118
7.3.9	Plant flume load estimation for the 99-00 season	119
7.4	Comparison and discussion of plant cane and ratoon sediment loads	120
<b>Chapter 8</b>		
<b>Headlands</b>		<b>123</b>
8.1	Introduction	123
8.2	Headland erosion and deposition processes	123
8.3	The erosion pin method	125
8.4	Pinplot distribution: capturing variation	126
8.4.1	Transect sampling	126
8.4.2	Pinplot distribution per season	127
8.5	Pinplot set up and measurements	128
8.6	Results	128
8.6.1	Variation of erosion and deposition rate	129
8.7	Alternative load estimates	136
8.7.1	Averages and medians	136
8.7.2	Estimate based on vegetation cover	138
8.7.3	Overview and discussion of estimates	140
8.8	Additional observations	141
8.8.1	Observations of sediment deposits	141
8.8.2	Variation within pinplots	142
8.9	Other factors influencing erosion and deposition rates	145
	<i>Other factors affecting surface level change</i>	145
	<i>Swelling and shrinking processes</i>	145
8.10	Conclusion: budget values	146
<b>Chapter 9</b>		
<b>Drains and Water furrows</b>		<b>147</b>
9.1	Introduction	147
9.2	Integrated Drainage Survey	148
9.3	Water furrows	149
9.4	Surface profile meter method	150
9.4.1	Profile meter design	150
9.4.2	Method disadvantages	151
9.5	Profile distribution: capturing variation	152
9.5.1	Erosion and deposition processes in drains and water furrows	152
9.5.2	Transect sampling	153

9.5.3	Profile distribution per season	153
9.5.4	Particle size adjustments	154
9.6	Results	155
9.6.1	Profile data availability	155
9.6.2	Variation of erosion and deposition rates for drain types	156
9.6.3	Variation of erosion and deposition rates for soil type	160
	<i>Drains</i>	160
	<i>Water furrows</i>	160
9.6.4	Variation of erosion and deposition rates for crop types	161
9.7	Input for the budget calculation	162
9.7.1	Drains	162
9.7.2	Water furrows	167
9.8	Additional observations	169
9.9	Other factors influencing erosion and deposition rates	170
9.10	Conclusion	171
<b>Chapter 10</b>		
<b>Budget Calculation</b>		<b>172</b>
10.1	Introduction	172
10.2	Particle size	172
10.2.1	Sediment size adjustment methods	173
	<i>Size adjustment headlands</i>	174
	<i>Particle size adjustment for drains and water furrows</i>	175
10.3	Soil bulk density	177
10.4	Surface area	178
10.5	Budget calculations and budget differences	180
10.6	Discussion	183
10.6.1	Best budget estimates	183
10.6.2	Discussion of individual landscape elements	184
10.6.3	Landscape elements not represented in the sediment budget	186
	<i>Fallow and melon fields</i>	187
	<i>Roads, tracks, built environment, and other sources</i>	187
<b>Chapter 11</b>		
<b>Uncertainty analysis</b>		<b>189</b>
11.1	Introduction	189
	<i>Uncertainty analysis methods</i>	189
11.2	Monte Carlo simulation of the budget uncertainty	191
	<i>Simulation procedures</i>	191
	<i>Uncertainty distribution functions</i>	191
11.3	Headlands	192
11.3.1	Overview	192
11.3.2	Measurement error	193
11.3.3	Interpolation methods	194
11.3.4	Time and Space	195
11.3.5	Total uncertainty in the budget input from headlands	197
11.4	Outlet drain gauging data	199
11.4.1	overview	199
11.4.2	Flow depth and cross-section	201
11.4.3	Flow velocity	201

11.4.4	Suspended solid concentration	202
11.4.5	Time and space	202
11.4.6	Missing data	202
11.4.7	Total uncertainty in the budget input from gauging data	203
11.5	Comments on the uncertainty estimates for the remaining budget components	204
11.6	The total uncertainty	204
11.6.1	Worst case estimate	204
11.6.2	Cumulative frequency distribution curves	205
11.6.3	Error correlation	207
11.7	Conclusion	208

### **PART III**

#### **Floodplain erosion and the case of the Lower Herbert River** **209**

*Outline* 209

#### **Chapter 12**

##### **Floodplain processes** **210**

12.1	Floodplain definition	210
12.2	Floodplain formation	211
12.2.1	Formation processes	211
12.2.2	Floodplain accretion rates	212
12.3	Floodplain development	213
12.3.1	Development processes	213
12.3.2	Floodplain degradation	214
12.4	The role of various floodwater sources	215
12.4.1	Sources of floodwater	216
12.4.2	Floodwater sources and floodplain formation	217
12.4.3	Floodwater composition and floodplain degradation	218
12.5	Summary and implications	218

#### **Chapter 13**

##### **Scenarios of erosion and deposition on a floodplain in the Lower Herbert River Catchment** **220**

13.1	The case of the Lower Herbert: a cultivated floodplain	220
13.2	Floodplain modification for land use	221
13.3	Potential impact	222
	<i>Erosion resistance</i>	222
	<i>Drainage efficiency</i>	222
	<i>Flood regulation</i>	222
13.4	Scenarios of flooding, erosion and deposition in the Ripple Creek Catchment	222
	<i>Scenario 1: local inundation</i>	223
	<i>Scenario 2: reverse flow from the Herbert River</i>	223
	<i>Scenario 3: blocking of floodwater by floodgates</i>	223
	<i>Scenario 4: the Herbert River overtops its banks</i>	224
	<i>Observed flow conditions</i>	224
13.5	Additional observations	226
13.6	Discussion: representativeness of the sediment budget results	230

**PART IV****Concluding Chapter****232****Chapter 14****Conclusions and recommendations****233**

- 14.1 Sediment export from low-lying sugarcane land on a tropical floodplain 233
- 14.2 Sediment sources and sinks 233
- 14.3 Accuracy of the budget 235
- 14.4 Floodplain erosion on a tropical floodplain 236
- 14.5 Future research 237
  - 14.5.1 Soil conservation practices 237
  - 14.5.2 Bedload quantity and origin 237
  - 14.5.3 Floodplain development 238
  - 14.5.4 Upland versus lowland input 238
  - 14.5.5 A budget based on direct measurement methods 238
- 14.6 In conclusion 239

**References****240****APPENDICES**

- Appendix A Water sample locations in the Ripple Corner Catchment. 259
- Appendix B Locations of erosion pin plots and drain surface profiles in the Ripple Corner Catchment during both budget seasons. 260
- Appendix C Data availability for the gauging sites during the 99-00 and 00-01 wet season. 262
- Appendix D Water sample analysis procedure for suspended solid concentration (SSC) and turbidity (including sub-sampling for future chemical analysis). 263
- Appendix E Data of flow velocity measurements in Post Creek 'wet cross-section' at gauging site. 263
- Appendix F Depth, Velocity and SSC (calculated from turbidity) recordings for each gauging station, in both budget seasons. 264
- Appendix G Average net surface level change (mm) and surface vegetation cover (%) on pinplots in the Ripple Corner Catchment over two periods (December to March and March to May) in both budget seasons. 275
- Appendix H Average net surface level change (mm), erosion, and deposition rate (mm) for drain and water furrow surface profiles in the Ripple Corner Catchment, over two periods (December to March and March to May) in both budget seasons. 275
- Appendix I Examples of graphs from both budget seasons, showing changes in the surface profile (distance relative to profiler datum, in mm) of drains and water furrows in the Ripple Corner Catchment. 282
- Appendix J Histograms for surface profile data (adjusted) from the 99-00 budget season. 292

## List of Tables

Table 2.1: Discharge and sediment loads of the Herbert River compared with the Rhine (Europe) and the Murray Darling (Australia).	22
Table 5.1: Data availability Ripple Drain 1999-2000.	56
Table 5.2: Availability Greenspan turbidity data Ripple Drain 99-00.	57
Table 5.3: Availability of Starflow velocity and depth, and Greenspan turbidity data 2000-2001.	58
Table 5.4: Availability Starflow depth and velocity data and Greenspan turbidity data Prosser Drain 99-00.	58
Table 5.5: Availability Starflow velocity and depth and Greenspan turbidity data 2000-2001.	58
Table 5.6: 00-01 Ripple Drain manual depth measurements and corresponding Starflow records.	60
Table 5.7: 00-01 Prosser Drain manual depth measurements and corresponding Starflow records.	61
Table 5.8: 00-01 manual velocity measurements and corresponding Starflow records for Ripple Drain and Prosser Drain.	63
Table 5.9: Manual velocity/Starflow velocity ratios for Ripple Drain.	65
Table 5.10: Manual velocity/Starflow velocity ratios for Prosser Drain	66
Table 5.11: 99-00 Prosser Drain water quality data and corresponding Greenspan turbidity records.	71
Table 5.12: 00-01 Prosser Drain water quality data and corresponding Greenspan records.	72
Table 5.13: Load calculations for the 99-00 Ripple Drain data. Best estimate is shaded.	82
Table 5.14: Load calculations for the 00-01 Ripple Drain data. Best estimate is shaded.	82
Table 5.15: Load calculations for the 99-00 Prosser Drain data. Best estimate is shaded.	84
Table 5.16: load calculations for the 00-01 Prosser Drain data. Best estimate is shaded.	84
Table 5.17: Summary of best estimates of sediment load, discharge values and runoff coefficients.	85
Table 6.1: Data availability Post Creek 1999-2000.	89
Table 6.2: Post Creek manual depth measurements and corresponding Dataflow records.	91
Table 6.3: Discharge estimates for Post Creek based on manual velocity profiles.	92
Table 6.4: Post Creek water quality data and corresponding Greenspan records.	96
Table 6.5: Post Creek load calculations for the 1999-2000 budget season. Best estimate shaded.	100
Table 6.6: Post Creek load calculation for the 2000-2001 budget season.	101
Table 6.7: Summary of best estimates of sediment load, discharge values and runoff coefficients.	101
Table 7.1: Availability of depth and velocity data from the south flume gauging site for the 99-00 and 00-01 season.	105
Table 7.2: Results of the sediment load estimation from the south flume	110
Table 7.3: Data availability for the plant flume 00-01 season.	113
Table 7.4: Turbidity and SSC in runoff from plant cane and ratoon rows.	119

Table 7.5: Plant cane field load estimate based on grab sample SSC and runoff coefficients.	120
Table 7.6: Summary of sediment loads estimated from plant cane and ratoon gauging sites.	121
Table 8.1: Distribution of pinplots across headland sites with different surface conditions.	127
Table 8.2: Results of Kruskal-Wallis tests for differences in surface level change due to differences in headland surface conditions.	133
Table 8.3: Different estimates of erosion and deposition rates and net surface level change on headlands in the Ripple Corner Catchment. Best estimate shaded.	140
Table 8.4: Pin height estimates for pins with rusty, stuck washers.	146
Table 9.1: Distribution of profiles across drains and water furrows with different characteristics (numbers used for data analysis).	154
Table 9.2: Results of Kruskal-Wallis tests for differences in surface level change in drain profiles due to differences in soil and drain type. Significance of original and adjusted data for each budget season are shown.	157
Table 9.3: Results of Kruskal-Wallis tests for differences in surface level change in water furrow profiles due to differences in soil type and crop conditions. Significance of original and adjusted data for each budget season are shown.	162
Table 9.4: Estimates of erosion and deposition rates and net surface level change for different drain types in the Ripple Corner Catchment.	166
Table 9.5: Different estimates of erosion and deposition rates and net surface level change in water furrows in the Ripple Corner Catchment.	168
Table 10.1: Different estimates of erosion and deposition rates and net surface level change on headlands in the Ripple Corner Catchment. Values adjusted for bedload fraction. Best estimate is shaded.	175
Table 10.2: Particle size distribution for soils in the Ripple Corner Catchment (Wood, 1984).	176
Table 10.3: Median particle size of soil surface samples (<10 cm) taken from the Ripple Corner Catchment.	177
Table 10.4: Bulk densities ( $\text{g cm}^{-3}$ ) of the Hamleigh soil in the Ripple Creek catchment (Wilson and Baker, 1990).	178
Table 10.5: Percentage area of cultivated lowland (= total catchment – forested upland) covered by each landscape element.	179
Table 10.6: Sediment budgets for 99-00 and 00-01 budget seasons for particles <20 $\mu\text{m}$ based on 'best estimate' results.	181
Table 10.7: Sediment budgets for 99-00 and 00-01 budget seasons for particles <20 $\mu\text{m}$ based on averages.	182
Table 10.8: Summary of all budget calculations (as shown in Figure 10.4). Best budget estimate shaded.	182
Table 11.1: The average, minimum and maximum value of the (absolute) difference between two subsequent measurements of all pins in an erosion pinplot.	193
Table 11.2: Reduction of variance for the distribution of plot surface level change averages compared to average surface level change for all individual pins.	195

Table 11.3: Worst case estimates of headland sediment load in tonnes and as percentage difference of best estimate based on all input uncertainty (Total) and on individual input uncertainties.	199
Table 11.4: Worst case estimates of catchment output in tonnes and as percentage difference of best estimate based on all input uncertainty (Total) and on individual input uncertainties.	203
Table 13.1: SSC ( $\text{mg l}^{-1}$ ) in water samples from four locations in the Ripple Corner Catchment and Ripple Drain, and discharge at time of sampling.	226



## List of Figures

- Figure 1.1: Map of North Queensland with sugarcane cultivation areas; seven of the major coastal catchments, including the Herbert River Catchment; and the Great Barrier Reef. 3
- Figure 1.2: Aerial photo of Ripple Creek Catchment, a tributary of the Herbert River. Photo of forested upland section was not available. The (mostly artificial) drainage network in the catchment lowlands is highlighted in blue. 4
- Figure 1.3: Schematic close-up of sugarcane land illustrating typical landscape elements: ratoon fields, plant cane fields, drains, headlands and water furrows. 12
- Figure 2.1: Herbert River Catchment and Ripple Creek Sub-catchment with sugarcane cultivation areas and approximate Upper and Lower Herbert River divisions and Herbert River Gorge. 15
- Figure 2.2: Geomorphology of the Lower Herbert River Catchment (after Wilson and Baker, 1990 in Johnson and Murray, 1997). 18
- Figure 2.3: Daily (top) and annual (bottom) discharge from the Herbert River between August 1915 and September 1995. Data source: Queensland Department of Natural Resources and Mines (Furnas and Mitchell, 2001). 22
- Figure 2.4: Map of Herbert River Catchment with an indication of the extent of the flood caused by heavy cyclonic rainfall in the Upper Herbert River Catchment (Cameron McNamara, 1980; Johnson and Murray, 1997). 23
- Figure 2.5: Topographic map of the Ripple Creek Catchment. 27
- Figure 2.6: Land-use in the Ripple Creek Catchment (after Johnson and Murray, 1997). 27
- Figure 2.7: Soils in the Ripple Creek Catchment (after Wood, 1984). 29
- Figure 2.8: Daily rainfall (mm) recorded by the weather station at Palmas' site in the Ripple Creek Catchment. The figures show data for two wet seasons: November 1999 – May 2000 and December 2000 – May 2001. 30
- Figure 3.1: Sediment budgets for Coon Creek, a 360 km<sup>2</sup> catchment in Wisconsin, USA, over the period 1853-1993. Numbers are annual averages in 10<sup>3</sup> Mg year<sup>-1</sup>. All values are direct measurements except "Net upland sheet and rill erosion," which is the sum of all sinks and the efflux minus the measured sources. The lower main valley and tributaries are sediment sinks, whereas the upper main valley is a sediment source' (Trimble, 1999, modified from Trimble, 1981). 35
- Figure 3.2: Sediment budget outline for low-lying sugarcane land. 39
- Figure 4.1 (next page): Aerial photo of the study area for the sediment budget study. The boundary of the cultivated lowland is indicated in red. 42
- Figure 5.1: Scatter diagram of turbidity versus SSC for all drain water samples taken in the Ripple Corner Catchment. Both budget seasons plotted separately. Also shown are linear regression curves for each data set. 54
- Figure 5.2: Profiles of cross-sections through Ripple Drain (a) and Prosser Drain (b) at gauging sites. 55
- Figure 5.3: Scatter diagram of Ripple Drain Dataflow depth data versus Starflow depth data and a linear regression curve for 99-00 season. 57
- Figure 5.4: Scatter diagram of Ripple Drain transducer depth (Starflow and Dataflow) versus manual depth at the gauging site for both budget seasons.

Regression curves for Starflow depth data (99-00 data thick, 00-01 data thin).	60
Figure 5.5: Ratios between manual velocity measurements as observed along the Ripple Drain surface profile and Starflow velocity as measured in the deepest part of the drain.	64
Figure 5.6: Ratios between manual velocity measurements as observed along the Prosser Drain surface profile and Starflow velocity as measured in the deepest part of the drain. Inaccurate 16/02/01 estimates plotted separately.	65
Figure 5.7: Profile of cross-sections through Ripple Drain with vertically extrapolated banks, used for discharge calculation during flood conditions.	67
Figure 5.8: Scatter diagram of Greenspan turbidity records versus grab sample Turbiquant turbidity and SSC, with regression curve for Turbiquant turbidity. All samples taken from Ripple Drain gauging site during the 99-00 season.	68
Figure 5.9: Scatter diagram of Greenspan versus Turbiquant turbidity data, for grab samples taken at Ripple Drain gauging site (D21) (with and without ) and at Palmas' site (D4) in the 00-01 season. Regression curve for D4 and D12 samples (without erroneous sample) included.	69
Figure 5.10: Scatter diagram of Greenspan turbidity versus Turbiquant turbidity and SSC for grab samples taken at Prosser Drain gauging site (D24) and downstream locations in Prosser Drain (D25+D28) in the 99-00 season. Regression curves for Turbiquant data from locations D24 (thick) and D25+D28 (thin) included.	70
Figure 5.11: Scatter diagram of Greenspan turbidity versus Turbiquant turbidity and SSC for grab samples taken at the Prosser Drain gauging site in the 00-01 season. Regression curve for turbidity data included.	72
Figure 5.12: Scatter diagram of Ripple Drain depth versus Ripple Drain discharge for both budget seasons. 00-01 data plotted both with and without suspect data records.	74
Figure 5.13: Scatter diagram of Ripple Drain depth versus Ripple Drain velocity for the 99-00 budget season.	74
Figure 5.14: Scatter diagram of Prosser Drain depth versus Prosser Drain discharge for both budget seasons, unadjusted data.	76
Figure 5.15: Scatter diagram of Prosser Drain depth versus Prosser Drain discharge for both budget seasons. Data adjusted for errors.	76
Figure 5.16: Scatter diagram of Ripple Drain depth versus Prosser Drain depth for both budget seasons, unadjusted data.	78
Figure 5.17: Scatter diagram of Ripple Drain velocity versus Prosser Drain velocity for both budget seasons.	78
Figure 5.18: Scatter diagram of Ripple Drain depth versus Prosser Drain depth for both budget seasons and a regression curve for the 99-00 data. Data adjusted for errors.	79
Figure 5.19: Scatter diagram of 99-00 Ripple Drain depth versus SSC.	81
Figure 6.1: Profile of cross-section through Post Creek at gauging site (December 2000).	88
Figure 6.2: Relationship between Prosser Drain depth and Post Creek depth data for both budget seasons, and different Post Creek depth adjustments.	92
Figure 6.3: Post Creek depth – discharge rating curve (n=4, P=0.08).	93
Figure 6.4: Scatter diagram Rainfall versus Post Creek Discharge for both budget seasons (n=196, P<0.01).	94

Figure 6.5: Scatter diagram of Turbidity versus SSC for Post Creek water samples and all Ripple Corner Catchment water samples (n=10 and n=261).	95
Figure 6.6: Scatter diagram for Post Creek turbidity versus SSC for both budget seasons (n=10 and n=3, P=0.09).	95
Figure 6.7: Calibration of Post Creek Greenspan turbidity probe with Turbiquant grab sample turbidity estimates and SSC estimates for both budget seasons (n=6 and n=3, P<0.01).	96
Figure 6.8: Regression curves Rainfall and Post Creek SSC for both budget seasons (n=488, P<0.01).	97
Figure 6.9: Scatter diagram of Post Creek Depth versus SSC for both budget seasons.	98
Figure 7.1: Set up of Parshall flume at the ratoon field site (side view).	104
Figure 7.2: Gauging data, south flume (2 – 5 April 1999).	106
Figure 7.3: Gauging data, south flume (15 – 19 March 2000).	106
Figure 7.4: Depth – discharge rating curve based on 99-00 south flume data. (n=189, P<0.01)	107
Figure 7.5: Relationship between Ripple Drain water levels and south flume water depth (separate regression equations for RD depths <1.0 m (n=429, P<0.01) and >1.0 m (n=58, P<0.01))	108
Figure 7.6: Suspended sediment concentration – water depth relationship for the south flume. Samples for each season and the first event of each season shown separately (n=78).	109
Figure 7.7: Set up of cutthroat flumes at the plant cane site.	112
Figure 7.8: Plant flume gauging data (13 – 21 February 2001).	114
Figure 7.9: South flume and Plant flume depth and SSC data (13-21 February 2001).	115
Figure 7.10: Scatter diagram of Ripple Drain (RD) versus plant flume (PF) water depth data (n=229, P<0.01).	116
Figure 7.11: Depth – discharge rating curve based on 00-01 plant flume (PF) data (n=247, P<0.01).	116
Figure 7.12: Suspended sediment concentration – water depth relationship for the south flume and plant flume. Samples for each season shown separately.	118
Figure 7.13 Suspended sediment concentration – water depth relationship for plant flume water depths >20 $\mu$ m (n=75).	118
Figure 8.1: Boxplots for the variation in erosion rate, deposition rate and net surface level change on headlands during the 99-00 season, grouped by soil type.	130
Figure 8.2: Boxplots for the variation in erosion rate, deposition rate and net surface level change on headlands during the 99-00 season, grouped by crop type.	131
Figure 8.3: Boxplots for the variation in erosion rate, deposition rate and net surface level change on headlands during the 99-00 season, grouped by drain type.	132
Figure 8.4: Boxplots for the variation in erosion rate, deposition rate and net surface level change on headlands during the 00-01 season, grouped by soil type.	134
Figure 8.5: Boxplots for the variation in erosion rate, deposition rate and net surface level change on headlands during the 00-01 season, grouped by drain type.	135

Figure 8.6: Histograms of erosion rate (a), deposition rate (b), and net surface level change (c) of all 99-00 pinplots from the Ripple Corner Catchment.	137
Figure 8.7: Histograms of the erosion rate (a) and deposition rate (b) of the logtransformed 99-00 pinplot data.	138
Figure 8.8: Scatter diagram of vegetation cover percentage and net surface level change (mm), with separate regressions for the 99-00 and 00-01 data (n=13, P=0.09, and n=6, P<0.01).	139
Figure 8.9: Headland along a plant cane (foreground right) and fallow (background) field. The headland section along plant cane is covered with sediment derived from the field after a heavy rainstorm in November 1999. The sediment buried the vegetation (see also inset; measuring-tape indicates 50 cm).	143
Figure 8.10: Spatial distribution of net surface level change on pinplots J and M between measurement sessions during the 99-00 season.	144
Figure 9.1: Signs of soil erosion in different drain types in the Ripple Creek Catchment; results from the Integrated Drainage Survey (Roth <i>et al.</i> , 2000).	149
Figure 9.2: Schematic representation of the surface profile meter.	151
Figure 9.3: Example of a surface profile through a water furrow in a ratoon field on grey sand (profile 1).	156
Figure 9.4: Boxplots for the variation in erosion rate, deposition rate and net surface level change (original data) in different drain types (and water furrows) during the 99-00 season.	158
Figure 9.5: Boxplots for the variation in erosion rate, deposition rate and net surface level change (original data) in different drain types (and water furrows) during the 00-01 season.	159
Figure 9.6: Net surface level change in the original 99-00 drain profile data, grouped by soil type (silty clay, clay and grey sand).	160
Figure 9.7: Net surface level change in the original 00-01 drain profile data, grouped by soil type (silty clay, clay and grey sand).	161
Figure 9.8: Boxplots for the variation in erosion rate, deposition rate and net surface level change (original data) in water furrows, grouped by soil type (99-00 season).	163
Figure 9.9: Boxplots for the variation in erosion rate, deposition rate and net surface level change (original data) in water furrows, grouped by soil type (00-01 season).	164
Figure 9.10: Boxplots for the variation in erosion rate, deposition rate and net surface level change (original data) in water furrows, grouped by crop type (00-01 season).	165
Figure 10.1: Particle size distribution of soil surface samples (<10 cm) taken from headlands along Ripple Drain (HRD), major drains (HMaj) and minor drains (HMin).	174
Figure 10.2: Sediment size distribution of soil surface samples (<10 cm) from fields (FG = grey sand, FS = silty clay, FC = clay)	176
Figure 10.3: Particle size distribution of soil surface samples (<10 cm) taken from the beds of Ripple Drain (DRD) and major drains (DMaj). Sandy top layer (<5 cm) at site DMaj6 is analysed separately.	177
Figure 10.4: Comparison of (Input – Storage) with catchment Output, showing budget difference, for each budget calculation method.	183
Figure 10.5: Input of sediment from individual landscape elements for each year's budget.	185

Figure 10.6: Storage of sediment in individual landscape elements for each year's budget.	186
Figure 10.7: Net input of sediment from individual landscape elements. Positive values indicated net sediment storage, negative values net erosion.	186
Figure 11.1: Histogram of the absolute differences (deviations) between repeated measurements of erosion pins in pinplot G in the 00-01 season.	194
Figure 11.2: Histogram of headland widths measured in the Ripple Corner Catchment.	196
Figure 11.3: Histogram of 1000 samples taken from a triangular distribution for % particles <20 $\mu\text{m}$ in headland surface soil.	197
Figure 11.4: Cumulative frequency distribution curves obtained from 1000 simulations of headland sediment load, by re-sampling the original surface level change data (dark) and sampling from a normal distribution (light). Load estimates based on average and median surface level change data indicated with dots.	198
Figure 11.5: Worst case uncertainty estimates for headland sediment load calculations. 'Total range' shows the effect of assuming minimum and maximum values for all uncertainties. The separate effect of uncertainty in surface level change (SLC), surface area, measurement error, particle size and bulk density is also shown.	199
Figure 11.6: Worst case uncertainty estimates for catchment output calculations. 'Total range' shows the effect of assuming minimum and maximum values for all uncertainties. The separate effect of uncertainty in SSC, cross-section, velocity and rating curve.	203
Figure 11.7: Worst case uncertainty estimates for the 99-00 sediment budget. 'Total range' (dark bars) shows the effect of assuming minimum and maximum values for all uncertainties. Light bars show separate effect on total sediment load of uncertainty in surface level change (SLC), surface area, measurement error, particle size and bulk density.	206
Figure 11.8: Cumulative frequency distribution curves obtained from 1000 simulations of the sediment budget components I-S (dark) and O (light). Best estimate values for each component are indicated with dots.	207
Figure 13.1: Scenarios of erosion and deposition processes under four different (flood) flow conditions on the Ripple Creek floodplain.	225
Figure 13.2: SSC ( $\text{mg l}^{-1}$ ) in water samples from four locations in the Ripple Corner Catchment (99-00 season). Dark bars indicate peak flow (backwater) conditions; Bright bars indicate free flow conditions.	226
Figure 13.3: Water depth (m), flow velocity ( $\text{m s}^{-1}$ ) and SSC ( $\text{mg l}^{-1}$ ) for a peak flow event in the Ripple Drain. Backwater effects cause reduction in flow velocity at greatest water depths. Dashed lines indicate times when water samples were taken (7 and 10 February 2000).	227
Figure 13.4: Water and sediment discharge estimates for 6 sample dates on four locations in the Ripple Corner Catchment. Dark bars indicate peak flow (backwater) conditions; Bright bars indicate free flow conditions.	229
Figure 13.5: Clockwise hysteresis in the discharge – SSC relationship for the peak flow event between February 4 and 12. Three minor flow events after the main event are also included.	229
Figure 14.1: Sediment budget diagram for the 1999-2000 wet season in the Ripple Corner Catchment.	234

---

**PART I**

**INTRODUCTORY CHAPTERS**

---

---

# Chapter 1

## Introduction

---

### 1.1 Humid tropics and sugarcane cultivation

Land use in the river catchments of tropical North Queensland appears to have increased the transport of sediment and nutrients to the coast. The increase is believed to threaten coastal and marine ecosystems as well as the freshwater ecosystems of the catchments. This thesis is focused on the transport of sediment in and from one type of land use in this region: sugarcane cultivation. A sediment budget is used to quantify rates of sediment production, deposition and export.

An outstanding feature of the North Queensland wet tropical coast is the concentration of high annual rainfall in a few months of the year; during this period several hundred millimetres of rain can fall within days or even hours. The intense rainfall causes large amounts of runoff and makes water levels in river drainage systems rise quickly. Because the rainstorms often persist for several days, flooding occurs frequently.

Large areas of sugarcane cultivation occupy the lowlands of North Queensland (Figure 1.1). Sugarcane crop needs 1500 mm of rainfall or irrigation each year and can survive under inundated conditions for several days. These characteristics make it a suitable crop for cultivation in the flood prone tropical lowlands. Production of sugarcane is now one of Australia's largest intensive agricultural industries. In the 2000-2001 season 424,350 hectares of cane was harvested (Canegrowers, 2002).

To make the lowlands of the North Queensland catchments suitable for sugarcane, several adjustments have been made to the landscape. The first requirement is the clearing of the original vegetation. In North Queensland native vegetation has been substantially reduced and replaced by sugarcane. Since 1988 the area used for sugarcane growing has increased by more than 40%.

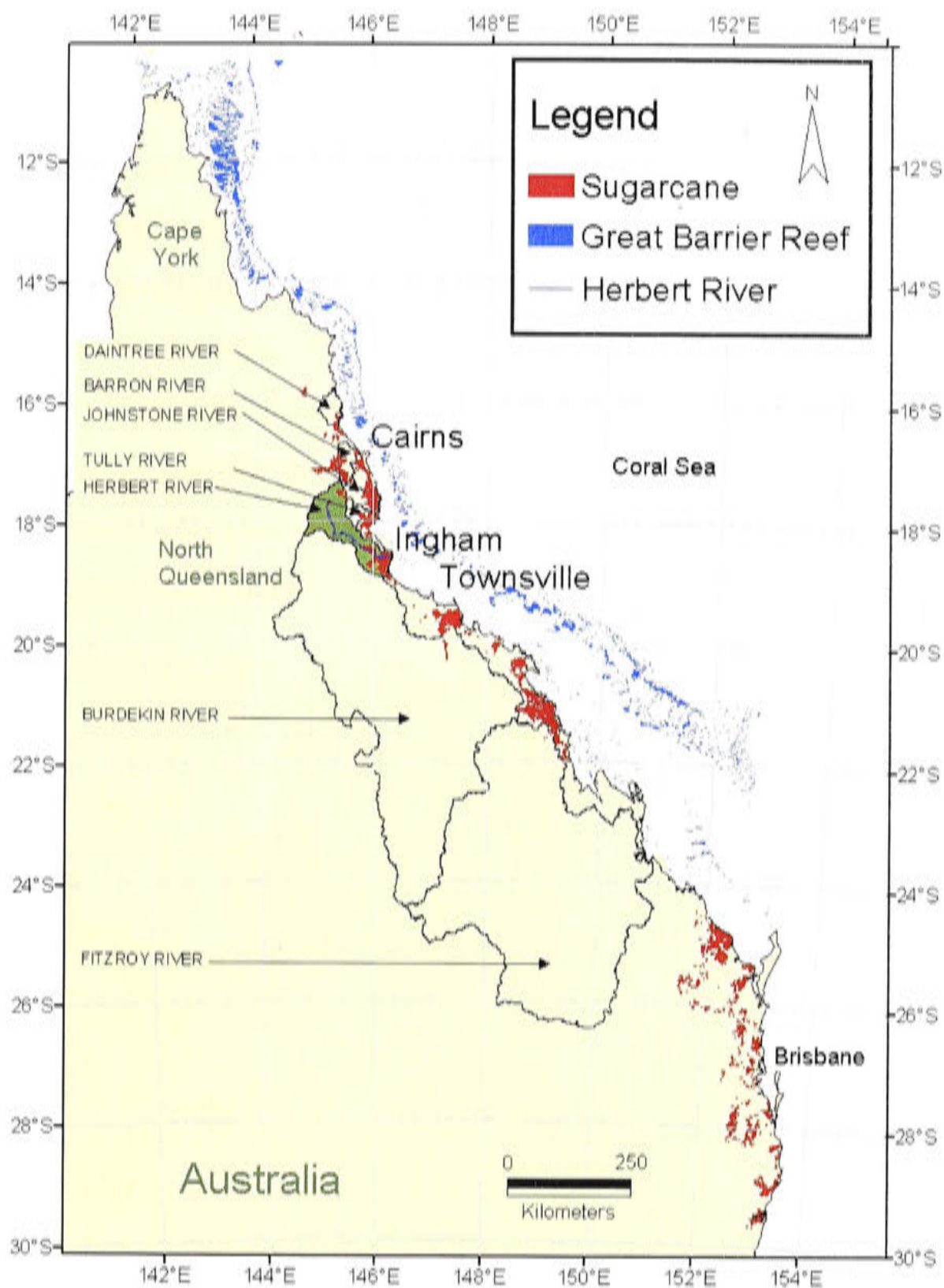


**Figure 1.1:** Map of North Queensland with sugarcane cultivation areas; seven of the major coastal catchments, including the Herbert River Catchment; and the Great Barrier Reef.

Johnson *et al.* (2000) studied vegetation changes in the lower part of the Herbert River Catchment, the largest wet tropical catchment in North Queensland. They observed that the three key vegetation types in the original landscape, which are Eucalyptus dominated forest, Melaleuca (paper-bark) dominated forest and Rainforest, have all been reduced, while the area under sugarcane has expanded. The highest loss was in the freshwater wetland Melaleuca communities (65%). According to these authors, similar trends are apparent in other North Queensland catchments.



A second requirement to prepare country for cane growing is drainage of the cultivated surface. The natural landscape has very low relief and contains many depressions where water accumulates for some time after a flood. Creeks drain most of the lowland, but to remove the ponded water additional drainage lines are necessary. The high tropical rainfall is very welcome for the thirsty sugarcane crop, but prolonged waterlogging or inundation is not desirable because it reduces the cane yield (Cameron McNamara, 1980; Dick, 1982, in Herbert River Improvement Trust, 1993; R. Burry pers. comm.) and makes access to the fields with heavy machinery difficult. Figure 1.2 shows an aerial photo of the Ripple Creek Catchment, a sub-catchment of the Herbert River, illustrating the typical cane land dissected by a dense network of drains (blue lines).

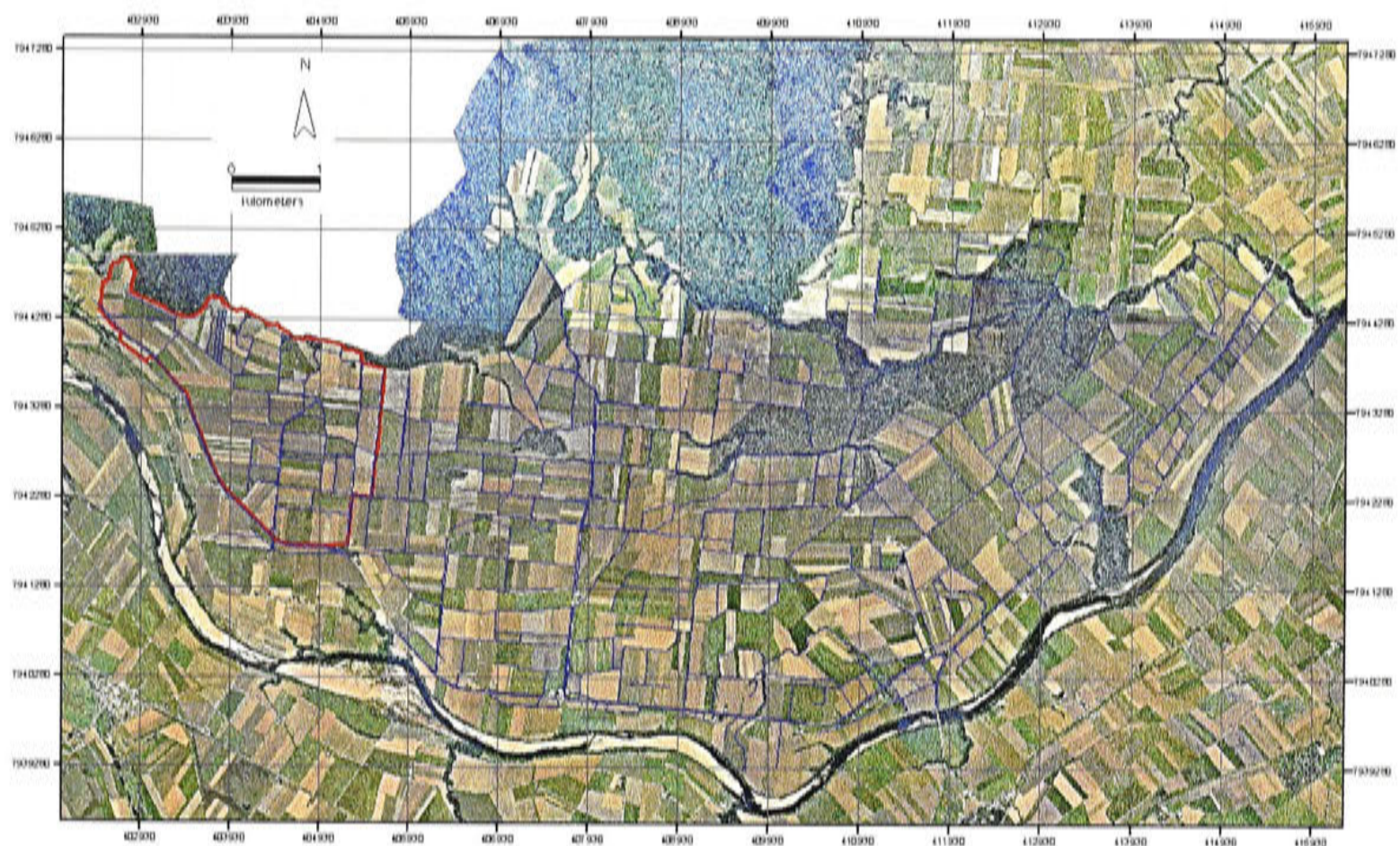


**Figure 1.2:** Aerial photo of Ripple Creek Catchment, a tributary of the Herbert River. Photo of forested upland section was not available. The (mostly artificial) drainage network in the catchment lowlands is highlighted in blue.

## 1.2 Increase in soil erosion since European settlement: the off-site effects

Similar to the Queensland sugarcane country, adjustments have been made to the landscape throughout Australia, mostly in the form of clearing of the native vegetation. A recent study estimates that about 32% of Australia's native vegetation

in the intensively used areas (primarily the agricultural and urban zones) has been cleared or substantially modified (Cofinas and Creighton, 2001).

The human disturbance has a significant impact on the health of the landscape. Johnson *et al.* (2000) for example describe the vegetation changes in the lower part of the Herbert catchment as a 'decline of the diversity, quality, and integrity of the tropical lowland ecosystems'. Many researchers have also noticed how clearing and subsequent introduction of European style agriculture has led to severe degradation of the soil and increased erosion rates (Wasson and Galloway, 1986; Moss *et al.*, 1992; Wasson *et al.*, 1996). Large parts of the eroded material are redeposited elsewhere in the river catchments (Wasson *et al.*, 1996), but a significant amount of sediment is exported to the catchment outlets, into the ocean. This has led to an increase of sediment, and associated nutrient, export to the coast from Australian river catchments. Moss *et al.* (1992) estimated a three to five-fold increase in sediment and nutrient export from the Queensland coastal catchments since European settlement.

On the land, degradation of the soil surface is not always recognized or acknowledged as a problem. In certain areas the effects of increased sediment loads from rivers, have become the first reasons for concern. This is the case in tropical North Queensland (Rayment and Neil, 1996; Wasson, 1996). All coastal catchments in this region drain directly into the Great Barrier Reef World Heritage Area (GBRWH). The concern about potential impacts of the increased sediment loads from these catchments has been growing among scientists, government management agencies, and among the general population.

The Great Barrier Reef Marine Park occupies the Queensland coastal zone between the tip of Cape York and the Mary River near Hervey Bay, approximately 200 km north of Brisbane (Figure 1.1). The area contains the world's largest system of coral reefs (GBRMPA, 2001). It is best known for the astonishing coral reefs out in the ocean, but it also comprises many reefs closer to the shore, large areas of mangrove forest, and coastal wetlands. Increase in water turbidity is thought to harm coral reefs and more recently researchers have also become aware of the potential impact of sediments on coastal mangrove and freshwater wetland and river (eco) systems, which are important in the functioning of the Marine Park. The following section reviews the information upon which the concern is based.

### **1.3 Effects of sediments and nutrients on the Great Barrier Reef World Heritage Area and riverine ecosystems**

#### **1.3.1 Increased sediment and nutrient inputs**

CRC Reef Research Centre (2001) provides a concise overview of the current state of knowledge on runoff from the land. On average 14 million tonnes of sediment, 49,000 tonnes of nitrogen and 9,000 tonnes of phosphorus are carried into the GBRWH each year. This is a threefold increase of sediments and nitrogen over the last 150 years and more than 10-fold for phosphorus. Slightly higher increases are listed in the recent report by the Great Barrier Reef Marine Park Authority (GBRMPA) (2001), which also states that the loads are still increasing without a sign of abatement. A large part of the nitrogen (40%) and phosphorus (80%) carried by the rivers is attached to fine sediment particles. River water concentrations of other chemicals used in agriculture such as pesticides and their components (e.g. Diuron, atrazine, mercury and cadmium) are very low, but can accumulate in sediment deposits and may have biological impacts (Bryan and Langston, 1992).

Over the last 15-20 years extensive research has been done to understand the effects on the reef and coastal wetland systems of changes in runoff from the land. Numerous reports have been published on this research by the involved organisations (e.g. GBRMPA, Australian Institute for Marine Science (AIMS), CSIRO, etc.) and regularly the findings are reviewed (Baldwin, 1990; Hillman, 1995; Crossland *et al.*, 1997; Hutchings and Haynes, 2000). The latest of such reviews are reported in (GBRMPA, 2001; Williams, 2001; WWF, 2001).

#### **1.3.2 Effects of sediment on coral reef systems**

It is generally assumed that the increase of sediments, nutrients and other chemicals will lead to increased degradation of coral reef systems (Wilkinson, 1999; Edinger *et al.*, 1998). Sediments are seen as a potential threat to coral reef systems, but the exact effect of increased sediment loads is however still not very well understood. The following reasons are given for concern about sediments.

- They can exclude light from corals (Well-developed outer reef systems occur only in seawater with low suspended particulate concentrations)
- They can smother corals (Wilkinson, 1999)

- They can prevent the settlement of coral larvae on the reef surface

Apart from direct threats there are possible indirect impacts, but their functioning is even less well known:

- Crown-of-thorns (starfish) outbreaks may be related to increased phytoplankton levels, caused by increased nutrient loads (partly associated with sediments) from terrestrial runoff (Day, 2000)
- Changes in habitat due to reduction in micro-topography can have an indirect effect on the survival of corals

The scientific literature on all of these impacts is both limited and contradictory (McClanahan and Obura, 1997; Williams, 2001; Marohasy and Johns, 2002).

Very recently some researchers have questioned the argument that higher sediment loads increase turbidity of the seawater and cause the problems mentioned above. Larcombe and Woolfe (1999) argue that turbidity levels and sediment accumulation rates are at most coral reefs currently not limited by sediment supply. Sediment input from rivers will not add significant extra turbidity to what is caused by regular seabed disturbance already. They do note that the seaward terrigenous sediment edges and coral reefs immediately adjacent to identified point sources of sediment input should be studied more closely.

#### *Effects of sediment related chemicals*

Besides impacts on coral reefs directly related to increased sediment concentrations in the seawater, there are problems caused by fertilizers and pesticides bound to particulate matter. Large amounts of these chemicals leave the land connected to soil particles and are transported into the ocean. When river water mixes with seawater there is a possibility that they are released from the soil particles. Brodie and Mitchell (1992) found a significant proportion of inorganic P in the flood plume of the Fitzroy River after mixing of the freshwater with seawater. The process of sorption and desorption of nitrogen and phosphorus from flood plumes into the seawater is however not sufficiently understood

Devlin and Taylor (1999) and GBRMPA (2001) list a number of observed increases in chlorophyll concentrations in flood plumes and in water with sediment resuspended by strong winds. Because phytoplankton and bacteria rapidly consume nutrients in seawater, nutrient levels are typically low and a poor indicator of the

nutrient status of reef water. Chlorophyll provides a better integrative measure of the amount of nutrients held and cycling in the reef ecosystems. The increased concentration among suspended sediment could indicate increased bioavailability of nutrients attached to sediments.

Cavanagh *et al.* (1999) failed to detect significant amounts of organochlorine in near-shore sediments, although easily detectable amounts were found in sugarcane soils in the Herbert and Burdekin catchments, and the chemicals are known to move attached to soil particles. There is no detectable organochlorine contamination of the GBRWH from historic agricultural activities in the catchments.

### **1.3.3 Effects of sediment on other marine ecosystems**

Seagrass beds are important ecosystems in the GBRWH, situated in coastal areas close to the input sources of terrestrial runoff. The beds can experience impacts from sediment in direct and indirect ways similar to the coral reefs. Some research has shown that seagrass beds can die due to light deprivation as a result of increased turbidity (Preen *et al.*, 1995; Longstaff and Dennison, 1999). Potential impacts of nutrients are assumed, but no clear proof of negative impacts is available (Williams, 2001).

Many marine species rely on the coastal freshwater wetlands and mangroves as breeding and nursery areas (Robertson and Lee Long, 1991; GBRMPA, 2001). Mixing between mangrove creek water and coastal seawater through tides ensures a strong dynamic link between mangroves and coastal waters (Wolanski *et al.*, 1990), making mangroves vulnerable to pollutants in the near shore waters. Trott and Alongi (1999) observed increased nutrient concentrations in mangrove creeks during the summer wet season, which are probably due to erosion, solubilization and transport of nutrients from adjacent catchments into creeks. Negative impacts of the elevated nutrient levels were not noted.

### **1.3.4 Effects of sediments on freshwater ecosystems**

Freshwater ecosystems also play an essential role in the functioning of the Great Barrier Reef Marine Park. Many organisms, for example, use the fresh river water as breeding grounds. Because increased input of sediments and nutrients are routed through the rivers, these freshwater systems are directly affected.

There are several potential problems related to increased sediment loads in rivers (Arthington *et al.*, 1997). Suspended sediment causes water turbidity, which can diminish the light that is available for photosynthesis of stream vegetation, and decrease water temperature through increased reflection. Suspended material can also inhibit respiration and feeding of stream biota (Ryan, 1991).

Crossland (1999) points out that aquatic organisms in tropical rivers are well adapted to short term events with high concentrations of sediments and nutrients, because disturbance by floods is a normal occurrence in North Queensland streams. It is, however, a continuing supply of enhanced levels of nutrients and sediments through the year via seepage, runoff, and irrigation tailwater that are likely to be of greater importance to aquatic communities.

### 1.3.5 Conclusion

The forgoing overview shows that there are potential direct and indirect impacts of increased sediment loads on many of the ecosystems of the GRBWH and the closely related freshwater systems. Firm evidence of a serious decline in any of the systems is however currently limited. This does not mean that terrestrial runoff can be ignored. Large-scale systematic studies on the GRBWH only started in the last 20 years or less and we do not know what the area looked like before European settlement. There are also studies from other parts of Australia and the rest of the world that indicate negative effects of sediments and nutrients on coral reefs and especially seagrass communities (Robertson and Lee Long, 1991; Edinger *et al.*, 1998; Corredor *et al.*, 1999). Similar effects could occur in the GRBWH and increase with continued or increasing inputs. Clearly most at risk are near-shore ecosystems such as near shore reefs and seagrass beds, because of their vicinity to the sites of sediment input.

A final very important concern is the potential cumulative effect of the increased (chronic and episodic) impacts of sediment pollution. Coral reefs and other ecosystems may be able to cope with impacts for a considerable time, but continued stress and unobserved sub-lethal effects can lead to fatal degradation in the longer term. Some studies worldwide have shown examples of systems that display such threshold effects (Williams, 2001).

#### 1.4 Soil erosion in low-lying sugarcane land

Sugarcane land is mainly located in the low-lying areas of the North Queensland catchments (see Figure 1.1). This industry is therefore situated adjacent to the many coastal and freshwater ecosystems that play a role in the survival of the Great Barrier Reef. The drainage water from the cane fields flows directly into these aquatic ecosystems. During storm flows the drainage water has a 'dirty' colour, which suggests that considerable amounts of sediments leave the catchment. Attached to the sediments will be fertilizers and pesticides that are used abundantly for cane growing.

The only published research on soil erosion from cane land in Australia was done on sloping cane land. In the Mackay region erosion rates in excess of  $200 \text{ t ha}^{-1}$  were measured (Sallaway, 1979). Prove and Hicks (1991) observed values ranging from  $50$  to  $500 \text{ t ha}^{-1}$  on the wet tropical coast, where the magnitudes of erosion depended on rainfall amount and intensity, not soil type and slope. Although no numbers are available for erosion from low-lying cane land, their location close to the coast and the observations of sediment export through river water provide grounds for public concern that sugarcane land is a major source of pollution. Even though decline of the Great Barrier Reef due to terrestrial runoff is not clearly demonstrated the sugarcane industry is often mentioned as, at least, a threat to the health of the Great Barrier Reef (Flannery, 1994; WWF, 2001).

As a result of early observations of erosion, and signs of pollutants leaving the cane lands, ameliorative action began in the 1980s (Prove and Hicks, 1991). Around that time Green Cane Trash Blanket (GCTB) harvesting was introduced in parts of the Queensland cane-growing region. This is a type of minimum-tillage harvesting, where the leaves of the cane plant are left on the fields as trash cover after the harvest of the cane stalks. GCTB harvesting now occurs in nearly 70% of the cane lands.

Prove *et al.* (1995) showed that the GCTB method reduces sediment runoff from sloping fields to levels comparable with those from rainforest, which were estimated at around  $4 \text{ t ha}^{-1}$  by Capelin and Prove (1983). Williams (2001) describes unpublished research on sediment cores from Hinchinbrook Channel and Missionary Bay that display a decline in terrestrial sediment supply rates over the last two decades, which could be related to green cane harvesting practices in the Herbert

River valley. Evidence of how much GCTB-harvesting reduces sediment export from the cane lands is however still not abundant, and criticism of cane growers continues by environmentalists.

#### 1.4.1 Sources of sediment: the first thesis objective

Erosion research in the cane district has paid little attention to sediment sources other than the cultivated fields, although there may be some of considerable importance. The establishment of a cane property in the tropical lowlands requires more than just the clearing of the original vegetation. One of the most important additional requirements is an artificial drainage system. In erosion studies on natural lowland drainage systems elsewhere in the world, bank erosion has been identified as an important source of sediment besides sheet erosion (Knighton, 1998; Laubel *et al.*, 1999). The same process can be expected in artificial drainage systems (Urban, 2002) and could be of particular importance in the sugarcane district with its high rainfall and runoff.

In addition to the drains there could be other unidentified sources of sediment in the modified cane lands. A number of landscape elements, which are schematically presented in Figure 1.3, are common in most of the low-lying sugarcane land. Each of these elements could be a sediment source:

- Plant cane fields: fields with a first year crop. The soil surface beneath the plant cane crop is still bare. Sheet erosion can be expected.
- Ratoon fields: sugarcane is grown for up to four return cycles called 'ratoon'. The soil surface beneath the ratoon crop is protected with a trash cover from earlier harvests, but sheet erosion might occur under extreme runoff.
- Water furrows: shallow trenches in fields for improved drainage. Concentrated field runoff that flows through furrows could easily scour the bare surface.
- Drains: because of the low gradient in a flood plain environment, a dense drainage network is necessary to quickly drain the high volumes of rainwater. Bank erosion can be a major sediment source in lowland drainage systems (Laubel *et al.* 1999).
- Headlands: 2 – 5 meter wide strips of land along the margins of cane fields, used for the turning of cane harvesters and as access roads. Their slightly sloping



surface and sometimes sparse grass cover can make them susceptible to rill and sheet erosion.

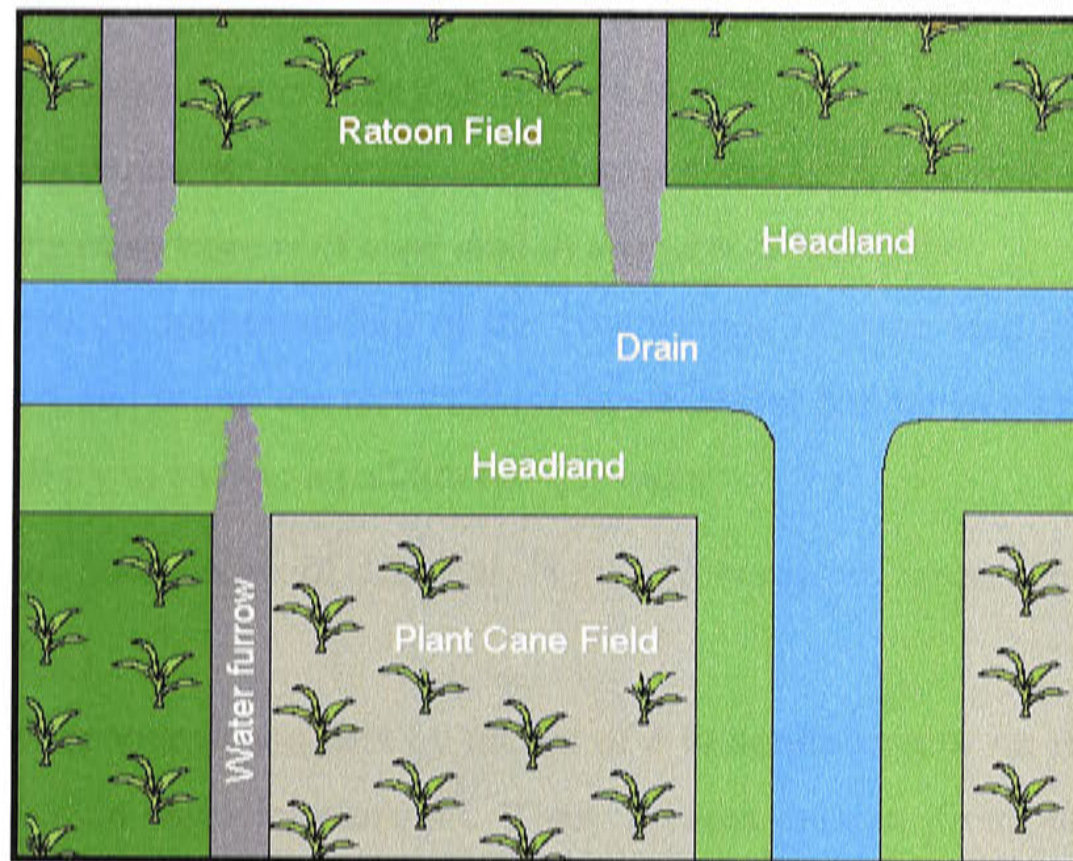


**Figure 1.3:** Schematic close-up of sugarcane land illustrating typical landscape elements: ratoon fields, plant cane fields, drains, headlands and water furrows.

If the sugar industry wants to further improve cane growing practices to reduce erosion and downstream impacts of runoff, they need to know the importance of the above mentioned potential sources. This thesis aims to assist improvements of cane land management by studying these sediment sources and provide an answer to the following questions:

- How much sediment is coming from low-lying sugarcane land?
- What are the important sources of sediment in low-lying sugarcane land?

The problem is approached by developing a sediment budget for an area of cane land in the Herbert River Catchment. In the budget the amount of sediment generated from the various sources is compared with the export of sediment from cane land. For the composition of the budget, measurement data are collected from a field site in the Herbert River Catchment.

If significant sources of sediment are identified and if processes are sufficiently understood, the answers to these questions can lead to recommendations for improved management of the sugarcane land. This will allow cane farmers to effectively protect their land and reduce off-site pollution.

#### **1.4.2 Soil erosion on floodplains: a second thesis objective**

Much of the cane land is situated in what has in previous pages been described as 'lowlands' or 'low-lying areas'. Most of these areas are actually floodplains. In a river catchment floodplains are usually sediment storage areas; areas that collect sediment, rather than generate it (Schumm, 1977; Alexander and Marriott, 1999), which contradicts the observations of cane land as a source of sediment.

To improve the understanding of the contribution of cane land to the sediment input of rivers and to put the results from the sediment budget in a broader context, the thesis will try to answer an additional question:

- How can floodplains of tropical North Queensland rivers be a source of sediment?

This problem is approached first by means of a literature review on the functioning of floodplains in river catchments. Then process insight from the review, in combination with information from local sources and the budget study results, is used to develop scenarios that describe erosion and deposition processes for part of the Herbert River floodplain. The scenarios will help answering the additional thesis question and give an indication of the representativeness of the results from the sediment budget study.

#### **1.5 Thesis outline**

This introductory part of the thesis will continue with a description of the Herbert River Catchment, which is the area on which the study focuses. Special attention is paid to Ripple Creek, the sub-catchment of the Herbert River, where most of the fieldwork is performed.

Part II of the thesis describes the approach and results of the sediment budget study that was performed in the Ripple Creek Catchment, with the aim to answer the first thesis questions. Part III comprises a literature review and a discussion of the information available from the Ripple Creek Catchment, which leads to the development of qualitative scenarios for erosion and deposition processes in this area, in answer to the additional thesis question.

In the final part (IV) the conclusions drawn from the previous parts will be combined and presented, together with recommendations for future research to assist management of the low-lying cane lands.

---

## Chapter 2

### The Herbert River Catchment: a site description

---

#### 2.1 Introduction

The Herbert River Catchment (Figure 2.1) is the largest catchment along the sub-humid to humid tropical coast of northeastern Australia and the fifth largest catchment draining into the Great Barrier Reef, providing 4.8% of the total input of freshwater runoff (Furnas and Mitchell, 2001). The catchment includes the largest area of cane land under wet tropical conditions. The canegrowing region extends further north along the coast under humid tropical conditions, but in smaller catchments (see Figure 1.1 in Chapter 1). Further south larger catchments such as the Burdekin River catchment also have considerable areas of cane land, but the climatic conditions are drier and the cane is often irrigated (Arthington *et al.*, 1997).

Because of its large area of typical low-lying cane land, the Herbert River Catchment is chosen as the study area for this research. Previously various Australian research organisations (e.g. CSIRO, Great Barrier Reef Marine Park Authority (GBRMPA) and Australian Institute of Marine Science (AIMS)) have concentrated research within this catchment (e.g. Horsley *et al.*, 1982; Hillman, 1995; Bramley and Johnson, 1996; Johnson and Murray, 1997; Mitchell *et al.*, 1997; Cavanagh *et al.*, 1999; Bramley and Wood, 2000; Johnson *et al.*, 2000; Bramley and Roth, 2002). There is, therefore, an existing base of knowledge that is of use to this project.

Within the Herbert River Catchment the Ripple Creek Sub-catchment is chosen as the main study site. The location of the Ripple Creek Sub-catchment is shown in Figure 2.1. This sub-catchment is thought to be representative for areas of 'low-lying cane land', and it is also the most intensively studied sub-catchment of the Herbert River.

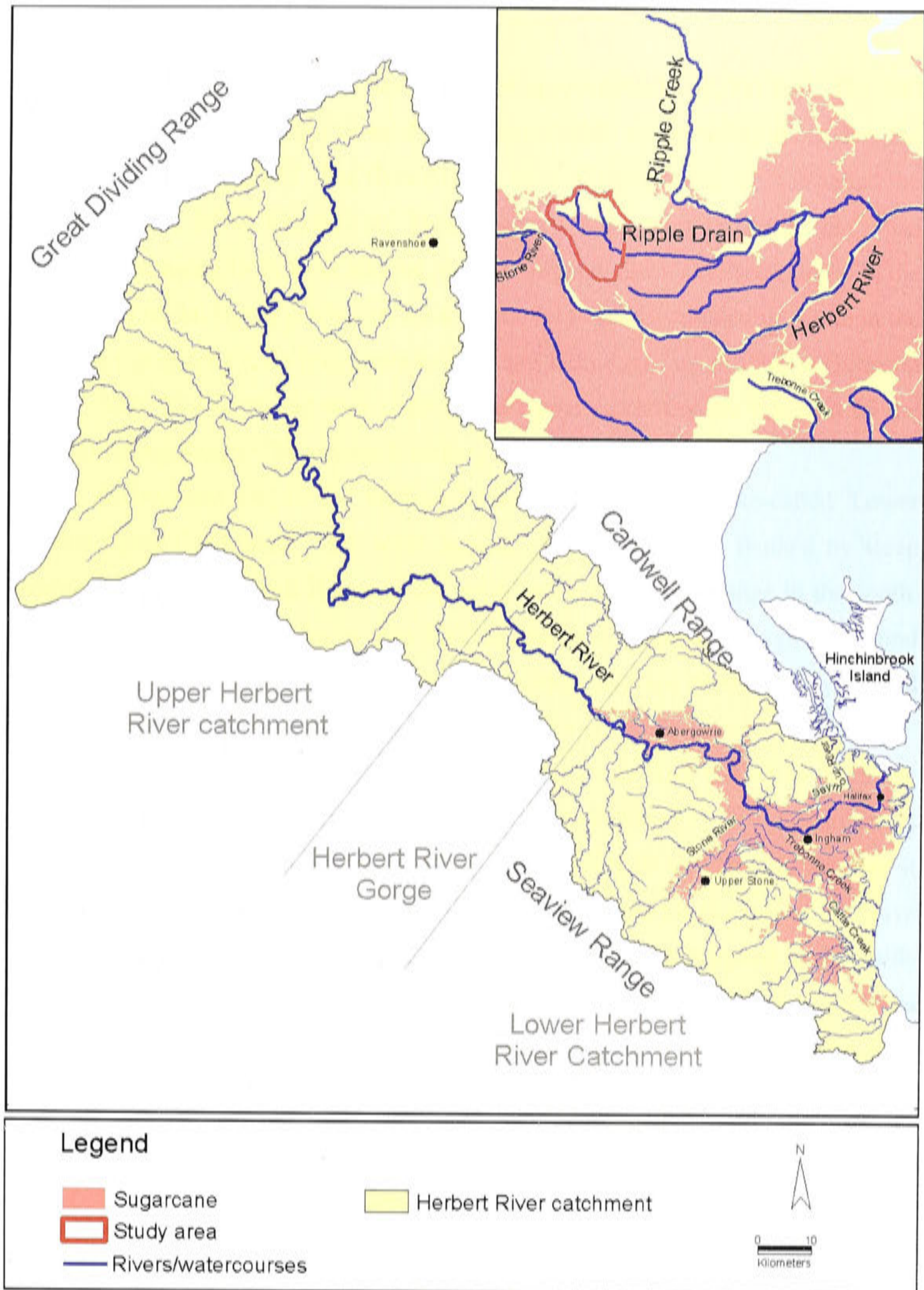


**Figure 2.1:** Herbert River Catchment and Ripple Creek Sub-catchment with sugarcane cultivation areas and approximate Upper and Lower Herbert River divisions and Herbert River Gorge.

## **2.2 General catchment description**

The Herbert River drains a catchment area of approximately 10,000 km<sup>2</sup>. The 340 km long river flows through three distinct geomorphic zones before it reaches the Coral Sea north of Halifax. The river rises at 1070 m elevation in what is called the 'Upper Herbert River Catchment'. This upstream zone (approx. 6,000 km<sup>2</sup>) has topography ranging from level alluvial plains to rugged, deeply incised ranges. In the eastern part of the Upper catchment the topography is gently undulating, while in the west, the topography rises irregularly and reaches altitudes of up to 1000 m (Johnson *et al.*, 2000). The north and west sides of the Upper catchment are bounded by the Great Dividing Range. The eastern boundary is the Cardwell Range.

The downstream end of the Herbert River flows through the so-called 'Lower Herbert River Catchment'. This zone consists of a coastal plain flanked by steep mountains of the Cardwell Range in the north and the Seaview Range in the south. The mountains reach altitudes of over 1000 m, but have an average height of around 750 m. The Upper and Lower Herbert River Catchment are connected by a third intermediate zone (1000 km<sup>2</sup>), the 'Herbert River Gorge'.

The lower part of the Herbert River Catchment was first settled in 1865 for pastoral use. Sugarcane production started in 1872 (Pulsford, 1996). Sugarcane is only grown on the alluvial soils of the Lower Herbert River Catchment. Here it occupies approximately 650 km<sup>2</sup> (Shrubsole *et al.*, 1999) and is the largest intensive agricultural industry in the catchment. Harvested sugarcane is supplied to two mills (Victoria and Macknade) for sugar production. Most cane is grown close to the mills near the catchment outlet. The growing area extends upstream along the main river towards Abergowrie and along the Stone River tributary to Upper Stone.

Other important industries in the Herbert River Catchment are forestry, beef cattle and small areas of crops such as pineapples, melons and pumpkins. Most of the Upper Herbert River Catchment remains under native vegetation with extensive cattle grazing. Grazing in the Lower catchment occurs mainly on improved pasture.

## **2.3 Geology**

The geology of the Herbert River Catchment is described by de Keyser and has been summarized in the Herbert River Catchment Atlas (Johnson and Murray, 1997). The following information is paraphrased from the Atlas.

The lowland of the Lower Herbert River Catchment consists largely of Quaternary alluvial deposits, beach sand, and mangrove muds. The deposits reach a depth of more than 96 m and are interbedded due to sea level oscillations. The steep mountains surrounding the deposits consist of Carboniferous granites, with rocks of various compositions and texture grading into one another. Palaeozoic basalt occurs within the Herbert Gorge. The Upper Herbert River Catchment consists of four units. The rugged highland in the north consists of incised Palaeozoic sediments, acid extrusives and granite. The level to gentle undulating plain in the centre has low rises of granite and metamorphic rock. The plain in the south and southwest consists of Cainozoic basalt, extruded from local craters. The geology of the Coastal Range along the eastern edge of the catchment boundary is complex. It consists of andesite, and rhyolite volcanics, locally intruded by granite, Cainozoic basalt flows and an area of undifferentiated granite.

## **2.4 Geomorphology**

No publications exist on the geomorphology of the Upper Herbert River Catchment. Because this part of the catchment is not relevant to the subject of this thesis, no attempt will be made to describe and explain the geomorphology in this area. Some understanding of the geomorphology of the Lower Herbert River Catchment is, on the other hand, essential for the research of this thesis. Moreover, there is information available from this area.

Wilson and Baker (1990, also presented in: Johnson and Murray, 1997) mapped the landforms and the closely related soil types in the Lower Herbert River Catchment. A copy of the map presented in Johnson and Murray (1997) (Figure 2.2) is added to illustrate the following geomorphological features.

The hills and mountains of the Cardwell and Seaview Ranges provide a clear geomorphic contrast with the lowland of the Lower Herbert River Catchment. The Ranges surrounding the lowland have a low to very high relief with gently inclined to precipitous slopes and fixed erosional stream channels (classification according to the Australian Soil and Land Survey Field Handbook (McDonald *et al.*, 1990). The main forces that shaped the mountains are probably water erosion and mass wasting, although so far no detailed geomorphological survey has been done here.

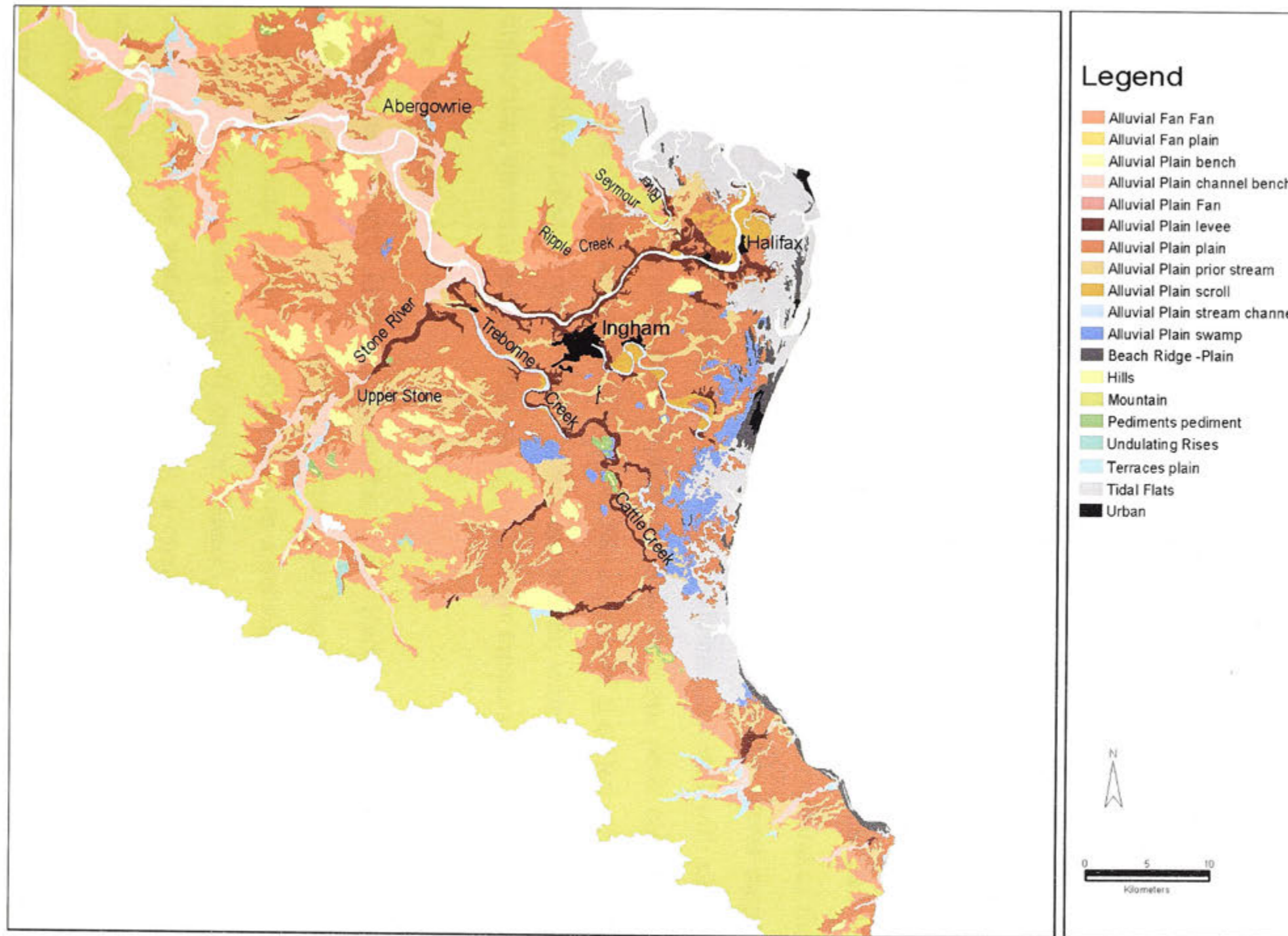


**Figure 2.2:** Geomorphology of the Lower Herbert River Catchment (after Wilson and Baker, 1990 in Johnson and Murray, 1997).

The lowland is a fan shape depositional area spreading out towards the Coral Sea. Within the lowland a geomorphic subdivision can be made between deposits of mainly fluvial origin and deposits of marine origin. A band of around 5 km wide from the coast consists of marine deposits. The most common depositional features here are tidal flats, mangrove muds, and beach ridges. Further inland the lowland consists of mainly fluvial deposits. Along the footslopes of the Ranges, runoff and debris from local slopes have created alluvial fans. The fans have slopes of up to 8% and are built on an alluvial plain. The alluvial plain consists of deposits from both the local creeks and the Herbert River.

The Herbert River has a channel pattern ranging from low sinuosity to meandering stretches. Scroll ridges formed during migration of the meander bends are visible in scroll plains of up to 300 m wide along the river (map unit 'Alluvial Plain channel bench' and 'Alluvial Plain scroll'). Excavations in several of the scroll plains in the Lower Herbert River Catchment showed that the lateral migration of meander bends has left behind mainly sandy floodplains covered with an up to 1 m of mud produced by over bank deposition (R.J. Wasson, pers. comm). Frequent floods have created levee deposits along these parts of the Herbert River and the Stone River tributary where scroll plains are absent, which are up to three meters higher than the surrounding plain. Along both rivers terraces also occur.

#### *The Herbert River delta*

Johnson and Murray (1997) describe the Lower Herbert River alluvial plain as an asymmetric delta. Most of the recent deposition happens towards the northern edge of the delta. Here the Herbert River ends in a network of minor branching channels. Russell (1967) argues that all major channel patterns in a delta are originally established under water. At its outlet a channel becomes divided by an island structure that forms through preferred deposition in the middle of the channel. With continuing sedimentation the channel splits and a distributary is created. The distributaries continue building their levees and finally surface. Some become closed off at point of branching by extensions of levees along more favoured channels. The creek patterns on the Lower Herbert alluvial plain are the remnants of a network of prior deltaic distributaries. The Seymour River is the only former major distributary that is still connected with the Herbert River and still carries part of its flow. The Trebonne and Cattle Creek systems are probably some of the earliest major



distributaries. From their, now cut-off, point of branching the Herbert River has migrated northward.

Most of the former deltaic plain is regularly inundated by floodwater from the Herbert River (see Section 2.6). During flood conditions the prior distributaries may still divert some of the Herbert flow. The delta area that consists of fluvial deposits can now be defined as the floodplain of the Herbert River, comparable to the delta area of the River Niger in West Africa, as described by Allen (1964). The Niger delta can be divided into three zones, which consist of terrestrial, transitional and marine sediment input. Like the Herbert River alluvial plain, the upper part of the delta is the terrestrial zone consisting of a floodplain environment with levees and backswamps.

## **2.5 Climate**

The rainfall in the North Queensland wet tropics is among the most intense by world and tropical standards. Daily totals can exceed 250 mm. For a site near Babinda (median annual rainfall 3600 mm) the mean number of days with rainfall greater than 100 mm is seven per year (Bonnell *et al.*, 1986, in Isbell and Edwards, 1988). The Herbert River Catchment is located at the southern edge of the wet tropics. Therefore, it does not receive as much rainfall as the central parts. The catchment average is 1500 mm (Bureau of Meteorology, 1988), but the actual amount varies considerably within the catchment. Totals in excess of 3000 mm occur on the top of the Cardwell Range, while areas in the west receive only 750 mm. Of the total annual rainfall 75% falls in the warm summer months between December and April. This period is referred to as the 'wet season'. In Ingham the temperatures during these months have a mean monthly maximum of 32 °C and a mean monthly minimum of 23 °C. The winter months are mild and dry, with maximum mean monthly temperatures of 25 °C and minimum mean monthly temperatures of 13 °C (Johnson and Murray, 1997).

In contrast to many of the world's humid tropical regions, in the North Queensland tropics the major source of the rainfall is not a zone of thunderclouds within the monsoon trough. This type of rainfall happens occasionally, but usually the monsoon trough does not extend far enough south. More significant is the development and movement of vortices on the monsoon trough in the vicinity of the wet tropical coast (Bonell, 1988). These systems occur generally as tropical depressions, but they can deepen and upgrade to tropical cyclones. The presence of a depression causes heavy

rainfall over a few days, followed by periods of little precipitation until the development of a new depression. Other important sources of rain are orographic and convergence systems. The latter causes most of the rainfall between April and November.

## **2.6 Hydrology of the Herbert River**

The hydrographs of the rivers draining the North Queensland wet tropical catchments closely follow the seasonal distribution of the rainfall, with the major part of the flow concentrated in the wet summer months (Gilmour, 1977). The rainfall patterns during the wet season cause variable river flow with infrequent, high-intensity flood events (Mitchell *et al.*, 1997). These flood events, especially extreme floods resulting from cyclonic activity, cause problems for agriculture (e.g. yield loss (Horsley *et al.*, 1982) and personal damage (Cameron McNamara, 1980; Hausler, 1991)). Extensive flooding usually occurs on the alluvial plains, at the downstream ends of the tropical rivers. These flat, low-lying and flood-prone areas are favoured locations for settlement and agricultural development.

### *Discharge patterns in the Herbert River Catchment*

The Herbert River has a highly variable discharge, seasonally, as well as between years and over decades, which is typical for the North Queensland catchments (see Figure 2.3 (Furnas and Mitchell, 2001)). The average annual discharge, since first recorded in 1915, is 3.3 km<sup>3</sup>, varying between 0.14 km<sup>3</sup> (1961) and 10.4 km<sup>3</sup> (1974) (Furnas and Mitchell, 2001).

In Table 2.1 the average discharge of the Herbert River is compared with those of the Rhine and the Murray Darling. The mean discharge to drainage area ratio of the Herbert River is similar to that of the Rhine, a river in the temperate part of Europe. However in high discharge years the Herbert can generate three times its mean annual discharge, while the Rhine rarely generates more than two times (Middelkoop, 1997). Most Australian rivers generate considerably less discharge per square kilometre. The Murray Darling River is Australia's largest river catchment, which drains an area that includes several drier climate zones. Its drainage area is more than 100 times larger than the Herbert River Catchment, but generates less than 10 times the amount of discharge.

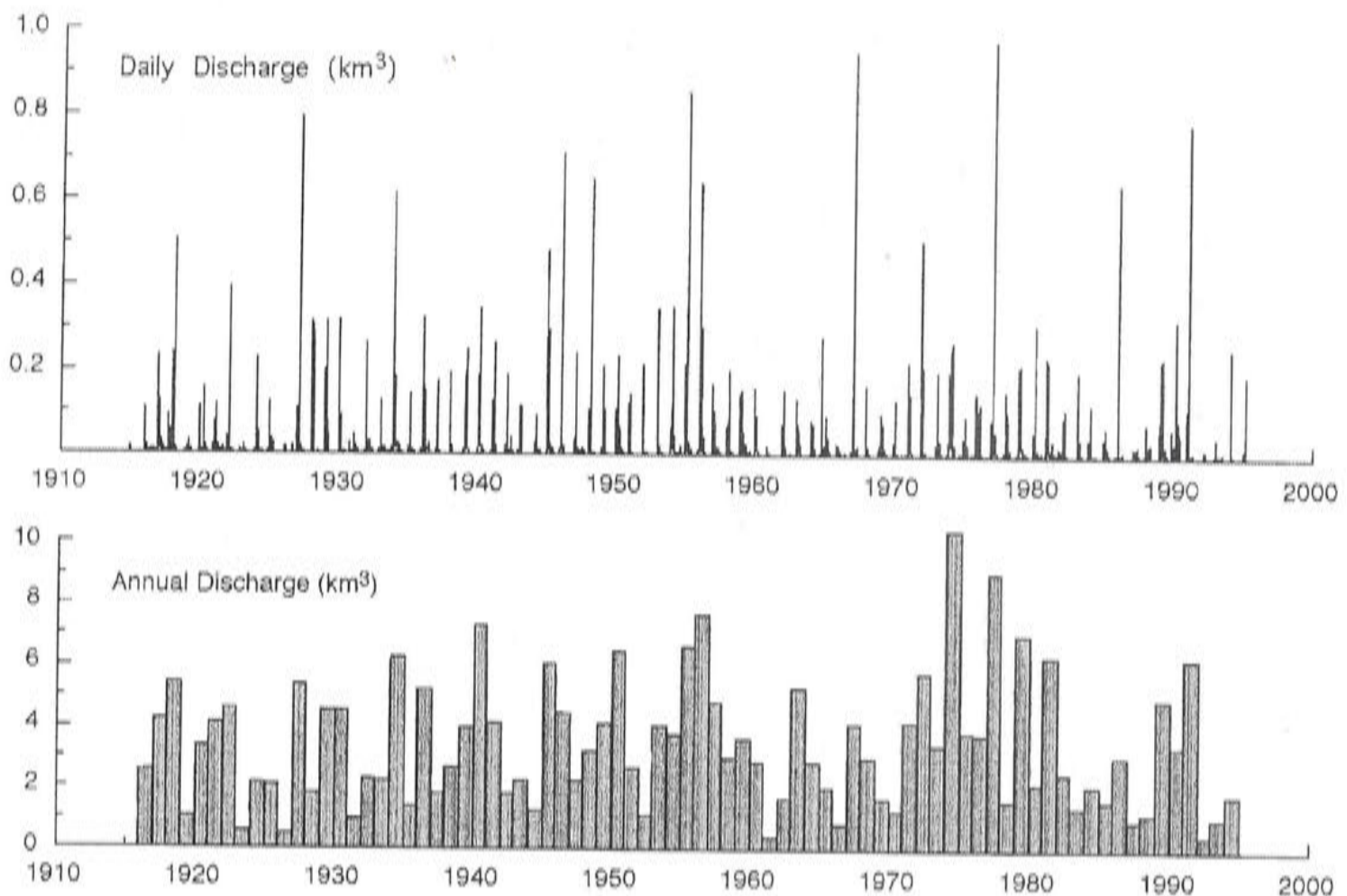


**Figure 2.3:** Daily (top) and annual (bottom) discharge from the Herbert River between August 1915 and September 1995. Data source: Queensland Department of Natural Resources and Mines (Furnas and Mitchell, 2001).

**Table 2.1:** Discharge and sediment loads of the Herbert River compared with the Rhine (Europe) and the Murray Darling (Australia).

	Drainage area ( $10^3 \text{ km}^2$ )	Mean discharge ( $\text{km}^3 \text{ y}^{-1}$ )	Mean suspended sediment load ( $10^6 \text{ t y}^{-1}$ )
Herbert River*	8,6	3.3 (0.4-10)	0.4
Rhine**	165	69	2.1
Murray Darling***	1,060	22	30

Based on: \*Furnas and Mitchell (2001), \*\*Middelkoop (1997), \*\*\*Knighton (1998)

Overall 60% of the water discharged from the Herbert River is derived from the Lower Herbert floodplain and the mountains surrounding the Herbert River gorge and floodplain (approx. 40% of the total catchment area). Only during the summer wet season is discharge at Ingham is significantly higher than at Abergowrie (see map in Figure 2.1). This reflects the increased contribution from the downstream tributaries in the wet season, when the downstream area receives much more rainfall (Bramley and Johnson, 1996). Because of the relatively high downstream input, the Herbert River behaves hydrologically like a wet tropical river, although the

catchment is seasonally dry and the land cover of the Upper catchment closer resembles the drier catchments of the rivers to the south (Furnas and Mitchell, 2001).

Large flood events, such as that caused by a cyclone in 1977, can inundate the alluvial plain of the Lower Herbert River Catchment (700 km<sup>2</sup>, was inundated in 1977) (Figure 2.4). Floods of the 1977 extent have a recurrence interval of 25 years. They will be referred to as 'major' floods. Floods of similar extent in the last century occurred in 1927, 1964, 1967, 1986 and 1991 (Johnson and Murray, 1997). These floods caused considerable change to the natural and damage to the built environment. Every year smaller flood events occur as a result of heavy rainfall. They will be referred to as 'minor' floods. These minor flood events usually only cause local inundation, but can do considerable damage to agriculture, depending on their timing, duration, and location.

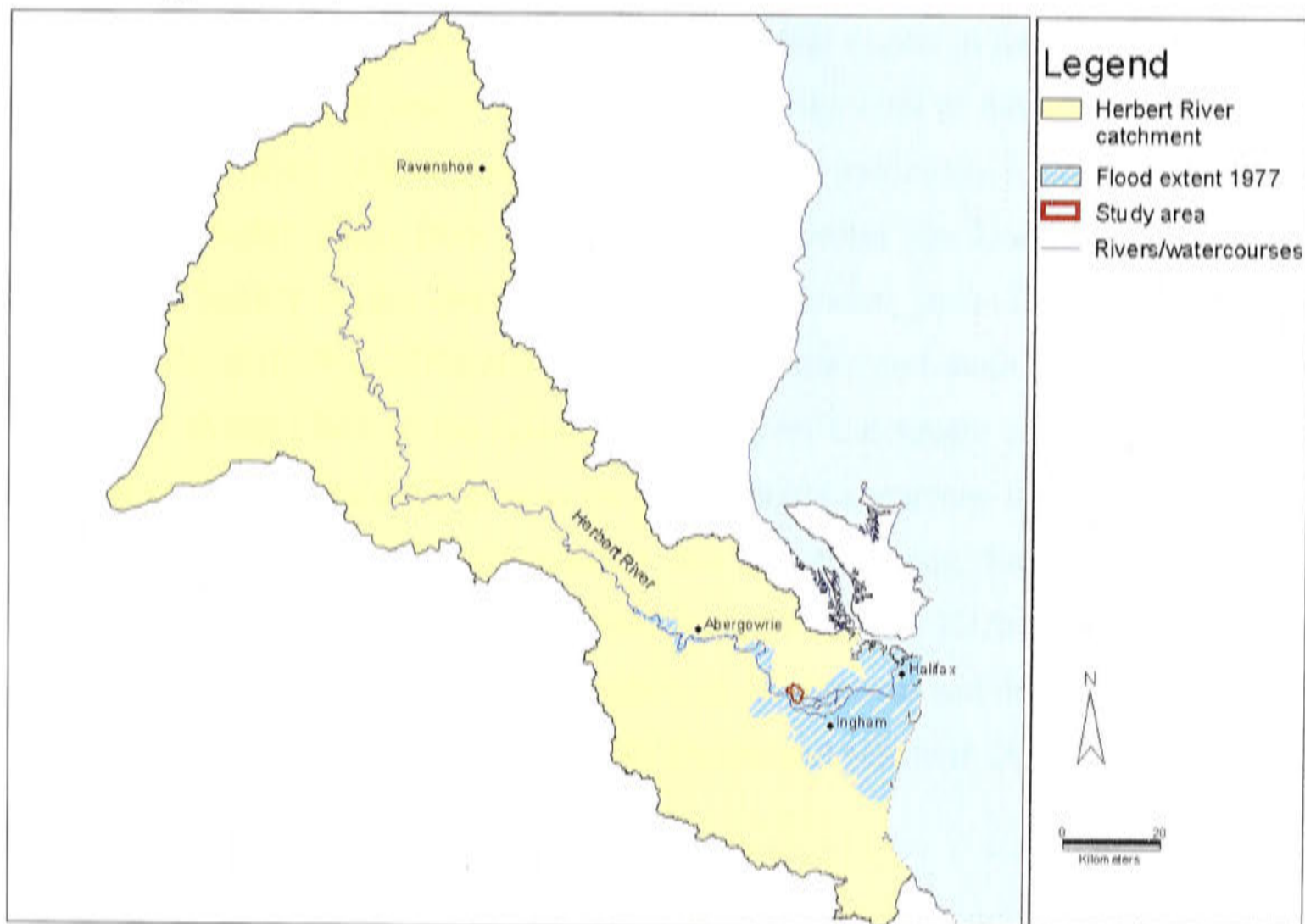


**Figure 2.4:** Map of Herbert River Catchment with an indication of the extent of the flood caused by heavy cyclonic rainfall in the Upper Herbert River Catchment (Cameron McNamara, 1980; Johnson and Murray, 1997).

#### *Sediment and nutrient runoff*

The bulk of sediments and the nutrients nitrogen and phosphorus leave the Herbert River Catchment in runoff during brief flood events, which are usually related to

cyclones. Relatively little material leaves the catchment during dry years. Furnas and Mitchell (2001) estimated for example 2,600 tonnes of N-export for the 1990-91 season and only 140 tonnes for the following season (1991-92). Phosphorus loads showed a similar difference between these seasons: 432 tonnes for the first season and 12 tonnes for the next. During seasons with below average rainfall and low flow periods in general, nutrient concentrations in the Herbert are below ANZECC 1992 target levels for protection of freshwater ecosystems and statutory levels for drinking water (Bramley and Johnson, 1996).

One cyclone event has been very well documented for the Herbert River Catchment. Cyclone Sadie in 1994 exported at least 600 t N, 65 t P and 100,000 t suspended sediment from the catchment over a period of six and a half days (Mitchell *et al.*, 1997). 85% of this occurred over just two days. Thus such events can produce as much or even more sediment and nutrient export in just a couple of days as produced in a whole year without cyclonic activity. Half of the N and 80% of the P in the runoff from cyclone Sadie was transported in particulate form.

Water samples taken from various locations within the Lower Herbert River Catchment mainly during low-flow or recession phases showed lower particulate fractions for both N (<25%) and P (<45%) (Bramley and Roth, 2002). The same study also showed how in the Lower Herbert River Catchment sediment as well as nutrient concentrations are higher in streams draining sugarcane land compared with streams draining predominantly grazing and forestry areas. Earlier research had already pointed out that nutrient concentrations in the Herbert River increase between the upstream end of the floodplain at Abergowrie and the downstream end near Ingham (Bramley and Johnson, 1996; Furnas and Mitchell, 2001).

## **2.7 The Ripple Creek Sub-catchment**

Most of the research described in this thesis has been performed in the Ripple Creek Catchment, a sub-catchment of the Lower Herbert River (Figure 2.1). The tributary joins the main river approximately 7 km northeast of Ingham. Ripple Creek rises in the Mount Leach Range, which forms the southeastern end of the Cardwell range on the north side of the Herbert River floodplain. The watershed of Mount Leach Range is the northern boundary of the Ripple Creek Catchment. The north part of the sub-catchment consists of rolling to steep mountains. The south part is a segment of the Herbert River alluvial plain. The boundary between the alluvial plain and footslopes

of the mountains causes a distinct change in topography. Along this border, the alluvial plain is locally covered with alluvial or colluvial fans derived from the mountains. The low-lying part of the Ripple Creek Catchment lies in a bend of the Herbert River. The levees of the river form the boundaries on the southwest, south, southeast and east side of the catchment.

#### *The Ripple Creek drainage system*

From its origin, Ripple Creek flows down the mountains towards the south until it reaches the alluvial plain. Here it turns to the east and continues in this direction until it joins with the Herbert River. Several tributary creeks drain the slopes of Mount Leach Range and join Ripple Creek on its way down. The low-lying part of the catchment is drained by a largely man-made drainage system. Ripple Drain is the main drain in this system. It drains the area of alluvial plain bounded by Hawkins Creek in the West and Ripple Creek in the east. Ripple Drain starts at the foot of mount Hawkins about 500 m southeast from the point where Hawkins Creek flows from the hill slopes onto the floodplain. At its origin Ripple Drain is fed with water from an upland creek. From here it flows in an easterly direction across the plains, more or less parallel to the Herbert River, until it meets Ripple Creek. On its way down numerous smaller drains join the main drain. Some of these are fed by creeks that drain the mountain slopes.

#### *Land use*

The area of cultivated land in the Ripple Creek Catchment (approx. 45%) is restricted to the alluvial plain (Figure 2.6). Almost all agriculture is sugarcane cultivation. The steeper mountain slopes are forested with mainly Eucalypt dominated vegetation and strips of rainforest along creek incisions. Most of the forested upland is National Park. Only in a few areas along Ripple Creek low input grazing under native vegetation occurs.

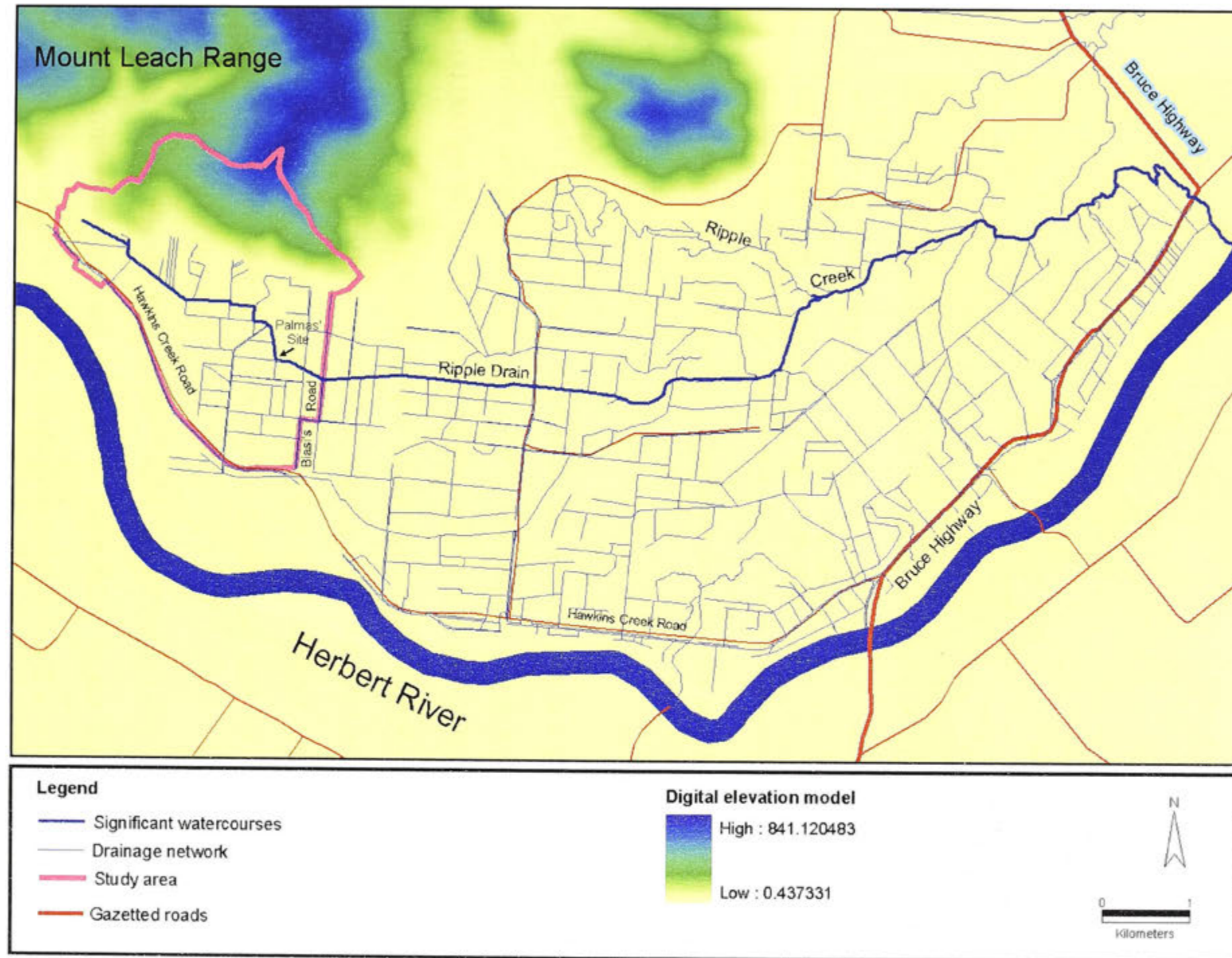


Figure 2.5: Topographic map of the Ripple Creek Catchment.

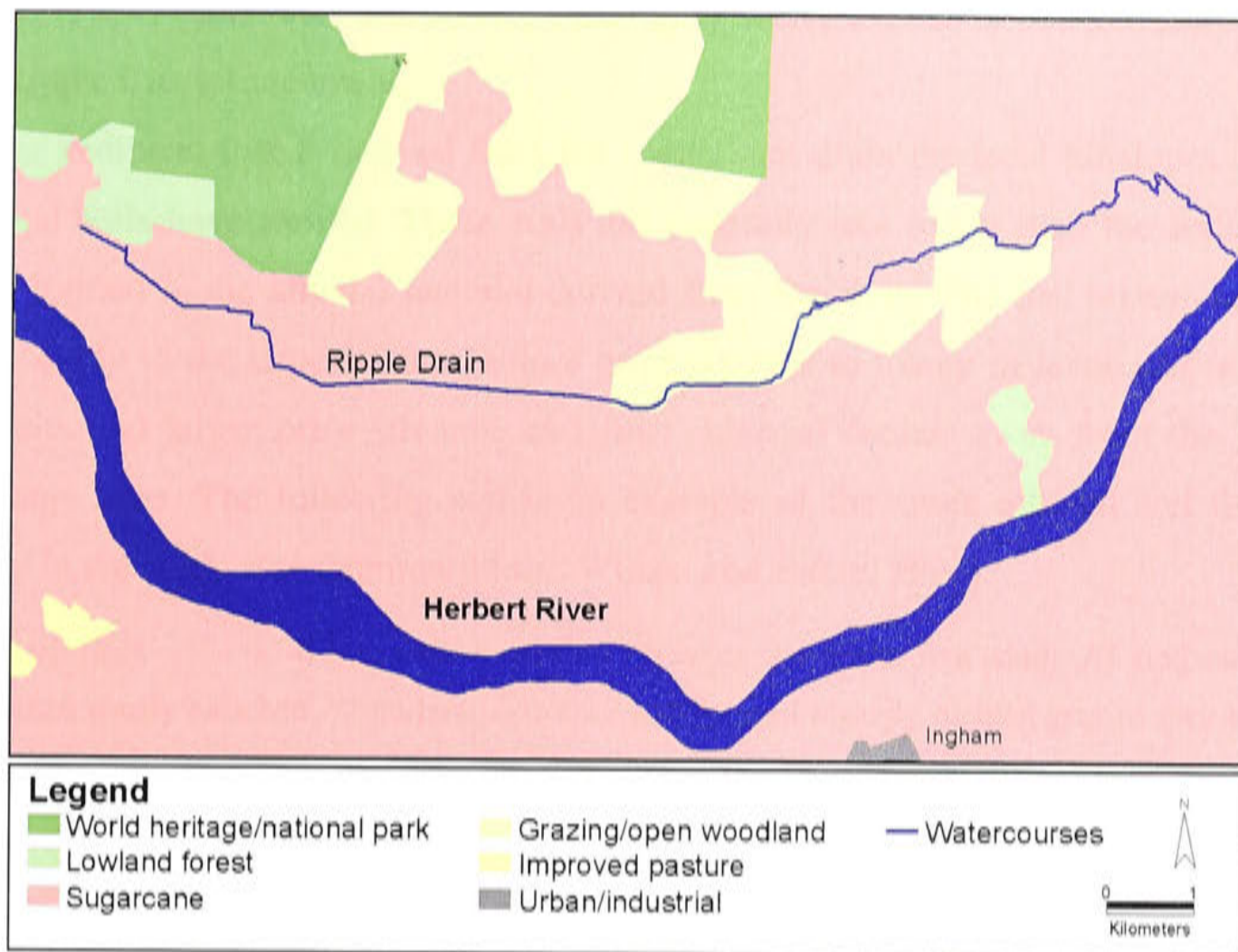


Figure 2.6: Land-use in the Ripple Creek Catchment (after Johnson and Murray, 1997).

### Soils

Several soil maps have been created for the Herbert River Catchment or parts of the catchment (Johnson and Murray, 1997). The Ripple Creek was mapped at a scale of 1:100,000 by Wilson and Baker (1990) and at 1:8,000 by Wood (1984). Figure 2.7 shows the soils in the catchment according to the classification by Wood. Both surveys only cover the catchment lowlands; no survey has been done in the forested upland. The soil types in the Ripple Creek Catchment are very similar to soils elsewhere in the Lower Herbert River Catchment and are closely related to the geomorphology of the area.

Soils in the alluvial fans at the footslopes of the granitic and acid volcanic hills contain fine gravel or sand throughout the profile. In the upper part of the alluvial fans the soils are generally red, while grey colours occur at the down slope end of the fans. The following soil type occurs in the alluvial fans of the study area (summary from Wilson and Baker (1990):

*Rungoo (Rg):* 0.05-0.15 m dark loamy sand to light sandy clay loam A1 horizon over conspicuously bleached A2 horizon to 0.4-0.75 m over acid mottled grey, yellow-brown to yellow fine gravelly sandy clay to medium clay B horizon to 1.2+ m.



Wood (1984) subdivides this soil type into 'grey sand', 'red sands' and 'red loams' for the Ripple Creek Catchment.

In the sediment that is derived from the creeks that drain the local hillslopes creek alluvial soils have formed. These soils are generally less fertile than the soils that have formed in the alluvial material derived from the river. The soil texture ranges from sandy in the deposits from minor prior streams to loamy in levee and terrace deposits and larger prior streams, and finer material further away from the prior drainage lines. The following soil is an example of the creek alluvial soil that is found in the study area (summary from Wilson and Baker, 1990):

*Ripple (Rp)*: 0.1-0.3 m dark loam fine sandy to clay loam, fine sandy A1 horizon over conspicuously bleached A2 horizon to 0.3-0.7 m over acid strongly mottled grey to grey-brown medium to heavy clay B horizon to 1.2+ m.

Most of this soil type is for the Ripple Creek Catchment classified by Wood (1984) as 'clays'.

The alluvial deposits derived from the Herbert River in the Ripple Creek Catchment are relatively young compared to the deposits further south in the Lower Herbert River Catchment. The soils in the river alluvium that occur in the Ripple Creek Catchment mainly have a silty clay, clay or clay loam texture. The following three soils are among the most common in the Ripple Creek Catchment and occur in the study area (summary from Wilson and Baker, 1990):

*Toobanna (Tb)*: 0.1-0.3 m dark to grey-brown loam fine sandy to clay loam fine sandy A1 horizon over conspicuously bleached A2 horizon to 0.3-0.8 m over acid to alkaline mottled yellow-brown to brown medium to heavy clay B horizon to 0.6-1.2 m over acid to alkaline mottled grey to yellow-brown sand to sandy clay loam D horizon to 1.2+ m.

*Hamleigh (Hl)*: 0.1-0.2 m dark to grey-brown hardsetting silty clay to medium clay A1 horizon over sporadically bleached A2 horizon to 0.35 m over acid to alkaline mottled grey to grey brown medium to heavy clay B horizon to 1.2+ m.

*Leach (Lh)*: 0.15-0.2 m dark to grey-brown light medium to medium clay A horizon over acid strongly mottled grey to grey-brown medium to heavy clay B horizon to 1.2+ m.

Wood (1984) classifies these soils mainly as 'silty clays' and 'terrace silt loam'.

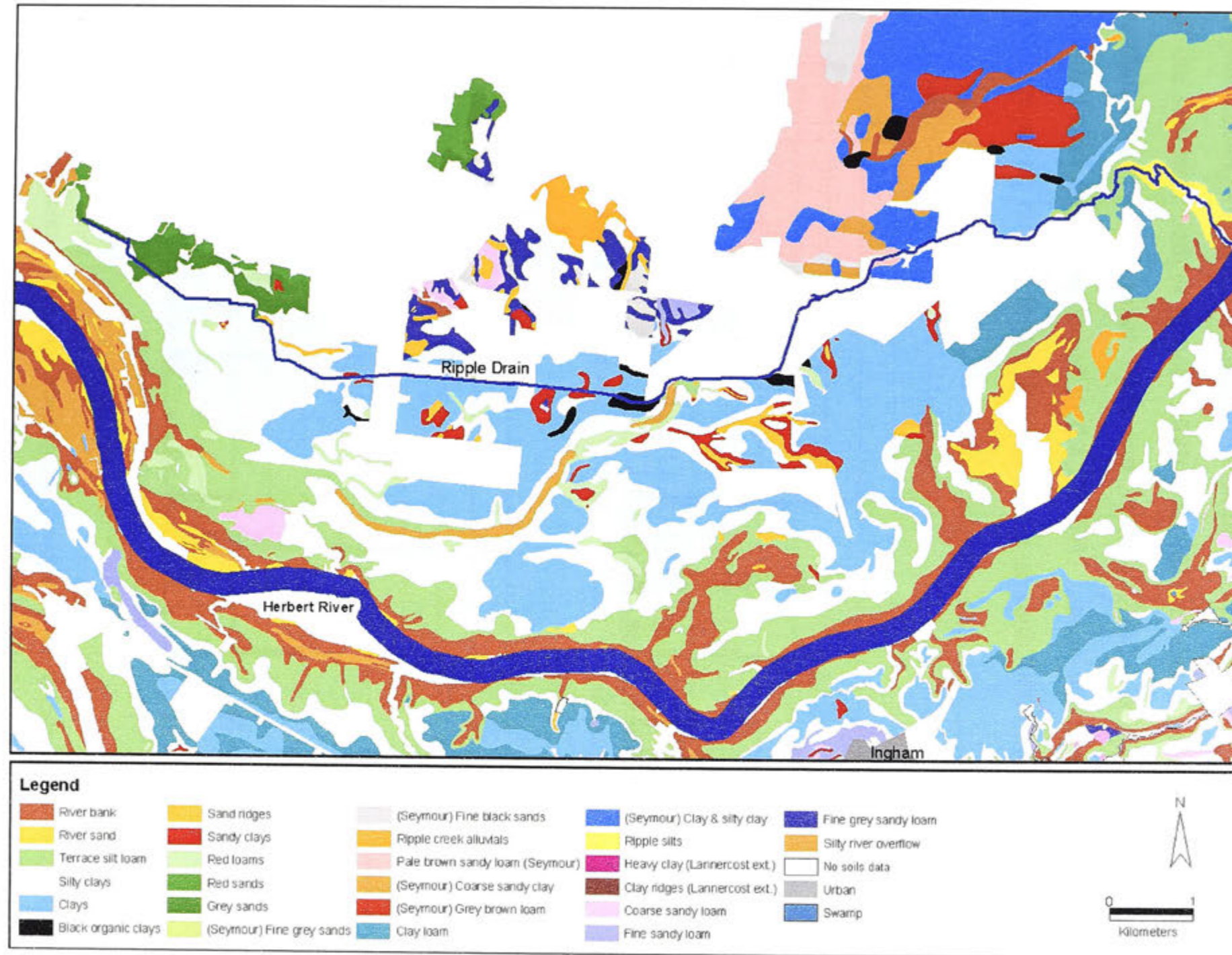
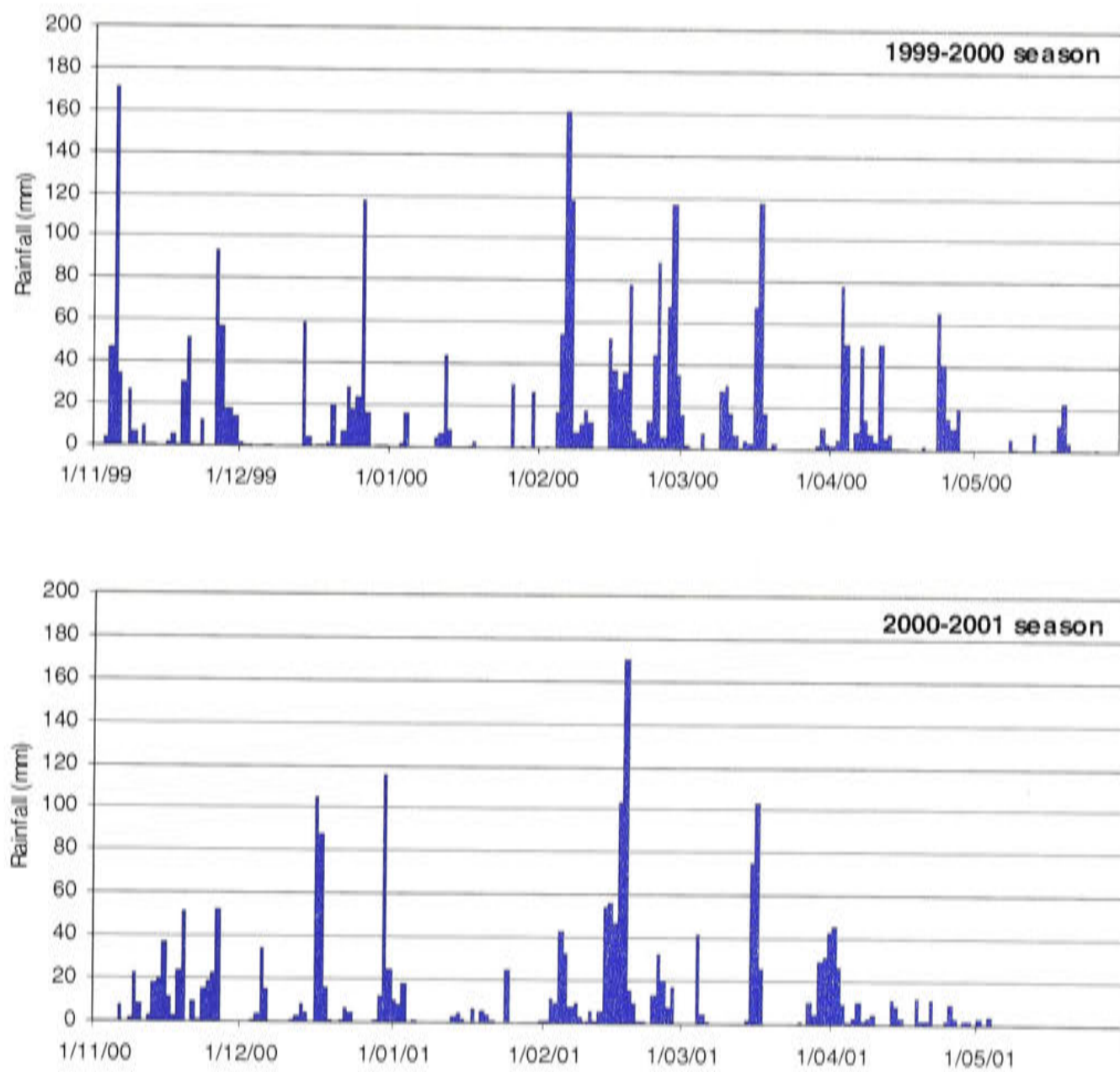


Figure 2.7: Soils in the Ripple Creek Catchment (after Wood, 1984).

*Palmas' site*

Research in the Ripple Creek Catchment has been concentrated around a location locally known as 'Palmas' site' (see Figure 2.5). This site was equipped with a weather station and two Parshall flumes that each drain a one hectare sugarcane field. Figure 2.8 shows the daily rainfall measured at Palmas' site during two field seasons of the sediment budget project. Both seasons had above average rainfall. The total rainfall between 1 October 1999 and 31 May 2000 was approximately 2950 mm. Rainfall over the same period in the 2000-01 season was approximately 2210 mm. Average yearly rainfall for the Palmas' site is around 2000 mm.



**Figure 2.8:** Daily rainfall (mm) recorded by the weather station at Palmas' site in the Ripple Creek Catchment. The figures show data for two wet seasons: November 1999 – May 2000 and December 2000 – May 2001.

---

## **PART II**

# **COMPOSITION OF A SEDIMENT BUDGET FOR LOW-LYING SUGARCANE LAND**

---

### *OUTLINE*

Comparison of sediment sources can be done by means of a sediment budget calculation. This approach is applied in this part of the thesis, to identify, quantify, and compare potential sediment sources in the highly modified sugarcane production landscape.

In chapter 3 the sediment budget concept is introduced and its advantages and limitations when applied in the sugarcane landscape are discussed. Chapter 4 describes the development of the sediment budget for the cane land in the Ripple Creek Catchment, considering the limitations discussed in the previous chapter. This includes a discussion of the methods that can be used to quantify the sediment budget components. In chapters 5 to 9 the specific field measurement methods are explained that were used to quantify input into the sediment budget from various sediment sources. The chapters cover fields, headlands, drains and water furrows, input from forested upland, and catchment output. Each chapter includes the results of the measurements and a discussion. In chapter 10 the sediment budget equation is composed using the results obtained from the previous chapters. The reliability of the results from individual components and the total budget equation are discussed in Chapter 11.

---

## Chapter 3

### The sediment budget approach

---

#### 3.1 Erosion and storage

When sediment is transported through a landscape it is not on the move continuously. At the field scale soil particles detached by rainsplash or flowing water will be transported down slope by overland flow. When during transportation the overland flow conditions change, for example reduction of flow velocity due to a change in slope or reduction of overland flow volume due to infiltration, particles can be deposited. The deposited sediment remains stored in the landscape for variable lengths of time. Transport could continue at the onset of a new rainstorm, but the sediment could also become buried by additional material and subsequently fixed by vegetation. When the sediment is fixed it will only be remobilized after a longer period of time as a result of some major 'disturbance' (e.g. a change in land-use or stream incision).

The sequences of deposition and re-mobilization occur at different scales. In a large catchment, for example, sediment generated in steep headwaters can be deposited under the slower flow conditions downstream on the floodplain. Changes in the hydrology or in the sediment transport regime of the river could however convert this storage area into a sediment source.

Trimble (1981, 1993, 1999) describes an example from the Coon Creek basin in the Driftless Area of Wisconsin, USA. In this catchment, improvement of agricultural land management led to a strong decrease in erosion of upland hillslopes, and consequently to a reduction of sediment supply into the catchment drainage system. Erosion of the tributary floodplains and upstream parts of the main river channel, that were initially important stores for the upland sediment, turned them into important sediment sources. In spite of the large changes in erosion and deposition processes in different parts of the catchment, it had remarkably little effect on the

sediment yield of the Coon Creek. During the studied period the low sediment yield of the catchment hardly changed.

## 3.2 The sediment budget approach

### 3.2.1 Analysing catchment systems

Due to the variable patterns of storage and remobilization of sediment, catchment yield is usually smaller than the erosion rate in a catchment. The discrepancy can be described as the catchment Sediment Delivery Ratio (SDR) (Glymph, 1954):

$$\text{SDR} = \text{Catchment yield} / \text{Gross catchment erosion.}$$

Both catchment yield and SDR are emergent properties of a catchment system, resulting from the interactions of many individual components.

The movement of material through a river catchment can be thought of as a complex system; that is, a system with many components and agents that interact in many ways. It is well known that complex systems cannot be understood by examining their emergent properties alone (e.g. yield or SDR), and require a whole system perspective (De Boer and Ali, 2002; Wasson, 2002). Such a perspective is provided by sediment budgets. A sediment budget is an accounting of the various sediment sources in a catchment and the possibilities of storage when the sediment is routed through that catchment, which results in the catchment sediment yield (Reid and Dunne, 1996; Knighton, 1998).

### 3.2.2 Sediment budget applications

Leopold *et al.* (1966) and Dietrich and Dunne (1978) are some of the earliest authors of sediment budgets. Since then numerous researchers have applied this approach, which provides a convenient means of presenting and analyzing erosion, deposition and sediment yields of river catchments (Walling, 1999). The sediment budget approach has particular advantages for resource management purposes. The budget principal ensures that all components in a catchment sediment transport system are examined, so that important sediment fluxes can be identified and management appropriately targeted. In addition it can provide information about the interactions between components of the system and therefore an understanding of how the system will respond to changes (Trimble, 1993; Reid and Dunne, 1996).

### 3.2.3 Sediment budget presentation

A sediment budget is usually described by the following mass balance equation (Roberts and Church, 1986; Slaymaker, 1993; Brunton and Bryan, 2000):

$$I - \Delta S = O$$

in which  $O$  is the output of sediment (the yield) from the studied catchment,  $I$  is the input of sediment from erosion sources and  $\Delta S$  is the change in amount of sediment stored in the catchment. Budget components  $I$  and  $\Delta S$  represent a range of sources and sinks depending on the processes acting in a particular catchment. More effective in presenting a sediment budget are the flux diagrams used by Trimble (1999) and Walling *et al.* (1998). This type of presentation (Figure 3.1) allows a quick assessment of the relative quantitative importance of sources and sinks, and can give some information on the spatial arrangement of sediment sources and sinks.

Figure 3.1 shows the sediment budgets for the study in Coon Creek by Trimble (1999). The figures show that erosion and deposition processes vary over three time periods as a result of the changes in land management. The budgets show how reduction of erosion by 75% in the catchment upland had no effect on the catchment yield, but was compensated by changes in erosion and storage processes elsewhere in the catchment.

## 3.3 Sediment budget limitations

### 3.3.1 Variation in time and space

The example of the Coon Creek catchment illustrates how sediment budgets can vary in time. Similarly, budgets will vary for different positions in space and at different spatial scales due to variation in environmental conditions. A sub-catchment of a river is likely to have a sediment budget that is different from that of the whole river system. For example, an upland sub-catchment could have relatively steep slopes and only a poorly developed floodplain. This will result in relatively little deposition within the sub-catchment compared to the whole river system.

Sediment budgets can also be applied to only a part of a river catchment. Roberts and Church (1986), for example, used a budget equation to describe erosion and storage along a single river stretch, and Brunton and Bryan (2000), and Oostwoud Wijdenes and Bryan (2001) limited their budget to describe geomorphic processes in

an individual gully. The budgets of sub-systems can be combined to obtain a budget that describes the sediment transport in a whole catchment (Sutherland and Rorke, 1991).

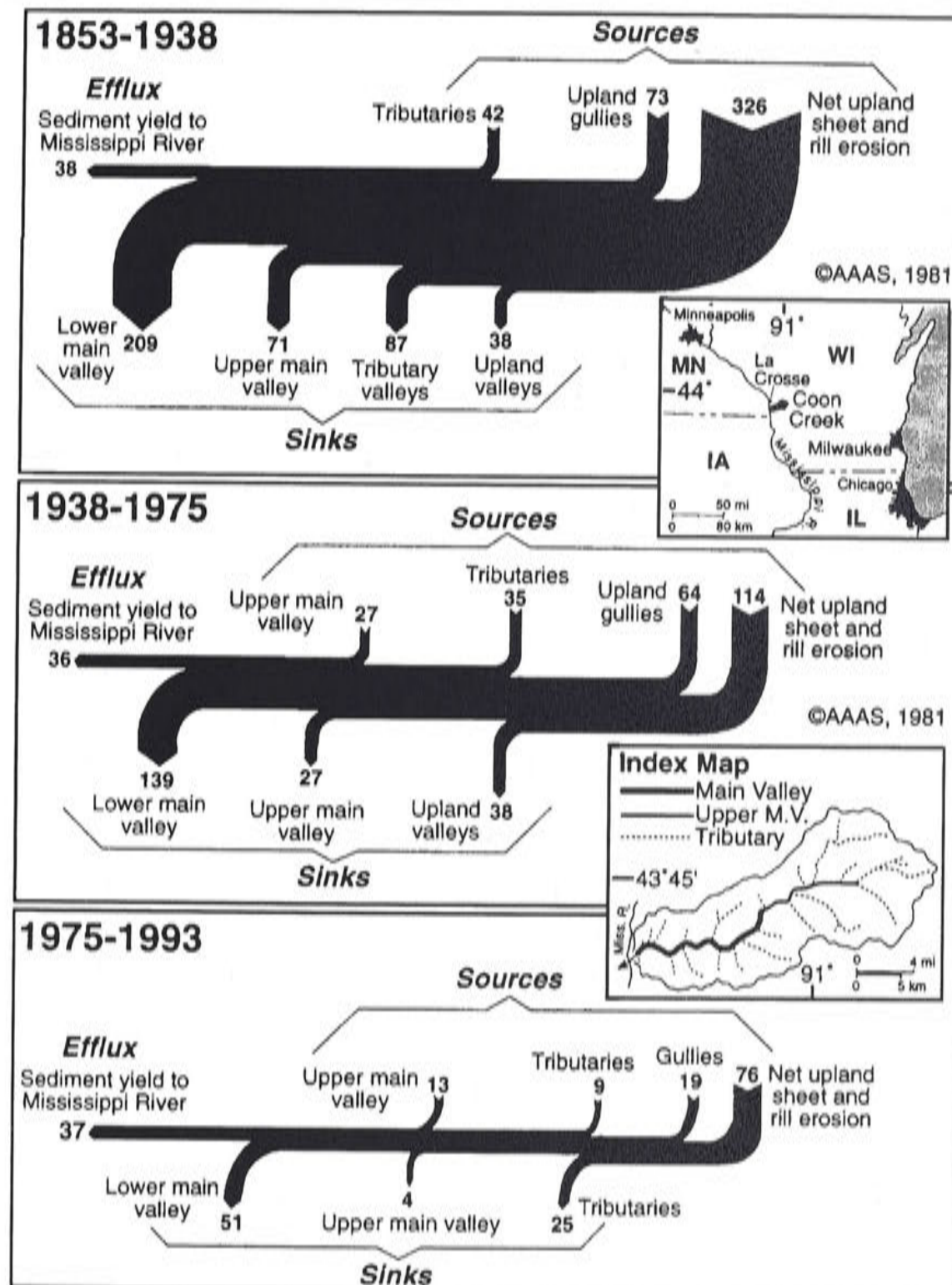


**Figure 3.1:** Sediment budgets for Coon Creek, a 360 km<sup>2</sup> catchment in Wisconsin, USA, over the period 1853-1993. Numbers are annual averages in 10<sup>3</sup> Mg year<sup>-1</sup>. All values are direct measurements except "Net upland sheet and rill erosion," which is the sum of all sinks and the efflux minus the measured sources. The lower main valley and tributaries are sediment sinks, whereas the upper main valley is a sediment source' (Trimble, 1999, modified from Trimble, 1981).

### 3.3.2 Budget balance and uncertainty

Although providing a useful framework to document and analyse sediment source, sink, transport and yield, the difficulty of quantifying sediment generated by different sources or stored in sediment sinks is often considerable. However, several authors



applied the sediment mass balance equation to obtain estimates of the magnitude of either unquantified or hard to measure budget components. Lehre (1982) for example obtains estimates of sediment storage on hillslopes by subtracting measured amounts of mobilized sediment and sediment input to the river channel. In the same way he obtains estimates of sediment storage in the riverbank and bed from input into the river channel and the sediment yield of the catchment. These residuals are for some years more than 80% of the total budget. Rondeau *et al.* (2000) use along-river differences of suspended sediment in the St. Lawrence River, Canada, to estimate the relative input from bank erosion, which amount to 65% of the total suspended load. Kern and Westrich (1997) also attribute the lack of balance in their budget to 'erosion' in the river reach.

Assumptions about the imbalance of sediment budgets are usually based on field experience and in many cases the researchers will be correct, but rarely is the magnitude of possible errors known. Kondolf and Matthew (1991) give several more examples of authors who ascribe the imbalance in their sediment budget to unmeasured budget components. They point out that a detailed error analysis is important in budgets that use such residual terms, because the residual will also include the net error of other budget terms. For the same reason they argue that budget error can not necessarily be considered equal to the sediment budget imbalance. The imbalance may underestimate actual sediment budget errors if they include compensating positive and negative errors. Recently more attempts have been made to quantify errors involved in budget studies; to design methods to test potential errors (Hill *et al.*, 1998); or to provide more detailed discussions of the possible sources of budget imbalance, as done by Loughran *et al.* (1992) in the first sediment budget for an Australian catchment.

Despite the large uncertainties involved in sediment budget studies, they should not discourage the development of sediment budgets; not even budgets that obtain one of their terms by subtraction. According to Kondolf and Matthews (1991) 'Budgets still give valuable information on the magnitude of erosion processes and the transport processes involved. And even budgets based on incomplete information can give an indication of the relative importance of different sources and linkages'.

### **3.3.3 Summary**

The previous overview of the sediment budget concept and its applications shows that it provides a useful approach to study complex catchment systems. In resource management, this type of approach is particularly necessary in order to make correct decisions. However, it becomes clear that several things need to be considered when developing a sediment budget:

- Budget balance: a sediment budget should preferably be closed by measuring all sources and sinks.
- Spatial variability: Spatial variability could cause misleading budget results. Measured quantities for both sides of the budget equation should come from the same area or catchment.
- Temporal variability. A budget will only apply to the time over which the components were estimated. All components should be quantified for the same time period.
- Accuracy and uncertainty: To make budget results most useful, the most accurate methods have to be chosen to quantify the budget components. Even a closed budget can obscure errors by cancelling positive and negative errors. To improve the value of the budget an estimate of uncertainty should be provided with the budget.

### **3.4 Considerations for a sediment budget in low-lying cane land**

The description of low-lying cane land in the introduction illustrated how canefarmers created several typical landscape elements. Viewed from a geomorphic perspective each of these elements has the potential to be either a source or store of sediment. Knowledge of the magnitude of both the erosion and deposition capacity of each landscape element is important for the management of sugarcane land. Besides reduction of erosion from sources in the landscape, the trapping capacity of other landscape elements could be managed to reduce sediment concentrations in the cane land runoff.

A sediment budget study can aid soil management in sugarcane land by showing the relative importance of the various landscape elements as sediment source and the importance of deposition of the material elsewhere in the catchment. The budget

balance can confirm adequate representation of processes in the sugarcane landscape or reveal unexpected sources as well as budget errors.

#### *Balancing the budget equation*

To create a balanced budget all sources and sinks in the studied area have to be known. In the case of low-lying cane land the important sources and sinks are not clear, because prior research has not been done. So, the a priori composition of an equation that includes only the quantitatively significant components for erosion input and sediment storage is not possible. The budget has to be composed in a different way. Instead, all typical landscape elements that make up the sugarcane landscape will initially become the components of the sediment budget. From what is known from the literature and field observations, all of these elements have the potential to be either a source or a sink of sediment, and in many cases both. Thus, erosion and deposition processes have to be quantified separately for each individual element and are separately included in the budget equation. The general budget equation is for this study therefore modified to:

#### **Equation 3.1**

$$I - S = O$$

in which I is the amount of sediment input into the drainage system from each landscape element, S is the amount of deposition within each landscape element and O is the total output of sediment from the studied area. Figure 3.2 illustrates the initial budget. The question marks indicate the information that is needed to establish the budget.

Because there is not sufficient knowledge of the erosion and deposition processes within each landscape element, the methods used to measure these processes should cover the total route of sediment transport through each element and record both erosion and deposition processes along that route. If this is not done properly, sources or sinks could remain unidentified and the budget will be unbalanced. In the drain landscape element, for example, material can erode from the drain bank and be directly transported to the catchment outlet by the drain water. It is however possible that the eroded material from the banks is deposited on the drain bed. The measurement method applied to estimate budget components I and S for landscape

element 'drain' must be able to distinguish and quantify both the erosion (from the banks) and subsequent deposition (on the drain bed).

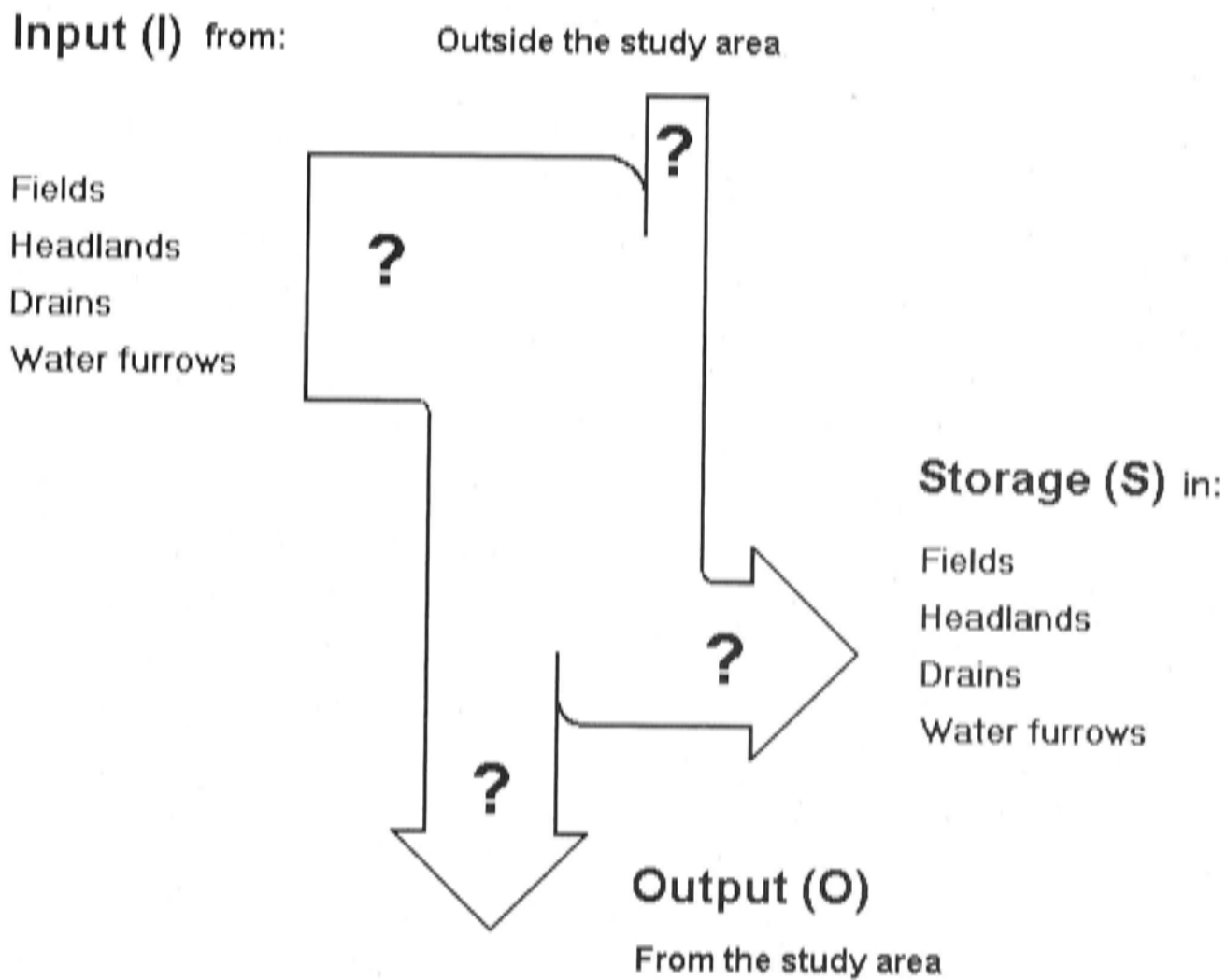


**Figure 3.2:** Sediment budget outline for low-lying sugarcane land.

### *Spatial variation*

Properties of each landscape element, such as soil type, slope or morphology will vary in space. Examples are differences in the shape of drains or changes in the slope of headlands. The variation in such properties will have an effect on the magnitude of erosion and deposition processes. Less vegetated headlands are for example likely to be more erodible. If spatial variation within landscape elements is not accounted for in the quantification of budget components, the relative importance of processes in landscape elements could be misinterpreted and compromise the budget results.

### *Temporal variation*

It is important that the budget is calculated over a short, recent time period. If farmers want to take action now and stop the degradation of cane land they need to know where sediment is coming from under present conditions. An average of processes acting over periods longer than ten years back will not be useful, because

agricultural practices and environmental condition have changed a great deal over that period of time. Also, all components have to be quantified for the same period of time. If, for example, one side of the sediment budget equation consists of catchment output averaged over 10 years, the other side of the equation should not be derived from average erosion and deposition rates in drains over only the last two years. The density of the drainage systems might have increased considerably over ten years. Consequently the average discharge over 10 years does not reflect the current contribution of the drainage system to the sediment budget and will create a budget imbalance.

#### *Budget uncertainty*

If a closed budget can be produced, than it is likely that all budget components have been included. It is however not guaranteed that all components are quantified correctly. As Kondolf and Matthews (1991) showed, cancelling of error on both sides of the budget equation can result in an apparent balanced budget, and in the same way a budget might be unbalanced by errors on one side of the equation. To avoid this problem, the most accurate methods to estimate the components have to be chosen and an estimate of the uncertainty should be made to understand the possible effects of errors on the mass balance.

---

## **Chapter 4**

# **Development of the sediment budget and methods for quantification of the budget components**

---

### **4.1 Introduction**

The previous chapter showed how sediment budgets are a useful framework for studies of sediment sources and storage. When this framework is applied to study the sediment sources in low-lying cane land, there are a number of requirements and restrictions for the design of the budget and the measurement methods that can be used. This chapter describes the further development of the sediment budget for low-lying cane land according to those requirements. It includes the definition of the budget area and reasons for the choice of methods used to quantify the budget components.

### **4.2 Budget Area**

To obtain a closed budget, the area described by the budget has to be well defined. There should be no sediment transport across the boundaries of the budget area, unless these can be quantified.

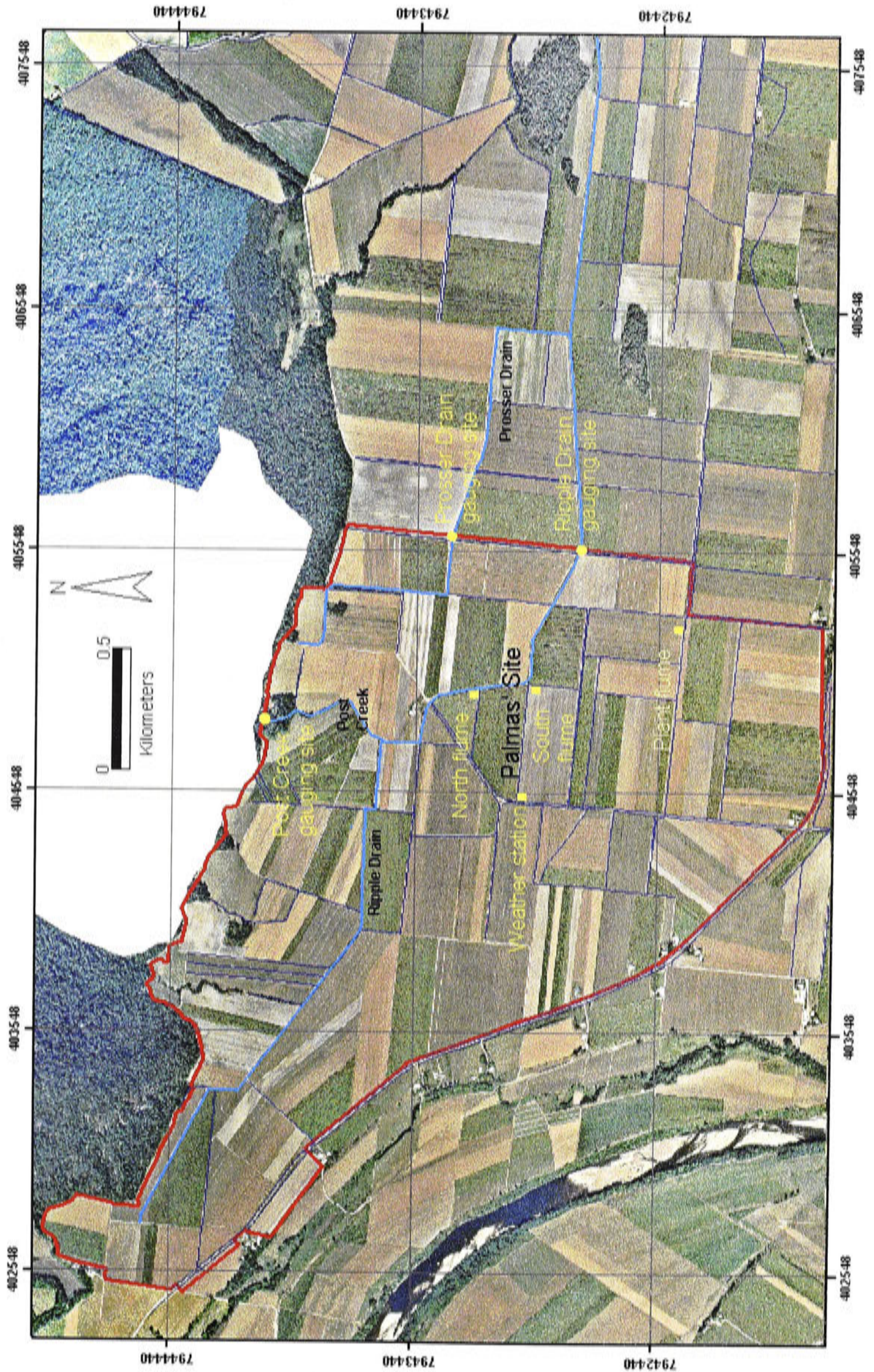
For practical reasons such as accessibility, equipment requirements and composition of the landscape (e. g. land use and geomorphology), it was decided to develop a budget for only a part of the Ripple Creek Catchment. The chosen site consists of a 5.4 km<sup>2</sup> sub-catchment in the westernmost corner of the Ripple Creek Catchment. For the purpose of this research the sub-catchment is called the Ripple Corner Catchment. Ripple Corner Catchment includes a distinct flat segment of the alluvial plain (3.2 km<sup>2</sup>) bordered on the south side by the Herbert River and on the north side by the piedmont and hills of the Mount Leach Range. All of the lowland is in use for sugarcane cultivation apart from farm buildings and some fields with pumpkin and melon cultivation. The bordering mountain slopes are forested.

The low-lying part of the study area is drained by a major drain, known as Ripple Drain, which discharges into Ripple Creek approximately 12 km east of the study area. Hawkins Creek Road forms the south boundary of the study area. The road is slightly elevated above the floodplain surface on a natural levee of the Herbert River. All water and sediment north of this road is expected to drain towards Ripple Drain. Water south of the road drains directly into the Herbert River via local drainage lines. On the northwest side of the study area, the Hawkins Creek Road approaches the mountain slopes to within 500 m. The catchment boundary leads from the road to the foot of the mountain approximately 250 m west from the point where Ripple Drain starts. From the foot of the mountain the boundary follows the watershed of the mountain slope towards the northeast. Water and sediment from the mountain slopes within the boundary are expected to drain towards the lowland, mostly via permanent creeks. At the foot of the mountain the creeks continue as straight artificial drains. The west boundary of the study area leads from Hawkins Creek Road, just east of Biasi's Road turn-off, more or less straight north to the foot of Mount Hawkins. The exact boundary on this side of the study area is determined by the drainage direction of the fields. Figure 2.5 and 4.1 show the boundaries of the sediment budget area in detail.

### **4.3 Budget output and upland input components**

All drains and creeks within the study area eventually discharge into either Ripple or Prosser Drain. Prosser Drain starts about 3 km downstream from the origin of Ripple Drain, and is fed by one of the smaller upland creeks that drain the mountain slope between Post Creek and Jap Creek. Prosser Drain flows parallel to Ripple Drain about 500 m to the north. After 1 km the drain turns 90° to the south and joins up with Ripple Drain. The west boundary of the Ripple Corner Catchment is located 500 m upstream from this point and thus intersects both drains. The drains form the outlet of the budget area. All water and sediment from the area is assumed to leave the catchment through the two drains, constituting the output component of the sediment budget.

**Figure 4.1 (next page):** Aerial photo of the study area for the sediment budget study. The boundary of the cultivated lowland is indicated in red.





Some sediment will be generated in the forested upland. This will be transported with the water that drains the mountain slopes and passes through the low-lying cultivated area before it reaches the outlet of the study area. Potential erosion and storage occurring within the forested upland is not relevant for this sediment budget, because it only aims at sources in the cultivated lowland. However, during transport to the outlet of the study area, sediment from the upland could get trapped and remain stored in the cultivated lowland and/or contribute to the output from the whole catchment. The forested upland therefore becomes an input component for the sediment budget. Only the net amount of sediment entering the cultivated lowland is part of the budget equation and has to be monitored.

In most sediment budgets the output component is derived from stream gauging data over the budget period (e.g. Trimble, 1981; Sutherland and Rorke, 1991; Walling *et al.*, 1998). In this budget the output can be obtained by monitoring the sediment load at the two outlet drains. Similarly the sediment input to the budget from the forested upland can be obtained by monitoring the sediment load of upland creeks. Details of the procedures applied for the quantification of these budget components will be described and discussed in Chapter 5 and 6.

## **4.4 Quantification of the sediment sources and sinks**

### **4.4.1 Introduction**

The most difficult task in the budget development is quantification of the remaining budget components. For all landscape elements within the cultivated lowland both sediment input and sediment storage have to be estimated. There are various methods to quantify erosion and deposition processes, and most have been applied to quantify components of sediment budgets. All methods however have their specific problems and limitations (Stocking, 1987; Loughran, 1990; Hudson, 1993). Loughran (1990) reviewed advances in the measurement of soil erosion. He concludes that of all techniques the caesium-137 (Cs-137) tracer method has shown the greatest potential. However, some methods are more suitable for certain situations than others. This section discusses the most commonly used methods and their appropriateness for the sediment budget constructed for the Ripple Creek Catchment.

#### 4.4.2 Caesium-137 tracer

To comply with the requirements for the cane land sediment budget that were pointed out in Section 3.4, the most accurate method should to be chosen to quantify the budget components, with the aim to avoid imbalance in the budget equation. Because many authors have argued that the use of the caesium tracer has a number of advantages that make it less sensitive to problems of spatial and temporal variation, and of measurement error, (Campbell *et al.*, 1988; Loughran, 1990; Walling and He, 1997; Collins *et al.*, 2001), this method is considered first.

Caesium was released into the atmosphere during nuclear testing from the end of World War II till the 1970s. The nuclide was distributed globally and deposited on the earth's surface as fallout both in precipitation and in dust, where it attached rapidly and strongly onto fine soil particles (Walling and Quine, 1992). Cs-137 is now used to trace redistribution of soil particles. An increase or decrease of total caesium in the soil profile compared to an undisturbed reference site allows identification of areas subject to deposition or erosion respectively (see Campbell *et al.*, 1988 for method description). Alternatively the annual variation in input over the period since the first atomic tests in 1945 might be visible in a soil profile and provide an indication of soil accumulation rates (Walling and He, 1997). The difference between the Cs-137 content of sub-soil and surface soil is also used to 'fingerprint' the source of sediment in river discharge. If the sediment in a river contains little Cs-137 this indicates it originates mostly from sub-surface sources, for example from bank erosion, while a high Cs-137 content indicates predominant surface sources (Wallbrink *et al.*, 1996).

Walling and Quine (1993) identified the following conceptual benefits of the Cs-137 technique for studies of rates and patterns of erosion and deposition:

- The technique permits retrospective assessment of decadal erosion rates
- Both rates and patterns of soil redistribution may be quantitatively assessed
- The estimated rates and patterns represent the sum of all erosive processes
- Estimated soil redistribution rates integrate extreme events

The Cs-137 technique is also the only technique that can be used to make actual measurements of soil loss and redeposition quickly and efficiently (Ritchie and

Ritchie, 2000). The benefits make the technique especially useful for assessment of the often slow process of sheet erosion. It can also be used to estimate rates of accumulation and degradation in floodplain environments if measured in depositional profiles (Walling and He, 1997).

Unfortunately some of these benefits make the caesium tracer unsuitable for use in a sediment budget for low-lying cane land. Firstly, the method averages soil redistribution over a 30-year time period. During that time the low-lying cane lands and sugarcane growing conditions have undergone major changes, so the caesium data can not provide information on the specific effects of recent changes and the present condition of cane land. Additionally it can not identify the origin of deposited sediment or the alternating occurrence of erosion and deposition. Using the Cs-137 content in runoff to 'fingerprint' the sources is not useful for this budget either, because it can not provide information about the detailed spatial variability of different sources. Finally Quine (1999) describes how tillage causes soil redistribution in addition to movement by water. This lead to an unexpected discrepancy between results from a water erosion model and results of caesium measurements. As a result of various maintenance practices on the different landscape elements in the cane land, soil is moved around. This might have similar unexpected effects on caesium measurements and make the method unreliable for this application.

#### **4.4.3 Other indirect erosion measurement methods**

Because of their long half-life most other radionuclide tracers, such as lead-210 (Blake *et al.*, 1999), are not suitable for this particular budget either. Blake *et al.* (1999) investigated the use of beryllium-7 in a field in the UK. This tracer has a half-life of only 53 days and can therefore give information on short-term erosion processes, for example sediment relocation over the duration of a single rainfall event. However the application of this short-term tracer has not been tested extensively, and its reliability is therefore uncertain.

Many other types of tracers or fingerprinting techniques have been suggested to identify sediment sources and erosion rates. Some examples are geochemical fingerprinting (Peart and Walling, 1988; Walling *et al.*, 1998), variation in sediment colour along suspended sediment – discharge curves (Grimshaw and Lewin, 1980), or mechanical tracers (e.g. magnetic beads (Ventura Jr. *et al.*, 2001). But, all

techniques appear to have some limitations that make them unsuitable in this particular application, mainly due to the extremely wet conditions in the study area or the lack of geochemical differences between the sources.

Another promising method to study sediment sources on a floodplain is the use of optical-infrared remote sensing images (CSIRO Land and Water, 1998). Variation in the optical characteristics of water, which are visible from remotely sensed images can be related to variation in water quality variables such as turbidity. With this type of information, areas of high sediment concentration can be indicated and quantified. Several studies have already provided insight into the dynamics of water and sediment movement in floodplain environments (Mertes, 1997; Mertes, 2002). The particular advantage of this method is that it avoids problems with ground access. However, the high costs of images, the coarse spatial and irregular temporal resolution, and the common presence of a thick cloud cover during the wet season in North Queensland make this method impractical.

#### **4.4.4 Modelling**

Soil erosion models could be applied to predict certain components of a sediment budget, but this also includes some problems. Firstly very little is known about erosion and deposition processes in tropical floodplain landscapes. Specific models for these conditions do not exist and the necessary values for model parameters of existing models are likely to lie outside the constraints under which these models were developed.

Furthermore erosion prediction through models is generally not very accurate, which is inconvenient for a floodplain landscape where erosion rates are likely to be small. In combination with empirical data, which is necessary to validate and calibrate a model, self-cancelling of larger errors in either the model or the data, could occur. This is the same problem that is described for sediment budget equations in Section 3.3.2 (Kondolf and Matthews, 1991). Nearing *et al.* (1999), Nearing (2000), Brazier *et al.* (2001) and Zehe *et al.* (2001) encountered the problem in the validation of their model studies. Obviously models are not likely to provide the verifiable accuracy needed for the construction of a reliable sediment budget for low-lying sugarcane land.

#### **4.4.5 Plot studies**

Direct field measurement methods, such as erosion pins and runoff plots, are the most common way to estimate soil erosion and deposition. These methods are however not thought to be very reliable. They are sensitive to measurement error and, especially in the case of plot scale measurements, their coverage of spatial and temporal variability is limited. Additional operational difficulties and cost of the surveys, make direct measurements only practical in small basins (Walling, 1999).

Clear advantages of direct field measurements are that they can be designed to separately quantify erosion and deposition processes. Also, observations made while carrying out the fieldwork can improve the understanding of the processes that are being measured.

#### **4.5 Budget composition**

The specific requirements of this study, to distinguish between many potential sediment sources as well as identifying both erosion and deposition processes, leave little choice in what method to use for quantification of the sediment budget components. Despite the problems involved with direct field measurements, it seems the only possible method to quantify different sediment sources as well as storage areas in the sugarcane landscape.

In summary, the inadequacies of (plot scale) direct field measurements can be related to some of the problems that have to be considered in the development of a sediment budget (Chapter 3):

- Direct measurements are not thought to be accurate, while accuracy of the budget components is important for the significance of the budget results.
- Especially plot scale measurements provide only limited representation of spatial variability, while insufficient representation of spatial variability for budget components can result in an unbalanced budget.
- Short-term measurements might not represent temporal variability. In the budget all components have to represent the same time period in order to achieve a sound budget. Temporal variation does not have to be a problem as long as all measurements provide a continuous record for the total budget period. However,

during interpretation of the budget results, attention has to be paid to the significance of the results beyond the budgeted period.

These points have to be taken into account in the further design of the measurement techniques, and their consequences will be evaluated in the discussion of the budget results.

Because all landscape elements are morphologically different and are affected by different erosion and sedimentation processes of different magnitudes, it is difficult to apply the same measurement design to all elements. Also for practical reasons one method will not suit all landscape elements. Chapter 7 to Chapter 9 separately discuss the measurements in landscape elements: headlands, fields, drains, and water furrows.

The field study was performed during three wet-seasons: in the summer of 1998-1999 (98-99), 1999-2000 (99-00), and 2000-2001 (00-01). During the 98-99 season only preliminary data were collected. In Chapter 10 the data from all budget components for the 99-00 and 00-01 season will be used to create a separate budget for each season. The budgets can be compared to obtain some indication of temporal (seasonal) variation. No measurements were performed during the winter seasons; the climate is too dry in winter for significant sediment movement.

#### **4.6 Particle size problems**

At the start of the project all researchers involved and people consulted were under the impression that most sediment in the catchment moves in suspension. Because bedload is also notoriously hard to measure (Gomez *et al.*, 1990; Thomas and Lewis, 1993; Gomez and Troutman, 1997), it was decided to restrict the budget to suspended load. The size fraction of material that moves in suspension was assumed to be particles  $<20\ \mu\text{m}$ . This assumption was confirmed by a set of water samples taken from various locations in the catchment (see Appendix A). For all samples, less than 1% of residue remained when passed through a  $20\ \mu\text{m}$  sieve.

The decision to restrict the budget to suspended sediment has the following limitations:

- Some observations during the fieldwork period contradicted the original belief, and bedload does seem to be an important component in the sediment load.

- Some of the applied methods provide information on the bulk of material eroding and depositing, including particles  $>20 \mu\text{m}$ . Such data have to be adjusted for sediment size.
- Erosion, deposition and sediment transport processes are particle size selective (Stone and Walling, 1997). Deposits can for example consist of different amounts of coarse material due to sorting. This complicates the adjustments of the budget calculations.

In Chapter 10 will be described how particle size adjustments have been made in the budget calculation. Here the importance of bedload in the sediment transport system will also be further discussed on the basis of observations made during the fieldwork for this project.

---

## **Chapter 5**

### **Output from the Ripple Corner Catchment**

---

#### **5.1 Introduction**

The Ripple Corner Catchment was described in Chapter 4, along with an account of how runoff leaves the catchment through two drains. The largest share of the water flows through the main Ripple Drain. A much smaller amount of water leaves through Prosser Drain. The total load of sediment transported by the water passing through both drains in a season makes up the output component for the sediment budget of the Ripple Corner Catchment. In this chapter the methods used to quantify the total sediment output from the drains during the 1999-2000 and 2000-2001 wet seasons are described.

#### **5.2 Water discharge estimation**

The sediment load of a stream is obtained by integrating sediment discharge over a defined time period. Instantaneous sediment discharge is calculated from the instantaneous water discharge and sediment concentration of the stream. These two variables can be measured in the field.

A common way to measure water discharge is by installing a weir in the stream cross-section (Gregory and Walling, 1973). From the weir dimensions and the head of the water above the weir crest, stream flow velocity can be calculated. By this method only water depth at the weir has to be measured to obtain discharge. Alternatively several velocity measurements can be performed in the stream at different water stages. These measurements can be used to create a depth – discharge rating curve. The curve can be used in combination with continuous depth measurements to estimate water discharge.

For various reasons neither of these methods was suitable to gauge the outlet drains of the Ripple Corner Catchment in the current project. The main problems are caused by the hydrology of the study area. Firstly, the tropical rainfall events



generate extremely large quantities of water. Especially in a large drain such as the Ripple Drain a very large weir structure would be needed to conduct the flood flows. Secondly, in the flat landscape of the study area backwater processes occur under flood conditions.

Backwatering means that water flow in a certain direction is restricted by a larger body of water (stagnant or flowing) or a structural element (e.g. bridge, culvert). The flow velocity can be reduced or completely blocked by the obstructing element. When, in the case of two water bodies, the pressure difference between the bodies becomes too large, the flow of the smaller body might be reversed and fed by water from the larger body. This process is called 'reverse flow'. Under backwater and reverse flow conditions the flow velocity of a stream may not be directly related to water depth, which could affect the development of a reliable depth – discharge rating curve. This method is therefore not considered suitable to gauge the outlet drains of the Ripple Corner Catchment.

Continuous velocity measurements in combination with continuous depth measurements can avoid the above problems with discharge estimation. Both outlet drains were therefore equipped with Unidata STARFLOW Ultrasonic Doppler meters. This type of velocity meter can measure reverse flow (Unidata, 1998). Discharge can be estimated directly from the flow velocity records and (wet) drain cross-sections based on continuous depth records. A single point velocity measurement might however not sufficiently represent velocity across the drain cross-section. In Section 5.7 the application of the method to estimate discharge from the outlet drains will be discussed in more detail.

### **5.3 Sediment concentration estimation**

A large amount of literature exists on the estimation of sediment concentration in streams to obtain sediment load values. Many techniques are proposed (NSW Environment Protection Authority, 1999). The suitability of a technique for a particular situation depends on practical factors (financial, logistic, etc.) and characteristics of the sampled stream (variability in the load, sediment size distribution, etc.). Because manual sampling for direct suspended solid concentration (SSC) estimates is prone to high uncertainty, a continuous automated method is favoured.

An often-proposed method uses continuous measurements of stream water turbidity to obtain sediment concentration data. Turbidity in streams is mainly caused by sediment in suspension, which can be measured with an optical device. In combination with a relationship between turbidity and SSC the turbidity meter can provide continuous sediment concentration records. However, in many cases it is not possible to establish a useful relationship between turbidity and SSC data or the relationship proves highly variable both in time and space (Gippel, 1995, 1989).

The sediment budget for the Ripple Corner Catchment consists only of the sediment fraction  $<20\ \mu\text{m}$ , which is suspected to move predominantly in suspension. If a relationship exists between turbidity and SSC in the Ripple Corner Catchment, continuous monitoring of the sediment concentration at the drain output should be possible using a turbidity probe.

### **5.3.1 SSC – turbidity relationship for the Ripple Corner Catchment**

During the budget study many water samples have been taken from the catchment. Most of these samples were analysed in the lab for both turbidity and SSC. SSC was analysed by pouring the water samples through a  $20\ \mu\text{m}$  sieve and drying and weighing duplicate 50 ml sub-samples at  $105\ \text{C}^\circ$ . Turbidity was measured from sub-samples with a Merck 'Turbiquant 1500' bench top turbidity meter.

From the sampling date, water samples have been stored in a fridge for periods of time varying from weeks up to several months. To resuspend settled material each sample is vigorously shaken by hand for 2 minutes (measurement procedures added in Appendix D).

The SSC and turbidity values of each sample are plotted in Figure 5.1. Samples from each budget season are plotted separately. There appears to be little difference between the relationships for each season. Similarly, little difference was observed between samples from individual rainfall events, and between samples from different locations in the catchment.

Both outlet drains were equipped with turbidity meters, which provided continuous turbidity records (see Section 5.4). The regression equation in Figure 5.1 based on all available water samples can be used to estimate SSC from the continuous records of stream turbidity at the drain outlets:

**Equation 5.1:**

$$\text{SSC} = 1.2 * \text{Turbidant turbidity} + 23.3 \quad (R^2 = 0.9)$$

Details of the SSC estimates from the outlet drains are described in Section 5.8.

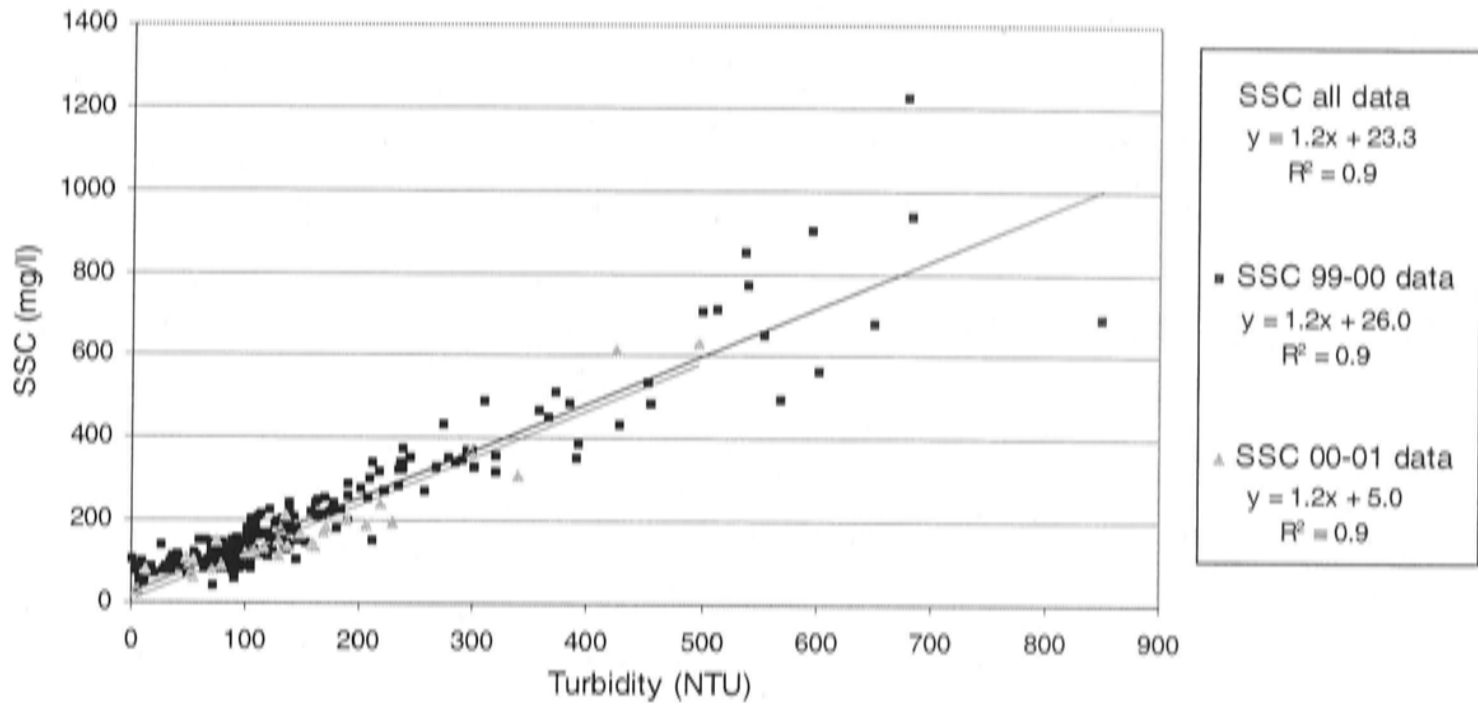


**Figure 5.1:** Scatter diagram of turbidity versus SSC for all drain water samples taken in the Ripple Corner Catchment. Both budget seasons plotted separately. Also shown are linear regression curves for each data set.

#### 5.4 Location and equipment

The gauging stations in Ripple and Prosser drain were installed at the catchment boundary (see Figure 4.1). The gauging equipment at both sites consists of a 'Dataflow Pressure Sensor (0-5 m)' connected to a 'Dataflow 392' data logger; a 'STARFLOW Ultrasonic Doppler Instrument' to measure water flow velocity, which has a built-in pressure transducer; and a 'Greenspan TS100' turbidity meter, connected to a 'Campbell CR10X' data logger. Thus velocity, turbidity and two sets of depth data are available for each outlet drain.

In Ripple Drain the depth and turbidity sensors were connected to the concrete base of a wooden bridge that leads across the drain. A few meters upstream from the bridge a concrete block was dug into the drain bed at the deepest point in the drain. The Starflow velocity meter was fixed on top of the block, level with the surrounding drain bed surface. From the bridge across the Ripple Drain, a track leads north along the cane paddocks straight to Prosser Drain. There is no bridge over this drain; the track simply continues across the drain bed. The gauging station for Prosser Drain was located about 5 m downstream from the drain crossing. The turbidity and depth

sensor were held in place with three-sided metal stakes (so called 'star pickets') at the edge of the drain. The velocity meter is again connected to a concrete block in the deepest part of the drain. Attempts to make the sensor level to the drain bed failed. The sensor remained slightly above the surrounding drain bed (<5 cm).

The track across Prosser Drain is only rarely used by traffic. So, increased turbidity as a result of disturbance of the drain bed by car wheels has not affected the observations. Water samples were always taken before crossing the drain.

Figure 5.2 shows the profiles of the drain cross-sections at the Ripple and Prosser Drain gauging sites. The profiles were estimated with a Dumpy Level between marked points on the drain banks.

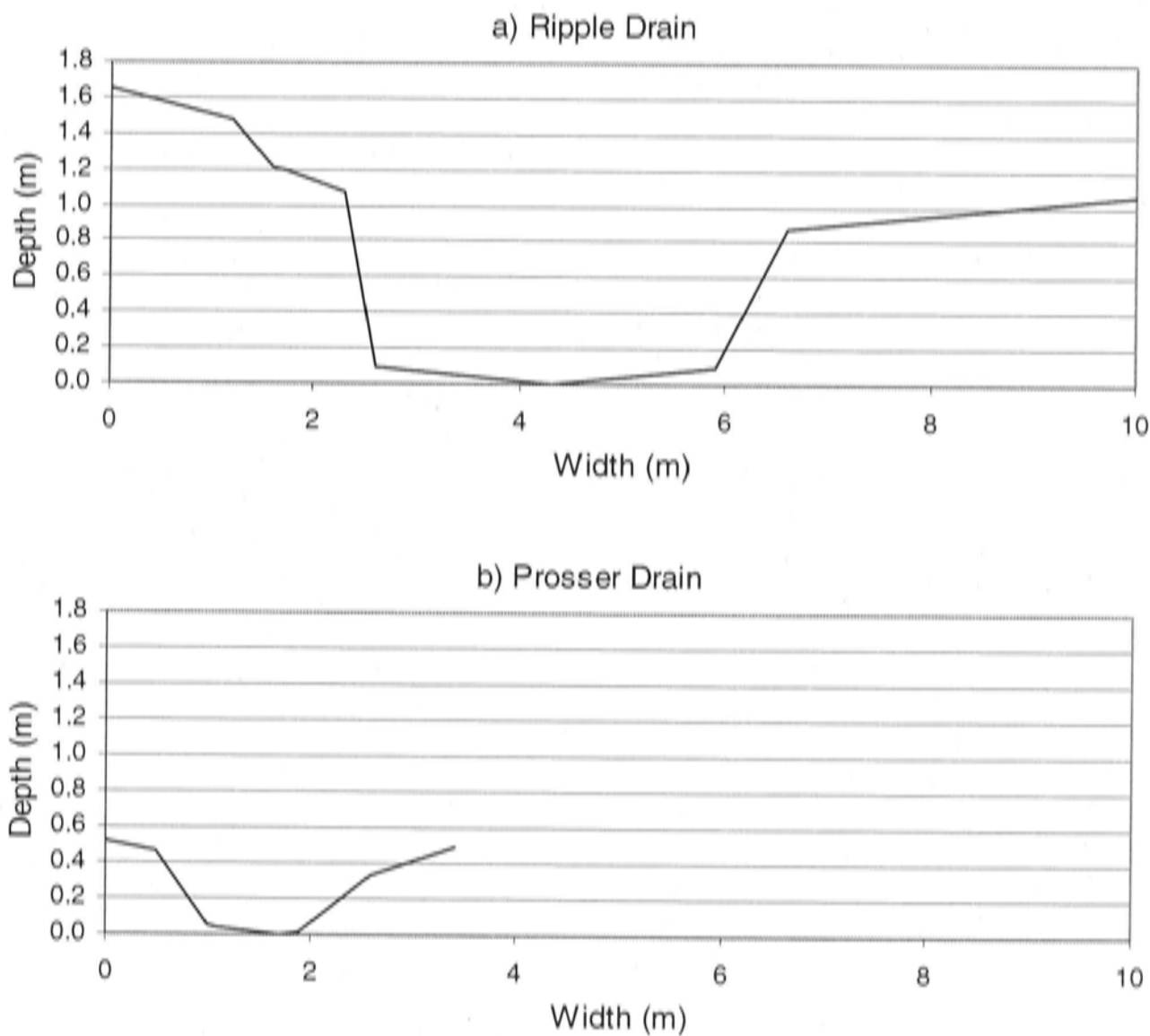


**Figure 5.2:** Profiles of cross-sections through Ripple Drain (a) and Prosser Drain (b) at gauging sites.

## 5.5 Raw data availability

All data sets collected at the gauging sites contain periods of missing data, mainly due to failure of the equipment. In the 00-01 season the gauging equipment was removed on 3/04/01, a month before the end of the budget period. In this section the availability of raw gauging data for the two budget periods, between 21/12/99 and

3/5/00 for the 99-00 wet season and between 7/12/00 and 15/5/01 for the 00-01 wet season, is reviewed. The significance of data gaps is assessed and whenever possible they are filled using original data. The quality of the raw data and the methods used to calculate the final loads when the original gauging data are not adequate, are also discussed in subsequent sections.

### 5.5.1 Ripple Drain 99-00

During the 1999-2000 wet season at both the Ripple and Prosser Drain gauging sites, Starflow and Dataflow depth and velocity data were logged every 5 minutes and Greenspan turbidity data every 30 minutes.

An overview of gaps in the depth data sets of Ripple Drain for the 1999-2000 season is listed in Table 5.1 and graphically presented in Appendix C. In addition to the listed gaps, the data also includes a number of smaller gaps with duration of less than an hour. Such gaps are ignored, because they become unimportant during later stages of the load calculations and will not affect the final budget figures.

The gap between 5/04/00 12:15 and 6/04/00 12:25 is probably a leap in the timestamps. Data before this gap shows peaks in depth around 12 hours before a rainstorm, the same length of time as the missing data period. The depth data series from the end of the previous gap (28/03/00 10:40) is therefore moved forward in time until the gap is filled. The resulting graph appears more realistic. As a result of the data adjustment, the gap that starts 22/03/00 12:55 now continues till 29/03/00 10:45.

**Table 5.1:** Data availability Ripple Drain 1999-2000.

Dataflow depth data		Starflow depth and velocity data		Starflow and Dataflow combined	
Start	End	Start	End	Start	End
4/02/00 20:15	15/02/00 12:30	17/12/99 14:45	13/01/00 0:55	17/12/99 15:00	22/03/00 12:55
16/02/00 12:20	22/03/00 12:55	13/01/00 10:25	10/02/00 2:50	28/03/00 10:40	5/04/00 12:15
28/03/00 10:40	5/04/00 12:15	15/02/00 12:30	3/03/00 4:30	6/04/00 12:25	21/07/00 10:55
6/04/00 12:25	7/06/00 11:40	8/03/00 17:30	9/03/00 14:30		
		10/03/00 1:35	19/03/00 17:50		
		23/04/00 6:05	20/05/00 8:10		
		7/06/00 11:55	10/06/00 9:05		

Data records from corresponding periods in the 99-00 Starflow and Dataflow depth data sets are plotted in Figure 5.3. A linear regression equation for Dataflow and Starflow values is used to estimate Starflow depth values from the Dataflow data and create one more complete depth data set for the season:

$$\text{Starflow depth} = 1.0 * \text{Dataflow depth} + 266 \quad (R^2 = 1.0)$$

Two gaps remain after combining the two data sets (Table 5.1). To fill these remaining gaps linear interpolation of the adjacent data is sufficient, because no rainfall was recorded over these periods.

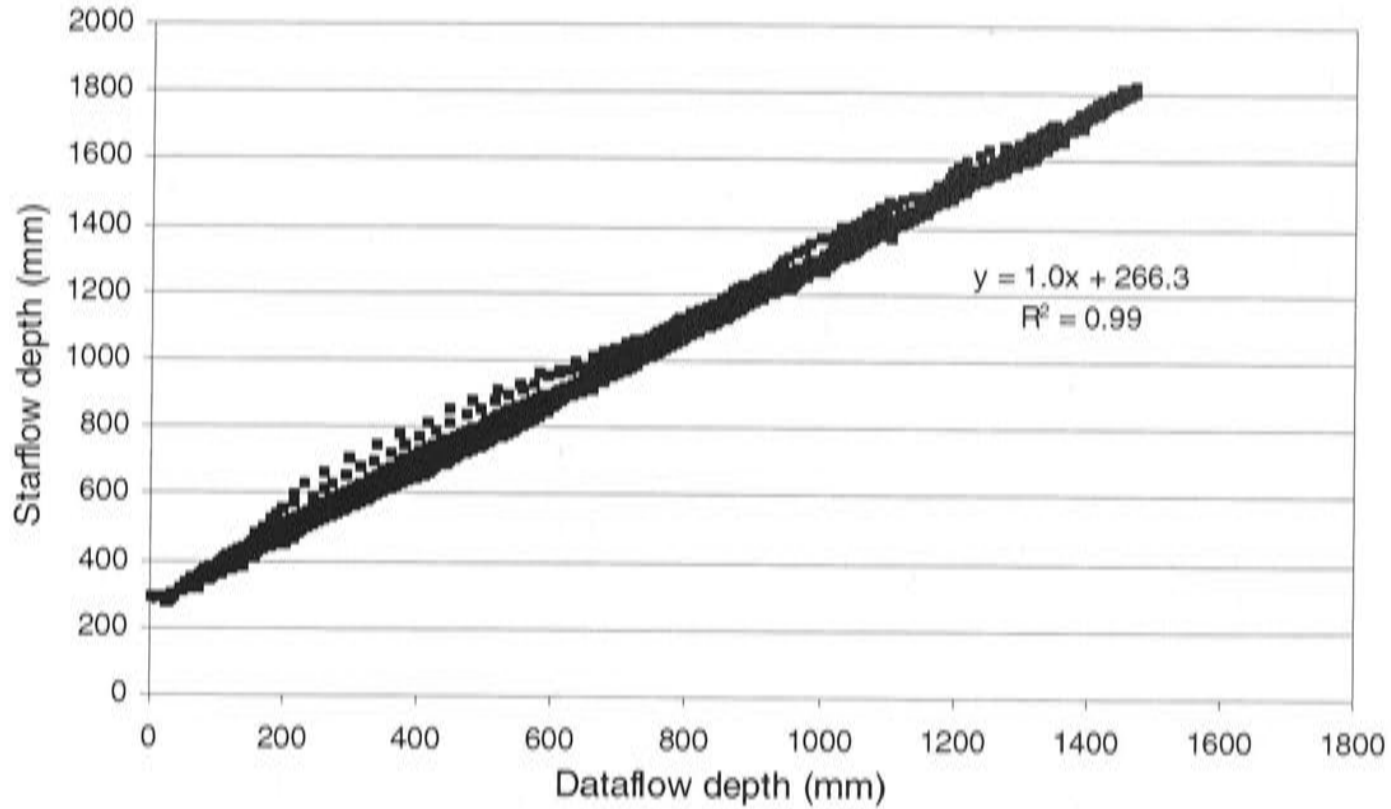


**Figure 5.3:** Scatter diagram of Ripple Drain Dataflow depth data versus Starflow depth data and a linear regression curve for 99-00 season.

Gaps in the 1999-2000 Starflow velocity data correspond with those in the Starflow depth data. Greenspan turbidity data are missing for two short time periods, during one rainfall event (see Table 5.2). Linear interpolation might not be sufficient for these gaps. Alternative possibilities to fill the gaps are described in Section 5.9.

**Table 5.2:** Availability Greenspan turbidity data Ripple Drain 99-00.

Greenspan turbidity data	
Start	End
20/12/99 16:45	3/04/00 12:15
3/04/00 18:45	3/04/00 20:45
6/04/00 12:30	7/06/00 11:15

### 5.5.2 Ripple Drain 00-01

In the 2000-2001 season all sensors at both gauging sites were logged every 15 minutes. The data from the Ripple Drain Starflow sensor contain a number of duplicate timestamps, but they have little effect on the overall data recording. Furthermore there is only one missing data period in the 2000-2001 data sets. This period is the same for all depth, velocity and turbidity data. Table 5.3 lists the availability of the 2000-2001 data.

The only gap in the 00-01 data is filled by linear interpolation of the neighbouring data. Some rain fell over the period of missing data, but this was only a small amount and it is not thought to have caused a significantly higher sediment load.

**Table 5.3:** Availability of Starflow velocity and depth, and Greenspan turbidity data 2000-2001.

Starflow velocity and depth, and Greenspan turbidity data	
Start	End
1/12/00 13:30	29/01/01 14:00
2/02/01 12:30	3/04/01 11:00

### 5.5.3 Prosser Drain 99-00

The Dataflow data from Prosser Drain for the 99-00 season is completely discarded. The data set contains too many gaps and periods with faulty records. The remaining useful data do not add any extra information to the more complete Starflow depth data set. The gaps in the Starflow depth and velocity data sets are listed in Table 5.4 (see also Appendix C). The 99-00 turbidity data contains only one gap, which is also shown in Table 5.4.

**Table 5.4:** Availability Starflow depth and velocity data and Greenspan turbidity data Prosser Drain 99-00.

Starflow depth data		Starflow velocity data		Greenspan turbidity data	
Start	End	Start	End	Start	End
20/12/99 18:30	22/03/00 12:00	20/12/99 18:30	27/02/00 17:25	20/12/99 18:15	10/03/00 20:15
17/04/00 6:00	21/07/00 10:40	28/02/00 22:35	3/03/00 20:20	22/03/00 12:45	16/07/00 15:15
		8/03/00 16:35	19/03/00 20:10		
		17/04/00 6:00	28/04/00 15:35		
		1/05/00 17:35	21/07/00 10:40		

### 5.5.4 Prosser Drain 00-01

Like the Ripple Drain data for this season, the Prosser Drain data sets all have one missing data period at the end of January (see Table 5.5).

**Table 5.5:** Availability Starflow velocity and depth and Greenspan turbidity data 2000-2001.

Starflow velocity and depth, and Greenspan turbidity data	
Start	End
1/12/00 14:30	29/01/01 13:45
2/02/01 12:15	3/04/01 0:30

## 5.6 Water depth and drain cross-sectional areas

For those periods covered by the data records, the availability of velocity data allows easy calculation of discharges by multiplying the velocity with the (wet) cross-

sectional areas of gauging sites. The cross-sectional areas of the Ripple and Prosser Drain gauging sites are estimated for the recorded water depth values with a 'water depth–cross-sectional area' function. The function is constructed from the drain cross-section profiles of the gauging sites (Figure 5.2). Cross-sectional surface areas are calculated from each of the profiles for 6 water depths. Fourth order polynomials are fit through the points calculated for each site. This type of function is chosen because it perfectly fits the data points ( $R^2 = 1.0$ ). The functions will only be used to interpolate between existing data points, not for further extrapolation of the data.

To relate the depth recorded by the pressure transducers to the drain profiles and their depth-cross-sectional area functions, manual measurements of the water level were taken from reference points close to the gauging sites. The heights of these reference points were included in the drain profile survey. The transducer depth record at the time of the manual measurement can therefore be related to a water depth and cross-sectional area in the drain profile. In some cases the manual measurements were not documented in enough detail, so some assumptions had to be made for the transformation of the transducer data. The next sections describe these assumptions and the transformations that were applied to the raw depth data for each drain and each season.

### **5.6.1 Depth adjustments Ripple Drain 99-00**

The reference point chosen for Ripple Drain is the bridge to which the gauging devices were connected. During the 99-00 season 7 manual water depth measurements were taken from this point. Figure 5.4 shows the regression curves for the manual depth measurements and the records from both pressure transducer types. The 'manual depth–Starflow' regression equation is used to transform the Starflow depth records to depth values that can be used to calculate drain cross-sectional areas:

#### **Equation 5.2**

$$\text{Manual depth} = 1.1 * \text{Starflow depth} - 0.2 \quad (R^2 = 1.0)$$



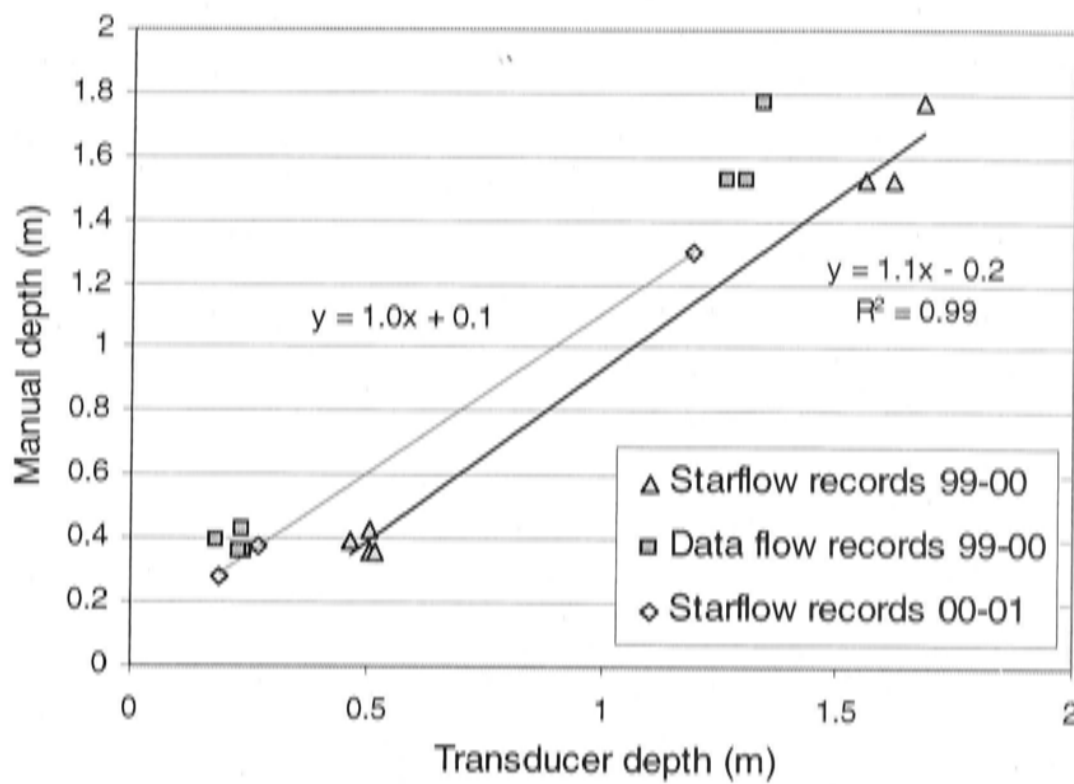


**Figure 5.4:** Scatter diagram of Ripple Drain transducer depth (Starflow and Dataflow) versus manual depth at the gauging site for both budget seasons. Regression curves for Starflow depth data (99-00 data thick, 0 0-01 data thin).

### 5.6.2 Depth adjustments Ripple Drain 00-01

During the 00-01 season only three manual measurements were taken and only Starflow data records exist, but documentation of the measurements is reliable and the manual depth–Starflow depth regression curve closely fits a 1:1 line. Because the regression of only three points is not significant, the decision was made to average the difference between the manual measurements and the Starflow measurements and add this average to all Starflow data. Table 5.6 shows the differences between all manual measurements and the corresponding Starflow records and the average of the differences. The measurements are also plotted in Figure 5.4.

**Table 5.6:** 00-01 Ripple Drain manual depth measurements and corresponding Starflow records.

Measurement date	Manual depth (m)	Starflow depth (m)	Difference (m)
3/01/01 12:00	0.3	0.2	0.1
16/02/01 12:00	1.3	1.2	0.1
26/02/01 12:25	0.4	0.3	0.1
		Average	0.1

### 5.6.3 Depth adjustments Prosser Drain 99-00 and 00-01

There is no obvious fixed reference point in the vicinity of the Prosser drain gauging site, therefore various different reference points were used. However, the

documentation of the reference points was inadequate for both gauged seasons. The reliability of the data from the Starflow sensor can not be checked either, because most of the matching Dataflow records are missing due to failure of the data logger.

Three of the 10 manual measurements are clearly documented, one for the 99-00 season and two for the 00-01 season. From the Ripple Drain depth calibration it appears that depth generated from the transducers is more or less proportional to the true water depth, and that the transducer data only need adjustment with a constant for the height of the sensor in the drain profile.

The only documented manual measurement in the 99-00 season (3/01/00) is taken from the concrete block on which the Starflow sensor is fixed. This measurement reads 33 cm deeper than the measurement by the Starflow sensor. One of the measurements is obviously incorrect. Adjusting all Starflow depth data by adding the 33 cm results in low flow depth greater than 30 cm. It is known from field observations that this is too deep. Thus, 'calibration' of the 99-00 Starflow data with this one manual measurement is not possible.

The 00-01 data have a similar problem. Of the three 'calibration' measurements from the 00-01 season, two (3/01/01 and 16/02/01) are sufficiently documented to relate them to the drain profile. A line drawn through the two points has a 1:1 slope, but the more than 40 cm difference in depth between the manual and the Starflow measurement is again not correct.

**Table 5.7:** 00-01 Prosser Drain manual depth measurements and corresponding Starflow records.

Measurement date	Manual depth (m)	Starflow depth (m)
3/01/01 12:39	0.6	0.1
16/02/01 12:30	1.0	0.5
26/02/01 12:45	0.3	0.4

Since the Starflow sensors are located almost level with the bed in the deepest part of the drains, depth records are expected to lie close to the true depth values. Only some deviation may be expected from either a slight elevation of the block above the drain bed or from errors in the profile survey. The two seasons of Ripple Drain data required a +0.16 m and a -0.09 m adjustment for the sensor depth. Based on these findings the manual measurements taken in the Prosser Drain were ignored and it was assumed that the Starflow records give the best representation with an error based on the variation in the Ripple Drain data. Because Prosser Drain is a much smaller drain, this variation will have a greater impact on the total load calculation

The concrete block with the Starflow meter was not level with the bed of the Prosser Drain. Section 5.10 on load calculations will discuss the effect of adding an extra 0.05 m to the depth records to compensate for the elevation of the sensor.

The adjusted depth curves from both Ripple Drain and Prosser Drain for each season are shown in Appendices F (1-6).

## **5.7 Water flow velocity**

The Starflow meters that were installed at the outlet drains record the average flow velocity of the water column above the sensor. The generated data in general appears very noisy (see velocity curves in Appendices F (1,3 and 5)). It is not clear whether this is the result of a sensor problem or whether it reflects natural variability in the drain flow velocity. The Starflow manual (Unidata, 1998) mentions the occurrence of signal noise, but only when flow velocities become very low, which is not likely to be the problem.

The 99-00 velocity data from the Ripple Drain contains a large number of gaps but it does not show any unexpected behaviour. The 00-01 data contains only one gap, but certain parts of the data appear to be unreliable. There are for example some periods of up to 18 hours during the flood peak between 16/02/01 and 20/02/01 when the velocity records do not change. Also the highest velocities measured in the 00-01 season are over  $3 \text{ m s}^{-1}$  compared to a maximum of  $1.8 \text{ m s}^{-1}$  in the previous season.

In general the Prosser Drain data appear noisier than the Ripple Drain velocity data. The higher short-term variation in the Prosser Drain data sets is probably due to the much shallower and more responsive flow in this drain. There do not seem to be any problems with the 99-00 data set. Flow velocity increases with increasing water depth during a rainfall event, as expected. Only towards the end of the season (after 15 May 2000) the flow velocity becomes zero in between rainfall events. This probably occurs when the water column above the Starflow sensor becomes either too shallow or disappears. The 00-01 velocity data appear different. There is some increase in velocity at the onset of rainstorms, but the increase is not as pronounced as during the previous season, and the noise in the data seems to overrule the event based variation.

These general observations indicate that some of the velocity data might not be reliable. If there are errors in the Starflow velocity data, this could mean that there are also errors in the Starflow depth data.

### 5.7.1 Velocity calibration

A few times during the two gauged seasons velocity measurements were taken with a hand-held 'OTT C2 current meter SN15721' (the pulse output of the device was captured using a PSION workabout). Table 5.8 compares the manual velocity estimates in the deepest part of the drain with the Starflow values recorded at the same time. At all measurement dates the Starflow velocity curves consist of a broad band of small scale noise with a width of about  $0.1 \text{ m s}^{-1}$ . Maximum changes in the noise can occur within half an hour. Considering this amount of variation in the Starflow velocity data, the manual measurements seem to correspond reasonably well and no calibration/transformation needs to be applied. The only measurement that does show a considerable difference is the one taken in Ripple Drain at 16/02/01. The Starflow records around this date have earlier been identified as unreliable.

### 5.7.2 Velocity distribution

Due to friction of the water along the drain bed and banks, flow velocity is not constant throughout a drain cross-section. The Starflow meter in each drain is located in the deepest part of the profile where the friction is lowest and flow velocities are highest. Therefore discharge calculated directly from raw Starflow data is likely to overestimate true flow.

**Table 5.8:** 00-01 manual velocity measurements and corresponding Starflow records for Ripple Drain and Prosser Drain.

Measurement date	Prosser Drain		Ripple Drain	
	Manual velocity ( $\text{m s}^{-1}$ )	Starflow velocity ( $\text{m s}^{-1}$ )	Manual velocity ( $\text{m s}^{-1}$ )	Starflow velocity ( $\text{m s}^{-1}$ )
18/02/00	0.4	0.5	0.8	0.6
8/03/00	0.1	n.a.	0.7	n.a.
17/03/00	0.5	0.4	1.4	1.1
03/01/01	0.3	0.3	0.4	0.3
16/02/01	0.6	0.6	1.5	2.6

To get an estimate of horizontal variation in flow velocity, manual measurements were done at several distances along the profile. Vertical variation was not measured; instead manual measurements were taken at  $2/3$  of the water depth, which is

generally considered to provide the average flow velocity of the water column (Shaw, 1983).

The variation of the velocity in the drain cross-section at Ripple Drain gauging site is studied from four velocity measurement sessions with the hand-held meter. For each manual measurement, the ratio between manual and Starflow velocity values is calculated. All ratios are plotted against the drain width in Figure 5.5. The graph shows that the manual measurements in the middle of the drain are always higher than those estimated by the Starflow meter. Only at the edges of the profile velocities are measured with the hand-held meter lower than the Starflow velocities. The information from the graph suggests that the Starflow data might *not* overestimate the true average velocity in the drain profiles.

In the same way velocity ratios are calculated from the Prosser Drain data. They show a similar pattern as the Ripple Drain ratios, with values higher than one in the middle of the profile and less than a half towards the edges. Because of the smaller size of the drain the influence of friction along the drain banks is more important. In this drain the Starflow values probably overestimate the average flow velocity for the whole cross-sectional area.

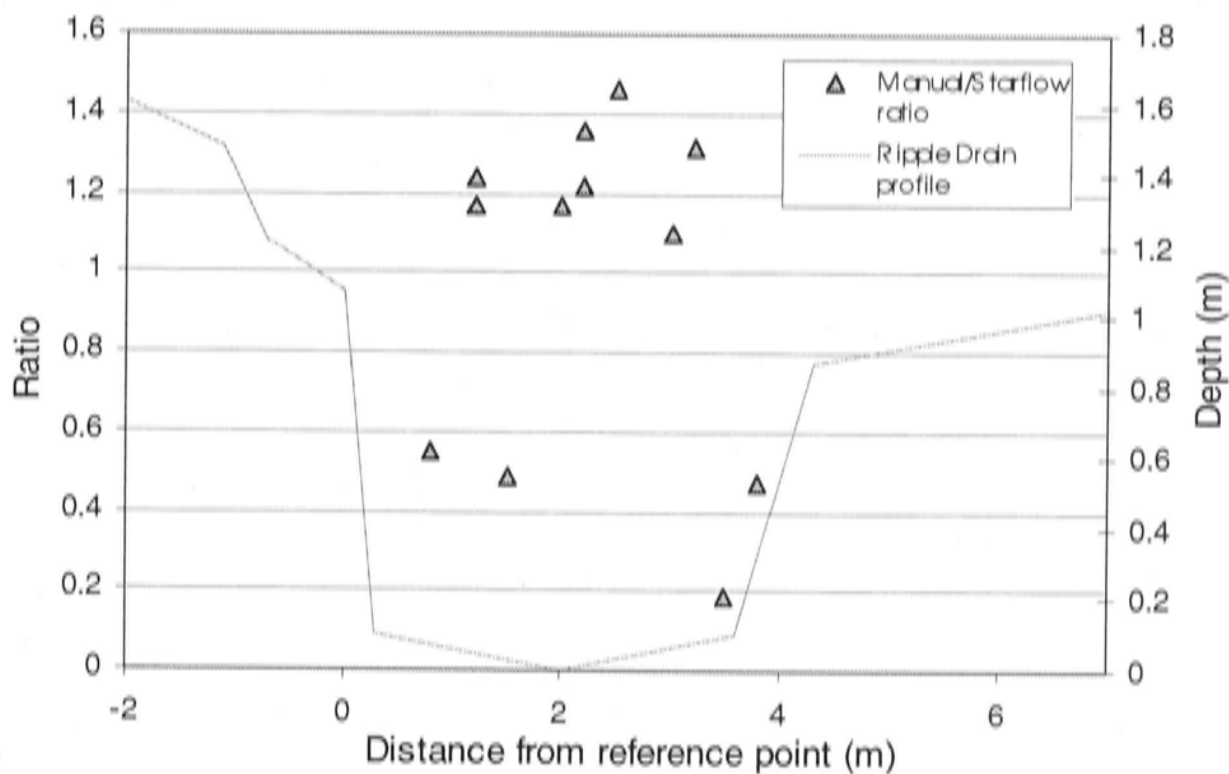


**Figure 5.5:** Ratios between manual velocity measurements as observed along the Ripple Drain surface profile and Starflow velocity as measured in the deepest part of the drain.

The most detailed velocity profile in Ripple Drain has only five points. This number of points does not give sufficient information on the width of the area affected by the friction of water along the drain bank. All other profiles consist of

**Table 5.9:** Manual velocity/Starflow velocity ratios for Ripple Drain.

Measurement date	Distance from reference point (m)	Manual velocity ( $\text{m s}^{-1}$ )	Starflow velocity ( $\text{m s}^{-1}$ )	manual/Starflow ratio
18/02/00	1.2	0.7	0.6	1.2
	2.2	0.8	0.6	1.4
	3.2	0.7	0.6	1.3
10/03/00	0.8	0.3	0.6	0.6
	1.2	0.7	0.6	1.2
	2	0.7	0.6	1.2
	3	0.7	0.6	1.1
	3.8	0.3	0.6	0.5
17/03/00	2.2	1.4	1.1	1.2
3/01/01	1.5	0.2	0.3	0.5
	2.5	0.4	0.3	1.5
	3.5	0.1	0.3	0.2
Average				1.0

even fewer points. It is also not known how representative the manual measurements are, because the reliability of the manual measurement device has not been tested and the exact vertical velocity distribution is not known. It is therefore impossible to develop a quantitative transformation of Starflow velocity records to account for velocity variation across the drain profiles. For the calculation of the sediment load Starflow records are assumed representative for the whole profile. This assumption is expected to be sufficient, because the average of the ratios in this profile is 1.0.

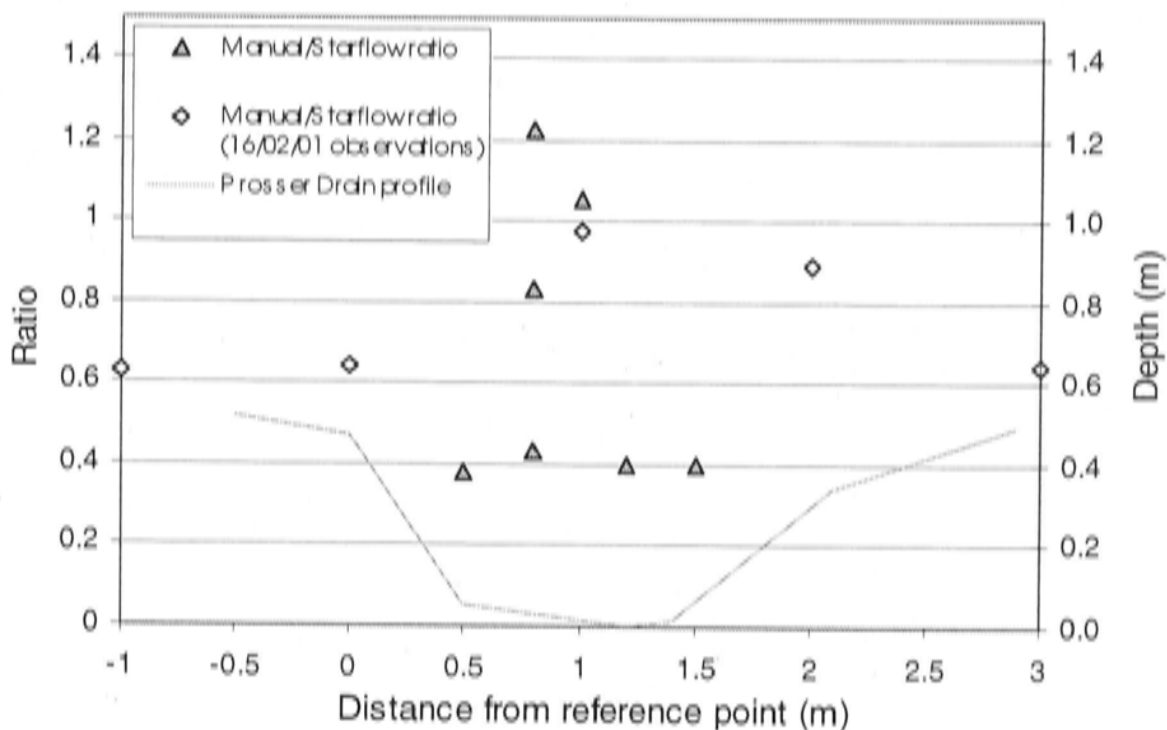


**Figure 5.6:** Ratios between manual velocity measurements as observed along the Prosser Drain surface profile and Starflow velocity as measured in the deepest part of the drain. Inaccurate 16/02/01 estimates plotted separately.

**Table 5.10:** Manual velocity/Starflow velocity ratios for Prosser Drain

Measurement date	Distance from reference point (m)	Manual velocity ( $\text{m s}^{-1}$ )	Starflow velocity ( $\text{m s}^{-1}$ )	manual/Starflow ratio
18/02/00	0.8	0.4	0.5	0.8
8/03/00	0.8	0.1	0.3	0.4
	1.2	0.1	0.3	0.4
17/03/00	0.8	0.5	0.4	1.2
3/01/01	0.5	0.1	0.3	0.4
	1	0.3	0.3	1.1
	1.5	0.1	0.3	0.4
16/02/01*	-1	0.4	0.6	0.6
	0	0.4	0.6	0.6
	1	0.6	0.6	1.0
	2	0.5	0.6	0.9
	3	0.4	0.6	0.6
Average				0.7

\*Distance from reference point and depth at which velocity measurements were taken are rough estimates. They were not measured. The data are however thought to be representative of the field conditions observed at this date.

Although the average ratio of 0.7 for the Prosser Drain (Table 5.10) suggests that the Starflow values overestimate the average flow velocity in the cross-sectional area, unadjusted Starflow records will be used in the load calculation. The average of the Manual/Starflow ratios is not based on sufficient data to represent the velocity distribution. To test the error that may be introduced this way, an additional load value based on reduced velocity values will be calculated in Section 5.10.2.

### 5.7.3 Flood events

The drain profiles are measured from the highest points of each drain bank. This is the point where the steep drain bank changes to a gentler sloping headland. During high flows water depths regularly exceed the maximum bank height. Under these conditions so called 'overbank flow' occurs. Excess water starts flowing across the headlands and often reaches into the cane fields. During field visits water levels of more than 1 metre were observed on the headlands along Ripple Drain. The drain profiles need to be extrapolated for such overbank flow periods. Initially the assumption is made that flow velocities of the water on the headlands and beyond are very small and the additional discharge from this excess water can be neglected. In this case the edges of the drain profiles are extrapolated vertically to provide cross-

sectional areas for water depths deeper than the maximum drain bank heights (Figure 5.7).

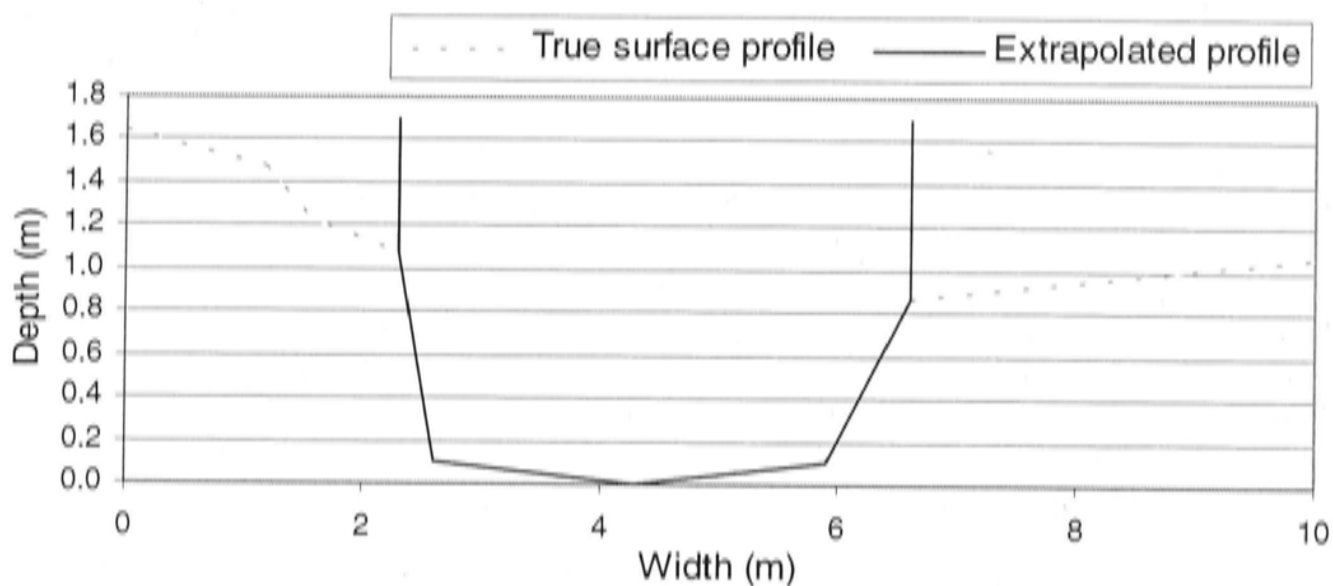


**Figure 5.7:** Profile of cross-sections through Ripple Drain with vertically extrapolated banks, used for discharge calculation during flood conditions.

Later observations showed that the water that flows over the headlands *can* have significant velocity and does contribute to the total discharge. At 16 February 2001 a profile of five velocity measurements was taken in the Prosser Drain under flood conditions. The exact position of the measurements along the width of the drain has not been determined, but their approximate position is indicated in Figure 5.6. The velocity of the two measurements taken in the flow on the headland surface is more than half of the velocity measured by the Starflow meter in the deepest part of the drain. After this observation, no more opportunities arose to make more precise estimates of overbank flow velocities. Calculation of the discharges is therefore based on the earlier assumptions.

## 5.8 Suspended sediment concentrations

The relationship between turbidity and SSC is dependent on the properties and the organic content of the sediment concentration and the specifications of the measurement device (Gippel, 1989). Although the Turbiquant hand held meter is regularly calibrated in the lab and the Greenspan in-stream device was calibrated at the factory before the 00-01 season, this does not mean they will measure the same values. Because the turbidity – SSC relationship (Equation 5.1) is based on turbidity values of water samples measured with the Turbiquant hand-held meter, SSC values can not be obtained directly from the continuous Greenspan data. First Greenspan



NTU has to be related to Turbiquant NTU. The following sections describe the procedures of the adjustments for each season.

### 5.8.1 Ripple Drain 99-00

During the 99-00 season 11 water samples were taken at the Ripple Drain gauging site (D21). After storage in a refrigerator for periods varying from days to months, the turbidity of the samples was measured in the lab with the Turbiquant turbidity meter (see Appendix D for procedures). Figure 5.8 shows the relationship between the Turbiquant sample turbidity and the Greenspan in-stream turbidity at the time of sampling. The regression equation for the data points is used to transform the Greenspan data records to Turbiquant values:

#### Equation 5.3

$$\text{Turbiquant turbidity} = 2.1 * \text{Greenspan turbidity} + 11.8 \quad (R^2 = 0.9)$$

The SSC can be estimated from the Turbiquant values with the Turbidity – SSC relationship (Equation 5.1, Section 5.3.1):

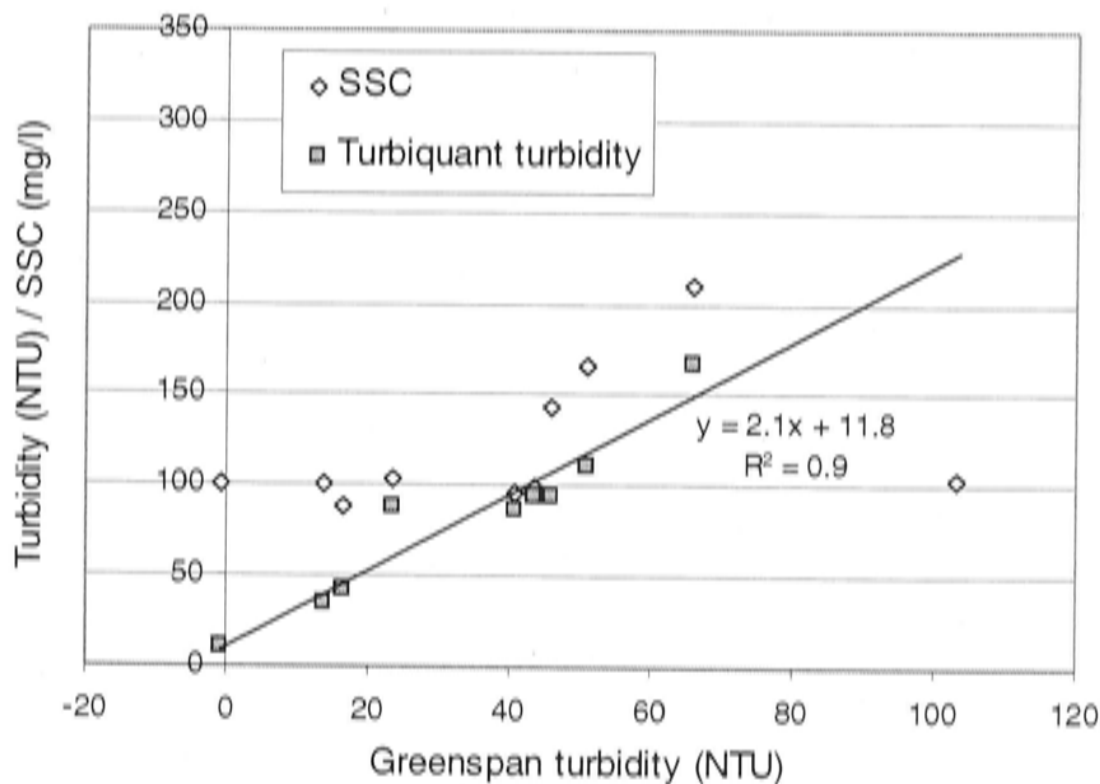


**Figure 5.8:** Scatter diagram of Greenspan turbidity records versus grab sample Turbiquant turbidity and SSC, with regression curve for Turbiquant turbidity. All samples taken from Ripple Drain gauging site during the 99-00 season.

### 5.8.2 Ripple Drain 00-01

Because the Greenspan turbidity probe had been calibrated at the beginning of the 00-01 season, a small number of water samples was thought to be sufficient to adjust the data. Four samples were taken. The grab sample Turbiquant turbidity values are plotted in Figure 5.9 against the Greenspan turbidity values in the drain at the time of sampling. The equation of a regression curve through these points does not provide a transformation that would make the 00-01 turbidity data comparable with the 99-00 data.

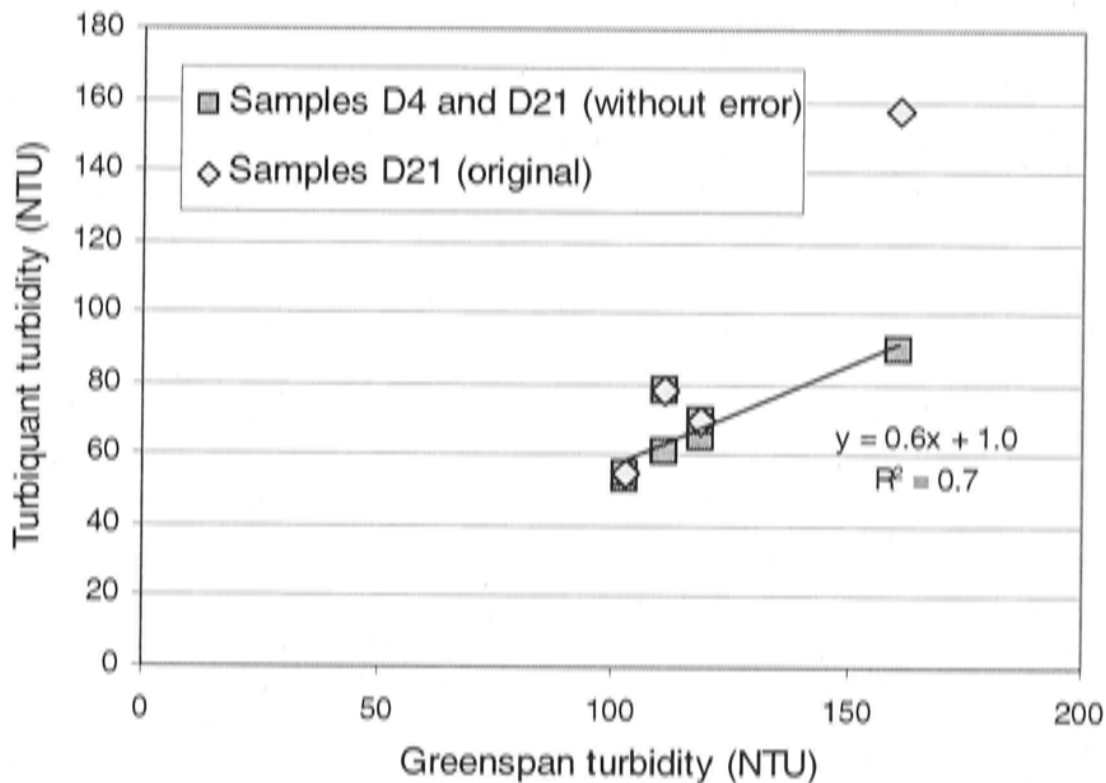


**Figure 5.9:** Scatter diagram of Greenspan versus Turbiquant turbidity data, for grab samples taken at Ripple Drain gauging site (D21) (with and without ) and at Palmas' site (D4) in the 00-01 season. Regression curve for D4 and D12 samples (without erroneous sample) included.

The Turbiquant values from grab samples taken upstream in Ripple Drain, at the Palmas' site (D4, see Appendix A) do generate a useful regression equation with the Greenspan values from the gauging site. Because there is no significant sediment input from tributary drains between the two sites, values are expected to be similar. This is confirmed by data from the previous season, when D4 and D21 samples have very similar turbidity values. Apparently an error occurred during the measurements of the sample turbidity for the 00-01 samples. A new regression was developed based on the D4 and D21 samples without the erroneous value. The following regression equation is used to transform the 00-01 Greenspan turbidity records to sample turbidity values, which can then be transformed to SSC with Equation 5.1:

## Equation 5.4

$$\text{Turbiquant turbidity} = 0.6 * \text{Greenspan turbidity} + 0.7 \quad (R^2 = 0.8)$$

The range of the resulting SSC-graphs for the two seasons is (more or less) similar. The SSC curves for each drain and each season are shown in Appendix F(1-6).

## 5.8.3 Prosser Drain 99-00

Eight water samples were taken at Prosser Drain gauging site (D24) and analysed with the Turbiquant meter in the 99-00 season (Table 5.11). One sample had to be discarded, because the corresponding Greenspan measurement fell outside the measurement range of the probe. This occurred because the probe had not been calibrated at the beginning of the season. The remaining samples do not result in a significant regression, see Figure 5.10 ( $P = 0.07$ ).

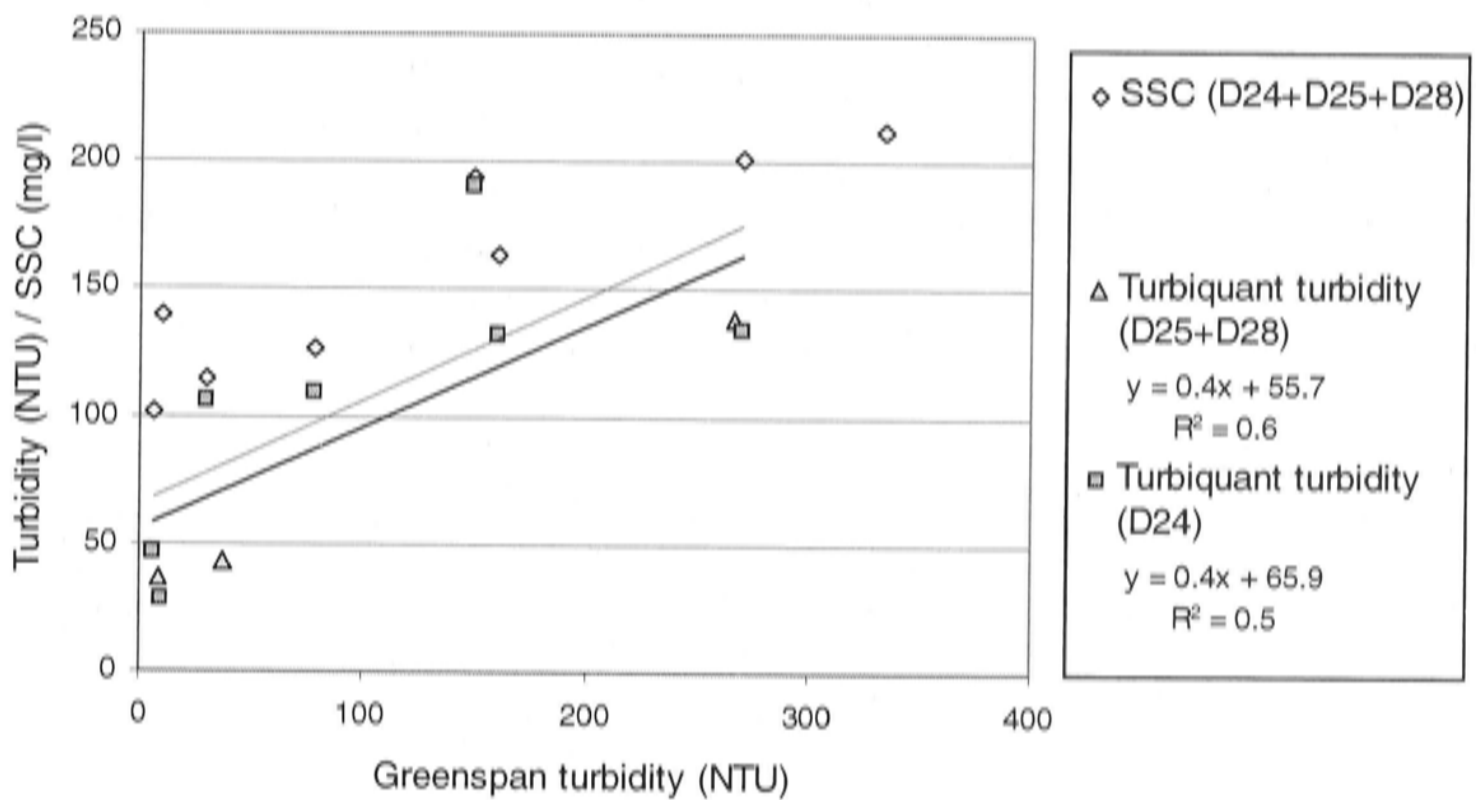


**Figure 5.10:** Scatter diagram of Greenspan turbidity versus Turbiquant turbidity and SSC for grab samples taken at Prosser Drain gauging site (D24) and downstream locations in Prosser Drain (D25+D28) in the 99-00 season. Regression curves for Turbiquant data from locations D24 (thick) and D25+D28 (thin) included.

The best explanation for the poorer relationship between the turbidity values from the in-stream sensor and the water samples is probably a combination of drain size, variation in the exact sample sites and time of sampling, and incomplete mixing of the drain water. A small tributary joins the Prosser Drain a few meters upstream from the gauging site. Under certain conditions the water from this tributary stream may

not have mixed sufficiently with the water from Prosser Drain and therefore caused unexpected variation of the in-stream or water sample turbidity values.

**Table 5.11:** 99-00 Prosser Drain water quality data and corresponding Greenspan turbidity records.

Measurement date	Greenspan turbidity (NTU)	Turbiquant turbidity D24 (NTU)	Turbiquant turbidity D25 + D28 (NTU)	SSC (D24 + D25 + D28) ( $\text{mg l}^{-1}$ )
3/2/00 12:00	38		43	94
3/2/00 12:40	6	46		102
4/6/00 12:00	9		37	108
2/25/00 12:00	30	106		115
4/4/00 12:00	78	109		127
1/18/00 14:10	11	28		140
2/7/00 15:15	161	132		163
2/10/00 10:45	267		138	191
2/16/00 13:25	150	191		194
2/10/00 11:10	270	134		201
2/18/00 12:33	333	164		212
2/18/00 13:13	333		175	218
2/18/00 13:00	333		178	222

Samples were also taken from Prosser Drain at two sites further downstream (D25 and D28, see Appendix A). Between the gauging site and these sample sites, no significant amount of water is supplied from tributaries. The measurements are consistent with both the D24 and Greenspan values, supporting the idea that the other manual samples are affected by local input, not observed at the gauging site. A regression curve for all Prosser Drain samples (D24, D25 and D28) is little different from the curve based on only D24 samples (see Figure 5.10), but its relationship is significant ( $P = 0.01$ ) The resulting equation (Equation 5.5) will be used to transform the 99-00 Prosser Drain turbidity data:

**Equation 5.5**

$$\text{Turbiquant turbidity} = 0.4 * \text{Greenspan turbidity} + 55.7 \quad (R^2 = 0.6)$$

#### 5.8.4 Prosser Drain 00-01

The records from the Greenspan sensor show extreme values that do not obviously relate to the grab sample data. These extreme values result from the strange behaviour of the sensor that has already been mentioned. No pattern is recognised that could explain the behaviour of the turbidity meter. The transformation suggested by the regression equation in Figure 5.11 obviously does not improve the data:

$$\text{Turbiquant turbidity} = 0.04 * \text{Greenspan turbidity} + 99.6 \quad (R^2 = 0.7)$$

The data have to be discarded. Other ways to obtain SSC data will be considered further on in the chapter.

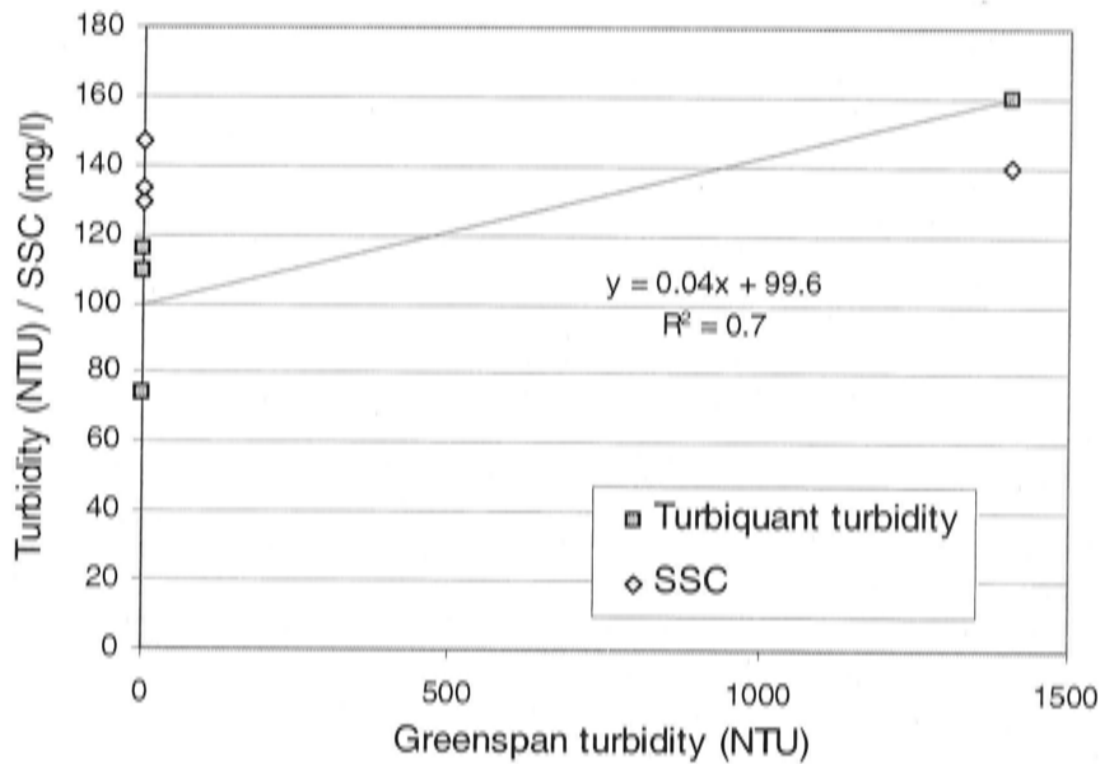


**Figure 5.11:** Scatter diagram of Greenspan turbidity versus Turbiquant turbidity and SSC for grab samples taken at the Prosser Drain gauging site in the 00-01 season. Regression curve for turbidity data included.

**Table 5.12:** 00-01 Prosser Drain water quality data and corresponding Greenspan records.

Measurement date	Greenspan turbidity (NTU)	Turbiquant turbidity (NTU)	SSC (mg l <sup>-1</sup> )
3/01/01 12:22	0.4	74	147
16/02/01 12:25	1404	160	140
26/02/01 12:45	0.4	109	129
3/04/01 10:55	0.4	116	133

## 5.9 Further data improvement

After the modifications of the raw gauging data, as described in the previous sections, the data are further studied with the aim to find possible relationships between the gauged variables that could help filling in remaining gaps in the data sets.

First, discharges are calculated from the transformed depth and velocity data for each gauging site. Next all data are averaged over 6-hourly periods. This is done to obtain comparable units of time that facilitate the study of relationships between seasons, between sites and between gauged variables, and the calculation of total

loads. It also smooths some of the fine scale noise (especially present in the velocity data) that does not contain important information. The averaging period of six hours was chosen because this time period does not affect the shape of the flow peaks.

The section on *raw data* (5.5) mentioned gaps that could be filled by simple linear interpolation of the existing data. Such interpolation is done after the data are transformed and averaged.

### 5.9.1 Depth-discharge rating curve Ripple Drain 99-00

The initial tidying of the Ripple Drain data resulted in an uninterrupted depth data set for the 99-00 season that covers the whole budget period. Because problems were expected due to backwater processes, depth discharge rating curves were not thought to be useful for the initial estimation of sediment load. However, with the now available depth and discharge data, such a curve can easily be established and studied and it might provide a good method to replace missing velocity data. A depth-discharge rating-curve is plotted from the depth and all available discharge data. A power function can be fitted through the data points (see Figure 5.12). The function is used to calculate 6-hourly discharges for periods with missing velocity data:

#### Equation 5.6

$$\text{Discharge} = 3.3 * \text{depth}^{2.0} \quad (R^2 = 1.0)$$

With this method all missing discharges for the 99-00 budget period can be calculated.

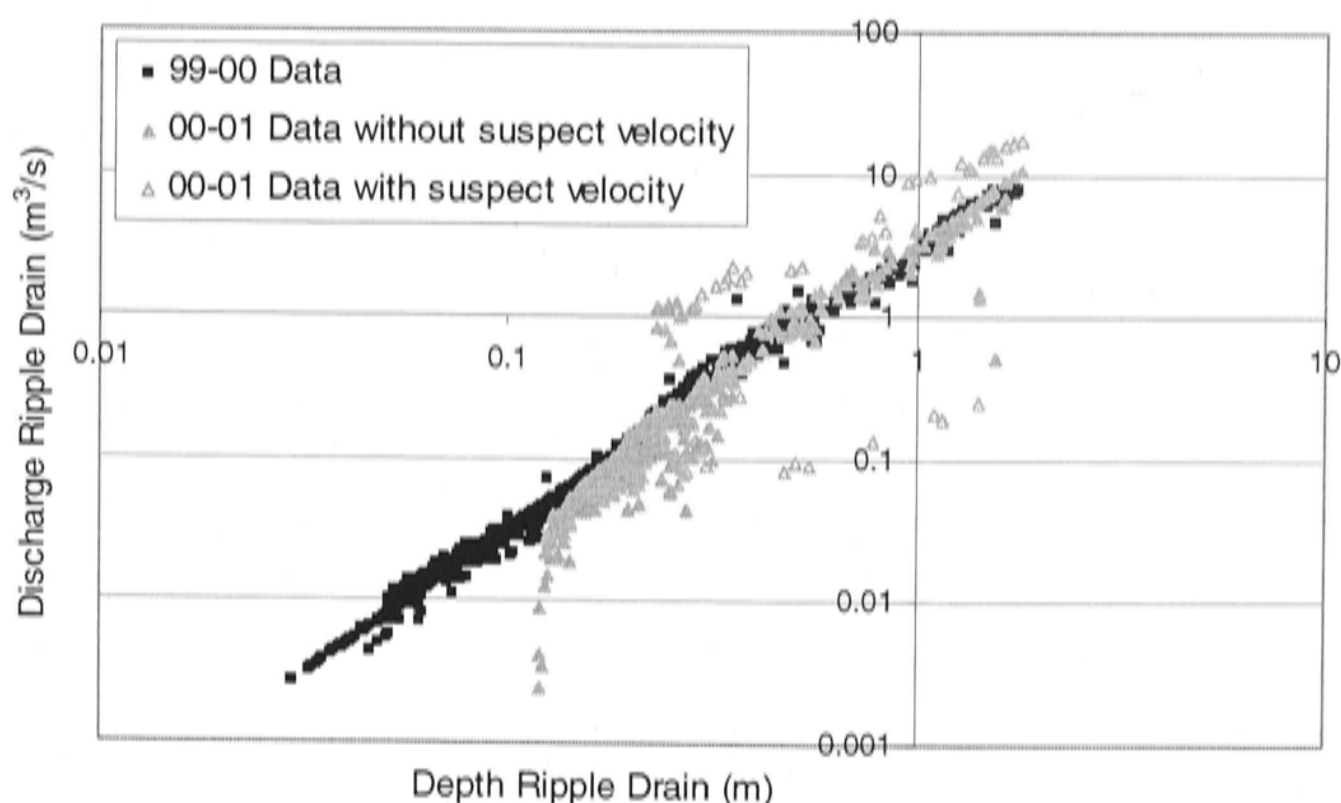


**Figure 5.12:** Scatter diagram of Ripple Drain depth versus Ripple Drain discharge for both budget seasons. 00-01 data plotted both with and without suspect data records.

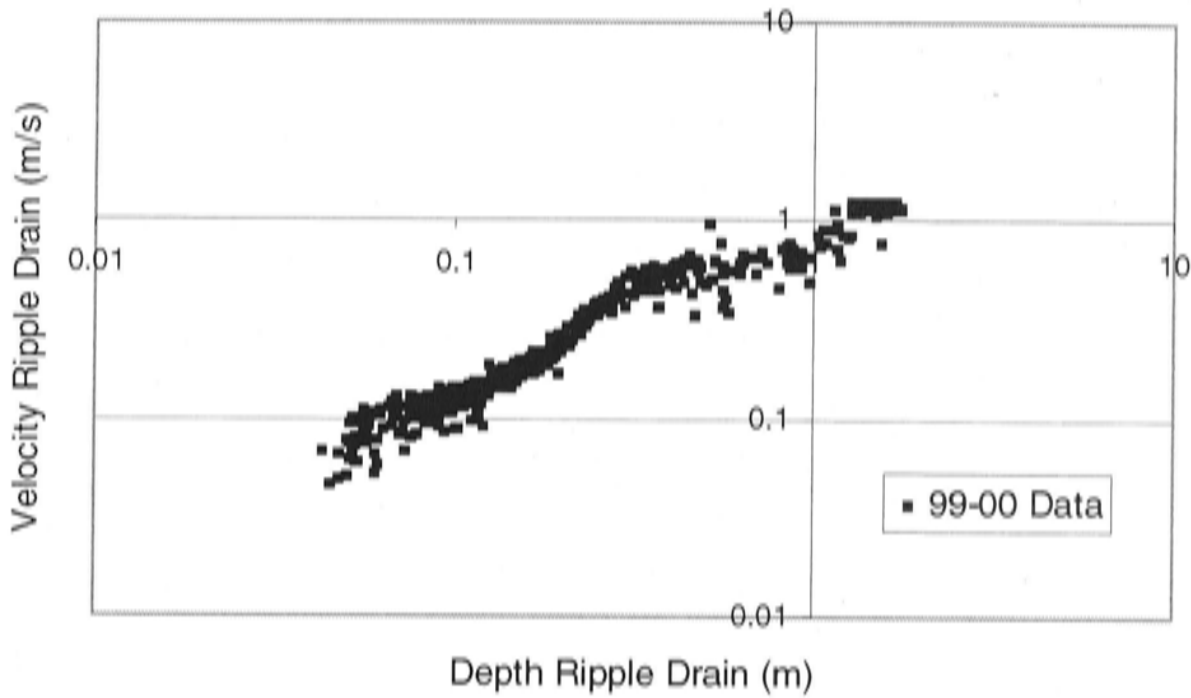


**Figure 5.13:** Scatter diagram of Ripple Drain depth versus Ripple Drain velocity for the 99-00 budget season.

Backwatering did not seem to significantly affect the relationship between depth and discharge. Some effect is however visible when the velocity data of Ripple Drain are plotted against water depth (Figure 5.13). At 0.3 m water depth in the Ripple Drain, the drain flow velocity temporarily stops increasing with water depth, probably because the drain flow is obstructed downstream by floodgates or river water.

### 5.9.2 Depth-discharge rating curve Ripple Drain 00-01

Although the 00-01 data sets for Ripple Drain are complete, a depth – discharge rating-curve is created for the 00-01 season as well. The curve is plotted in the same graph as the 99-00 curve (Figure 5.12), to enable comparison. The rating curve of the 00-01 season follows the same trend as the 99-00 curve, but there is more scatter in the data. A possible explanation for the deviant behaviour of the 00-01 discharge curve is the quality of the velocity data for this season, as was already commented on in Section 5.7. To test whether the suspicious periods in the velocity data cause the diversion in the 00-01 depth–discharge rating-curve, a third curve is plotted in the same graph. This curve shows the 00-01 data from which the suspicious records are omitted. Some of the major anomalies have disappeared in the new curve. This confirms the idea that the depth–discharge rating curve for the two seasons should be

similar. Especially in the higher depth and discharge ranges both curves follow a similar line. The deviation that is still present in the lower ranges could be the result of other, less obvious errors in the velocity or depth data.

### 5.9.3 Depth-discharge rating curve Prosser Drain 99-00

Missing velocity data in the 99-00 Prosser Drain data set can be estimated in the same way as for the Ripple Drain by creating a depth–discharge rating curve. From the data plotted in Figure 5.14 the following Depth – discharge rating curve is estimated for Prosser Drain Starflow depth:

#### Equation 5.7

$$\text{Prosser Drain discharge} = 1.0 * \text{Prosser Drain depth}^{2.0} \quad (R^2 = 0.9)$$

To test the effect of the elevation of the depth sensor, a total sediment load value has been calculated based on the original depth data plus an extra 5 centimetres to account for the difference between the drain bed surface and the sensor. A rating curve is calculated for this condition too. The depth – discharge rating curve for Prosser Drain Starflow depth accounting for 5 cm elevation of the depth sensor above the drain bed is as follows:

#### Equation 5.8

$$\text{Prosser Drain discharge} = 1.1 * \text{Prosser Drain depth}^{2.2} \quad R^2 = 0.9$$

The loads generated by these different relationships will be discussed in section 5.10. The combined presentation and discussion of all load calculations in this last section enables quick evaluation of the various data adjustments.

After fixing the minor gaps in the velocity data, one gap with a length of almost a month remains. The only other continuous data that are available over this period are rainfall and turbidity, but neither of these variables shows a clear relationship with depth or discharge. An alternative is to estimate the water depth/discharge in Prosser Drain from the Ripple Drain water depth/discharge. This possibility will be examined below.



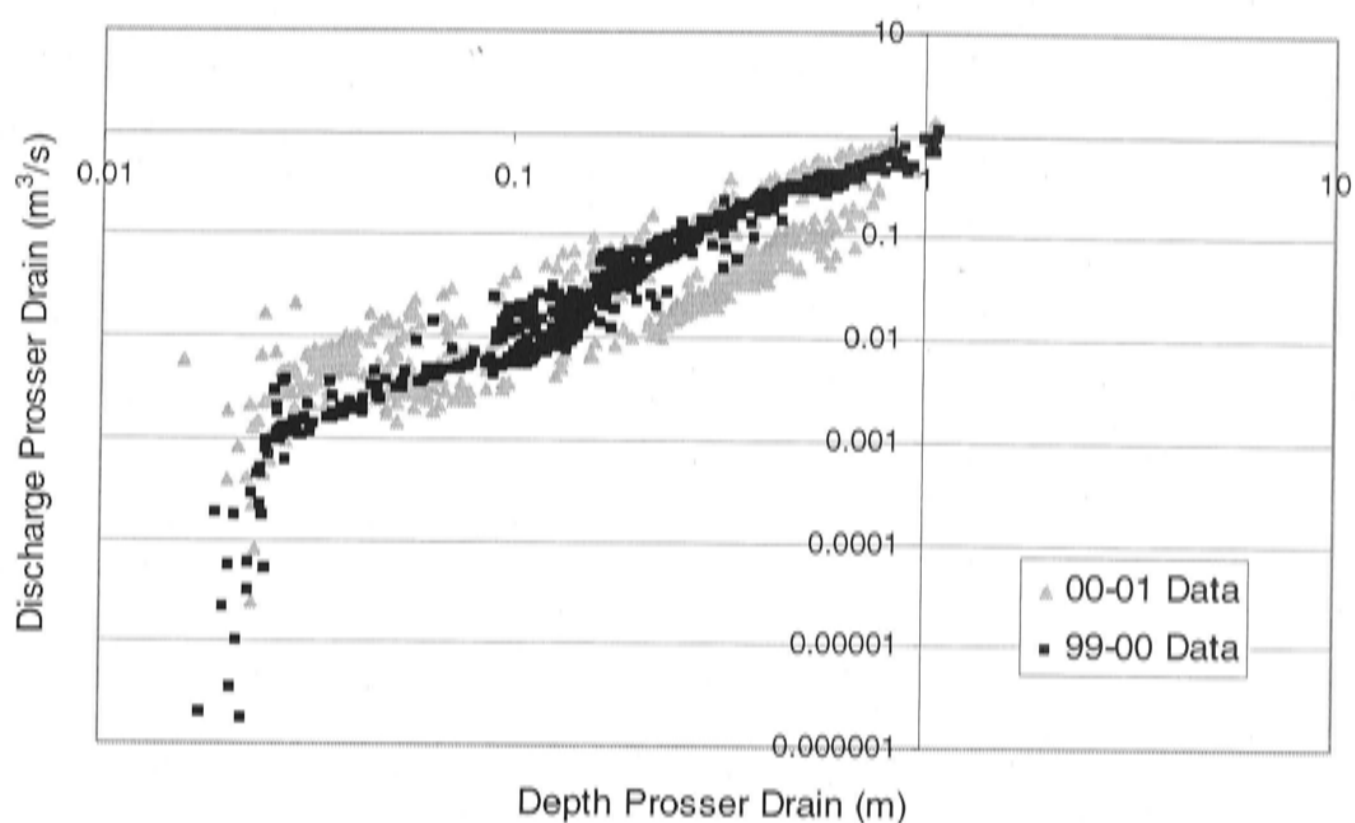


**Figure 5.14:** Scatter diagram of Prosser Drain depth versus Prosser Drain discharge for both budget seasons, unadjusted data.

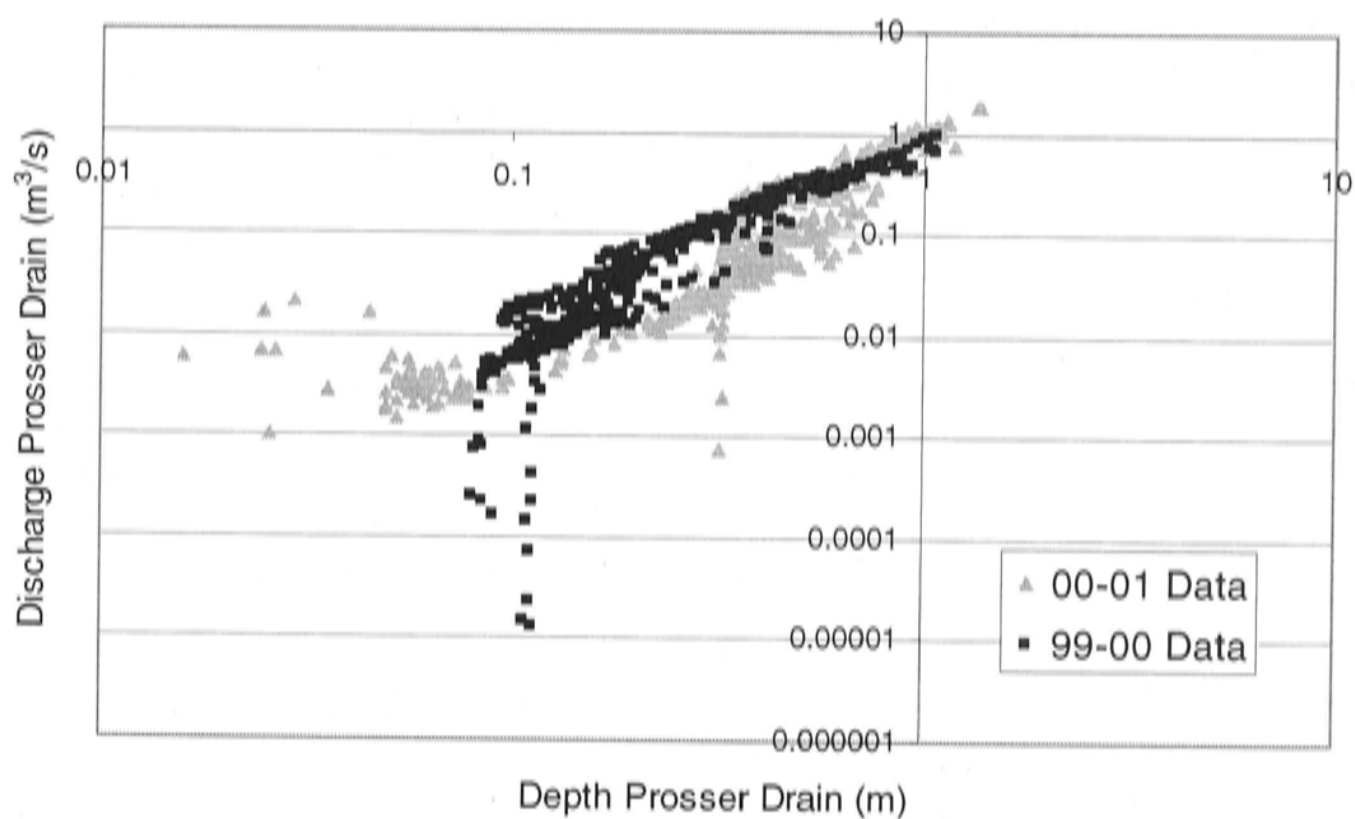


**Figure 5.15:** Scatter diagram of Prosser Drain depth versus Prosser Drain discharge for both budget seasons. Data adjusted for errors.

#### 5.9.4 Depth-discharge rating curve Prosser Drain 00-01

For both seasons of Ripple Drain data and for the 99-00 Prosser Drain data the depth – discharge rating curves were shown to provide some information on the gauging data quality. A similar rating curve is thus created to check the 00-01 Prosser Drain data. When both Prosser Drain curves are plotted in the same graph they show a

distinct difference. The trend of both curves is similar, but the 00-01 data cover a much wider range of discharge values. At a closer inspection it shows that the 00-01 curve consists of two separate sections. One section consists of data collected before 28/12/00, the other section of data collected after this date. It is not completely clear whether the split in the depth – discharge curve is caused by a change in the velocity data and/or by a change in depth data. The following section compares the available data for both drains. This will provide more insight into the origin of the errors.

The vertical tails of the Prosser Drain depth–discharge curves (Figure 5.14) cover periods of zero velocity. When the water depth above the Starflow sensor becomes too low, the sensor is not able to detect flow velocity and the velocity recordings fall to zero. This sudden fall causes the sharp change in the depth – discharge curve. For the estimation of the rating curve equations these low discharge values were discarded. The same effect is shown in the 00-01 curve for Ripple Drain (Figure 5.12).

#### **5.9.5 Comparison of Ripple and Prosser Drain data**

Since Prosser Drain is a tributary of Ripple Drain, there may be some relationship between the gauged variables. Potential relationships between the drains can help solve the problem of missing discharge data in the 99-00 season for Prosser Drain and explain the difference between the depth – discharge rating curves for both seasons. Figure 5.16 and 5.17 show how depth and velocity are related in both outlet drains, for both seasons.

The lack of relationship between both drains for velocity (Figure 5.17) might be a result of the backwatering in the system or perhaps because of unreliable data. Depth does show some relationship (Figure 5.16), but the curves for both seasons are split. This split indicates a sudden change in the Prosser Drain depth relative to the Ripple Drain data, which could be caused by a change in the position of the depth sensor.

The split in the 00-01 data corresponds with the moment of sudden change in the Prosser drain data around 28/12/00, as identified in the section above. At that date the depth suddenly decreases by approximately 30 cm. The 99-00 data are affected by two depth changes. One change of approximately 6 cm (it is not possible to reconstruct the exact change) coincides with a sudden fall in the Prosser drain hydrograph at 8/03/00 that was not previously considered of importance. The second change of approximately 3 cm is added to the previous one and starts after the

22/03/00 gap in the data. This change is undone at the end of the measuring period (6/07/00).

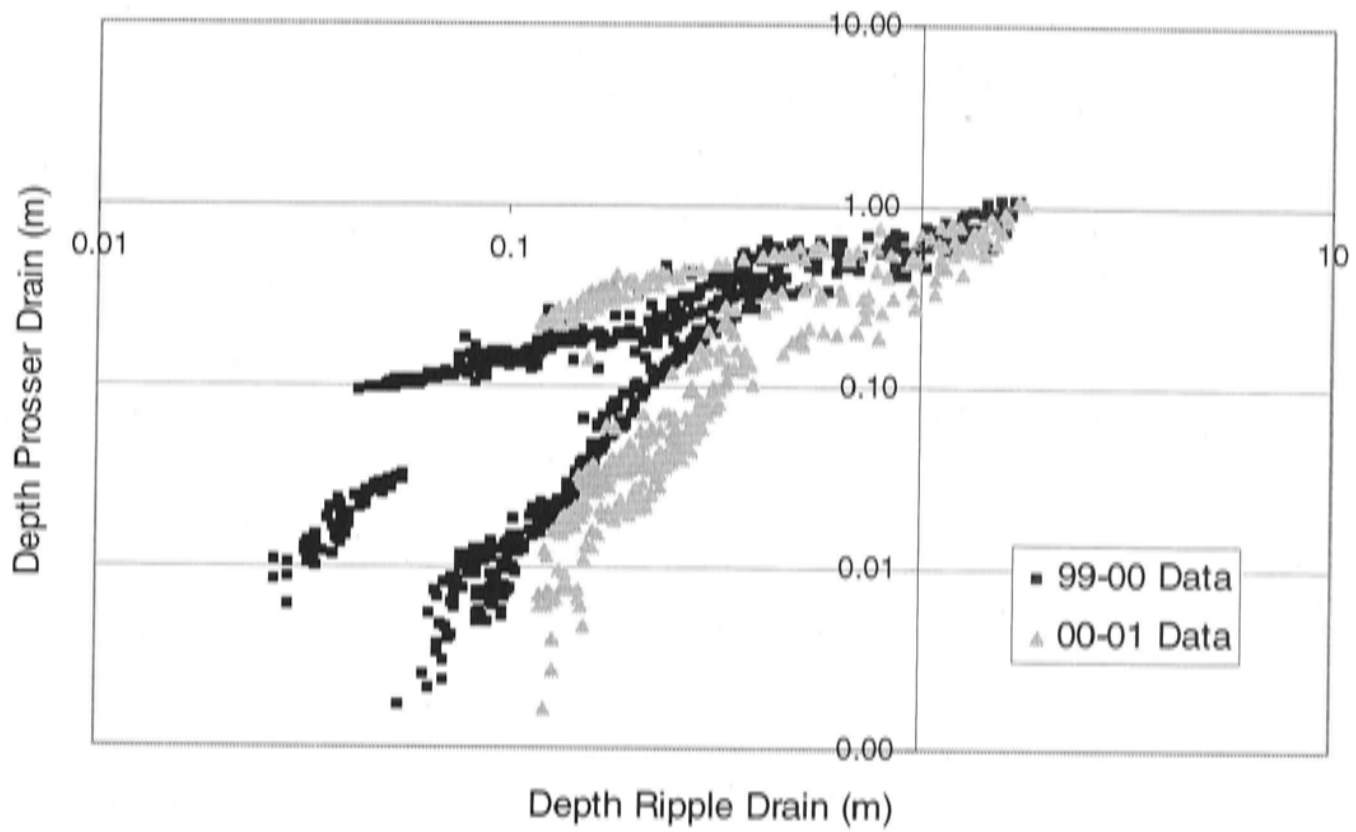


**Figure 5.16:** Scatter diagram of Ripple Drain depth versus Prosser Drain depth for both budget seasons, unadjusted data.

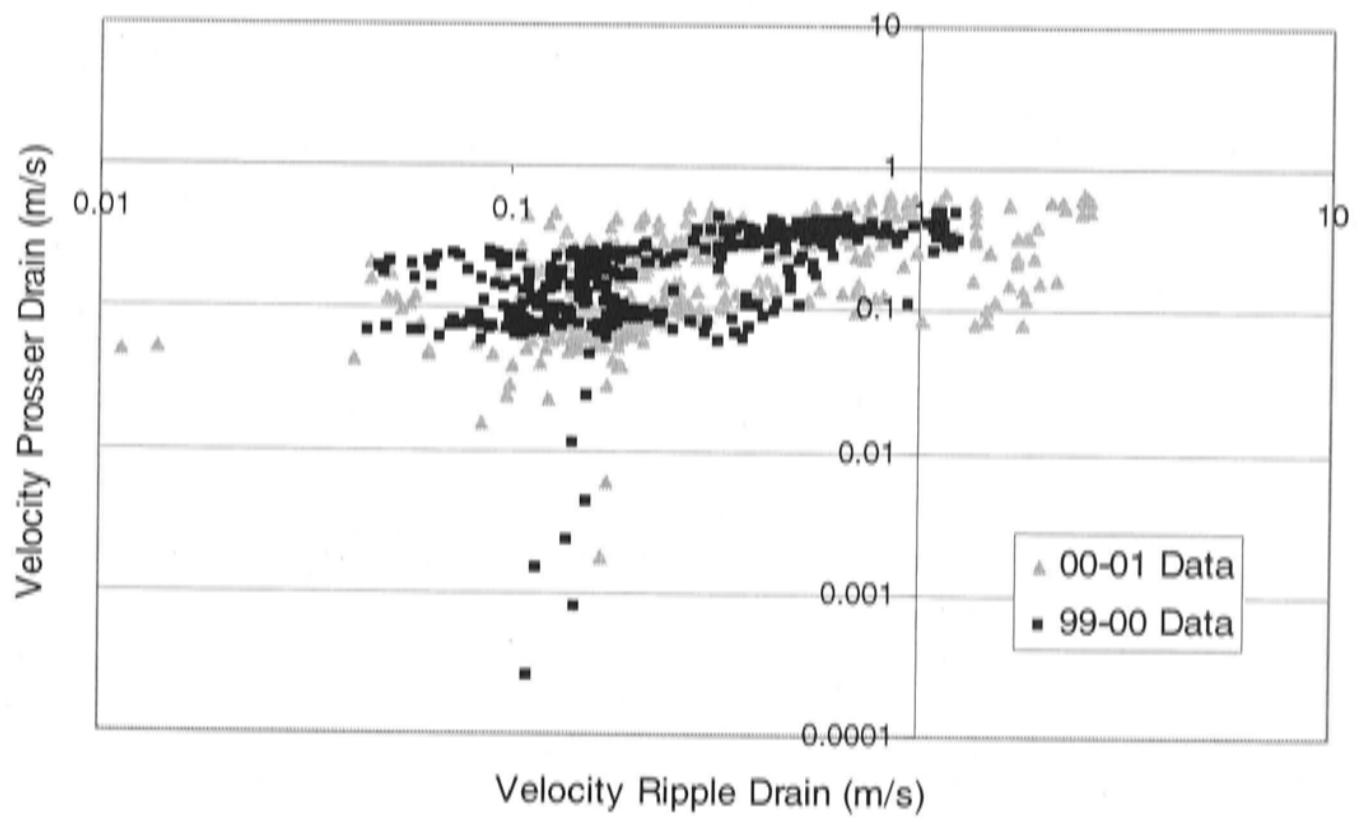


**Figure 5.17:** Scatter diagram of Ripple Drain velocity versus Prosser Drain velocity for both budget seasons.

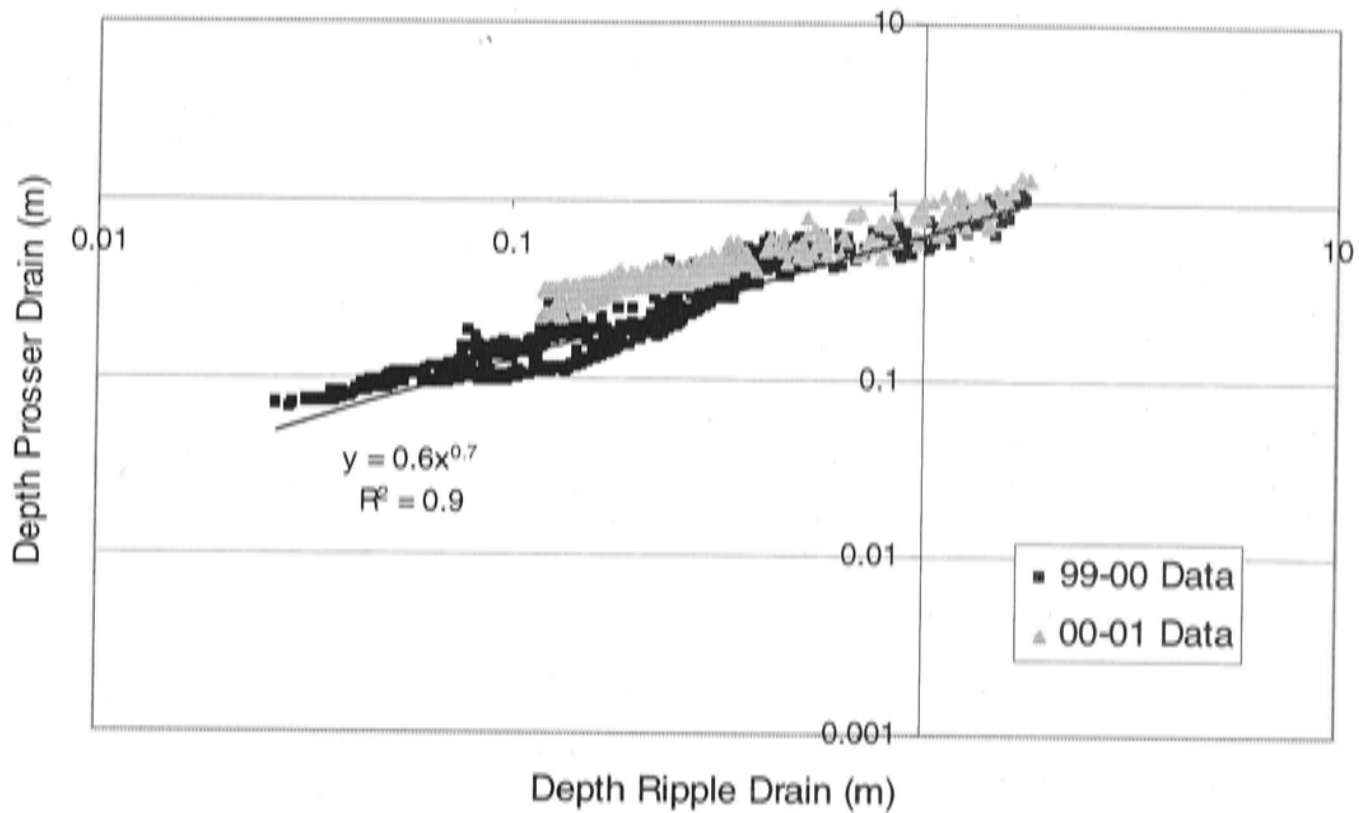


**Figure 5.18:** Scatter diagram of Ripple Drain depth versus Prosser Drain depth for both budget seasons and a regression curve for the 99-00 data. Data adjusted for errors.

After the discovery of these errors, the depth data sets have been adjusted and new discharges and averages have been calculated. Figure 5.18 shows the new relationships between the Ripple and Prosser Drain depth data. A power function now fits the data for both seasons:

**Equation 5.9**

$$\text{Depth Ripple Drain} = 0.6 * (\text{Depth Prosser Drain})^{0.7} \quad R^2 = 0.9$$

This function is used to estimate the missing Prosser Drain data.

There is some doubt about the correctness of the adjusted depth data. Figure 5.15 shows how the depth changes affected the depth - discharge rating curves for Prosser Drain. The trend in the curves is similar for both seasons, but the biggest part of the 00-01 depth-discharge curve lies lower than the 99-00 curve. The Ripple Drain – Prosser Drain curve also suggests that the Prosser Drain depth is not correct, because at low flows Prosser Drain depths are higher than Ripple Drain depths (Figure 5.16). It could be questioned whether the assumed 30 cm decrease in the second half of the 00-01 depth data actually meant that the earlier data records were too high. A 30 cm decrease in the first half of the curve would however make parts of the data negative, which is impossible. The only other explanation could be a gradual change in depth.

### **5.9.6 Missing turbidity data**

Apart from periods of missing data there is another problem with the turbidity data. Because the Greenspan sensors were not calibrated at the beginning of the 99-00 season, the settings of the sensors were not suited to record high turbidity values. The measured values go 'out of range' during periods with high turbidity. Unfortunately no significant relationship between turbidity and any of the other gauged variables was found for both the Ripple and Prosser Drain. Turbidity in Ripple Drain is not related to the turbidity in Prosser Drain and, unlike the upland creeks (see Chapter 6), turbidity in the lowland drains is not clearly related to rainfall. The lack of any relationship is probably a result of backwatering in the drainage system and the big difference in the size between the drains.

As an example the SSC and depth of Ripple Drain are plotted in a graph (Figure 5.19). The graph suggests an increase in the suspended sediment concentration with water levels up to 0.8 m. At higher water levels the sediment concentration remains relatively constant with further increase of the water depth in Ripple Drain. More comments on the relationships between velocity, discharge and SSC will be given in Chapter 13.

Ripple Drain turbidity data do not contain any significant gaps. The 99-00 data have periods of 'out of range' values, but they only occur for a significant amount of time during a low flow period between 4/01/00 and 5/01/01, not during high flow events. Under high flow conditions turbidity values are relatively low probably due to dilution, backwatering and/or source depletion. The problem of the 'out of range' values is therefore not thought to cause a significant reduction of the total calculated sediment load for this season.

The 99-00 Prosser Drain data contain one major gap, and 'out of range' values occur under peak flow conditions. The exact behaviour of sediment concentrations during peak flows is therefore not known for the 99-00 season. Comparison with the turbidity/flow peaks of the following season is not possible because of the poor quality of the 00-01 data. This means that only some indication of the sediment load for the 99-00 season exists, which can only be corrected roughly for the missing information. The data from 00-01 are useless and no possibility exists to replace them.

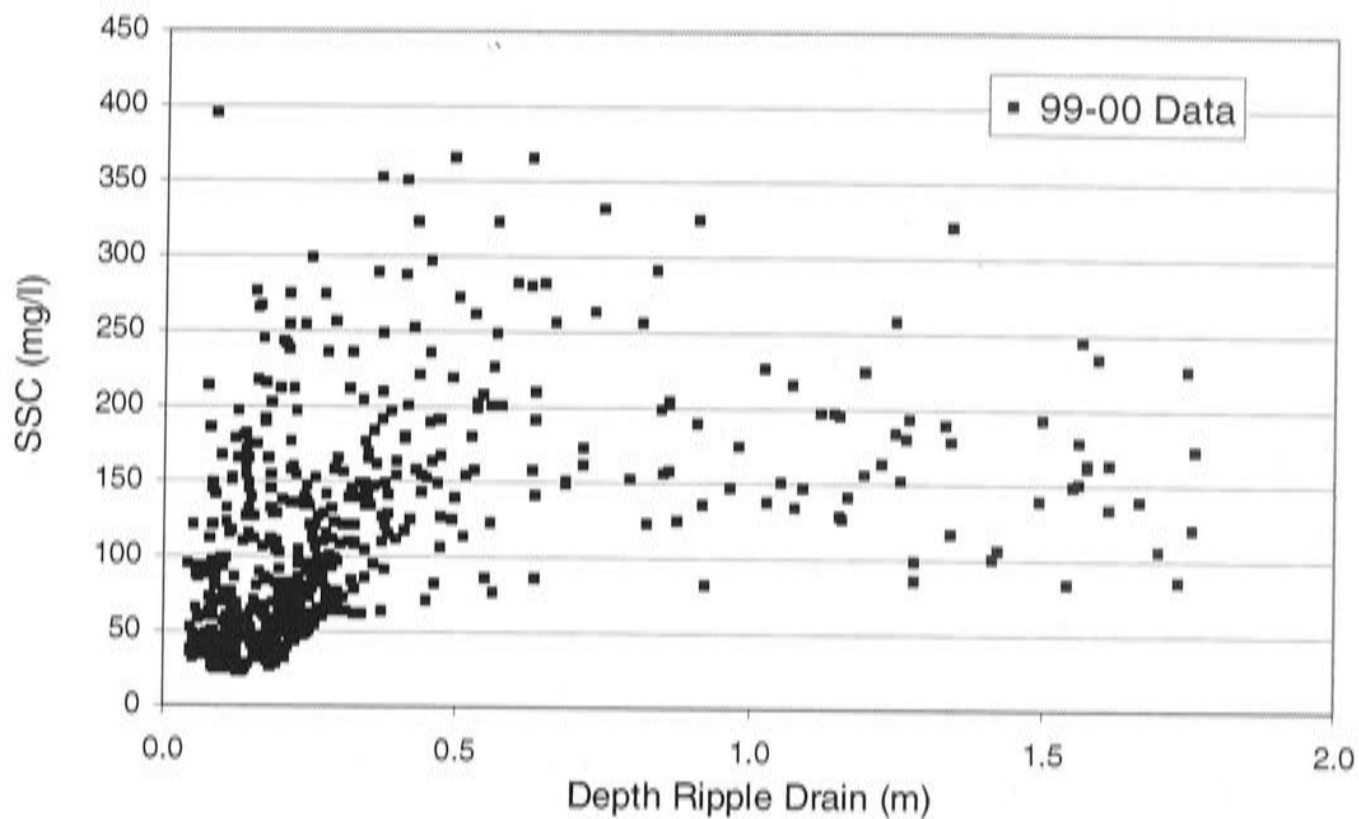


**Figure 5.19:** Scatter diagram of 99-00 Ripple Drain depth versus SSC.

## 5.10 Load calculations

The transformed, substituted and averaged data will now be used to calculate total sediment loads, total discharges and runoff coefficients for each drain and each season. Total loads are calculated by multiplying the discharge with the SSC for each 6-hourly interval and summing these for the whole season. For each season several different loads are calculated to compare the effects of the various data adjustments and transformations. The total discharges and runoff coefficients are used to assess the reliability of the data.

### 5.10.1 Ripple Drain load calculations

Table 5.13 lists all estimates of the Ripple Drain 99-00 sediment load and water discharge. Load calculation 1 is based on all available depth and velocity data. Periods of missing data are not included. In calculation 2 the missing discharge data are estimated from the depth – discharge rating curve (Equation 5.6). In calculation 3 remaining gaps in the turbidity data are linearly interpolated. The difference between calculation 2 and 3 is relatively small so the gap in the turbidity data has little effect on the total sediment load. Calculation 3 is expected to be the best estimate of water discharge and sediment output through the Ripple Drain over the 99-00 budget period.

**Table 5.13:** Load calculations for the 99-00 Ripple Drain data. Best estimate is shaded.

<b>Ripple Drain 99-00 season</b> Discharge and sediment load calculated from:	Unit area sediment load* (t ha <sup>-1</sup> )	Sediment load (t)	Runoff coefficient	Total discharge (10 <sup>6</sup> m <sup>3</sup> )
1. All available depth, velocity and turbidity data	3.8	1226	0.6	7.3
2. Depth and depth – discharge rating curve	4.7	1509	0.8	9.5
3. Linear interpolation of the turbidity data	4.9	1580	0.8	9.5
Total rainfall (x10 <sup>6</sup> m <sup>3</sup> ) = 11.7				

\* Sediment load per unit area cane land = Sediment load (tonnes) minus 269 t of sediment originating from forested upland

Sediment load and water discharge for the 00-01 season are listed in Table 5.14. Calculation 1 is based on all available depth and velocity data. Periods of missing data are not included. SSC is calculated directly from the Greenspan records with Equation 5.4. Calculation 2 is done in the same way, but periods with suspect velocity data are excluded. This significantly reduces the discharge at Ripple Drain outlet. For calculation 3, SSC is estimated with a regression equation based only on water sample data from the 00-01 season (Figure 5.1). This makes little difference to

**Table 5.14:** Load calculations for the 00-01 Ripple Drain data. Best estimate is shaded.

<b>Ripple Drain 00-01 season</b> Discharge and sediment load calculated from:	Unit area sediment load (t ha <sup>-1</sup> )	Sediment load (t)	Runoff coefficient	Total discharge (10 <sup>6</sup> m <sup>3</sup> )
1. All available data; Turbidity – SSC regression based on all SSC data; original Greenspan records	6.5	2080	1.1	9.3
2. Suspect velocity data excluded; Turbidity – SSC regression based on all SSC data; original Greenspan records	3.7	1184	0.5	4.1
3. Suspect velocity data excluded; Turbidity – SSC regression based on just 00-01 SSC data; original Greenspan records	3.5	1120	0.5	4.1
4. Suspect velocity data excluded; Turbidity – SSC regression based on all SSC data; Greenspan records adjusted	2.3	736	0.5	4.1
5. Greenspan records adjusted; All discharge data calculated with the 99-00 depth – discharge rating curve	3.8	1216	0.9	7.5
6. Greenspan records adjusted; Only suspect velocity data replaced with discharge based on 99-00 rating curve	3.5	1120	0.8	7.0
Total rainfall (10 <sup>6</sup> m <sup>3</sup> ) = 8.8				

the total sediment load. In calculation 4 the Greenspan data are transformed with Equation 5.4 before the SSC is calculated. This significantly reduces the sediment load estimate. For calculation 5 all discharge is estimated from the depth data with the 99-00 Ripple Drain depth – discharge rating curve. The best estimate for the 00-01 sediment load is given by calculation 6, which consists of calculation 4 combined with estimates for the missing data based on the 99-00 Ripple Drain depth – discharge rating curve.

The fact that the runoff coefficients for both seasons are equal gives some confirmation that the discharge estimates are correct, although it is no proof. For some missing Ripple Drain data no replacement was found and therefore can not be included in the final load calculations:

- All data from the last month of the 00-01 budget period is missing. Some rain fell during this period, but no major events occurred. The error for the total sediment load is expected to be less than 10%.
- Some of the 99-00 turbidity data go 'out of range', but this occurs under low flow conditions so the effect of the underestimated sediment concentrations is insignificant for the sediment load.

#### **5.10.2 Prosser Drain load calculations**

The 99-00 sediment load and water discharge calculations for Prosser Drain are listed in Table 5.15. Calculation 1 is based on all available depth, velocity and turbidity data. For calculation 2 the depth data are adjusted by 5 cm to assess the possible error as a result of the elevation of the sensor above the drain bed. Apparently it can cause an error of approximately 15%. In the further calculations the sensor is assumed to be level with the drain bed. In calculation 3, depth is adjusted for the displacement of the sensor as proposed in Section 5.9.5. This adjustment has little effect on the total load. For load calculation 4 the gap in depth data between 22 March and 18 April 2000 has been filled with data based on the Ripple Drain depth values, using Equation 5.9. This significantly increases the sediment load and discharge values. This calculation is thought to best represent the output through Prosser Drain over the 99-00 budget period. Load 5 shows the considerable effect that misrepresentation of the velocity could have on the sediment



load estimate. For this calculation flow velocity is assumed to be 0.7 times the measured velocity.

**Table 5.15:** Load calculations for the 99-00 Prosser Drain data. Best estimate is shaded.

<b>Prosser Drain 99-00 season</b> Discharge and sediment load calculated from:	Unit area sediment load (t ha <sup>-1</sup> )	Sediment load (t)	Runoff coefficient	Total discharge (10 <sup>6</sup> m <sup>3</sup> )
1. All available depth, velocity and turbidity data	3.1	143	1.5	1.3
2. Depth + 0.05 m and velocity, gaps filled	3.6	166	1.7	1.5
3. Depth adjusted for two jumps and velocity, gaps filled	3.2	147	1.5	1.3
4. Depth gap filled based on Ripple data	3.7	170	1.6	1.6
5. Depth gap filled based on Ripple data; velocity x 0.7 to account possible overestimate	2.6	119	1.1	1.1
Total rainfall (10 <sup>6</sup> m <sup>3</sup> ) = 1.0 (0.9 with open gap)				

All 99-00 calculations result in discharges that are at least 1.6 times higher than the rainfall in the catchment, which is not possible. There are several possible explanations for the high runoff coefficients. The discharge might be overestimated due to errors in depth and/or velocity values. If the discharge is overestimated this means that the true sediment load from the Prosser Drain will be lower. Another possibility is underestimation of the rainfall. As a result of its proximity to the mountains the Prosser Drain catchment is likely to receive more rainfall than that measured at Palmas' site. Finally the catchment boundary might not be correctly delineated and additional discharge might be derived from outside what is thought to be the catchment boundary. During field visits under extreme flood conditions it was observed how water from the Ripple Drain diverted into the Prosser Drain.

**Table 5.16:** load calculations for the 00-01 Prosser Drain data. Best estimate is shaded.

<b>Prosser Drain 00-01 season</b> Discharge and sediment load calculated from:	Unit area sediment load (t ha <sup>-1</sup> )	Sediment load (t)	Runoff coefficient	Total discharge (10 <sup>6</sup> m <sup>3</sup> )
1. Original depth and velocity data			1.0	0.8
2. Depth + 0.05 m and velocity			1.2	0.9
3. Depth corrected for jump and velocity			2.3	1.7
4. Original depth and 99-00 PD rating curve			1.0	0.8
5. Corrected depth and 99-00 PD rating curve			2.9	2.2
Total rainfall (10 <sup>6</sup> m <sup>3</sup> ) = 0.7				

For the 00-01 season sediment loads can not be calculated for Prosser Drain, because the turbidity data are unreliable. Water discharges are listed in Table 5.16.

Calculation 1 is based on all available depth and velocity data. For calculation 2 the depth is increased with 5 cm to assess the effect of the raised depth sensor. This results in a maximum error of 20%. In calculation 3 the depth is adjusted for the jump in the depth data. This significantly increases the discharge. In calculation 4 and 5 discharge is estimated from the corrected and uncorrected depth with the 99-00 Prosser Drain depth – discharge rating curve (Equation 5.7).

The calculations with adjusted depth data result in extremely high runoff coefficients, indicating that the depth adjustment is not correct. The high baseflow depths of the Prosser Drain depth curve and the difference between the Prosser Drain – Ripple Drain relationships for each budget season already suggested this. It is not possible to reconstruct what went wrong with the depth data in the 99-00 season.

The following data are still missing in the Prosser Drain data sets:

- No substitute has been found for the missing turbidity data between 10 and 23 March 2000. The missing load is expected to be significant (error >10%).
- Due to 'out of range' values for the 99-00 season in the Prosser Drain turbidity data, sediment concentrations during peak flows were underestimated. It is hard to quantify the importance of this error, because there is no information available on the behaviour of sediment concentrations during peak flows.
- Turbidity data of the 00-01 season is unreliable for calculation of SSC.

### 5.10.3 Summary of the load calculations and implications for the sediment budget

Table 5.17 gives a summary of the best estimates of the load and discharge values for each season and each outlet drain.

**Table 5.17:** Summary of best estimates of sediment load, discharge values and runoff coefficients.

	Ripple Drain		Prosser Drain	
	99-00	00-01	99-00	00-01
Total Discharge ( $10^6 \text{ m}^3$ )	9.5	7.0	1.6	1.7
Total Rainfall ( $10^6 \text{ m}^3$ )	11.7	8.8	0.9	0.7
Runoff Coefficient	0.8	0.8	1.6	2.3
Sediment load (t)	1580	1120	170	-
Sediment load ( $\text{t ha}^{-1}$ )	4.9	3.5	3.7	-

The sediment load data from the Prosser Drain are insufficiently accurate for the sediment budget study. The 5 cm elevation of the depth sensor above the drain bed

could cause a more than 10% error in the final sediment load and there are obviously more factors that cause even larger errors.

Prosser Drain drains a separate catchment that can be subdivided from the Ripple Corner Catchment. The budget study can then be restricted to only the 'Ripple Drain catchment'. When this is done there is a possibility of errors due to diversion of water between the Prosser and Ripple Drain under flood conditions. However, the total discharge through Prosser Drain is 17% of the Ripple Drain discharge and the total sediment load is little more than 10%. Less than half of this is expected to be derived from Ripple Drain. Reduction of the sediment load at the Ripple Drain outlet due to diversion will therefore be insignificant.

---

## **Chapter 6**

### **Upland input**

---

#### **6.1 Introduction**

Suspended sediment in runoff from the forested upland becomes an input component of the sediment budget as pointed out in Chapter 4. Within the budget area there are nine points along the foot of Mt Hawkins where drainage water enters the alluvial plain in distinct channels. The total amount of sediments added to the Ripple Drain drainage system from these streams is assumed to represent the upland input. The amount of sediment that enters the cultivated lowland via overland flow is assumed to be insignificant for the budget, since the mountain slopes are well vegetated.

The most reliable way to estimate total sediment input from the forested upland into the floodplain drainage system would be through continuous monitoring of the sediment discharge from all input streams. For practical reasons this is not possible. Instead only one of the streams is instrumented and the data from this stream are extrapolated to obtain the sediment input from the remaining upland area.

The stream gauging site was not equipped with a velocity meter that provides continuous data like the gauging sites in Ripple and Prosser Drain at the catchment outlet. Water discharge data have been estimated from a depth – discharge rating curve, which was obtained from velocity profiles measured at the site. Since the gauged creek drains the steep slopes of Mt Hawkins, its flow is not expected to be influenced by backwater processes and there should be no difficulty in establishing a rating curve. Sediment concentrations are estimated from a turbidity – SSC relationship.

#### **6.2 Gauging location and equipment**

Only two creeks drain most of the upland area, and both are suitable for gauging. Both creeks have a catchment area of similar size. Of the two creeks 'Post Creek' is chosen for observation, because this creek is most accessible under flood conditions.

The gauging station is situated at the distinct transition between hillslopes and alluvial plain. The vegetation on the west (right) bank of the drain changes at this point from forest to sugarcane. On the east bank the forest continues for another 100 m, and the creek retains its natural sinuous course. At the point where the vegetation changes to sugarcane the channel is a straight man-made drain. The exact location of the gauging station is indicated on the map in Figure 4.1

Post Creek flow depth is gauged with a pressure transducer and Dataflow data logger, and turbidity is recorded by a Greenspan turbidity meter similar to that at the gauging sites described previously. At the gauging site the creek is about 8 m wide and 2 m deep with very steep banks and an approximately 2.5 m wide sandy bed. The gauging equipment was placed in the stream channel several cm above the stream bed at 2 m distance from a reference point on the west bank of the creek. The pressure transducer was located in a perforated PVC pipe. The pipe was fixed to an overhanging tree. The Greenspan turbidity meter was fixed to a tree root nearby. Figure 6.1 shows the profile of the creek cross-section, as measured with a Dumpy level in between fixed reference points on each bank. It also shows the location of the gauging instrumentation.

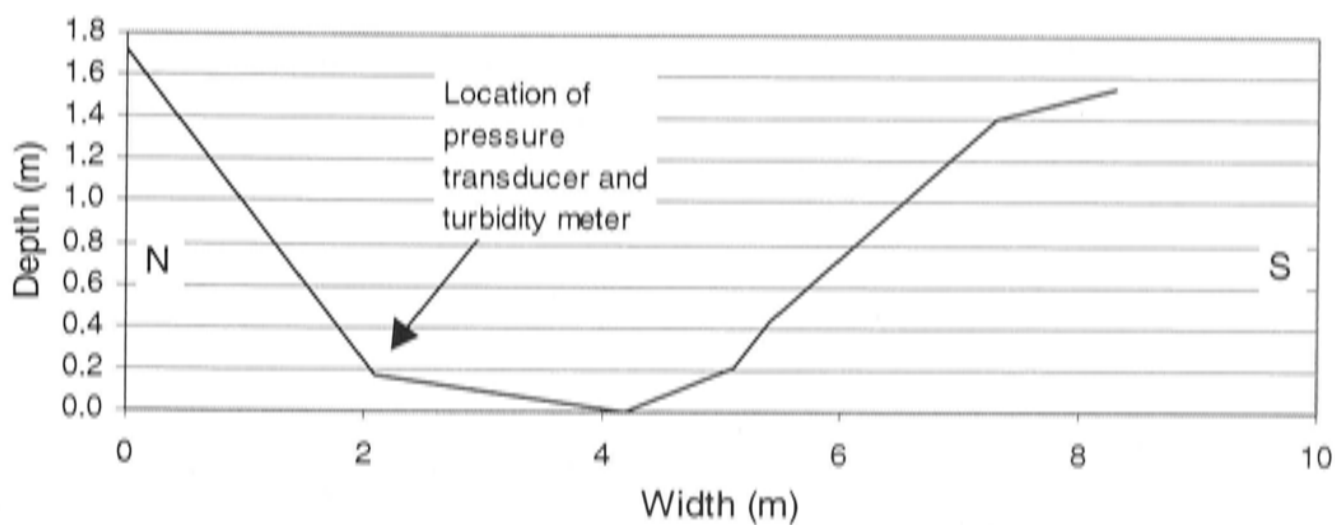


**Figure 6.1:** Profile of cross-section through Post Creek at gauging site (December 2000).

### 6.3 Raw data Post Creek

The gauging station in Post Creek was operational during both budget seasons. Appendix C shows the availability of the data for each season and Appendices F (7 and 8) show the hydrographs for each season.

### 6.3.1 1999-2000 data

During the first wet-season water depth in Post Creek was logged every 5 minutes between 3/12/99 23:00 and 12/05/00 13:19. The data from the first season contain many gaps due to malfunctioning of the data logger. Table 6.1 lists the availability of the depth data.

**Table 6.1:** Data availability Post Creek 1999-2000.

99-00 Post Creek Depth data		99-00 Post Creek Turbidity data	
Start	End	End	Start
21/12/99 13:50	5/01/00 13:25	5/01/00 13:30	16/03/00 21:45
6/01/00 13:35	31/01/00 10:45	22/03/00 12:00	12/05/00 12:45
31/01/00 13:50	15/02/00 15:10		
8/03/00 11:33	22/03/00 11:34		
6/04/00 10:40	12/05/00 13:19		

The turbidity data for the same season starts at 5/01/00 13:30 and ends at 12/05/00 12:45. Data were logged every 30 minutes. There is only one major gap in these data (Table 6.1). Five times during the season the turbidity data logger took a 15-minute time step, instead of a 30-minute step. There is no explanation for these incidents and they do not seem to significantly affect the correspondence between the turbidity and rainfall peaks throughout the season (after adjustment of the major data gap, as described in the next section).

### 6.3.2 Gap filling 1999-2000 data

The original flow depth and turbidity curves show a discrepancy between 31/01/00 13:50 and 15/02/00 15:10. Over this period turbidity peaks about three hours before water depth peaks and rainfall. Later data do not show a similar delay between peaks. The most probable explanation for the discrepancy is a jump in the depth data timestamps. The missing data between 31/01/00 10:45 and 31/01/00 13:50 approximately covers the three hours delay between depth and turbidity maxima. When the timestamps for depth are adjusted by three hours, the turbidity peaks correspond with water depth peaks.

Data gaps of less than one day or with insignificant amounts of rain were filled by linear interpolation of existing data. The coverage of the remaining data gaps is discussed later in this chapter (see Section 6.5.2 and 0).

### **6.3.3 2000-2001 data**

During the 2000-2001 wet-season, depth data were recorded every 5 minutes from 12/11/2000 10:20 to 22/03/01 9:45. Turbidity measurements were taken every 15 minutes between 12/11/00 10:30 and 22/03/01 9:45. There are no major gaps in the data sets for this season. A number of gaps of less than an hour length were filled by linearly interpolating the adjacent data, and some double timestamps and 'out of range' values were removed.

### **6.3.4 Raw data appearance**

The available depth and turbidity data are plotted in Appendices F (7 and 8). The depth data for both seasons show some anomalies that may need to be considered in further analysis:

- The baseflow level of the last part of 99-00 depth curve is approximately 5 cm lower than that of the first part of the curve. Furthermore the depth data for this season appear to be reliable.
- The first 10 days of the 00-01 hydrograph appear to be similar to the 99-00 hydrograph, but after 23/11/00 the diurnal variation in the depth data becomes much more pronounced and the baseflow suddenly increases by approximately 8 cm
- Base flow increases towards the end of the 00-01 season
- Some flow peaks (e.g. 8/12/00 – 14/12/00) do not coincide with rainfall peaks.
- In general the 00-01 data are unreliable and are expected to affect the load calculations that are presented in this chapter.

## **6.4 Depth data adjustment**

In the 1999-2000 wet-season five manual water depth measurements were taken. Only two of the measurements can be used to relate the Dataflow data records to true flow depth in Post Creek (Table 6.2). For the other depth measurements corresponding Dataflow records are missing, due to failure of the data loggers. In the 2000-2001 season only two measurements were taken. The difference between manual depth and Dataflow depth varies considerably between each measurement

date. To solve this problem the values can either be averaged per season or applied separately to different parts of the depth curve.

**Table 6.2:** Post Creek manual depth measurements and corresponding Dataflow records.

Season	Date	Manual depth (m)	Dataflow depth (m)	Difference	Average
1999-2000	10/02/00	0.33	0.14	0.19	0.22
	17/03/00	0.64	0.40	0.24	
2000-2001	3/01/01	0.24	0.17	0.07	0.00
	26/02/01	0.27	0.33	-0.06	

The strong decrease in base flow depth in the last months of the 99-00 observations suggests that different adjustments might be necessary for different parts of the curve. New depth data are calculated with both the average depth adjustment and separate adjustments for parts of the curve. When the calibrated data are related to the Prosser Drain depth data it appears that separate adjustments are more appropriate (Figure 6.2). Depth adjusted with the average value results in a greater scatter, which suggests that this method partly overestimates and partly underestimates the data.

For the 00-01 data there is no clear point in the depth curve where a sudden change in depth could have occurred. The only possibility in this case is to apply the average depth difference. The 00-01 relationship with Prosser Drain depth is plotted in Figure 6.2. The scatter is slightly lower than the 99-00 curve. This suggests that some of the data from either Post Creek or Prosser Drain are still not properly corrected.

## 6.5 Discharge estimation

### 6.5.1 Depth – Discharge rating curve

Discharge in Post Creek is estimated from the adjusted depth data and a depth – discharge rating curve. The rating curve is based on a number of single discharge estimates, which are obtained from manual flow velocity measurements and creek cross-sectional areas.

Although accessibility was taken into consideration when choosing the upland-input monitoring site, it was still a problem to reach the site during flood events. The number of velocity measurements is therefore small (4) and covers only a limited



range of flow conditions. Appendix E lists all velocity data that are available for the Post Creek gauging station.

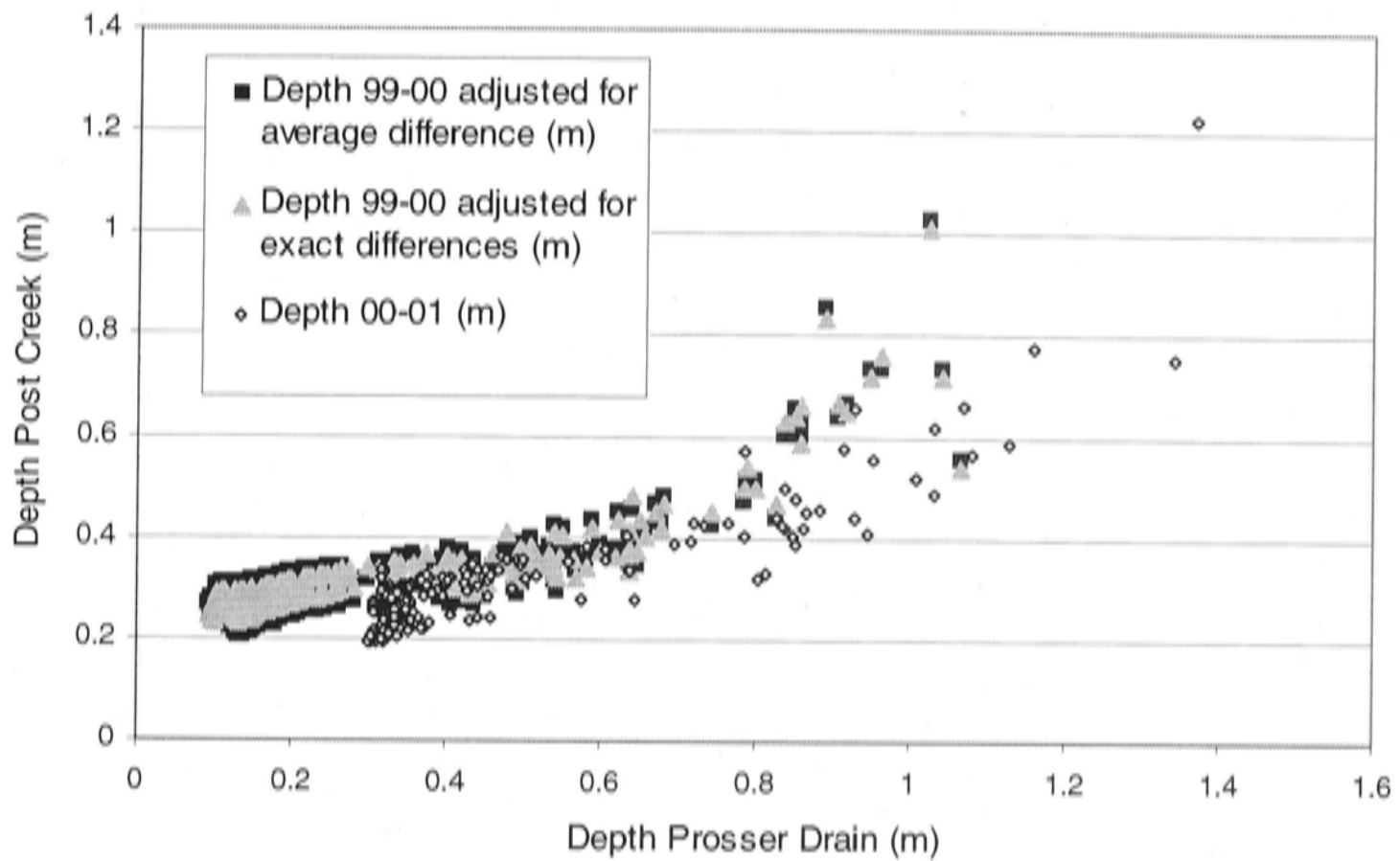


**Figure 6.2:** Relationship between Prosser Drain depth and Post Creek depth data for both budget seasons, and different Post Creek depth adjustments.

For three of the four velocity estimates, the creek cross-section is divided into several segments. In each segment velocity is measured separately. Because depth estimates for individual segments are unavailable at most sample dates, it is not possible to calculate separate discharges for each segment. Instead the measurements are averaged and assumed constant across the whole creek cross section. Wet cross-sectional areas are estimated from the adjusted Dataflow depth and the creek profile in the same way as for the outlet drains (see Section 5.6). The resulting discharges are listed in Table 6.3.

**Table 6.3:** Discharge estimates for Post Creek based on manual velocity profiles.

Date	Number of measurements	Dataflow depth (m)	Adjusted depth (m)	Wet creek cross-section (m <sup>2</sup> )	Average velocity (m s <sup>-1</sup> )	Discharge (m <sup>3</sup> s <sup>-1</sup> )
18/02/00	1	0.17	0.41	1.01	0.65	0.65
8/03/00	7	0.05	0.29	0.60	0.16	0.10
17/03/00	5	0.28	0.52	1.44	0.42	0.60
3/01/01	3	0.17	0.17	0.29	0.20	0.06

Figure 6.3 shows the Post Creek depth – discharge rating curve. The regression equation for the curve is used to estimate continuous discharge from the true depth data records. Although the regression is not significant ( $P = 0.08$ ), it is accepted, because it provides the only means to calculate Post Creek discharge.

**Equation 6.1**

$$\text{Discharge Post Creek} = 3.4 * (\text{Water depth})^{2.4} \quad (R^2 = 0.9)$$

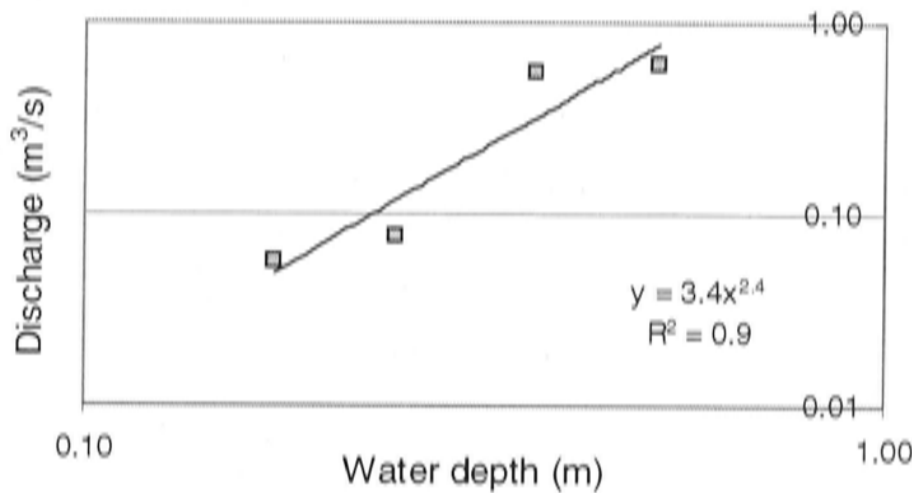


**Figure 6.3:** Post Creek depth – discharge rating curve ( $n=4$ ,  $P=0.08$ ).

### 6.5.2 Missing discharge data substitution

Considerable parts of the 99-00 depth data are missing and thus can not be used to estimate discharge. Other available data have been investigated to find methods for discharge data substitution. For this purpose data are averaged over 6-hourly periods, as was done for the study of the outlet drains. The missing 99-00 data are directly substituted by discharge values estimated from the regression curve for discharge and rainfall (Figure 6.4). A polynomial function is fitted though the curve (Equation 6.2). Data from the 00-01 season, which are plotted in the same graph, do not follow the same curve. This might be due to the strange behaviour of the 00-01 depth data.

**Equation 6.2**

$$\text{Post Creek Discharge} = 0.01 * (\text{Rainfall})^2 + 0.08 * (\text{Rainfall}) + 0.2 \quad (R^2 = 0.8)$$

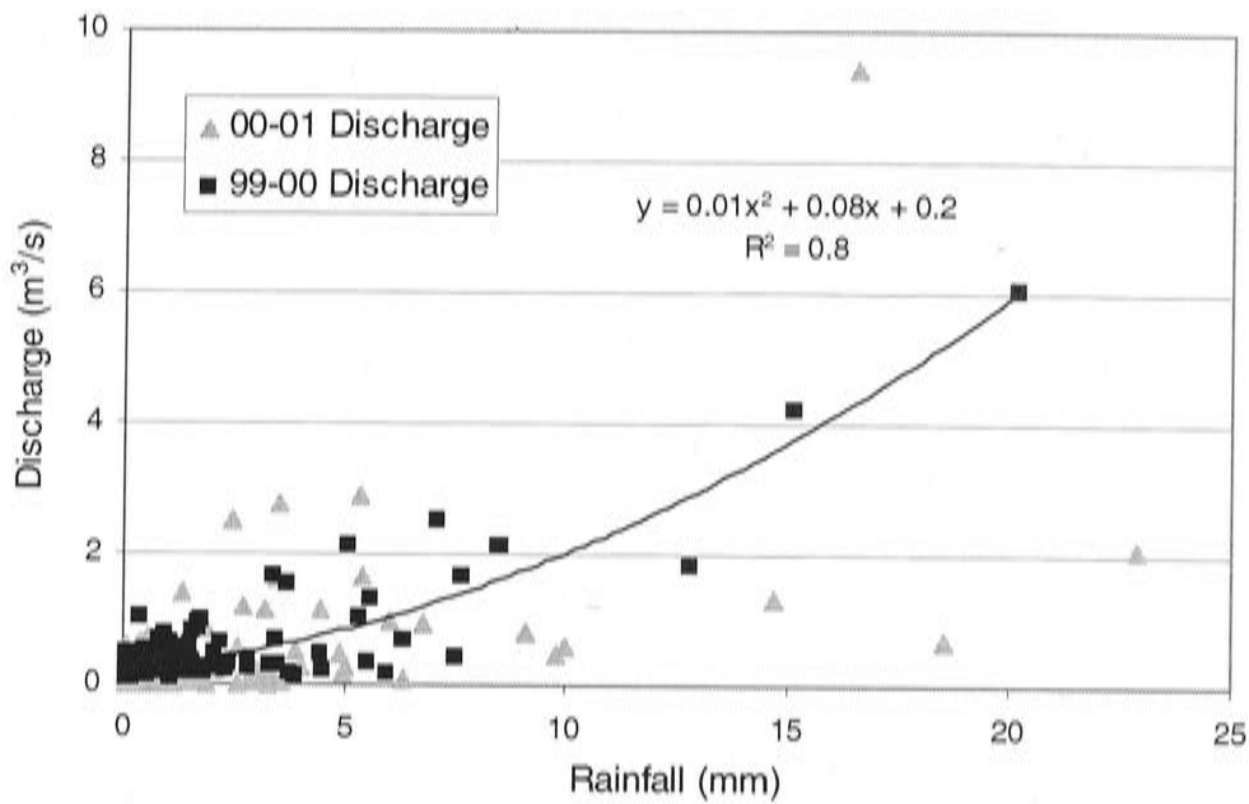


**Figure 6.4:** Scatter diagram Rainfall versus Post Creek Discharge for both budget seasons ( $n=196$ ,  $P<0.01$ ).

## 6.6 Sediment concentration estimation

### 6.6.1 SSC estimation

The SSC in the Post Creek discharge can be estimated from the turbidity in the same way as was done for the outlet drains in Chapter 5. The water of the Post Creek is however much less turbid than the water in the lowland drains. When water samples taken from the creek are plotted in a turbidity – SSC curve together with samples from the lowland part of the catchment, they occupy only the lowest sediment concentration ranges (Figure 6.5). When the samples from Post Creek are plotted as a separate turbidity – SSC graph, the relationship between the variables is less clear and results in a rather different regression curve, which has a low significance ( $P = 0.09$ , see Figure 6.6):

#### Equation 6.3

$$\text{Turbidity} = 0.4 * \text{SSC} + 73 \quad (R^2 = 0.3)$$

Because the range of creek flow conditions that is sampled was restricted due to poor accessibility, the turbidity – SSC curve is not thought representative. The regression equation based on all samples (Equation 5.1 in Chapter 5) will therefore be used to estimate the sediment concentrations from the Post Creek turbidity

records. The effect of this assumption on the sediment load calculations is tested in Section 0.

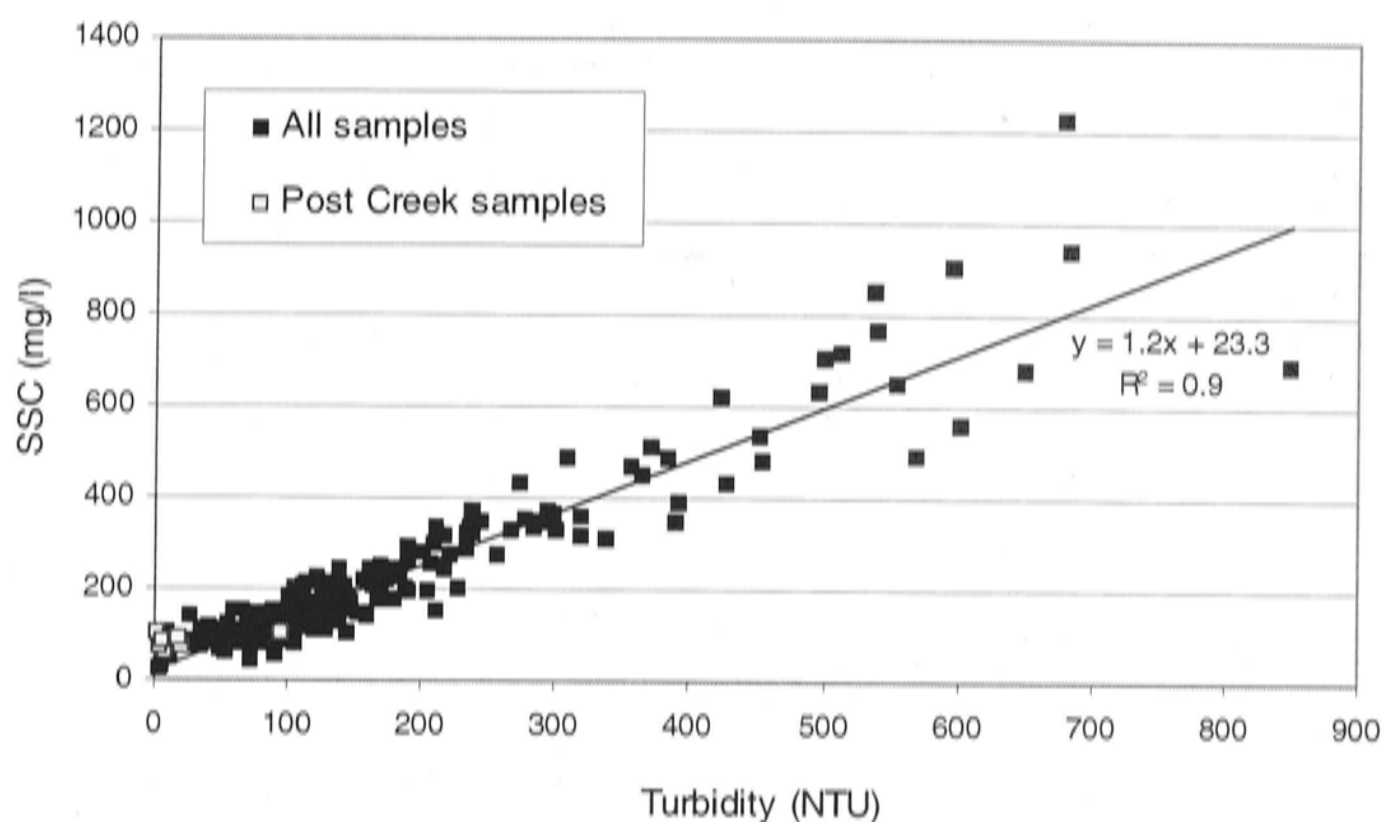


**Figure 6.5:** Scatter diagram of Turbidity versus SSC for Post Creek water samples and all Ripple Corner Catchment water samples (n=10 and n=261).

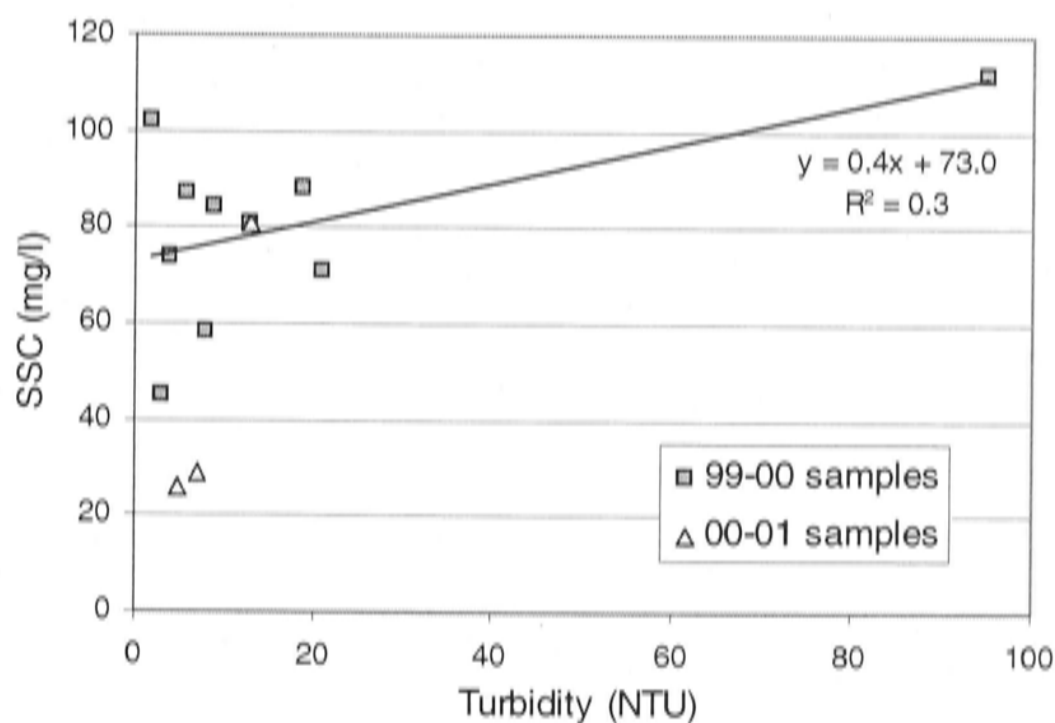


**Figure 6.6:** Scatter diagram for Post Creek turbidity versus SSC for both budget seasons (n=10 and n=3, P=0.09).

### 6.6.2 Turbidity meter calibration

For the 99-00 season Greenspan records are calibrated with turbidity values from water samples as measured by the Turbiquant bench top meter. Turbiquant turbidity and SSC data for the water samples and the corresponding Greenspan records are

listed in Table 6.4. The Greenspan-Turbiquant relationship for 99-00 season is presented in Figure 6.7. The following regression equation is obtained from the data and will be used to transform the Greenspan turbidity records:

**Equation 6.4**

$$\text{Turbiquant turbidity} = 1.8 * (\text{Greenspan turbidity}) + 11.7 \quad (R^2 = 0.9)$$

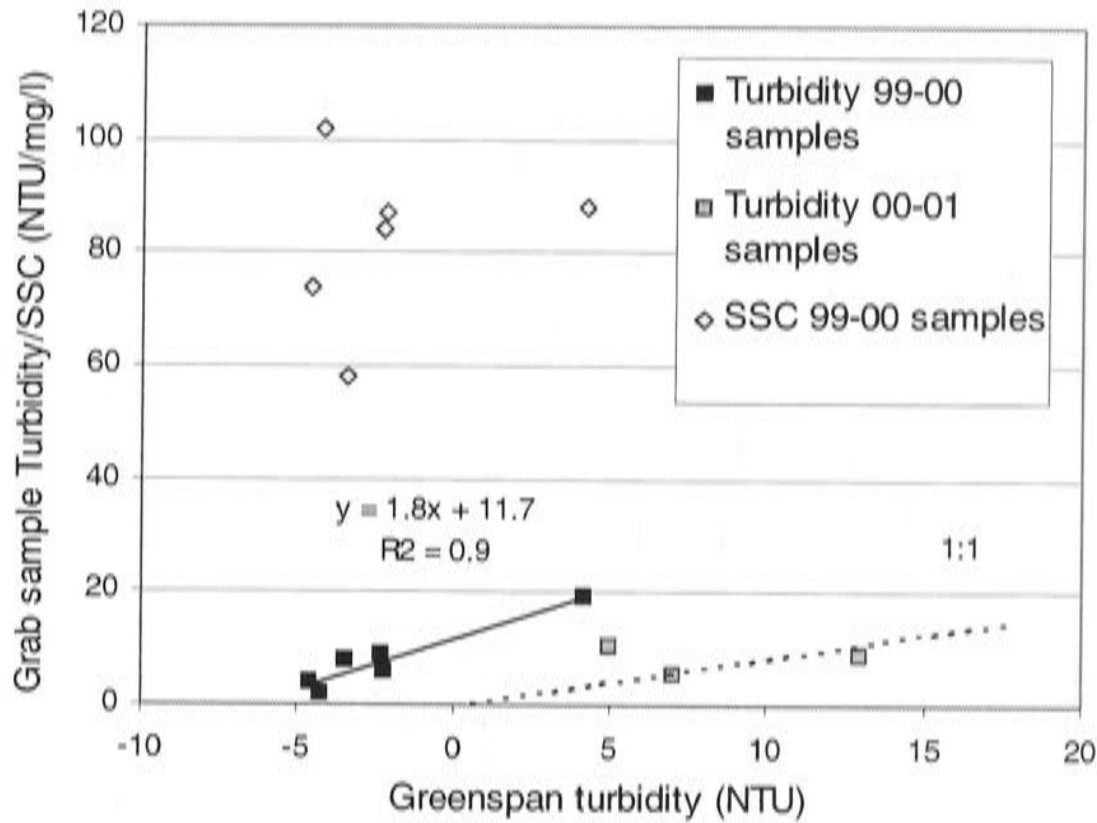


**Figure 6.7:** Calibration of Post Creek Greenspan turbidity probe with Turbiquant grab sample turbidity estimates and SSC estimates for both budget seasons (n=6 and n=3, P<0.01).

**Table 6.4:** Post Creek water quality data and corresponding Greenspan records.

Date	Greenspan (NTU)	Turbidity (NTU)	SSC (mg l <sup>-1</sup> )
5/11/99	-	21	71
19/11/99	-	3	45
1/18/00 15:30	-4.2	2	102
2/16/00 12:13	-2.3	9	84
2/18/00 12:00	-2.2	6	87
2/25/00 14:10	4.21	19	88
3/2/00 12:26	-3.41	8	58
3/17/00 10:50	-	95	112
4/6/00 12:00	-4.6	4	74
1/3/00 11:40	-	13	81

The Greenspan probe used for the turbidity measurements in Post Creek was calibrated before installation for the 00-01 season. Laboratory calibration of the

device does not necessarily mean that the Greenspan NTU values correspond with Turbiquant NTU's as pointed out in Chapter 5. Three grab samples taken during the 00-01 season can not provide a significant relationship with the Greenspan records and they do not fit the regression of the 99-00 data. Because there are no other means of calibrating the turbidity data, Turbiquant and Greenspan values are assumed equal, which is supported by the fact that the available values fit close around a 1:1 line (dashed) through the origin of Figure 6.7.

### 6.6.3 Missing turbidity data

The relationship between Post Creek turbidity and rainfall data, which is used to estimate the two periods of missing turbidity data for the 99-00 season, is as follows (see Figure 6.8):

#### Equation 6.5

$$\text{SSC} = 5.2 * (\text{Rainfall}) + 34.4 \quad (R^2 = 0.5)$$

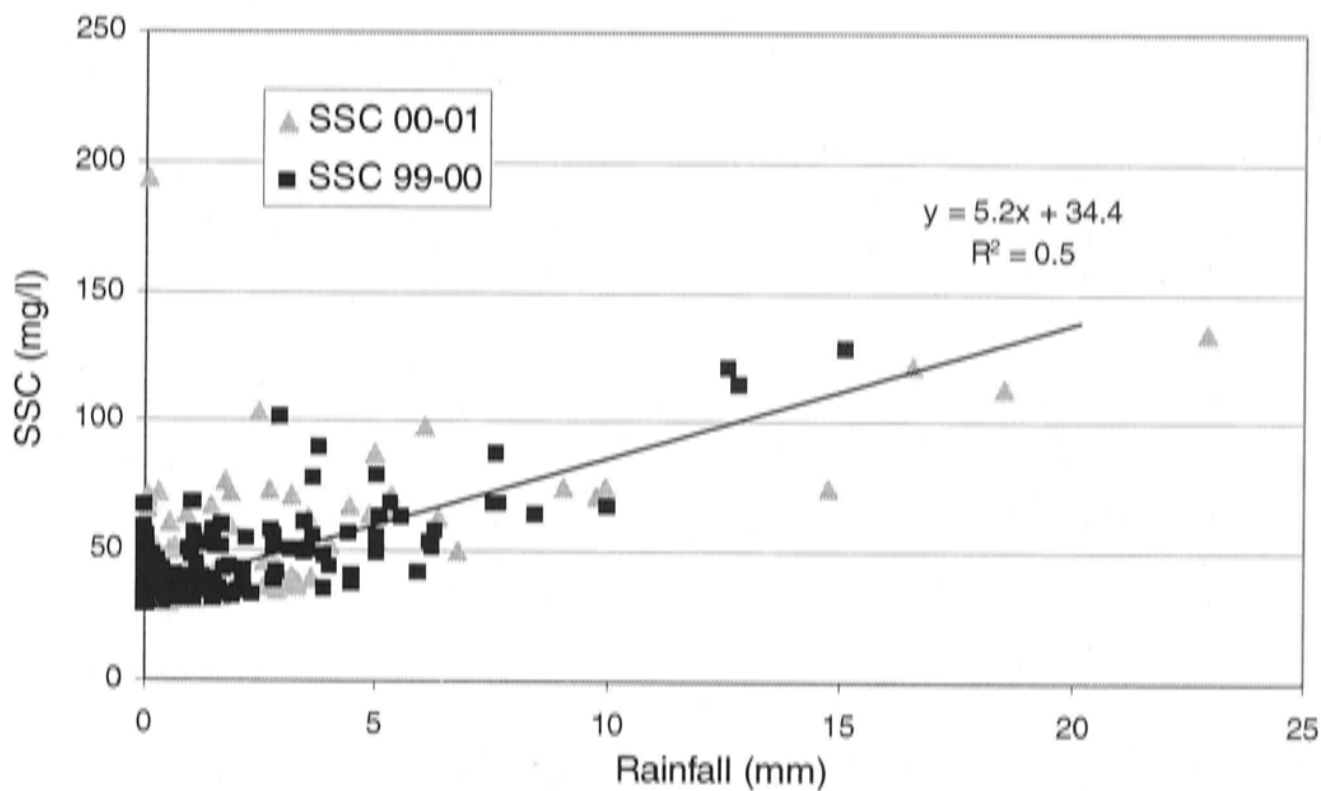


**Figure 6.8:** Regression curves Rainfall and Post Creek SSC for both budget seasons (n=488, P<0.01).

The relationship between Post Creek turbidity and depth for the same season (99-00) in Figure 6.9 shows an increase in NTU values at the lowest water depths. These low water depths only occur at the end of the season, between the end of April and the beginning of May. Although it is not verified with observations in the field, the most obvious explanation is a drop in water level below the sensor surface. According to the Greenspan manual (Greenspan Technology, 2002) noise of up to

20NTU can occur in the records when the turbidity meter is not covered with water. Exclusion of the affected data does not significantly change the rainfall – depth regression equation (Equation 6.5), used to substitute missing turbidity data.

The 00-01 data are different from the 99-00 data. This could again be the result of the dubious depth data quality.

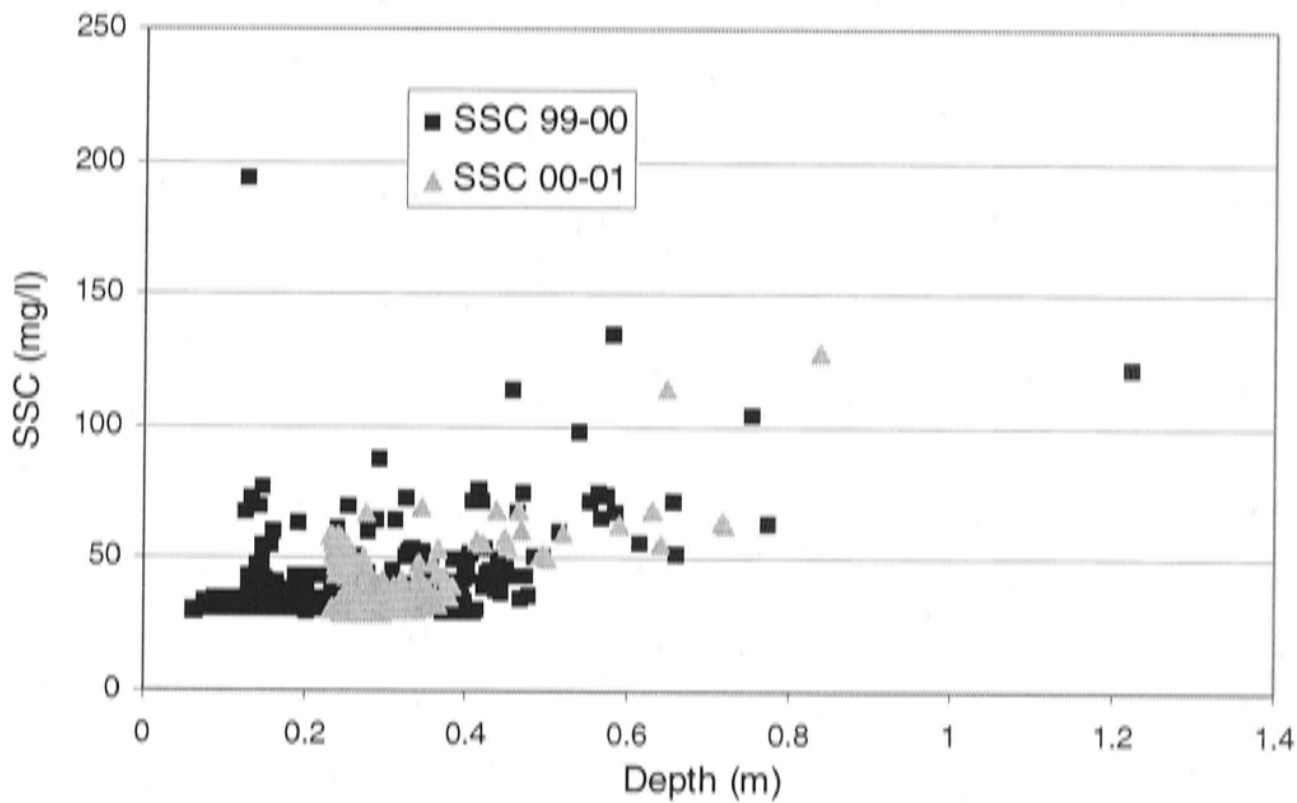


**Figure 6.9:** Scatter diagram of Post Creek Depth versus SSC for both budget seasons.

## 6.7 Load calculations

According to the methods presented in the previous section, missing depth and turbidity data are estimated from rainfall. Discharge is estimated from adjusted depth data and the rating curve based on velocity measurements. SSC is estimated from the turbidity records. With this information sediment discharge has been estimated and summed over the budget period, which results in the total sediment load for the Post Creek catchment. A number of different calculations are made to test and illustrate the effect of some of the assumptions and data adjustments that were made. All loads are listed in Table 6.5.

The first calculation (1) is based on the original data without adjustments for depth. A specific depth – discharge rating curve is estimated for this calculation:

### Equation 6.6

$$\text{Post Creek Discharge} = 3.3 * (\text{Original water depth})^2 \quad (R^2 = 0.9)$$

Gaps in the data are filled with a rainfall – discharge regression equation estimated from the unadjusted depth data:

**Equation 6.7**

$$\text{Post Creek Discharge} = 0.1 * (\text{Rainfall}) - 0.06 \quad (R^2 = 0.7)$$

For calculation 2 all discharge data are estimated from this rainfall – discharge curve (Equation 6.7). The results for both calculation methods are very similar. It is not likely that this method of data substitution produces a large error.

For calculation 3 all depth data are adjusted with the average calibration value of 0.22 m (see Section 6.4). A specific depth – discharge rating curve is estimated from the adjusted data:

**Equation 6.8**

$$\text{Post Creek Discharge} = 5.3 * (\text{Original water depth} + 0.22)^3 \quad (R^2 = 0.7)$$

Gaps are filled using a specific depth – rainfall regression.

**Equation 6.9**

$$\text{Post Creek Discharge} = 0.2 * (\text{Rainfall}) + 0.1 \quad (R^2 = 0.7)$$

In calculation 4 different calibrations are applied to different parts of the depth curve, using the depth – discharge rating curve (Equation 6.1) presented in Section 6.5.1 and the rainfall – discharge relationship (Equation 6.2) from Section 6.5.2.

Calculation 5 shows the importance of estimating missing data. The calculation is similar to 4, but without the gaps filled. The approximately 15% reduction of the total load shows that filling of the gaps is necessary and gives an indication of the maximum error that could be introduced when the gaps are filled. Calculation 6 shows the load estimated completely from the rainfall – discharge equation (Equation 6.2). In this case the estimate from rainfall is much lower than the estimate based mainly on depth (4). However, if the method is only used to substitute a limited amount of missing data, the estimate based on the rainfall data are not thought to produce a more than 10% error in the load estimate.

Calculation 7 is similar to calculation 4, except for the regression equation used to calculate SSC from the turbidity records. This calculation uses Equation 6.3 from Section 6.6.1. The big difference in sediment load stresses the potential error that is



introduced by assuming that the relationship between SSC and turbidity is uniform throughout the Ripple Corner Catchment.

Discharge and consequently sediment transport vary considerably with the different adjustments of the depth data. Calculation 4 is assumed to be the best estimate, because this calculation uses depth data adjusted in what is thought to be the best possible way, as pointed out in Section 6.4. However the relatively high low flow water levels and the extremely high runoff coefficients make the correctness of the large depth adjustment questionable. The runoff coefficient from the original data is more realistic.

**Table 6.5:** Post Creek load calculations for the 1999-2000 budget season. Best estimate shaded.

<b>Upland input 99-00 season</b> Discharge and sediment load calculated from:	Unit area sediment load* (t ha <sup>-1</sup> )	Sediment load (tonnes)	Runoff coefficient	Total discharge (x10 <sup>6</sup> m <sup>3</sup> )
1. Original data (missing data estimated from rainfall – discharge regression)	0.7	48	0.5	0.6
2. Only rainfall data and rainfall – discharge regression	0.7	42	0.4	0.6
3. Depth data adjusted with 0.216 m (missing data estimated)	2.5	162	2.3	3.2
4. Depth with two adjustments (missing data estimated)	2.3	148	2.1	3.0
5. Depth with two adjustments (missing data not replaced)	1.9	124	1.6	2.4
6. Only rainfall data and rainfall – discharge regression	1.6	99	1.7	2.4
7. Depth with two adjustments (missing data estimated). Alternative turbidity – SSC relationship	3.9	247	2.1	3.0
Total rainfall (x10 <sup>6</sup> m <sup>3</sup> ) = 1.5				

Table 6.6 shows the best Post Creek load estimate for the 00-01 season. Despite the fact that depth data for this season were not adjusted, it also has a high runoff coefficient. This could indicate that the 00-01 depth data were correct and adjustment of the 99-00 data was necessary, while other factors caused the high runoff coefficients. Possible factors are underestimation of the Post Creek catchment surface area, errors in the depth – discharge rating curve or underestimation of the total rainfall in the catchment. However, the quality of the depth data remains dubious and some anomalies have not been explained.

**Table 6.6:** Post Creek load calculation for the 2000-2001 budget season.

<b>Upland input 00-01 season</b> Discharge and sediment load calculated from:	Unit area Sediment load (t ha <sup>-1</sup> )	Sediment load (tonnes)	Runoff coefficient	Total discharge (x10 <sup>6</sup> m <sup>3</sup> )
Original data	1.8	115	2.1	2.0
Total rainfall (x10 <sup>6</sup> m <sup>3</sup> ) = 1.0				

The best estimates of the Post Creek sediment load and discharge are summarized in Table 6.7, together with the best estimates of the Ripple Drain and Prosser Drain. Post Creek catchment consists completely of forested upland and receives a considerably larger amount of rainfall than estimated at the weather station in the cultivated lowland. David Post (pers. comm.) estimated from rainfall surfaces that the yearly rainfall in the upland areas is approximately 1.2 times higher than in the lowlands (2400 mm compared to 2000 mm) around Palmas' site. According to these numbers excess rainfall only partly explains the high runoff coefficient. The coefficient for adjusted rainfall is 1.75. To get a more realistic input for the sediment budget, the load is reduced, assuming a maximum likely runoff coefficient of 0.85. The loads used as input for the budget calculation then become 72 t (99-00) and 56 t (00-01).

**Table 6.7:** Summary of best estimates of sediment load, discharge values and runoff coefficients.

	<b>Ripple Drain*</b>		<b>Prosser Drain*</b>		<b>Post Creek (based on data)</b>		<b>Post Creek (used in the budget calculation)</b>	
	99-00	00-01	99-00	00-01	99-00	00-01	99-00	00-01
Total Discharge (10 <sup>6</sup> m <sup>3</sup> )	9.5	7.0	1.6	1.7	3.0	2.0	-	-
Total Rainfall (10 <sup>6</sup> m <sup>3</sup> )	11.7	8.8	0.9	0.7	1.5	1.0	-	-
Runoff Coefficient	0.8	0.8	1.6	2.3	2.1	2.1	0.85	0.85
Sediment load (t)	1580	1120	170	-	148	115	72	56
Sediment load (t ha <sup>-1</sup> )	4.9	3.5	3.7	-	2.3	1.8	1.1	0.9

\* Ripple Drain and Prosser Drain data are discussed in Chapter 5

To obtain the upland input value for the sediment budget, the information obtained from the Post Creek catchment has to be extrapolated across the remaining upland surface. This procedure will be described with the budget calculation in Chapter 10.

---

## Chapter 7

### Fields

---

#### 7.1 Introduction

The budget component that covers the largest surface area in the catchment is 'fields'. There are three types of fields: plant cane fields with first year crop, ratoon fields with return crops and fallow fields without crop. Ratoon crops are grown from the stubble left behind after the harvest. Two or three ratoon crops follow a plant cane crop before the land is rested (fallow), ploughed and replanted.

Fields under different crop stages are expected to generate different sediment loads, because of the presence or absence of a cane trash cover beneath the crop. The different crop stages will also require different erosion control management. In order to apply most effective management, it is necessary to know the relative contribution of each type of field to the sediment budget. The input from plant cane and ratoon fields is therefore quantified separately in this chapter. Fallow fields were not studied, because there was no suitable fallow field available for study during the field seasons. Field observations suggested that the sediment export from fallow fields lies in between that from plant cane and ratoon. In Chapter 10 is explained how the area of fallow fields is incorporated in the sediment budget.

At the start of the budget study it was assumed that sediment transport from fields would only occur down slope via inter-rows and water furrows. It was also assumed that, because of the dense network of drains, runoff from each field would drain directly into a drain at the down slope end. No lateral exchange of sediment was expected to occur between neighbouring fields. If these assumptions are correct it means that fields do not serve as storage space for sediment from external sources. They will only (temporarily) store sediment generated within the field. For the sediment budget, only knowledge of its significance as a net sediment source is

important, although for management purposes storage processes within the fields are of importance to enable reduction of the export from fields.

The measurement design for the budget input from fields, described in this chapter, is based on these assumptions. However, in later stages of the research they proved only partly correct. Under flood conditions reverse flow from drains onto the fields occurs and during extreme flood conditions completely different flow scenarios could occur. Under these conditions sediment from external sources could be stored on the fields. The effect this has on the interpretations of the sediment budget will be discussed in Chapter 13.

A common way to estimate discharge and sediment export from fields is with the use of runoff flumes (Hudson, 1993). This method does not allow separate identification of erosion and storage rates within this landscape element, but this information is not necessary as pointed out above. An important reason why this method was chosen is that two fields at the Palmas' site were already equipped with runoff flumes at the start of the project. Furthermore the method can provide information on the average surface level change for a whole field and thus avoids problems of small-scale spatial variation within that field.

## **7.2 Ratoon data**

### **7.2.1 Set up**

The two flumes at the Palmas' site are referred to as 'north flume' (NF) and 'south flume' (SF). Each drains a field of approximately one hectare. The fields are located along Ripple Drain at approximately 100 m distance from each other (see Figure 4.1). The positions of the flumes were chosen for their accessibility under inundated conditions.

Both flumes at Palmas' site are Parshall flumes with an 80 cm wide neck. Each is located at the downstream end of a water furrow. Sheets of zinc bunding 40 cm high (inserted  $\pm 10$  cm into the soil) direct water from seven rows on each side of the water furrow towards the mouth of the flume. The total width of the banded funnel is 20 m. The length of the field drained by the north flume is 480 m. A part of the upstream end of the field is cleared to accommodate the weather station. To clearly define the

area gauged, bunding was installed upstream at 450 m distance from the flume. The total area drained by this flume therefore is 0.9 ha.

A cabin above each flume contains an ISCO automatic water sampler. A depth sensor, located in a stilling well at the flume entrance, triggers the sampler at a set flume water depth (see Figure 7.1). The sampler then takes water samples every two hours until the water in the stilling well drops below the threshold level. A data logger records the water depths in the stilling well. During the second field season (99-00), the south flume was also equipped with a STARFLOW Doppler velocity meter (Unidata, 1998). This instrument was placed in the centre of the flume entrance (see Figure 7.1).

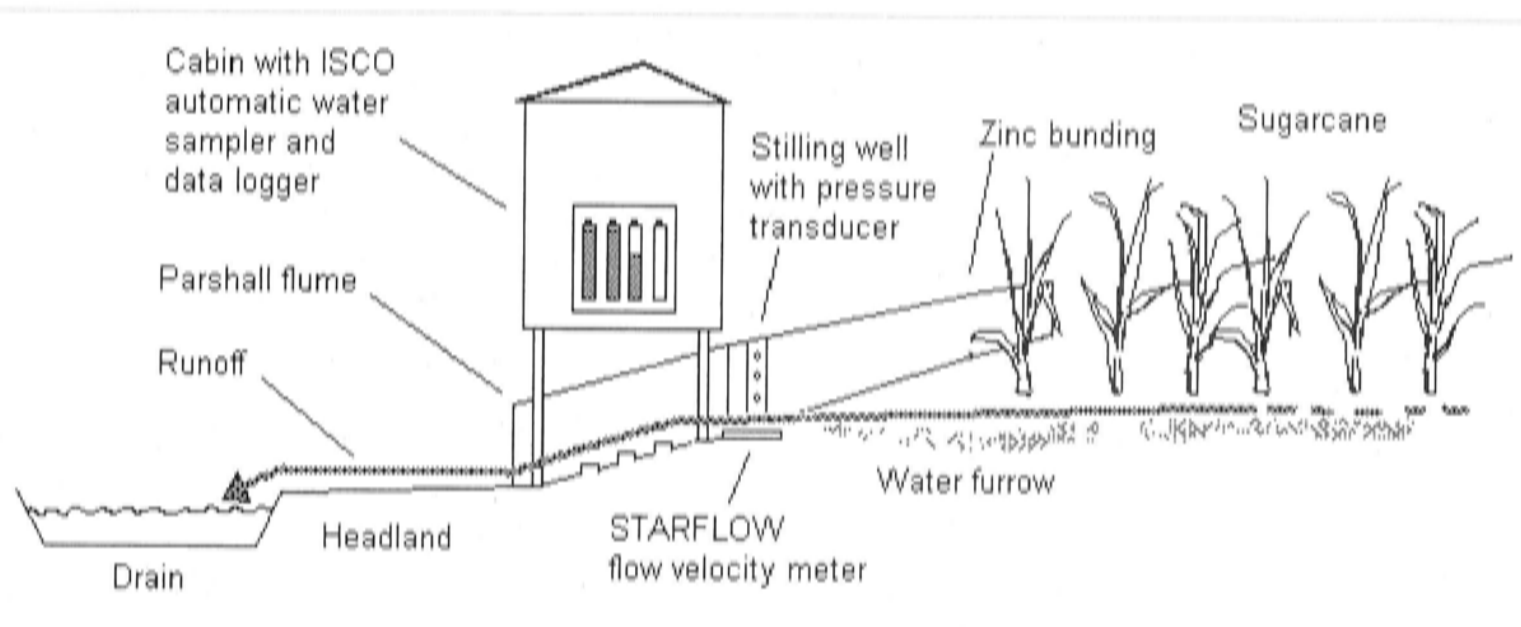


**Figure 7.1:** Set up of Parshall flume at the ratoon field site (side view).

In the original design one flume would drain a ratoon field and one flume a plant cane field each season. However, due to the weather and the crop conditions neither of the gauged fields was replanted over the duration of the project. The flumes at Palmas' site therefore only provided information on sediment runoff from ratoon fields. For the last field season an alternative set up was created to also obtain data for plant cane fields. This set up is presented in Section 7.3.2.

### 7.2.2 Raw data

During the first two budget seasons (98-99 and 99-00) both flumes were operating. During the last season (00-01) only the south flume was in use. Because the data from the 98-99 season is not used for the calculation of a sediment budget, it will not be discussed at length, although some of the data will be used for clarification. The availability of the data for both budget seasons is listed in Table 7.1 and also illustrated in Appendix C. Daily changes in temperature cause small fluctuations in

the 00-01 Dataflow depth data. These fluctuations are removed prior to use. All available and corrected data for each season are plotted in Appendices F (9 and 10).

The appendices also show the turbidity and SSC results from the flume water samples. The first samples for the 99-00 season were taken in December when the gauges were not yet operating. All events are fully sampled, apart from the 6-8 February event, for which only the last half is sampled. There were three rainfall events during the gauged period of the 00-01 season. No water samples were taken during the first event, and the first few samples of the last two events are missing, due to problems with the ISCO sampler.

**Table 7.1:** Availability of depth and velocity data from the south flume gauging site for the 99-00 and 00-01 season.

	Start	End
99-00 Starflow velocity and depth data	31/01/00 10:05	12/5/00 12:35
00-01 Dataflow depth data	20/12/00 18:00	20/02/01 2:15

### 7.2.3 Flume hydrographs and backwatering

During the first field season (98-99) it was recognized that backwatering affects the flow through the flumes at Palmas' site. Runoff from the fields is reduced when the water level in the adjacent drains rises above the mouth of the flumes. Because the standard stage/discharge formula of the flumes assumes unimpeded flow of water, it can in this situation not be used to calculate discharge from the flume water depth. Towards the end of the season the south flume was equipped with a flow velocity meter, to overcome this problem.

Figure 7.2 shows an example of a storm event for the south flume from the first field season (2 – 4 April 1999). The flow depth curve shows a peak as a result of the rainfall over this time period. The flow velocity does however not increase with increasing flow depth. After an initial increase the velocity suddenly decreases. At peak water depth, flow velocity is lowest. This indicates that runoff through the flume was impeded. The sudden change in flow velocity and thus the start of backwatering occurs at a water depth between 5 and 6 cm. A similar pattern is shown in Figure 7.3, although less pronounced, partly because of faulty data. With

increasing water levels the flow velocity in the flume decreases, due to increasing pressure from the drain water.

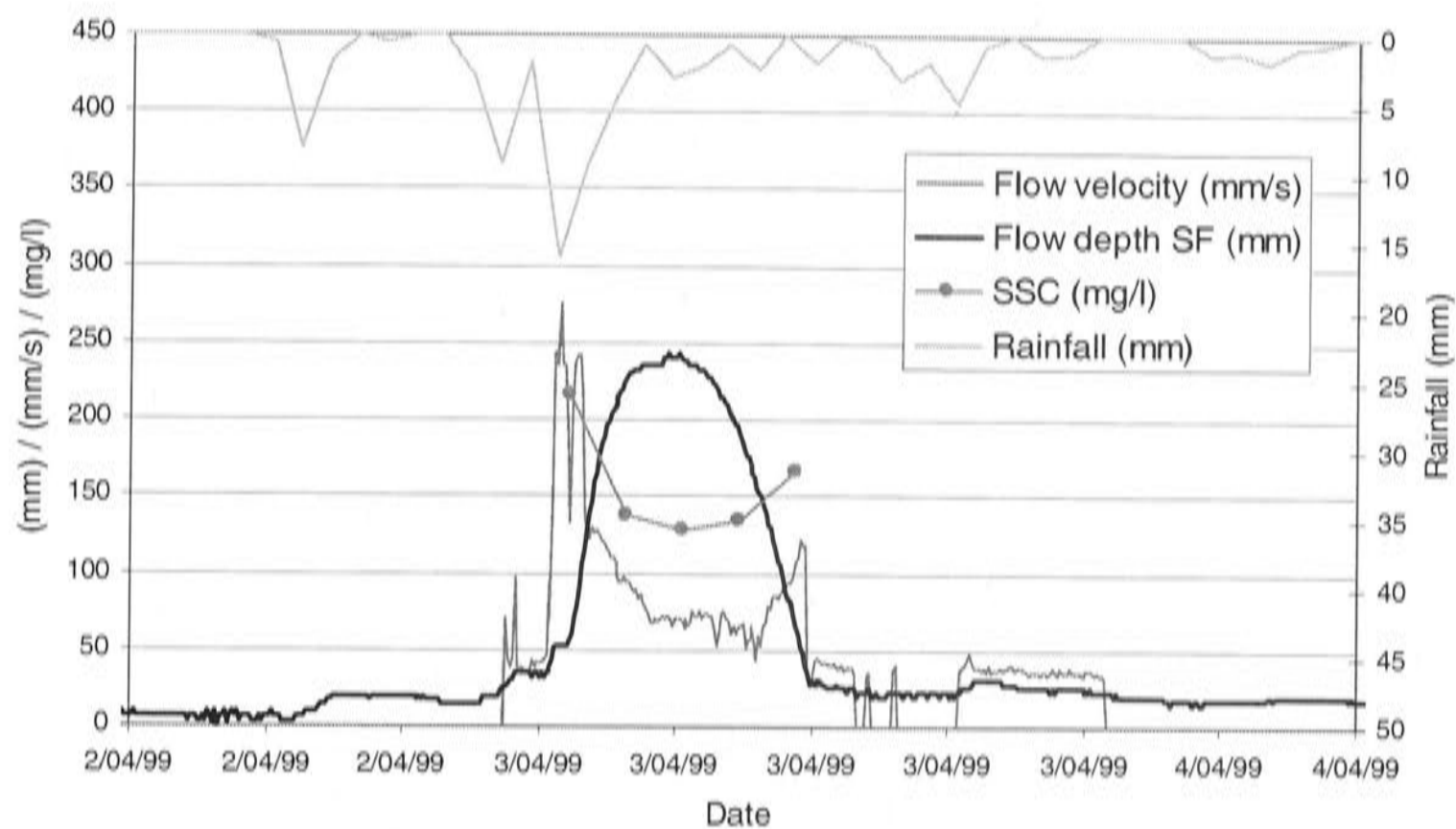


Figure 7.2: Gauging data, south flume (2 – 5 April 1999).

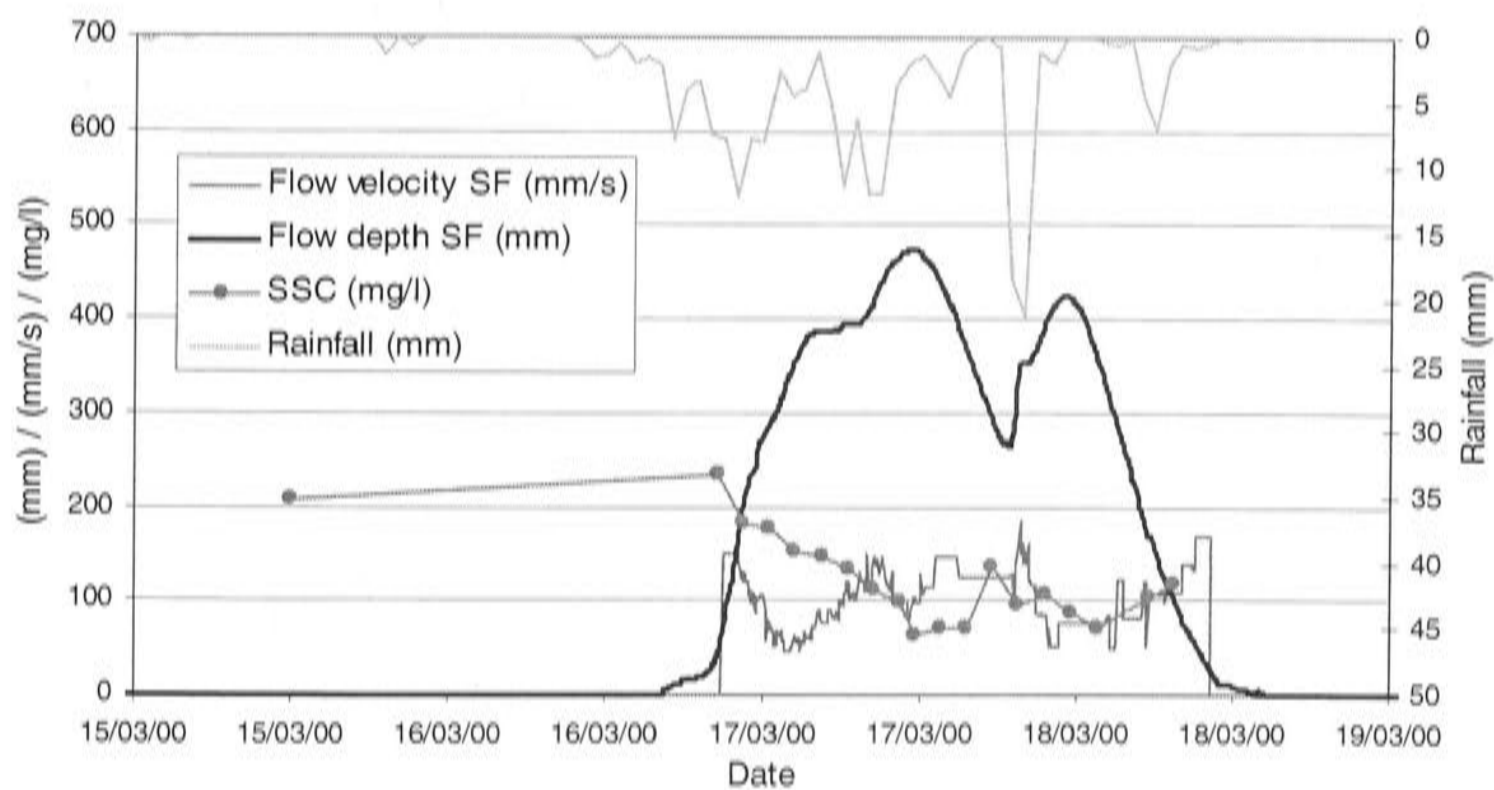


Figure 7.3: Gauging data, south flume (15 – 19 March 2000).

#### 7.2.4 Rating curves

To calculate the sediment load from the south flume, discharges are first calculated from the depth and velocity data. Next, all depth, velocity, turbidity and discharge

data are averaged over periods of six hours, in the same way as for the gauging data from the outlet drains (Chapter 5).

The velocity meter was only installed in the flume during the 99-00 season. For this season, discharge can be calculated directly from velocity data, water depth records and the flume cross-section. Flume discharge for the 00-01 season is estimated from a rating curve, which was established with the 99-00 averaged depth and discharge data. The curve is shown in Figure 7.4.

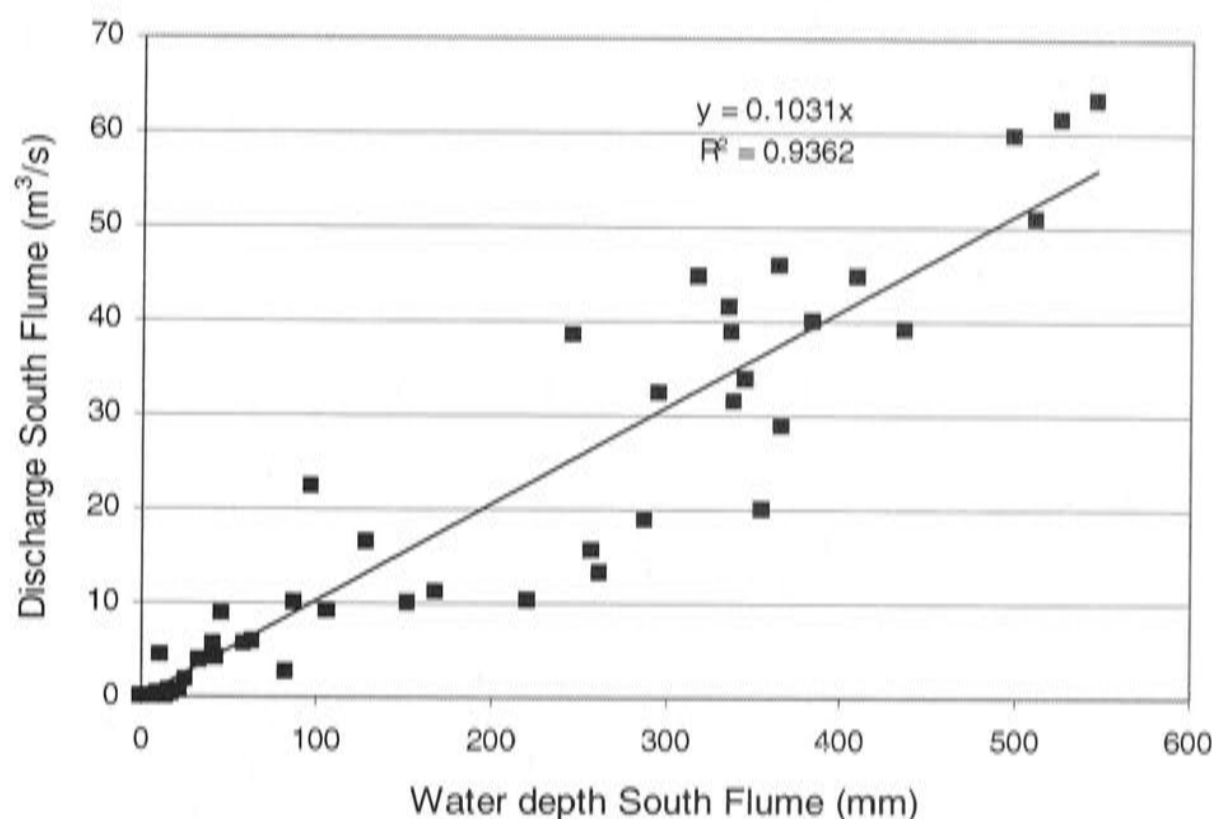


**Figure 7.4:** Depth – discharge rating curve based on 99-00 south flume data. (n=189, P<0.01)

Because of the backwater conditions, the water depth in the flume is strongly dependent on the depth of Ripple Drain. The relationship based on 6-hourly 99-00 Ripple Drain and south flume depth data are shown in Figure 7.5. The curve consists of two obviously different sections. The kink in the curve represents the point where the water level from the nearby drain reaches the flume mouth and starts obstructing the runoff from the field. For water depths above this point there appears to be a close relationship between the drain and flume depth. For the lower depths the relationship is not clear. For the two parts of the curve two different regression equations are established. For both seasons missing south flume depth data at the beginning and the end of the budget periods are estimated from Ripple Drain data.



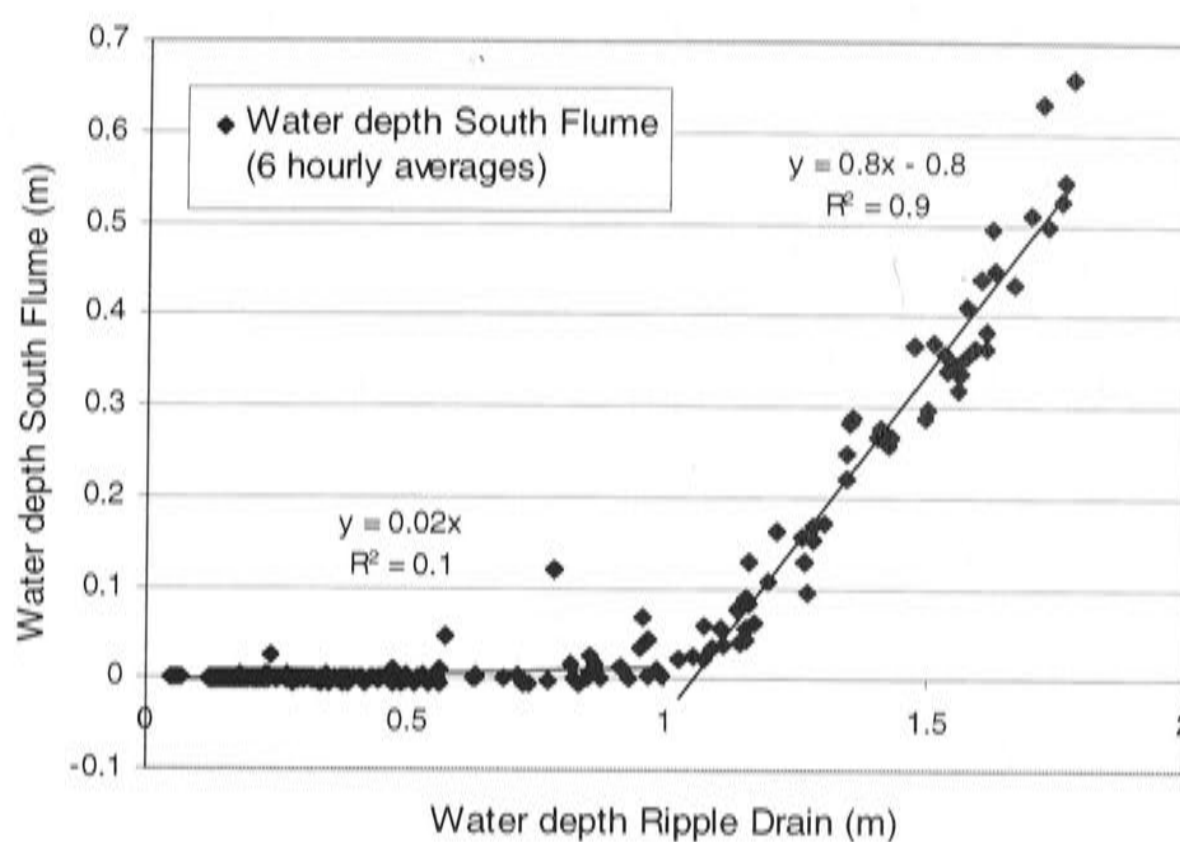


**Figure 7.5:** Relationship between Ripple Drain water levels and south flume water depth (separate regression equations for RD depths <1.0 m (n=429, P<0.01) and >1.0 m (n=58, P<0.01))

### 7.2.5 Sediment export

The flume water samples were analysed for SSC and turbidity in the same ways as the drain samples (see Section 5.3.1). Figure 7.2 and 7.3 show how the sediment concentration of the flume runoff is affected by backwatering. The SSC of the flume samples follows the flow velocity curve of the runoff. Concentrations are highest at the shallowest flume depths, when the runoff is not yet impeded by drain backwatering and runoff velocities are highest. During the peak water depths the concentrations are lowest, because the flow velocities are low, so sediment is allowed to settle and the flow has least erosive power. At the end of the flow peak when the water level lowers and the flow velocity increases again, the sediment concentration increases as well, which indicates that the concentration decreases under peak flow conditions is not just source depletion as is often seen under unimpeded flow conditions.

To obtain a continuous SSC record for the calculation of the sediment load, a rating curve has been developed. Due to the backwater conditions sediment concentration is not well related to discharge. A better rating curve is obtained from the depth data. For each water sample the flume depth at time of sampling is plotted against the SSC. The regression equation for the 99-00 data is used to calculate continuous sediment concentration data for the final load estimation (see Figure 7.6):

## Equation 7.1

$$\text{SSC} = -43 * \ln(\text{Depth SF}) + 365 \quad (R^2 = 0.7)$$

The logarithmic relationship was chosen, because it best represents the elevated concentrations at low flow depths.

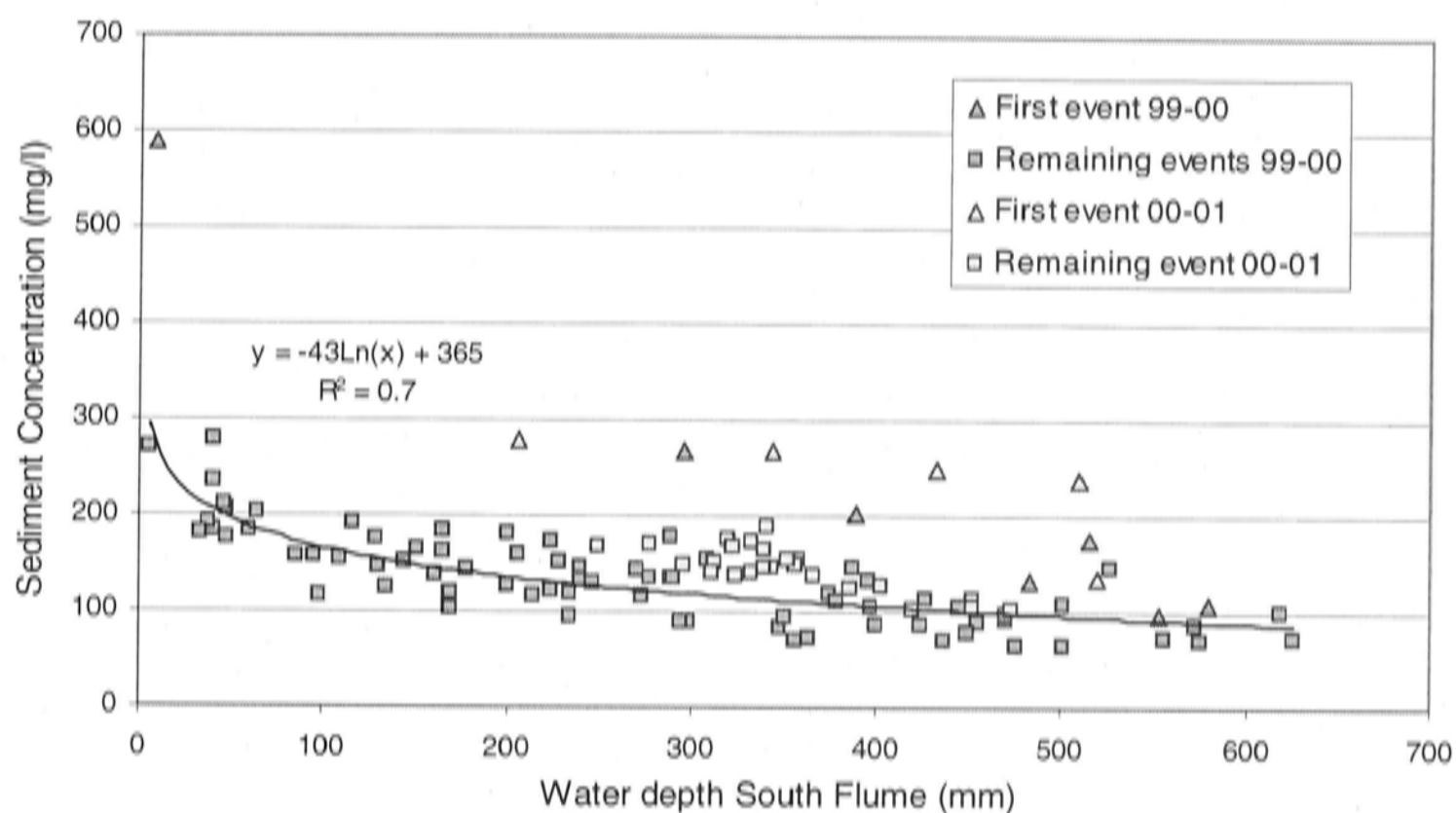


**Figure 7.6:** Suspended sediment concentration – water depth relationship for the south flume. Samples for each season and the first event of each season shown separately (n=78).

Figure 7.6 shows the samples for the first events of both seasons separately. When the samples for the first event of the 99-00 season were taken, water depth was not yet being recorded. The flume water depth at the time of sampling is therefore estimated from the Ripple Drain depth with the equations in Figure 7.5. Most of the first event samples have relatively high sediment concentrations. This is thought to be the result of disturbance of the surface after installation of the bunding each season. It could also be due to the so-called 'first flush' effect, which is a high sediment concentration in the first runoff after the dry season. This effect will be discussed in more detail in Section 7.3.9. Because the results from these samples are not representative for the sediment concentrations during the budget period, they are not used in the calculation of the rating curve.

### 7.2.6 Ratoon fields load calculation

All missing depth data at the beginning and end of both seasons is substituted with data estimated from Ripple Drain depth (Figure 7.5) where possible. All discharge

data for the 00-01 season and the missing periods of the 99-00 season are estimated from the rating curve in Figure 7.4. With the equation from Figure 7.6 sediment concentrations are estimated for the runoff from both seasons. The cumulative sediment discharge results in 3.2 tonnes sediment load from the south flume ratoon field in the 99-00 season and 2.5 tonnes in the 00-01 season.

Because the gauged field includes a water furrow, the estimated load includes sediment derived from the water furrow. In the budget study, water furrows are considered separate budget components that require specific soil conservation management. To obtain the export solely from the ratoon field surface, the amount of sediment expected to originate from the furrow is subtracted from the total sediment load measured at the flume outlet (see Table 7.2). The estimate of the furrow input is derived in Chapter 9. The water furrows occupy 12.5% of the field surface. (2.5 m furrow width per 20 m field width). Thus for the 99-00 season:

$$\text{Soil loss field without furrow (t)} = \text{Soil loss field} - (12.5\% * (\text{Soil loss furrow}))$$

$$1.4 = 3.6 - (12.5\% * 18) \text{ for the 99-00 season and}$$

$$0.7 = 2.8 - (12.5\% * 20) \text{ for the 00-01 season.}$$

**Table 7.2:** Results of the sediment load estimation from the south flume

South flume whole budget period	Sediment load (t)	Sediment load (t ha <sup>-1</sup> )	Load minus furrow component (t ha <sup>-1</sup> )	Runoff coefficient
99-00	3.2	3.6	1.4	1.2
00-01	2.5	2.8	0.7	1.0

To obtain the total input for the sediment budget, the results from the ratoon flume are considered representative for all ratoon fields and extrapolated across the budget area. Further details on the extrapolation methods are described and discussed in Chapter 10.

So far only data from the south flume have been discussed. Because the north flume has never been equipped with a velocity meter, it was not possible to calculate discharges for this flume. It is therefore not possible to make a second estimate the sediment load that could confirm the south flume result. However, both the depth and the suspended sediment measurements from both flumes were very similar.

## 7.3 Plant cane data

### 7.3.1 Introduction

During the first budget season several observations were made of much higher sediment concentrations in the runoff from plant cane fields compared with runoff from ratoon fields. This suggested that the plant cane fields were potentially an important source of sediment; and sediment load data from ratoon fields alone would not sufficiently represent the sediment export from cane fields. Unfortunately the gauged fields at Palmas' site were not replanted during the remainder of the project. To obtain some information on the sediment export from plant cane fields, an additional flume gauging site was installed during the last season elsewhere in the catchment. The only field suitable and available for this purpose was 1 km downstream from the Palmas' site (Figure 4.1).

There are a number of important differences between the ratoon field gauging site and the new gauging site for plant cane fields. These differences are likely to influence comparison of results between the two sites and will have to be taken into consideration in the interpretation of the budget results. Firstly the soil texture of the plant cane site is classified by Wood (1984) as clay, while the soils at Palmas' site are silty clay. The difference in soil texture is likely to cause differences in erodibility of the field surface, which will influence the measured sediment loads. Secondly the plant cane field was laser levelled and therefore does not contain water furrows. This required a change in design of the flume set-up. It also means that the flume runoff does not contain sediment derived from water furrows. Finally the field was located along a farm drain at 1.2 km distance from Ripple Drain, while Palmas' site is located along Ripple Drain. The difference in distance from the main drain has an effect on the hydrology and erosiveness of the field runoff.

To illustrate the difference between the sites and the effect it might have on the load calculation, the hydrology and SSC data from the plant cane site will be compared with the data from the ratoon site that was presented above.

The plant flume site was only installed at the beginning of the 00-01 season. There is no plant cane gauging data for the 99-00 season. Section 7.3.9 describes an

alternative method that is used to estimate plant cane budget input for the first budget season.

### 7.3.2 Set up

The gauging installation at the plant cane site consisted of two small cutthroat flumes with 30 cm wide throat (Walker and Skogerboe, 1987) (see Figure 7.7). Each flume collected the runoff from seven rows. Runoff at the downstream end of the rows was directed to the throat of the flume with zinc bunding (similar to the ratoon set-up). The rear and sides of the area were not bounded. The total area drained by each flume is approximately 0.6 ha.

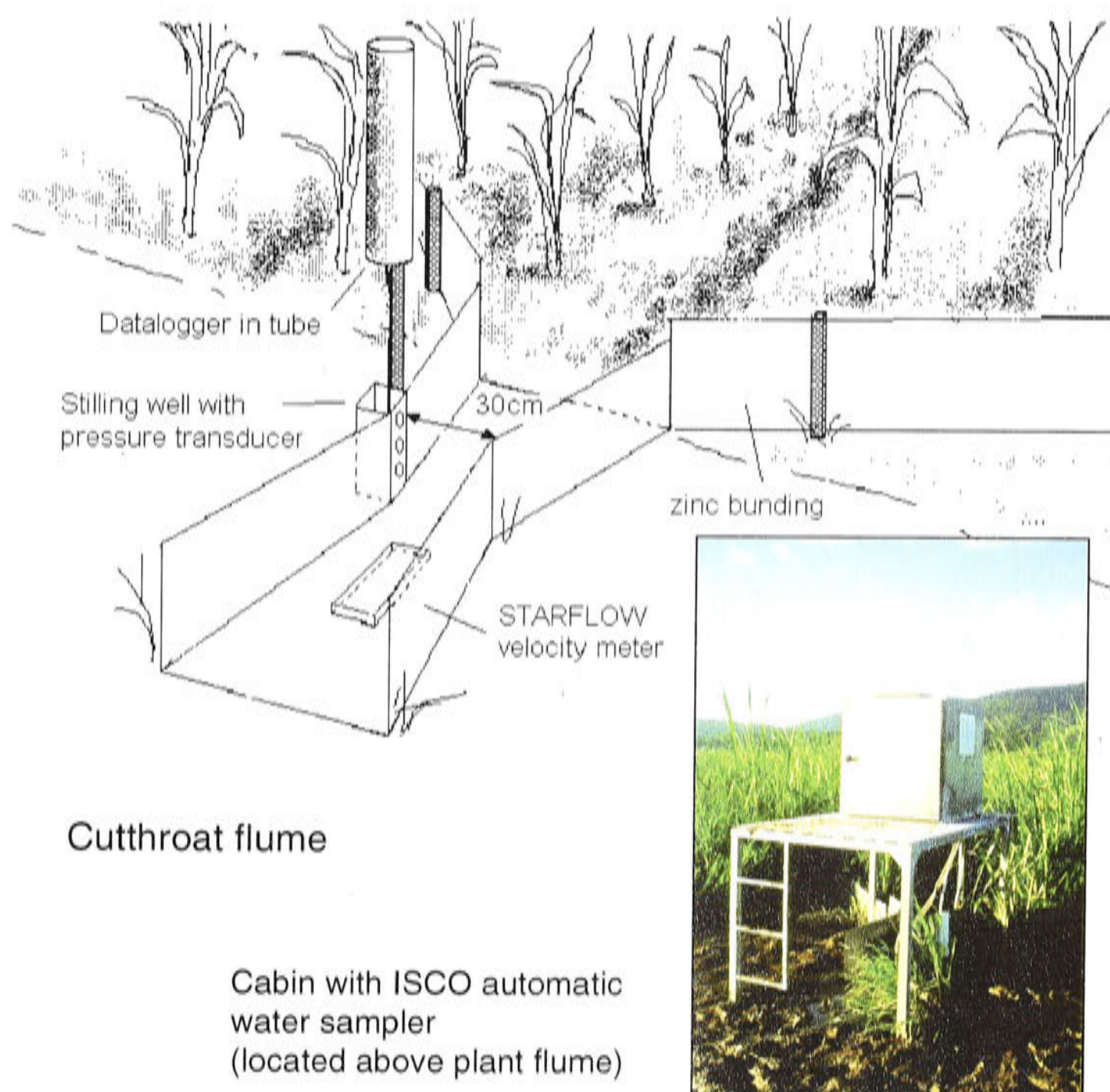


**Figure 7.7:** Set up of cutthroat flumes at the plant cane site.

Water depth in each flume was gauged with depth sensors in a stilling well connected to Dataflow data loggers. One of the flumes was also equipped with an ISCO water sampler and a Starflow Doppler velocity meter, similar to those used for

the flumes at Palmas' site. The fully gauged flume at the plant cane field will be referred to as plant flume (PF).

### 7.3.3 Raw data

Velocity and depth data from the Starflow meter at the plant flume covers the whole period between 20 December 2000 and 20 February 2001 (Table 7.3). The Dataflow data from the same flume do not add any extra information and will be discarded. Three storms occurred over the gauging period. The depth and velocity curves for these storms are shown in Appendix F (11). Between 2 and 6 January 2001 both velocity and depth data show suspect behaviour.

All events were sampled. Only the last samples of the last event are missing, because there were no spare bottles left in the ISCO sampler. Sample SSC-s are also plotted in Appendix F (11).

The purpose of the second flume at the plant cane site was to provide a back up for the runoff depth recordings of the first flume. Because SSC and velocity data are not recorded at this flume it cannot be used to confirm the estimate of the sediment load. The depth graphs of both flumes are identical. The data from the second flume will therefore not be discussed any further.

**Table 7.3:** Data availability for the plant flume 00-01 season.

	Start	End
00-01 Starflow velocity and depth data	20/12/00 18:00	20/02/01 2:15

### 7.3.4 Reverse flow

Figure 7.8 shows the plant flume gauging data for the storm period between 13 and 20 February 2001. During this event the plant flume velocity data often become negative. This also occurs during the other recorded events. There are two possible explanations for the negative flow velocities. It could be an artefact of the velocity meter, or for very low flow velocities the sensor might produce signal noise. However the instrument can measure velocities as little as  $21 \text{ mm s}^{-1}$  and the noise should consist of very high velocity signals ( $<3 \text{ m s}^{-1}$ , Unidata, 1998), which is not

the case. It is more likely that the flume experienced reverse flow, which means that overbank water from the drain flows through the flume onto the field.

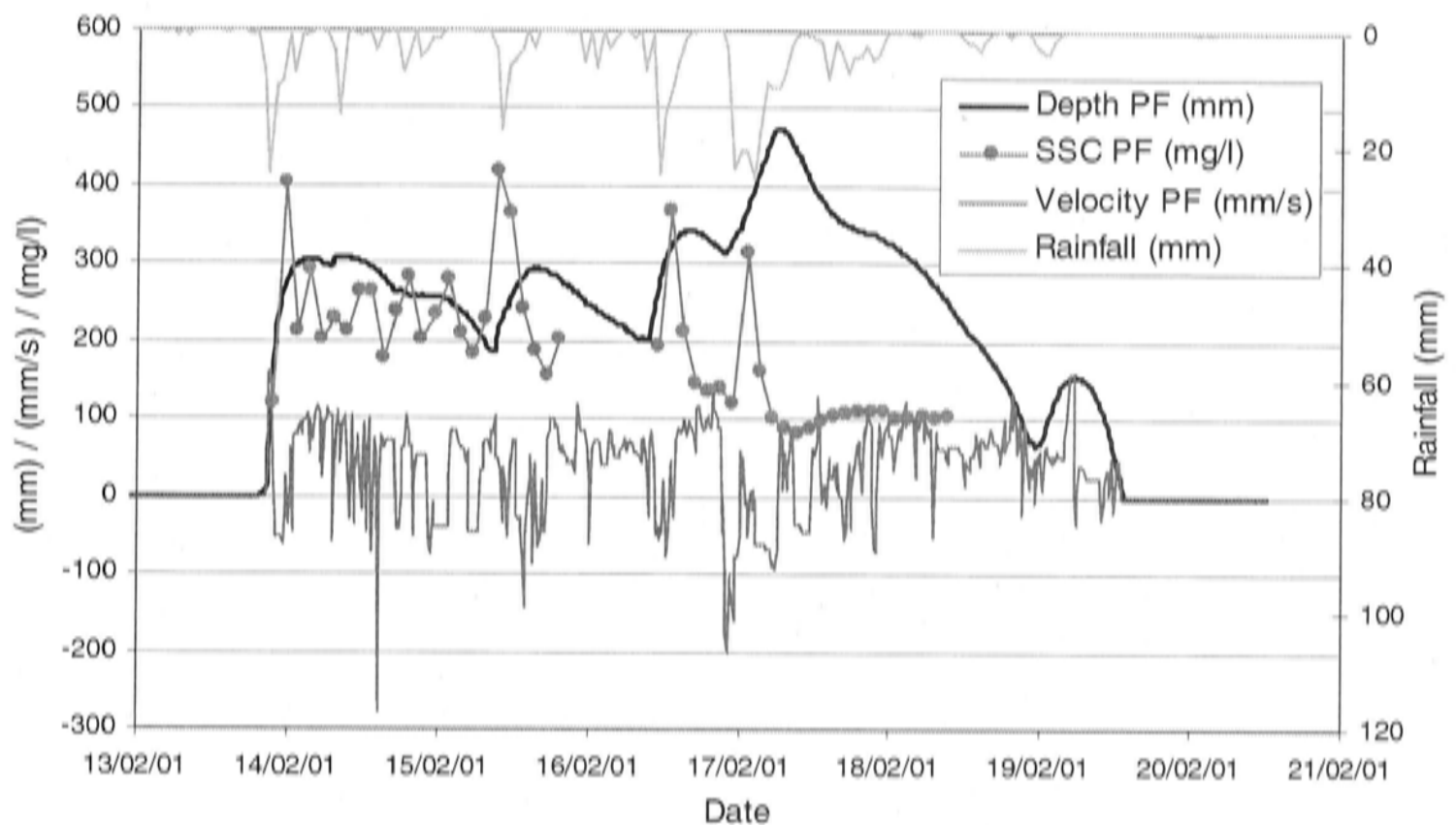


**Figure 7.8:** Plant flume gauging data (13 – 21 February 2001).

Reverse flow seems to occur especially during and just after rainstorms, when the water depth in the flume rises. Only when the flow peak lowers and the pressure difference between drain and field runoff decreases, water starts draining from the field. The signal is however very noisy, with many switches between normal and reverse flow. It is not possible to fully explain the shape of the velocity curve.

In addition, the position of the flumes in the catchment could have an effect on the hydrographs. Runoff from the plant cane field further downstream may be blocked for a longer period of time.

### 7.3.5 Comparing hydrographs

Figure 7.9 shows the flow depth curves for both the south flume and the plant flume. The graph does not reveal anything about the total water discharge from the fields, because the flumes have different dimensions, but it does show how drainage from the ratoon is much more efficient. The recession of the plant flume hydrograph takes longer than that of the south flume. The most likely cause is the design of the fields. The ratoon field is drained with water furrows, in contrast to the laser-levelled plant cane field. The water furrows allow faster drainage of the field surface and will produce higher peak runoff.

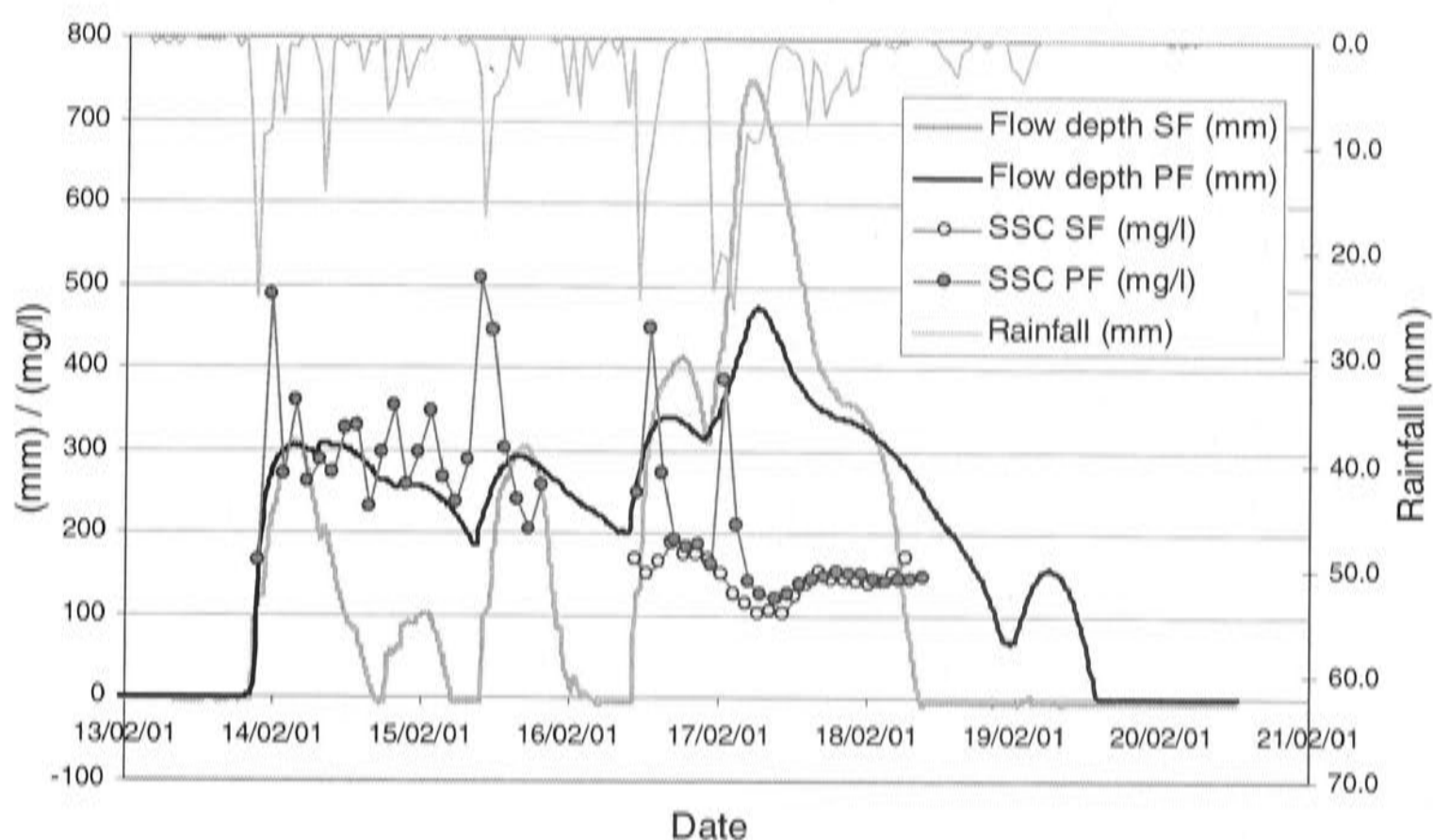


**Figure 7.9:** South flume and Plant flume depth and SSC data (13-21 February 2001).

Reverse flow was never recorded in the flumes at Palmas' site. At peak water levels in the South flume flow velocity was reduced, but never reached zero or became negative. The south flume reached flow velocities of up to  $0.6 \text{ m s}^{-1}$ . Velocities in the plant flume were predominantly between  $0.1$  and  $-0.1 \text{ m s}^{-1}$ .

### 7.3.6 Rating curves

Because the 00-01 plant flume data do not cover the full budget period, the existing data have to be extrapolated. Similar to the ratoon load calculations, rating curves are developed based on all available, averaged data. The plant flume depth – Ripple Drain depth curve is shown in Figure 7.10 and the depth – discharge curve in Figure 7.11.

The depth relationship with Ripple Drain is not as distinct as for the ratoon flume. There appears to be a hysteresis effect. The drainage from the field is relatively slow compared with the water level decrease in Ripple Drain. This could be partly due to the slow drainage from laser-levelled fields and partly due to a delayed response because the site is not in direct contact with the main drain. The depth – discharge rating curve is especially unreliable. This is again caused by the particular backwatering and reverse flow conditions at the gauging site. The suspect data pointed out in Section 7.3.3 do not seem to significantly change the relationship shown in Figure 7.11.



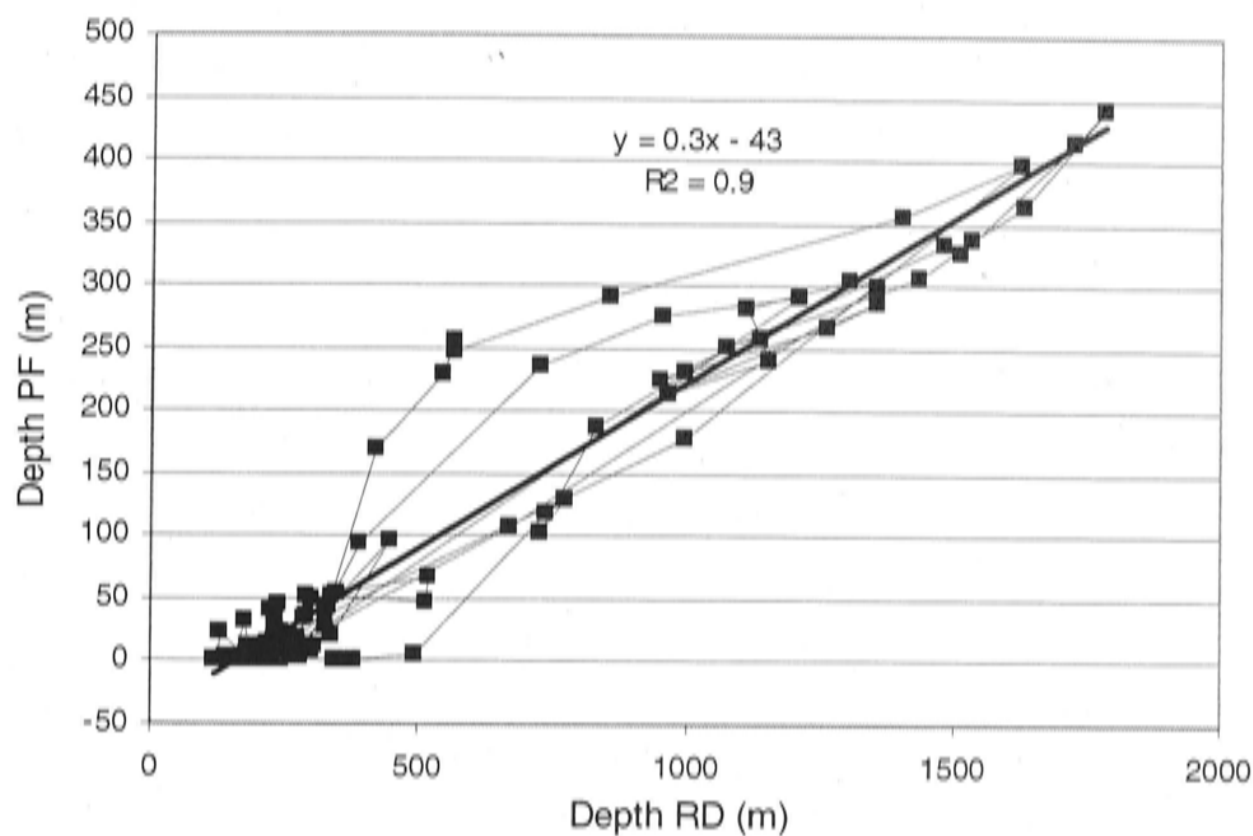


**Figure 7.10:** Scatter diagram of Ripple Drain (RD) versus plant flume (PF) water depth data (n=229,  $P < 0.01$ ).

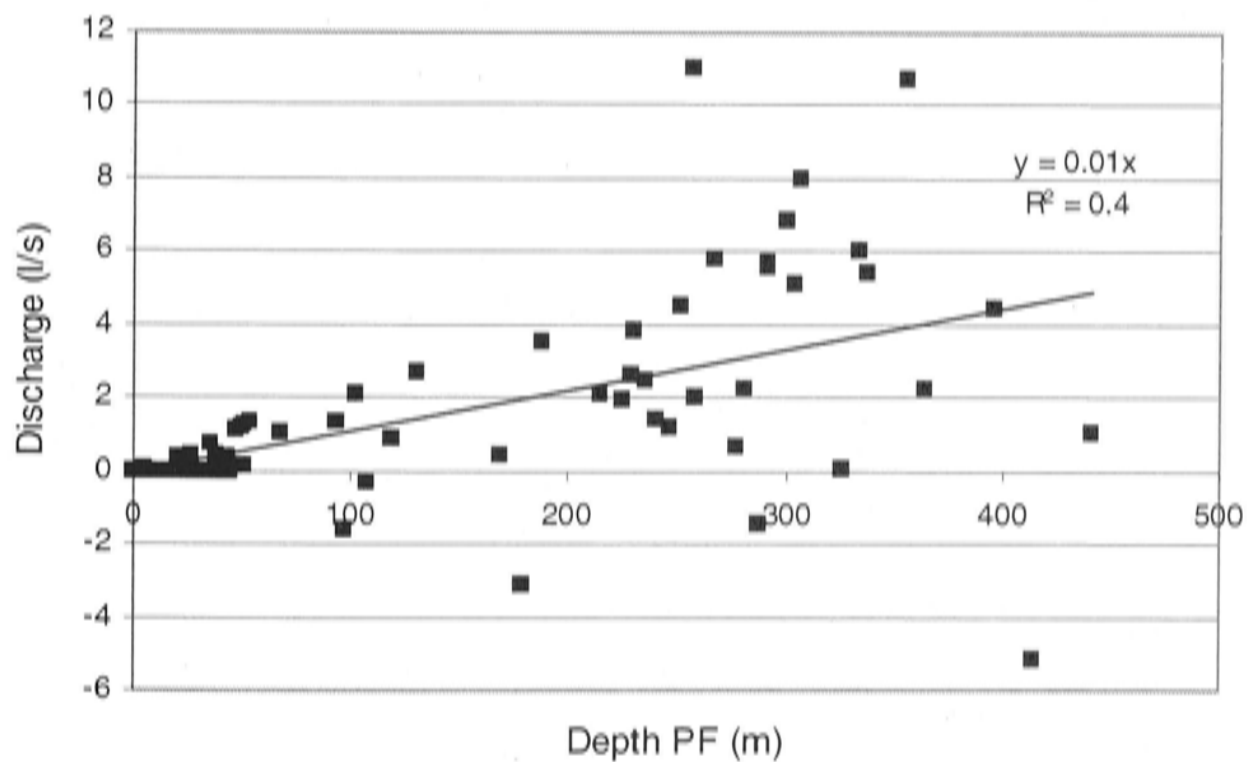


**Figure 7.11:** Depth - discharge rating curve based on 00-01 plant flume (PF) data (n=247,  $P < 0.01$ ).

### 7.3.7 Sediment export

Concluding from the analysis of the raw data, there are only three storm events recorded at the plant flume in the 00-01 season. The SSC of the samples taken from the flumes every two hours during the 14-18 February storm event are plotted in Figure 7.8. Other events are plotted in Appendix F (11).

A remarkable aspect of Figure 7.8 is that the sediment concentration peaks in the plant flume seem to coincide with both rainfall and reverse flow velocity peaks. It is not clear why these three processes occur at the same time. High sediment concentrations during a rainstorm are understandable, because the rainfall detaches new sediment from the field surface, which is transported with the runoff. However, the reverse flow that appears to occur at the same time, indicates that water from the drain flows back into the flume. Drain water is expected to be less turbid than water draining directly from the field, which contradicts the high sediment concentrations in the water samples. The flow velocity pattern is however rather noisy, which makes interpretation of the flume data difficult.

In the south flume, SSC was reasonably well related to flume water depth. When the plant flume samples are plotted in the same graph (Figure 7.12), it shows that some of the samples have relatively high sediment concentrations. Most of the high concentration samples are taken at intermediate flume flow depths of 20 to 30 cm. Samples taken at higher water levels have concentrations comparable to the south flume samples. This effect is also shown in the hydrograph of the only event during which both the plant and south flume were sampled (14-18 February 2001, see Figure 7.9).

It is difficult to explain the variation in sediment concentration from plant flume samples with the current data. It could indicate that water with relatively high sediment concentrations is still draining from the fields at intermediate drain water levels, while at higher flows this water is impeded and sediment-poor drain water is sampled. However, the velocity pattern of the flume does not confirm this interpretation.

It is hard to fit a curve through the Plant flume SSC data. This means that the sediment load from the plant flume will remain much more uncertain than the load from the South flume. To get some estimate of the total load a composite 'model' is used to estimate SSC from flume depth. For flume depths smaller than 200 mm the South flume equation is used and for all depths greater than 200 mm a new power function is fitted (see Figure 7.13).

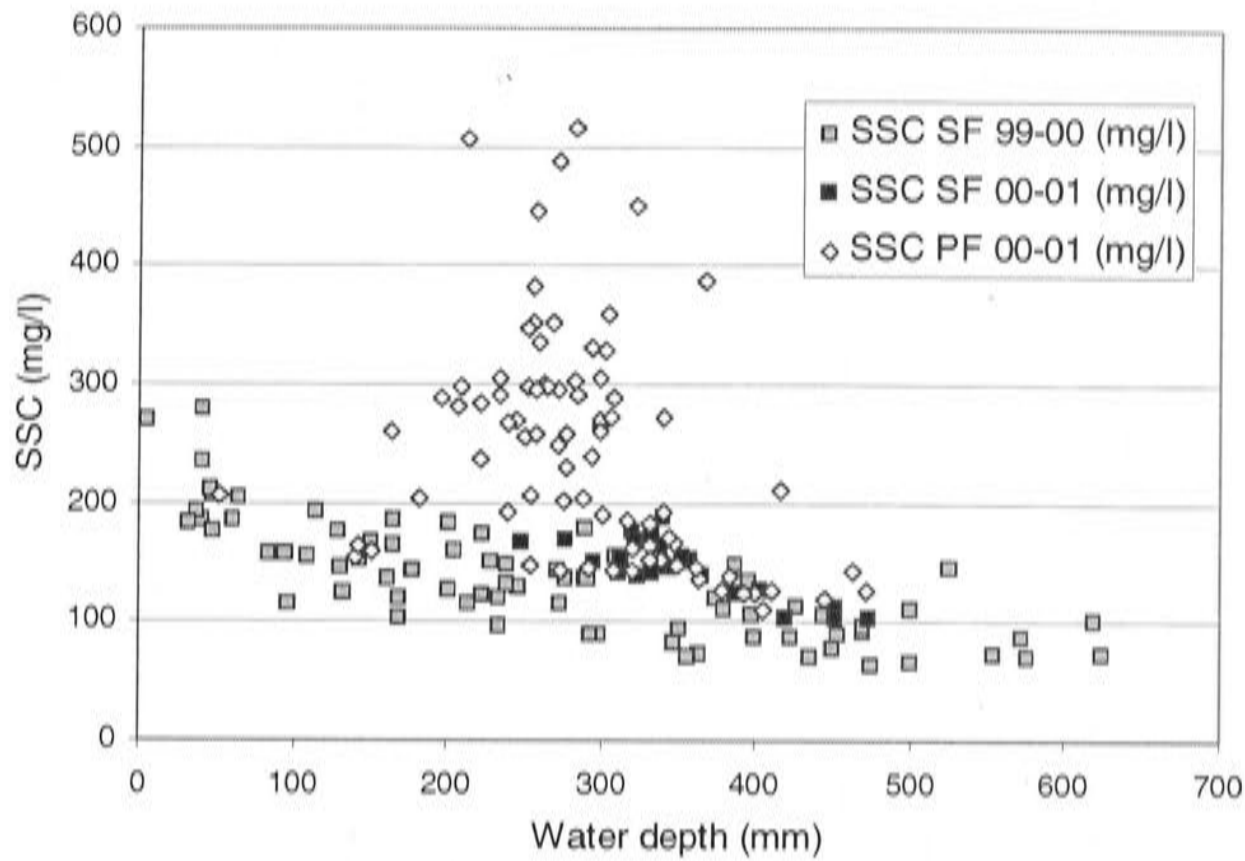


**Figure 7.12:** Suspended sediment concentration – water depth relationship for the south flume and plant flume. Samples for each season shown separately.

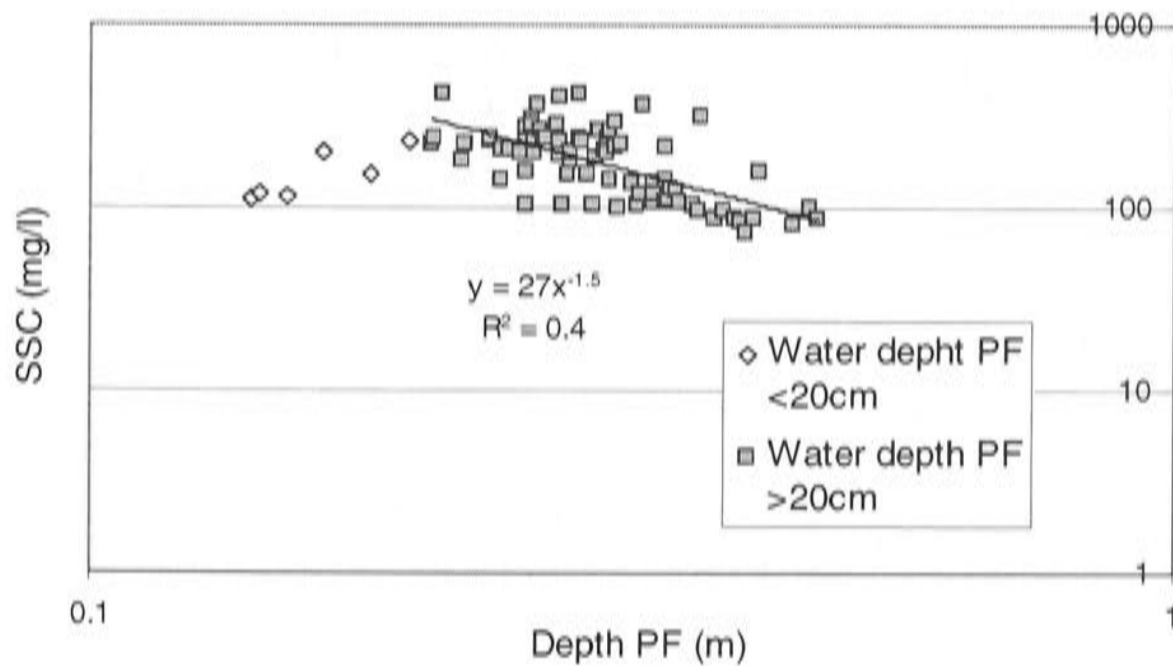


**Figure 7.13** Suspended sediment concentration – water depth relationship for plant flume water depths  $>20 \mu\text{m}$  ( $n=75$ ).

### 7.3.8 Plant flume load estimation for the 00-01 season

To obtain plant flume sediment discharge for the whole budget period, missing depth data are estimated from the equation in Figure 7.10, where possible. Missing discharge data are estimated from the rating curve in Figure 7.11. With the 'model' proposed in Section 7.3.7, the sediment concentration of the runoff is estimated.

Based on these estimates a total sediment load for the season is estimated, which is presented in Table 7.6.

Negative sediment discharge is treated as such in the load calculation. Negative discharge means that sediment is imported onto the field from elsewhere instead of exported from the field, so there will be accretion rather than erosion. The observed amount of reverse flow might not be representative, because the bunding funnel blocked most of the flow from the drain onto the field and concentrated the runoff.

### 7.3.9 Plant flume load estimation for the 99-00 season

There is no gauging data for a plant cane field for the 99-00 season, but during this season a large number of grab samples were taken in the catchment. Some of these samples were taken directly from the runoff that leaves the fields via inter-rows. Based on these water samples an estimate is made of the sediment export from plant cane fields during that season.

The SSC of all grab samples taken from plant cane rows are averaged. The average sample concentration is multiplied with the monthly runoff, providing an estimate of monthly sediment loads. The monthly runoff is calculated from rainfall and monthly runoff coefficients estimated for plant cane fields (David Mitchell, pers. comm.) (see Table 7.5) This method indicates a total sediment load of 5.9 tonnes per hectare plant cane.

**Table 7.4:** Turbidity and SSC in runoff from plant cane and ratoon rows.

Grab samples plant cane runoff 99-00				Grab samples ratoon runoff 99-00			
Field number	Date	Turbidity (NTU)	TSS (mg l <sup>-1</sup> )	Field number	Date	Turbidity (NTU)	TSS (mg l <sup>-1</sup> )
102 (PC)	7-Feb-00	164	136	28 (RG)	5-Nov-99	35	190
102 (PC)	5-Nov-99	131	278	29 (RG)	7-Feb-00	102	140
47 (PS)	7-Feb-00	103	127	48 (RS)	5-Nov-99	104	199
50 (PS)	5-Nov-99	325	394	58 (RS)	5-Nov-99	41	149
59 (PS)	25-Feb-00	190	170	80 (RS)	5-Nov-99	95	147
62 (PS)	5-Nov-99	1030	969				
84 (PS)	5-Nov-99	1001	922				
95 (PS)	5-Nov-99	318	324				
average SSC			415	average SSC			165
stdev SSC			341	stdev SSC			97

P = Plant cane field; R = Ratoon field; C = Clay; S = Silty clay; G = Grey sand

**Table 7.5:** Plant cane field load estimate based on grab sample SSC and runoff coefficients.

Month	Rainfall (mm)	Runoff coefficient (Mitchell, pers. comm.)	Runoff (mm)	Plant cane sediment load based on sample SSC of 415 mg l <sup>-1</sup> (kg)	Ratoon sediment load based on sample SSC of 165 mg l <sup>-1</sup> (kg)
from 21/12/1999	232	0.5	116	481	191
Jan-00	98	0.2	20	81	32
Feb-00	1027	0.8	821	3409	1355
Mar-00	337	0.7	236	978	389
Apr-00	442	0.5	221	917	365
till 3/05/2000	0	0.1	0	0	0
Total	2189		1414	5867	2332

A similar calculation based on the ratoon samples gives a sediment load of 2.3 t ha<sup>-1</sup> from a ratoon field. The 2.3 t ha<sup>-1</sup> is not very different from the estimate of 1.4 t ha<sup>-1</sup>, based on total seasonal discharge and SSC information from all flume water samples adjusted for furrow contribution.

It has to be stressed that most of the water samples used in the calculations of both the plant cane and ratoon load were taken early in November 1999, during one of the first summer rainstorms (see Table 7.4). Sediment concentrations in the runoff were relatively high compared to concentrations later in the season. This has two causes. Firstly, early in the wet-season the cane crop is still very small and does not provide a protective cover for the field surface. Secondly, the North Queensland wet tropics experience what is known as the 'first flush' effect (Mitchell *et al.*, 1991; Devlin *et al.*, 2000; Williams, 2001). The runoff from the first significant rainstorms of the wet season usually contain high sediment and nutrient concentrations, reflecting the mobility of oxidised N (and P to a lesser extent), and easily erodible soil material that has become available over the dry-season. Later in the season this source becomes depleted and sediment concentrations decrease. The total load calculated from samples predominantly taken in November is therefore likely to overestimate the 'true' load.

#### 7.4 Comparison and discussion of plant cane and ratoon sediment loads

Table 7.6 summarizes the sediment load estimates in tonnes per hectare for both plant cane and ratoon fields, based on the methods described above.

**Table 7.6:** Summary of sediment loads estimated from plant cane and ratoon gauging sites.

	Sediment load (t ha <sup>-1</sup> )	Runoff coefficient
<b>Ratoon</b>		
99-00	1.4	1.3
00-01	0.7	1.0
<b>Plant cane</b>		
99-00	5.9	n/a
00-01	1.7	1.1

For both seasons the amount of sediment coming from plant cane fields is clearly higher than that coming from ratoon fields. However, the methods used to estimate the sediment load are very different, and comparison of the ratoon and plant cane values and the differences between the seasons must be made cautiously. The method used to obtain the 99-00 sediment load for plant cane is thought to have the highest uncertainty and is likely to overestimate the true load, because of the biased sampling strategy.

The method used to obtain the 99-00 sediment load for ratoon is thought to be most accurate. The discharge used to calculate the load results however in a runoff coefficient of 1.3, which is impossible. If the rain gauge provides representative data, there are two possible explanations for the overestimated discharge. Either the runoff was over estimated due to errors in the calculation methods or data measurements, or runoff from outside the assumed catchment area was measured at the flume. Either of these explanations means that the sediment load is overestimated.

In Section 7.3.1 it was mentioned how differences in field characteristics between the plant cane and ratoon gauging site can complicate comparison and application of the data. The effects of the differences occur in combination; it is not possible to assess them separately. The following observations suggest how they may affect the sediment load estimates:

Soil type will affect erosion rates. The clay soil is thought to be less erodible than the silty clay soil (Timmer, 1998). This is confirmed by the water samples taken from field runoff (see Table 7.5). The samples taken from clay fields have relatively low SSC. Because the soil in the catchment is predominantly silty clay, the plant flume in clay soil would therefore underestimate the average sediment load from plant cane fields.

The effect of the differences in the hydrology between the site has been commented on earlier. Overall flow velocity from the plant cane field is lower, allowing less sediment transport and erosion by the runoff. This suggests that the plant cane site yields less sediment compared to the ratoon site.

The effect of the difference between the set up of the two gauging sites is unknown. Adjustment of the load from the ratoon flume for water furrow erosion will increase the error at this site, but it is not known whether this would cause either over or underestimation of the load.

An important observation made at the plant flume is the reverse flow of drain water onto the fields. This process violates the assumption made in Section 7.1, that fields do not serve as storage for sediment from external sources. In the load calculation for plant cane fields in 00-01 (Section 7.3.8), reverse flow has been taken into account. However, the results have been affected by the flume structure that blocked the flow. It is not possible to quantify this effect, but it should be noted that overbank flow does not only cover the headlands, but can also reach into the field beyond.

Potential errors in the gauging data due to movement of sensors, similar to what was observed at the drain outlets, have been ignored, because they cannot be quantified. There were some indications that parts of the depth data might be incorrect, but there were no ways to check this.

---

## **Chapter 8**

### **Headlands**

---

#### **8.1 Introduction**

Headlands are common elements of cane growing areas. They are strips of grassland along the margins of the cane fields with a width of 2-5 meters. The purpose of headlands is in the first place to allow turning space for the large cane harvesters, but they are also used to allow access into areas without roads and tracks. To improve drainage from the fields towards the drains, headlands usually slope several degrees in the direction of the drain.

Long grass on the headlands tends to attract cane rats. Cane rats feed on the sugarcane stalks and can considerably reduce the cane yield (Bureau of Sugar Experimental Stations, 2002). Canegrowers therefore prefer to maintain the shortest possible grass cover on their headlands. In most of the study area the grass is cut with 'slashers'. These machines cut the grass to the base of the plant and often leave patches of bare soil with a little grass stubble.

The combination of intensive vegetation management and a slightly sloping surface creates a situation that can be susceptible to erosion. At the start of the research some headlands showed clear signs of soil erosion such as rills and soil pedestals. Headlands were therefore identified as a potentially important source of sediment in sugarcane land. Reduction of sediment export from this landscape unit would require specific alterations of management practices. It therefore becomes a separate component in the sediment budget. In this chapter sediment export and sediment storage processes on headlands are quantified, so that their share in the sediment budget can be estimated.

#### **8.2 Headland erosion and deposition processes**

Preliminary erosion and deposition measurements were done on the headlands during the 98-99 season. The results of these measurements and additional observations in



the catchment provided a first insight into the erosion and deposition processes on the headlands. The experimental design that was used to quantify the headland budget component in the following seasons is based on these first impressions.

Erosion and deposition processes on headlands are thought to occur by two types of water flow. The first type of flow consists of water that drains from the inter-row spaces of fields across the headland towards the drain. This flow creates rills, which develop mainly from the margin of fields where concentrated runoff flows onto the headland surface. In situations where runoff from a field is rich in sediment, deposition occurs rather than erosion, and fan shaped deposits have been observed at the field margins. The second type of flow occurs when drains overflow onto the headlands during flood events. This process deposits coarse sediment in the vegetation along the edge of the drains and causes some surface scouring in the direction of the flow.

The combined effect of the two types of water flow causes a variable pattern of erosion and deposition across the headlands. The effects of both sediment deposition and scouring by overbank flow are expected to decrease further away from the drain, as velocity decreases. Runoff from the fields has most effect closest to the field margin. At the catchment scale, the magnitude of erosion and deposition processes probably varies as a result of spatial variation in headland surface conditions, drain proximity and drain size. The following headland surface conditions were identified as factors that potentially influence variation in erosion and deposition on headlands:

- Soil type: The texture of the soil in the catchment varies from clay to sand. Soil type has in earlier studies been identified as an important erosion controlling factor (Morgan, 1986; Timmer, 1998).
- Type of drain along which the headland stretch is located: Overbank flow from Ripple Drain and other major drains has high velocities and is therefore erosive and can transport more sediment than minor drains.
- Crop cover on the fields bordering the headlands: More sediment is expected to be transported onto the headlands from plant cane fields compared to ratoon fields.

- 
- Vegetation cover: Sites with clear signs of surface erosion often have low vegetation cover.

### 8.3 The erosion pin method

Erosion pins have been used to measure erosion and deposition on headlands during the two budget seasons. Pins are put into the ground as reference points from which changes of the soil surface level can be recorded. The method has been widely used in soil erosion research, because it is a fast and cheap way to obtain direct estimates of surface level change (Haigh, 1977; Stocking, 1987). An important reason for the application of the method in this study is also that it can provide separate information on both erosion and deposition rates.

Sutherland and Rorke (1991) applied erosion pins to measure several components of their sediment budget for the Katorin drainage basin in Kenya. The application was not completely successful, because most of the pins were disturbed, which reduced available data and hampered analysis. In his review of the use of erosion pins, Haigh (1977) mentions this as a matter that requires attention, together with the accuracy of the method; the interpretation of the measured surface level changes; and the potential influence of erosion pins on the measured processes. In addition to this Loughran (1990) notes how the method can not be used for long-term experiments in cultivated areas. All these matters have been taken into consideration for the erosion pin study on headlands and will be discussed in the following description of the application.

Often erosion pins are used in combination with washers, which serve as a solid base for the estimates of the pin height. In some studies the washers are not permanent but only applied at the time of measurement (Sirvent *et al.*, 1997). Haigh (1977) describes in his review how the continuous presence of the washer can have several advantages. By either collecting sediment on top of the washer in case of deposition or maintaining a soil pedestals beneath the washers in case of erosion, the washer can provide additional information on processes acting on the studied surface.

During trials on the headlands in the 98-99 season, both deposition on top of the washer as well as soil pedestal beneath the washer were observed. Disturbance of the

processes due to the presence of the washer was not apparent. The use of washers is therefore thought beneficial in this study.

## **8.4 Pinplot distribution: capturing variation**

### **8.4.1 Transect sampling**

Erosion pins can be used in a flexible set up, although they are usually installed as plots consisting of an array of pins. The measurements from the plot serve as a random sample of the local variation in surface level change. In this project it is important that the pin measurements sufficiently represent the variation in erosion and deposition processes on the headlands, because misrepresentation of the headland component will cause imbalance in the sediment budget.

The spatial variation in the type and magnitude of erosion and deposition processes on headlands, combined with the typical elongate shape of the landscape element determined the decision to use a transect type sampling plan. Pinplots were laid out as transects, which extend from the edge of the field to the drain. Each plot is five pins wide and seven to nine pins long depending on the width of the headland. Thirteen plots were spread throughout the catchment in the 99-00 season to include all surface conditions that were pointed out above. In the 00-01 season only seven plots were installed. For each plot an erosion and deposition rate is calculated. Statistical tests are then used to determine whether these rates are significantly different for plots on headlands with different surface conditions. If this is the case, the rates can be averaged across-catchment for areas with similar surface conditions, in order to obtain total amounts of erosion and storage on headlands in the budget area.

There are however a few difficulties with this method. On the headlands in the study area a wide range of different surface conditions occur that have the potential to influence erosion and deposition rates. For practical reasons it is not possible to compare the effects of all these conditions separately. The total number of sites that can be sampled and their distribution throughout the catchment is restricted by the following issues:

- Time to install, measure and remove plots is limited

- Pinplots prohibit access of vehicles to headlands or parts thereof and can thus only be in place when access is not required (that is during the wet season)
- Not all farmers allow access to their properties

#### 8.4.2 Pinplot distribution per season

In the 99-00 budget season 13 pinplots were installed in the Ripple Corner Catchment. Because soil type is thought to have much influence on the magnitude of erosion and deposition, the initial distribution of the plots was based on the three main soil types in the area. Two plots were located on clay soils, four plots on grey sand, and seven plots on silty clay. The boundaries of the soil types were taken from the Wood soils map (Wood, 1984). Within the three soil classes, plot sites were distributed among headland stretches along different drain orders. In total six plots were located along Ripple Drain, four plots along other major drains, and three plots along minor drains. At each of the selected headland sites two plots were installed. Where possible one of the plots was located along a field with plant cane crop and one along a ratoon field. This resulted in a total of seven plots along plant cane fields and six along ratoon fields. The number of plots that cover each surface condition are listed in Table 8.1 and the location of each plot is shown in Appendix B.

In the second season (00-01) the number of plots within the Ripple Corner Catchment was reduced to save operating time. However, the same sites were used to allow comparison between the seasons. None of the sites contained a plant cane crop so no plots were present along plant cane fields in the 00-01 season. The number of plots that represent each of the surface conditions for this season are listed in Table 8.1. The site locations are plotted in Appendix B.

**Table 8.1:** Distribution of pinplots across headland sites with different surface conditions.

Surface condition		1999-2000	2000-2001
Soil type	Silty clay	7	3
	Grey sand	4	2
	Clay	2	2
Drain type	Ripple Drain	6	2
	Major drain	4	2
	Minor drain	3	3
Crop type	Plant cane	7	-
	Ratoon	6	7

Vegetation cover of the headland surface was not taken into account in the distribution of the pinplots. Cover percentage is a continuous variable with a high spatial variability and is therefore studied in a different way. The cover percentage is estimated for each plot at the end of the season and its relationship with the erosion and deposition rates studied with a regression analysis.

### **8.5 Pinplot set up and measurements**

Each erosion pin plot is five pins wide. The number of rows varies between seven and nine depending on the width of the headland. The distance between pins is 50 cm. The decision for this plot size is based on visual observations of the small scale spatial variation and magnitude of the erosion processes. The pins consist of 350 mm long steel rods with a 5 mm diameter. They are driven into the soil with a hammer. The force used may have slightly disturbed the surrounding surface, but this is not thought to have significantly affected the measured processes. A 12 mm zinc washer is put on each pin.

The distance from the top of the erosion pin to the surface of the washer is measured with a digital calliper at a precision of 0.1 mm. The height of each erosion pin above the soil surface is measured twice on opposite sides of the washer. The mid-point of the two measurements is taken as the soil surface level at an erosion pin. This method handles measurement variation when the washer is not horizontal. When a washer is obviously affected by erosion or deposition processes, this is taken into account by taking additional measurements from the new soil surface level. The height values of all pins are averaged to obtain the net surface level change in mm for a pinplot. Erosion and deposition rates are obtained by separately summing positive and negative values and dividing them by the total number of pins in a plot.

### **8.6 Results**

In the 99-00 season the headland plots were installed in December, one week before the start of the stream/flume gauging. No rainfall was recorded on these first days, so the surface level change that occurred over this period is assumed insignificant and will not affect the total erosion and deposition rates.

All pinplots were measured at least twice after installation each season, in March and May. The successive measurement sessions provide information on temporal variation in the erosion and deposition processes, and disturbance of the plots can be

detected and corrected. Appendix G lists for both budget periods the net surface level change on each plot. Changes between individual measurement sessions within each season are also listed.

The 00-01 erosion value of plot M has an exceptionally high average erosion rate, considering its high vegetation cover of 99%. During the February measurements there was a clear sign of removal of soil around the pins, probably through digging by animals. The data from this plot are therefore excluded from further analysis.

### 8.6.1 Variation of erosion and deposition rate

The variation in erosion rates, deposition rates and net surface level changes for the different headland surface conditions is presented in boxplots. The boxplots for the 99-00 pinplot data are shown in Figure 8.1, 8.2 and 8.2. They are interpreted as follows:

- There appears to be more deposition on plots on clay soil, resulting in a relatively high net surface level change.
- There appears to be more deposition on plots along minor drains, resulting in a relatively high net surface level change.
- There appears to be a difference in both erosion and deposition rates between plots adjacent to plant cane and ratoon fields, resulting in a relatively high net surface level change on plots adjacent to plant cane fields.

Because the number of plots that could be installed was restricted and because their distribution was not random, the data are not appropriate for analysis using parametric statistics. Instead non-parametric statistics are used to test if there are differences in erosion and deposition rates between headland stretches with different surface conditions. The Kruskal-Wallis test, which is a non-parametric alternative for the one-way ANOVA test, is used.

The test results indicate that none of the erosion rates, deposition rates or net surface level changes is significantly different ( $\alpha = 0.05$ ) due to differences in any of the studied headland surface conditions (Table 8.2). The only difference is in the net surface level change on plots adjacent to fields with different crop types. In this case the Kruskal-Wallis test indicates a significantly higher positive surface level change

adjacent to plant cane fields relative to ratoon fields. Table 8.2 shows the probability (P) for all tests.

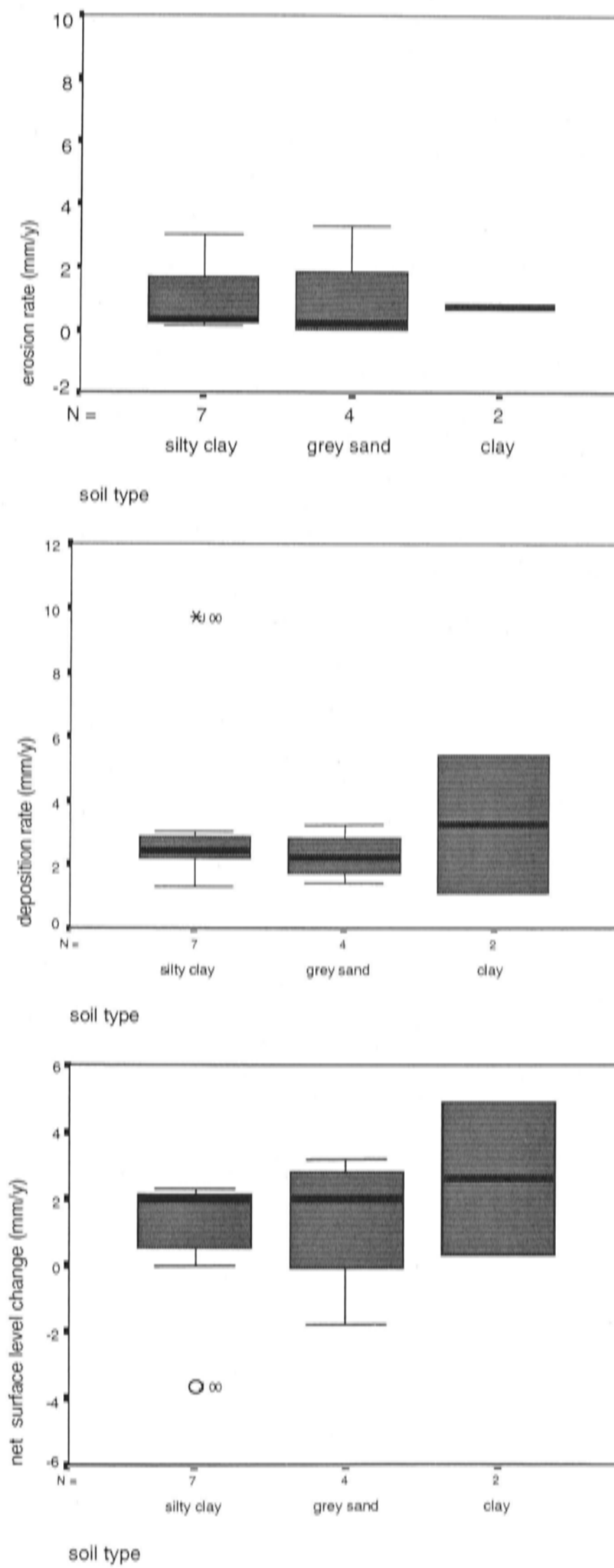


**Figure 8.1:** Boxplots for the variation in erosion rate, deposition rate and net surface level change on headlands during the 99-00 season, grouped by soil type.

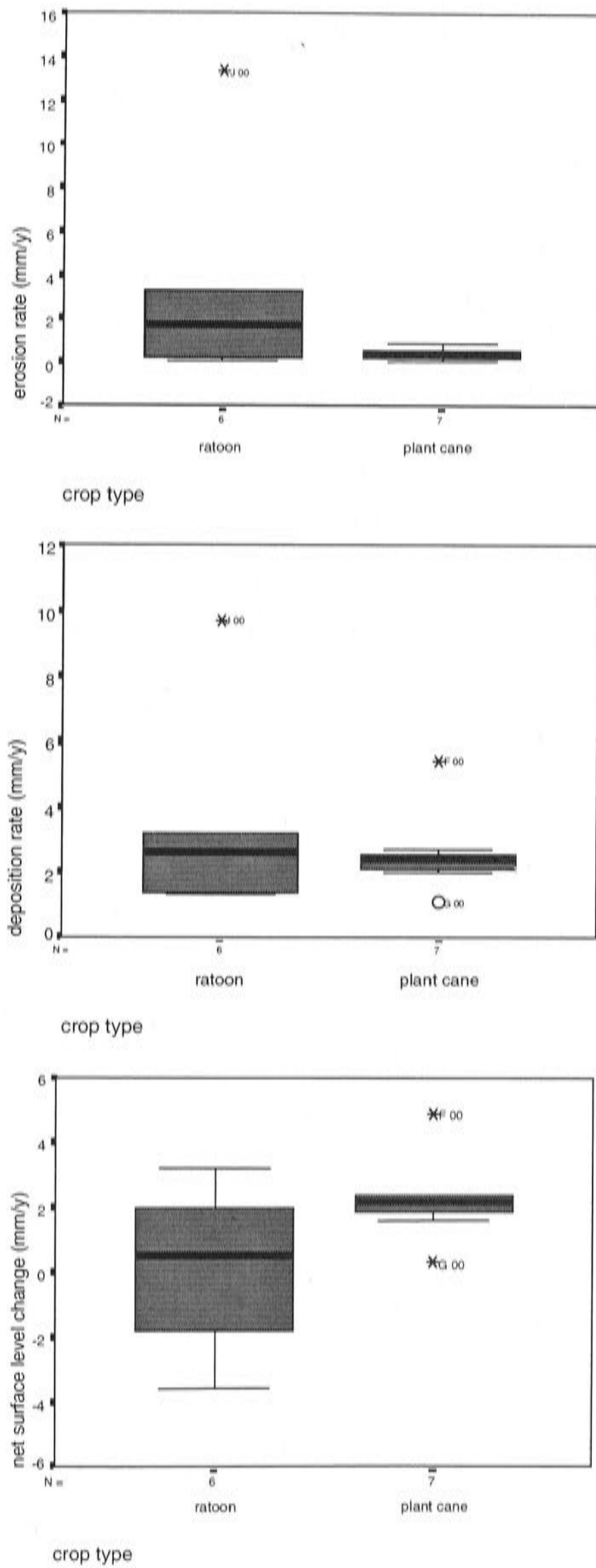


**Figure 8.2:** Boxplots for the variation in erosion rate, deposition rate and net surface level change on headlands during the 99-00 season, grouped by crop type.



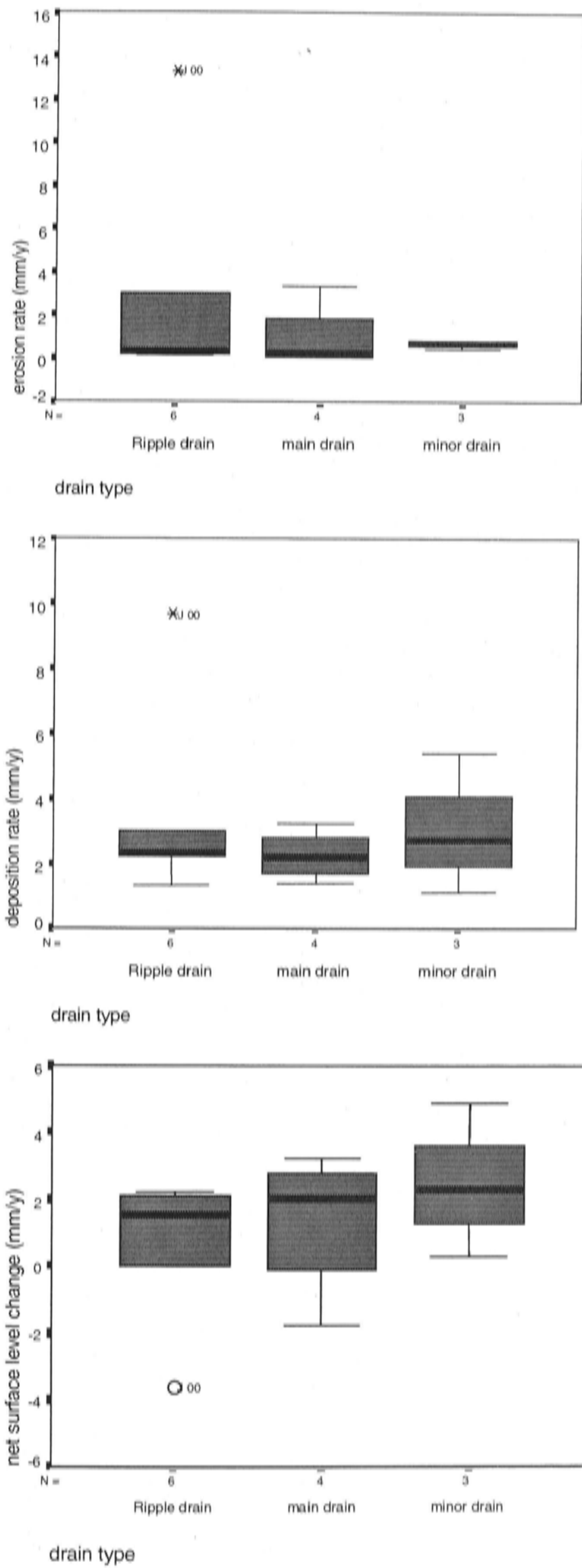


**Figure 8.3:** Boxplots for the variation in erosion rate, deposition rate and net surface level change on headlands during the 99-00 season, grouped by drain type.

From the boxplots in Figure 8.1, 8.2 and 8.3, deposition rates for headlands along minor drains and headlands on clay appear to be higher than for other surface conditions. These observed differences are however not significant, perhaps because of low sample numbers. Because the rates of change along minor drains are the same as those on clay soils, it is also not possible to say which of these conditions is likely to be more important in causing the difference in deposition rates.

**Table 8.2:** Results of Kruskal-Wallis tests for differences in surface level change due to differences in headland surface conditions.

Headland surface conditions	Surface level change	P for 99-00 data	P for 00-01 data
Soil type	Net	0.08	0.12
	Erosion	0.50	0.14
	Deposition	0.17	0.15
Crop type	Net	0.04	-
	Erosion	0.51	-
	Deposition	0.72	-
Drain order	Net	0.06	0.07
	Erosion	0.55	0.07
	Deposition	0.21	0.15

The boxplots for the 00-01 season are shown in Figure 8.4 and 8.5. The plots suggest that there is variation between the variables, but this is not confirmed by the Kruskal-Wallis test. The test indicates that none of the erosion rates, deposition rates and net surface level changes is significantly different ( $\alpha = 0.05$ ) due to differences in any of the studied headland surface conditions (Table 8.2). The sample sizes are, however, small and may not sufficiently represent surface conditions (see Table 8.1).

The difference between headlands adjacent to plant cane and ratoon fields could not be tested for this season, because none of the plots was located adjacent to plant cane. The total area of plant cane was less in this season: 20% compared to 34% in the 99-00 season (see Chapter 10) and there were no plant cane fields near sites suitable for the installation of pinplots.

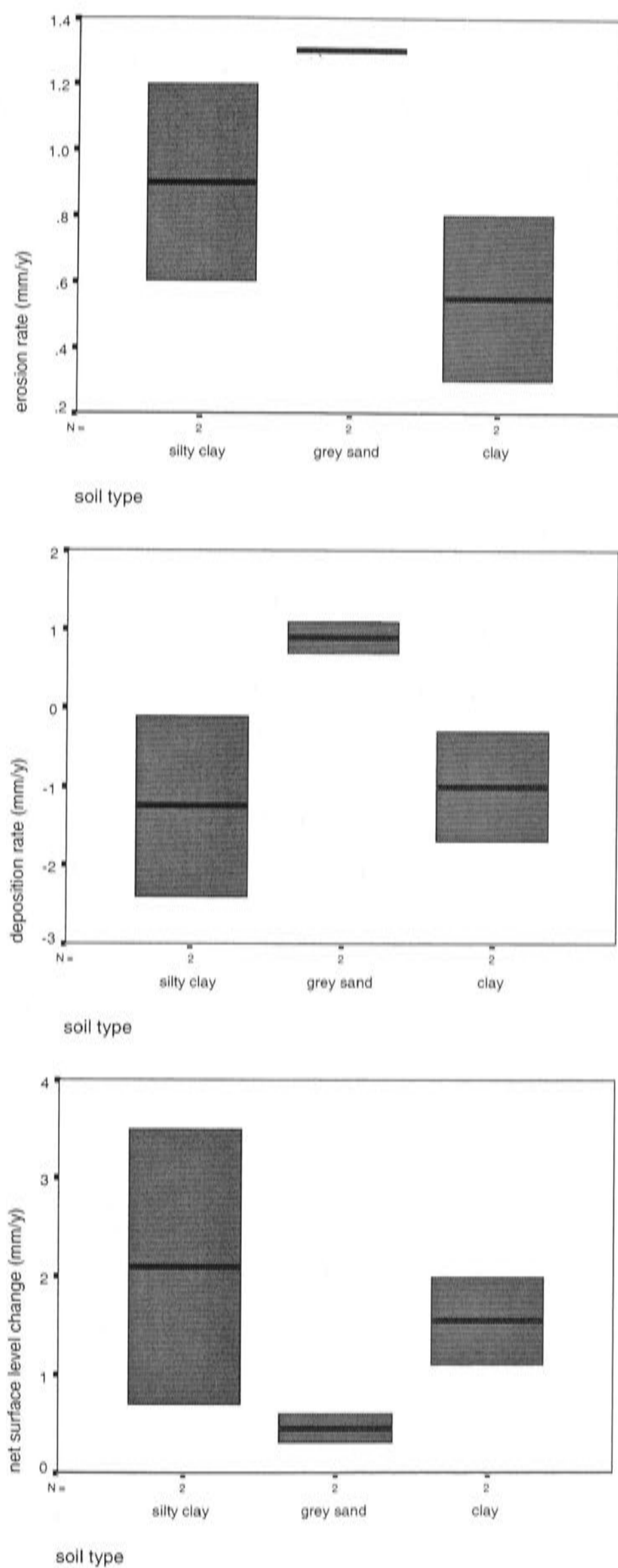


**Figure 8.4:** Boxplots for the variation in erosion rate, deposition rate and net surface level change on headlands during the 00-01 season, grouped by soil type.

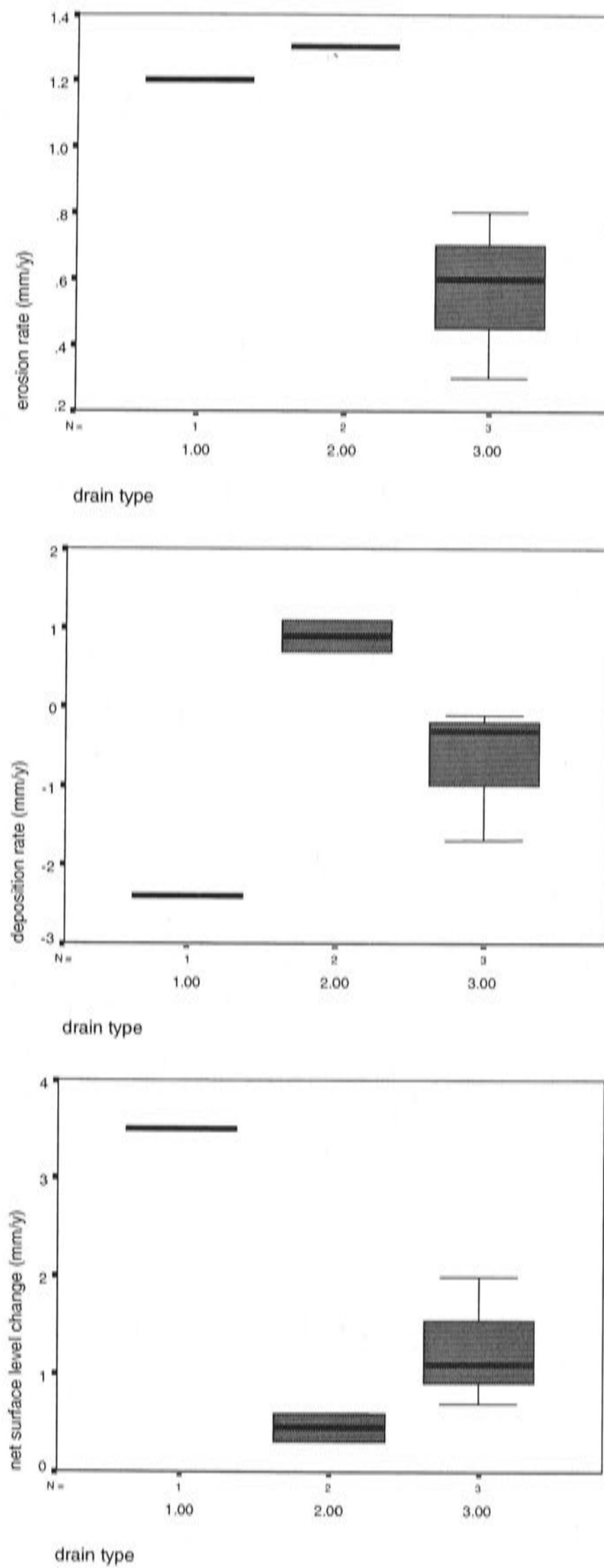


**Figure 8.5:** Boxplots for the variation in erosion rate, deposition rate and net surface level change on headlands during the 00-01 season, grouped by drain type.

## 8.7 Alternative load estimates

Surface level change on headlands was expected to vary with certain variable headland surface conditions, so that generalization to catchment scale based on those variables would be possible. However, there are no significant differences in erosion and deposition rates for any of the surface conditions, based on the available data. Total headland erosion and storage, which are required to estimate the sediment budget components, therefore have to be estimated in a different way.

### 8.7.1 Averages and medians

Given that spatial variation of erosion and deposition cannot be ascribed to headland condition, the most straightforward estimate could be based on averaging of erosion and deposition rates for all pinplots. However, the practical constraints for the location of pinplots resulted in a biased spread of pinplots across the catchment. Some extreme outliers are included in the data (see histograms in Figure 8.6). Because of the small sample numbers, these outliers will strongly affect the estimates of the average and cause significant overestimates of the total erosion and deposition rates.

The distributions of the 99-00 erosion and deposition rates appear lognormal. For the erosion rate data, logarithmic transformation results in a near normal distribution (Figure 8.7). A new average is calculated from the transformed data. The same transformation does not improve the distribution of the deposition rate data. In this case the median of the samples will best represent the total headland storage, because this statistic is not so much affected by the data outliers.

For the 00-01 data, totals are calculated from both the sample averages and medians. The sample size of the 00-01 data is too small to allow meaningful study of the sample distribution. The results of all described estimates are presented and discussed in Section 8.7.3.

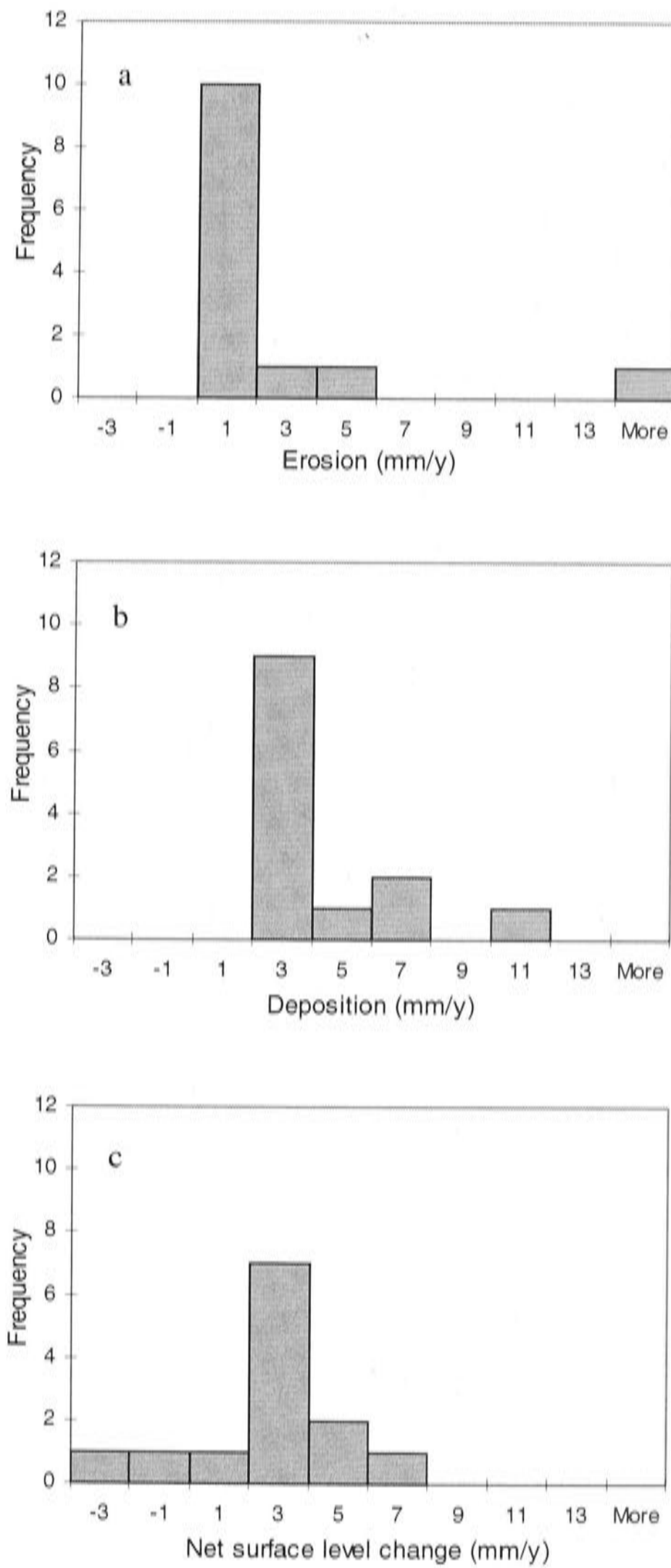


**Figure 8.6:** Histograms of erosion rate (a), deposition rate (b), and net surface level change (c) of all 99-00 pinplots from the Ripple Corner Catchment.

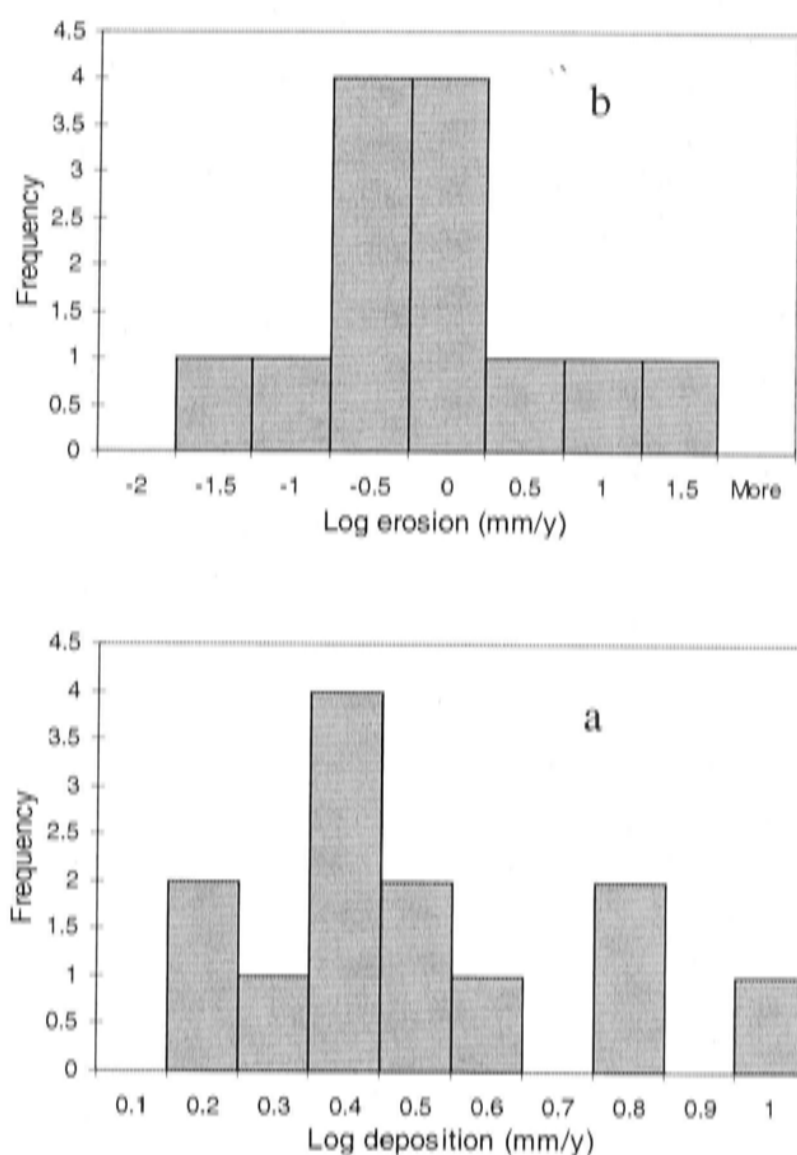


**Figure 8.7:** Histograms of the erosion rate (a) and deposition rate (b) of the logtransformed 99-00 pinplot data.

### 8.7.2 Estimate based on vegetation cover

Vegetation cover influences the occurrence of erosion and deposition (De Ploey, 1981; Morgan, 1986). Observations from the pinplots in the Ripple Corner Catchment indicate that high erosion rates occur on bare headland patches, while more deposition is observed on well-vegetated surfaces.

At the end of each budget period the vegetation cover percentage was estimated for each pinplot. The estimates consisted of simple visual assessment of the covered surface by two people. The average of the two independent estimates was used for the analysis. In addition to that a survey was made of vegetation cover percentages on headland stretches in a large part of the Ripple Corner Catchment during the 99-00 budget season. This survey was done in a similar way by the same two people.

The data from the pinplots has been studied to find out if it can be used in combination with the vegetation cover survey to predict the spatial distribution of headland surface level change. Based on the survey an alternative estimate of total headland erosion and storage could then be made.

For each season the pinplot vegetation cover estimates (VC) are plotted against the values for net surface level change (NSLC) (Figure 8.8). Both seasons show increasing surface level (deposition) with increasing vegetation cover and severest erosion with lowest vegetation cover as was expected. The trend in the 99-00 season data is however not significant ( $\alpha = 0.05$ ), because two outliers (G and F) affect the regression. If the data from these plots are excluded the regressions for both seasons become very similar. This is not necessarily expected, because yearly surface level changes could be different due to different weather conditions.

The following equations were derived from the regression curves.

For the 99-00 season:

**Equation 8.1**

$$\text{NSLC} = 0.06 * \text{VC} - 2.8 \quad (R^2 = 0.2, \text{ not significant})$$

For the 00-01 season:

**Equation 8.2**

$$\text{NSLC} = 0.06 * \text{VC} - 4.3 \quad (R^2 = 0.9)$$

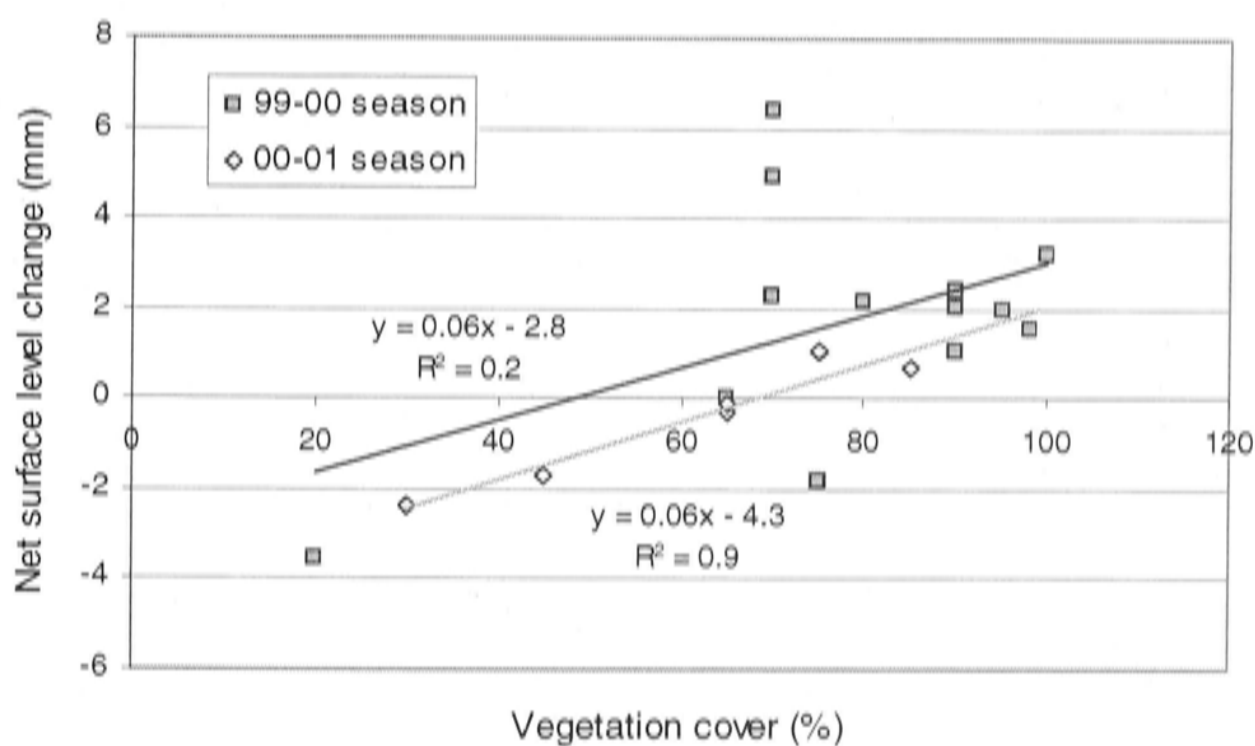


**Figure 8.8:** Scatter diagram of vegetation cover percentage and net surface level change (mm), with separate regressions for the 99-00 and 00-01 data ( $n=13$ ,  $P=0.09$ , and  $n=6$ ,  $P<0.01$ ).

During the vegetation cover survey, vegetation cover percentages were estimated for stretches of headland. A stretch usually extends along a drain segment, in between two side drains. From the cover percentages, net surface level change can be



estimated with Equation 8.1. Thus, for each surveyed stretch of headland a total sediment load (erosion or deposition) can be calculated from its surface area and surface level change estimate. Surface area is calculated from headland width (measured in the field) and length (estimated from an aerial photo). When the loads for all surveyed headland stretches are added and divided by the total headland surface area this results in an average net surface level change of 1.7 mm (deposition).

The vegetation survey was only done for approximately 75% of headland surface in the Ripple Corner Catchment, but the information is thought to be representative for the whole catchment.

The surface level change value obtained this way is not very reliable because it is based on the 99-00 regression, which is not significant. The relationship for the 00-01 season is significant, but the headland cover survey was not repeated. For this season an estimate is therefore made based on the 99-00 cover data, assuming that the overall cover was similar for both seasons. There is no reason to expect a significant difference between the seasons, although local variation between the seasons was observed. The estimate results in a net surface level change of 0.7 mm (deposition) for the 00-01 budget period.

### 8.7.3 Overview and discussion of estimates

The methods described above resulted in different values for net surface level change and erosion and deposition rates on the headlands. All values are listed in Table 8.3. The cells with values that are considered best estimates are shaded.

**Table 8.3:** Different estimates of erosion and deposition rates and net surface level change on headlands in the Ripple Corner Catchment. Best estimate shaded.

Rates in mm $y^{-1}$	Average	Log transformed	Median	Vegetation cover based
99-00				
Erosion	1.7	0.4	0.4	-
Deposition	3.3	-	2.4	-
Net	1.7	-	2.1	*1.7
00-01				
Erosion	1.4	-	1.1	-
Deposition	0.9	-	0.8	-
Net	-0.5	-	-0.2	**0.7

\*Calculated from insignificant regression equation

\*\*Estimated using 99-00 cover survey data

All estimates for the 99-00 season result in a positive net surface level change (deposition) on the headlands that ranges from 1.7 to 2.1 mm. The differences between estimates based on averages and medians show that the erosion rate, in particular for this season is strongly affected by outliers in the data. Logarithmic transformation of these data corrects the problem. The deposition rate is also considerably higher, but transformation does in this case not improve the data distribution, so an alternative deposition rate can not be calculated. For the net surface level change, which does not have a skewed distribution, the difference between averaged and median estimates is still more than 10%. The surface level change estimated from the vegetation cover information is equal to the estimate based on average data. This provides some confirmation of the results, although the uncertainties around each of the estimates are likely to be considerable.

Surface level changes estimated from the average and median of the 00-01 data indicate -0.5 and -0.2 mm headland erosion. Apart from the estimates for the deposition rate, differences between averages and medians are much greater than 10% percent for the 00-01 season. The value estimated from the vegetation cover data results in a positive surface level change. Because the estimates for this season are based on insufficient data and possibly incorrect assumptions, it is difficult to say which of these estimates is most reliable and will best represent the surface level change rates.

## **8.8 Additional observations**

The measurement design used to quantify the seasonal rates of surface level change on headlands did not aim to provide information on the processes that cause erosion and deposition. In order to apply effective sediment control measures it is however useful to understand the functioning and importance of the different processes. Several observations made during the fieldwork period give some insight into the processes and might be of help for the design of soil management strategies.

### **8.8.1 Observations of sediment deposits**

During the field study it became apparent that headlands can be important sediment stores. The material that is being stored originates from both types of water flow described in Section 8.2. The origin of the sediment influences the condition of

deposition and its size characteristics. Several observations were made of different types of sediment storage on headlands.

Thick deposits were often observed in dense grass cover close to the edge of Ripple Drain and the major drains. Analysis of soil surface samples from these locations showed that the material was sandier and better sorted than other headland surface samples (see Section 10.2). These deposits obviously originated from the drain water. Observations of sediment deposits on washers further away from the drain generally appeared to have finer texture, although they have not been analysed for sediment size. These deposits could have come from both field runoff and drain water.

Striking observations of sediment deposition on headlands were made after the first rainstorms in November of the 99-00 wet season. Especially headland stretches adjacent to plant cane fields were covered with sediment, while stretches along ratoon and fallow fields were not (Figure 8.9). The obvious source of this material is the runoff from plant cane fields. These sudden large amounts of deposition have never been quantified with erosion pin measurements, because installation of the pinplots was only possible later in the season when cultivation of the fields had finished.

Much of this observed sediment storage is likely to be only short term. In some situations the excessive deposition seemed to have smothered the headland vegetation cover, leaving a highly erodible surface.

### **8.8.2 Variation within pinplots**

The average values of erosion and deposition estimated from the pinplots disguise variation within a plot. Because this small-scale information is not of direct importance for the sediment budget calculation, it has not been studied in detail. However, the pinplot measurements confirmed some of the observations of headland processes that were described above.

Figure 8.10 shows spatial representations of the surface level changes on well vegetated (95% cover) pinplot M and bare (20% cover) pinplot J between four measurement sessions in the 99-00 season. Plot M shows slight and near uniform sediment accumulation and erosion across the plot. In contrast plot J gives an extreme example of severe erosion on the side of the plot that borders the cane land, probably caused by runoff from the fields. At the same time large amounts of

deposition occur along the edge of the drain, which probably consists of sediment trapped from overbank flow in grass patches.

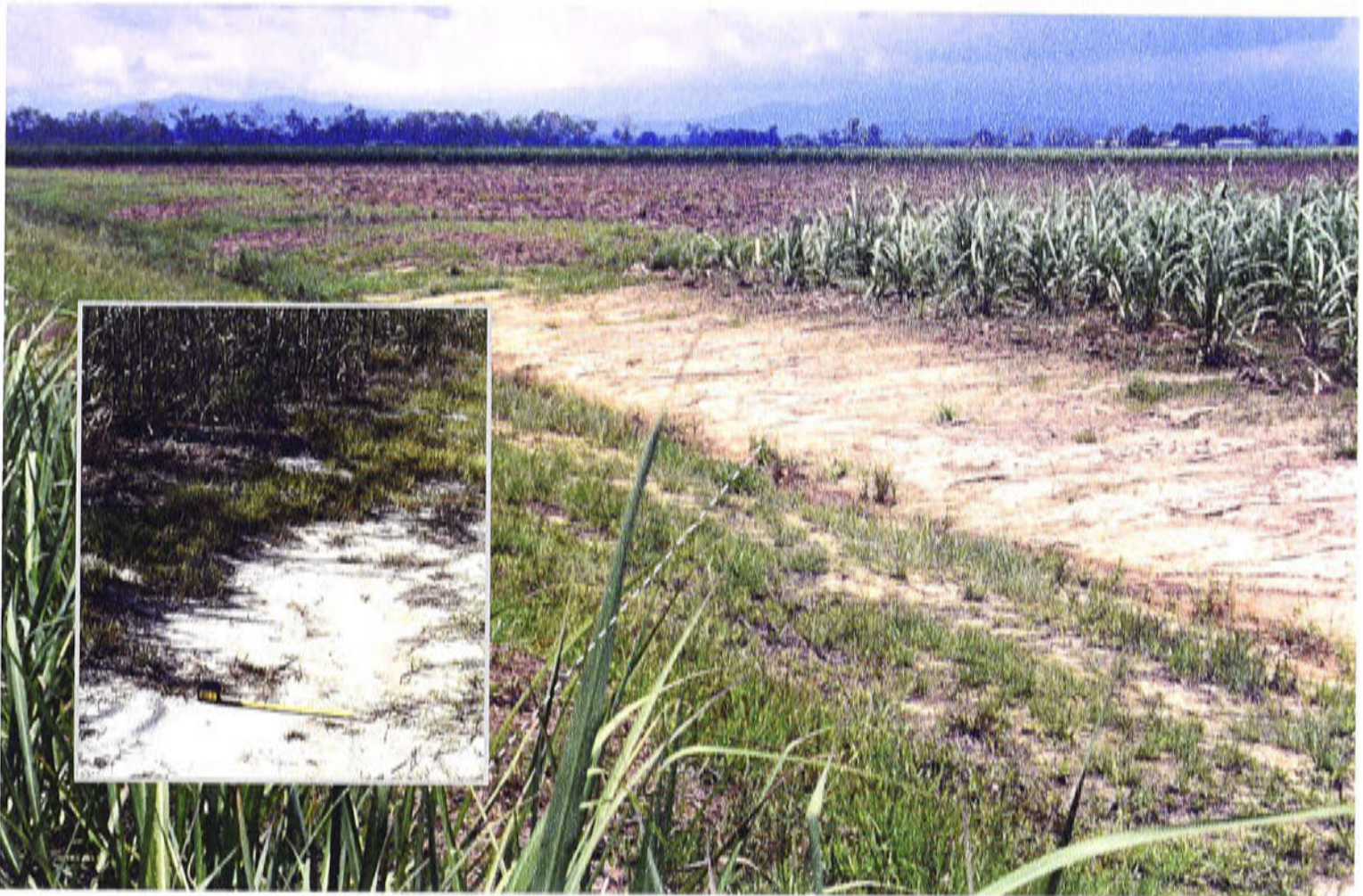


**Figure 8.9:** Headland along a plant cane (foreground right) and fallow (background) field. The headland section along plant cane is covered with sediment derived from the field after a heavy rainstorm in November 1999. The sediment buried the vegetation (see also inset; measuring-tape indicates 50 cm).

With the exception of plot J, which on average only erodes, plots do not show consistent erosion or deposition. There is also no consistency between different parts of a season, between separate seasons, or between adjacent plots. For individual pins, consistency is also unclear. Some plots (D and J) show evidence of alternating erosion and deposition between subsequent measurement sessions. In these cases the distance between the washer and the top of the pin had increased compared to the previous measurement session (indicating erosion), but a considerable layer of sediment had also accumulated on top of the washer. The high temporal variability is also visible from Figure 8.8.

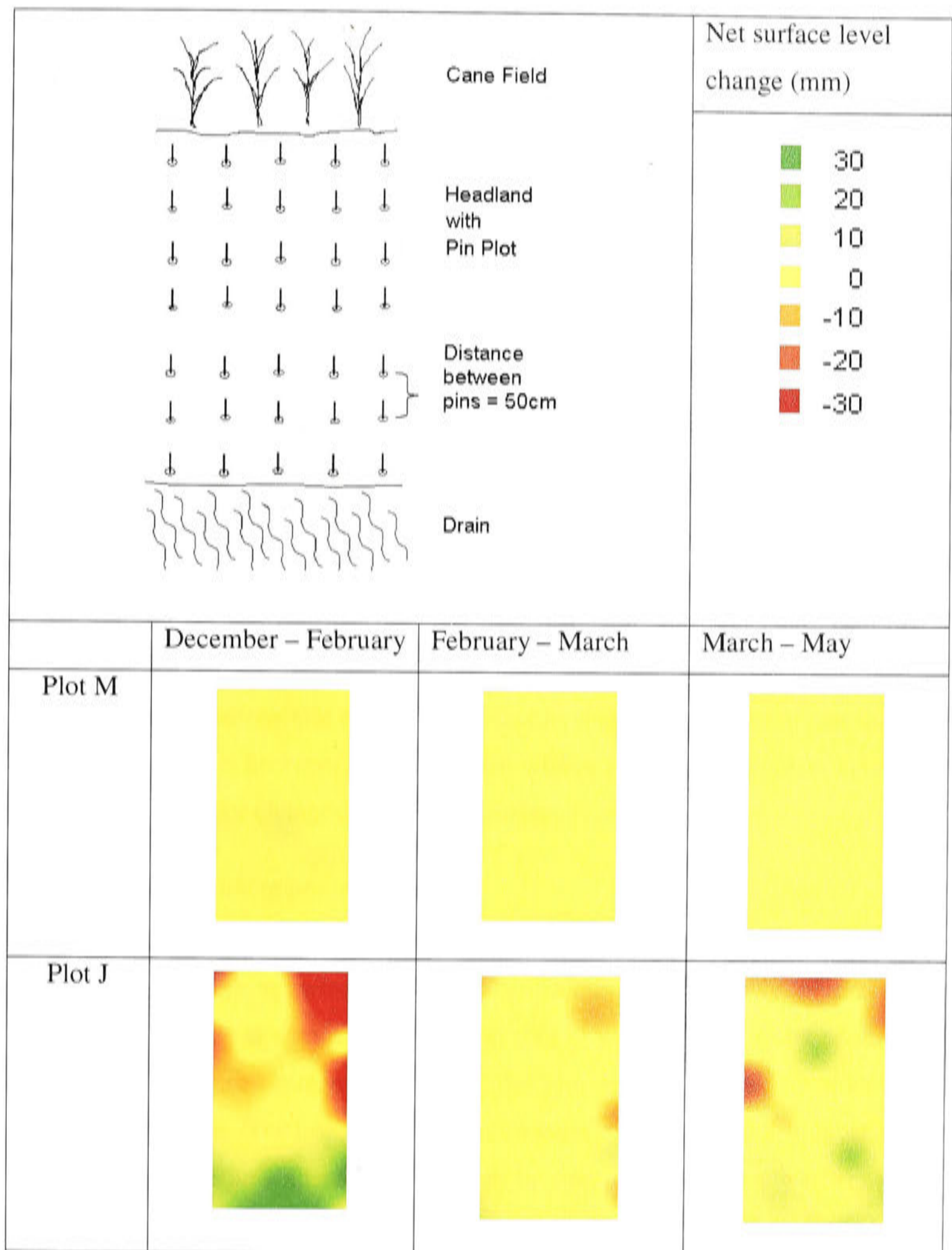


**Figure 8.10:** Spatial distribution of net surface level change on pinplots J and M between measurement sessions during the 99-00 season.

## 8.9 Other factors influencing erosion and deposition rates

### *Other factors affecting surface level change*

There are a number of other factors that have not been addressed previously, but which might play a role in the observations that were made on the headlands:

- Slope of the headland: Headland slope could especially influence the effect of field runoff. An increase in slope will increase flow velocities and thus reduce the possibilities for deposition.
- To improve field drainage a height difference is maintained between the field surface and the headland surface: A high step from the field onto the headlands may increase the possibility of scouring and rill formation by field runoff.
- Orientation of the headland relative to the rows (parallel or perpendicular). Headlands perpendicular to the rows receive most of the runoff from the fields. Headlands parallel to the field will be hardly influenced by this type of flow.

There were indications that each of these factors might affect erosion and deposition processes. There is however not sufficient evidence to make quantitative estimates of their importance for changes in headland surface level.

### *Swelling and shrinking processes*

The results of erosion pin measurements can be affected by the process of soil swelling and shrinking, which occurs in certain clay soils. Initially the process was not thought to be important, and potential effects were thought to be precluded by performing all measurement sessions under similar soil moisture conditions. An observation in the 00-01 season however changed this idea. On a number of plots some washers became attached to the pins by rust. Some of these washers were no longer level with the surface at the time of the last measurement session. They got stuck a few millimetres above the soil surface. For this to happen soil could have either eroded from underneath the washer or the soil could have shrunk. Also at the time of measurement, cracks were observed in the soil surface of the plots, confirming the possibility of shrinkage.

The plots with most of the 'raised' washers were F, G, M, and P, which are on silty clay and clay soils. For a few pins both the distance to the washer was measured

while it was still attached to the pin and after it had been pushed level with the surface. Table 8.4 shows the difference between these measurements for three pins.

**Table 8.4:** Pin height estimates for pins with rusty, stuck washers.

	Pin height from stuck washer (mm)		Average	Pin height from washer when level with surface (mm)		Average	Difference
Pin 1	92.6	92.4	92.5	95.9	96.9	94.1	3.9
Pin 2	130.6	130.4	130.5	134.8	135.4	132.3	4.6
Pin 3	143.4	143.3	143.4	146.3	145.9	144.5	2.7

Only a few pins in the concerned plots had their washers stuck, so it was not possible to say if similar surface level lowering occurred across the plot. Average surface level lowering across the plots is less (-1.3, 0.2, -1.4, and 0.0) than the values obtained from the pins with stuck washers; and pins showing deposition occur as well.

### 8.10 Conclusion: budget values

Various observations indicate that there are at least two different processes causing erosion and deposition on headlands (i.e. water draining from the fields and overbank flow from the drains). A wide range of factors potentially influences the magnitude of these processes, for example vegetation cover. As a result, both erosion and deposition rates show highly variable patterns in space and time. There is, however, a general indication that headlands can be a net store for sediment, especially when sufficient vegetation cover is present

Quantitatively only one of the headland surface conditions was identified to have a significant effect on headland erosion and deposition processes. Net surface level change was found to be greatest on headlands along plant cane fields. Several other observations also indicated increased sediment storage in relation to plant cane fields, stressing both the importance of sediment transport from plant cane fields and the importance of headlands in reducing sediment transport to the drains.

---

## Chapter 9

### Drains and Water furrows

---

#### 9.1 Introduction

Sugarcane production in a low-gradient floodplain landscape that receives large amounts of high intensity rainfall requires an efficient drainage network. Without this network runoff from the fields is slow and crops could be damaged when the soil remains waterlogged for too long. Figure 1.2 shows an example of the dense network of drains that accommodates the runoff from the cane fields in the Ripple Creek Catchment. The drains represent another landscape element and therefore another component of the cane land sediment budget.

Several sediment budget studies have shown that stream banks can account for more than 50% of the sediment export from a catchment (Walling and Woodward, 1992; Wallbrink *et al.*, 1998; Laubel *et al.*, 1999). However, the occurrence and magnitude of bank erosion processes, depends on many factors, which vary by location. For sections of several British rivers, Hooke (1979) showed that peak discharge and soil moisture condition are dominant factors in the occurrence of different types of bank erosion processes. Other authors also showed the importance of, for example, vegetation (Abernethy and Rutherford, 1998, 2000), frost (Stott, 1997; Prosser *et al.*, 2000) or livestock (Trimble, 1994) for bank erosion. In most situations the importance and interactions between the factors that cause bank erosion are still not fully understood (Stott, 1997; Green *et al.*, 1999; Laubel *et al.*, 1999).

If peak discharge and soil moisture control bank erosion processes under the wet tropical conditions in the Lower Herbert River Catchment, like they do in the British rivers studied by Hooke (1979), drain banks have a particularly high potential to be an important sediment source. The high frequency and prolonged periods of tropical rainfall will cause high moisture levels in the banks, which can promote the



occurrence of bank slumping. The high magnitude of peak discharge in the drains will cause direct scouring.

In addition to the climatic factors, the design of the drainage systems could also be of importance. Man-made drainage systems are not always able to drain the large amounts of runoff on floodplains. In such cases drainage systems have been shown to be sources of sediment (Lee, 1968).

## **9.2 Integrated Drainage Survey**

Within the Ripple Creek Catchment there are drains at the down slope end of most fields. All drains are connected and ultimately discharge into Ripple Drain, which is the main drain in the area. The size, catchment area, and design of all drains in the Ripple Creek Catchment were surveyed in detail as a part of the Integrated Drainage Survey (ID Survey) (BSES and CSIRO, 1997). During this survey information on the shape of the drains, their vegetation status, and signs of (bank) erosion were also documented.

Drains vary in size depending on their position in the drainage network, and thus the amount of discharge they carry. The results from the ID Survey indicated that the shape of the drains is closely related to their size and position in the system. Of the total length of drains in the catchment, the largest percentage has a 'spoon' shape. The cross-sectional profile of this drain type is curved (like a spoon). Spoon-shaped drains are usually the smallest drains, which form the lowest order branches in the network. They are shallow and their surface is usually covered with grass. These drains will be referred to as 'minor drains'.

The larger drains that discharge directly into Ripple Drain and that are fed by the minor drains will be referred to as 'major' drains. Ripple drain and most of the major drains have a 'regular' profile, which is a trapezoidal shape with relatively steep, straight banks. Less than 20% of the drains have more complex shapes. The profiles of the drain types that occur in the catchment are illustrated in the legend of Figure 9.1 (Roth *et al.*, 2000).

The information that was obtained from the ID Survey on bank erosion along the drains in Ripple Creek Catchment is summarized in Figure 9.1. The survey results show that spoon shaped drains show few signs of erosion, while most signs of severe erosion are observed in the regular drain type with steep banks.

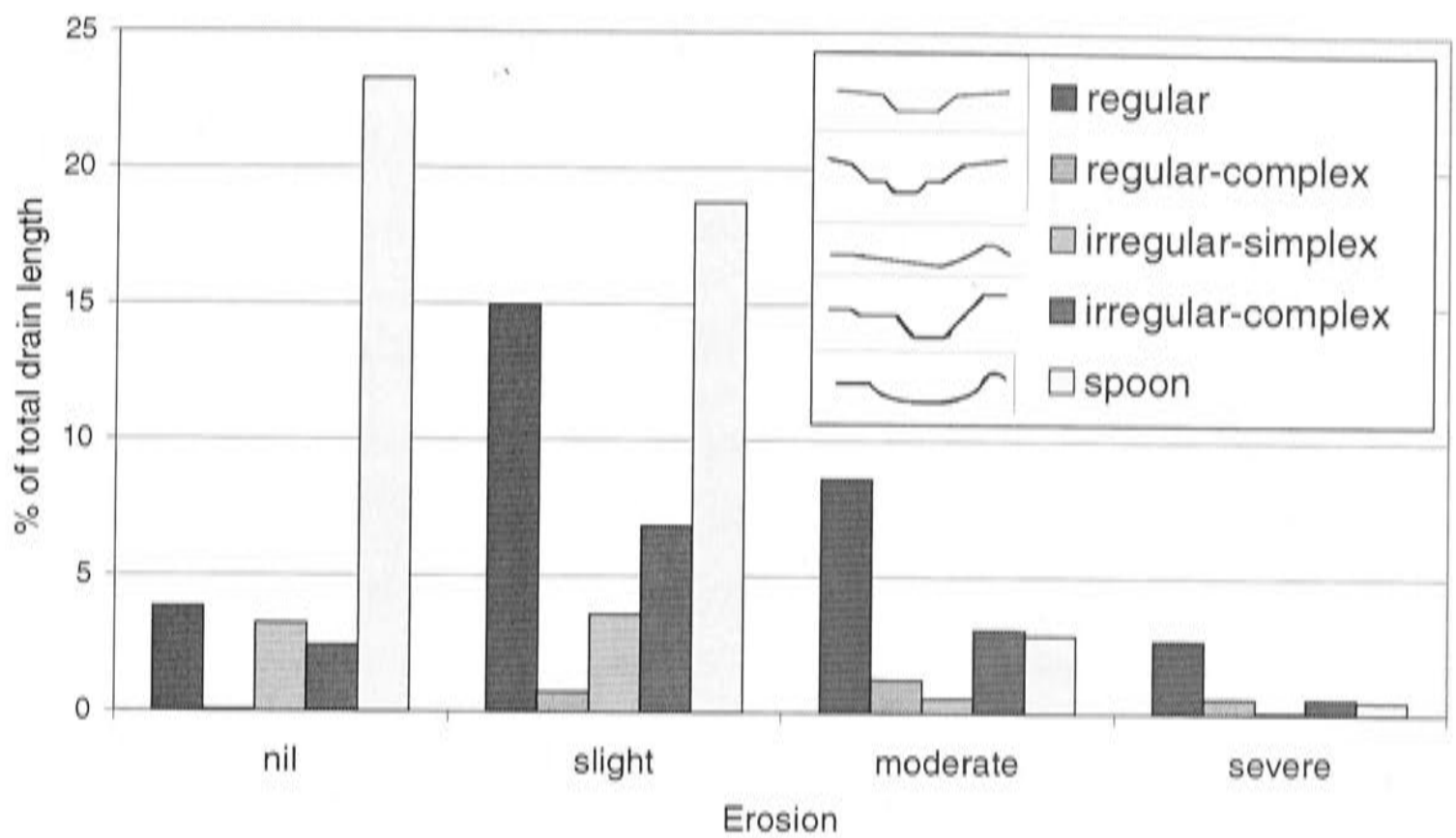


**Figure 9.1:** Signs of soil erosion in different drain types in the Ripple Creek Catchment; results from the Integrated Drainage Survey (Roth *et al.*, 2000).

### 9.3 Water furrows

In addition to the drainage structures in between cane fields, drainage is also improved within the fields through the installation of water furrows. Water furrows are drainage structures that extend over the full length of a field. They are spaced at intervals of approximately 20 meters. Water furrows have a spoon-shaped profile, but are narrower than drains and do not have a vegetation cover. The recommended size of water furrows is 2.5 m wide and 0.25-0.5 m deep, usually set by the size of the laser-controlled scoop, with which they are created (Kingdon, 1991). Water furrows are regularly re-worked to maintain sufficient depth and to remove vegetation.

In-field drainage structures such as water furrows are rarely discussed in the literature, although they can be important sediment sources (Alonso *et al.*, 1988). The processes that occur in water furrows are distinctly different from most river and drain erosion, where bank collapse is important. They are also different from field runoff, because runoff in water furrows is concentrated and might become more powerful.

Because erosion and deposition processes are likely to be different and because of their particular position within the cane fields, water furrows require soil

management procedures different from those for drains. In the sediment budget they will be represented as individual budget components. However, the same methods were used to quantify erosion and deposition rates in these landscape elements, therefore water furrows and drains are discussed together in this chapter.

## 9.4 Surface profile meter method

Erosion in rivers is often quantified with erosion pins in the riverbank (Hooke, 1979; Lawler, 1993; Stott, 1997; Laubel *et al.*, 1999; Couper *et al.*, 2002). This method is similar to that applied in the study of erosion and deposition rates on headlands (Chapter 8). However, erosion as well as deposition processes in rivers and drains can also occur on the riverbed. To obtain a closed sediment budget of the Ripple Corner Catchment, erosion and deposition rates on both the bed and banks need to be quantified. In the larger drains, which carry water throughout the year, measurements of pins placed in the drain bed will be difficult. Pins in the drain cross-sections will also catch vegetation debris, such as grass and logs, which are likely to cause significant disruption of the position of the pins (Lawler, 1993). In some situations erosion pins can even modify erosion processes by reinforcing the riverbanks (Thorne, 1981).

An alternative method for the direct measurement of erosion and deposition processes on stream profiles is the surface profile meter (Hudson, 1993; Sirvent *et al.*, 1997; Prosser *et al.*, 2000). A profile meter is a datum from which changes in surface level are measured. The datum usually consists of a horizontal bar, which can be attached to supports, fixed in the ground. From the bar a rod is lowered down to the soil surface. The fixed supports enable repeated measurements at exactly the same location each time.

### 9.4.1 Profile meter design

Based on the principle outlined above, a new profile meter was designed and built for the budget study. A schematic drawing of this profile meter is shown in Figure 9.2. The horizontal bar (the datum) of the profile meter consists of a square aluminium pipe. Holes are drilled in the pipe at 10 cm intervals. An aluminium rod fits tightly through the holes, so lateral variation in the position of the rod is minimized. The bar has a total length of 5 m but can be split to facilitate transportation. For short drain and furrow profiles it is sufficient to use only one half of the bar. The bar rests on

two aluminium legs. The legs fit tightly into aluminium supports, which are installed at fixed positions in the soil on either side of a drain or water furrow. The supports are 35 cm long aluminium tubes with pointy tips, which are driven into the ground until the opening on top is level with the soil surface. The aluminium rod that is used to measure the distance from the profile meter bar to the ground surface is 2 cm in diameter and contains a mm scale.

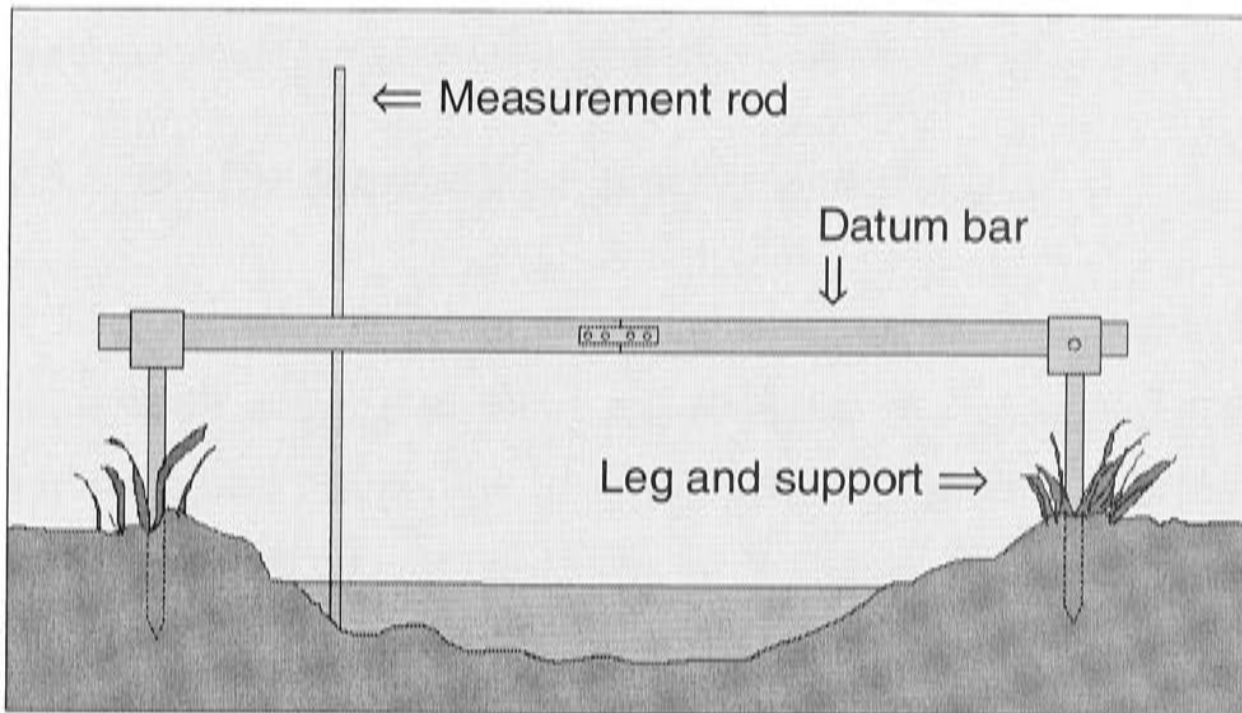


**Figure 9.2:** Schematic representation of the surface profile meter.

#### 9.4.2 Method disadvantages

It was mentioned before that the surface profile method has the advantage over the erosion pin method that the method of measurement does not disrupt erosion and deposition processes. The design of the two permanent supports, which are level with the soil surface, also ensures that the method interferes less with farming practices. Besides advantages, the method also has the following important disadvantages:

- (Undetected) disturbance/movement of the profile supports can influence the measurements.
- Movement of the profile bar and rod during measurements will cause variation in the measurements.
- The weight of the measurement rod can compact the soil surface during measurement, causing an underestimation of net surface level change.
- The analogue scale is less precise than the digital calliper used for the pin measurements.

- The method does not provide an additional opportunity to detect erosion and deposition processes, like the washers do for the erosion pin method.

These disadvantages mainly cause the method to be considerably less accurate. However, because the rates of erosion and deposition are expected to be larger in the drains and water furrows compared to the rates observed on the headlands, the percentage error for each method might be similar. The effect of error in the measurement of budget components will be further discussed in Chapter 11.

## 9.5 Profile distribution: capturing variation

### 9.5.1 Erosion and deposition processes in drains and water furrows

In the 98-99 season, preliminary measurements were carried out in drains and water furrows around Palmas' site. The observations from this season combined with the information that was obtained from the Integrated Drainage Survey suggested that the following drain characteristics were important factors in the control of the erosion and deposition processes in drains and water furrows.

- Soil type: The texture of the soil in the catchment varies from clay to sand. Soil composition is thought to be a major factor that determines the occurrence of bank erosion (Hooke, 1979; Green *et al.*, 1999).
- Size of drain: Ripple Drain and the major drains carry more water with higher flow velocities. In these drains erosion is likely to be higher than in the minor drains.
- Shape of the drain: This could influence erosion and deposition processes in different ways. Steep drain banks might, for example, be more prone to undercutting and collapse than gently sloping banks.
- Crop type: For water furrows the crop type of the field in which they are situated might affect erosion and deposition rates, mainly because of the different composition of the runoff they conduct. This factor is not expected to have significant effect on drain erosion and deposition processes, however.

### **9.5.2 Transect sampling**

Erosion and deposition processes will vary across the drain, particularly in drains with a regular shape where there is a distinct difference between drain bank and drain bed. With the surface profile meter a transect of sample points is measured. The average erosion and deposition rates calculated from a profile are assumed to represent processes at the point in the drain or water furrow where the profile was taken. The magnitude of these processes will change throughout the drainage system as a result of variation in the drain and water furrow characteristics pointed out in Section 9.5.1. For profiles in drains and water furrows with similar characteristics, the average erosion and deposition rates are expected to be similar and will be used to calculate the final sediment budget value.

Erosion rate is calculated from the surface profile data by adding all records of soil surface level decrease and dividing them by the total number of records in the profile. Deposition rate is calculated in the same way by adding all records of surface level increase. Net surface level change is obtained by adding all records and dividing them by the total number of records.

The profile method does not obstruct cultivation activities, like the erosion pin method does (Section 8.4.1). The distribution of measurement sites through the Ripple Corner Catchment was therefore more representative. However, the number of profiles was still limited because of time constraints and limited access to certain areas. For practical reasons clusters of three or four profiles were located in the same stretch of drain. The stretches were chosen to represent a wide range of drain characteristics (soil type, drain order). The data were not sufficient to compare each of the drain characteristics separately, and because many profiles are taken in the same stretch of drain or water furrow, it is in many cases not possible to single out factors influencing erosion and deposition rates. However, a general analysis of the data is performed using non-parametric statistics.

### **9.5.3 Profile distribution per season**

The distribution of the profiles through the Ripple Corner Catchment in the 99-00 season firstly aimed to cover all drain types (main, major and minor), because this was assumed to be the most important factor influencing erosion and deposition processes. Next, profiles for each drain type were located in the different soil types.

This was not always possible, because in the study area not all drain types were present in each soil type. There were only Ripple Drain profiles in silty clay. There were no major drain profiles in clay, and no minor drain profiles in grey sand.

In the second season (00-01) the number of profiles was reduced to save operating time. The same sites were used to allow comparison between the seasons and the same combinations of drain type and soil type were covered. Four profiles are exactly the same as in the 99-00 season (profiles 18-21).

The number of profiles that represent the various drain and furrow characteristics in each season are listed in Table 9.1. Initially more profiles were installed, but the data from these became useless in the course of the field season for the reasons listed in Section 9.6. The location of the profiles in each budget season are indicated on the maps of Appendix B.

**Table 9.1:** Distribution of profiles across drains and water furrows with different characteristics (numbers used for data analysis).

		1999-2000	2000-2001
Drain type	Ripple drain	4	5
	Major drain	11	5
	Minor drain	8	8
Soil type drains	Silty clay	14	14
	Grey sand	7	2
	Clay	2	2
Soil type water furrow	Silty clay	8	3
	Grey sand	11	3
	Clay	8	3
Crop type water furrow	Plant cane	8	-
	Ratoon	19	-

#### 9.5.4 Particle size adjustments

The profile measurements provide estimates of the volumes of soil being eroded or deposited. Because the budget will only include particles  $<20 \mu\text{m}$ , the profile meter data have to be adjusted, in order to represent this sediment size. For each measured profile, adjustments are made based on the type of soil in which the profile was located. In the major drains, further adjustment is also made for particle size differences in bank and bed material, because sediment samples from the drain beds were significantly sandier than those from banks (see Section 10.2). Adjustments are made to individual data records in a profile before erosion and deposition rates are

calculated. A description of the exact methods used is given in Chapter 10.

The adjustments change the data from different profiles in different ways. They will therefore influence statistical tests on differences in surface level change in relation to soil type as well as in relation to drain type.

## **9.6 Results**

### **9.6.1 Profile data availability**

In the 99-00 season the profiles were installed in December, one week before the start of the stream/flume gauging. No rainfall was recorded on these days, so the surface level change that occurred over this period is assumed insignificant and will not affect the total erosion and deposition rates.

All profiles were measured twice after installation, in March and May. Subsequent measurements provide information on temporal variation in the erosion and deposition processes, and disturbance of the site could be detected. During the two field seasons several profile supports were lost, disturbed or for other reasons not useful. Some profiles were measured only once after installation. These profiles are listed below, and it is noted whether or not a profile is included in further analysis.

99-00 Season:

- Profile supports 4,5 and 6 had been lifted after March measurement. May measurements have been adjusted by assuming that the first record of the affected side should be equal to the same record of the March measurement and that the first record on the unaffected side is correct. All records in between are adjusted proportionally and are included in the analysis.
- Profile 21 (lost), 30 (bent), and 31 (bent) were not measured in May. Profiles are included in analysis, because considerable changes were recorded between December and March. Potential misestimation of processes due to the missing May data are taken into consideration with the interpretation of results.
- There are no profile numbers 22 and 23.
- Profile 24 first installed in March and is not included in the analysis.
- Profile meter leg did not fit in support of profile 55 after installation and is not included in the analysis.



- 44-47 Removed and re-installed in January and included in analysis.
- 5,6,11, 25-27, and 36-43 not measured in March and included in analysis.
- 12 lost after installation and not included in analysis.

00-01 Season:

- Profile 1 and 2 supports lost, so no May measurement and not included in analysis.
- Profile 15 support removed and re-installed in March and not included in analysis.
- Profile 21 support damaged and not included in analysis.
- Profile 8 disturbed and not included in analysis.

All drain and water furrow measurements are shown as surface profile graphs in Appendix I. Figure 9.3 gives an example of a profile for a water furrow in a ratoon field on grey sand (profile 1). The difference between the profile records on the three measurement dates show how during the 99-00 season certain parts of the water furrow surface were eroding, while deposition occurred in other parts.

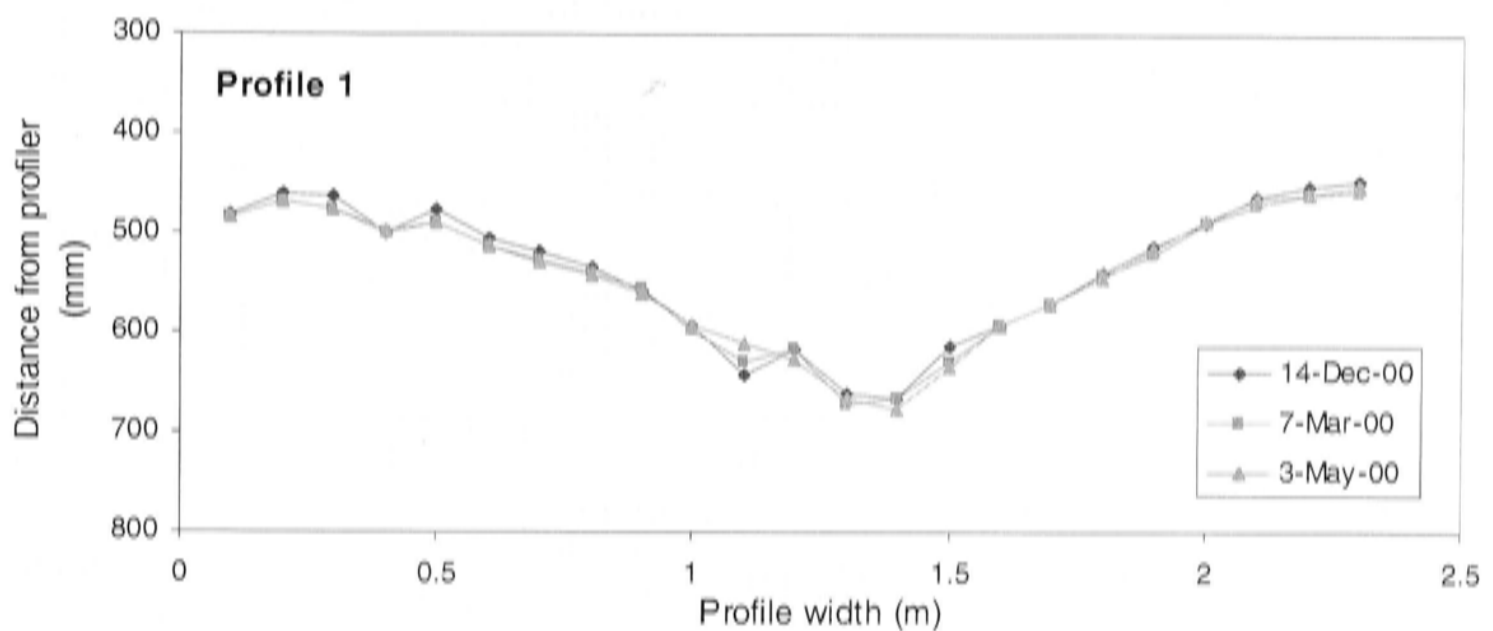


**Figure 9.3:** Example of a surface profile through a water furrow in a ratoon field on grey sand (profile 1).

### 9.6.2 Variation of erosion and deposition rates for drain types

Because there is a close relationship between drain type and drain shape, these factors are not studied separately. Only different drain types are studied to find out if there are significant differences in erosion and deposition processes. The boxplots in

Figure 9.4 and 9.5 show the variation in (original) net surface level change and erosion and deposition rates for all drain types in the 99-00 and 00-01 season. Water furrows are also included in the graphs for comparison. The data for both seasons is listed in Appendix H. The appendix also shows the data after adjustment for sediment size.

The data from profiles taken in Ripple Drain stands out in both seasons, because of the high deposition rates. Field observations show that most of the deposition is sandy material on the bed of Ripple Drain. After adjustment of the data for sediment size the amount of deposition is considerably reduced. The high deposition rate in the 00-01 season is not reflected in the net surface level change, because its effect is offset by a high erosion rate. Minor Drains show net deposition for both seasons. Furrows show net erosion for both seasons.

The non-parametric Kruskal-Wallis test indicates for both seasons that the erosion and deposition rates on the profiles calculated from the original data are significantly different ( $\alpha = 0.05$ ) for at least one of the drain types (Table 9.2). The data from Ripple Drain is obviously most different. Only the net surface level change of the 00-01 season does not show a significant difference. In this season erosion and deposition cancel-out. When the data are adjusted for sediment size the different magnitude in erosion and deposition processes in the Ripple Drain is masked, because it mainly consists of coarse material.

**Table 9.2:** Results of Kruskal-Wallis tests for differences in surface level change in drain profiles due to differences in soil and drain type. Significance of original and adjusted data for each budget season are shown.

Profile surface conditions	Surface level change	P for 99-00 original data	P for 99-00 adjusted data	P for 00-01 original data	P for 00-01 adjusted data
Soil type	Net	0.82	0.17	0.30	0.23
	Erosion	0.27	0.08	0.08	0.07
	Deposition	0.43	0.20	0.70	0.24
Drain type	Net	0.01	0.12	0.40	0.49
	Erosion	0.01	0.18	0.01	0.17
	Deposition	0.01	0.01	0.03	0.80

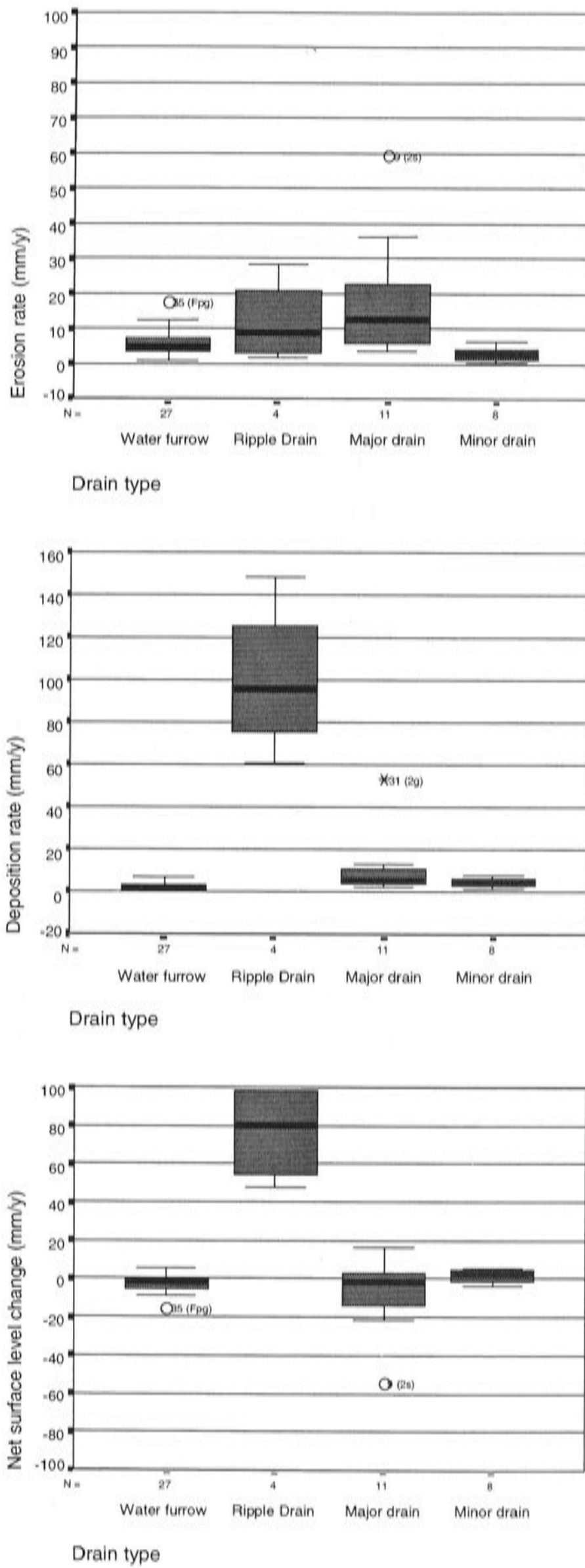


**Figure 9.4:** Boxplots for the variation in erosion rate, deposition rate and net surface level change (original data) in different drain types (and water furrows) during the 99-00 season.

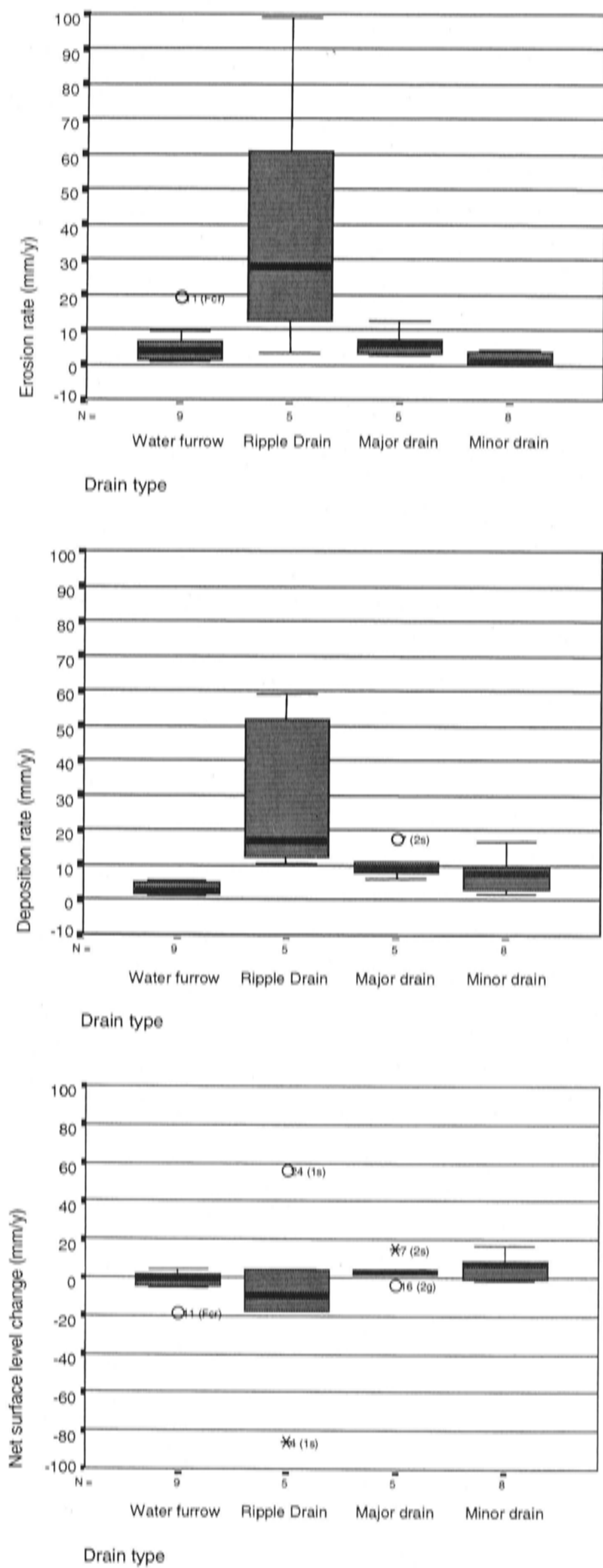


**Figure 9.5:** Boxplots for the variation in erosion rate, deposition rate and net surface level change (original data) in different drain types (and water furrows) during the 00-01 season.

### 9.6.3 Variation of erosion and deposition rates for soil type

#### Drains

When the drain profiles are grouped by soil type, the Kruskal-Wallis test does not show a significant difference ( $\alpha = 0.05$ ) between the groups for net surface level change, erosion or deposition rates (see Table 9.2). This is the case for both the original and adjusted data from each season. The boxplots for the original data by soil type group in Figure 9.6 show that there is more variation between profiles in silty clay than profiles in clay and grey sand in the 99-00 season. This could however be caused by the fact that there are no Ripple Drain profiles in clay or sand. Ripple Drain profiles generally have highest erosion and deposition rates, which is more likely to be due to the size and shape of the drain. The difference in variation is not as large for the 00-01 season data (Figure 9.7), but in this season the erosion and deposition rates in Ripple Drain cancel-out. Also, the number of samples for clay and grey sand are too small to be representative.

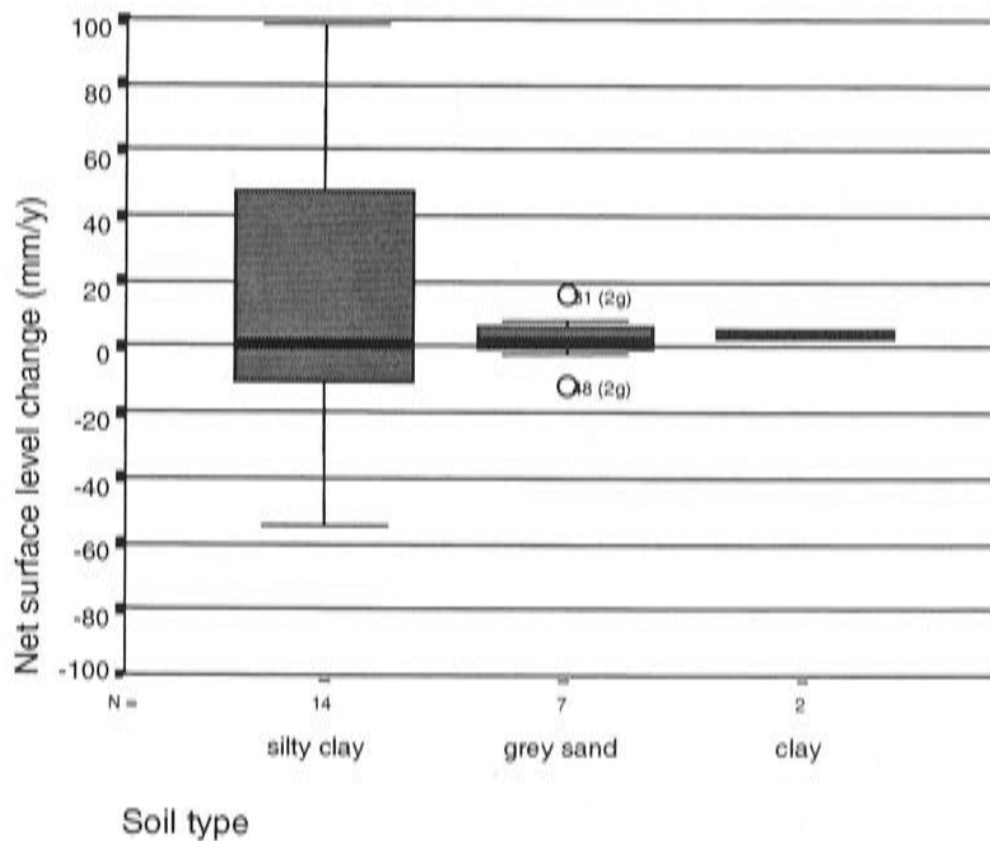


**Figure 9.6:** Net surface level change in the original 99-00 drain profile data, grouped by soil type (silty clay, clay and grey sand).

#### Water furrows

When the original 99-00 water furrow profile data are grouped by soil type, there is a significant difference between the groups for erosion rate and net surface level change (Table 9.3). After adjustment of the data, only the deposition rates show a

significant difference. The original 00-01 profile data are significantly different for both erosion and deposition rates. For the adjusted data this changes to the net surface level change and erosion rates.

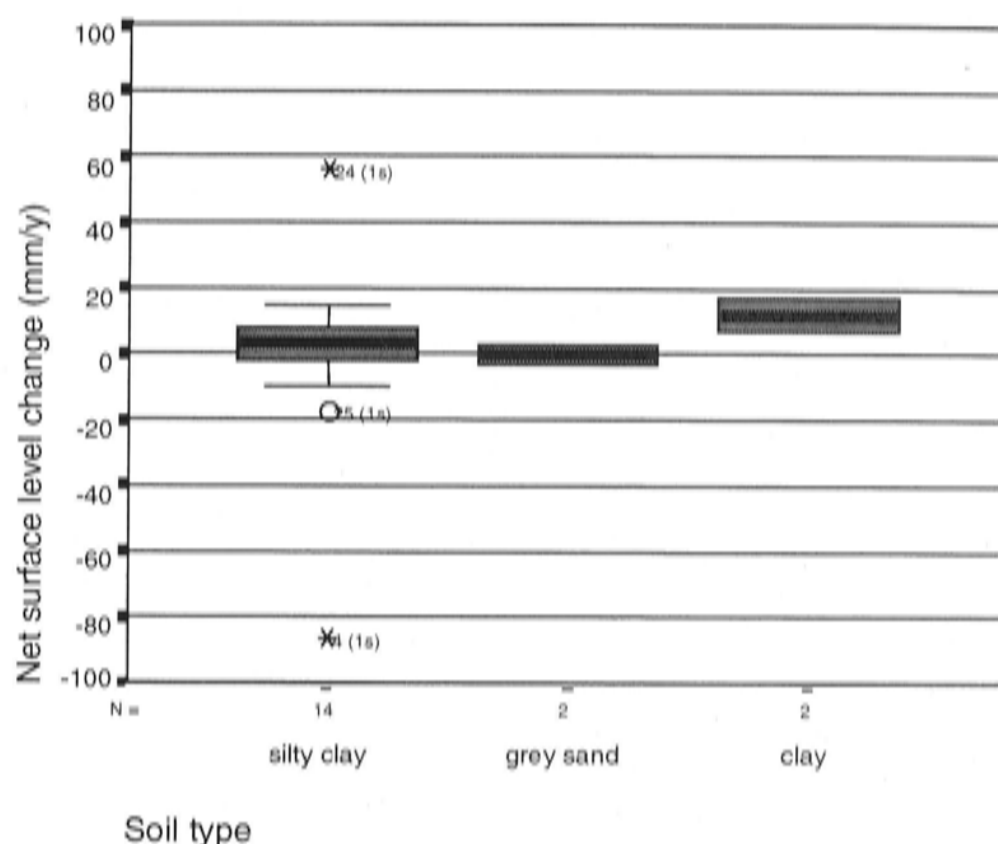


**Figure 9.7:** Net surface level change in the original 00-01 drain profile data, grouped by soil type (silty clay, clay and grey sand).

The boxplots for water furrows grouped by soil type are shown in Figure 9.8 and 9.9. The 00-01 profile data (Figure 9.9) shows a remarkably high erosion rate for furrows in clay soil, which is not expected because clay is thought to be the least erodible of the three soil types. The number of furrow samples for this season is however rather small and samples for each soil type were taken from only one furrow. It is therefore possible that other factors are responsible for the differences between the groups (e.g. maintenance).

#### 9.6.4 Variation of erosion and deposition rates for crop types

The furrow data of the 99-00 season are also tested for differences in relation to the crop type of the field in which they are located. This information was not available for the 00-01 season, because there were no profiles in plant cane fields during this season. The boxplots for the original water furrow data grouped by crop type are shown in Figure 9.10. The Kruskal-Wallis test shows a significant difference in erosion rate and net surface level change for both the original and the adjusted data (Table 9.3). For soil type clay and sand, both plant cane and ratoon fields were sampled. Furrows in silty clay were only sampled on ratoon fields. The difference

between ratoon and plant cane fields is therefore not caused by the same samples that cause the difference between the soil type groups.

**Table 9.3:** Results of Kruskal-Wallis tests for differences in surface level change in water furrow profiles due to differences in soil type and crop conditions. Significance of original and adjusted data for each budget season are shown.

Profile surface conditions	Surface level change	P for 99-00 original data	P for 99-00 adjusted data	P for 00-01 original data	P for 00-01 adjusted data
Soil type	Net	0.04	0.26	0.06	0.05
	Erosion	0.00	0.09	0.04	0.04
	Deposition	0.58	0.02	0.03	0.06
Crop type	Net	0.02	0.03	-	
	Erosion	0.00	0.00	-	
	Deposition	0.58	0.96	-	

## 9.7 Input for the budget calculation

### 9.7.1 Drains

Data analysis in Section 9.6.2 and 9.6.3 indicated that there are several factors that seem to influence the erosion and deposition rates measured in the drains and water furrows. For drains the results can be summarized as follows:

- In both budget seasons: surface level change calculated from original data was significantly dependent on drain type
- In both budget seasons: surface level change was not dependent on soil type

Field observations confirmed that there was an obvious difference in erosion and deposition processes between drain types, as indicated by the unadjusted data. Although the adjusted data did not show the difference, it was considered necessary to study the contribution of the drains in the sediment budget separately. The different processes in the drain types are, for example, likely to need different management.

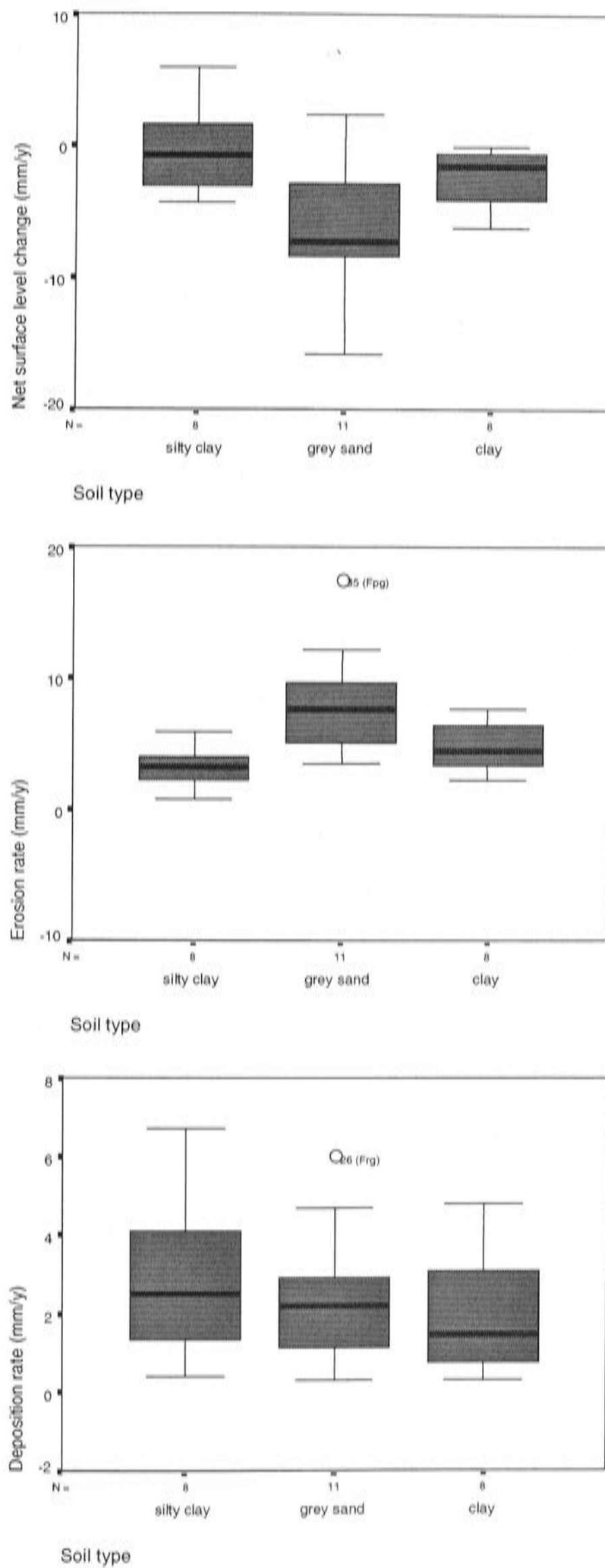


**Figure 9.8:** Boxplots for the variation in erosion rate, deposition rate and net surface level change (original data) in water furrows, grouped by soil type (99-00 season).



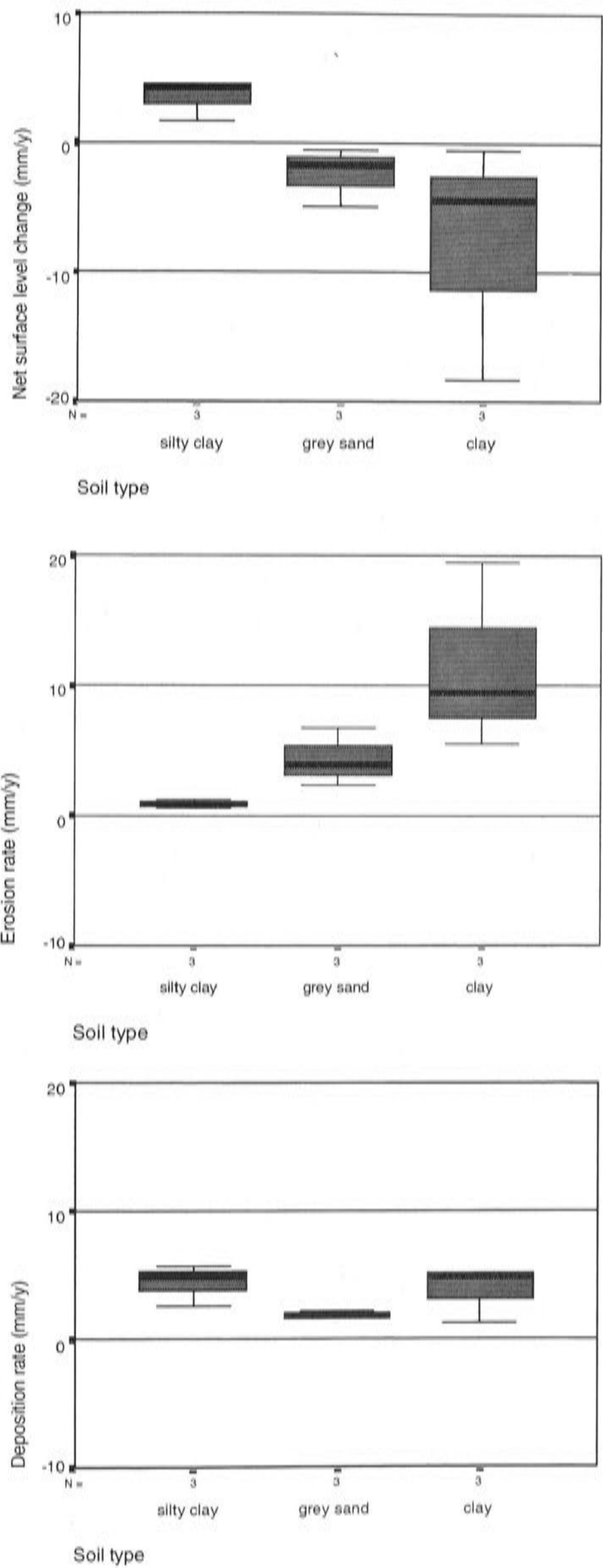


**Figure 9.9:** Boxplots for the variation in erosion rate, deposition rate and net surface level change (original data) in water furrows, grouped by soil type (00-01 season).

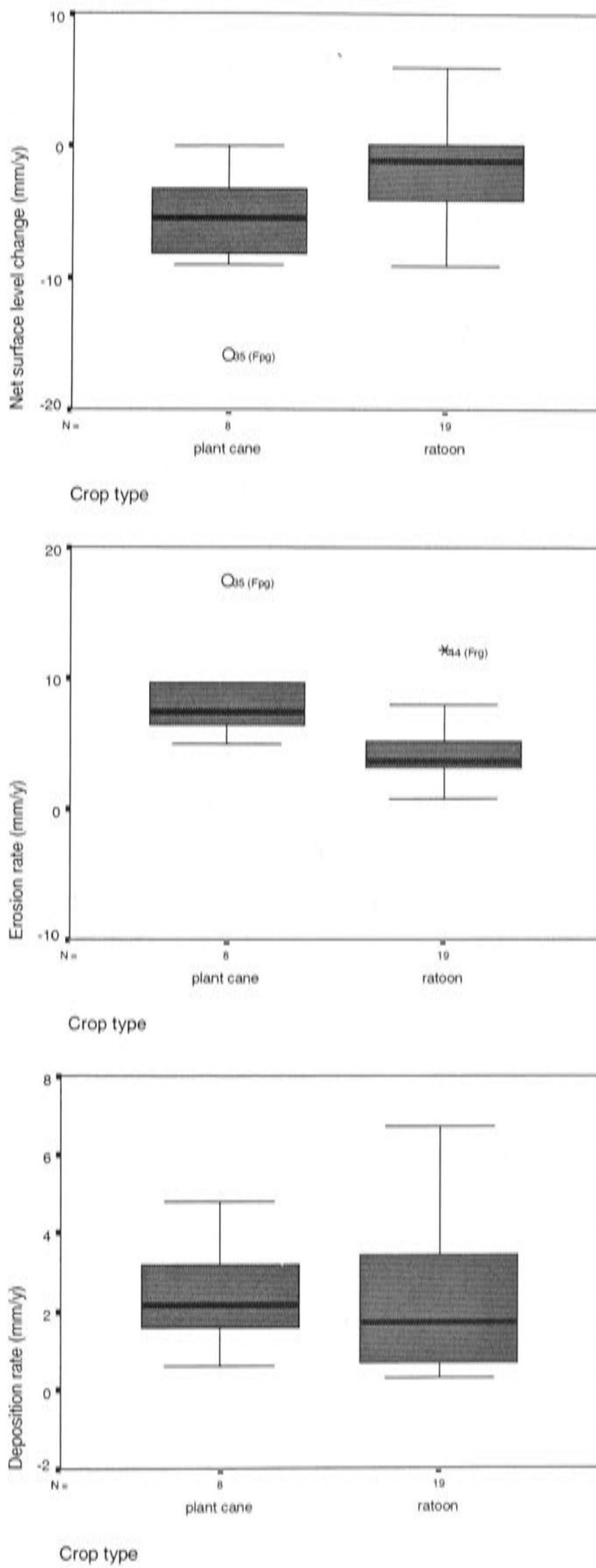


**Figure 9.10:** Boxplots for the variation in erosion rate, deposition rate and net surface level change (original data) in water furrows, grouped by crop type (00-01 season).

To obtain the sediment load from the total drain landscape element, individual erosion and deposition rates are calculated for the different drain types because there appears to be a significant difference. Soil type is clearly not the most important factor that causes variation in the erosion and deposition processes within the drainage network. No further subdivision for soil type was attempted for individual drain types, because the data were insufficient.

The erosion and deposition rate and the net surface level change are calculated as follows. Data records for each profile are first adjusted for sediment size (see Chapter 10). Next the records for each profile are averaged, assuming that the data records from a profile can be considered a random sample and that their distribution is near-normal. The averages of the profiles are then grouped for different drain types. From each group average erosion and deposition rate, and net surface level change are calculated. The average rates can be used to calculate the final sediment budget input, which is explained in Chapter 10. The averages for each drain type are listed in Table 9.4.

**Table 9.4:** Estimates of erosion and deposition rates and net surface level change for different drain types in the Ripple Corner Catchment.

Rates in mm y <sup>-1</sup> :	Average Ripple Drain	Median Ripple Drain	Average major drains	Median major drains	Average minor drains	Median minor drains
99-00						
Erosion	5.6	5.3	5.6	2.0	1.6	1.6
Deposition	7.5	7.4	1.9	1.8	2.7	2.7
Net surface level change	1.9	2.4	-3.7	-0.4	1.1	1.5
00-01						
Erosion	5.8	3.9	2.4	2.7	1.1	0.7
Deposition	6.3	3.0	5.0	4.5	4.6	4.9
Net surface level change	0.5	-0.9	2.6	1.3	3.5	4.5

It is questionable whether the average erosion and deposition rates will result in the best estimates of sediment load from the drains, for the following reasons: few of the histograms for the (adjusted) drain data indicate a normal distribution (see examples for the 99-00 season in Appendix J); variation in the data may have been introduced with variation in the amounts of adjustment; the samples may be biased because many were taken from the same drain sections; and the sample sizes for each drain type are small. It is possible that outliers have a strong influence on the average data

values. The medians of the data might better represent the export and storage in the drain landscape element.

Median values are also listed in Table 9.4. The table shows that in several cases there is a big difference between the average and median estimates. The average erosion rate for major drains in the 99-00 season is for example very high, mainly as a result of three profiles (profiles 7, 8 and 9) with 8-27 mm erosion rates, which were located in the same drain. Field observations suggested that the high erosion rates in this drain were not representative of the whole catchment area.

It is difficult to decide which of the estimates best represents the surface level changes in the drains. The median will be applied as best estimate, but the average will also be used in the budget calculations in chapter 10.

### **9.7.2 Water furrows**

Analysis of the furrow data (Section 9.6.2 and 9.6.3) provide the following results:

- In both budget seasons: either erosion rate, deposition rate or net surface level change was significantly dependent upon soil type for the original data as well as the adjusted data.
- In the 99-00 season: net surface level change and erosion rate were significantly dependent upon crop type for the original and adjusted data

For the calculation of surface level change rates in water furrows, data records for each profile are first adjusted for sediment size (see Chapter 10). Next the records in each profile are averaged, assuming that the data records from a profile can be considered a random sample and that their distribution is near normal. From the profile averages, erosion rate, deposition rate and net surface level change are then estimated in four different ways. In the same way as for the drains and headland the average and median values are compared. In addition to these, rates are estimated using separate median values for soil type, weighted by percentage area of each soil type. For the 99-00 data a fourth method is applied, which uses the different medians for crop types, weighted, by the area of each type. The results of the different estimates are listed in Table 9.5.

**Table 9.5:** Different estimates of erosion and deposition rates and net surface level change in water furrows in the Ripple Corner Catchment.

Rates in mm $y^{-1}$ :	Average	Median	Different medians per soil type	Different medians per crop type
99-00				
Erosion	2.4	2.1	2.0	2.9
Deposition	1.2	1.0	1.4	0.9
Net surface level change	-1.2	-1.1	-0.6	-1.5
00-01				
Erosion	3.2	1.1	1.0	-
Deposition	1.8	1.5	2.7	-
Net surface level change	-1.3	-0.4	1.9	-

Because of the relatively large number of furrow samples, which have a near normal distribution for all studied variables (see Appendix J), the average and median results for the 99-00 season are comparable. However, when some of the spatial variation, as a result of differences in soil type or crop type, are taken into account, variation in the estimates is larger. It is not known which estimate is best, but the average estimate will be used in the budget calculation, because it lies mid-way between the extreme results.

All three estimates of surface level change in the 00-01 season show substantial variation, because of the small sample numbers. An estimate based on crop type is not available, because no profiles were measured in furrows on plant cane fields. As a result of the limited data, the following problems arise:

Of the 9 furrow samples from the 00-01 season three samples show relatively high erosion rates (4-13  $\text{mm } y^{-1}$  compared to  $<2 \text{ mm } y^{-1}$ , see boxplots in Figure 9.9). These three samples were all taken from the same furrow in clay soil. Profiles in the same water furrow during the 99-00 season also show relatively high erosion rates (see Appendix H). Because of the three outliers in the erosion rate data, there is a big difference between the average and median erosion rate (see Table 9.5). The average erosion rate is higher than the average deposition rate, resulting in net erosion. On the contrary the median erosion rate is lower than the median deposition rate, indicating net deposition. However the median value of the net surface level change results in net erosion, and thus contradicts the median erosion and deposition values.

This problem is caused by the different distributions for erosion and deposition rates due to outliers in the erosion rate data.

When erosion and deposition rates for the water furrows are calculated, using medians per soil type, the 00-01 data are very different from either the average or the median. The estimate for deposition rate is particularly rather high. This is the result of the high deposition rates measured in the furrow in silty clay. Silty clay covers most of the budget area. The high deposition rates therefore dominate the calculation.

In the case of the 00-01 water furrow data it is clear that the sample method has too much influence on the results. The variation between the different estimates will have significant effect on the sediment budget, and will be evaluated in chapter 10.

## **9.8 Additional observations**

The Integrated Drainage Survey suggested that steeper drain banks in particular, which occur in Ripple Drain and other major drains, are susceptible to bank erosion. Profiles across these drains confirmed that considerable amounts of soil material can erode from the banks of this type of drain. Clear example are the left bank of Ripple Drain in profile 19 (99-00), and the left bank in profiles 8 (99-00) and 9 (99-00), which are profiles through a major drain near Palmas' site. With the large amounts of soil that erode quickly, considerable amounts of sediment are added to the runoff.

The profile study also indicated various possibilities for sediment storage within the drain profiles. Even the steep banks of Ripple Drain store considerable amounts of sediment. An example of this is the deposition recorded on the banks of profile 25 (00-01). The deposits trapped in clumps of vegetation growing on the banks were clearly noticed during the measurements. The most striking deposition processes were observed on the bed of Ripple Drain. In the month of March, between the March and May measurements, up to 25 cm thick, sandy deposits occurred in Ripple Drain. The sand appeared to be supplied by Post Creek and thus originates from the forested upland (see also Section 10.2). Similar sandy deposits were recorded in profile 31 in Prosser Drain. This drain is also directly connected with an upland creek.

It has to be stressed that the sandy deposits on the drain beds only provide short-term storage. This was shown by profiles 1-4 through Ripple Drain. The supports of these profiles were not removed during the dry season between the 99-00

and 00-01 budget seasons. They therefore provide a longer data record and show how in the 00-01 season much of the deposition on the bed of Ripple Drain profiles was removed (profile 20) or partly rearranged into a bar on one side of the profile (profile 19). The profiles across Ripple Drain further downstream (24-26) show less movement of material in this season.

In smaller amounts, sediment also accumulates in the well-vegetated spoon shaped drains. Drain profiles 18-20 in the 00-01 season are examples of this. Because of the grass cover in these drains, the sediment is thought to be stored for longer than the material on the bed of Ripple Drain. This is confirmed by the fact that all minor drains show net deposition during both budget seasons. For individual drains the evidence is however not obvious. Profiles 18-20, for example, showed net erosion during the previous season.

### **9.9 Other factors influencing erosion and deposition rates**

The observations described in the section above indicated the effect of vegetation on sediment export and storage in drains. The deposition in vegetation on the relatively steep banks of Ripple Drain is a surprising example. The presence of a vegetation cover in most of the minor drains might also be the reason why these drains show net deposition, while water furrows, which have a similar shape, show net erosion. The vegetation factor was not considered in the design of the study, so its effect has not been quantified. It is however thought to be important. For management purposes the observations can be useful.

Another factor that is likely to have a significant effect on erosion and deposition processes in drains as well as water furrows is maintenance. In the case of water furrows, maintenance practices will mainly result in removal of vegetation and disturbance of the soil. Disturbance of the soil means that fresh soil becomes available for transportation by runoff. On the other hand it also increases micro-topography of the furrow or drain surface, which promotes re-deposition.

Flow velocity or stream power will have an important effect. This factor was not monitored separately, but is indirectly included in the drain type classes

Finally the process of swelling and shrinking, which was discussed for headlands, could have affected the profile measurements. The influence of this process was minimized by taking all measurements under similar soil moisture conditions.

Practically this was not always possible. The process might explain the high erosion rates that were observed in the water furrows on clay soils. Unfortunately the profile meter did not provide a measure to check whether swelling and shrinking occurred.

### **9.10 Conclusion**

Various factors influence the erosion and deposition processes in the drains of the Ripple Corner Catchment. The present study showed that drain type is an important factor that causes a significant difference in erosion and deposition rates among the drains. Ripple Drain in particular showed relatively high erosion and deposition rates.

Most drain types appear to both generate and store sediment. The magnitude of erosion and deposition rates varies between seasons. It also depends on the calculation method used, which indicates that there is considerable uncertainty in the results of the present study. Only minor drains were net sediment sinks for both budget seasons, regardless of the method used.

The estimates for surface level change in water furrows indicate that this landscape element is a net sediment source. Only one estimate for the 00-01 season, based on data stratified by soil type, resulted in positive surface level change. This result illustrates the consequences of insufficient representation of spatial variation



---

## Chapter 10

### Budget Calculation

---

#### 10.1 Introduction

In Chapters 5 to 9, erosion and deposition processes in the landscape elements of low-lying sugarcane land have been quantified. With this information a sediment budget can be composed. However, to obtain comparable budget components the data need further adjustment. Part of the data have thus far not been adjusted for particle size; part of the data have to be adjusted for soil bulk density; and all data have to be extrapolated across the budget area.

#### 10.2 Particle size

Early in this research project, it was believed that most sediment moving through the catchment was in suspension. Bedload was not expected to move far in the low gradient catchment. The sediment budget therefore only includes material likely to move in suspension. The size class of material moving in suspension was assumed to be particles smaller than 20  $\mu\text{m}$ .

Contrary to these early assumptions several observations indicated the importance of bedload, with implications for the sediment budget. Firstly considerable transport of coarse material was observed in some drains. These observations were confirmed by measurements of high deposition rates on the drain beds during a single season, especially in Ripple Drain (see Section 9.6). Secondly some material covering the washers of the erosion pins on the headlands, predominantly along Ripple Drain, consisted of mainly coarse material. Such deposits were often very thick (up to several centimetres) and occurred amongst tall grass, so they were not thought to originate from splash erosion processes. Finally sediment size analysis of the local soils by Wood (1984) showed that the size fraction  $>20 \mu\text{m}$  in the local soils varies from 73% in sandy soils to 44% in clay soils (see Table 10.2).

The sandy deposits on the drain beds were observed in Ripple Drain and the major drains directly fed by upland creeks. Several times after heavy rainfall in the 99-00 season, input of sandy bedload from Post creek into Ripple Drain was unambiguously observed. At the point where the creek joins Ripple Drain the creek bed was elevated more than 5 cm above the drain bed, as a result of bedload supply from the creek into the drain. These observations suggest that much of the coarse material originates from the forested upland. The bed material appeared to move in pulses through the drainage system.

The sandy material observed in the drain bed and on the headlands was recorded in the drain profiles and on the headland pinplots. In contrast, only the particle fraction finer than 20  $\mu\text{m}$  was included in the sediment load calculations at the catchment outlet. An internally consistent sediment budget must be based upon the same sediment size range for each component. The soil erosion and deposition measurements are therefore adjusted to the same particle size, using the procedures described in the next section.

Although the observations suggest the movement of considerable amounts of bedload, insufficient time was available in the current project for the composition of an additional budget for bedload. Furthermore, proper estimation of bedload is proven very difficult (Gomez *et al.*, 1990; Thomas and Lewis, 1993; Gomez and Troutman, 1997).

### 10.2.1 Sediment size adjustment methods

The erosion and deposition rates measured in the drains and on headlands could be adjusted directly, using the particle size data that are available for soils in the region from Wood (1984). These data are listed in Table 10.2. However, the observations of the sandy deposits in the drains and on the headlands suggested that some of the thickest deposits were well sorted and consisted of coarse material. It is therefore unlikely that an adjustment based on the soil particle size distribution will be sufficient.

To support the observations, soil samples were taken from the headland surface and fields as well as from the beds of several drains. Samples were taken with 10 cm soil cores and analysed for sediment size composition using the sieve and pipette method. Figure 10.1 to 10.3 show the results of the analysis grouped by landscape

element. The total number of samples taken and analysed was rather small. This will affect the accuracy of the sediment size adjustments based on these data.

#### *Size adjustment headlands*

Figure 10.1 shows the particle size distributions of surface soil samples taken from headlands. Three of the samples were taken along Ripple Drain, two along minor drains, and one along a major drain. Sample RDH1 was taken at approximately 0.5 m from the edge of Ripple Drain, where a thick sandy deposit had been recorded in an erosion pin plot. Sample RDH2 was taken at the same location midway between the drain edge and the cane field.

The particle size distribution of the RDH1 sample shows enrichment of very fine to fine sand ( $\phi 2 - 4$ ). This material is likely to be a sorted deposit derived from overbank flow of the drain. The particle size fraction  $<20 \mu\text{m}$  of the deposit is 36%. The other headland surface samples have around 50% fine material, with the exception of sample HMin1, which contains more than 70% of particles  $<20 \mu\text{m}$ . This sample was taken from a headland in silty clay. Hence, variation in the particle size distribution of the headland surface samples is not clearly related to the soil type of the headlands.

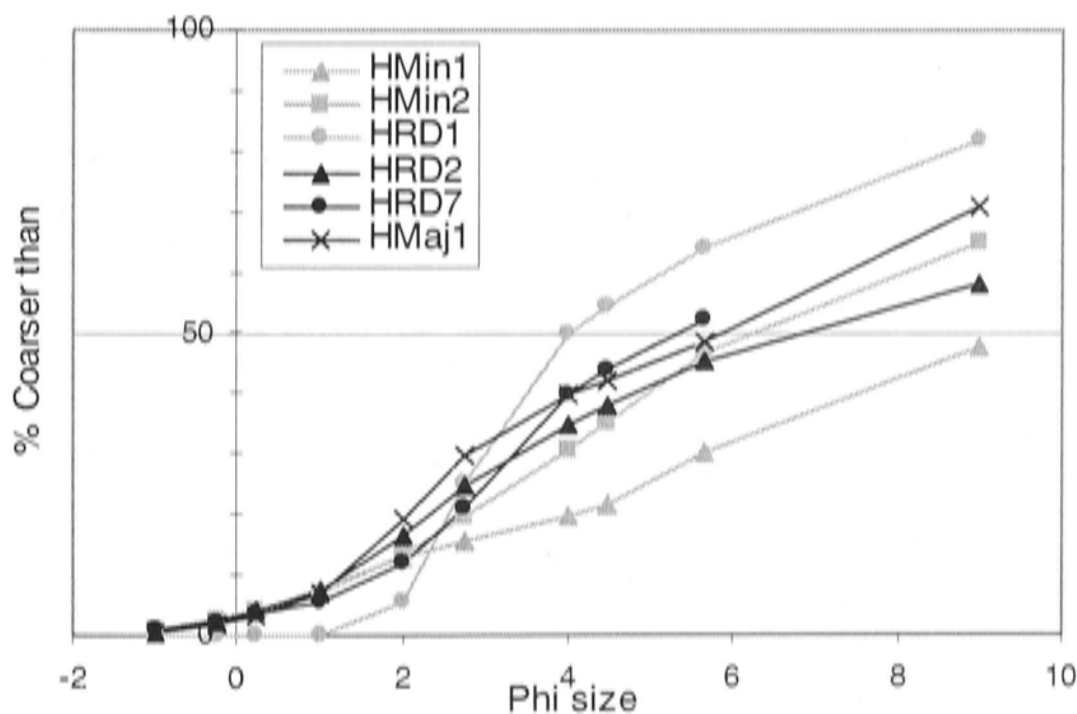


**Figure 10.1:** Particle size distribution of soil surface samples ( $<10 \text{ cm}$ ) taken from headlands along Ripple Drain (HRD), major drains (HMaj) and minor drains (HMin).

The median of all headland samples is equal to the silty clay topsoil value in the Wood data set (Table 10.2). Because most of the headland surface in the budget area

is silty clay, using the Wood data to adjust the surface level change measurement will not be significantly different from using the sample median (52.6%). Thus, the headland net surface level change, erosion and deposition rates that were presented in Table 8.3 are multiplied by 0.526. The resulting surface level change rates are listed in Table 10.1.

The headland sample median is higher than the field sample median. This is surprising; the headland median was expected to be lower as a result of sorting processes on the headland surface. The sample size is however too small to draw firm conclusions.

**Table 10.1:** Different estimates of erosion and deposition rates and net surface level change on headlands in the Ripple Corner Catchment. Values adjusted for bedload fraction. Best estimate is shaded.

Rates in mm $y^{-1}$	Average	Log transformed	Median	Cover based
99-00				
Erosion	0.9	0.2	0.2	-
Deposition	1.7	-	1.3	-
Net surface level change	0.9	-	1.1	*0.9
00-01				
Erosion	0.7	-	0.6	-
Deposition	0.5	-	0.4	-
Net surface level change	-0.3	-	-0.1	**0.4

\*Calculated from insignificant regression equation

\*\*Estimated using 99-00 cover survey data

#### *Particle size adjustment for drains and water furrows*

The surface level changes in the water furrows are adjusted using the topsoil particle size information from the Wood data set (Table 10.2). The median percentage particles  $<20 \mu\text{m}$  for the field samples from each soil type (Table 10.3) lie within 10% of the values documented by Wood. Because of the small number of samples the field data are expected to be less reliable than the Wood data.

Surface level changes in minor drains are adjusted in the same way as those in water furrows. However, profiles in Ripple Drain and major drains are separated into bed and bank segments so each can be adjusted for a different percentage of fine material. Figure 10.3 shows the particle size distributions of samples taken from the beds of Ripple Drain and Prosser Drain. The distributions indicate that the bed

material contains little fine material. If this is not taken into account in the calculation of erosion and deposition rates from the profile data, it could significantly overestimate input and storage of suspended solids in this landscape element.

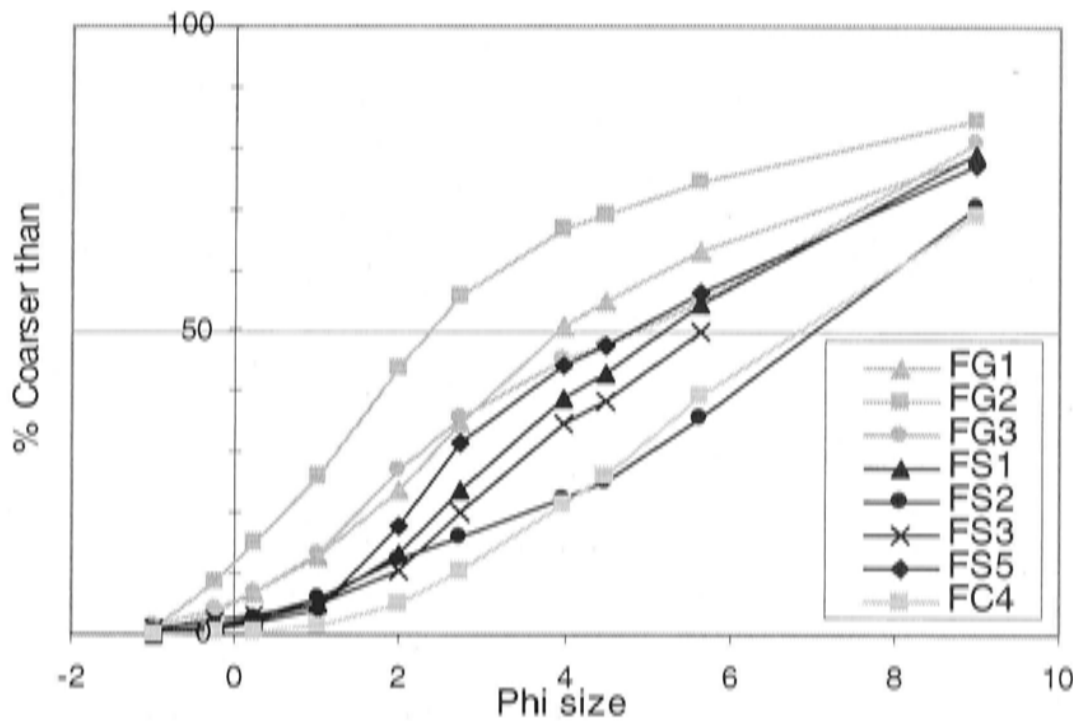


**Figure 10.2:** Sediment size distribution of soil surface samples (<10 cm) from fields (FG = grey sand, FS = silty clay, FC = clay)

**Table 10.2:** Particle size distribution for soils in the Ripple Corner Catchment (Wood, 1984).

Soil Type (Top and Sub Soil)	% Coarse sand	% Fine Sand	% Silt	% Clay	% <20 $\mu\text{m}$ (= % Silt + % Clay)
Silty Clay	14.1	33.3	27.3	25.3	52.6
	13.7	29.2	24.0	33.1	57.1
Clay	12.0	21.9	32.2	33.9	66.1
	12.4	19.6	28.0	40.0	68.0
Grey Sand	46.5	26.6	12.0	14.8	26.8
	48.0	24.9	10.9	16.2	27.1
Red Sand	44.7	27.1	12.6	15.6	28.2
	45.3	23.5	10.9	20.3	31.2

Data records from the bed segment of a drain profile are adjusted by assuming 2.2% of the particles are finer than 20  $\mu\text{m}$  for Ripple Drains and 8.6% for major drains. These adjustments are based on the medians of the drain bed sediment samples (Table 10.3). Data records that represent the bank segments of the profiles were adjusted, using the percentage of particles <20  $\mu\text{m}$  for the sub soil of the appropriate soil type as documented by Wood (Table 10.2).

The load estimates for drains and water furrows presented in Chapter 9 had already been calculated from adjusted profile measurement data. Therefore, the

information from Table 9.4 and 9.5 can be used directly in further sediment budget calculations.

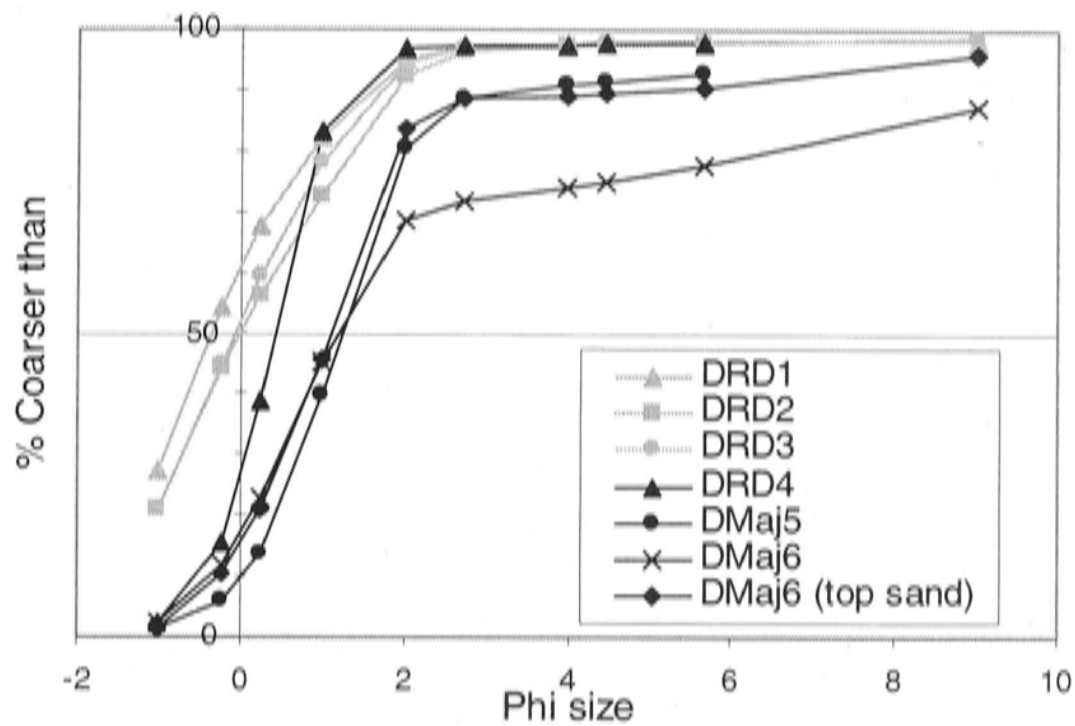


**Figure 10.3:** Particle size distribution of soil surface samples (<10 cm) taken from the beds of Ripple Drain (DRD) and major drains (DMaj). Sandy top layer (<5 cm) at site DMaj6 is analysed separately.

**Table 10.3:** Median particle size of soil surface samples (<10 cm) taken from the Ripple Corner Catchment.

% < 20 $\mu\text{m}$	Median	Count
Headland	52.6	6
All Fields	45.1	8
Fields in grey sand	37.0	3
Fields in silty clay	45.5	5
Fields in clay	60.6	1
Bed Ripple Drain	2.2	2
Bed Major Drain	8.6	2

### 10.3 Soil bulk density

To calculate the mass of the sediment load that has been estimated using erosion pins and profiles, information on the soil bulk density is required. Bulk density was not measured during this study, but data are available from literature. Table 10.4 lists the bulk densities as documented by Wilson and Baker (1990) for the Hamleigh soil type, which is the most prominent in the Ripple Corner Catchment. Wilson and Baker (1990) gives different values for the A-horizon of row and inter-row areas on (cane) fields, which indicates variation in compaction. The compaction of the headlands is probably similar to the inter-row area of a field. For erosion and

deposition in the drain profiles the bulk density observations from the deeper horizons are more appropriate. There is however no information on the spatial variation of any of the properties. It has been decided to use a value of  $1.5 \text{ g cm}^{-3}$  to transform all volumetric measurements. The effect of variation in bulk density on the sediment budget results is evaluated in Chapter 11.

**Table 10.4:** Bulk densities ( $\text{g cm}^{-3}$ ) of the Hamleigh soil in the Ripple Creek catchment (Wilson and Baker, 1990).

Soil type/Location	Horizon	Bulk density ( $\text{g cm}^{-3}$ )
Hamleigh (Wilson and Baker, 1990)	ARow	1.36
	AIR	1.52
	B2	1.58
	D1	1.52
	D2	1.87

#### 10.4 Surface area

In order to obtain a closed sediment budget, erosion and deposition rates for each landscape element are multiplied by the surface area that each occupies in the catchment. The surface areas of the landscape elements are listed as percentages of the total catchment area without forested upland, in Table 10.5.

The total surface area of the Ripple Corner Catchment is  $536 \text{ km}^2$ . The cultivated lowland covers  $320 \text{ km}^2$ , and the remaining  $216 \text{ km}^2$  consist of forested upland. The boundary of the catchment is described in Section 4.2 and shown in Figure 4.1. The upstream boundary is defined in ArcInfo from a 20 m DEM (Queensland Department of Natural Resources & Mines, 1980). The lowland boundary is derived from a 1 m DEM and the drainage directions of the fields as they were documented for the Integrated Drainage Survey (see Section 9.2).

The surface area covered by drains is calculated from the drain dimensions that were measured for the Integrated Drainage Survey. The area coverage is calculated separately for each of the drain type. The results are listed in Table 10.5.

Headland surface area is estimated by adding a 3.5 m wide strip of land on each side of a drain section. The average headland width of 3.5 m is estimated from the headland erosion survey (see Section 8.7.2). This results in a headlands cover of 6.9% of the total lowland surface area.

Field boundaries in the Ripple Creek Catchment have been surveyed for the Integrated Drainage Survey. From this survey an accurate estimate can be made of the total surface area of fields. Each budget season the crop cover of the fields in the Ripple Corner Catchment was mapped for this project, allowing the calculation of relative percentages of plant cane, ratoon and fallow.

**Table 10.5:** Percentage area of cultivated lowland (= total catchment – forested upland) covered by each landscape element.

Landscape element	% cultivated lowland 99-00	% cultivated lowland 00-01
Building	0.2	0.2
Ripple Drain	0.7	0.7
Major drains	1.1	1.1
Minor drains	0.7	0.7
Water furrow	6.4	7.7
Fallow	9.4	9.9
Formed roads	1.0	1.0
Headland	6.9	6.9
Melon	2.2	-
Other	1.2	2.8
Plant cane	34.1	19.6
Ratoon	36.4	48.9
Total*	103	102

\*Total can become more than >100% due to rounding errors.

During the 00-01 crop cover survey also the presence of water furrows in fields was mapped. Of the total surface area covered by fields that contain water furrows, the furrows occupy 12.5%. This percentage is based on the surface area covered by a water furrow of 2.5 m in a 1-hectare field section of 20 x 500 m. The total water furrow cover of the cultivated lowland is 6.4%. The percentage of water furrows can change each year depending on the percentage fallow fields and the application of laser-levelling for field drainage rather than water furrows. In subsequent years the differences are not expected to be very big, therefore the 00-01 percentage is also used for the 99-00 season, for which information on exact water furrow coverage is not available.

The surface area covered by the remaining landscape components, roads and built environment, is estimated from aerial photos.

Summation of the surface areas of all landscape components leaves part of the catchment area undefined. This area mainly consists of spaces between fields, spaces



along roads and irregular spaces between cane land and forested upland. These spaces are collected under the heading 'Other'. In total they take up 1.2% of the cultivated lowland. Roads, built environment and other area are not included in the budget calculation. The consequences of this will be discussed in Section 10.6.

### 10.5 Budget calculations and budget differences

The best estimates of the erosion and deposition rates and net surface level change in each landscape element for both budget seasons for particles  $<20 \mu\text{m}$  are listed in Table 10.6. Both the volumetric ( $\text{mm y}^{-1}$ ) rates and the rates per unit surface area ( $\text{t ha}^{-1} \text{y}^{-1}$ ) are shown. The table also lists the total loads for the catchment surface area. For the 99-00 season the methods on which the best estimates are based, are indicated. For the 00-01 season all best estimates are based on medians. Net input for the sediment budget from each landscape element can be obtained by subtracting the erosion and deposition loads. Alternatively it can be calculated directly from the net surface level change rates. The measurement methods used to quantify the budget input from fields and the forested upland did not provide separate information on erosion and deposition rates.

According to the sediment budget equation (Equation 3.1), the sum of the net sediment input from each landscape element ( $I - S$ ) should equal the output from the catchment ( $O$ ). The sum of the net sediment inputs for the 99-00 season is 1015 tonnes. The catchment output for this season, which was quantified in Chapter 5, is 1580 tonnes. Evaluation of the budget equation, at the bottom of Table 10.6, shows that the output from the catchment (1580 t) is larger than the net input from sediment sources (945 t). This results in a budget difference of 635 tonnes for the 99-00 season. For the 00-01 season the budget output is also higher (1120 t) than the net input (634 t), resulting in a budget difference of 486 tonnes.

For several landscape elements the difference between erosion and deposition loads is different from the net budget input, calculated from the net surface level change, despite being based on the same original data. This is caused by the use of the median of data. The median value is strongly influenced by the skewed distribution of the erosion and deposition rate data. Subtraction of the two medians is therefore likely to result in a different value than the median directly calculated from the net surface level change data. The budget evaluation in Table 10.6 is based on the results

from the net surface level change data. A summary of the budget calculated from the erosion and deposition rates is listed in Table 10.8.

**Table 10.6:** Sediment budgets for 99-00 and 00-01 budget seasons for particles <20 µm based on 'best estimate' results.

Source	Values 1999-2000 season			Values 2000-2001 season		
	mm	t ha <sup>-1</sup>	t	mm	t ha <sup>-1</sup>	t
Headlands erosion <sup>3</sup>	0.2	3	70	0.6	9	192
Headlands deposition <sup>1</sup>	1.3	19	419	0.4	6	140
Headlands net <sup>2</sup>	0.9	13	297	-0.1	-2	-35
Water furrows erosion <sup>2</sup>	2.4	36	738	1.1	17	406
Water furrows deposition <sup>2</sup>	1.2	18	369	1.5	23	554
Water furrows net <sup>2</sup>	-1.2	-18	-369	-0.4	-6	-148
Ripple Drain erosion <sup>1</sup>	5.3	79	174	3.9	59	128
Ripple Drain deposition <sup>1</sup>	7.4	110	242	3.0	45	98
Ripple Drain net <sup>1</sup>	2.4	35	77	-0.9	-14	-30
Major drain erosion <sup>1</sup>	2.0	30	104	2.7	40	139
Major drain deposition <sup>1</sup>	1.8	27	92	4.5	68	234
Major drain net <sup>1</sup>	-0.4	-6	-22	1.3	19	67
Minor drain erosion <sup>1</sup>	1.6	24	51	0.7	10	21
Minor drain deposition <sup>1</sup>	2.7	40	85	4.9	73	155
Minor drain net <sup>1</sup>	1.5	22	46	4.5	67	142
Ratoon		-1.4	-157		-2.1	-336
Plant		-5.9	-644		-1.7	-107
Upland		-1.1	-243		-0.9	-189
<b>Total (Input - Storage)</b>			<b>-1015</b>			<b>-634</b>
<b>Ripple Drain Output</b>			<b>1580</b>			<b>1120</b>
<b>Difference</b>			<b>565</b>			<b>486</b>

Methods used to obtain best estimate for 99-00 season: <sup>1</sup> Median; <sup>2</sup> Average; <sup>3</sup> Log transformed. All 00-01 season data based on medians.

For a number of landscape elements (headlands, drains and water furrows, Chapter 8 and 9) the budget input based on medians has been compared with budget input based on data averages. Table 10.7 lists the results for all budget components based on data averages. The I – S components are 1210 t for the 99-00 season and 714 t for the 00-01 season, which results in budget differences smaller than those for the best estimates: 370 and 407 tonnes respectively. The calculation method for I – S, either by directly using surface level change or by using erosion and deposition separately, does not affect the results of these budgets. The remaining difference between the

calculations is the result of rounding errors. The results of these budget calculations are also summarized in Table 10.8.

**Table 10.7:** Sediment budgets for 99-00 and 00-01 budget seasons for particles <20  $\mu\text{m}$  based on averages.

Source	Values 1999-2000 season			Values 2000-2001 season		
	mm	t ha <sup>-1</sup>	t	mm	t ha <sup>-1</sup>	t
Headlands erosion	0.9	13	297	0.7	11	244
Headlands deposition	1.7	26	576	0.5	7	157
Headlands net	0.9	13	297	-0.3	-4	-87
Water furrows erosion	2.4	36	738	3.2	48	1181
Water furrows deposition	1.2	18	369	1.8	27	664
Water furrows net	-1.2	-18	-369	-1.3	-20	-480
Ripple Drain erosion	5.6	84	184	5.8	87	190
Ripple Drain deposition	7.5	113	246	6.3	95	207
Ripple Drain net	1.9	29	62	0.5	8	16
Major drain erosion	5.6	84	289	2.4	36	124
Major drain deposition	1.9	29	98	5	75	258
Major drain net	-3.7	-56	-191	2.6	39	134
Minor drain erosion	1.6	24	51	1.1	17	35
Minor drain deposition	2.7	41	86	4.6	69	147
Minor drain net	1.1	17	35	3.5	53	112
Ratoon		-1.4	-157		-0.7	-114
Plant		-5.9	-644		-1.7	-107
Upland		-1.1	-243		-0.9	-189
<b>Total (Input - Storage)</b>			<b>-1210</b>			<b>-714</b>
<b>Ripple Drain Output</b>			<b>1580</b>			<b>1120</b>
<b>Difference</b>			<b>370</b>			<b>406</b>

Methods used to obtain best estimate: <sup>1</sup> Median; <sup>2</sup> Average; <sup>3</sup> Log transformed

**Table 10.8:** Summary of all budget calculations (as shown in Figure 10.4). Best budget estimate shaded.

	99-00	99-00	99-00	99-00	00-01	00-01	00-01	00-01
	best estimate	best estimate	averages	averages	best estimate	best estimate	averages	averages
	I - S	net surface level change	I - S	net surface level change	I - S	net surface level change	I - S	net surface level change
Input (I)	2181		2603		1518		2184	
Storage (S)	1206		1375		1180		1433	
I - S (or net)	975	1015	1228	1210	338	634	751	714
Output (O)	1580	1580	1580	1580	1120	1120	1120	1120
Budget difference	605	565	352	370	782	486	369	406

The relative differences between the budget component values for the various calculation methods and the resulting budget differences are illustrated in Figure 10.4.

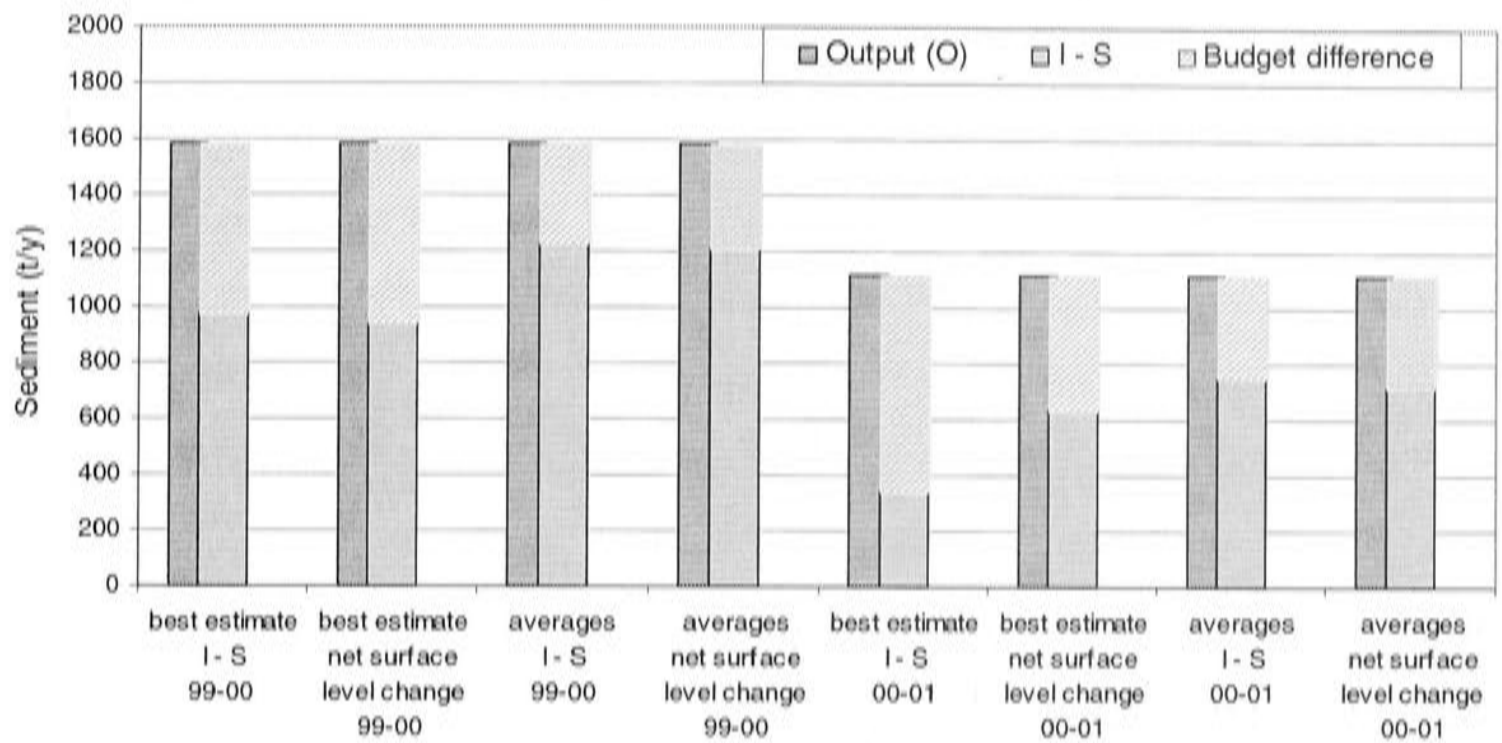


**Figure 10.4:** Comparison of (Input – Storage) with catchment Output, showing budget difference, for each budget calculation method.

## 10.6 Discussion

### 10.6.1 Best budget estimates

All budget calculations, which are summarized in Table 10.8, result in differences between net input and catchment output, varying from 25% to more than 50% of the sediment output from the catchment. For both seasons the differences for budgets based on median data values are bigger than for those based on data averages. It is however incorrect to assume that the average data better represent the erosion and deposition rates in the landscape. It is likely that the uncertainty in the output estimate is so large that the difference with the I – S component falls within error ranges.

The budgets calculated from the 'best estimates' of surface level change rates are still expected to provide the best approximation of actual erosion, deposition and sediment transport processes in the catchment. Among the budget calculations with best estimate data, budgets calculated from net surface level change data are expected to be most reliable. Splitting plot and profile data into erosion and deposition rates has caused 'artificial' distributions. If these distributions are not

symmetrical, their median values will not add up to the median of the original data. However, the separate erosion and deposition rates are needed to understand processes within the landscape elements.

### 10.6.2 Discussion of individual landscape elements

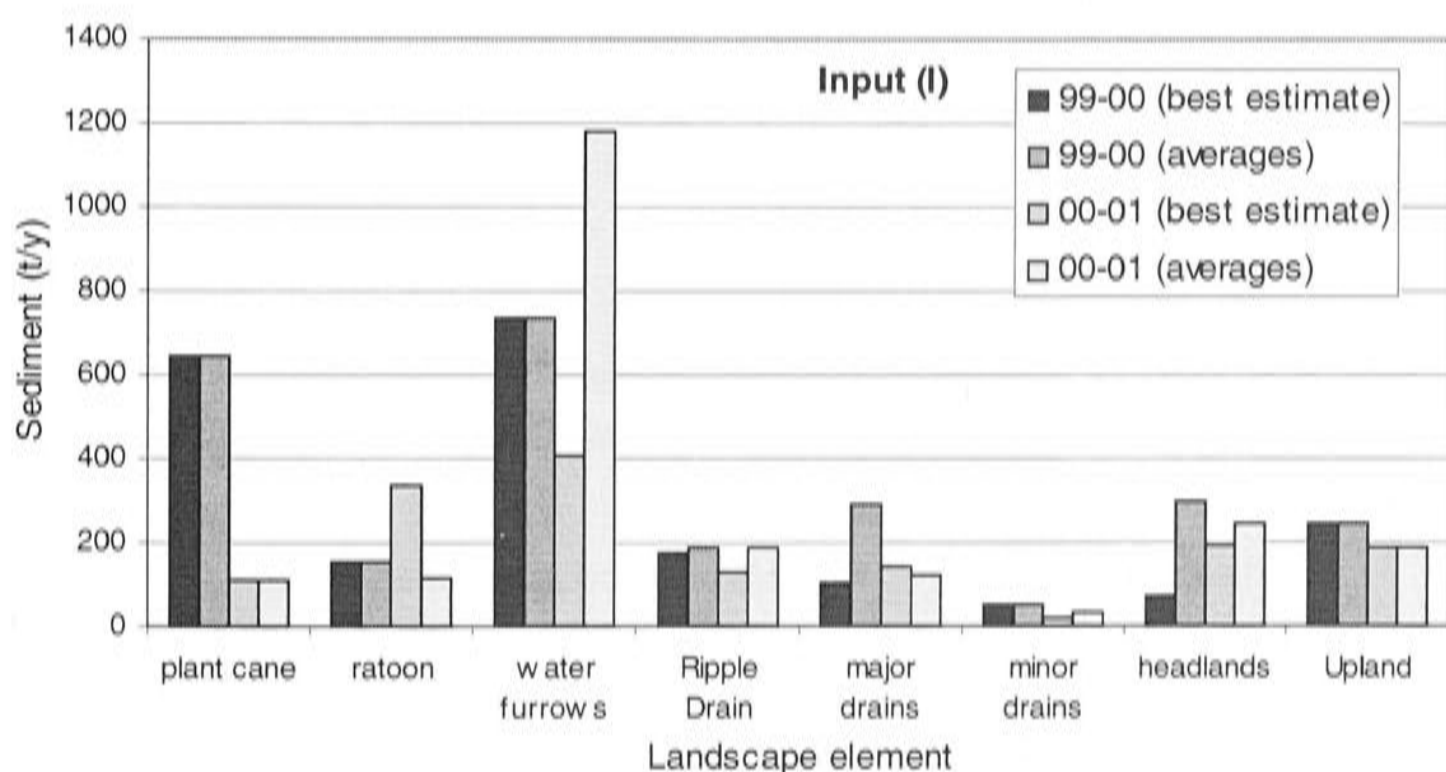
Figure 10.5, 10.6 and 10.7 give an overview of the input and storage values for all landscape elements in different seasons and for different calculation methods. The error ranges for the input and storage estimates of individual landscape elements will be considerable. However, if the data are assumed to be representative of the processes in the catchment, the following comments can be made about the budget results:

- Highest erosion rates are measured in Ripple Drain (see Table 10.6 and 10.7). However, water furrows generate most sediment input in both seasons, because they cover a larger surface area. Fields cover most surface area, but their (net) input is variable.
- The highest net input of sediment was generated from plant cane fields in the 99-00 season. However, the input for the subsequent season is relatively small. The different measurement methods that were used in the different seasons might be (partly) responsible for the different results.
- The combination of high erosion and high deposition rates in water furrows indicates that much soil is moving through this landscape element. Their connectivity with the drainage system is however low. Much of the eroded material redeposits within the furrows, which reduces the input in the sediment budget.
- Headlands appeared to be the most effective sediment store during the first budget season. This could be related to a high frequency of overbank flow events during this season.
- Both input and storage are relatively low in drains. Only minor drains are a net sediment sink in both seasons.
- Although the estimated contribution of upland input to the total sediment load is higher than was expected from the field observations of clear creek water, there

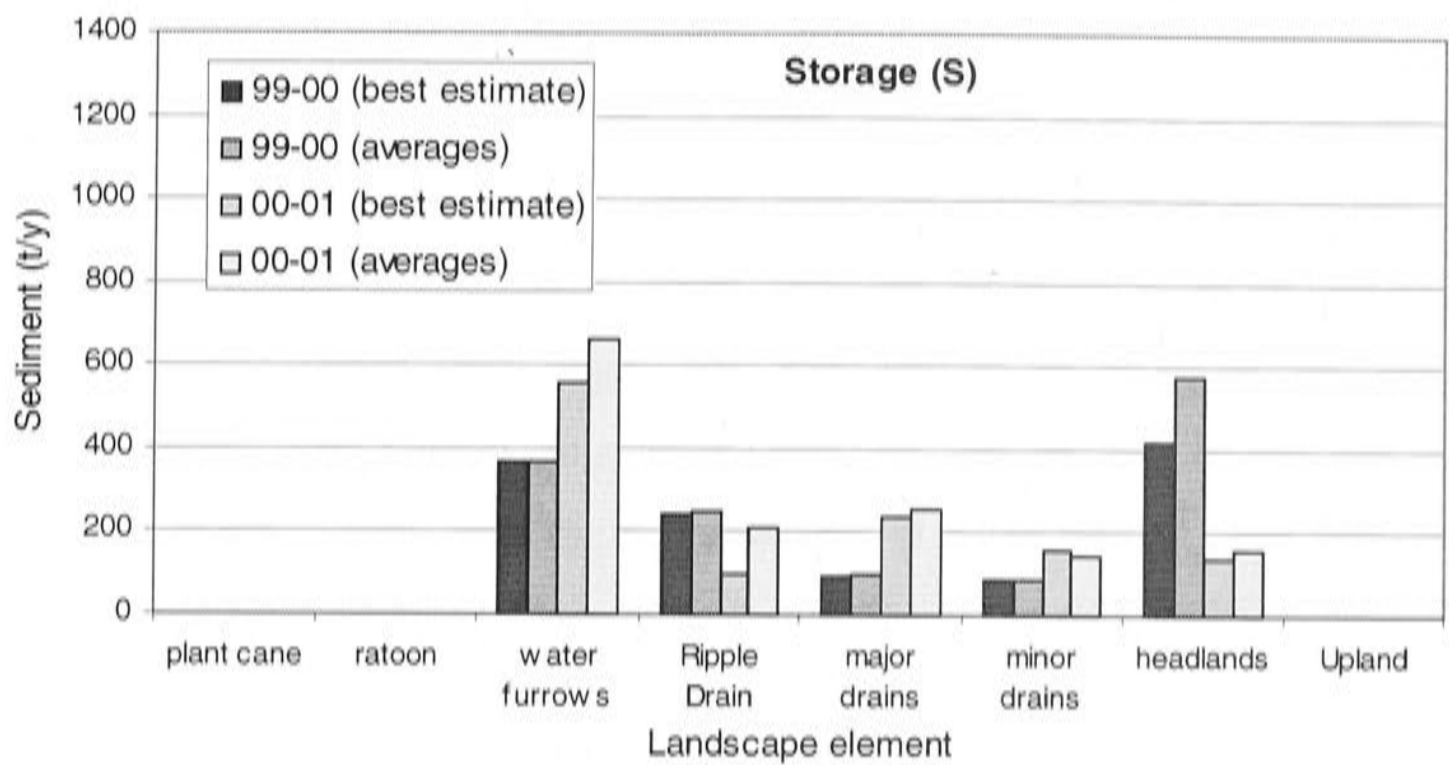
is reason to believe that the actual contribution is even higher. The estimated input was reduced, because the high runoff coefficient did not seem realistic (see Chapter 6). That reduction is based on extrapolated rainfall data, and could therefore be incorrect. If the unadjusted data from the Post Creek is extrapolated over the total upland, the budget input becomes 500 t for the 99-00 season and 390 t for the 00-01 season, which reduces the budget difference.

Figure 10.5 to Figure 10.7 also clarify some of the differences between budget calculation methods. For the 99-00 budget the higher budget difference in the 'best estimate' budget, compared to the average budget is mainly caused by a decrease of erosion from headlands and 2<sup>nd</sup> order drains. Both of these components have some outliers in the erosion rates, which are likely to 'underestimate' the actual surface level change.

The relatively large difference between the 'best estimate' and average budget for 00-01 is caused by the water furrow component. The average value probably 'overestimates' the actual erosion rate. As a result of the high furrow input, the input from the ratoon fields decreases; since the measured ratoon field input includes material from the water furrow, which has to be subtracted to obtain input exclusively from the field.



**Figure 10.5:** Input of sediment from individual landscape elements for each year's budget.



**Figure 10.6:** Storage of sediment in individual landscape elements for each year's budget.

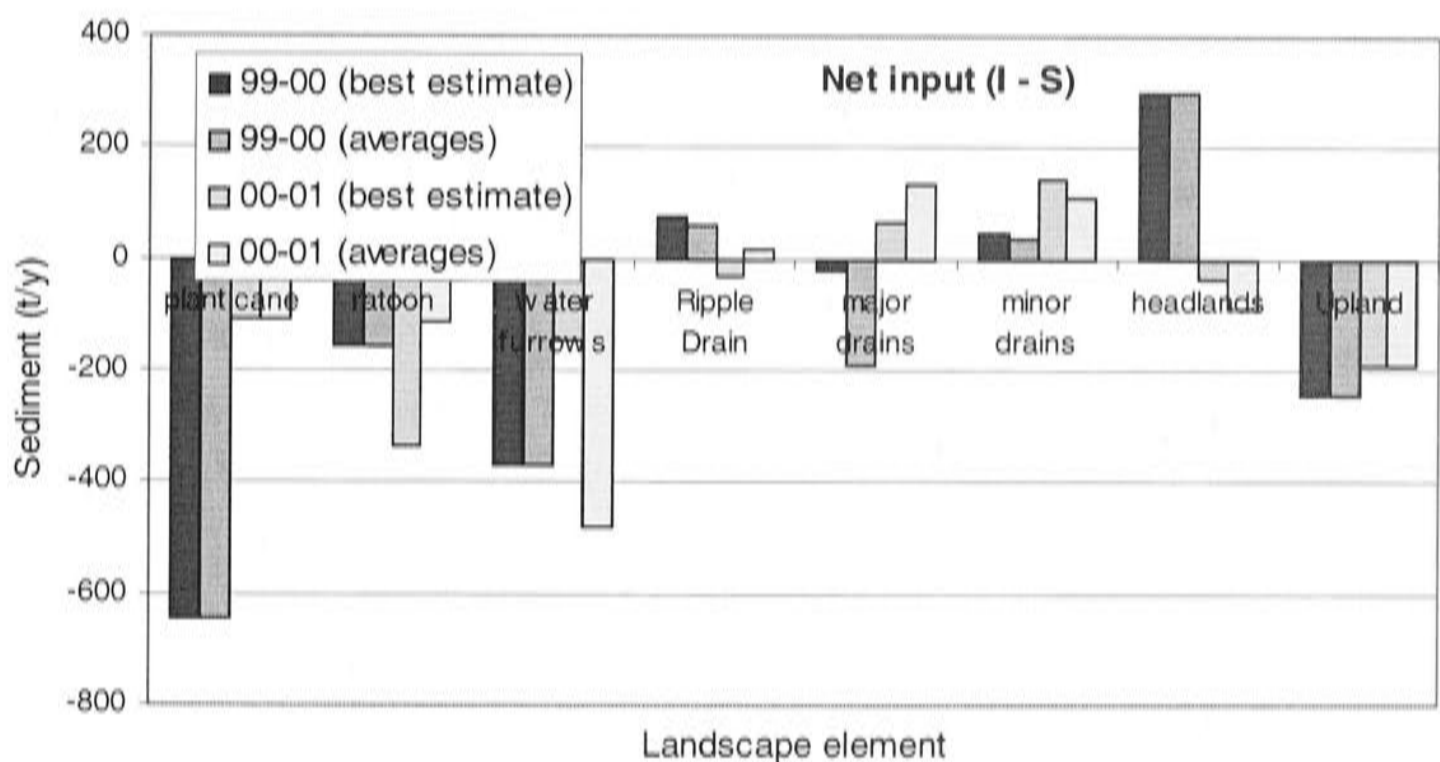


**Figure 10.7:** Net input of sediment from individual landscape elements. Positive values indicated net sediment storage, negative values net erosion.

### 10.6.3 Landscape elements not represented in the sediment budget

Several landscape elements have not been included in the sediment budget calculation. These elements are listed below with a discussion on their potential share in the catchment sediment budget.

*Fallow and melon fields*

No erosion and deposition data were collected from fallow fields. The cover survey each year indicated that 9-10% of the cultivated lowland consists of fallow. Field observations suggested that fallow fields will not generate as much sediment as plant cane fields, because the coarse aggregates/soil lumps of the recently ploughed surface do not appear as erodible as the much finer plant cane aggregates. Aggregates with diameters of up to 30cm are common on the fallow fields while the average size of the plant cane aggregates is only in the order of a few centimetres. The stability has not been tested. Erosion from fallow fields might be higher than from ratoon fields, because the surface cover is lacking. However, the coarse microtopography due to the aggregates will also trap a lot of sediment.

2.2% of the catchment surface area in the 99-00 season consisted of fields with melon crop. Because of their small area in the catchment no measurements were carried out on these fields. Erosion rates are expected to be less than from plant cane field, because the vegetation cover is higher, but there is no surface cover.

To estimate the amount of sediment that might be missing from the budget equation, because export from fallow and melon fields was not included, it is assumed that the sediment export from both types of field in tonnes ha<sup>-1</sup> lies approximately mid-way between export from ratoon and plant cane fields. This results in 140 t more input for the 99-00 season and 75 t for the 00-01 season. This increases the I – S component of the budgets for both seasons, but considerable budget differences remain.

*Roads, tracks, built environment, and other sources*

Roads and tracks have been shown elsewhere to be significant sources of sediment (Croke *et al.*, 1999; Croke and Mockler, 2001). In the Ripple Corner Catchment signs of erosion were observed on the roads especially after large flood events. The total input of sediment from roads is, however, thought to be relatively small. There are no 'high input' processes such as bank erosion or rilling, and the input will mainly be in the form of coarse sediment (gravel).

No major input is expected from the built environment. Overall input and storage will be insignificant due to the small area of buildings and few connections with major sediment sources.



The remaining catchment surface area, classified as 'other', mostly consists of uncultivated grassland. It is not likely to generate a significant amount of sediment, because it is well vegetated, and probably acts as sediment sink.

---

## Chapter 11

### Uncertainty analysis

---

#### 11.1 Introduction

Error is introduced in sediment budgets during measurements and because of problems in both temporal and spatial representation of rates of erosion and deposition (see Chapter 3). These errors will be propagated when data are extrapolated to times and locations not adequately estimated, and can produce large uncertainties around the final budget numbers. Although both sides of the budget equation for the Ripple Corner Catchment appear to balance, self-cancelling of large errors in individual budget inputs could be masked (Kondolf and Matthews, 1991). To draw valid conclusions from the budget results, and use these for resource management purposes, a good understanding of the uncertainty related to the results is necessary.

#### *Uncertainty analysis methods*

Uncertainty analysis in empirical erosion studies as well as erosion modelling studies is not common. There is no standard method for such an analysis; various approaches are possible, but each has specific limitations (Bárdossy and Fodor, 2001; Lall *et al.*, 2002). A number of methods were considered for the assessment of the reliability of the Ripple Creek budget and are discussed below.

A conventional method for uncertainty analysis is first-order variance propagation (Taylor, 1982). This method has the limitations that it only applies to uncertainties with a coefficient of variation of less than 10 – 20% and requires knowledge of the probability distribution of the error. These assumptions are not met in the data available for the sediment budget. For many of the uncertainties in the budget study the coefficients of variation are higher, and there is not sufficient data to estimate their probability distribution without making unverifiable assumptions. When the large uncertainties are propagated through repeated addition and multiplication in the

budget calculation, this method will also result in very large total uncertainty for the budget numbers, which may be unrealistic.

A very simple approach is the 'worst case analysis' approach (Morgan *et al.*, 1990), which only uses the upper and lower bounds of data or model parameter distributions. This method also has the disadvantage that it produces hyper-conservative results and will therefore not greatly help with the interpretation of the sediment budget results. It is known beforehand that the results represent the worst case scenario and that more confidence in the results is warranted. The method is, however, very simple. It can give a quick indication of the maximum effect of error and variation in the budget data, and the contribution from various sources of error and variability can be shown separately.

The probabilistic Monte Carlo simulation method provides a more flexible alternative to the above-mentioned methods, which might produce a less extreme budget uncertainty. It allows the combination of more and less clearly defined uncertainty in the data, so optimal use can be made of available information. In the process of simulation the sensitivity of the output to various uncertainties can be tested. Because of these advantages and its relative simplicity, this method is often used for uncertainty analysis in modelling, environmental decision-making and risk analysis. Guidelines of good practice have been developed for the application of the method (US Environmental Protection Agency, 1999; Intergovernmental Panel on Climate Change, 2000; Lall *et al.*, 2002).

There are several other uncertainty analysis methods besides those described above, such as Fuzzy and Bayesian techniques (Burrough, 1998; Freissinet *et al.*, 1999; Bárdossy and Fodor, 2001). They have been considered, but will not be further discussed, because the methods were not thought to provide additional insight into the uncertainty compared to any of the above methods.

In this study mainly the 'worst case analysis' will be applied, to analyse the uncertainty in the sediment budget, because of the nature of the available data. However, where possible the Monte Carlo method will also be applied to see if this method provides smaller uncertainties.

Because of the advantages of the Monte Carlo method it was thought to be particularly useful to evaluate the budget results from the Ripple Corner Catchment. The application of the method should however conform to certain conditions as

noted above. In this analysis these conditions were not always met. Therefore the analysis will be restricted to the following very general aim: to obtain an indication of the reliability of the budget values and the relative magnitude of uncertainty on each side of the budget equation, and to compare these results with those from the 'worst case' analysis.

## **11.2 Monte Carlo simulation of the budget uncertainty**

### *Simulation procedures*

Budget variables from each landscape element are simulated 1000 times using random samples (with replacement) from ranges of values (e.g. surface level change, bulk density, measurement error). 1000 simulations were assumed plentiful to obtain a stable output, considering the simple structure of the budget calculation.

From each set of simulations for all landscape elements, the I – S component of the budget equation is calculated. The resulting 1000 realisations of I - S can be plotted as a cumulative frequency distribution, which gives an indication of the likelihood of occurrence of different total sediment loads from sediment sources in the Ripple Corner Catchment. In the same way a cumulative frequency distribution is created from 1000 simulations of the sediment load at the catchment outlet, based on the uncertainty in the input data.

### *Uncertainty distribution functions*

Monte Carlo simulation assumes complete representation of the population distribution of data or model parameters. Population distributions are usually presented as a probability density function (PDF). For each simulation parameter or data, values are randomly sampled from their probability density function. For many uncertainties in the budget calculation an exact probability distribution is however not known, and in many cases only an estimate of the maximum and minimum value is available. Because Monte Carlo simulation can handle distributions of any shape, several authors suggest that, for situations where the probability distribution is unknown, either a uniform distribution between a minimum and maximum value or a triangular distribution based on a minimum, maximum and the most likely value should be assumed. The triangular distribution is applied when it is believed that values close to the most likely value will occur more often than values

near the extreme ends of the range (Hession, 1996; Hession *et al.*, 1996; Hession and Storm, 2000; Lall *et al.*, 2002).

Another alternative for fitting or assuming a PDF is the empirical distribution function (EDF), which is obtained from the cumulative frequency of available data. The EDF method completely describes the data values and their probability of being encountered, while no assumptions have to be made about their distribution. Using this alternative includes the risk that the EDF poorly represents population variability and percentiles. A well-chosen PDF can reduce that risk, but its choice requires some theory and professional judgment, and the result may be incorrect (US Environmental Protection Agency, 1999). An empirical distribution function can be used in Monte Carlo simulations by resampling (with replacement) the original data.

In this study, uniform and triangular as well as empirical distribution functions have been used. In most cases there were few alternatives, because insufficient data were available to obtain PDFs without making unverifiable assumptions.

The following sections describe in detail the sources of error in the budget input estimates for the example of headlands and the outlet drains. The same methods have been used for all other budget components. Some comments on these analyses are included in Section 11.5. A detailed analysis is only done for the 99-00 data. Possible differences for the 00-01 data will be commented on in Section 11.7.

## 11.3 Headlands

### 11.3.1 Overview

The sediment budget value for headlands was obtained from erosion pin plots across the headlands in the budget area (Chapter 8). From the measurements of each separate pin in the field, until the final appearance of the data in the budget equation, the following factors add uncertainty:

1. Erosion pin measurement error
2. Error in the estimate of total headland surface area
3. Error in the length of observation period
4. Interpolation of pin values within a pinplot
5. Extrapolation of plot values across the headland surface area
6. Error in the headland soil bulk density

7. Error in the soil particle size distribution

Numbers 1 to 3 are knowledge uncertainties (Morgan and Henrion., 1990), which could be reduced by improved measurement of the system. Uncertainty from sources 4 to 7 is the result of spatial variability, the quantification of which is limited by both adequacy of the measurement methods used and the current level of understanding of soil processes. In the Monte Carlo simulation of the budget components, all types of uncertainty will be combined to obtain total uncertainty for the budget results.

The sources of uncertainty in the estimates of net input for the budget from drains and water furrows are similar to those of the headland input calculation. Only the value ranges for some variables in the load calculation are different.

**11.3.2 Measurement error**

During the measurement of erosion pins, positioning of the callipers on the washers varied slightly with each measurement resulting in random measurement error. Calibration errors or malfunctioning of the callipers could have caused systematic errors. The systematic errors are ignored in the uncertainty analysis, because they are expected to be insignificant compared to other sources of error. To estimate the random measurement error, four pinplot measurements were repeated after short time intervals. In the final measurement session of the 99-00 season, the measurements of three plots were repeated after a two-week interval. No rainfall or flooding was recorded over this period, so the true soil surface change was thought to be insignificant. During the final 00-01 measurement session one plot was repeated immediately after the first measurement. The average of the (absolute) differences between repeated measurements of all the pins in a plot is used to represent the uncertainty due to measurement error in this measurement method. This is assumed to be comparable to using the standard deviation of repeated measurements as an estimate of uncertainty as described by Taylor (1982).

**Table 11.1:** The average, minimum and maximum value of the (absolute) difference between two subsequent measurements of all pins in an erosion pinplot.

	Average (mm)	Minimum (mm)	Maximum (mm)
Plot G 99-00	1.4	-2.2	6.2
Plot O 99-00	1.1	-9.2	2.1
Plot P 99-00	1.5	-6.5	13.7
Plot G 00-01	0.8	-3.7	1.6

Table 11.1 shows the uncertainties estimated from repeated pinplot measurements. The deviations of the 99-00 plot measurements are slightly higher than the deviation of the 00-01 plot measurements. Because of the rather long time period between the 99-00 repeated measurement, the 00-01 value is thought to be more reliable and will be used in the remainder of the uncertainty analysis.

In the Monte Carlo simulation of the sediment load from headlands, uncertainty through measurement error is included by sampling from the empirical distribution function of the deviation estimates of plot G. This means that the simulation input is randomly sampled from the original data, which was not clearly normally distributed. The Kolmogorov-Smirnov and Shapiro-Wilk test of normality (Chakravarti *et al.*, (1967); Shapiro and Wilk, 1965) showed only low significance for the K-S and W test statistics ( $P = 0.1$  and  $0.02$ ). Figure 11.1 shows the histogram of the deviation data.

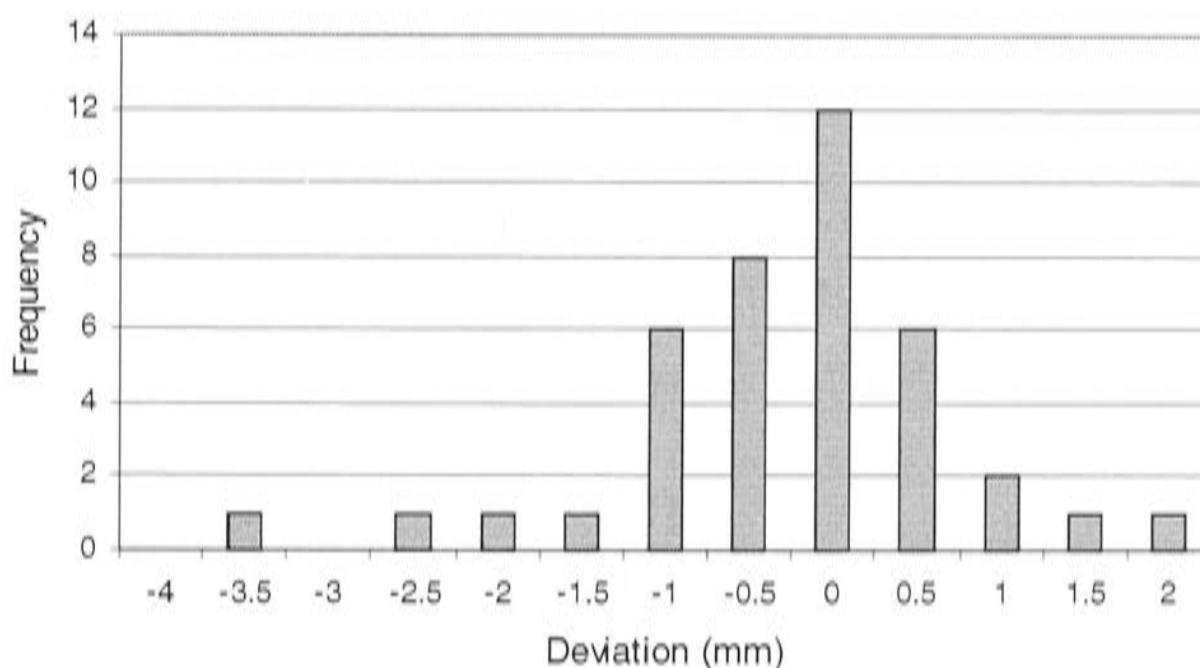


**Figure 11.1:** Histogram of the absolute differences (deviations) between repeated measurements of erosion pins in pinplot G in the 00-01 season.

### 11.3.3 Interpolation methods

Uncertainty from sources 4 and 5, as mentioned in the overview in Section 11.3.1, is the result of the spatial variation of the headland surface level change values. In Section 8.7.3 the representation of the headland surface level changes by the pinplot data was discussed. It was concluded that the sample average best represented the net surface level change. The variance of the data is assumed to represent the spatial variability and thus the uncertainty around the net surface level change estimate. The validity of this assumption can however be questioned, because 'spatial variation of

any continuous attribute is often too irregular to be modelled by a simple smooth mathematical function' (Burrough, 1998). This means that the uncertainty in the headland load value due to spatial variation might not be sufficiently quantified. The consequences of this depend on the contribution of this source for the total uncertainty, and will be discussed in Section 11.6.

Both the Kolmogorov-Smirnov and Shapiro-Wilk tests indicate that the data are normally distributed ( $P = 0.2$  and  $0.56$ ). The sample number is however rather small ( $n = 13$ ), which reduces the reliability of the test results. For this source of uncertainty the difference will be tested between the use of a normal distribution as well as random sampling from the original data.

Extrapolating the average pin plot data across the catchment area ignores the variability within the plots. The variability within some plots is as high or higher than variability between plots. The clustering of pin measurements by plot and assuming the plot value is representative for a particular headland area therefore reduces the variance of the data (Table 11.2). The variance within pinplots is not taken into consideration in the error propagation. Relying on field observations it is assumed that the grid size was sufficiently dense to obtain an accurate interpolation of the surface by simple averaging of the data. The spatial variation of surface level change at this scale is not thought to cause uncertainty in the sediment budget results.

**Table 11.2:** Reduction of variance for the distribution of plot surface level change averages compared to average surface level change for all individual pins.

	Plot averages	Individual pins
n	13	279
Average	1.7	1.7
Standard error	2.6	11
Variance	6.6	112

#### 11.3.4 Time and Space

Uncertainty sources 2 and 3 result from inaccuracy in the total length of the time and the area over which surface level change on headlands is estimated. The pinplots were not all measured at the same date, so the results will cover different lengths of time. This error is assumed to be insignificant, because installation and measurement of the plots were performed under dry conditions over a relatively short time period, so no significant change would have occurred.



Area data could be a significant source of error, particularly for headlands, because their surface area was not properly mapped. The method for estimation of total headland surface area is presented in Section 10.4. The uncertainty in this estimate is different for headland length and width. Uncertainty for width is estimated from the observed frequency of headland widths (Figure 11.2). This information is included in the Monte Carlo budget equation simulation as an empirical distribution function. Total headland length is thought to be equal to total drain length. Total drain length is known from the Integrated Drainage Survey. Although these data are thought to be accurate, a 5% error in the estimate is not unlikely. This assumption is included in the simulation as a uniform distribution around the best estimate of total headland length.

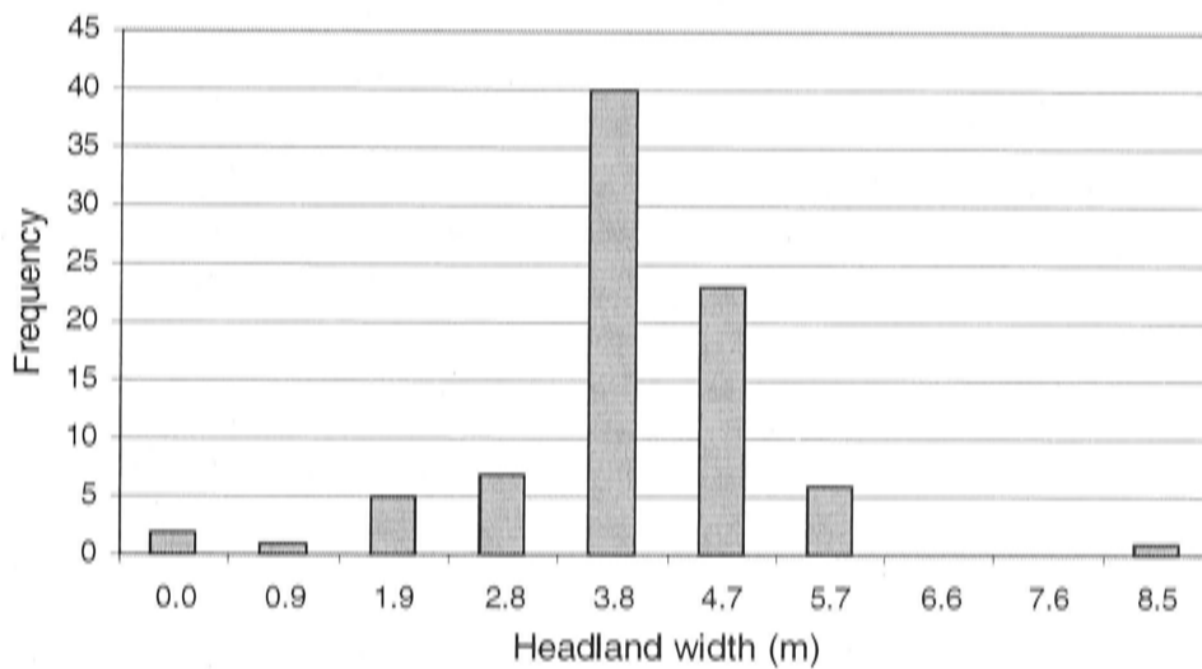


**Figure 11.2:** Histogram of headland widths measured in the Ripple Corner Catchment.

### Soil properties

For both bulk density and the particle size fraction  $<20\ \mu\text{m}$ , a single value was used in the headland budget input calculation. In reality these properties vary throughout the budget area, for example with changes in soil type or with varying degrees of compaction.

The particle size distribution used to calculate the suspended solid fraction from the total sediment input for headlands is estimated from 6 headland samples as described in Section 10.2.1. The fraction of particles  $<20\ \mu\text{m}$  in these samples ranges from 36% for a sandy headland deposition and 70% for a sample taken from silty clay soil, with a median of 53%. Both extreme values in the measured range are expected to represent the maximum and minimum possible values and the median, to

represent the best estimate. Therefore, a triangular distribution represents the uncertainty due to particle size adjustment in the Monte Carlo simulation. A histogram obtained from 1000 random samples from the triangular distribution is presented Figure 11.3.

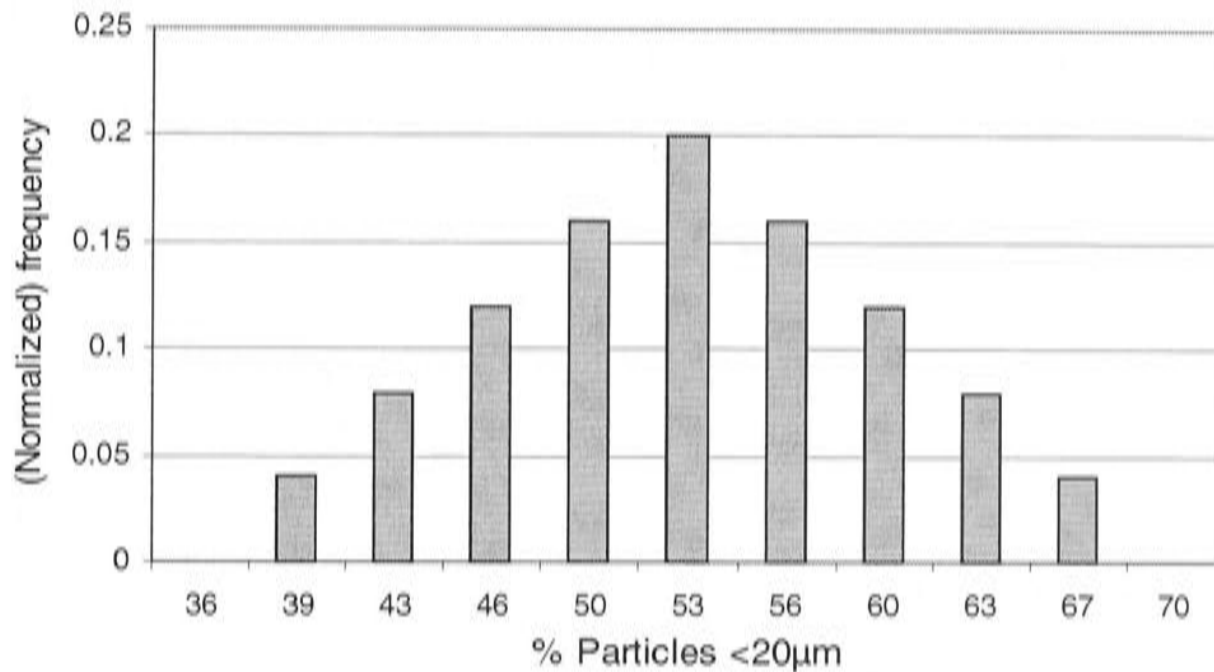


**Figure 11.3:** Histogram of 1000 samples taken from a triangular distribution for % particles <20 µm in headland surface soil.

Table 10.4 in Section 10.3 showed the bulk density values for the dominant soiltype in the Ripple Creek Catchment. The topsoil and upper subsoil bulk densities varied between 1.36 and 1.58 g cm<sup>-3</sup>. In the budget calculation a bulk density of 1.5 g cm<sup>-3</sup> is applied for all landscape elements. Nothing is known about the spatial variation of this property. The minimum expected value is 1.4 and the maximum 1.6 g cm<sup>-3</sup>, with a most likely value of 1.5 g cm<sup>-3</sup>. This information is also represented with a triangular distribution in the Monte Carlo simulation.

### 11.3.5 Total uncertainty in the budget input from headlands

In the calculation of the sediment load from headlands, the uncertainties are combined as follows:

$$\text{Uncertainty headland load estimate} = (\text{Spatial variability} + \text{Measurement error}) \\ * \text{Uncertainty bulk density} * \text{Uncertainty particle size} * \text{Error headland length} * \\ \text{Error headland width}$$

From the 1000 realizations of the simulation of net sediment input from headlands, cumulative frequency distribution curves can be plotted. Figure 11.4 shows the different curves obtained from simulations by re-sampling the original net surface

level change data and by sampling from a normal distribution. There is a maximum difference of approximately 150 t between the curves.

With the currently available data and information, 95% of the realizations of sediment load from headlands (estimated from the EDF) have a value between -750 t and 1400 t; 68% of the realizations (comparable with one standard deviation) have a value between -25 t and 750 t. The former range indicates a variation of  $\pm 300\%$  around the average estimate, and the latter a variation of  $\pm 100\%$ .

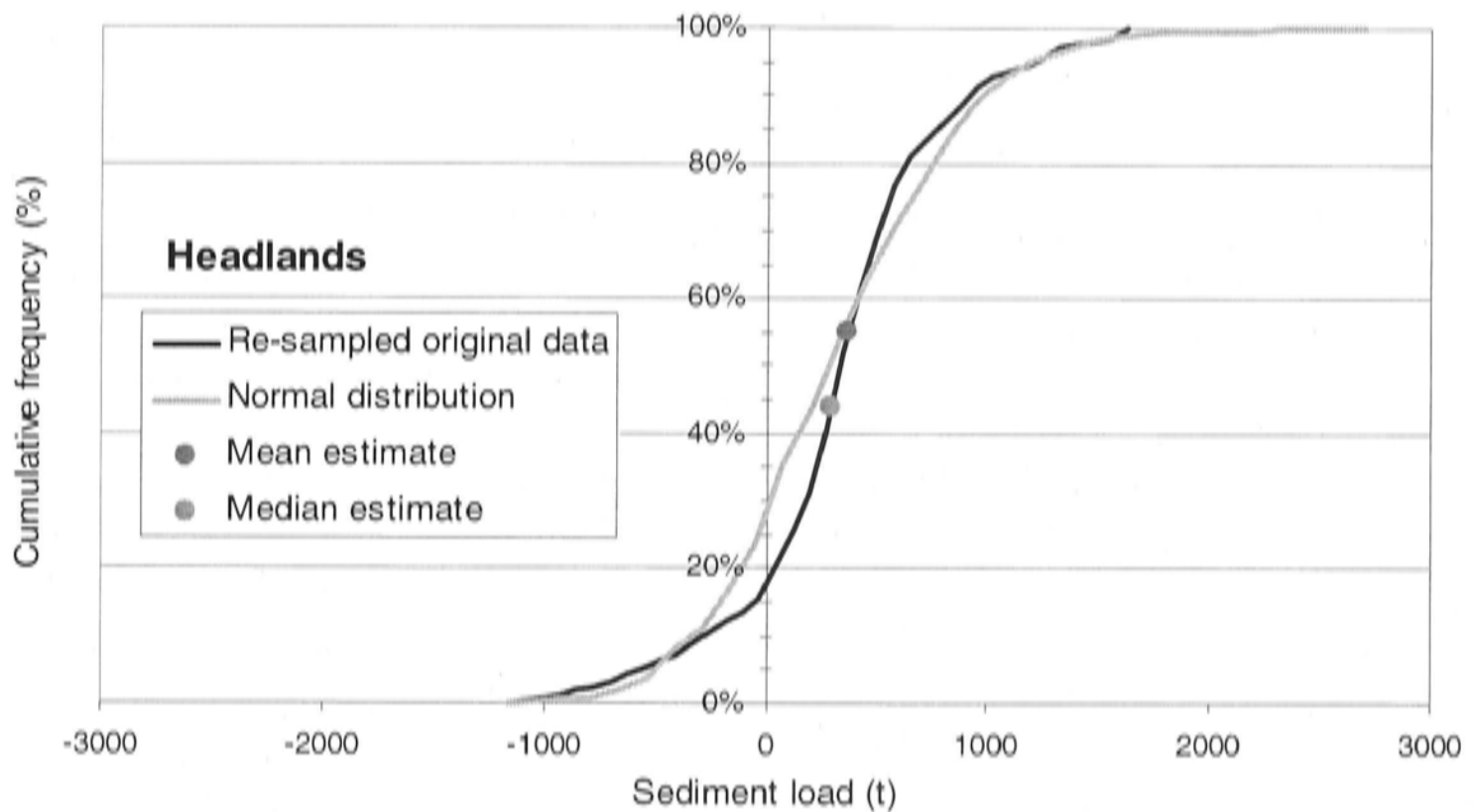


**Figure 11.4:** Cumulative frequency distribution curves obtained from 1000 simulations of headland sediment load, by re-sampling the original surface level change data (dark) and sampling from a normal distribution (light). Load estimates based on average and median surface level change data indicated with dots.

The worst case analysis is performed by calculating a highest and lowest headland sediment input. The highest input calculation uses plus one standard deviation of the net surface level change, headland width, and measurement error distributions (assuming normal data distributions), and the maximum likely value for bulk density and particle size (as described above). The lowest input calculation uses minus one standard deviation and minimum likely values. This results in a maximum likely range for the headland input, shown in Figure 11.5 and Table 11.3. The Figure also shows the relative contribution of the individual uncertainties, using best estimate values for the other variables.

The total range is considerably larger than the 68% range from the Monte Carlo simulation. The spatial variation in net surface level change causes most uncertainty. The effect of the measurement error appears to be small, contrary to expectations.

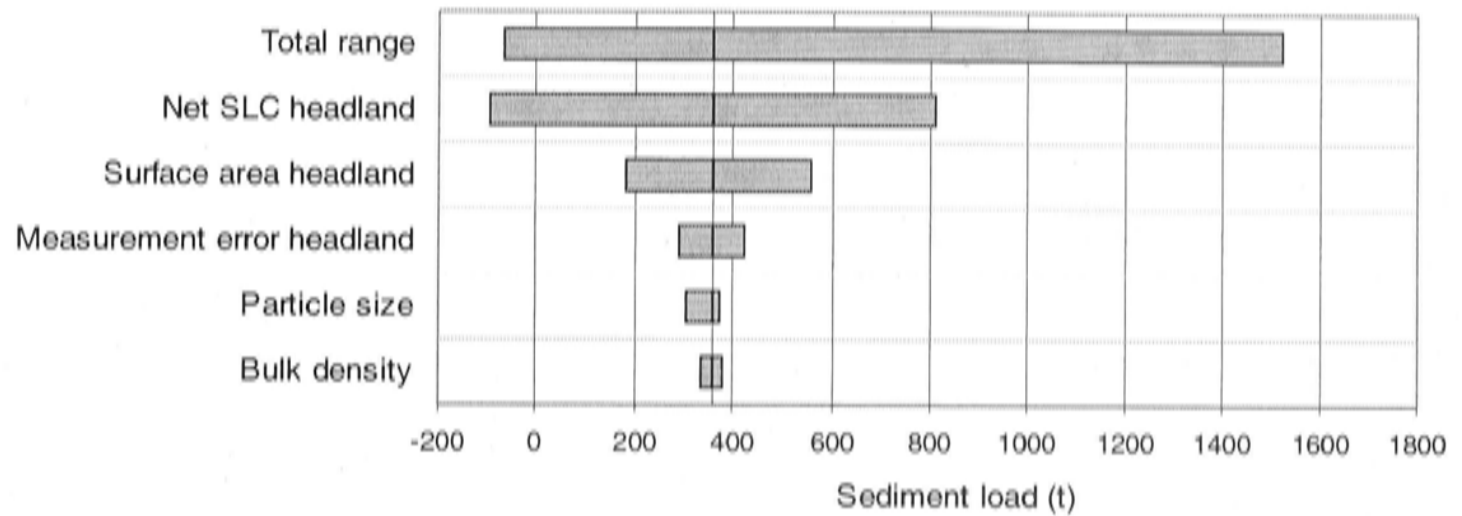


**Figure 11.5:** Worst case uncertainty estimates for headland sediment load calculations. 'Total range' shows the effect of assuming minimum and maximum values for all uncertainties. The separate effect of uncertainty in surface level change (SLC), surface area, measurement error, particle size and bulk density is also shown.

**Table 11.3:** Worst case estimates of headland sediment load in tonnes and as percentage difference of best estimate based on all input uncertainty (Total) and on individual input uncertainties.

	Maximum load (t)	Minimum load (t)	Difference from best estimate (%)	
Total uncertainty	-65	1525	-118	327
Net surface level change	-96	810	-127	127
Surface area	182	558	-49	56
Measurement error	293	422	-18	18
Particle size	306	374	-14	5
Bulk density	333	381	-7	7

## 11.4 Outlet drain gauging data

### 11.4.1 overview

The budget values obtained from gauging data (i.e. forested upland, ratoon fields and catchment output) have different sources of uncertainty than the plot scale erosion and deposition measurements. In summary the following sources of error can be identified:

1. Error in flow depth estimates
2. Error in flow cross-section estimates

3. Error in flow velocity estimates
4. Error resulting from the use of rating curves
5. Error in SSC estimates
6. Error due to temporal resolution of measurements
7. Error in catchment boundary definition
8. Missing data

This section discusses the uncertainty in the catchment output in detail. Procedures for the other gauged variables (upland input and ratoon fields) are very similar and will only be commented on in Section 11.5.

The total load at the catchment outlet is estimated from continuous sediment discharge measured over the budget period. Each sediment discharge record is obtained from depth, SSC, and velocity data records, which all contain errors. The uncertainty in the output will never be larger than the sum of the fractional uncertainties whether or not they are independent and whether or not they are normally distributed (Taylor, 1982), as follows:

$$\delta SD \leq \left| \frac{\partial SD}{\partial d} \right| \delta d + \left| \frac{\partial SD}{\partial v} \right| \delta v + \left| \frac{\partial SD}{\partial SSC} \right| \delta SSC$$

in which  $\delta SD$  is the uncertainty in the sediment discharge;  $\partial SD/\partial d$  is the partial derivative of sediment discharge with respect to depth;  $v$  is velocity; and  $SSC$  is suspended solid concentration. Uncertainty is estimated for each sediment discharge record, and added for all data records in the season, which results in the total uncertainty around the final output value. The contribution from individual variables is also estimated in this manner, assuming zero uncertainty for other variables. The resulting error for the total output is assumed to be the standard deviation of a normal distribution around the best estimate value.

For further error propagation in the I – S estimate, values will be randomly sampled from the uncertainty distributions for upland input and fields. To compare the uncertainty range in the catchment output component with the I – S component, a cumulative frequency curve is obtained from the catchment output uncertainty distribution by taking 1000 random samples.

### 11.4.2 Flow depth and cross-section

Discharge in the outlet drain is estimated using the change in the flow cross-sectional area over time. The cross sectional area is estimated from continuous depth data recorded by a pressure transducer. The pressure transducers installed at the gauging sites are expected to record depth so accurately that their (random) measurement error can be ignored in the presence of other errors in the discharge calculation. However significant uncertainty arises when relating the sensor records to actual drain depths. The 'calibration' measurements used for this purpose showed considerable variation. The uncertainty introduced in the output data this way is calculated from the 'calibration' data presented earlier in Figure 5.4, using the following equation (Taylor, 1982):

$$\sigma_y^2 = \frac{1}{N-2} \sum_{i=1}^N (y_i - A - Bx)^2$$

in which A and B are the parameters obtained from the linear regression between the manual samples and the transducer records. The uncertainty in the depth measurements calculated this way is 7 cm.

The calculation of cross-sectional area from depth includes errors from the initial cross-section estimate. A repeated measurement of the Ripple Drain cross section showed on average a 0.1 m difference in the width on each side of the profile. This estimate is based on only four data points, but is used in the error propagation assuming it is normally distributed. The models used to represent change in profile cross-section with depth have an exact fit ( $R^2 = 1$ ). Because the data are not extrapolated, the model error is thought to be insignificant.

### 11.4.3 Flow velocity

In Section 5.7 the velocity measurements in the outlet drain are described. There is continuous noise in the data with a width of approximately  $1 \text{ m s}^{-1}$ . Results from the automatic Starflow velocity device are compared with a manual velocity meter. Up to  $0.3 \text{ m s}^{-1}$  difference is observed between measurements from each device in the deepest part of the drain. Nothing is known about the accuracy of each, and variation within the drain profile has not been taken into account. In the propagation, the error is assumed to be normally distributed with a standard deviation of  $\pm 1 \text{ m}^{-1}$ .

#### 11.4.4 Suspended solid concentration

The turbidity – SSC calculations are based on two subsequent regressions. Transformation from Greenspan to Grabsample turbidity includes a  $\pm 15$  NTU error for the outlet data and a  $\pm 4$  NTU for the upland input. Transformation of NTU to SSC includes a  $\pm 64$  mg l<sup>-1</sup> error for all data. There could be an additional error because of the method used to measure the total sediment fraction  $< 20$   $\mu\text{m}$  (sieve mesh, balance error, etc.). This was not tested, but the error is expected to be relatively small, adding insignificant uncertainty.

#### 11.4.5 Time and space

Because the temporal resolution of all gauging data is better than 15 minutes, errors through interpolation between data records will be insignificant. Errors in the definition of catchment area (6) could be more problematic. The total load measured at the outlet can only be equal to the load from individual landscape components if all are based on the same catchment and if the catchment boundaries are clear. The boundaries of the total catchment are estimated from the topography in the upland area and from drainage directions, as identified in the Integrated Drainage Survey (see Section 9.2), in the low-lying areas. It is uncertain if these assumed boundaries are correct. Subsurface flow paths of water in the uplands might be different from the surface topography and the accuracy of the topographic map is not known. In the lowlands, drainage directions might change under storm flow conditions. This effect was observed at the Ripple Drain gauging site.

The inputs estimated from the gauging data of the flumes and the upland creek have an increased uncertainty, because the output per unit area, estimated from an area with inaccurate boundaries, is extrapolated over an area with similar inaccurate boundaries.

With the current knowledge of the area it is impossible to make accurate estimates of the additional uncertainty in the sediment budget as a result of the uncertainties in the catchment, sub-catchment and field area boundaries.

#### 11.4.6 Missing data

For the periods that velocity data were missing and parts of the discharge curve have been estimated from a depth – discharge relationship, uncertainty is assumed to lie in the depth data plus uncertainty in the estimate from the relationship. Error included

in this relationship through discharge estimates is ignored. No uncertainty is included for the linear interpolation of the missing turbidity data. The effect of this on the total output value was already shown in Section 5.10.1.

### 11.4.7 Total uncertainty in the budget input from gauging data

The best estimate for the catchment output plus or minus the total uncertainty obtained by propagating the above errors through the flow data, gives the 'worst case' range of uncertainty. The range indicates  $\pm 82\%$  variation around the best estimate (see Figure 11.6 and Table 11.4).

The contribution of uncertainty from the suspended solid concentration estimates is slightly higher than the total uncertainty from discharge estimates (which consists of uncertainty in velocity, cross-section and rating curve estimates).

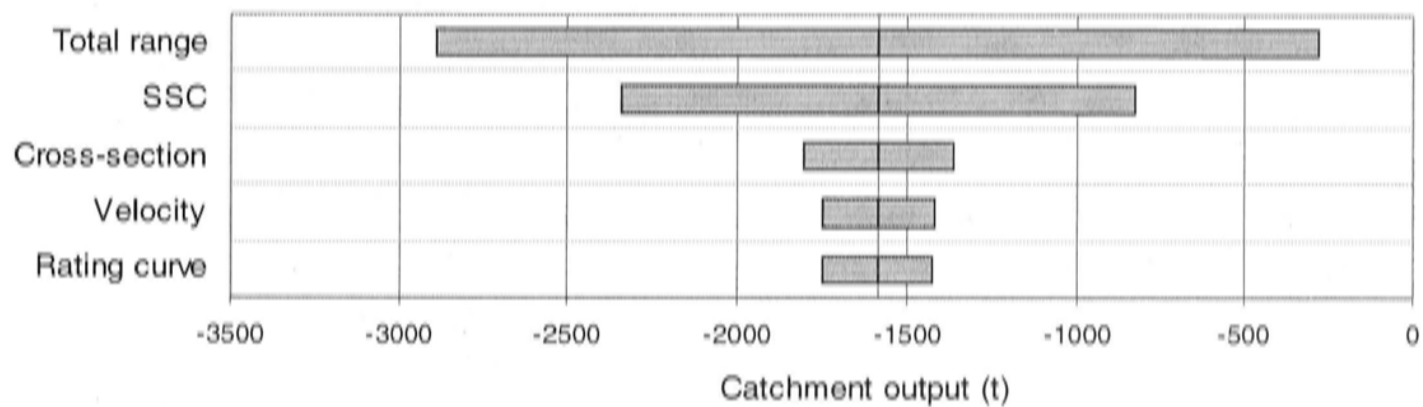


**Figure 11.6:** Worst case uncertainty estimates for catchment output calculations. 'Total range' shows the effect of assuming minimum and maximum values for all uncertainties. The separate effect of uncertainty in SSC, cross-section, velocity and rating curve.

**Table 11.4:** Worst case estimates of catchment output in tonnes and as percentage difference of best estimate based on all input uncertainty (Total) and on individual input uncertainties.

	Maximum load (t)	Minimum load (t)	Deviation from best estimate (%)	
Total range	-282	-2890	-82	82
SSC	-827	-2345	-48	48
Cross-section	-1366	-1806	-14	14
Velocity	-1423	-1749	-10	10
Rating curve	-1424	-1748	-10	10



## 11.5 Comments on the uncertainty estimates for the remaining budget components

Drains, water furrows, fields and upland input have been analysed in a similar way as described for headlands and catchment output. Some differences and unresolved difficulties that were encountered are commented on below:

- The uncertainty around the plant cane input was included in the Monte Carlo simulation by resampling the water sample data. Uncertainty in the monthly runoff coefficients, used to calculate a total sediment load for the season, has been ignored. There was not sufficient information to make an estimate of uncertainty in this part of the calculation.
- As a result of large uncertainty in the suspended sediment concentration data the distribution of the upland sediment load data contains negative sediment loads. This results in an obvious overestimate of uncertainty.
- Velocity for the Post creek was calculated directly from the water depth with a rating curve. The uncertainty related to the rating curve is  $0.2 \text{ m}^3 \text{ s}^{-1}$ . However, it is suspected that much more uncertainty has been included in the estimate by the use of the velocity profiles and the drain cross section. This uncertainty has been ignored, because there were no means to quantify it.

## 11.6 The total uncertainty

### 11.6.1 Worst case estimate

The effect that uncertainty in each budget variable has on the total budget result is shown in Figure 11.7. The light bars show the uncertainty ranges obtained by calculating a budget result from the minimum and maximum uncertainty value for each budget variable, while assuming best estimate values for all other variables. The dark bars show the combined effect of the minimum and maximum uncertainty values for all budget variables. The upper bar shows the range for the catchment output component and the lower bar for the Input – Storage component.

The total uncertainty range is highest for the Input – Storage components of the budget. The bar indicates an uncertainty of around  $\pm 300\%$  of the best estimate. The

total uncertainty range for the catchment output is only  $\pm 80\%$  of the best estimate value.

Most uncertainty is introduced through the estimate for the sediment load from plant cane fields. This was expected, because the grab samples on which the estimate is based had very low spatial and temporal coverage. The uncertainty range indicated here is not even complete. After uncertainty in the plant cane estimate, the variability in net surface level change for water furrows, headlands, and major drains causes most uncertainty in the budget calculation. Because the method that was used to estimate these uncertainties is questionable, it is not clear how representative these ranges are.

### 11.6.2 Cumulative frequency distribution curves

With the uncertainty ranges for all budget variables as defined in the first part of this chapter, Monte Carlo simulation is performed to obtain cumulative distribution functions for the budget components. The resulting curves are shown in Figure 11.8. The simulations for the catchment output (O) cover a wider range of values than the simulations of the I-S budget components. Contrary to the worst case scenario results, this suggests that the I-S components are more reliable. However for both the I-S and O component, 68% of the realizations (comparable with one standard deviation) lie within a range of  $\pm 80\%$  of the best estimate. Also, the curves should be interpreted with caution. There are several reasons to believe that the cumulative distribution curves are not representative for the uncertainty in the sediment budget, for several reasons.

Firstly, it is likely that the tails of the I-S distribution are not as strongly represented as those of the catchment output curve. The empirical distribution functions that were used for the I-S curve exclude the simulation of values outside the range available data, which reduces the tails.

Secondly, the method used to estimate the uncertainty in the catchment output (O) is only valid for small uncertainties (Taylor, 1982). The uncertainties in the outlet data are likely to be too large for the method to be appropriate. It also is the worst case scenario, because no other method was found that could deal with it otherwise. The distribution for catchment output is therefore likely to be relatively wide.

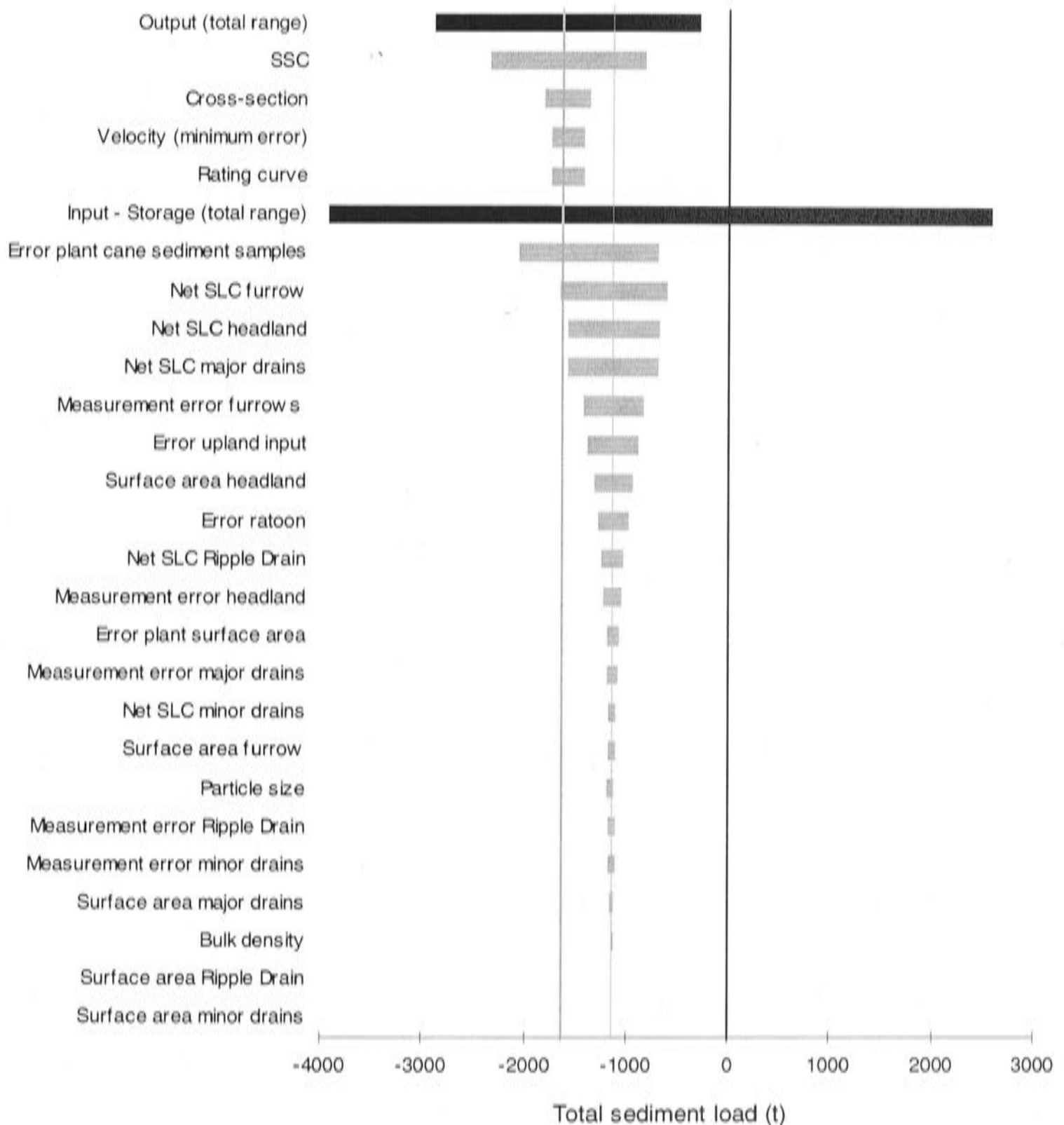


**Figure 11.7:** Worst case uncertainty estimates for the 99-00 sediment budget. 'Total range' (dark bars) shows the effect of assuming minimum and maximum values for all uncertainties. Light bars show separate effect on total sediment load of uncertainty in surface level change (SLC), surface area, measurement error, particle size and bulk density.

Finally, Hession *et al.* (1996) describe a Monte Carlo uncertainty analysis for an application of the Universal Soil Loss Equation. They show how discretization of the modelled area causes a reduction in the variance of the simulated erosion rates, if independence of the sub-areas is assumed. The variance of the simulation results when the model is applied to a whole field, is higher than the total variance of separate simulations for parts of the field. The authors show that this is a mathematical artefact.

The I – S value for the budget area is also composed of separate sub-areas; it is the sum of the values for individual landscape elements. Simulation of this addition might therefore reduce the total uncertainty in the results for the same reason as described by Hession *et al.* (1996).

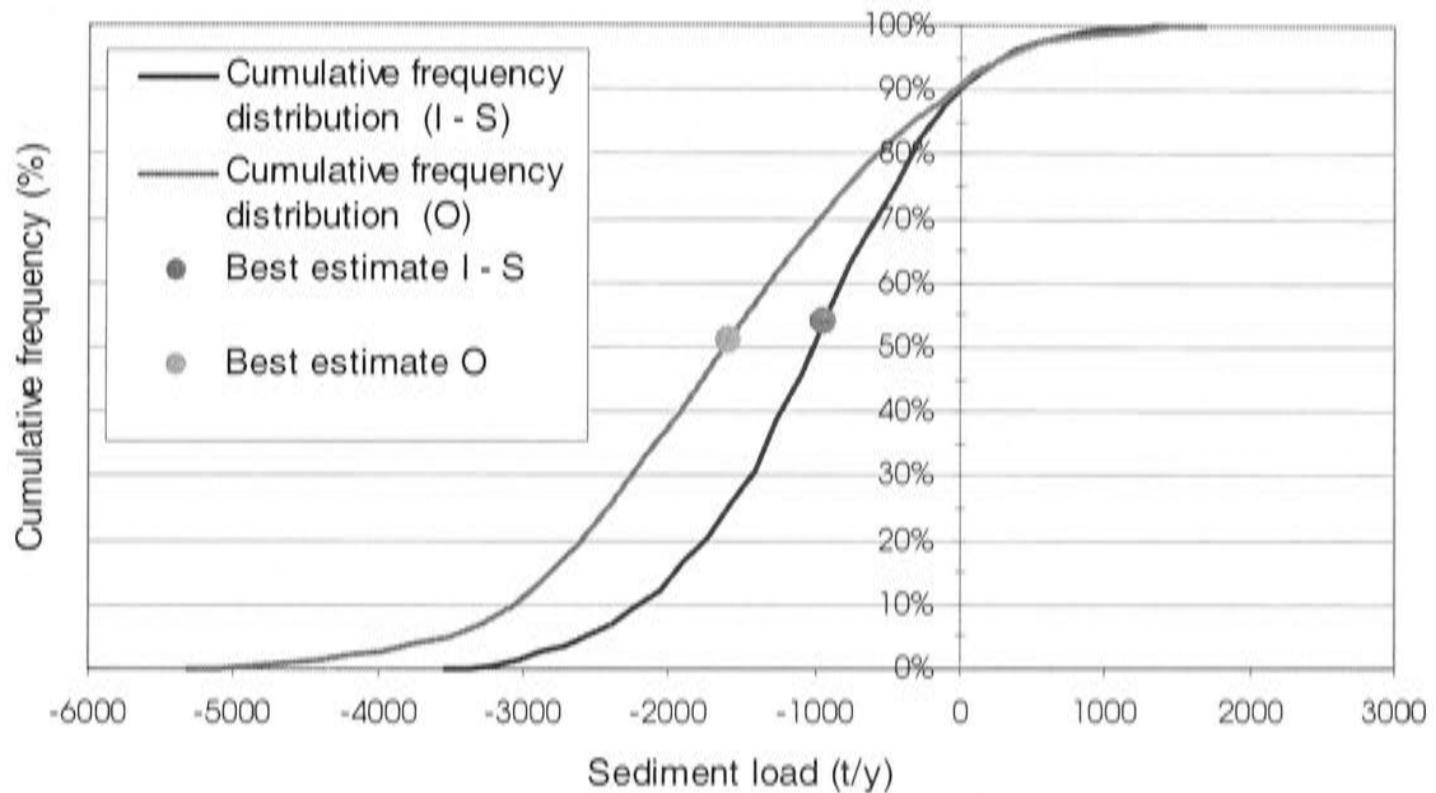


**Figure 11.8:** Cumulative frequency distribution curves obtained from 1000 simulations of the sediment budget components I-S (dark) and O (light). Best estimate values for each component are indicated with dots.

### 11.6.3 Error correlation

Correlation between variables in the budget calculation should be included in the Monte Carlo simulation, because it can have an effect on the total variation in the budget output. Several of the variables used in the composition of the budget calculation are correlated. The surface area of each landscape element is an example of this. If the area of one landscape element increases, another area has to decrease. The total surface area always has to add up to 100%. Other correlations are less well known, but likely to exist. Field observations, for example, showed that headland surface level change was influenced by runoff from the field, and that field runoff was on the other hand related to drain discharge.

Because of the complex interactions between budget variables, a sufficient study of correlations is beyond the scope of this thesis and not included in the simulation of the budget results. Disregarding correlation is, however, likely to be a cause of the relatively small range of uncertainty resulting from the Monte Carlo simulation of

the I – S budget component. Hession *et al.* (1996) show how the reduction of variance as a result of discretization of the modelled surface area becomes smaller with increasing correlation across sub-areas. The same is likely to occur when correlation between budget variables in the various landscape elements is taken into account.

## 11.7 Conclusion

All methods presented to quantify the uncertainty in both sides of the sediment budget equation for low-lying sugarcane land indicate that there is a range of at least 80% uncertainty around the best estimates. This means that the budget difference lies within the error ranges of the estimates for both sides of the equation, and could therefore be the result of an error in the estimates of each of the components. Because of the large error ranges, it is not possible to say whether the budget equation was complete and whether all potential sources and sinks in the budget area were included. However, field observations show that all components have been included.

Two different ways to determine the uncertainty in the I-S component of the budget resulted in rather different uncertainty ranges. A large uncertainty, as shown by the 'worst case' estimate, was expected because of the plot scale methods that were used to quantify this budget component. Applying the Monte Carlo method resulted in a remarkably smaller uncertainty range. It is however likely that it is not wholly appropriate to use this method in the present situation. There are several unresolved problems, such as correlation in the data and the significance of reduced variation as a result of area discretization.

When a similar uncertainty analysis is performed with the 00-01 budget data, uncertainty ranges will become wider. Most of the budget input will be based on less data and less reliable data. Only the input from plant cane fields has been quantified more accurately during this season, but this will not significantly reduce the total uncertainty.

---

## **PART III**

# **FLOODPLAIN EROSION AND THE CASE OF THE LOWER HERBERT RIVER**

---

### *OUTLINE*

An important result of Part II of this thesis is the observation that the Ripple Corner Catchment is a net source of sediment. This observation confirmed the idea, presented in Chapter 1, that sugarcane land can be a source of the sediment in North Queensland rivers that drain into the Great Barrier Reef. From the sediment budget study for the Ripple Corner Catchment it is now known how much sediment comes from sugarcane land. It is however not known how representative the findings are for all areas of low-lying cane land.

The observation of a floodplain as a sediment source contradicts the general understanding that floodplains are areas of sediment storage within river catchments (Schumm, 1977; Alexander and Marriott, 1999). Erosion on floodplains is usually insignificant compared to sediment deposition, which makes them sediment sinks. This raises the questions why the study area acts as a net sediment source and if the sediment budget observation is representative for processes in larger parts of the Herbert River Catchment.

In the following Chapter (Chapter 12) literature on the geomorphology and hydrology of river floodplains is reviewed. The review focuses particularly on processes of floodplain erosion. With this insight into floodplain erosion processes and additional material from local reports, the possibility of erosion of the Herbert River floodplain in the Ripple Creek Catchment is considered in the light of human modifications to the floodplain surface characteristics and hydrology. This leads to the development of a number of qualitative scenarios that describe how different (flood) flow conditions in the Herbert River Catchment can result in local degradation of the floodplain surface (Chapter 13). It will also provide an indication of the representativeness of the observed degradation rates for the whole floodplain of this tropical catchment.

---

## Chapter 12

### Floodplain processes

---

#### 12.1 Floodplain definition

There is no exact definition of a floodplain. The main reason for this is that there are various ways in which the boundaries of a floodplain can be defined. Differences surround the inclusion of river channels and tidal areas, and the minimum frequency of inundation, so that the landform can still be called a floodplain. In their description of floodplains, Alexander and Marriott (1999) cite a number of studies that apply various definitions. Most of these include the following general characteristics:

- Floodplains are rather flat landscape elements adjacent to a river.
- Floodplains are built up from unconsolidated alluvial material deposited by the river.
- Floodplains serve as a store for water and sediment when the regular river channel can not handle the supply from upstream and overtops its banks.

Alexander and Marriott (1999) use these general characteristics, limited to those areas periodically inundated at least every 100-200 years, to define active floodplain systems. Their definition does not only include yearly-inundated wetlands close to the river channel, but also areas which are defined on the basis of flood risk and therefore can not always be clearly delineated. The definition used by Alexander and Marriott (1999) will apply to the floodplains discussed in this review. Also, using this definition, most of the alluvial plain in the Lower Herbert River Catchment is a floodplain.

## 12.2 Floodplain formation

### 12.2.1 Formation processes

Nanson and Young (1981) studied the floodplains of small coastal streams in the Illawarra region in New South Wales, Australia. At their downstream ends these rivers have formed floodplains as gently sloping coastal plains. The floodplains are built entirely by deposition of layers fine sediment, derived from overbank flow during flood events. The river channels maintain a stable position within this cohesive sediment. By contrast, the floodplain of the Watts Branch in Maryland, USA, studied by Wolman and Leopold (1957) shows a different type of formation. This lowland floodplain was built by the continuous lateral movement of a meandering river, through deposition of point-bars at convex meander banks and consumption of earlier deposits by erosion of the concave banks.

The different appearance and sedimentary composition of these two examples of floodplains are typical results of two different dominant floodplain formation processes: formation through vertical accretion by overbank deposition in the Australian case, and formation through point-bar accretion and lateral movement of the river channel in the USA case. Many floodplains are formed by a combination of these two processes. The existence of both processes has long been identified, but lateral migration was often seen as most important for the building of floodplains (Wolman and Leopold, 1957). Only recently, more situations have been studied in which vertical accretion appears to be the major floodplain building process (Nanson and Young, 1981; Nanson, 1986; Lambert and Walling, 1987; Gomez *et al.*, 1998).

Researchers have become aware that each floodplain type is the result of a different combination of factors such as stream power, transport capacity, sediment texture and channel resistance. Nanson and Croke (1992) distinguished a wide range of types and classified them based on the energy environments in which they were formed. They proposed a primary classification by three classes of specific stream power: high ( $>300 \text{ Wm}^{-2}$ ), medium ( $10\text{-}300 \text{ Wm}^{-2}$ ) and low ( $<10 \text{ Wm}^{-2}$ ). The three classes can occur within reaches of a single river, from an upstream high-energy environment in a steep bedrock channel to a downstream low-energy environment on a low-gradient coastal plain. Different environmental conditions will cause



differences in energy levels between streams. Likewise a change in environmental conditions can change energy levels and thus the types of floodplain formation within a stream.

A decrease in specific stream power in the classification of Nanson and Croke (1992) implies a decrease in particle size of the transported sediment, which determines the composition of the floodplain. The floodplain composition will in turn determine the extent of lateral movement of the river through resistance of the stream banks. The Illawarra rivers in the introductory example are, due to their low stream power, only able to transport fine material. This has resulted in cohesive floodplains. Because of the cohesiveness and the low stream power the river is not able to move laterally. The higher stream power of the Watts Branch allows transport of coarser sediment and has resulted in a less cohesive composition of the floodplain. In this environment the river does move laterally.

### **12.2.2 Floodplain accretion rates**

Through trapping and accretion of sediment during their formation, floodplains become zones of sediment storage in a river system (Schumm, 1977). In this process a large part of the sediment generated upstream is captured, before it can reach the catchment outlet. The capacity of a floodplain to serve as a sediment store can become especially clear when the sediment load in a catchment suddenly increases, for example due to severe erosion of upland hillslopes after logging of the forest cover. In the Coon Creek catchment in Maryland (USA), Trimble (1981, 1999) documented an increased sediment load from hillslope soil erosion. The increased load did not reach the catchment outlet. Instead accelerated floodplain accretion was observed, indicating that most sediment was trapped before reaching the outlet.

Many estimates have been made of the efficiency of floodplains to trap sediment generated elsewhere in a catchment. These estimates vary widely, but usually comprise a considerable part of the total sediment load. For the River Waal in The Netherlands, Middelkoop and Asselman (1998) calculated floodplain deposition as 19% of the total suspended load for one year. Lambert and Walling (1987) estimated that 28% of the sediment load from the River Culm in Devon (UK), remained in floodplain deposits. For the Ganges-Brahmaputra catchment, Allison *et al.* (1998) estimated that up to 71% of the sediment load is stored on the floodplains. A low value has been estimated for the Waipaoa River floodplain in New Zealand. Gomez

*et al.* (1999) observed that most of the sediment load for this river is transported during flow below bankfull stage. The amount of material deposited on the floodplain during overbank flows is only 5% of the total load.

The thickness of deposition on the floodplain surface depends on several factors such as the sediment concentration of the floodwater, the width of the floodplain and the frequency and duration of flood events (Dietrich *et al.*, 1999; Gomez *et al.*, 1999). Mertes, (1994) gives values for central Amazonian rivers in the order of centimetres per day, which equals annual amounts of metres. Gomez *et al.* (1999) estimate average vertical accretion of 4-6 cm per year for the Waipaoa River. In contrast Lambert and Walling (1987) measured yearly thicknesses of less than a millimetre for a British lowland river.

## 12.3 Floodplain development

### 12.3.1 Development processes

When some tectonic, climatic, or human (e.g. massive re-vegetation) change alters the (flow or sediment) regimen of a river, a floodplain surface can be transformed into a terrace by entrenching itself below its established bed and associated floodplain (Wolman and Leopold, 1957). Without interruption by such major environmental change, a river channel could gradually become deeper as the alluvium it deposits gets thicker during repeated overbank flows. In the case of laterally migrating rivers this does not occur, because, in a time period that can range from a few hundreds to more than a thousand years (Leopold *et al.*, 1964; Walling *et al.*, 1996), the moving river channel will remobilize earlier floodplain deposits. This way the floodplain system remains in equilibrium with its channel (Leopold *et al.*, 1964).

Floodplains that are predominantly formed by vertical accretion can respond to continued sediment supply in different ways. Gomez *et al.* (1999) suggest two types of development for rivers that build floodplains by vertical accretion. For the Waipaoa River in New Zealand they demonstrate how the progressive accretion of the floodplain surface is complemented by channel aggradation. The channel capacity of this river remained constant, while the bankfull channel width was reduced and the depth increased (Gomez *et al.*, 1998). Alternatively the authors

suggest that increasing bank height could increase the channel capacity of a river. This will reduce the flood frequency and thus lead to reduction of the floodplain accretion rate. For both types of development, however, sediment deposition on the floodplain continues, which means that the system establishes a quasi-equilibrium.

Leopold *et al.* (1964) suggest a third option, which is vertical floodplain degradation, as opposed to vertical floodplain aggradation. He argues that this could occur due to irregular distribution of floodwater flow over the floodplain surface. The turbulent water flow could erode the surface by scouring.

### 12.3.2 Floodplain degradation

Degradation of floodplains by lateral migrating channels is seen as most important (Dunne *et al.*, 1998) and is usually studied in combination with lateral accretion processes. Studies of vertical floodplain degradation are less common and very few estimates are made of the net effect of degradation and accumulation.

For a floodplain in a high-energy stream environment, Nanson (1986) describes a case of catastrophic vertical floodplain degradation. He found that clusters of major floods caused erosion of enormous volumes of floodplain alluvium along the Manning River in Australia. The laterally stable channel of this river continuously builds its floodplain by vertical accretion. This increases the channel capacity and reduces the frequency of overbank flow. High magnitude flow events subsequently cause catastrophic erosion of the steep gradient floodplains. Variation in the growth rate of the floodplain and the intensity of floods along the river reach cause different flood events to affect different parts of the floodplain.

Ferguson and Brierley (1999) describe similar stripping of the floodplain surface for the lower Tuross River in New South Wales. They noticed that this type of floodplain erosion occurred especially in the sandier floodplain surfaces that are affected by floods of relatively high streampower ( $\pm 300 \text{ Wm}^{-2}$ ). The same factors appeared to be important reasons for the occurrence of severe floodplain destruction by channel widening along a semiarid river in Kansas (Schumm and Lichty, 1963).

Systematic vertical floodplain degradation in the medium and low energy environments of the classification by Nanson and Croke (1992), with cohesive floodplain surfaces and lower stream power, has not been described in the

geomorphological literature. The only form of vertical floodplain degradation, documented for this type of floodplain, is scouring as suggested by Leopold *et al.* (1964). Examples of floodplain scouring are mostly the result of high magnitude flood events, and the extent of destruction is often restricted. Kochel (1988) and Miller (1990) list a number of authors that describe floodplain erosion as a result of high-magnitude events.

The factors that affect the extent of floodplain destruction through scouring by major floods are not well understood. In some cases the resistance of the floodplain surface is considered as the reason for the insignificant impact. Gomez *et al.* (1995) observe that certain parts of the Upper Mississippi River valley did not show considerable floodplain erosion after a rare high magnitude event, while other areas were severely affected. They argue that the locally higher resistance of the floodplain material is an important factor, which should be taken into account when evaluating the sensitivity of floodplains to rare high-magnitude events. Schumm and Lichty (1963) provide a similar example where dense cohesive alluvium may have offered considerable resistance to floodplain destruction.

Vegetation cover can also provide resistance to a floodplain surface. In various studies vegetation is mentioned as a factor that influences the selective preservation of floodplain deposits. Gupta and Fox (1974) describe the erosive effects of four catastrophic floods on the floodplains of the temperate Patuxent River in Maryland, USA. They observed that the only significant scouring on the silty clay floodplain particularly occurred in areas with sparse vegetation. Similar effects were mentioned by Baker (1988), Prosser *et al.* (1994) and Ferguson and Brierley (1999).

Apart from surface resistance, other factors might be of equal importance. Miller (1990), for example, shows how erosion features are not the simple result of the unit stream power in a river, and how they are associated with specific configuration of channel and valley form, and flow patterns.

#### **12.4 The role of various floodwater sources**

Nanson and Croke (1992) show how the sediment size of material transported by a river determined the composition and consequently also the type of floodplain. They assume that floodwater on the floodplain is the water that is derived from the main river channel by overbank flow, as do most of the floodplain studies cited in the previous sections. However, across a floodplain surface, different types of floodwater

can occur. The composition and distribution of the types may be factors that influence the geomorphic development of a floodplain. Variations in floodwater have received attention only recently, especially because of their influence on the ecology of floodplain environments (Amoros and Bornette, 2002; Mertes, 2002). Less is known about their geomorphic importance.

#### 12.4.1 Sources of floodwater

Mertes (1997) shows, for a number of large river systems across the world, that floodplain inundation can be composed of water from different input sources. Apart from overbank flow from the main channel he distinguishes floodwater from:

- Catchment scale tributaries
- Local tributaries at the scale of the floodplain
- Groundwater
- Direct precipitation
- Slopes draining directly onto the floodplain

Before water from the main channel overflows onto the floodplain, these other sources could have already inundated parts or even most of the floodplain surface. This can result in mixing of the river water with the already present local floodwater.

The extent of the mixing depends strongly on the morphology of the floodplain surface. Mertes *et al.* (1995) demonstrate this in a study of three reaches of the Amazon River. When floodwater from the river enters the floodplain as diffuse overbank flow it readily mixes with the already present locally derived floodwater. Entrance of the river water onto the floodplain via tributary channels on the other hand reduces the opportunities for mixing with local floodwater. In some cases the local water can completely prevent overbank water from entering the floodplain, and the local water might even enter the river channel (Dietrich *et al.*, 1999). Mertes (1997) calls the mixing zone of river and local floodwater the “perirheic zone” meaning the zone surrounding (“peri”) the flowing river water (“rheo”).

The distribution and temporal variation of rainfall in a catchment will have great influence on the hydrologic variability of the perirheic zone (Mertes, 1997; Alexander *et al.*, 1999; Dietrich *et al.*, 1999; Stewart *et al.*, 1999). These factors

control the amount of water that is available from different sources, and the relative arrival time of each on the floodplain surface.

#### **12.4.2 Floodwater sources and floodplain formation**

The various types of floodwater that can inundate a floodplain will have different sediment and nutrient compositions, depending on their origin. Using remotely sensed optical infrared-images, Mertes (1994, 1997) showed differences in sediment concentration of floodwater on floodplains. Mertes (1997) suggested that the differences in the sediment composition of floodwater and its distribution across the floodplain could affect the floodplain geomorphology. The following observations by Dietrich *et al.* (1999) and Alexander *et al.* (1999) confirm her suggestion.

Through qualitative analysis of remote sensing data for the Fly River in Papua New Guinea, Dietrich *et al.* (1999) distinguished three types of processes that deliver sediment to the floodplain: advection through overbank flow; diffusive transport due to a sediment concentration gradient between the river source and floodplain sink; and transport upstream in tie channels and tributaries. For only for one month of the year water from the main river rather than local runoff seemed to contribute significantly to the storage of water on the floodplain. Dietrich *et al.* (1999) assume that this causes the low overbank deposition rates estimated for the floodplain. Continuously high water levels on the floodplain prevent the development of pressure gradients from the main channel to the floodplain and therefore inhibit sediment deposition.

For much drier conditions in the semi-arid to sub-humid tropical Burdekin catchment in Australia, Alexander *et al.* (1999) document the inundation of channel margins and floodplains solely as a result of intense local rainfall. The authors suggest that some of the finer deposits on the floodplain might come from local runoff as a result of the intense rainfall. However, such finer sediments are not common. The short duration of the flood waves in the Burdekin River and the high flow velocities of the floodwater, supply coarse (up to gravel size) overbank deposits. The floods that transport this coarse sediment might erode some of the fine sediments of local origin.

### 12.4.3 Floodwater composition and floodplain degradation

For the Fly River Dietrich *et al.* (1999) suggested that restricted mixing of sediment rich and sediment-deficient floodwater was reflected in the low rates of floodplain accretion. Leopold *et al.* (1964) identified erosive sediment-deficient floodwater as one of the mechanisms that can counteract the depositional tendency of floodplains. A few floodplain studies show how low sediment concentrations in the floodwater can even have an erosive effect: Graf *et al.* (1991) and Burkham (1981, in Graf *et al.*, 1991) noticed the increased ability of sediment-deficient floodwater to erode the channel banks. Baker (1988) mentions how this water can also be erosive when it moves onto a floodplain surface.

Two additional noteworthy examples of sediment-deficient floodwater types counteracting floodplain accretion are given by Mertes (1997) and Bornette *et al.* (1994). Mertes (1997) points out how scouring during extreme floods may never be repaired in areas on the floodplain side of the perirheic zone, due to a lack of sediment. Bornette *et al.* (1994) showed how water supplied by groundwater seepage in a floodplain can remove fine sediment and might reduce the overall tendency towards infilling of certain floodplain areas.

## 12.5 Summary and implications

Laterally migrating river systems continuously rework their floodplains. The erosion is however offset by simultaneous deposition, and the net change in floodplain volume and height is small. Other rivers form their floodplains mainly through vertical aggradation. If continuing deposition makes a system unstable, erosion follows on these floodplains. In high-energy environments, this has been shown to happen by several authors. For low-energy environments the development of such floodplains is however not well known. Only localized degradation by severe floods is reported.

The extent of floodplain degradation appears to depend on different factors such as the stream power of the floodwater and the resistance of the floodplain surface both through its sedimentary composition and the vegetation cover.

A factor that is rarely considered in floodplain formation studies is the source of the floodwater, and, related to this, the variation in distribution of water with different sediment composition across the floodplain. This has an effect on

floodplain accretion, and it might even directly affect degradation. The examples are most striking for tropical situations, where local runoff is significant as a result of high intensity rainfall.

For all cases in which deposition is followed by erosion, floodplains only provide a temporary store for sediments. The storage time depends on the rate of floodplain development.

Remobilization of floodplain sediment can in certain situations cause environmental problems. Marron (1992) gives a clear example of this from the Belle Fourche River in South Dakota, USA. Goldmining introduced 100 million tonnes of arsenic contaminated sediment into this river system. Marron found more than one third of these mine tailings in floodplain deposits along the river. Although the mining ceased in 1978 contaminants are still being released into the environment through the migration of the river channel, and this is expected to continue for many more centuries. These problems have also been pointed out by Walling *et al.* (1996), Knighton (1998), and Owens (2001). The processes of floodplain development and especially the role of floodplain degradation deserve more attention for this reason alone.



---

## **Chapter 13**

# **Scenarios of erosion and deposition on a floodplain in the Lower Herbert River Catchment**

---

### **13.1 The case of the Lower Herbert: a cultivated floodplain**

The Lower Herbert River has a mixed channel pattern: from low sinuosity to meandering with evidence of avulsion. As a result of the lateral movement of the channel, the riverbanks are locally eroding. There is no evidence that the meander bends are widening, or that the channel is doing so. Sediment export from bank erosion is offset by sediment deposition on other banks. Certain human activities might have increased the erosion rate, for example, by reduction of riparian vegetation or boating on the river (Herbert River Improvement Trust, 1993).

The sediment input into the Herbert River that is specifically derived from the areas of sugarcane cultivation is however generated on the floodplain surface. Under the conditions studied in thesis, parts of the cultivated floodplain are a net source of sediment. This type of erosion is not related to meandering processes and could therefore be described as a form of vertical erosion, distinct from lateral erosion of the floodplain.

From the review of floodplain processes in Chapter 12 it became clear that there is little known about the processes and magnitude of vertical floodplain erosion. Also, the effect of cultivation on the geomorphic development of floodplains is hardly ever discussed in the literature, so processes in the Herbert River can not be compared with similar cases. There are however a number of reasons to believe that human activity on the floodplain has modified the processes of floodplain erosion and deposition in the Lower Herbert River Catchment and specifically Ripple Creek.

### **13.2 Floodplain modification for land use**

Since European settlement in the Herbert River Catchment, the floodplain has been altered in several ways. Gutteridge, Haskins and Davey (1976, in Cameron McNamara, 1980) describe some of the alterations in a drainage study for the North Queensland sugar industry:

Development of farming activities has altered the general environment, increasing the rate of runoff and encouraging erosion and siltation. Much of the original natural drainage network and channels have been altered as the areas have been progressively developed for cane fields. Drainage lines have been levelled to provide farm lands, and small creeks have been filled in and diverted without adequate thought having been given to the consequences, or action having been taken to provide alternative watercourses.

More recently drainage has been improved through further development of the drainage network (Cameron McNamara, 1980):

Improved drainage also results in less infiltration of water and flow volumes are greater than they were prior to development.

Before cultivation of the floodplain started, Herbert River water would flow 'upstream' into Ripple Creek during minor floods. Cameron McNamara (1984) described this as follows:

...The outflow capacity of Ripple Creek is also affected by the water level of the Herbert River adjacent to the mouth of Ripple Creek ... as Herbert River rises, the backwater effect up Ripple Creek firstly reduces outflow and ultimately reverses the flow. Ripple Creek has greater capacity in reverse flow than it does in its natural flow direction...

In the case of extreme floods, when the Herbert River level rises above the height of the levee banks, reverse flow through the Ripple Creek outlet is not large enough to divert all excess river water. Instead the river overtops its banks.

To improve drainage and prevent Herbert River water from entering the floodplain, floodgates have been installed at the outlet of Ripple Creek. The floodgates hold back Herbert River floods with a recurrence interval of up to three years. The heavy tropical rainfall and large amounts of runoff from local uplands, however, still causes a large amount of water directly onto the Ripple Creek floodplain. This water now gets ponded against the floodgates and causes inundation during minor floods. During major floods the Herbert River still overtops its banks and floodwater enters the floodplain.

### **13.3 Potential impact**

The modifications of the surface characteristics and the flooding patterns of the Herbert River will affect the geomorphic development of the floodplain. In the light of the review in Chapter 12, in which floodplain degradation processes and the factors that appear to influence them were discussed, the modifications could have the following effects:

#### *Erosion resistance*

Several studies have shown how a vegetation cover can protect a floodplain surface against scouring (Gupta and Fox, 1974; Baker, 1988; Prosser *et al.*, 1994; Ferguson and Brierley, 1999). Cultivation of the Herbert River floodplain has generally lowered the erosion resistance of the floodplain, and has made the surface more prone to erosion and scouring by flowing water from any source.

#### *Drainage efficiency*

Artificial drainage systems and surface levelling have increased drainage volumes and flow velocities. This has increased the possibility of erosion and scouring of both the drainage system and the floodplain surface, and it has increased the possibilities of sediment export from the floodplain, while the likelihood of settling of mobilized sediment through ponding has decreased.

#### *Flood regulation*

Installation of floodgates in the Ripple Creek Catchment prevents entry of Herbert River water onto the floodplain during minor flood events. Under these conditions inundation of parts of the floodplain occurs, but the floodwater consists only of local runoff. This indicates that there are distinct types of floodwater similar to those observed by Mertes (1997) and Dietrich *et al.* (1999). Differences in the composition of the floodwater types could affect floodplain development in different ways, as was shown in Section 12.4.

### **13.4 Scenarios of flooding, erosion and deposition in the Ripple Creek Catchment**

In the Ripple Creek Catchment, reduced resistance of the floodplain surface as a result of cultivation and the altered drainage and flooding patterns have a combined

effect on floodplain erosion and deposition rates. Observations made during the sediment budget study in part II of this thesis combined with information from local sources described in Section 13.2, have led to a set of four qualitative scenarios for erosion and deposition in the Ripple Creek Catchment under different flow conditions. Each scenario is described below and all scenarios are illustrated schematically in Figure 13.1.

*Scenario 1: local inundation*

At the onset of a tropical rainstorm, local runoff from the steep forested hillslopes (E) and high intensity rainfall directly onto the floodplain is directed through the artificial drainage system (D) via Ripple Creek (E) into the Herbert River (A). High intensity rainfall on the floodplain surface generates considerable runoff, which causes sheet erosion on bare fields and scouring in water furrows and drains (C+D). The eroded material is removed from the floodplain into the Herbert River, via Ripple Creek. This situation continues until the floodgates close with rising water levels in the Herbert River, and it recommences when the gates reopen as the Herbert River falls below the Ripple Creek outflow level.

*Scenario 2: reverse flow from the Herbert River*

Before installation of floodgates at the Ripple Creek outlet, Scenario 1 would continue until the water level of the Herbert River rose above the outflow from the Ripple Creek; usually as a result of high rainfall input from elsewhere in the Herbert River Catchment. This would cause reverse flow of Herbert River water via the outlet of Ripple Creek as described by Cameron McNamara (1984). In this situation, Herbert River water mixes with locally derived floodwater. The drainage system can not contain the large volumes of flow, and excess water spreads onto the floodplain. When the Herbert floodwater spreads out, its flow velocity is reduced and the sediment it contains can settle. Local floodwater will be blocked by the inflow from Herbert River water and will also deposit part of the sediment it contains.

*Scenario 3: blocking of floodwater by floodgates*

The installation of floodgates caused a modification of Scenario 2. When the floodgates are closed, Herbert River water can not enter the floodplain via the Ripple Creek outlet. At the same time export of local runoff into the Herbert is impeded and

water ponds behind the floodgates. Ponding reduces both flow velocities in the drains and, at high water levels, runoff from the fields. The erosive power of runoff is reduced and locally eroded sediment is redeposited. This situation was observed several times during the sediment budget study. With lowering of the Herbert River levels and reopening of the floodgates, scenario 1 recommences until the floodplain is completely drained.

*Scenario 4: the Herbert River overtops its banks*

Under extreme flood conditions in the Herbert River the river water level rises above the levee banks and spills onto the floodplain. Cameron McNamara (1984) reports cases of severe scouring near levee banks due to spillage. The power and quantity of the floodwater might also cause major scouring in the artificial drainage system and on unprotected surfaces of the floodplain (particularly at falling stage of the flood). The flow velocities are however low compared to the river water and sediment derived from upstream in the Herbert River Catchment settles out. Any effect of locally derived floodwater is thought to be insignificant under these conditions, because the volume of local floodwater will be much smaller.

*Observed flow conditions*

Only the flow conditions of Scenario 1 and 3 were observed during the sediment budget study. Scenario 1 occurs frequently as a result of the regular heavy rainfall. Scenario 3 occurs several times each wet season, with persistent heavy rainfall, when minor flooding occurs. Scenario 2 no longer occurs since installation of the floodgates, but is included to illustrate change. Scenario 4 was not observed. This condition is less common, occurring during major flood events, for example during the 1977 flood, the extent of which is shown in Figure 2.4. The flow condition of Scenario 4 has a return period of less than 25 years, but probably greater than 3 years, which is the flood size for which the floodgates have been designed.

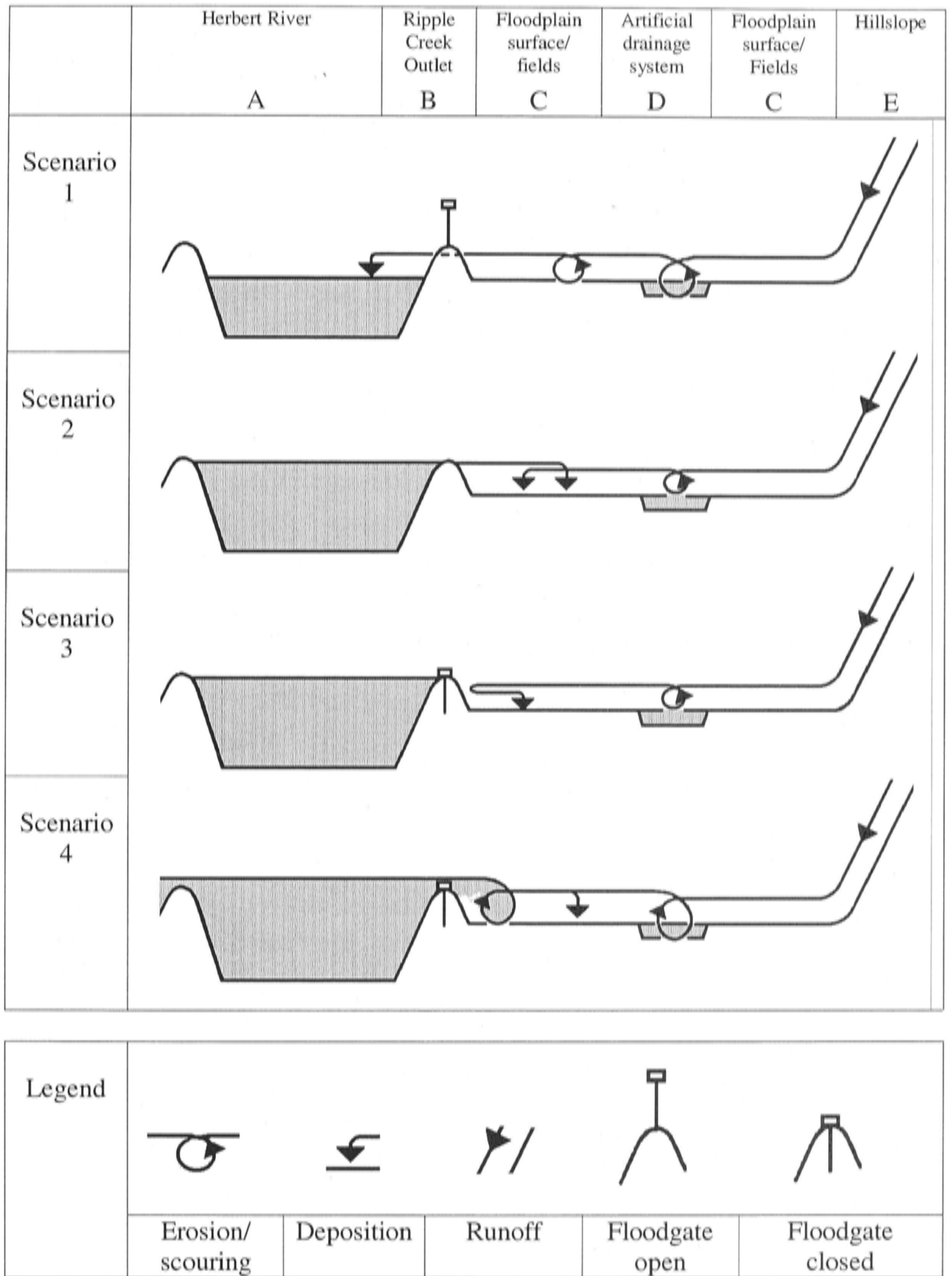


**Figure 13.1:** Scenarios of erosion and deposition processes under four different (flood) flow conditions on the Ripple Creek floodplain.

### 13.5 Additional observations

During the various field visits in the wet season, distinct differences were observed in the turbidity of the drain water. At times of peak flow the water appeared generally less turbid than during lower flow conditions. At various locations in the catchment water samples were taken. The suspended solid concentrations of samples from four locations are shown in Figure 13.2 and the data are presented in Table 13.1. Sample location DG3 and DG6 were in minor drains, location DG17 was in a major drain, and DG21 was in Ripple Drain at the outlet of the Ripple Corner Catchment (see map in Appendix A).

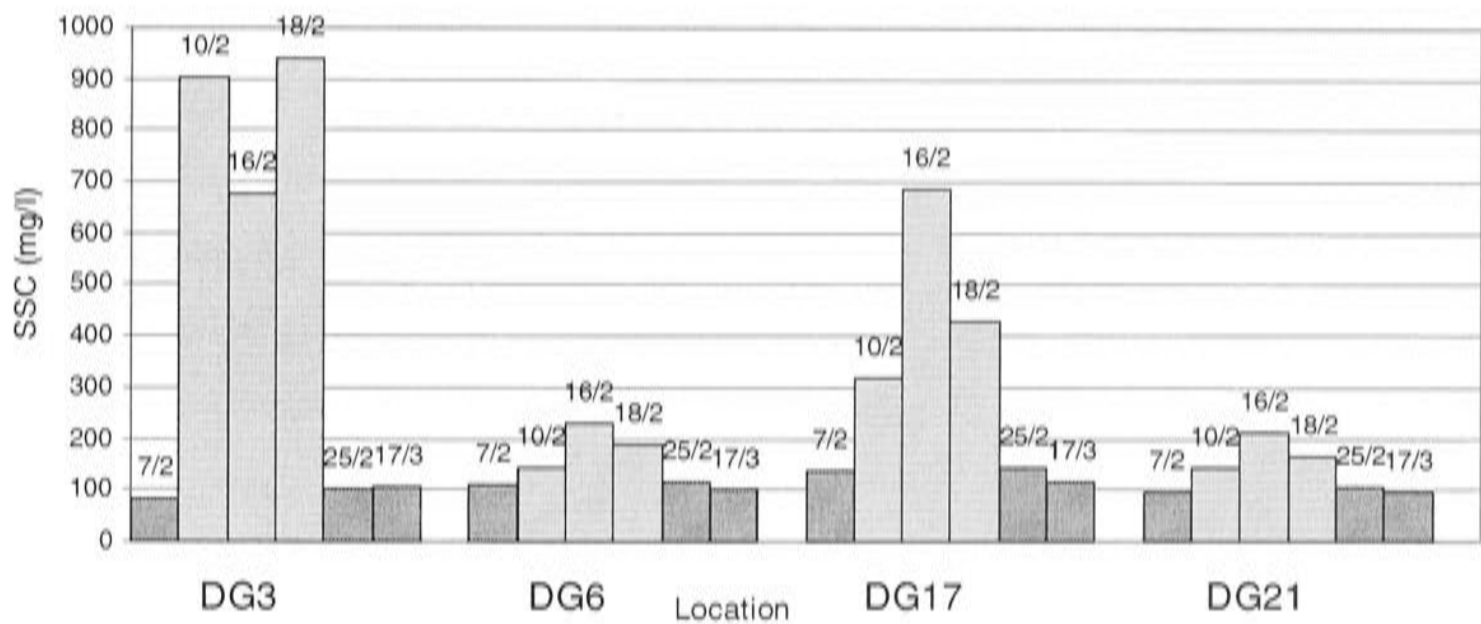


**Figure 13.2:** SSC ( $\text{mg l}^{-1}$ ) in water samples from four locations in the Ripple Corner Catchment (99-00 season). Dark bars indicate peak flow (backwater) conditions; Bright bars indicate free flow conditions.

**Table 13.1:** SSC ( $\text{mg l}^{-1}$ ) in water samples from four locations in the Ripple Corner Catchment and Ripple Drain, and discharge at time of sampling.

	SSC DG3 Minor drain ( $\text{mg l}^{-1}$ )	SSC DG6 Minor drain ( $\text{mg l}^{-1}$ )	SSC DG17 Major drain ( $\text{mg l}^{-1}$ )	SSC DG21 Ripple Drain ( $\text{mg l}^{-1}$ )	Ripple Drain discharge at time of sampling ( $\text{m}^3 \text{s}^{-1}$ )
7/02/00	81	109	138	99	7.5
10/02/00	903	145	318	143	0.5
16/02/00	677	230	688	210	0.7
18/02/00	938	188	430	166	0.7
25/02/00	102	114	143	104	6.2
17/03/00	106	102	114	96	7.0

On February 7, 25, and March 17 samples were taken under peak flow conditions when backwater occurred in the drains, as described by Scenario 3. Discharge in Ripple Drain at the moment of sampling was high (see Table 13.1). Sediment concentrations in all drains were relatively low. Figure 13.3 shows a fragment of the Ripple drain depth, velocity and SSC curves, in which the sampling time of the February 7 and February 10 samples is indicated. The curves show how under peak flow conditions, flow velocity in Ripple Drain stops increasing due to backwater effects at the outlet of Ripple Drain.

On February 10, 16 and 18, samples were taken under lower flow conditions (see February 10 example in Figure 13.3), when the tributary drains could freely discharge into Ripple Drain. In some tributary drains, sediment concentrations under these conditions are up to ten times higher than under backwater conditions. The high sediment input into Ripple Drain is however not strongly reflected in the Ripple Drain sediment concentrations. They are only up to two times higher than under the high flow conditions, while discharge is many times lower.

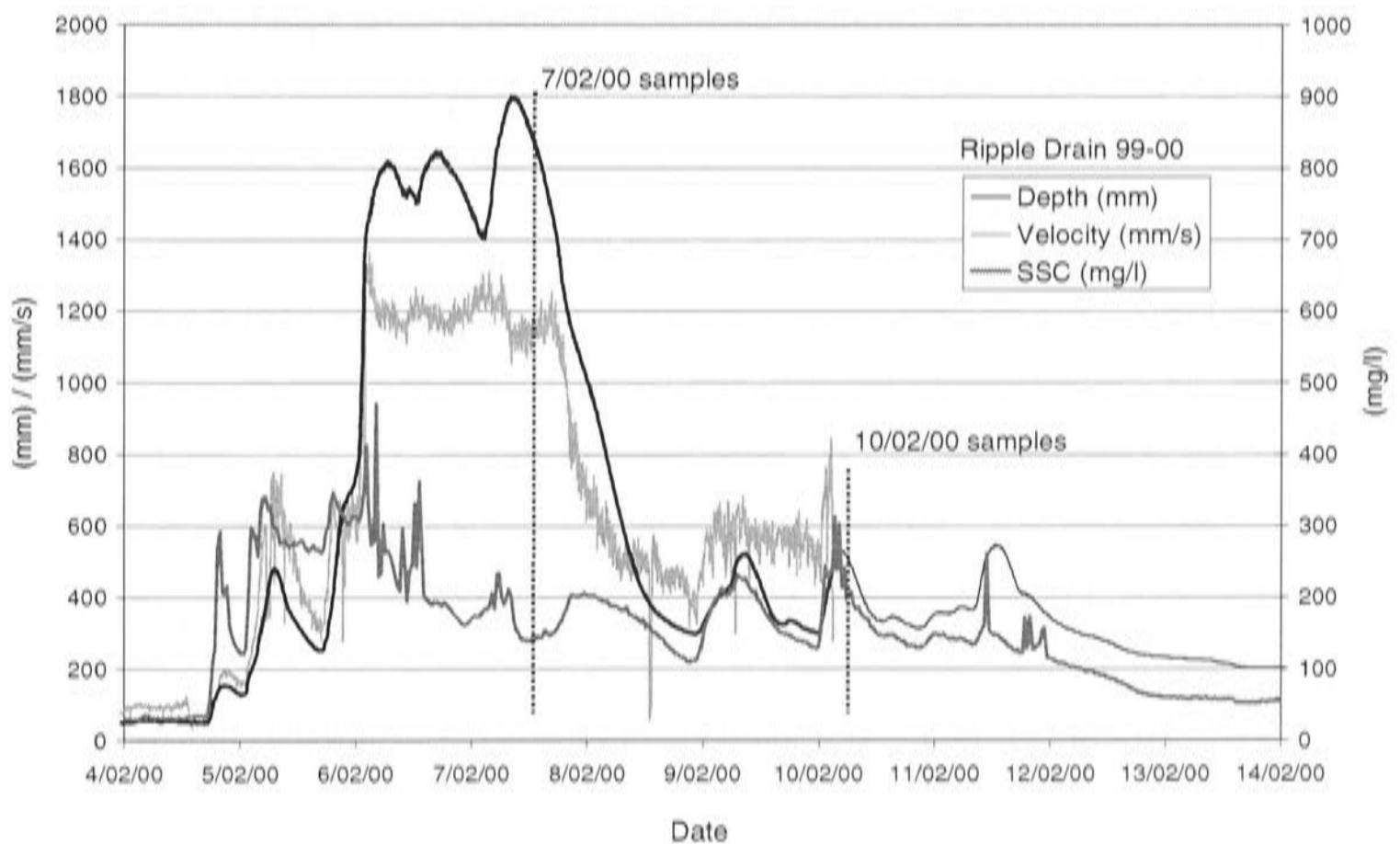


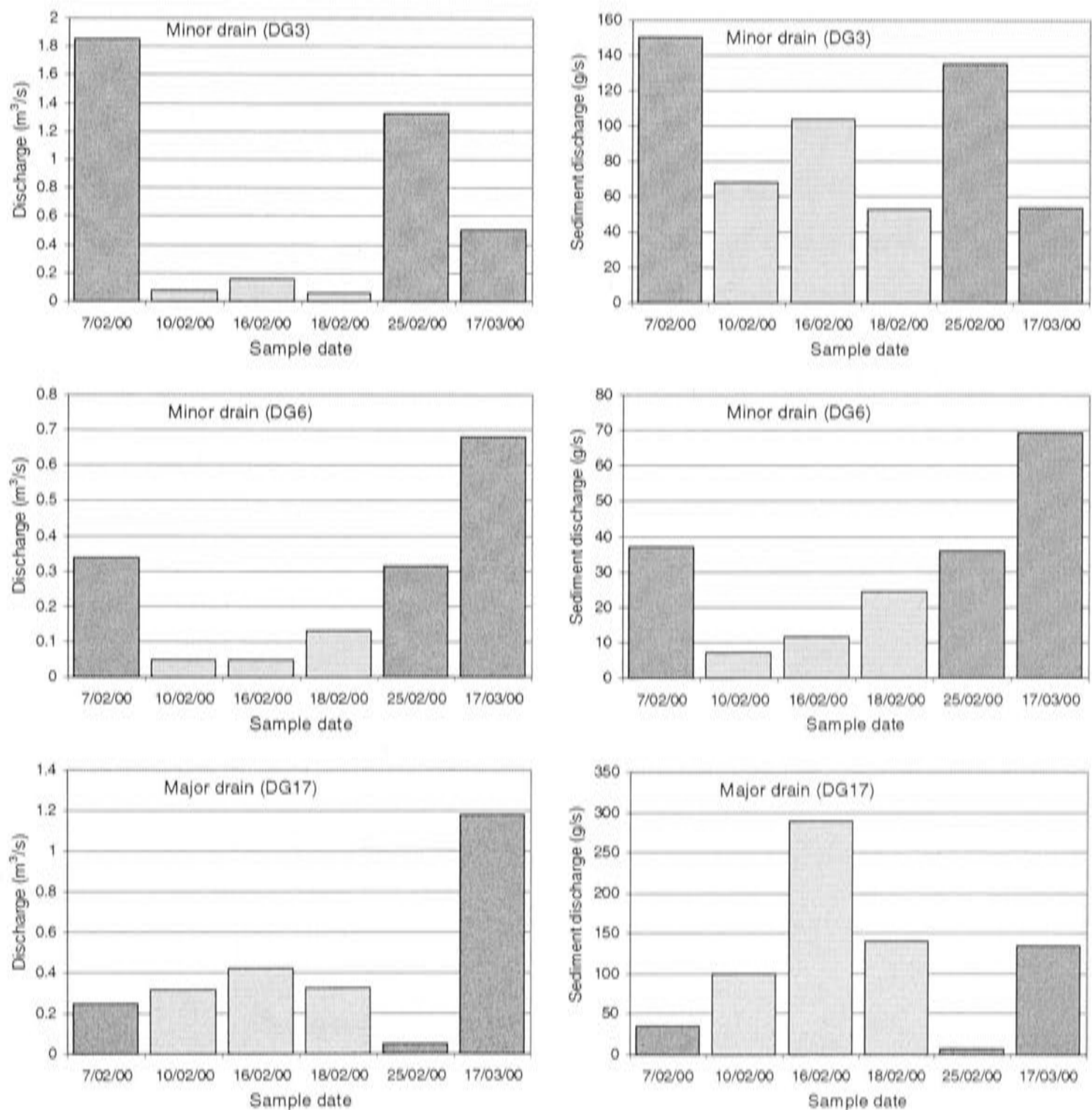
**Figure 13.3:** Water depth (m), flow velocity ( $\text{m s}^{-1}$ ) and SSC ( $\text{mg l}^{-1}$ ) for a peak flow event in the Ripple Drain. Backwater effects cause reduction in flow velocity at greatest water depths. Dashed lines indicate times when water samples were taken (7 and 10 February 2000).

At the time the water samples were taken, water depth and flow velocity were also recorded. From these data, water and sediment discharge for the sampling points at



the time of sampling have been estimated. The water and sediment discharges of four sample locations are presented in Figure 13.4. The bright bars represent samples taken under peak flow (backwater) conditions; dark bars show samples under low flow conditions. Despite backwater in the drains, discharges are relatively high in most drains under peak flow conditions, compared to low flow conditions. Only outflow from major drain DG17 is considerably reduced. Sediment discharges however show less difference between peak flow events and lower flow conditions, due to the much higher sediment concentrations. The sediment discharge in the major drain at location DG17 is even higher under the lower flow conditions.

Although sediment input from tributary drains can be considerable under the lower flow conditions, the output through Ripple Drain (DG21) remains much lower than under peak flow conditions.



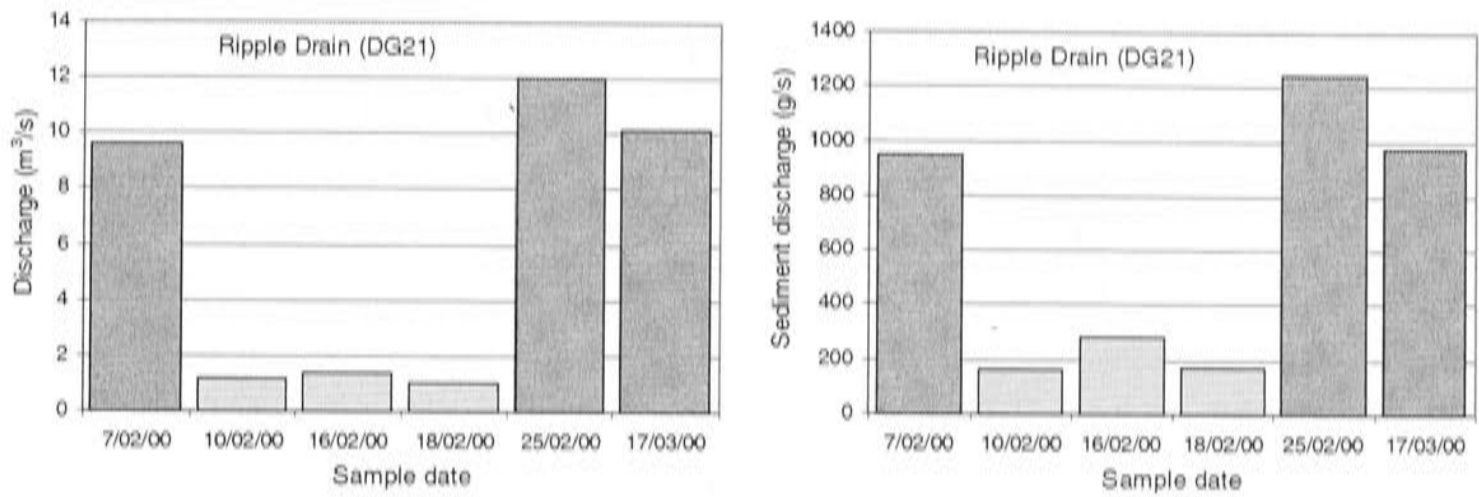


**Figure 13.4:** Water and sediment discharge estimates for 6 sample dates on four locations in the Ripple Corner Catchment. Dark bars indicate peak flow (backwater) conditions; Bright bars indicate free flow conditions.

The flow event shown in Figure 13.3 has a clockwise sediment concentration hysteresis curve. This type of curve indicates depletion of available sediment before discharge has peaked. This can be due to a small sediment supply or a long-lasting and/or intense flood (Williams, 1989). In the case of the Ripple Creek Catchment there are (at least) two other factors that cause the clockwise sediment hysteresis. Firstly the high intensity tropical rainfall will detach a lot of soil material and will thus provide a large amount of sediment at the start of a rainstorm. Secondly the quick rise in water level under the peak flow conditions will cause backwater effects in the tributary drains, which is likely to reduce their flow velocity and thus their sediment transport capacity and sediment supply to Ripple Drain.

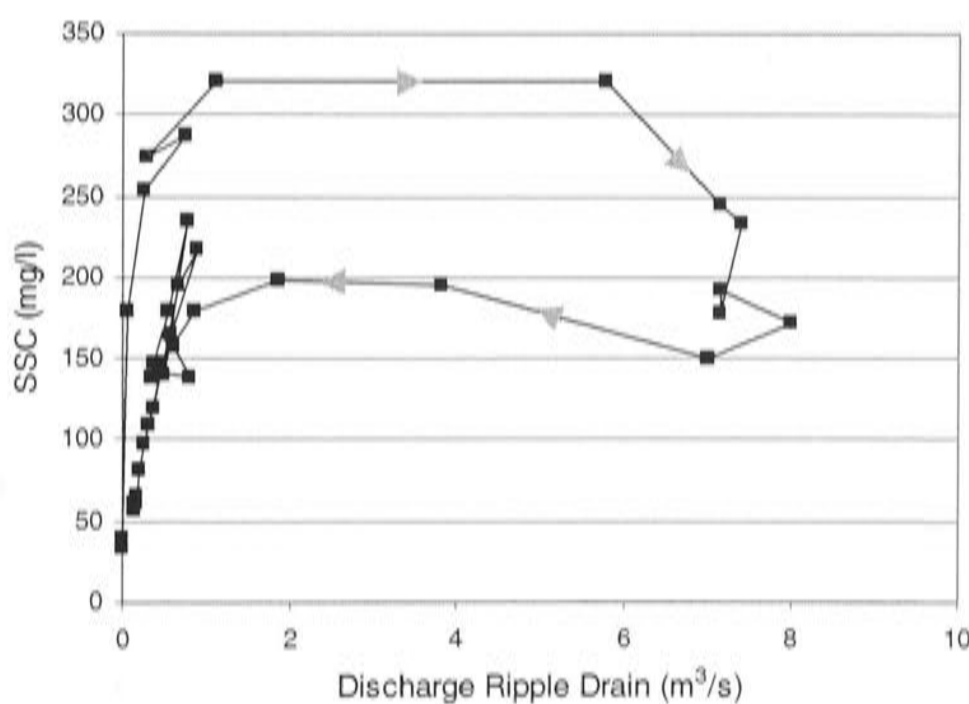


**Figure 13.5:** Clockwise hysteresis in the discharge – SSC relationship for the peak flow event between February 4 and 12. Three minor flow events after the main event are also included.

### **13.6 Discussion: representativeness of the sediment budget results**

The observations during rainfall events in the Ripple Creek Catchment, presented in the previous section, indicate that sediment discharge in the Ripple Drain is highest under Scenario 3 (Figure 13.1), despite backwater effect in the drainage system. The observations of relatively high sediment concentrations under unimpeded flow conditions (Scenario 1) and the strong hysteresis effect in the discharge – SSC relationship of Ripple Drain, suggests that backwater effects to a certain extent reduces the sediment export from the catchment.

The high sediment concentrations in the drains during the 'free flow' events might not be very important compared to sediment export during the peak flow events. However, sediment export during 'free flow' is likely to be a result of decreased resistance and increased erodibility of the floodplain surface. The sediment budget results show the importance of the unprotected plant cane field surface as sediment source. Furthermore the mobilized sediment has an increased opportunity to leave the catchment, because of the efficient system of water furrows and drains.

No research on erosion and deposition rates in the catchment was done before the floodgates were installed. The extent of floodwater that may have been introduced by reverse flow from the Herbert River, as described by Scenario 2, is not known. Neither is the amount of sediment that might have been left on the floodplain by this water.

Sediment deposition on the floodplain surface as a result of large floods, when the Herbert overtops its banks, has not been quantified. However sediment supply from upstream parts of the Herbert River Catchment is thought to be high, so deposition under overbank conditions is expected to be important. The artificial drainage system will have an effect on the time of floodwater storage on the floodplain and therefore the amount of deposition. Large amounts of Herbert River floodwater can, on the other hand, also cause severe scouring. Rates of scouring might have been increased due to lower surface resistance of the floodplain as a result of cultivation.

The relative importance of each type of event can only be determined when more information is available about the effect of the large floods. The sediment budget values will thus not represent the long-term development of the floodplain surface.

*Spatial variation*

The area of the sediment budget study is at the 'upstream' end of the Ripple Creek floodplain. The budget results therefore might not be representative for the entire floodplain surface in the Ripple Creek Catchment. Under the ponding conditions of Scenario 3, the area will experience relatively more erosion and less deposition compared to areas further downstream on the floodplain. Downstream areas will remain inundated for longer periods of time and receive more sediment from upstream parts of the floodplain. It is likely that the downstream areas are sediment sinks.

The Scenarios only focus on flow conditions in the Ripple Creek Catchment. Little is known about the representativeness of these conditions for other parts of the Herbert River floodplain. However, the effects of more efficient drainage and decreased surface resistance as a result of cultivation of the floodplain surface will be similar throughout the catchment.

## **PART IV**

## **CONCLUDING CHAPTER**

---

---

## Chapter 14

### Conclusions and recommendations

---

#### 14.1 Sediment export from low-lying sugarcane land on a tropical floodplain

In the study described in this thesis a sediment budget was developed for sugarcane land in tropical North Queensland, Australia, as a contribution to efforts to identify the principal sources of sediment reaching the Great Barrier Reef, as well as to design soil conservation strategies for the cane lands. Sugarcane cultivation is predominantly practiced on the floodplains of the North Queensland river catchments. The original floodplain landscape in these areas has been substantially modified to make it suitable for cultivation of sugarcane. The floodplains now comprise a number of specific elements that all have the potential to be a source of sediment, as well as a store. The sediment budget approach provides an appropriate technique to assess sediment transport and storage among these landscape elements.

Data were collected during two wet seasons and resulted in two sediment budgets. The budgets indicate that the 536 ha study area is a net source of sediment. In the 99-00 season 1580 tonnes of sediment left the study area. The contribution from the 320 ha area of cultivated lowland was  $4.9 \text{ t ha}^{-1}$ . In the 00-01 season the total output from the area was 1120 tonnes, or  $3.5 \text{ t ha}^{-1}$  from sugarcane land.

#### 14.2 Sediment sources and sinks

Figure 14.1 presents a diagram of the 99-00 sediment budget, which illustrates the magnitude of input and storage components in the studied cane land area. It indicates the relative importance of each landscape element as sediment source or sink and the difference between sediment input minus storage and sediment output from the catchment. It is difficult to create a similar figure for the 00-01 season, because estimates of erosion and deposition rates based on median values, result in different net input values ( $I - S$ ) to those based directly on net surface level change (see

Section 10.5). This highlights one of the notable challenges of this type of budget. Whereas most budgets tend to directly measure net surface level change in terms of either erosion or deposition, for this budget there was no a priori knowledge of which component was source or sink. There for both had to be estimated for each component.

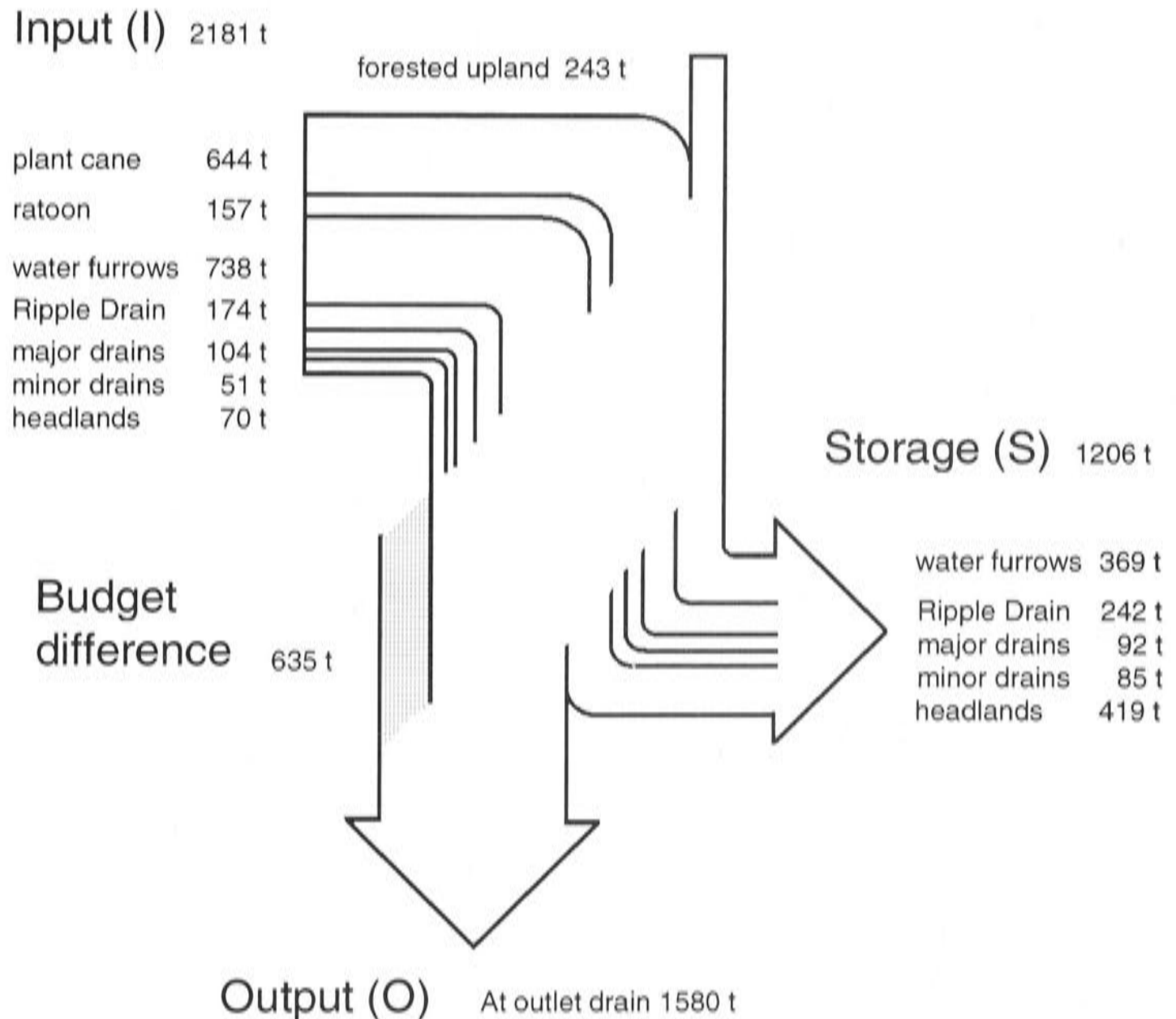


**Figure 14.1:** Sediment budget diagram for the 1999-2000 wet season in the Ripple Corner Catchment.

The sediment budget study identified the following sediment sources and sinks:

- Plant cane fields were the most important net source of sediment in the first budget season (99-00). During the second season the contribution from this landscape element was however considerably less. The difference between the seasons can be largely attributed to the application of different measurement methods.

- Water furrows were the second most important source of sediment during the 99-00 season. The results from the 00-01 season are strongly affected by uncertainty in the data.
- Headlands were the most important sediment sink during the 99-00 season. During the 00-01 season however, they became a minor source of sediment. The data for this season is however less reliable.
- Minor drains were the only landscape element that acted as sediment sink during both budget seasons.
- Contrary to expectation drains with steep banks, such as Ripple Drain and the major drains, were not major sources of sediment (c.f. Walling and Woodward, 1992; Wallbrink *et al.*, 1998; Laubel *et al.*, 1999). They even showed net deposition
- Ratoon fields appear to be a considerable source of sediment despite their protective trash cover, although the estimate of the contribution by the field surface is dependent on the estimate made for water furrows and therefore becomes less reliable.

### 14.3 Accuracy of the budget

The estimated output (O) from the study area and the erosion from the different landscape elements (I) minus the storage (S) within each element show a discrepancy in both seasons. In the 99-00 season O is 635 t higher than I – S. In the 00-01 season this difference is 486 t. The discrepancy could indicate that an important source of sediment has been overlooked and not included in the I – S components. However, it could also be the result of errors in the estimates of the budget components, which is a common problem in the development of sediment budgets.

An estimate of the uncertainty in the budget components shows that the potential variation in the output estimate is around  $\pm 80\%$ . The total uncertainty in the estimates of input and storage is almost  $\pm 300\%$ . The difference between the two sides of the sediment budget equation and between seasons falls within these uncertainty ranges and is therefore most likely to be the result of budget error. All significant processes of sediment transport and deposition have been measured.



Although the error ranges are large, two different ways of calculating net sediment export from cane land obtained very similar results for two measurement seasons. The net sediment export estimates vary between  $2.0 \text{ t ha}^{-1}$  for the I – S component of the 00-01 budget and  $4.9 \text{ t ha}^{-1}$  for the output component of the 99-00 budget. Some of the variation between the two seasons has been caused by differences in rainfall regimes between the seasons.

Thus, despite the uncertainty, the order of magnitude of the budget components is strongly confirmed, and is believed to be useful for the purpose of the thesis and the uses of the results.

#### **14.4 Floodplain erosion on a tropical floodplain**

The observation of a floodplain as net source of sediment contradicts the general understanding that floodplains store sediment. Under specific conditions however erosion can occur on floodplains. The tropical rainfall/flood conditions on the Ripple Creek floodplain and the modification of the floodplain surface for the cultivation of sugarcane provide such conditions.

From literature and local reports, four different qualitative scenarios of erosion and deposition have been developed that describe the development of the floodplain surface under different flood conditions, and the role of human influences on the floodplain. Two of these scenarios were experienced during the budget study, involving runoff from local hillslopes and heavy rainfall, which caused floodplain erosion (Scenario 1 and 3). In the longer term larger flood events, involving floodwater from the Herbert River, may lead to different erosion and deposition processes (Scenario 4).

Measurement during events described Scenario 4 will be necessary to construct budgets representative of longer term processes. With increased input of sediment from elsewhere in the catchment, the floodplain may become a sediment sink. Also, the observations from the budget study do not necessarily represent processes in other areas of the Herbert River Catchment.

## 14.5 Future research

### 14.5.1 Soil conservation practices

To reduce the potential threat to the environment of excess runoff of sediment, nutrients, and pesticides, future research on sediment sources in low-lying sugarcane land should firstly focus on further improvement of cane land management practices. This research can now be focussed on the important sources, and make use of the knowledge gained in this thesis on erosion and deposition processes.

Since plant cane fields and water furrows are the major sources of sediment it is recommended that conservation practices that reduce sediment export from these sources are developed. An already widely applied alternative for the water furrows is laser levelling of field surfaces. However, to obtain sufficient drainage, laser levelled fields might require an increase in slope. On plant cane fields in particular this could considerably increase sediment export and potentially offset the reduction achieved by eliminating the water furrows. Several other practical problems are encountered when fields are laser levelled, mainly related to field drainage efficiency, for which solutions have to be found (Roth, 2001).

Research should also focus on ways to exploit the sediment trapping capacity of headlands and minor drains. This could, for example, follow along the lines of research by Karssies and Prosser (1999) and Muñoz-Carpena *et al.* (1999), which has looked into sediment storage capacity of grass buffer strips.

### 14.5.2 Bedload quantity and origin

Bedload has not been included in the present study. The budget consisted only of particles  $<20 \mu\text{m}$ . This means that the total erosion rates are higher, as is the total sediment export from sugarcane land.

Much of the observed bedload appeared to originate from the densely forested upland, which is counter intuitive. It was expected that most coarse sediment would be derived from bank erosion in the lower sandy colluvial slopes. The exact origin however invites further study, as does the relative contribution of the uplands compared to the input from lowland sources. The percentage coarse particles in the floodplain soils suggest that, considering the amount of suspended material exported, at least  $2 \text{ t ha}^{-1}$  of coarse material should also leave the catchment, and has the potential to cause harm to freshwater ecosystems (Campbell and Doeg, 1989).

### **14.5.3 Floodplain development**

The observation of erosion of floodplains is interesting. The next thing that needs to be explored is how representative this observation is for the sediment yield of the whole Herbert River Catchment.

Extremely high sediment concentrations were only observed under flow conditions of Scenario 1. Water samples taken during the budget study showed that the highest sediment concentrations occurred during runoff events caused by frequent local severe rainstorms. Despite these high concentrations, sediment discharge at the outlet of the budget area is however highest during irregular peak flow events. The relative importance of each type of event for the yearly sediment load from the area needs further study.

No quantitative information exists on the sediment export from sugarcane land under major flood conditions (Scenario 4). Because this information is not available, it is not possible to say whether the floodplain is a source of sediment in the longer term. Also, the observations from the budget study may not represent processes in other areas of the Herbert River Catchment. More hydrological observations and modelling is required to test the hypothesis on the spatial and temporal variation of erosion and deposition processes presented in this thesis.

### **14.5.4 Upland versus lowland input**

Although recent studies have shown a significant increase of both sediment and nutrients in streams draining sugarcane land (Bramley and Roth, 2002), several studies have shown the relative importance of the uplands when it comes to sediment export from the catchment. To shed more light on the relative importance between upland and lowland input a sediment budget should be created for the whole Herbert River catchment.

### **14.5.5 A budget based on direct measurement methods**

Considerable measurement difficulties were encountered during this study, for example, with gauging equipment. Careful analysis of data has been necessary to properly identify such problems, which can otherwise lead to significant errors in the results. This problem becomes less important with increasing size of the gauged watercourse, when a few centimetres variation in water depth becomes negligible.

All too often researchers suffice with single plot studies to represent highly variable processes as erosion and deposition. It would be beneficial if such studies could be accompanied by a proper estimate of uncertainty involved. Despite the problems with the plot measurements, the method provided valuable insight into the erosion and deposition processes that occur in the sugarcane landscape.

#### **14.6 In conclusion**

In conclusion, this study provides the first estimates of sediment export from low-gradient sugarcane land as well as from tropical floodplain environments in general. It shows how modification of these tropical, high rainfall environments for cultivation, makes them susceptible to soil erosion. Bare fields and water furrows are/have in particular become important sources of sediment.

The results obtained from the sediment budget confirm the concern that sugarcane land on the floodplains of the Herbert River is eroding and therefore possibly contributes to negative impacts of sediment off-site, for example on the ecosystems of the Great Barrier Reef World Heritage Area. However, the budget observations only represent a snapshot in time.

Because of the likely temporal and spatial variability, the obtained budget results can not simply be extrapolated to all low-lying cane land and over longer time periods. More, longer term studies are needed. Possible impacts of the frequent high sediment concentrations (and slightly elevated concentrations in the major drains) under the conditions observed during the budget study, have to be sought in local aquatic environments. Although the rates might not be high compared to rates observed on sloping cane fields, they can not be ignored. Particularly not, because the soils used for sugarcane cultivation have stores of fertilizer and pesticide residues that are released together with the sediment.

---

## References

- Abernethy, B. and Rutherford, I.D. (1998). Where along a river's length will vegetation most effectively stabilise stream banks? *Geomorphology*, 23(1), 55-75.
- Abernethy, B. and Rutherford, I.D. (2000). The effect of riparian tree roots on the mass-stability of riverbanks. *Earth Surface Processes and Landforms*, 25(9), 921-937.
- Alexander, J., Fielding, C.R. and Pocock, G.D. (1999). Flood behaviour of the Burdekin River, tropical North Queensland, Australia. In: Marriott, S.B. and Alexander, J. (eds.), *Floodplains: interdisciplinary approaches*. Geological Society Special Publication. The Geological Society, London, pp. 27-40.
- Alexander, J. and Marriott, S.B. (1999). Introduction. In: Marriott, S.B. and Alexander, J. (eds.), *Floodplains: interdisciplinary approaches*. Geological Society Special Publication. The Geological Society, London, pp. 1-13.
- Allen, J.R.L. (1964). Sedimentation in the modern delta of the River Niger, West Africa. In: van Straaten, L.M.J.U. (ed.), *Deltaic and shallow marine deposits*. Elsevier, Amsterdam, pp. 26-34.
- Allison, M.A., Kuehl, S.A., Martin, T.C. and Hassan, A. (1998). Importance of flood-plain sedimentation for river sediment budgets and terrigenous input to the oceans: Insights from the Brahmaputra-Jamuna River. *Geology*, 26, 175-178.
- Alonso, C.V., Meyer, D.L. and Harmon, W.C. (1988). Sediment losses from cropland furrows. In: Bordas, M.P. and Walling, D.E. (eds.), *Sediment Budgets*. Proceedings of the Porto Alegre Symposium, IAHS Publication 174, pp. 3-9.
- Amoros, C. and Bornette, G. (2002). Connectivity and biocomplexity in waterbodies of riverine floodplains. *Freshwater Biology*, 47(4), 761 - 776.
- Arthington, A.H., Marshall, J.C., Rayment, G.E. and Hunter, H.M. (1997). Potential impact of sugarcane production on riparian and freshwater environments. In: Keating, B.A. and Wilson, J.R. (eds.), *Intensive sugarcane production: meeting the challenges beyond 2000*. CAB International, Wallingford, UK, pp. 403-421.
- Baker, V.R. (1988). Flood erosion. In: Baker, V.R., Kochel, C.R. and Patton, P.C. (eds.), *Flood geomorphology*. Wiley, New York.

- Baldwin, C. (1990). *Impact of elevated nutrients in the Great Barrier Reef*. Research Publication 20, Great Barrier Reef Marine Park Authority, Townsville, June 1990, 76 pp.
- Bárdossy, G. and Fodor, J. (2001). Traditional and new ways to handle uncertainty in geology. *Natural Resources Research*, 10(3), 179-187.
- Blake, W.H., Walling, D.E. and He, Q. (1999). Fallout beryllium-7 as a tracer in soil erosion investigations. *Applied Radiation and Isotopes (Incorporating Nuclear Geophysics)*, 51(5), 599-605.
- Bonell, M. (1988). Hydrological processes and implications for land management in forests and agricultural areas of the wet tropical coast of North-East Queensland. In: Warner, R.F. (ed.), *Fluvial geomorphology of Australia*. Academic Press, pp. 41-68.
- Bornette, G., Amoros, C. and Chessel, D. (1994). Effect of allogenic processes on successional rates in former river channels. *Journal of Vegetation Science*, 5, 237-246.
- Bramley, R.G.V. and Johnson, A.K.L. (1996). Land use impacts on nutrient loading in the Herbert River. In: Hunter, H.M., Eyles, A.G. and Rayment, G.E. (eds.), *Downstream effects of land use*. Department of Natural Resources, Queensland, pp. 93-96.
- Bramley, R.G.V. and Wood, A.W. (2000). *Risk assessment of phosphorus (P) loss and guidelines for P use in lower Herbert soils*. Final report on SRDC Project No CLW010, CSIRO Land and Water, August 2000, 20 pp.
- Bramley, R.G.V. and Roth, C.H. (2002). Land-use effects on water quality in an intensively managed catchment in the Australian humid tropics. *Marine and Freshwater Research*, 53, 931-940.
- Brazier, R.E., Beven, K.J., Anthony, S.G. and Rowan, J.S. (2001). Implications of model uncertainty for the mapping of hillslope-scale soil erosion predictions. *Earth Surface Processes and Landforms*, 26(12), 1333 - 1352.
- Brodie, J.E. and Mitchell, A.W. (1992). Nutrient composition of the January (1991) Fitzroy River flood plume. In: Byron, G.T. (ed.), *Workshop on the impacts of flooding, Rockhampton, Australia*. Great Barrier Reef Marine Park Authority Workshop Series 17, pp. 56-74.
- Brunton, D.A. and Bryan, R.B. (2000). Rill network development and sediment budgets. *Earth Surface Processes and Landforms*, 25(7), 783 - 800.

- Bryan, G.W. and Langston, W.J. (1992). Bioavailability, accumulation and effects of heavy metals and sediments with special reference to United Kingdom estuaries: a review. *Environmental Pollution*, 76, 89-131.
- BSES and CSIRO (1997). Project BS181: Increasing sugarcane productivity through development of integrated surface drainage systems for low-lying cane lands.
- Bureau of Meteorology, Department of Administrative Services (1988). *Climatic averages, Australia*. Australia Government Publication Service, Canberra, 532 pp.
- Bureau of Sugar Experimental Stations (2002). *Meet the climbing rat*. Fact sheets, Website (Access Date: 1/12/02), URL: <http://www.bses.org.au/Fact%20Sheets/>.
- Burrough, P.A. (1998). *Principles of geographical information systems*. Oxford University Press, Oxford, 333 pp.
- Chakravarti, I.M., Laha, R.G and Roy, J.(1967). *Handbook of Methods of Applied Statistics, Volume I*, Wiley & Sons, New York, pp. 392-394.
- Cameron McNamara (1980). *Herbert River Flood Management Study*, Herbert River Improvement Trust and Queensland Water Resources Commission, September 1980.
- Cameron McNamara (1984). *Hinchinbrook Rural Drainage Plan Volume 1: Report*, Hinchinbrook Shire Council.
- Campbell, B.L., Loughran, R.J. and Elliott, G.L. (1988). A method for determining sediment budgets using caesium-137. In: Bordas, M.P. and Walling, D.E. (eds.), *Sediment Budgets*. Proceedings of the Porto Alegre Symposium IAHS Publication 174, pp. 171-180.
- Campbell, I.C. and Doeg, T.J. (1989). Impact of timber harvesting and production on streams: a review. *Australian Journal of Marine and Freshwater Research*, 40, 519-539.
- Canegrowers (2002). *Industry Overview*. Website (Access Date: 1/12/02), URL: <http://www.canegrowers.com.au/overview.htm>.
- Capelin, M.A. and Prove, B.G. (1983). Soil conservation problems of the Humid Coastal Tropics of North Queensland. *Proceedings of Australian Society of Sugarcane Technologists Conference*, 5, 125-130.
- Cavanagh, J.E., Burns, K.A., Brunskill, G.J. and Coventry, R.J. (1999). Organochlorine pesticide residues in soils and sediments of the Herbert and Burdekin River regions, North Queensland - Implications for contamination of the Great Barrier Reef. *Marine Pollution Bulletin*, 39, 367-375.

- Cofinas, M. and Creighton, C. (2001). *Australian Native Vegetation Assessment 2001*. Commonwealth of Australia, Turner, Australian Capital Territory.
- Collins, A.L., Walling, D.E., Sickingabula, H.M. and Leeks, G.J.L. (2001). Using  $^{137}\text{Cs}$  measurements to quantify soil erosion and redistribution rates for areas under different land use in the Upper Kaleya River basin, southern Zambia. *Geoderma*, 104(3-4), 299-323.
- Corredor, J.E., Howarth, R.W., Twilley, R.R. and Morell, J.M. (1999). Nitrogen cycling and anthropogenic impact in the tropical interamerican seas. *Biogeochemistry*, 46, 163-178.
- Couper, P., Stott, T. and Maddock, I. (2002). Insights into river bank erosion processes derived from analysis of negative erosion-pin recordings: Observations from three recent UK studies. *Earth Surface Processes and Landforms*, 27, 59-79.
- CRC Reef Research Centre (2001). *Land use and the Great Barrier Reef World Heritage Area*, CRC Reef Research Centre and The Myer Foundation, November 2001.
- Croke, J., Hairsine, P. and Fogarty, P. (1999). Sediment transport, redistribution and storage on logged forest hillslopes in south-eastern Australia. *Hydrological Processes*, 13(17), 2705-2720.
- Croke, J. and Mockler, S. (2001). Gully initiation and road-to-stream linkage in a forested catchment, southeastern Australia. *Earth Surface Processes and Landforms*, 26(2), 205-217.
- Crossland, C.J., Done, T.J. and Brunskill, G.J. (1997). Potential impacts of sugarcane production on the marine environment. In: Keating, B.A. and Wilson, J.R. (eds.), *Intensive sugarcane production: meeting the challenges beyond 2000*. CAB International, Wallingford, UK, pp. 423-437.
- Crossland, M. (1999). Assessing the effects of cane field drainage on stream ecology private, *Aquaterrain*, Newsletter of the Australian Centre for Tropical Freshwater Research, Townsville, pp. 1-2.
- CSIRO Land and Water (1998). *Monitoring of large-area water quality with remote sensing tools*. Research Project Information from CSIRO Land and Water, Sheet No. 1.
- Day, K. (2000). Summary of investigations into a possible link between terrestrial run-off and crown-of-thorns starfish outbreaks on the Great Barrier Reef. Paper submitted to GBRMPA Water Quality Reef Advisory Committee, meeting no. 4.



- De Boer, D.H. and Ali, K.F. (2002). Sediment budget self-organization in a cellular landscape model. In: Dyer, F.J., Thoms, M.C. and Olley, J.M. (eds.), *The structure, functioning and management implications of fluvial sedimentary systems*. Proceedings of the Alice Springs Symposium, IAHS Publication 276, pp. 365-372.
- De Ploey, J. (1981). The ambivalent effects of some factors of erosion. *Mémoires de l'Institute Géologique de la Université de Louvain*, 31, 171-181.
- Devlin, M. and Taylor, J. (1999). Impacts of rivers and plumes on the Great Barrier Reef. *Rivers for the future*, Land and Water Resources Research and Development Corporation Magazine, Issue 10, Spring 1999, pp. 12-18.
- Devlin, M., Waterhouse, J., Taylor, J. and Brodie, J. (2000). *Flood plumes in the Great Barrier Reef: Spatial and temporal patterns in composition and distribution*. Great Barrier Reef Marine Park Authority, Research Publication 68, 113 pp.
- Dietrich, W.B. and Dunne, T. (1978). Sediment budget for a small catchment in mountainous terrain. *Zeitschrift für geomorphologie*, Supplementband 29, 191-206.
- Dietrich, W.E., Day, G. and Parker, G. (1999). The Fly River, Papua new Guinea: Inferences about river dynamics, floodplain sedimentation and fate of sediment. In: Miller, A.J. and Avijit, G. (eds.), *Varieties of Fluvial Form*. Wiley & Sons, Chichester, pp. 345-376.
- Dunne, T., Mertes, L.A.K., Meade, R.H., Richey, J.E. and Forsberg, B.R. (1998). Exchanges of sediment between the floodplain and channel of the Amazon River in Brazil. *Geological Society of America Bulletin*, 110(4), 450-467.
- Edinger, E.N., Jompa, J., Limmon, G.V., Widjatmoko, W. and Risk, M.J. (1998). Reef degradation and coral biodiversity in Indonesia: Effects of land-based pollution, destructive fishing practices and changes over time. *Marine Pollution Bulletin*, 36(8), 617-630.
- Ferguson, R.J. and Brierley, G.J. (1999). Downstream changes in valley confinement as a control on floodplain morphology, Lower Tuross River, New South Wales, Australia: a constructivist approach to floodplain analysis. In: Miller, A.J. and Gupta, A. (eds.), *Varieties of Fluvial Form*. Wiley & Sons, pp. 377-407.
- Flannery, T.F. (1994). *The future eaters: an ecological history of the Australasian lands and people*. Reed Books, Port Melbourne, 423 pp.

- Freissinet, C., Vauclin, M. and Erlich, M. (1999). Comparison of first-order analysis and fuzzy set approach for the evaluation of imprecision in a pesticide groundwater pollution screening model. *Journal of Contaminant Hydrology*, 37, 21-43.
- Furnas, M. and Mitchell, A. (2001). Runoff of terrestrial sediment and nutrients into the Great Barrier Reef World Heritage Area. In: Wolanski, E. (ed.), *Oceanographic processes of coral reefs: Physical and biological links in the Great Barrier Reef*. CRC Press, Boca Raton, pp. 37-51.
- GBRMPA (2001). Great Barrier Reef catchment water quality action plan. A report to Ministerial Council on targets for pollutant loads. Great Barrier Reef Marine Park Authority, Townsville, September 2001.
- Gilmour, D.A. (1977). Effect of rainforest logging and clearing of water yield and quality in a high rainfall zone of North-East Queensland, *The hydrology of Northern Australia: preprints of papers, Hydrology Symposium 1977*. Brisbane Institution of Engineers, Australia National Conference Publication No. 77/5, pp.156-160
- Gippel, C.J. (1989). *The use of turbidity instruments to measure stream water suspended sediment concentration*. Department of Geography and Oceanography, University College, Australian Defence Force Academy, Campbell, Australian Capital Territory, 204 pp.
- Gippel, C.J. (1995). Potential of turbidity monitoring for measuring the transport of suspended solids in streams. *Hydrological Processes*, 9, 83-97.
- Glymph, L.M. (1954). Studies of sediment yields from watersheds. *Assemblée Générale de Rome*, IAHS Publication 36, 173-191.
- Gomez, B., Hubbell, D.W. and Stevens Jr., H.H. (1990). At-a-point bed load sampling in the presence of dunes. *Water Resources Research*, 26(11), 2717-2731.
- Gomez, B., Mertes, L.A.K., Phillips, J.D., Magilligan, F.J. and James, L.A. (1995). Sediment characteristics of an extreme flood: 1993 upper Mississippi River valley. *Geology*, 23(11), 963-966.
- Gomez, B. and Troutman, B.M. (1997). Evaluation of process errors in bed load sampling using a dune model. *Water Resources Research*, 33(10), 2387-2398.

- Gomez, B., Eden, D.N., Peacock, D.H. and Pinkney, E.J. (1998). Floodplain construction by recent, rapid vertical accretion: Waipaoa River, New Zealand. *Earth Surface Processes and Landforms*, 23(5), 405-413.
- Gomez, B., Eden, D.N., Hicks, M.D., Trustrum, N.A., Peacock, D.H. and Wilmshurst, J. (1999). Contribution of floodplain sequestration to the sediment budget of the Waipaoa River, New Zealand. In: Marriott, S.B. and Alexander, J. (eds.), *Floodplains: interdisciplinary approaches*. Geological Society Special Publication. The Geological Society, London, pp. 69-88.
- Graf, J.B., Webb, R.H. and Hereford, R. (1991). Relation of sediment load and floodplain formation to climatic variability, Paria River drainage basin, Utah and Arizona. *Geological Society of America Bulletin*, 103, 1405-1415.
- Green, T.R., Beavis, S.G., Dietrich, C.R. and Jakeman, A.J. (1999). Relating stream-bank erosion to in-stream transport of suspended sediment. *Hydrological Processes*, 13, 777-787.
- Greenspan Technology (2002). Turbidity Sensor TS100, User Manual, Edition 2.0.
- Gregory, K.J. and Walling, D.E. (1973). *Drainage basin form and process, a geomorphological approach*. Edward Arnold, London, 456 pp.
- Grimshaw, D.L. and Lewin, J. (1980). Source identification for suspended sediments. *Journal of Hydrology*, 47, 151-162.
- Gupta, A. and Fox, H. (1974). Effects of high-magnitude floods on channel form: A case study in Maryland Piedmont. *Water Resources Research*, 10(3), 499-509.
- Haigh, M.J. (1977). The use of erosion pins in the study of slope evolution. In: Group, B.G.R. (ed.), *Shorter Technical methods (II)*, Technical Bulletin No. 18. Geo Books, Norwich, UK, 31-49.
- Hausler, G. (1991). Hydrology of North Queensland coastal streams and their groundwaters. In: Yellowlees, D. (ed.), *Land use patterns and nutrient loading of the Great Barrier Reef region*. James Cook University of North Queensland, Townsville, pp. 90-107.
- Herbert River Improvement Trust (1993). *Stream management plan Herbert River and district*. Consultancy, Ian Drummond and Associates Pty. Ltd., Wangaratta, Victoria, June 1993, 151 pp.
- Hession, W.C. (1996). A watershed-level ecological risk assessment methodology. *Water Resources Bulletin, American Water Resources Association*, 32(5), 1039-1054.

- Hession, W.C., Storm, D.E. and Haan, C.T. (1996). Two-phase uncertainty analysis: an example using the Universal Soil Loss Equation. *Transactions of the American Society of Agricultural Engineers*, 39(4), 1309-1319.
- Hession, W.C. and Storm, D.E. (2000). Watershed-level uncertainties: Implications for phosphorus management and eutrophication. *Journal of Environmental Quality*, 29(4), 1172-1179.
- Hill, B.R., Decarlo, E.H., Fuller, C.C. and Wong, M.F. (1998). Using sediment 'fingerprints' to assess sediment-budget errors, North Halawa valley, Oahu, Hawaii, 1991-92. *Earth Surface Processes and Landforms*, 23, 493-508.
- Hillman, S. (1995). Inventory of coral reefs in the area affected by the Herbert River (and others) catchments: technical working document for EAS-35. Staff Paper 1995-053, Great Barrier Reef Marine Park Authority, Townsville.
- Hooke, J.M. (1979). An analysis of the processes of river bank erosion. *Journal of Hydrology*, 42, 39-62.
- Horsley, D.R., Wood, A.W. and Stewart, R.L. (1982). Drainage of the Herbert Valley cane lands: an overview, *Proceedings of the Australian Society of Sugarcane Technologists Conference*, pp. 67-70.
- Hudson, N.W. (1993). *Field measurement of soil erosion and runoff*. FAO Soils Bulletin, 68. Food and Agriculture Organization of the United Nations, Rome, 139 pp.
- Hutchings, P. and Haynes, D. (2000). Sources, fates and consequences of pollutants in the Great Barrier Reef. *Marine Pollution Bulletin*, 41, 265-266.
- Intergovernmental Panel on Climate Change (2000). Good Practice Guidance and Uncertainty Management in National Greenhouse Gas Inventories (Good Practice Report), Montreal, May 2000.
- Isbell, R.F. and Edwards, D.G. (1988). Soils and their management in the Australian Wet Tropics. In: Loveday, J. (ed.), *National Soils Conference, Canberra*, Australian Society of Soil Science Incorporated.
- Johnson, A.K.L. and Murray, A.E. (1997). *Herbert River Catchment Atlas*. CSIRO Tropical Agriculture, Townsville, 48 pp.
- Johnson, A.K.L., Ebert, S.P. and Murray, A.E. (2000). Land cover change and its environmental significance in the Herbert River Catchment, North-east Queensland. *Australian Geographer*, 31(1), 75-86.

- Karssies, L. and Prosser, I. P. (1999). Sediment storage capacity of grass buffer strips. *Second Australian Stream Management Conference*, Adelaide.
- Kern, U. and Westrich, B. (1997). Sediment budget analysis for river reservoirs. *Water, Air and Soil Pollution*, 99, 105-112.
- Kingdon, B. (1991). Surface drainage essential for sugar cane growth. *Bureau of Sugarcane Experimental Stations Bulletin*, 35, 12-13.
- Knighton, D. (1998). *Fluvial forms and processes: a new perspective*. Arnold, London, 383 pp.
- Kochel, C.R. (1988). Geomorphic impact of large floods: review and new perspectives on magnitude and frequency. In: Baker, V.R., Kochel, C.R. and Patton, P.C. (eds.), *Flood geomorphology*. Wiley, New York.
- Kondolf, M.G. and Matthews, W.V.G. (1991). Unmeasured residuals in sediment budgets: A cautionary note. *Water Resources Research*, 27(9), 2483-2486.
- Lall, U., Phillips, D.L., Reckhow, K.H. and Loucks, D.P. (2002). *Quantifying and Communicating Model Uncertainty for Decision Making in the Everglades*. Report of the Comprehensive Everglades Restoration Plan's Model Uncertainty Workshop, US Army Corps of Engineers, South Florida Water Management District, West Palm Beach, Florida, 81 pp.
- Lambert, C.P. and Walling, D.E. (1987). Floodplain sedimentation: A preliminary investigation of contemporary deposition within the lower reaches of the river Culm, Devon, UK. *Geografiska Annaler*, 69A, 393-404.
- Larcombe, P. and Woolfe, K.J. (1999). Increased sediment supply to the Great Barrier Reef will not increase sediment accumulation at most coral reefs. *Coral Reefs*, 18, 163-169.
- Laubel, A., Svendsen, L.M., Kronvang, B. and Larsen, S.E. (1999). Bank erosion in a Danish lowland stream system. *Hydrobiologia*, 410, 279-285.
- Lawler, D.M. (1993). The measurement of river bank erosion and lateral change: a review. *Earth Surface Processes and Landforms*, 18, 777-821.
- Lee, K.W. (1968). Problems of secondary drainage on the Macleay floodplain, and their possible solution by the Macleay River County Council with extended powers. Department of Geography, University of New England for the Macleay River County Council, Armidale, New South Wales, 96 pp.
- Lehre, A.K. (1982). Sediment budget in a small coast range drainage basin in north-central California. In: Swanson, F.J., Janda, R.J., Dunne, T. and Swanston, D.N.

- (eds.), *Sediment budgets and routing in forested drainage basins*. Forest Service, US Department of Agriculture, Portland, Oregon, pp.123-139.
- Leopold, L.B., Wolman, M.G. and Miller, J.P. (1964). *Fluvial processes in geomorphology*. W.H. Freeman, San Francisco, 522 pp.
- Leopold, L.B., Emmett, W.W. and Myrick, R.M. (1966). *Channel and hillslope processes in a semiarid area, New Mexico*. US Geological Survey Professional Paper, 352-G.
- Longstaff, B.J. and Dennison, W.C. (1999). Seagrass survival during pulsed turbidity events: the effects of light deprivation on the seagrasses *Halodule pinifolia* and *Halophila ovalis*. *Aquatic Botany*, 65, 105-121.
- Loughran, R.J. (1990). The measurement of soil erosion. *Progress in physical geography*, 13, 216-233.
- Loughran, R.J., Campbell, B.L., Shelly, D.J. and Elliott, G.L. (1992). Developing a sediment budget for a small drainage basin in Australia. *Hydrological Processes*, 6, 145-158.
- Marohasy, J. and Johns, G. (2002). *WWF says 'jump!', governments ask 'how high?'*. Publication of the Institute for Public Affairs' NGO Project, March 2002.
- Marron, D.C. (1992). Floodplain storage of mine tailings in the Belle Fourche River system: a sediment budget approach. *Earth Surface Processes and Landforms*, 17(7), 675-685.
- McClanahan, T.R. and Obura, D. (1997). Sedimentation effects on shallow coral communities in Kenya. *Journal of Experimental Marine Biology and Ecology*, 209, 103-122.
- McDonald, R.C., Isbell, R.F., Speight, J.G., Walker, J. and Hopkins, M.S. (eds.) (1990). *Australian soil and land survey field handbook*. Inkata Press, Melbourne, 198 pp.
- Mertes, L.A.K. (1994). Rates of flood-plain sedimentation on the central Amazon River. *Geology*, 22(2), 171-174.
- Mertes, L.A.K., Daniel, D.L., Melack, J.M., Nelson, B., Martinelli, L.A. and Forsberg, B.R. (1995). Spatial patterns of hydrology, geomorphology, and vegetation on the floodplain of the Amazon River in Brazil from a remote sensing perspective. *Geomorphology*, 13, 215-232.
- Mertes, L.A.K. (1997). Documentation and significance of the perirheic zone in inundated floodplains. *Water Resources Research*, 33, 1749-1762.

- Mertes, L.A.K. (2002). Remote sensing of riverine landscapes. *Freshwater Biology*, 47(4), 799-816.
- Middelkoop, H. (1997). Embanked floodplains in the Netherlands, Geomorphological evolution over various time scales. *Nederlandse Geografische Studies*, 224, Utrecht, 341 pp.
- Middelkoop, H. and Asselman, N.E.M. (1998). Spatial variability of floodplain sedimentation at the event scale in the Rhine-Meuse delta, The Netherlands. *Earth Surface Processes and Landforms*, 23, 561-573.
- Miller, A.J. (1990). Flood hydrology and geomorphic effectiveness in the Central Appalachians. *Earth Surface Processes and Landforms*, 15, 119-134.
- Mitchell, A., Rasmussen, C., Blake, S., Congdon, R., Reghenzani, J., Saffinga, P. and Sturmeijer, H. (1991). Nutrient concentrations and fluxes in North Queensland coastal rivers and streams. In: Yellowlees, D. (ed.), *Land use patterns and nutrient loading of the Great Barrier Reef region*. James Cook University of North Queensland, Townsville, pp. 108-161.
- Mitchell, A.W., Reghenzani, J.R., Hunter, H.M. and Bramley, R.G.V. (1996). Water quality and nutrient fluxes from river systems draining to the Great Barrier Reef Marine Park. In: Hunter, H.M., Eyles, A.G. and Rayment, G.E. (eds.), *Downstream effects of land use*. Department of Natural Resources, Queensland, pp. 23-33.
- Mitchell, A.W., Bramley, R.G.V. and Johnson, A.K.L. (1997). Export of nutrients and suspended sediment during a cyclone-mediated flood event in the Herbert River Catchment, Australia. *Marine and Freshwater Research*, 48(1), 79-88.
- Morgan, M.G. and Henrion, M. (1990). *Uncertainty: a guide to dealing with uncertainty in quantitative risk and policy analysis*. Cambridge University Press, Cambridge, 332 pp.
- Morgan, R.P.C. (ed.), (1986). *Soil erosion and conservation*. Longman Scientific & Technical, Essex, 298 pp.
- Moss, A.J., Rayment, G.E., Reilly, N. and Best, E.K. (1992). *A preliminary assessment of sediment and nutrient exports from Queensland coastal catchments*, Queensland Department of Environment and Heritage, Brisbane, January 1992.
- Muñoz-Carpena, R., Parsons, J.E. and Gilliam, J.W. (1999). Modeling hydrology and sediment transport in vegetative filter strips. *Journal of Hydrology* 214, pp. 111-129.

- Nanson, G.C. and Young, R.W. (1981). Overbank deposition and floodplain formation on small coastal streams of New South Wales. *Zeitschrift für geomorphologie*, 25(3), 322-347.
- Nanson, G.C. (1986). Episodes of vertical accretion and catastrophic stripping: A model of disequilibrium flood-plain development. *Geological Society of America Bulletin*, 97, 1467-1475.
- Nanson, G.C. and Croke, J.C. (1992). A genetic classification of floodplains. *Geomorphology*, 4, 459-486.
- Nearing, M.A., Govers, G. and Norton, L.D. (1999). Variability in soil erosion data from replicated plots. *Soil Science Society of America Journal*, 63(6), 1829-1835.
- Nearing, M.A. (2000). Evaluating soil erosion models using measured plot data: accounting for variability in the data. *Earth Surface Processes and Landforms*, 25(9), 1035-1043.
- NSW Environment Protection Authority (1999). *Review of techniques to estimate catchment exports*. Technical Report, NSW Environment Protection Authority, Sydney, October 1999, 139 pp.
- Oostwoud Wijdenes, D.J. and Bryan, R. (2001). Gully-head erosion processes on a semi-arid valley floor in Kenya: a case study into temporal variation and sediment budgeting. *Earth Surface Processes and Landforms*, 26(9), 911 - 933.
- Owens, P.N. (2001). Downstream changes in the transport and storage of sediment-associated contaminants (P, Cr and PCBs) in agricultural and industrialized drainage basins. *The Science of the Total Environment*, 266, 177-186.
- Peart, M.R. and Walling, D.E. (1988). Techniques for establishing suspended sediment sources in two drainage basins in Devon, UK: a comparative assessment. In: Bordas, M.P. and Walling, D.E. (eds.), *Sediment Budgets*, Proceedings of the Porto Alegre Symposium, IAHS Publication 174, pp. 269-279.
- Preen, A.R., Long, W.J.L. and Coles, R.G. (1995). Flood and cyclone related loss, and partial recovery, of more than 1000 km<sup>2</sup> of seagrass in Hervey Bay, Queensland, Australia. *Aquatic Botany*, 52(1-2), 3-17.
- Prosser, I.P., Chappell, J. and Gillespie, R. (1994). Holocene valley aggradation and gully erosion in headwater catchments, south-eastern highlands of Australia. *Earth Surface Processes and Landforms*, 19, 465-480.



- Prosser, I.P., Hughes, A.O. and Rutherford, I.D. (2000). Bank erosion of an incised upland channel by subaerial processes: Tasmania, Australia. *Earth Surface Processes and Landforms*, 25(10), 1085 - 1101.
- Prove, B.G. and Hicks, W.S. (1991). Soil and nutrient movements from rural lands of north Queensland. In: Yellowlees, D. (ed.), *Land use patterns and nutrient loading of the Great Barrier Reef region*. James Cook University of North Queensland, Townsville, pp. 70-76.
- Prove, B.G., Doogan, V.J. and Truong, P.N.V. (1995). Nature and magnitude of soil erosion in sugarcane land on the wet tropical coast of north-eastern Queensland. *Australian Journal of Experimental Agriculture*, 35, 641-649.
- Pulsford, J.S. (1996). Historical nutrient usage in coastal Queensland river catchments adjacent to the Great Barrier Reef Marine Park. Research Publication 40, Great Barrier Reef Marine Park Authority, Townsville.
- Quine, T.A. (1999). Use of caesium-137 data for validation of spatially distributed erosion models: the implications of tillage erosion. *Catena*, 37(3-4), 415-430.
- Rayment, G.E. and Neil, D.T. (1996). Sources of material in river discharge, *The Great Barrier Reef science, use and management, a national conference, Proceedings Vol. 1*. Townsville, pp. 42-58.
- Reid, L.M. and Dunne, T. (1996). *Rapid evaluation of sediment budgets*. Catena Verlag, Reiskirchen, 164 pp.
- Ritchie, J.C. and Ritchie, C.A. (2000). *Bibliography of publications of 137-caesium studies related to erosion and sediment deposition*. Website (Access Date: 1/12/02), URL: <http://hydrolab.arsusda.gov/cesium137bib.htm>.
- Roberts, R.G. and Church, M. (1986). The sediment budget in severely distributed watersheds, Queen Charlotte Ranges, British Columbia. *Canadian Journal of Forest Research*, 16, 1092-1106.
- Robertson, A.I. and Lee Long, W.J. (1991). The influence of nutrient and sediment loads on tropical mangrove and seagrass ecosystems. In: Yellowlees, D. (ed.), *Land use patterns and nutrient loading of the Great Barrier Reef region*. James Cook University of North Queensland, Townsville, pp. 197-208.
- Rondeau, B., Cossa, D., Gagnon, P. and Bilodeau, L. (2000). Budget and sources of suspended sediment transported in the St. Lawrence River, Canada. *Hydrological Processes*, 14, 21-36.

- Roth, C.H., Visser, F., Prosser, I. and Reghenzani, J. (2000). *Quantifying and managing sources of sediments and nutrients in low-lying cane lands*. Milestone Report, CSIRO Land and Water, Townsville, May 2000, 16 pp.
- Roth, C.H. (2001). Recommendations to enhance environmental performance of drainage works proposed in the Lower Herbert Water Management Scheme. Consultancy, CSIRO Land and Water, Townsville, November 2001.
- Russell, R.J. (1967). *River plains and sea coasts*. (The Hitchcock lectures, 1965), Berkeley, University of California Press, Los Angeles, 173 pp.
- Ryan, P.A. (1991). Environmental effects of sediment on New Zealand streams: a review. *New Zealand Journal of Marine and Freshwater Research*, 25, 207-221.
- Sallaway, M.M. (1979). Soil erosion studies in the Mackay district, *Proceedings of the Australian Society of Sugarcane Technologists Conference*, pp. 125-132.
- Schumm, S.A. and Lichty, R.W. (1963). Channel widening and flood-plain construction along Cimarron River in southwestern Kansas. *Erosion and sedimentation in a semiarid environment: Geological Survey Professional Paper*, 352-D, pp. 71-88.
- Schumm, S.A. (1977). *The Fluvial System*. Wiley & Sons, New York. 338 pp.
- Shapiro, S.S. and Wilk, M.B. (1965). An analysis of variance test for normality (complete samples), *Biometrika*, 52, pp. 591-611.
- Shaw, E.M. (1983). *Hydrology in practise*. Van Nostrand Reinhold, New York, 569 pp.
- Shrubsole, D., Johnson, A., Murray, A., Ebert, S., Chalk, P., Jones, P. and Green, M. (1999). Ecologically sustainable development in a global economy: environmental management in the sugarcane assignment process - Herbert River District, Queensland Australia 1993-1996. Evaluation of integrated catchment management in a wet tropical environment: collected papers of LWRRDC R&D Project CTC7, Vol. 3, Brisbane.
- Sirvent, J., Desir, G., Gutierrez, M., Sancho, C. and Benito, G. (1997). Erosion rates in badland areas recorded by collectors, erosion pins and profilometer techniques (Ebro Basin, NE-Spain). *Geomorphology*, 18(2), 61-75.
- Slaymaker, O.(1993). The sediment budget of the Lillooet River basin, British Columbia. *Physical Geography*, 14(3), 221-224.

- Stewart, M.D., Bates, P.D., Anderson, M.G., Price, D.A. and Burt, T.P. (1999). Modelling floods in hydrologically complex lowland river reaches. *Journal of Hydrology*, 223, 85-106.
- Stocking, M.A. (1987). Measuring land degradation. In: Blaikie, P.M. and Brookfield, H. (eds.), *Land degradation and society*. Methuen, London, 296 pp.
- Stone, P.M. and Walling, D.E. (1997). Particle size selectivity considerations in suspended sediment budget investigations. *Water, Air and Soil Pollution*, 99, 63-70.
- Stott, T. (1997). A comparison of stream bank erosion processes on forested and moorland streams in the Balquhider catchments, Central Scotland. *Earth Surface Processes and Landforms*, 22, 383-399.
- Sutherland, R.A. and Rorke, B.B. (1991). Sediment budgeting: a case study in the Katorin Drainage Basin, Kenya. *Earth Surface Processes and Landforms*, 16, 383-398.
- Taylor, J.R. (1982). An introduction to error analysis: the study of uncertainties in physical measurements. University Science Books, Mill Valley, 270 pp.
- Thomas, R.B. and Lewis, J. (1993). A new model for bed load sampler calibration to replace the probability-matching method. *Water Resources Research*, 29(3), 583-597.
- Thorne, C.R. (1981). Field measurements of rates of bank erosion and bank material strength, *Erosion and sediment transport measurement*. Proceedings of the Florence Symposium IAHS Publication 133, pp. 503-512.
- Timmer, J. (1998). Die hydraulischen Eigenschaften der Böden und die Pedohydrotypen im Ripple Creek Teileinzugsgebiet in Queensland, Australien. Diplomarbeit Thesis, Universität Hannover.
- Trimble, S.W. (1981). Changes in sediment storage in the Coon Creek Basin, Driftless Area, Wisconsin, 1853 to 1975. *Science*, 214, 181-183.
- Trimble, S.W. (1993). The distributed sediment budget model and watershed management in the paleozoic plateau of the upper midwestern United States. *Physical Geography*, 14(3), 221-224.
- Trimble, S.W. (1994). Erosional effects of cattle on steambanks in Tennessee, USA. *Earth Surface Processes and Landforms*, 19, 451-464.
- Trimble, S.W. (1999). Decreased rates of alluvial sediment storage in the Coon Creek basin, Wisconsin, 1975-93. *Science*, 285, 1244-1246.

- Trott, L.A. and Alongi, D.M. (1999). Variability in surface water chemistry and phytoplankton biomass in two tropical, tidally dominated mangrove creeks. *Marine and Freshwater Research*, 50(5), 451-457.
- Unidata (1998). STARFLOW Ultrasonic Doppler Instrument plus version 3 software. Manual 6241 Revision E. Lynn MacLaren Publishing, Willetton, Western Australia.
- Urban, M.A. (2002). Conceptualizing anthropogenic change in fluvial systems: drainage development on the Upper Embarras River, Illinois. *The Professional Geographer*, 54(2), 204-217.
- US Environmental Protection Agency (1999). *Report of the Workshop on Selecting Input Distributions For Probabilistic Assessments*. EPA/630/R-98/004, Risk Assessment Forum, US Environmental Protection Agency, New York, January 1999.
- Ventura Jr., E., Nearing, M.A. and Norton, L.D. (2001). Developing a magnetic tracer to study soil erosion. *Catena*, 43(4), 277-291.
- Walker, W.R. and Skogerboe, G.V. (1987). *Surface Irrigation Theory and Practice*. Prentice-Hall, Englewood Cliffs, New Jersey, 386 pp.
- Wallbrink, P.J., Olley, J.M., Murray, A.E. and Olive, L.J. (1996). The contribution of subsoil to sediment yield in the Murrumbidgee River basin, New South Wales, Australia. In: Walling, D.E. and Webb, B.W. (eds.), *Erosion and sediment yield: Global and regional perspectives*. Proceedings of the Exeter Symposium IAHS Publication 236, pp. 347-355.
- Wallbrink, P.J., Murray, A.S., Olley, J.M. and Olive, L.J. (1998). Determining sources and transit times of suspended sediment in the Murrumbidgee River, New South Wales, Australia, using fallout <sup>137</sup>Cs and <sup>210</sup>Pb. *Water Resources Research*, 34, 879-887.
- Walling, D.E. and Quine, T.A. (1992). The use of caesium-137 measurements in soil erosion surveys. In: Bogen, J., Walling, D.E. and Day, T.J. (eds.), *Erosion and Sediment Transport Monitoring Programmes in River Basins*. Proceedings of the Oslo Symposium, IAHS Publication 210, pp. 143-152.
- Walling, D.E. and Woodward, J.C. (1992). Use of radiometric fingerprints to derive information on suspended sediment sources. In: Bogen, J., Walling, D.E. and Day, T.J. (eds.), *Erosion and sediment transport monitoring programmes in river basins*. Proceedings of the Oslo Symposium, IAHS publication 210, pp. 153-164.

- Walling, D.E. and Quine, T.A. (1993). Using Chernobyl-derived fallout radionuclides to investigate the role of downstream conveyance losses in the suspended sediment budget of the river Severn, United Kingdom. *Physical Geography*, 14(3), 239-253.
- Walling, D.E., He, Q. and Nicholas, A.P. (1996). Floodplains as suspended sediment sinks. In: Anderson, M.G., Walling, D.E. and Bates, P.D. (eds.), *Floodplain processes*. Wiley & Sons, London, pp. 399-440.
- Walling, D.E. and He, Q. (1997). Use of fallout  $^{137}\text{Cs}$  in investigations of overbank sediment deposition on river floodplains. *Catena*, 29(3-4), 263-282.
- Walling, D.E., Owens, P.N. and Leeks, G.J.L. (1998). The role of channel and floodplain storage in the suspended sediment budget of the River Ouse, Yorkshire, Uk. *Geomorphology*, 22, 225-242.
- Walling, D.E. (1999). Linking land use, erosion and sediment yields in river basins. *Hydrobiologia*, 410, 233-240.
- Wasson, R.J. and Galloway, R.W. (1986). Sediment yield in the Barrier Range before and after European settlement. *Australian Rangelands Journal*, 8(2), 79-90.
- Wasson, R.J. (1996). Run-off from the land to the rivers and the sea, *The Great Barrier Reef science, use and management, a national conference, Proceedings, Vol. 1*, Townsville, pp. 23-40.
- Wasson, R.J., Olive, L.J. and Rosewell, C.J. (1996). Rates of erosion and sediment transport in Australia. In: Walling, D.E. and Webb, B.W. (eds.), *Erosion and Sediment yield: global and regional perspectives*, Proceedings of the Exeter Symposium, IAHS Publication 236, pp. 139-148.
- Wasson, R.J. (2002). Sediment budgets, dynamics, and variability: new approaches and techniques. In: Dyer, F.J., Thoms, M.C. and Olley, J.M. (eds.), *The structure, functioning and management implications of fluvial sedimentary systems*. Proceedings of the Alice Springs Symposium, IAHS Publication 276, pp. 471-478.
- Wilkinson, C.R. (1999). Global and local threats to coral reef functioning and existence: review and predictions. *Marine and Freshwater Research*, 50, 867-878.
- Williams, D.M. (2001). *Impacts of terrestrial run-off on the Great Barrier Reef World Heritage Area (review)*. CRC Reef Research Centre, Australian Institute of Marine Science, Townsville, August 2001, 50 pp.

- Williams, G.P. (1989). Sediment concentration versus water discharge during single hydrologic events in rivers. *Journal of Hydrology*, 111, 89-106.
- Wilson, P.R. and Baker, D.E. (1990). *Soils and agricultural land suitability of the wet tropical coast of North Queensland: Ingham area*. Land Resources Bulletin, Queensland Department of Primary Industries, Brisbane.
- Wolanski, E., Yoshihiro, M., King, B. and Gay, S. (1990). Dynamics, flushing and trapping in Hinchinbrook Channel, a giant mangrove swamp, Australia. *Estuarine, Coastal and Shelf Science*, 31, 555-579.
- Wolman, M.G. and Leopold, L.B. (1957). River flood plains: some observations on their formation. *Physiographic and Hydraulic Studies of Rivers, Geological Survey Professional Paper*, 282-C, 87-107.
- Wood, A.W. (1984). *Soils of the Herbert Valley*, CSR, Ingham.
- WWF (2001). Clear? ...or present danger? Great Barrier Reef Pollution Report Card, WWF Great Barrier Reef Campaign, June 2001, 40 pp.
- Queensland Department of Natural Resources & Mines (1980). Contour topology and hydrology (ArcInfo coverages), Lucinda (8160-4) 01/07/1980 & Ingham (8160-1) 01/07/1980, scale 1:50,000.
- Zehe, E., Maurer, T., Ihringer, J. and Plate, E. (2001). Modeling water flow and mass transport in a loess catchment. *Physics and Chemistry of the Earth, Part B: Hydrology, Oceans and Atmosphere*, 26(7-8), 487-507.

---

## **APPENDICES**

---

**APPENDIX A** Water sample locations in the Ripple Corner Catchment.





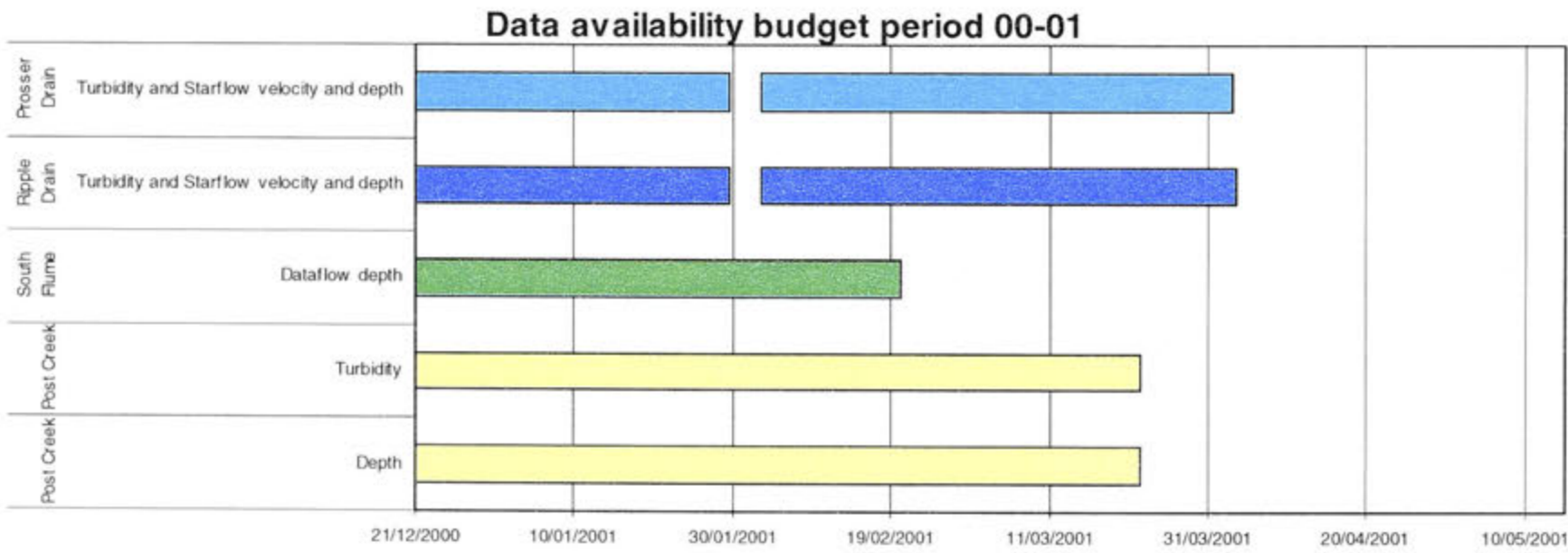
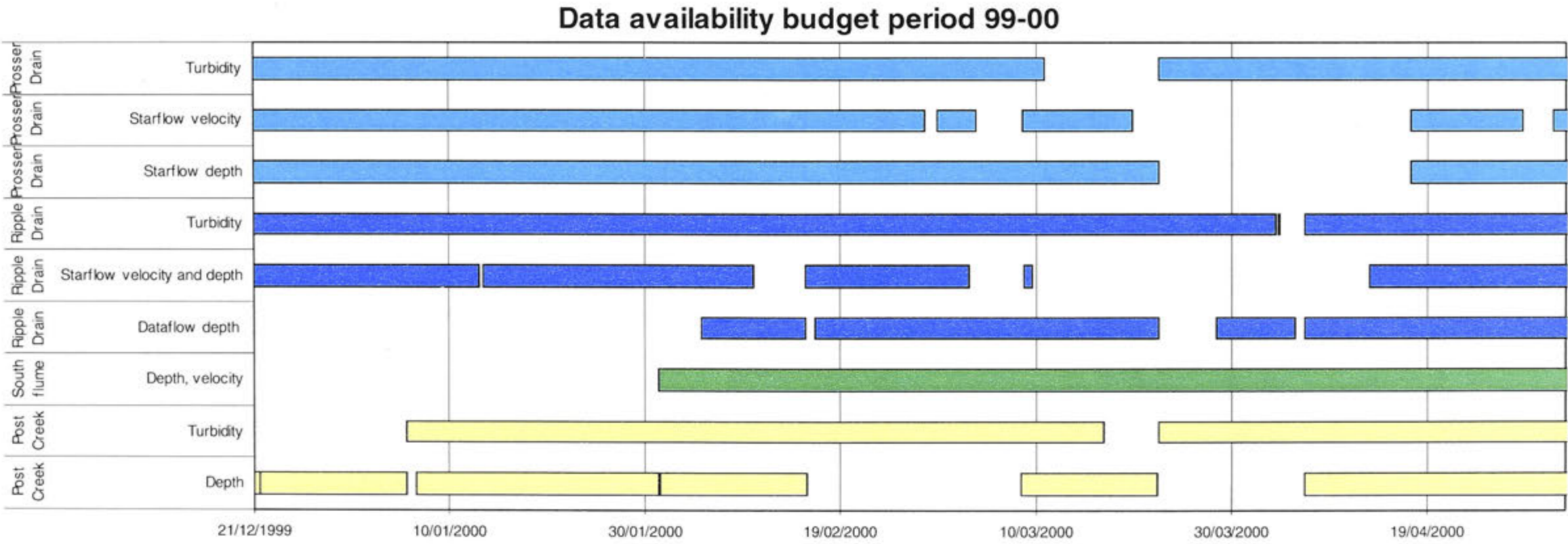
**APPENDIX B (1)** Locations of erosion pin plots and drain surface profiles in the Ripple Corner Catchment during the 99-00 budget season.



**APPENDIX B (2)** Locations of erosion pin plots and drain surface profiles in the Ripple Corner Catchment during the 00-01 budget season.



**APPENDIX C** Data availability for the gauging sites during the 99-00 and 00-01 wet season.



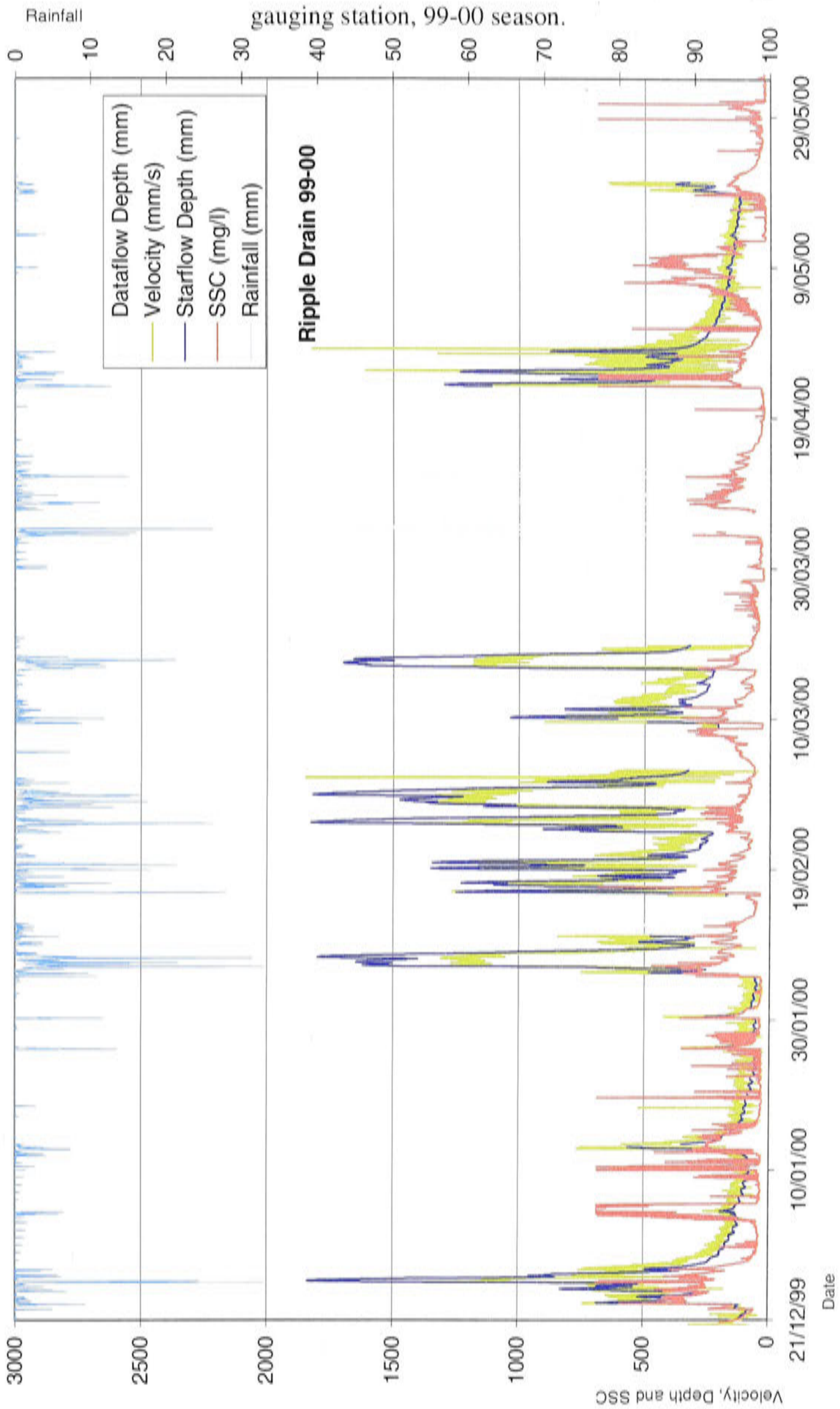
**APPENDIX D** Water sample analysis procedure for suspended solid concentration (SSC) and turbidity (including sub-sampling for future chemical analysis):

1. Wash 50 ml glass beakers and put in oven at 105 C° overnight.
2. Put beakers in desiccator for two hours.
3. Shake sample for 1 minutes.
4. Split samples in two parts (2 x 250 ml). Leave one part in original bottle.
5. Sieve sub-samples in original bottle through 20 µm sieve (use beaker).
6. Weigh 50 ml beakers.
7. Shake sample bottle for 2 minutes.
8. Rinse turbidity-sample-tube and 50ml pipette with sample.
9. Shake bottle for 0.5 minutes.
10. Fill turbidity sample tube and put in turbidity meter.
11. Take 50 ml sample with pipette
12. Put pipetted sample in beaker and dry at 105 C° for two nights.
13. Weigh beakers with dry sample after two hours in desiccator.

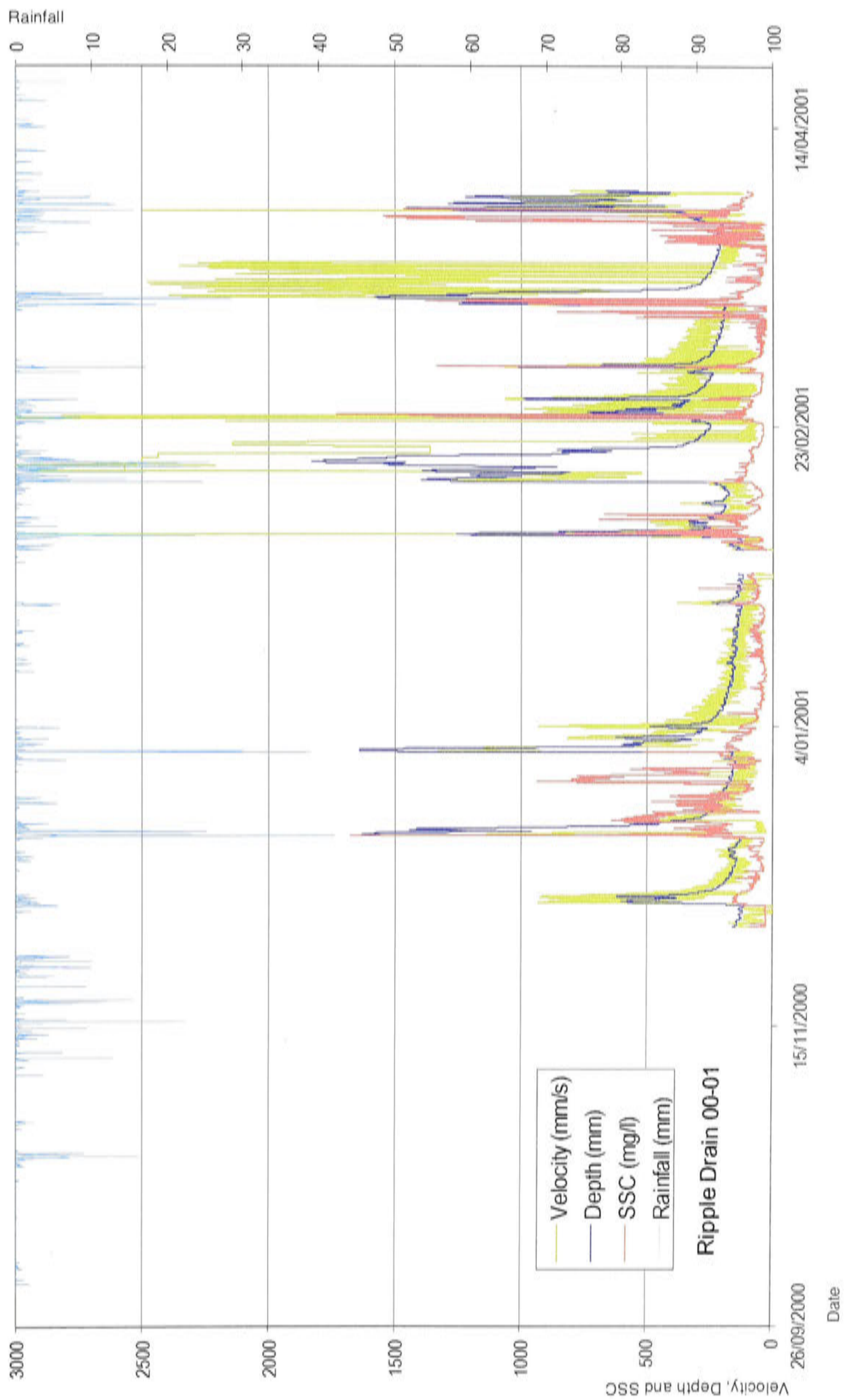
**APPENDIX E** Data of flow velocity measurements in Post Creek 'wet cross-section' at gauging site.

Date	Creek depth Dataflow (m)	Creek width (m)	Creek depth manual (m)	Flow velocity (m s <sup>-1</sup> )	Adjusted Dataflow depth (m)	Total wet Creek cross-section (m <sup>2</sup> )	Average velocity (m s <sup>-1</sup> )	Flux (m <sup>3</sup> s <sup>-1</sup> )
8/03/00	n/a	3.00 3.30 3.60 3.90 4.20 4.50 4.80	0.07 0.07 0.15 0.21 0.17 0.16 0.06	0.08 0.00 0.09 0.36 0.32 0.23 0.07	0.29	0.48	0.16	0.08
18/02/00	0.17				0.41	0.09	0.65	0.55
17/03/00	0.28	2.90 3.40 3.90 4.40 4.90	n/a n/a n/a n/a n/a	0.16 0.62 0.52 0.50 0.31	0.52	1.44	0.42	0.60
3/01/01	0.17	4.05 3.55 3.05	n/a n/a 0.24	0.06 0.19 0.34	0.17	0.29	0.20	0.06

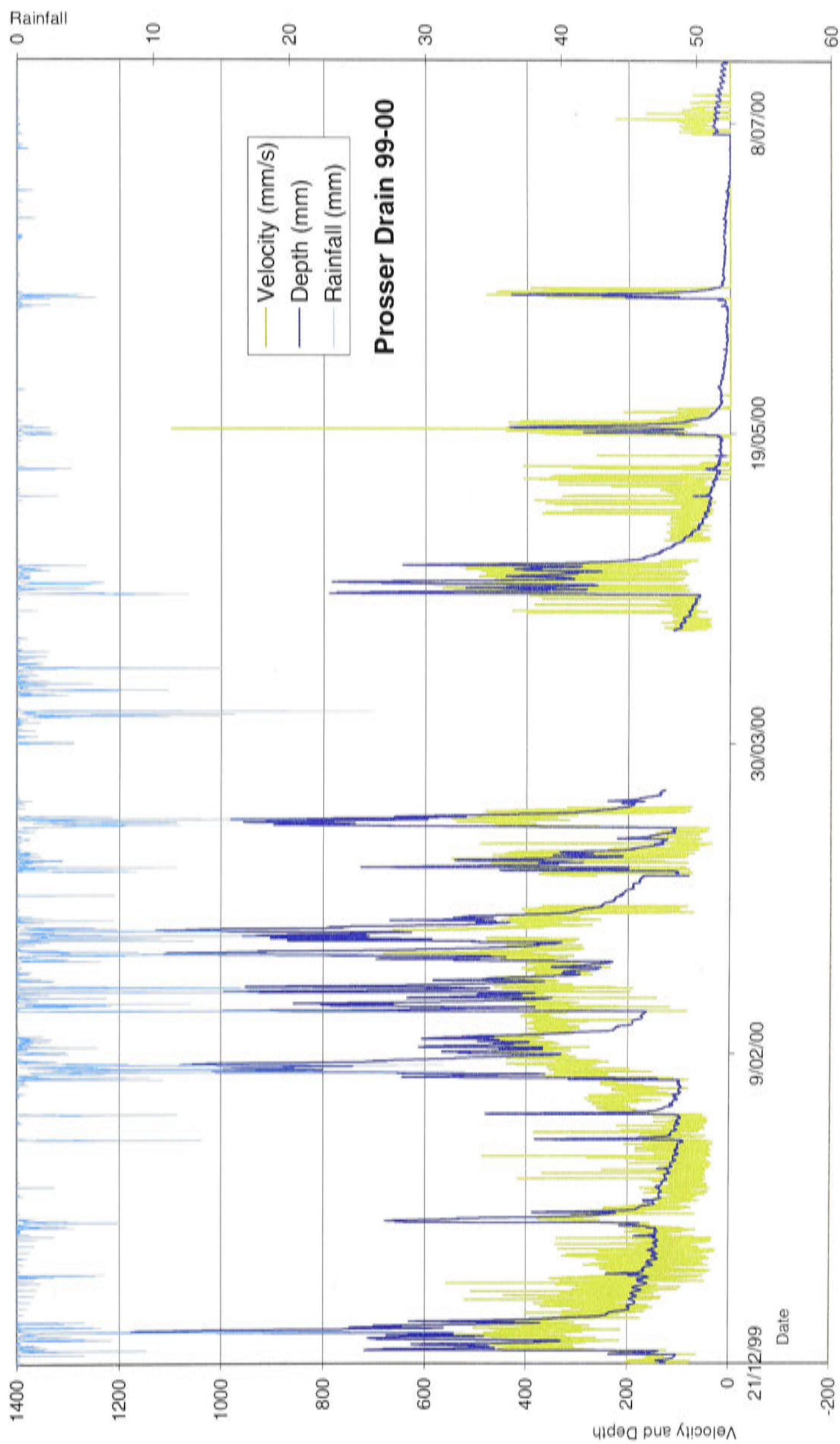
**APPENDIX F (1)** Depth (Dataflow and Starflow), Velocity and SSC (calculated from turbidity) recordings at Ripple Drain gauging station, 99-00 season.



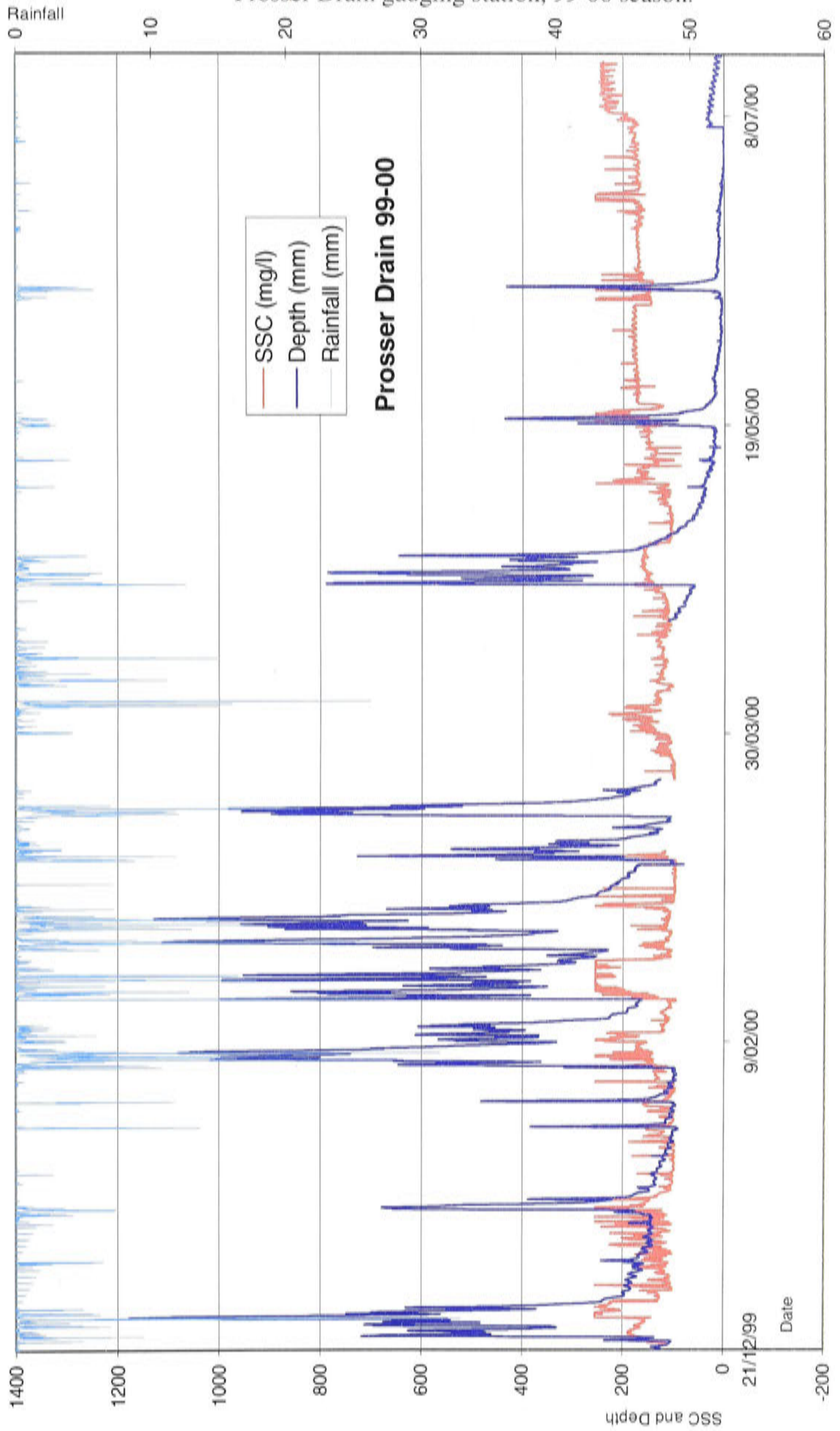
**APPENDIX F (2)** Depth, Velocity and SSC (calculated from turbidity) recordings at Ripple Drain gauging station, 00-01 season.



**APPENDIX F (3)** Depth and Velocity recordings at Prosser Drain gauging station, 99-00 season.

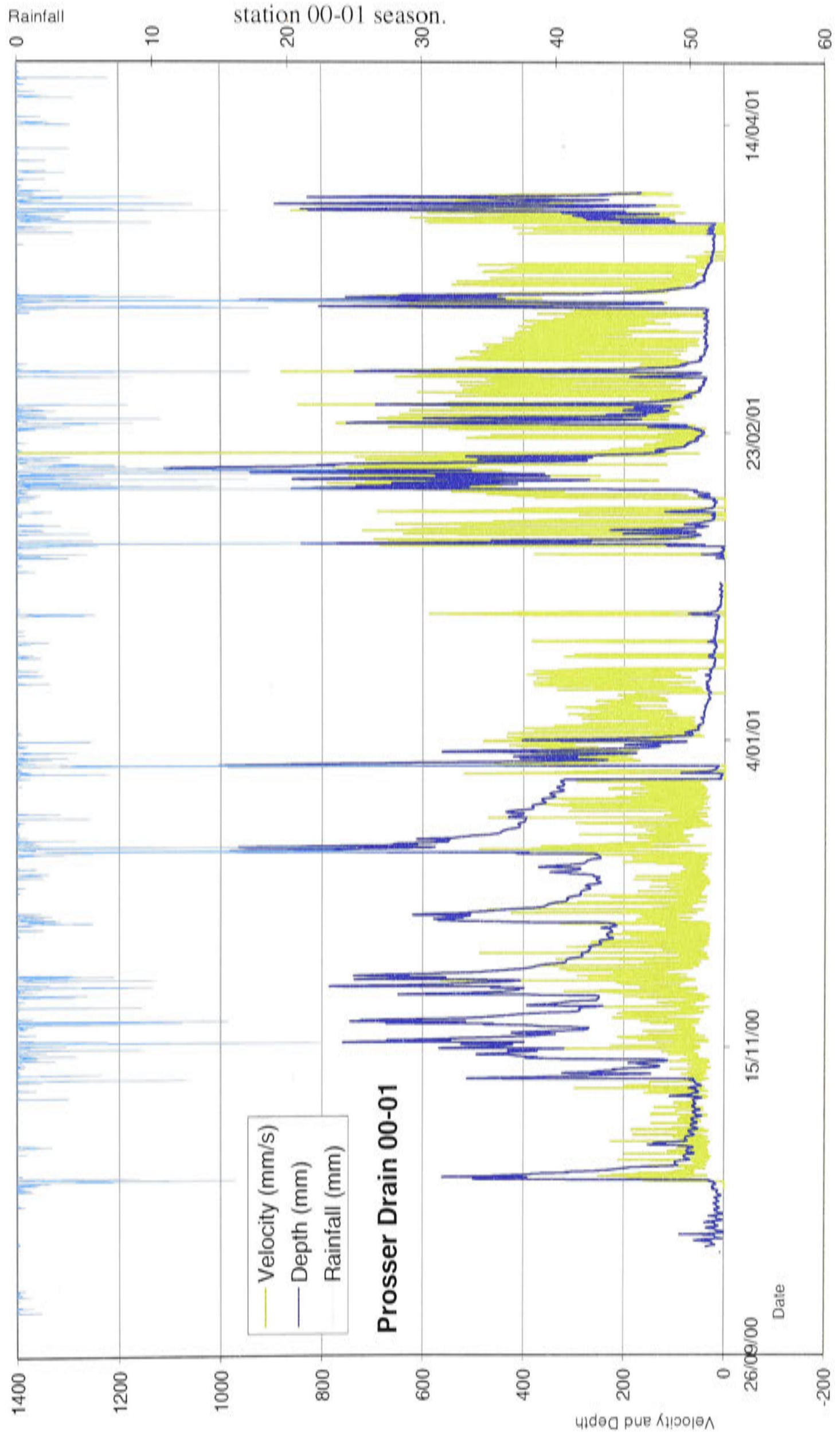


**APPENDIX F (4)** Depth and SSC (calculated from turbidity) recordings at Prosser Drain gauging station, 99-00 season.

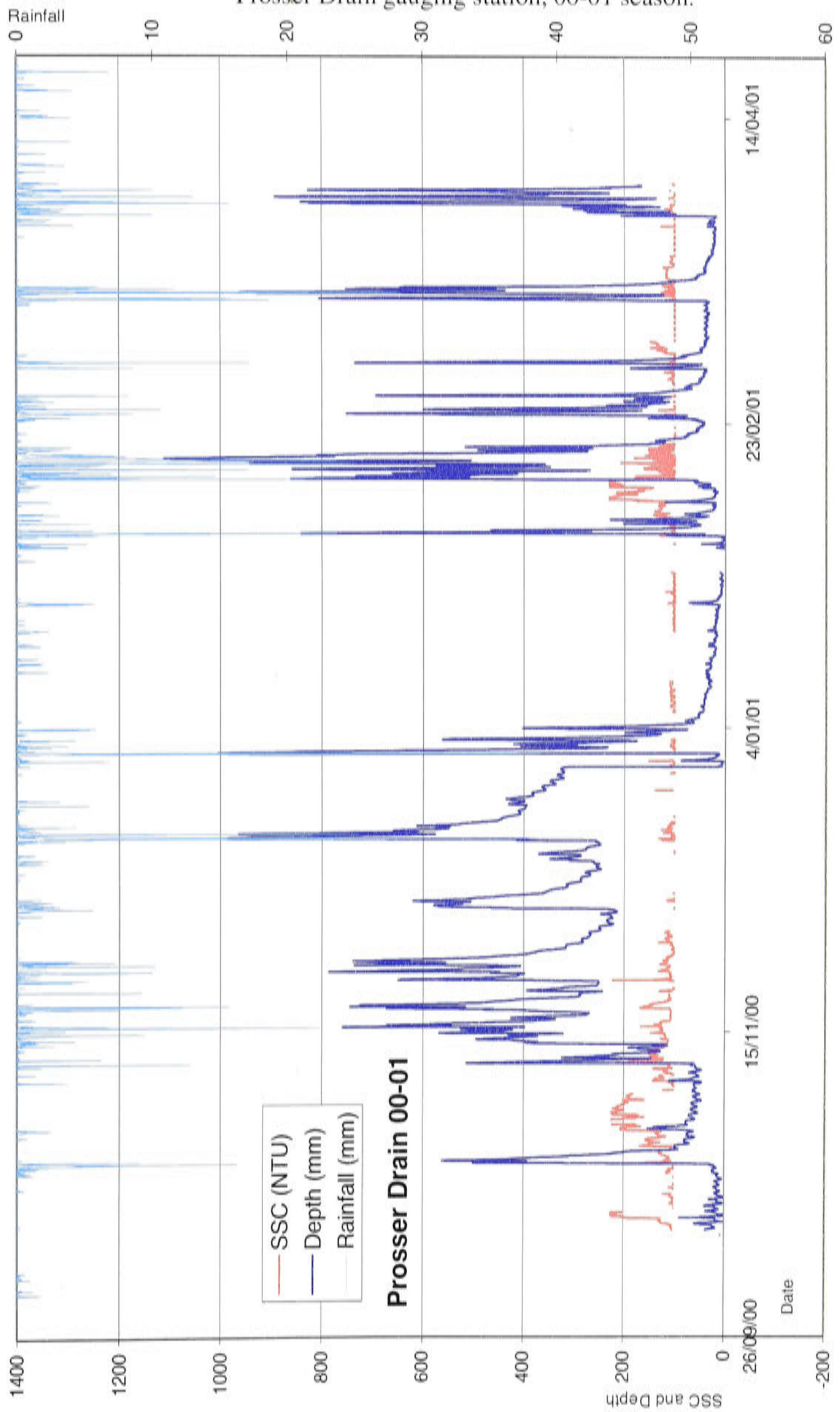




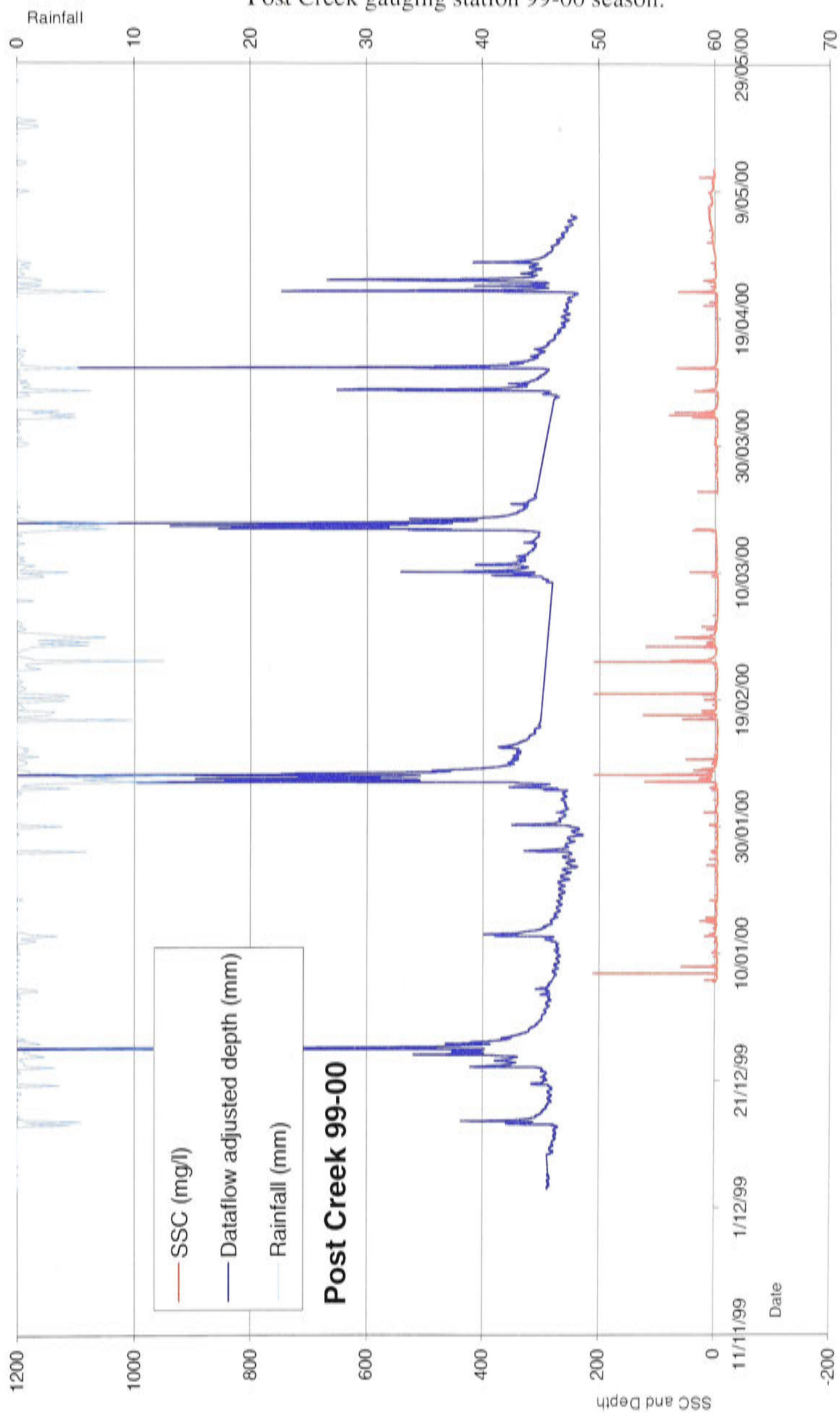
**APPENDIX F (5)** Depth and Velocity recordings at Prosser Drain gauging station 00-01 season.



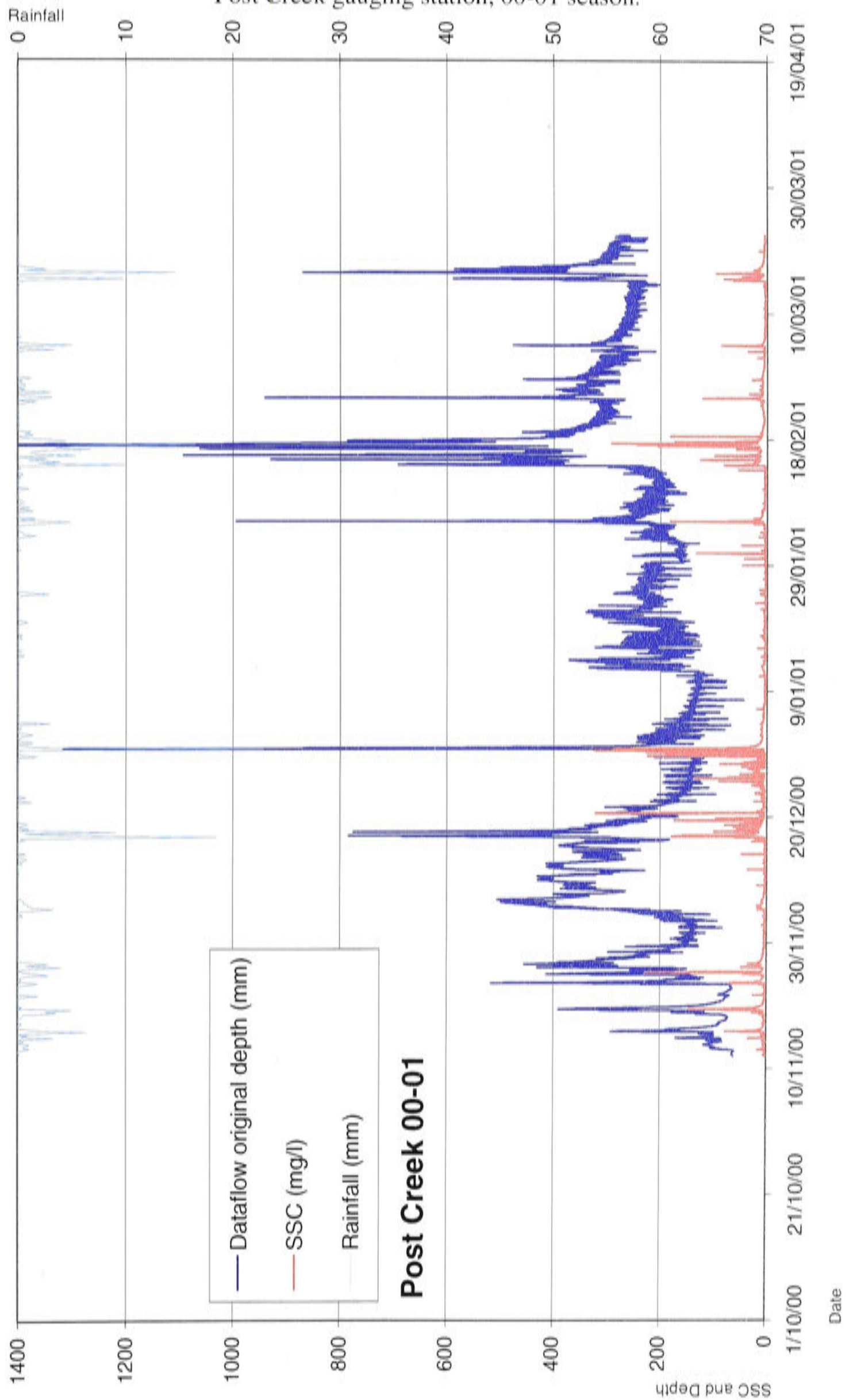
**APPENDIX F (6)** Depth and SSC (calculated from turbidity) recordings at Prosser Drain gauging station, 00-01 season.



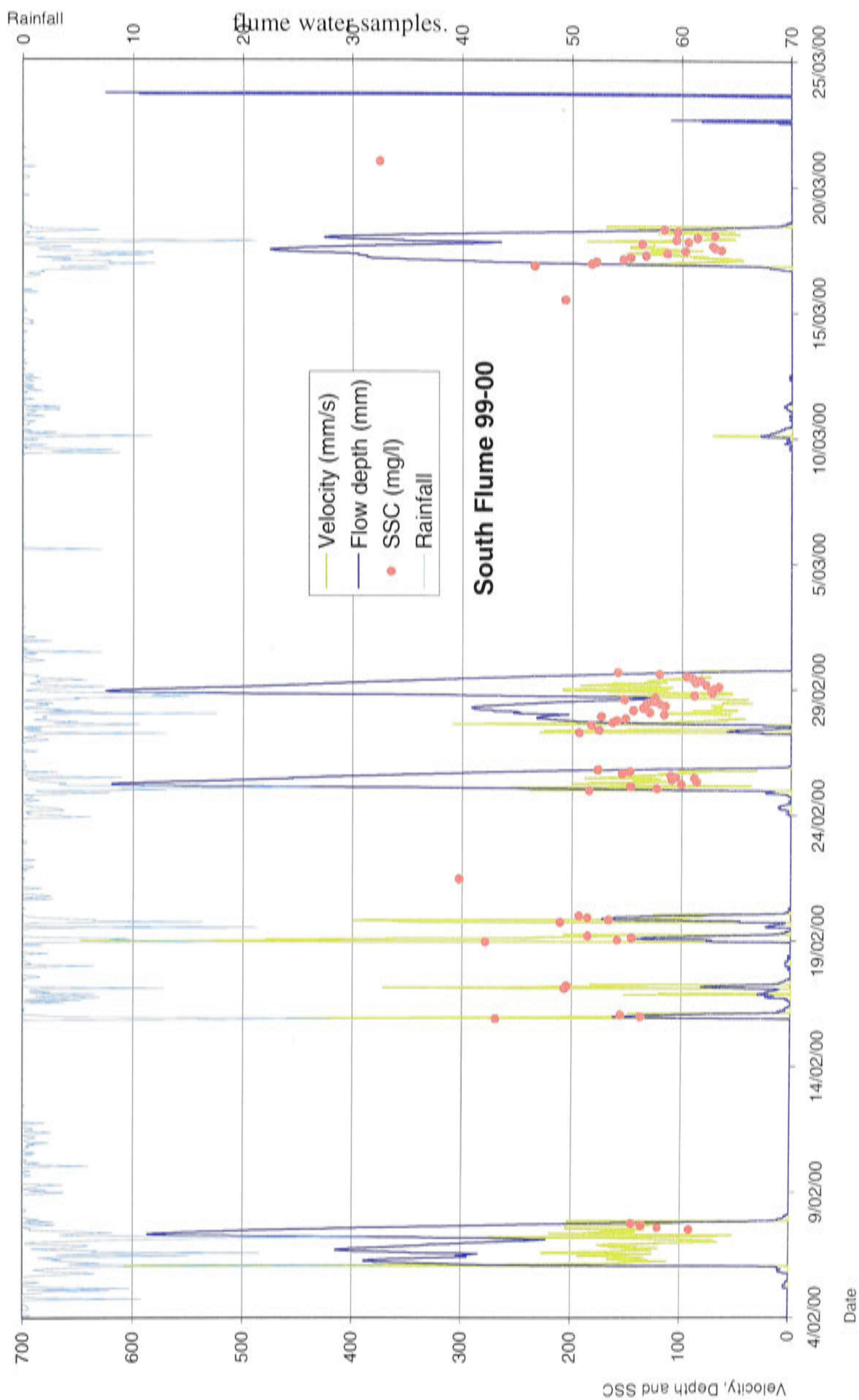
**APPENDIX F (7)** Depth and SSC (calculated from turbidity) recordings at Post Creek gauging station 99-00 season.



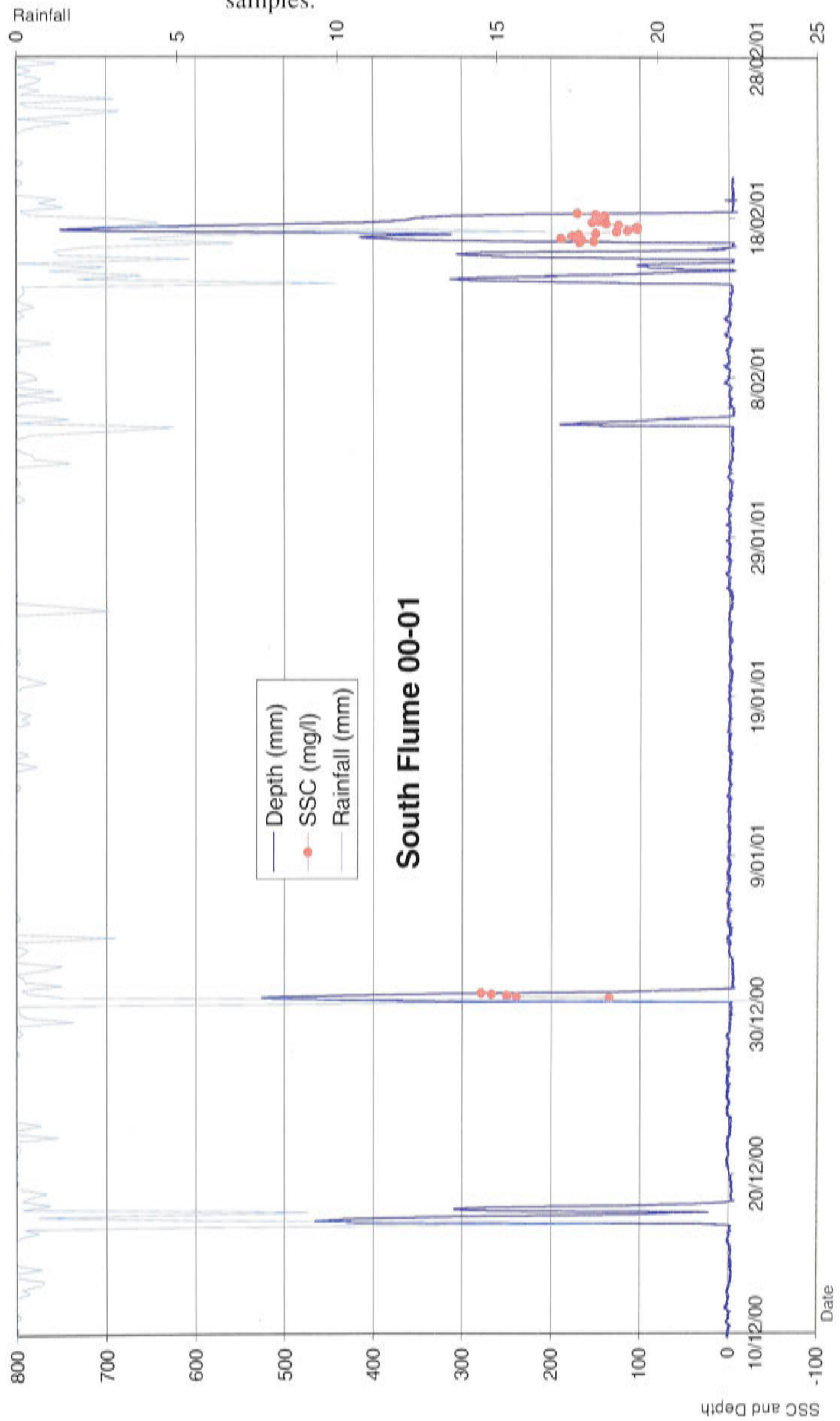
**APPENDIX F (8)** Depth and SSC (calculated from turbidity) recordings at Post Creek gauging station, 00-01 season.



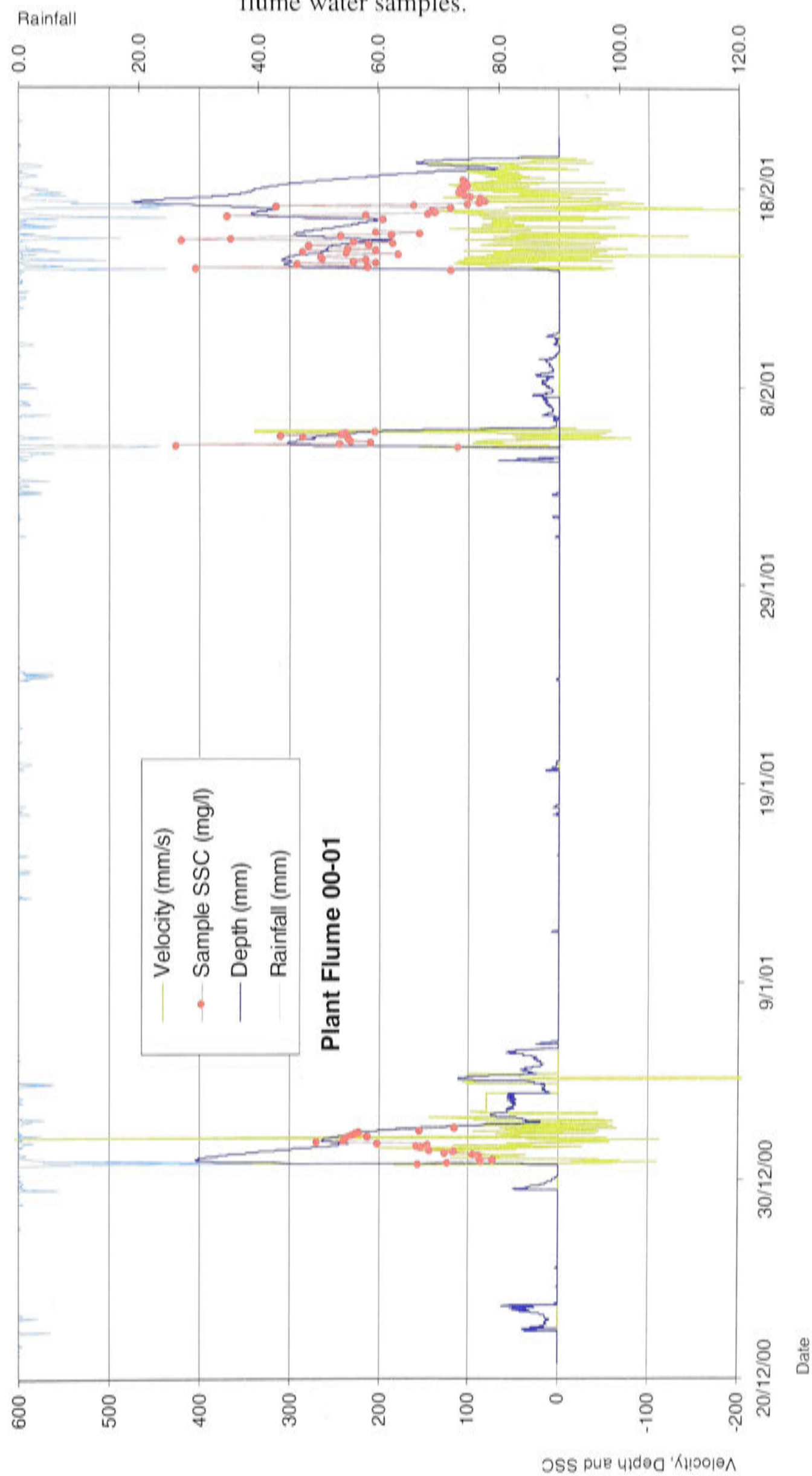
**APPENDIX F (9)** Depth and Velocity recordings at South Flume gauging station, 99-00 season, and SSC values measured from flume water samples.



**APPENDIX F (10)** Depth recordings at South Flume gauging station, 00-01 season, and SSC values measured from flume water samples.



**APPENDIX F (11)** Depth and Velocity recordings at Plant Flume gauging station, 00-01 season, and SSC values measured from flume water samples.



**APPENDIX G**

Average net surface level change (mm) and surface vegetation cover (%) on pinplots in the Ripple Corner Catchment over two periods (December to March and March to May) in the 99-00 (a) and 00-01 (b) season. Negative values indicate net soil loss.

a) Pinplots 1999-2000				
	Dec-Mar	Mar-May	total (mm)	Cover (%)
C	-0.3	-1.6	-1.9	75
D	1.1	0.5	1.6	98
F	4.4	1.3	5.7	70
G	6.2	1.1	7.3	70
H	1.8	0.6	2.4	90
I	1.0	2.2	3.2	100
J	-4.1	0.6	-3.6	20
K	-0.5	0.8	0.0	65
L	1.1	0.4	1.0	90
M	1.8	0.0	2.0	95
N	1.3	0.5	2.1	90
O	1.8	0.5	2.1	80
P	1.6	0.7	2.2	70
Mean:	1.1	0.3	1.4	
Median:	1.3	0.6	2.1	

b) Pinplots 2000-2001				
	Dec-Mar	Mar-May	total (mm)	Cover (%)
F	-0.4	-1.3	-1.7	45
G	-0.5	0.2	-0.3	65
H	1.8	-1.2	0.7	85
I	2.7	-1.6	1.1	75
J	-1.7	-0.6	-2.4	30
M	-2.4	-1.4	-3.8	99
P	-0.1	0.0	-0.1	65
Mean:	0.3	-0.8	-0.5	
Median:	-0.2	-0.9	-0.2	

**APPENDIX H**

(next pages) Average net surface level change (mm), erosion, and deposition rate (mm) for drain and water furrow surface profiles in the Ripple Corner Catchment, over two periods (December to March and March to May) in the 99-00 (a) and 00-01 (b) season.

RD = Ripple Drain  
 Maj = major drain  
 Min = minor drain  
 f = water furrow

g = grey sand  
 s = silty clay  
 c = clay

r = ratoon  
 p = plant cane



**a) Profile data 99-00 (unadjusted)**

Profile	Drain type	Soil type	Crop type	Deposition rate (mm)	Erosion rate (mm)	Net surface change (mm)	Deposition rate (mm)	Erosion rate (mm)	Net surface change (mm)	Deposition rate (mm)	Erosion rate (mm)	Net surface change (mm)
				Dec – Mar				Mar – May				Dec – May
1	f	s	r	0.7	-5.3	-4.5	2.2	-2.0	0.3	1.7	5.9	-4.3
2	f	s	r	1.3	-2.9	-1.6	2.2	-1.0	1.2	2.9	3.3	-0.4
3	f	s	r	1.3	-5.0	-3.8	1.7	-2.0	-0.3	0.4	4.5	-4.1
10	f	s	r	0.9	-2.5	-1.6	1.4	-1.7	-0.3	1.0	2.9	-2.0
11	f	s	r							2.1	3.2	-1.1
14	f	s	r	5.1	-1.2	3.9	0.9	-1.8	-1.0	4.4	1.5	2.9
15	f	s	r	6.2	-0.5	5.7	1.8	-1.7	0.1	6.7	0.8	5.9
16	f	s	r	4.0	-6.9	-2.8	5.0	-2.0	3.1	3.8	3.5	0.3
25	f	g	r							2.7	4.3	-1.6
26	f	g	r							5.8	3.6	2.2
27	f	g	r							4.4	3.6	0.8
32	f	g	p	4.1	-2.2	1.9	1.3	-8.1	-6.7	2.3	7.1	-4.8
33	f	g	p	9.6	-7.6	2.0	2.7	-12.2	-9.5	2.2	9.7	-7.4
34	f	g	p	0.9	-6.6	-5.7	0.3	-3.6	-3.3	0.6	9.5	-9.0
35	f	g	p	0.5	-16.7	-16.2	2.7	-2.2	0.4	1.7	17.5	-15.8
36	f	c	p							1.5	7.7	-6.2
37	f	c	p							4.1	6.2	-2.0
38	f	c	p							2.1	6.7	-4.5
39	f	c	p							4.8	4.9	0.0
40	f	c	r							2.5	3.6	-1.0
41	f	c	r							0.7	4.4	-3.7
42	f	c	r							1.5	2.5	-1.0
43	f	c	r							2.6	2.8	-0.2
44	f	g	r	2.5	-6.4	-4.0	2.5	-7.6	-5.1	3.1	12.2	-9.1
45	f	g	r	3.4	-2.0	1.4	0.6	-9.7	-9.1	0.3	8.0	-7.7
46	f	g	r	0.4	-3.7	-3.3	1.4	-5.4	-4.0	0.3	7.6	-7.3
47	f	g	r	0.8	-4.3	-3.5	1.8	-2.4	-0.6	1.7	5.8	-4.1
18	RD	s		34.8	-16.3	18.5	84.5	-1.4	83.0	114.7	13.2	101.5
19	RD	s		37.6	-30.9	6.7	86.8	-3.6	83.2	110.1	20.2	89.9

<b>a) Profile data 99-00 (unadjusted, continued)</b>												
Profile	Drain type	Soil type	Crop type	Deposition rate (mm)	Erosion rate (mm)	Total surface change (mm)	Deposition rate (mm)	Erosion rate (mm)	Total surface change (mm)	Deposition rate (mm)	Erosion rate (mm)	Total surface change (mm)
				Dec – Mar			Mar – May			Dec – May		
20	RD	s		42.5	-4.1	38.4	63.0	-2.2	60.8	102.6	3.4	99.2
21	RD	s								61.7	7.6	54.1
7	Maj	s		4.0	-29.2	-25.2	10.0	-1.3	8.7	4.3	20.2	-15.9
8	Maj	s		3.0	-23.8	-20.8	1.7	-2.7	-1.0	3.1	25.0	-21.8
9	Maj	s		2.7	-55.8	-53.1	7.8	-9.3	-1.5	4.8	59.4	-54.6
17	Maj	s		2.5	-11.6	-9.1	2.2	-3.4	-1.2	2.1	12.4	-10.3
28	Maj	g		13.9	-2.4	11.5	4.2	-7.6	-3.3	12.9	4.8	8.2
29	Maj	g		10.7	-3.6	7.1	2.0	-4.1	-2.1	10.3	5.3	5.1
30	Maj	g		10.9	-9.5	1.4				10.9	9.5	1.4
31	Maj	g		19.5	-2.8	16.7				19.5	2.8	16.7
48	Maj	g		4.6	-16.9	-12.3	4.3	-3.8	0.5	6.6	18.4	-11.8
49	Maj	g		4.0	-2.5	1.5	3.1	-3.1	0.0	5.0	3.5	1.5
50	Maj	g		5.0	-4.5	0.5	1.4	-4.0	-2.6	4.0	6.1	-2.1
4	Min	s		3.3	-3.0	0.4	2.0	-2.0	0.0	4.0	3.6	0.4
5	Min	s								5.6	0.1	5.5
6	Min	s								5.3	1.1	4.3
51	Min	s		2.5	-3.5	-1.1	0.7	-2.4	-1.7	1.5	4.3	-2.8
52	Min	s		2.6	-2.0	0.7	1.4	-1.3	0.2	2.9	2.0	0.8
53	Min	s		2.4	-5.5	-3.1	1.4	-1.9	-0.5	2.5	6.1	-3.6
54	Min	c		5.7	-2.5	3.1	2.9	-1.9	1.0	7.7	3.6	4.1
56	Min	c		6.4	-0.5	5.9	1.5	-2.1	-0.6	6.3	0.9	5.4

<b>a) Profile data 99-00 (adjusted)</b>												
Profile	Drain type	Soil type	Crop type	Deposition rate (mm)	Erosion rate (mm)	Total surface change (mm)	Deposition rate (mm)	Erosion rate (mm)	Total surface change (mm)	Deposition rate (mm)	Erosion rate (mm)	Total surface change (mm)
				Dec – Mar			Mar – May			Dec – May		
1	f s	r		0.4	-3.0	-2.6	1.3	-1.1	0.1	0.9	3.4	-2.4
2	f s	r		0.7	-1.7	-1.0	1.3	-0.6	0.7	1.6	1.9	-0.2
3	f s	r		0.7	-2.9	-2.2	1.0	-1.1	-0.2	0.2	2.6	-2.3

a) Profile data 99-00 (adjusted, continued)												
Profile	Drain type	Soil type	Crop type	Deposition rate (mm)	Erosion rate (mm)	Total surface change (mm)	Deposition rate (mm)	Erosion rate (mm)	Total surface change (mm)	Deposition rate (mm)	Erosion rate (mm)	Total surface change (mm)
				Dec – Mar			Mar – May			Dec – May		
10		f s	r	0.5	-1.4	-0.9	0.8	-1.0	-0.2	0.5	1.7	-1.1
11		f s	r							1.2	1.8	-0.6
14		f s	r	2.9	-0.7	2.2	0.5	-1.0	-0.5	2.5	0.9	1.7
15		f s	r	3.6	-0.3	3.3	1.0	-1.0	0.1	3.8	0.4	3.4
16		f s	r	2.3	-3.9	-1.6	2.9	-1.1	1.8	2.2	2.0	0.1
25		f g	r							0.7	1.2	-0.4
26		f g	r							1.6	1.0	0.6
27		f g	r							1.2	1.0	0.2
32		f g	p	1.1	-0.6	0.5	0.4	-2.2	-1.8	0.6	1.9	-1.3
33		f g	p	2.6	-2.1	0.6	0.7	-3.3	-2.6	0.6	2.6	-2.0
34		f g	p	0.2	-1.8	-1.5	0.1	-1.0	-0.9	0.2	2.6	-2.4
35		f g	p	0.1	-4.5	-4.4	0.7	-0.6	0.1	0.5	4.7	-4.3
36		f c	p							1.0	5.2	-4.2
37		f c	p							2.8	4.2	-1.4
38		f c	p							1.4	4.5	-3.1
39		f c	p							3.3	3.3	0.0
40		f c	r							1.7	2.4	-0.7
41		f c	r							0.4	3.0	-2.5
42		f c	r							1.0	1.7	-0.7
43		f c	r							1.8	1.9	-0.1
44		f g	r	0.7	-1.7	-1.1	0.7	-2.1	-1.4	0.8	3.3	-2.5
45		f g	r	0.9	-0.6	0.4	0.2	-2.6	-2.5	0.1	2.2	-2.1
46		f g	r	0.1	-1.0	-0.9	0.4	-1.5	-1.1	0.1	2.1	-2.0
47		f g	r	0.2	-1.2	-0.9	0.5	-0.7	-0.2	0.5	1.6	-1.1
18		RD s		7.2	-6.9	0.2	5.1	-0.8	4.3	11.8	7.3	4.5
19		RD s		4.1	-9.2	-5.1	4.4	-1.1	3.3	8.0	9.8	-1.8
20		RD s		2.5	-2.3	0.1	5.9	-1.2	4.7	6.7	1.9	4.8
21		RD s								3.5	3.2	0.2
7		Maj s		2.3	-11.2	-8.9	3.5	-0.7	2.7	2.3	8.3	-5.9

<b>a) Profile data 99-00 (adjusted, continued)</b>												
Profile	Drain type	Soil type	Crop type	Deposition rate (mm)	Erosion rate (mm)	Total surface change (mm)	Deposition rate (mm)	Erosion rate (mm)	Total surface change (mm)	Deposition rate (mm)	Erosion rate (mm)	Total surface change (mm)
				Dec – Mar			Mar – May			Dec – May		
8	Maj	s		1.7	-11.9	-10.1	0.7	-1.4	-0.7	1.8	12.6	-10.8
9	Maj	s		0.6	-24.5	-23.9	3.0	-4.9	-2.0	1.0	26.9	-25.9
17	Maj	s		1.4	-3.5	-2.1	0.7	-1.7	-0.9	1.2	4.2	-3.0
28	Maj	g		3.5	-0.7	2.9	1.2	-1.5	-0.4	3.5	0.9	2.5
29	Maj	g		2.7	-0.8	1.9	0.5	-1.0	-0.4	2.6	1.1	1.4
30	Maj	g		1.6	-2.3	-0.8				1.6	2.3	-0.8
31	Maj	g		2.6	-0.7	1.9				2.6	0.7	1.9
48	Maj	g		1.3	-2.0	-0.7	1.1	-0.6	0.5	1.8	2.0	-0.2
49	Maj	g		0.8	-0.6	0.2	0.8	-0.7	0.1	1.2	0.9	0.3
50	Maj	g		1.1	-1.2	-0.1	0.4	-0.7	-0.3	1.0	1.5	-0.4
4	Min	s		1.9	-1.7	0.2	1.2	-1.2	0.0	2.3	2.0	0.2
5	Min	s								3.2	0.1	3.1
6	Min	s								3.1	0.6	2.4
51	Min	s		1.4	-2.0	-0.6	0.4	-1.4	-1.0	0.9	2.5	-1.6
52	Min	s		1.5	-1.1	0.4	0.8	-0.7	0.1	1.6	1.2	0.5
53	Min	s		1.4	-3.2	-1.8	0.8	-1.1	-0.3	1.4	3.5	-2.1
54	Min	c		3.9	-1.7	2.1	2.0	-1.3	0.7	5.2	2.4	2.8
56	Min	c		4.4	-0.4	4.0	1.0	-1.4	-0.4	4.3	0.6	3.6

<b>b) Profile data 00-01 (unadjusted)</b>												
Profile	Drain type	Soil type	Crop type	Deposition rate (mm)	Erosion rate (mm)	Net surface change (mm)	Deposition rate (mm)	Erosion rate (mm)	Net surface change (mm)	Deposition rate (mm)	Erosion rate (mm)	Net surface change (mm)
				Dec – Mar			Mar – May			Dec – May		
9	f	c	r	7.0	-4.3	2.7	3.5	-10.7	-7.2	5.0	-9.5	-4.5
10	f	c	r	1.4	-6.7	-5.3	7.0	-2.3	4.7	5.0	-5.5	-0.6
11	f	c	r	2.8	-10.2	-7.4	1.6	-12.5	-10.9	1.3	-19.5	-18.3
12	f	g	r	2.8	-0.9	1.8	1.0	-3.4	-2.4	1.8	-2.3	-0.5
13	f	g	r	1.9	-2.2	-0.3	2.0	-3.4	-1.4	2.2	-4.0	-1.7

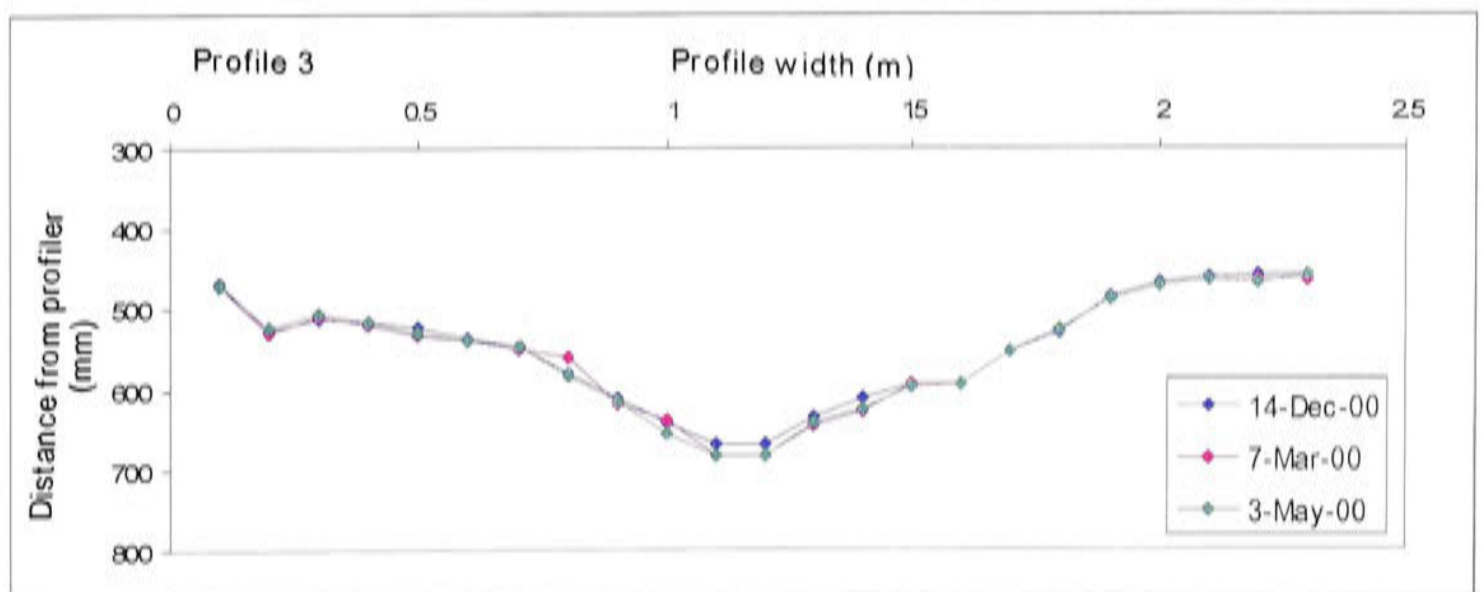
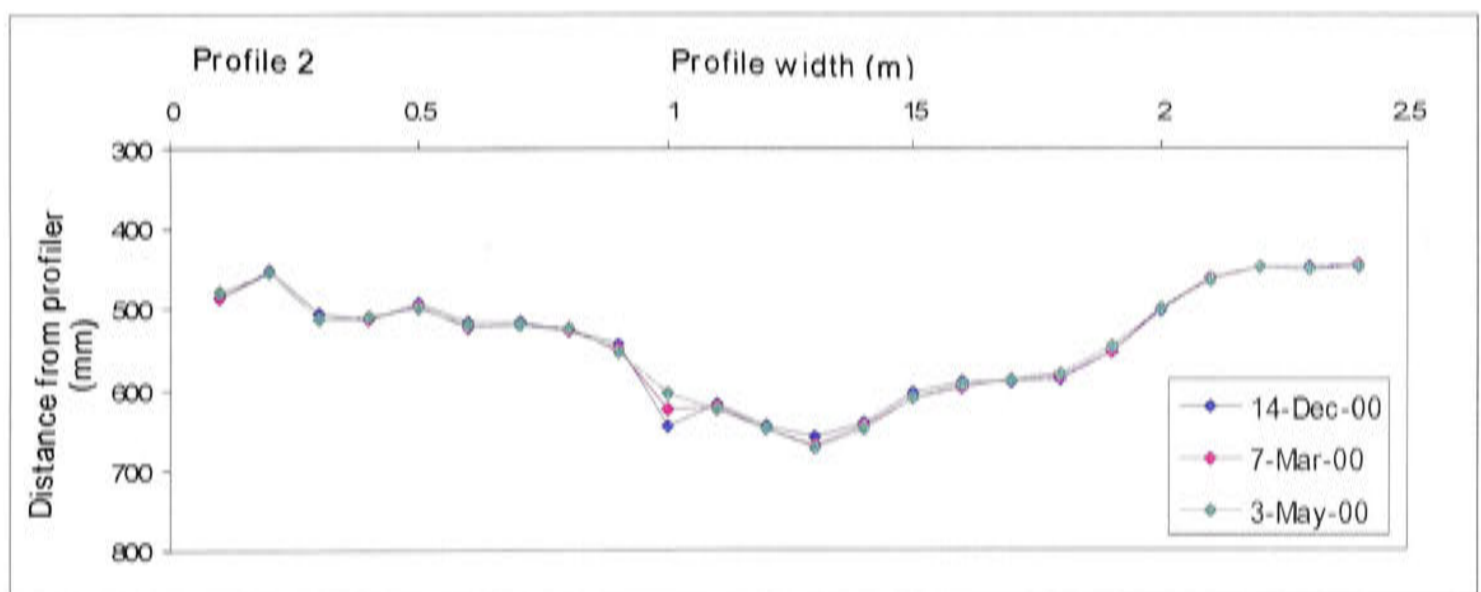
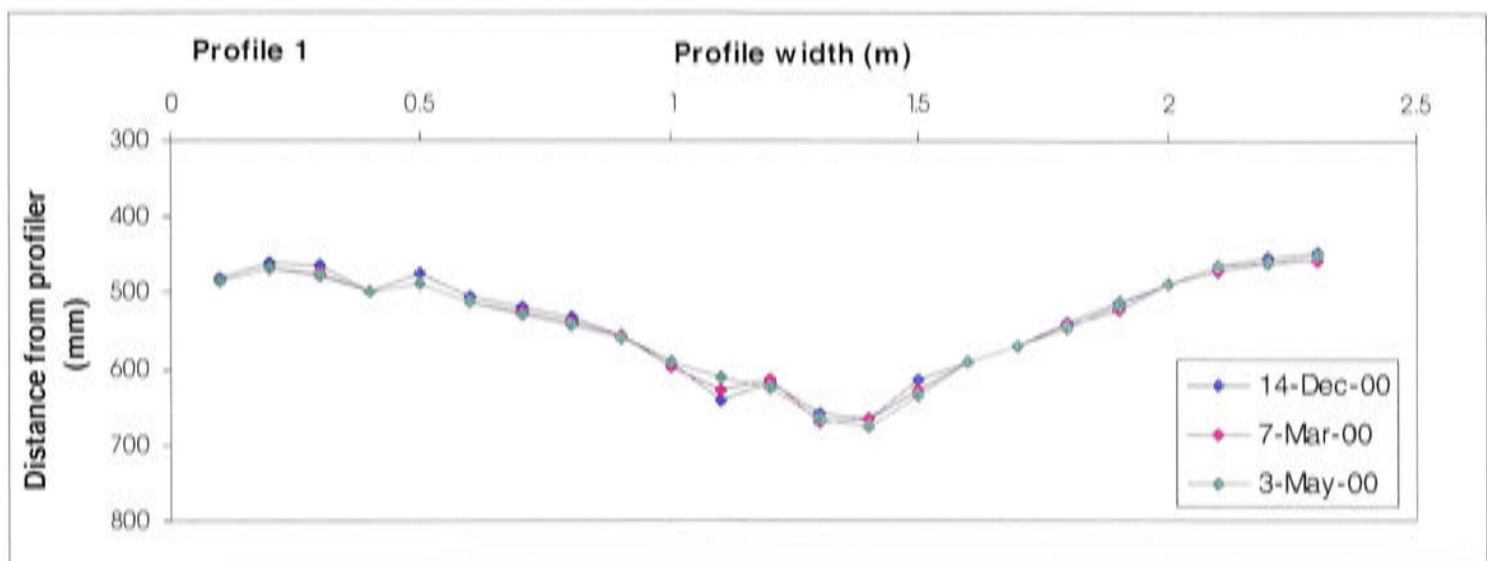
<b>b) Profile data 00-01 (unadjusted, continued)</b>												
Profile	Drain type	Soil type	Crop type	Deposition rate (mm)	Erosion rate (mm)	Net surface change (mm)	Deposition rate (mm)	Erosion rate (mm)	Net surface change (mm)	Deposition rate (mm)	Erosion rate (mm)	Net surface change (mm)
				Dec – Mar			Mar – May			Dec – May		
14	f	g	r	3.0	-3.3	-0.3	1.0	-5.8	-4.7	1.7	-6.7	-5.0
27	f	s	r	1.8	-1.0	0.8	2.8	-1.9	0.9	2.6	-1.0	1.7
28	f	s	r	3.8	-0.5	3.3	2.4	-1.3	1.1	5.7	-1.2	4.5
29	f	s	r	5.8	-0.8	5.0	3.7	-4.5	-0.7	4.9	-0.6	4.3
3	RD	s		40.9	-45.9	-5.0	17.5	-22.0	-4.5	51.6	-61.1	-9.5
4	RD	s		9.4	-91.5	-82.1	7.2	-11.3	-4.1	12.5	-98.8	-86.3
24	RD	s		27.1	-11.6	15.4	42.3	-1.7	40.6	59.2	-3.1	56.1
25	RD	s		3.1	-58.2	-55.1	39.8	-1.5	38.3	10.5	-28.1	-17.6
26	RD	s		6.7	-27.9	-21.2	28.5	-2.3	26.2	16.8	-12.3	4.5
5	Maj	s		7.6	-3.0	4.6	5.7	-8.3	-2.6	7.9	-6.0	2.0
6	Maj	s		4.2	-6.1	-1.9	16.1	-10.0	6.0	11.1	-7.0	4.2
7	Maj	s		17.8	-7.0	10.7				17.7	-2.7	15.0
16	Maj	g								9.2	-12.3	-3.1
17	Maj	g		6.0	-4.3	1.8	4.3	-3.4	1.0	6.1	-3.4	2.7
18	Min	s		3.8	-1.9	1.9	7.2	-1.0	6.2	8.7	-0.6	8.1
19	Min	s		6.6	-0.7	6.0	5.5	-2.5	3.0	10.4	-1.4	8.9
20	Min	s		5.3	-0.6	4.8	4.8	-2.0	2.8	8.5	-0.9	7.6
22	Min	c		8.3	-0.3	8.0	2.4	-3.3	-1.0	7.2	-0.2	7.0
23	Min	c		10.8	-0.2	10.7	7.1	-0.8	6.3	17.0	0.0	17.0
30	Min	s		1.6	-2.4	-0.8	4.4	-3.5	0.9	3.9	-3.9	0.0
31	Min	s		2.0	-2.7	-0.7	2.7	-4.0	-1.4	2.1	-4.2	-2.1
32	Min	s		1.9	-2.4	-0.5	2.1	-3.4	-1.3	1.8	-3.6	-1.8

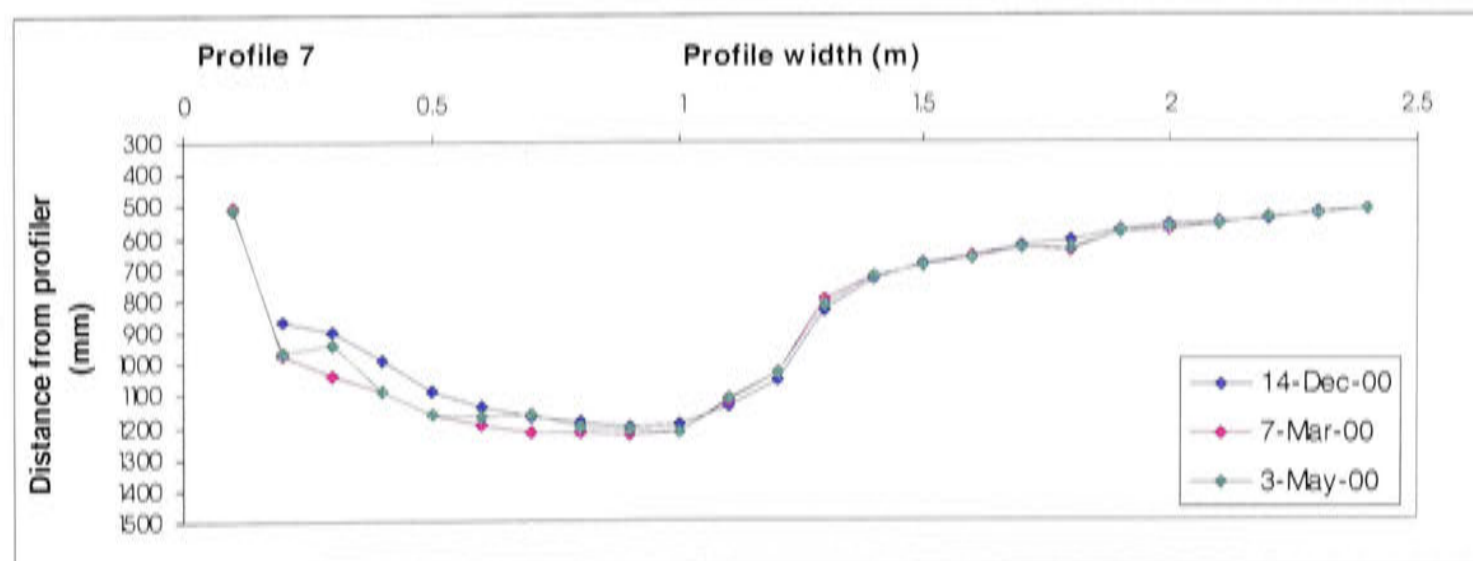
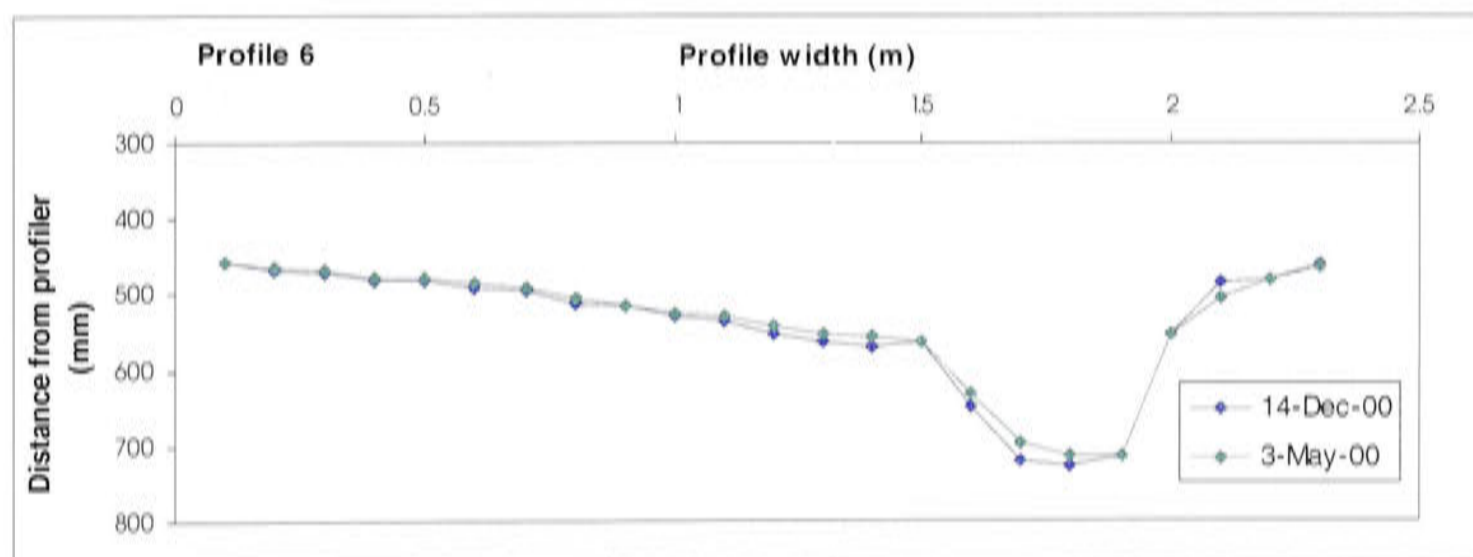
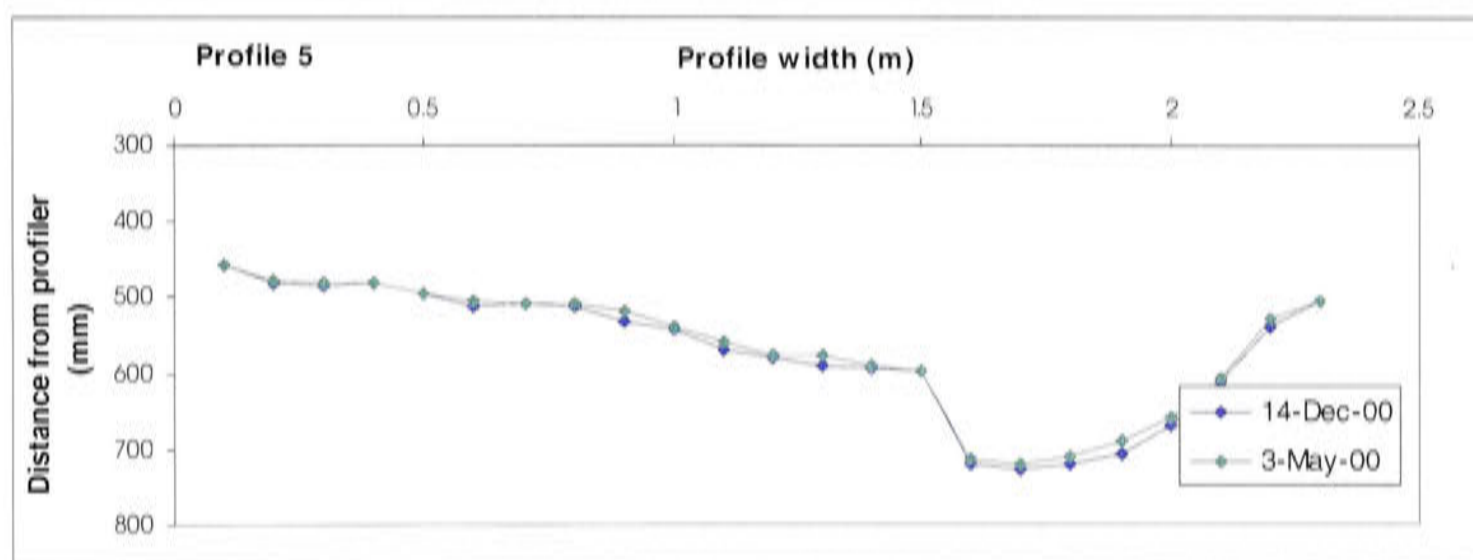
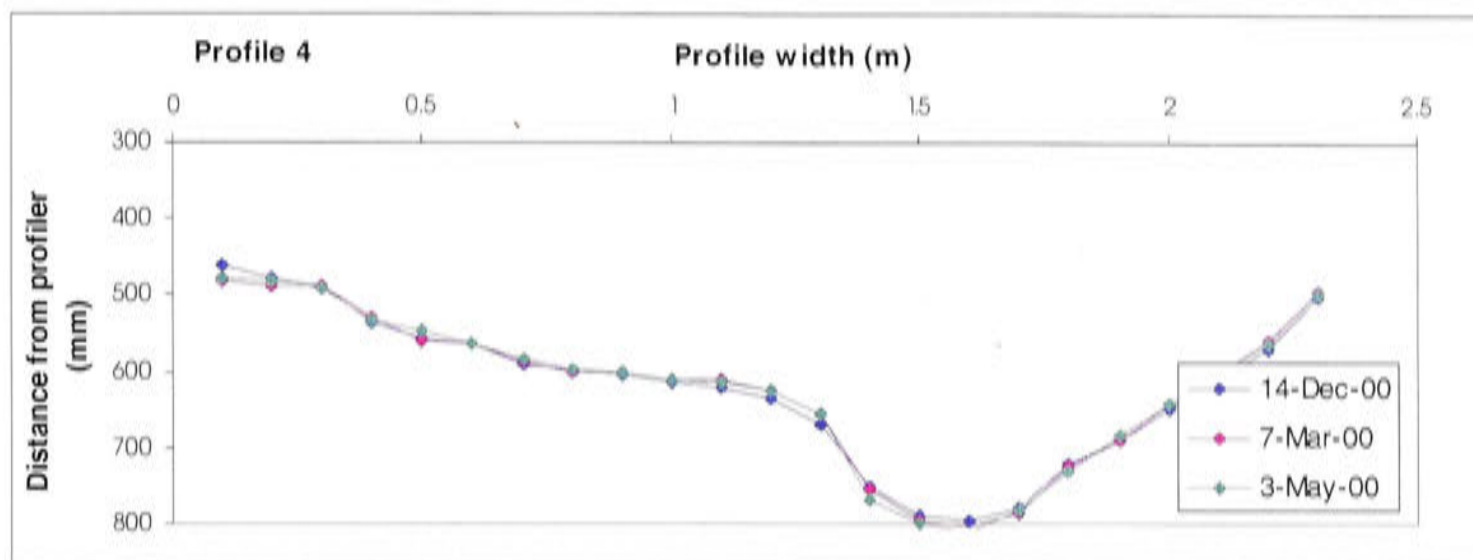
b) Profile data 00-01 (adjusted)												
Profile	Drain type	Soil type	Crop type	Deposition rate (mm)	Erosion rate (mm)	Net surface change (mm)	Deposition rate (mm)	Erosion rate (mm)	Net surface change (mm)	Deposition rate (mm)	Erosion rate (mm)	Net surface change (mm)
				Dec – Mar			Mar – May			Dec – May		
9	f	c	r	4.7	-2.9	1.8	2.4	-7.2	-4.9	3.4	-6.4	-3.1
10	f	c	r	0.9	-4.6	-3.6	4.8	-1.6	3.2	3.4	-3.8	-0.4
11	f	c	r	1.9	-6.9	-5.0	1.1	-8.5	-7.4	0.9	-13.3	-12.4
12	f	g	r	0.7	-0.2	0.5	0.3	-0.9	-0.6	0.5	-0.6	-0.1
13	f	g	r	0.5	-0.6	-0.1	0.5	-0.9	-0.4	0.6	-1.1	-0.5
14	f	g	r	0.8	-0.9	-0.1	0.3	-1.6	-1.3	0.5	-1.8	-1.4
27	f	s	r	1.0	-0.6	0.4	1.6	-1.1	0.5	1.5	-0.5	0.9
28	f	s	r	2.2	-0.3	1.9	1.4	-0.7	0.6	3.2	-0.7	2.6
29	f	s	r	3.3	-0.5	2.9	2.1	-2.6	-0.4	2.8	-0.3	2.4
3	RD	s		2.3	-3.3	-1.0	1.5	-1.4	0.1	3.0	-3.9	-0.9
4	RD	s		0.5	-12.7	-12.2	0.8	-4.2	-3.4	0.4	-16.0	-15.6
24	RD	s		14.3	-2.5	11.9	10.5	-0.7	9.8	22.0	-0.3	21.6
25	RD	s		1.8	-13.2	-11.4	8.6	-0.8	7.7	4.3	-8.3	-4.0
26	RD	s		1.4	-0.7	0.7	1.5	-0.5	1.0	1.8	-0.5	1.3
5	Maj	s		4.3	-1.7	2.6	3.2	-4.7	-1.5	4.5	-3.4	1.1
6	Maj	s		2.4	-3.5	-1.1	9.2	-5.7	3.5	6.4	-4.0	2.4
7	Maj	s		10.2	-4.0	6.1				10.1	-1.6	8.5
16	Maj	g								2.5	-2.7	-0.2
17	Maj	g		1.6	-0.6	1.0	1.0	-0.7	0.3	1.6	-0.4	1.3
18	Min	s		2.2	-1.1	1.1	4.1	-0.6	3.5	5.0	-0.4	4.6
19	Min	s		3.8	-0.4	3.4	3.1	-1.4	1.7	5.9	-0.8	5.1
20	Min	s		3.0	-0.3	2.7	2.7	-1.1	1.6	4.8	-0.5	4.3
22	Min	c		5.7	-0.2	5.4	1.6	-2.3	-0.7	4.9	-0.1	4.8
23	Min	c		7.4	-0.1	7.2	4.8	-0.5	4.3	11.6	0.0	11.6
30	Min	s		0.9	-1.4	-0.5	2.5	-2.0	0.5	2.2	-2.2	0.0
31	Min	s		1.1	-1.5	-0.4	1.5	-2.3	-0.8	1.2	-2.4	-1.2
32	Min	s		1.1	-1.4	-0.3	1.2	-2.0	-0.8	1.0	-2.1	-1.0

**APPENDIX I**

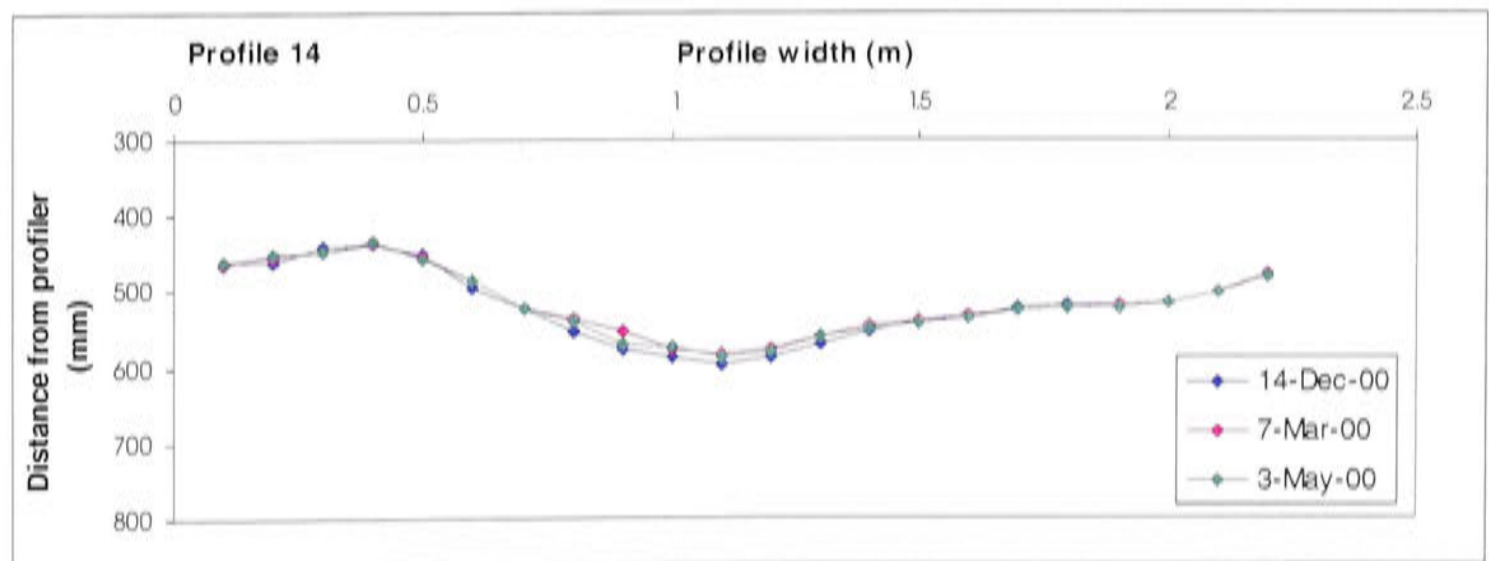
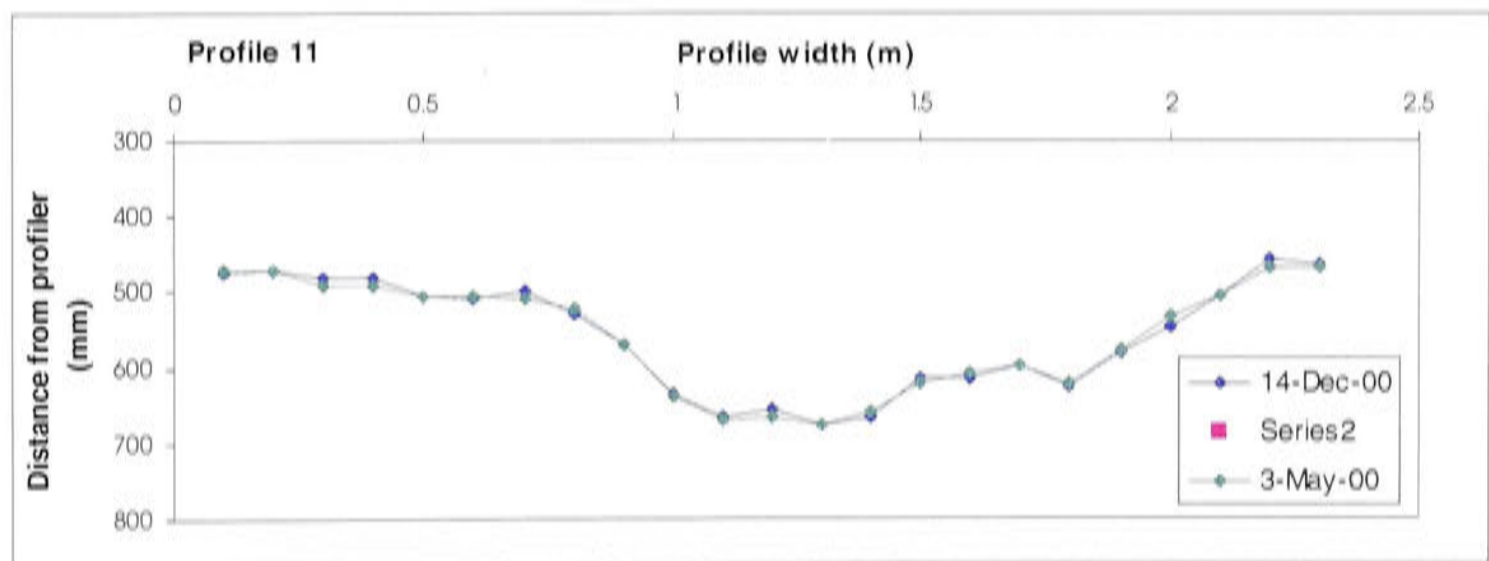
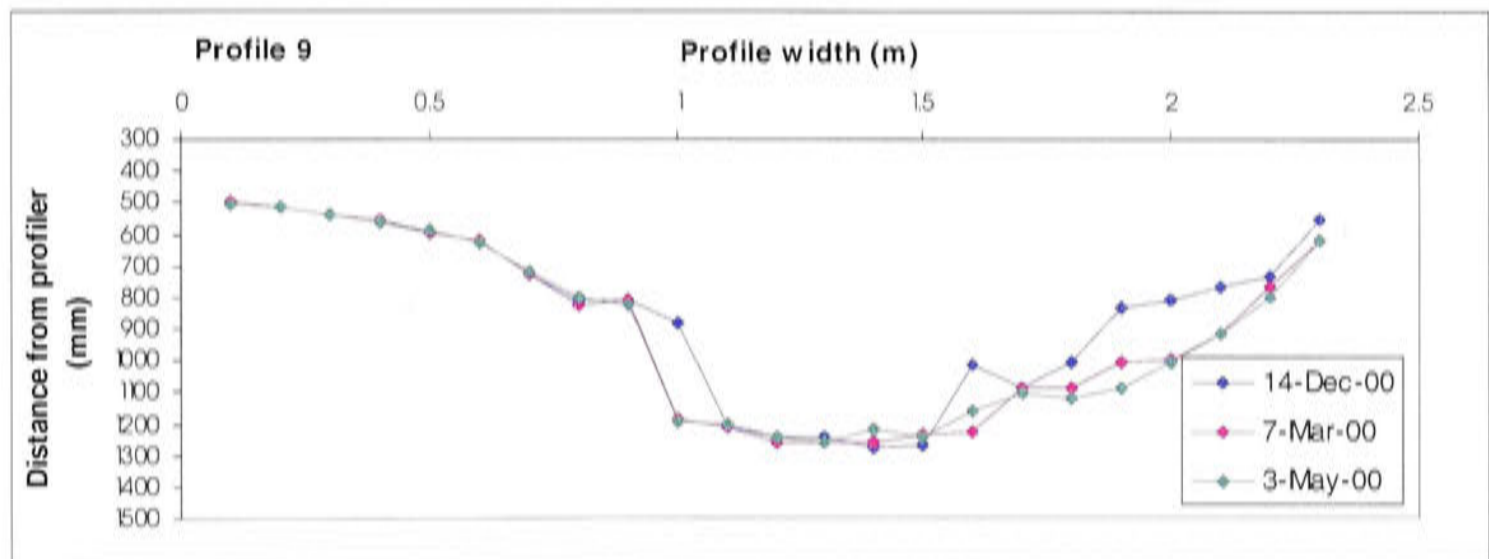
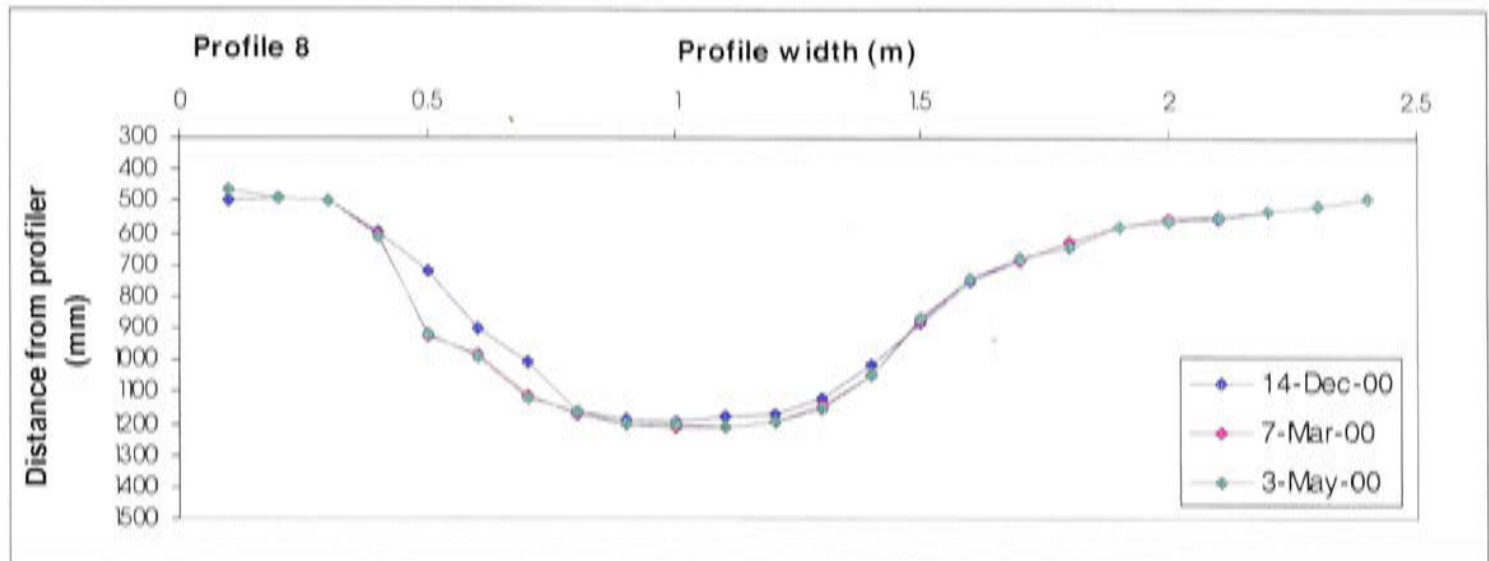
Examples of graphs from both budget seasons, showing changes in the surface profile (distance relative to profiler datum, in mm) of drains and water furrows in the Ripple Corner Catchment.

**Profiles 1-9, 11, 14: Season 99-00**

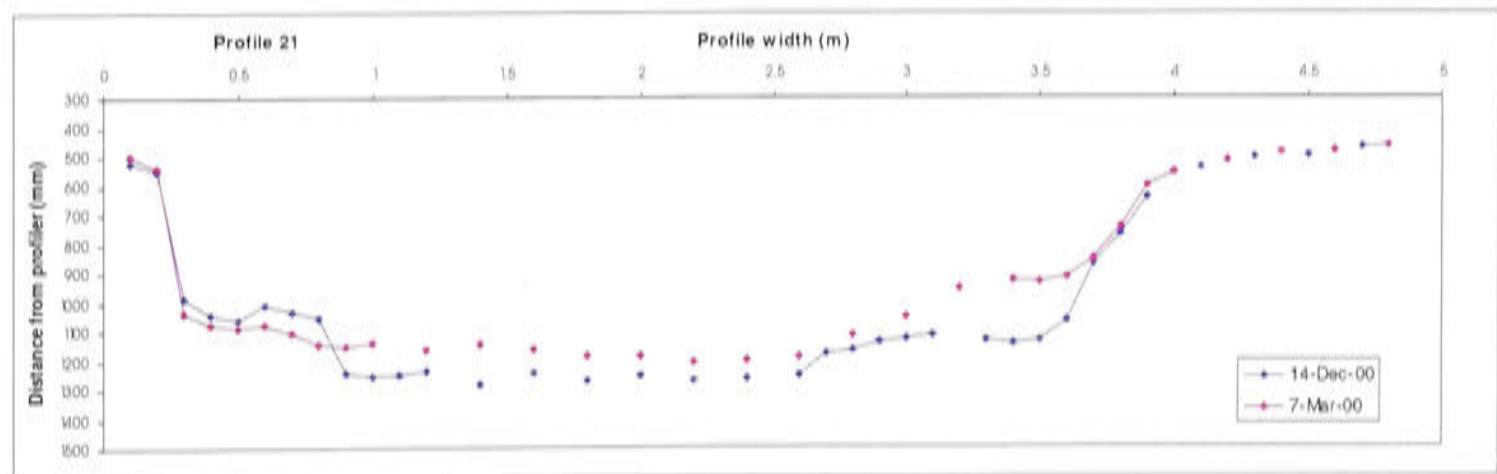
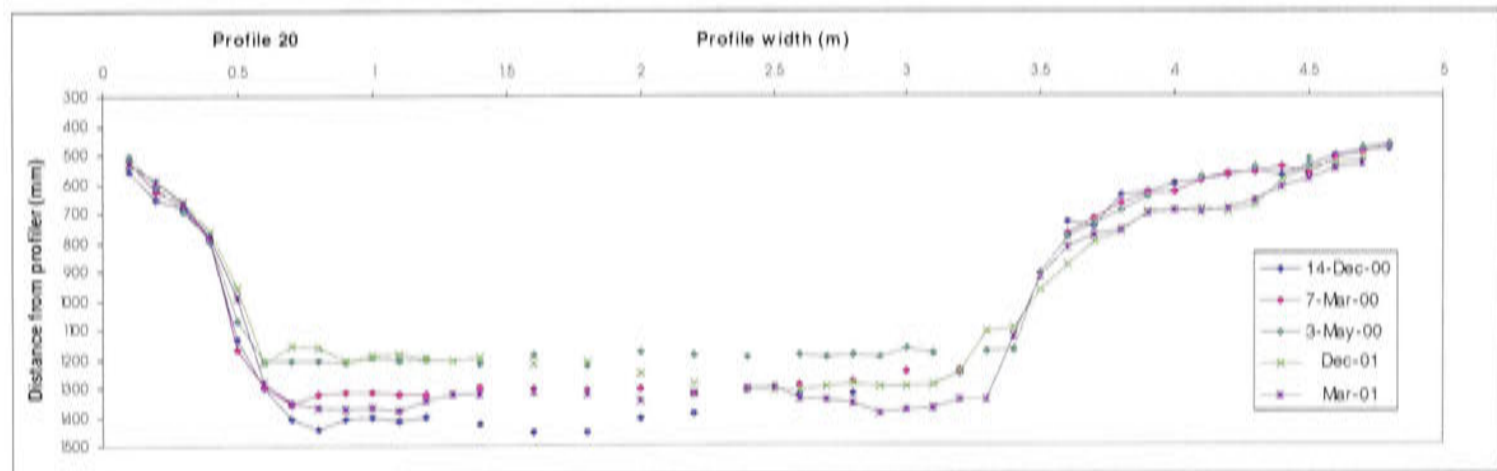
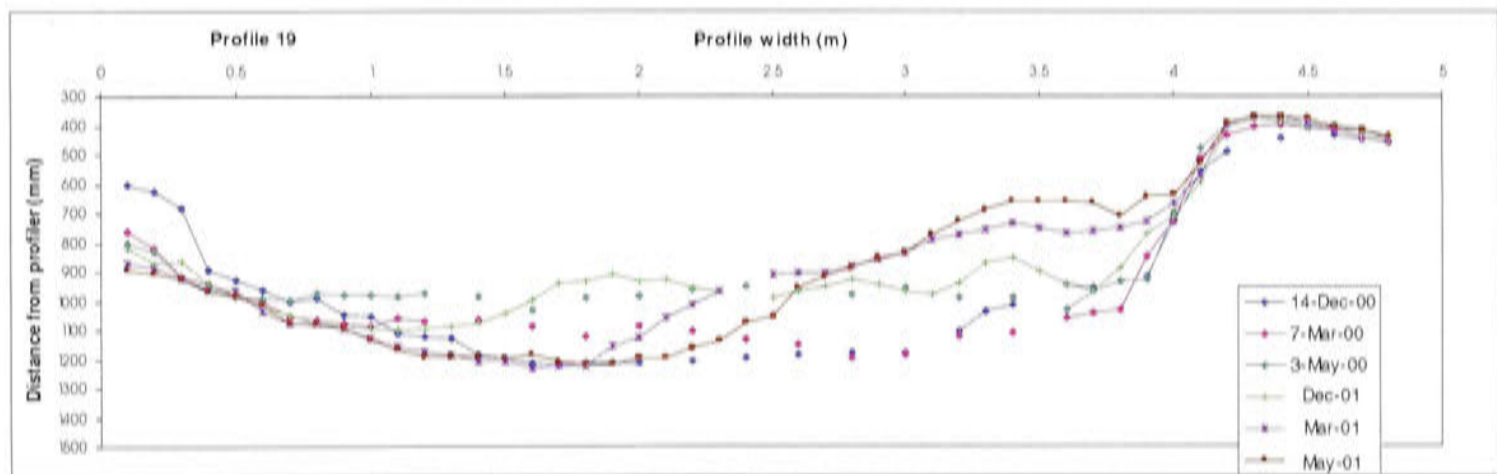
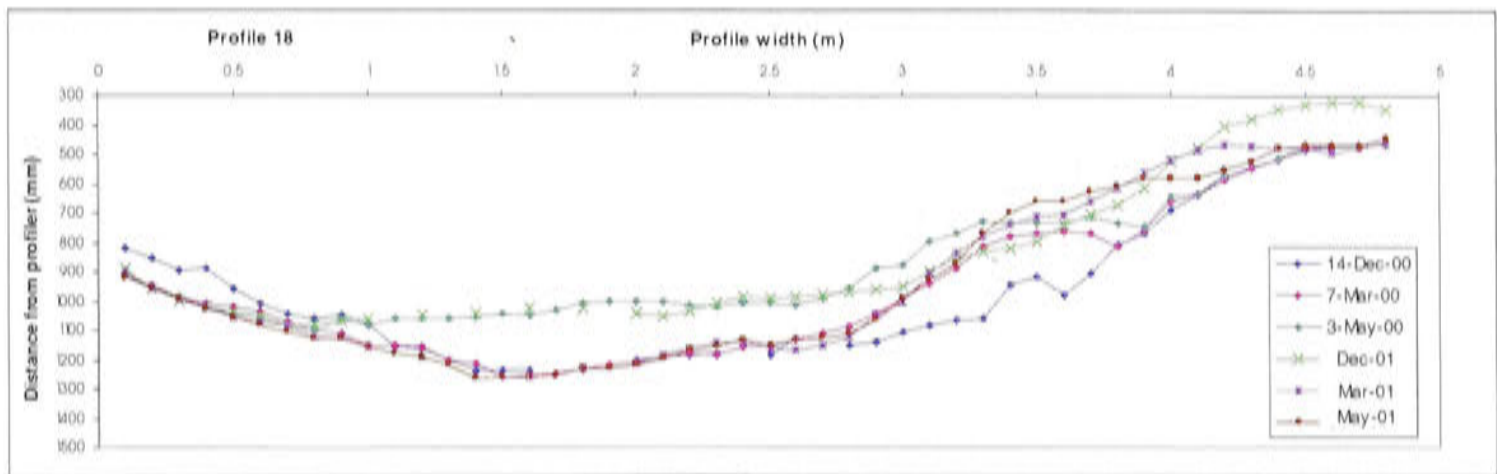


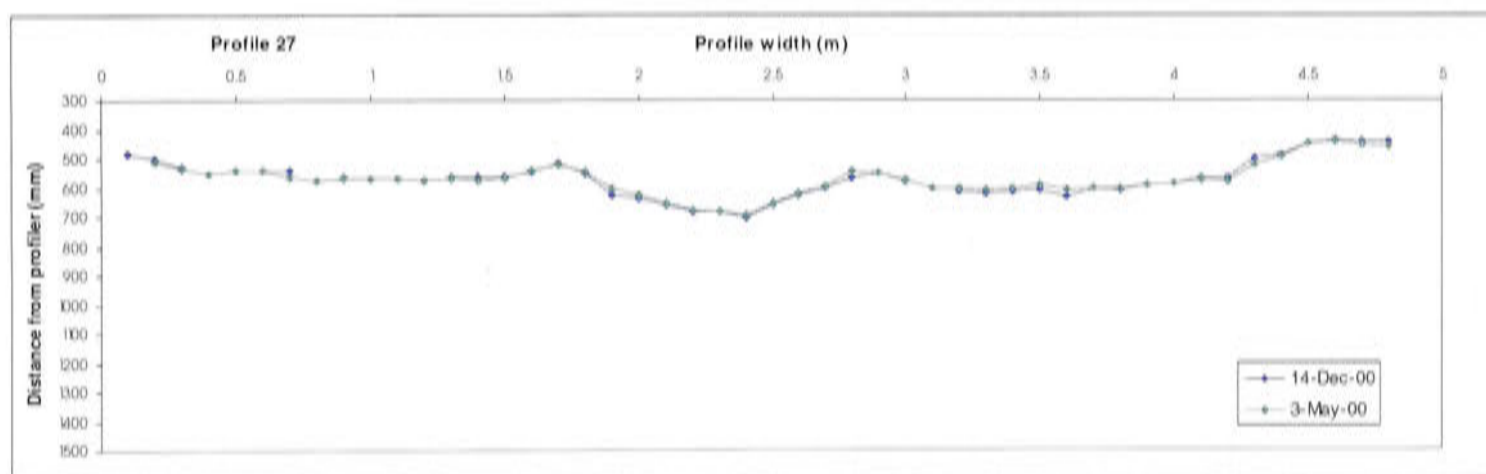
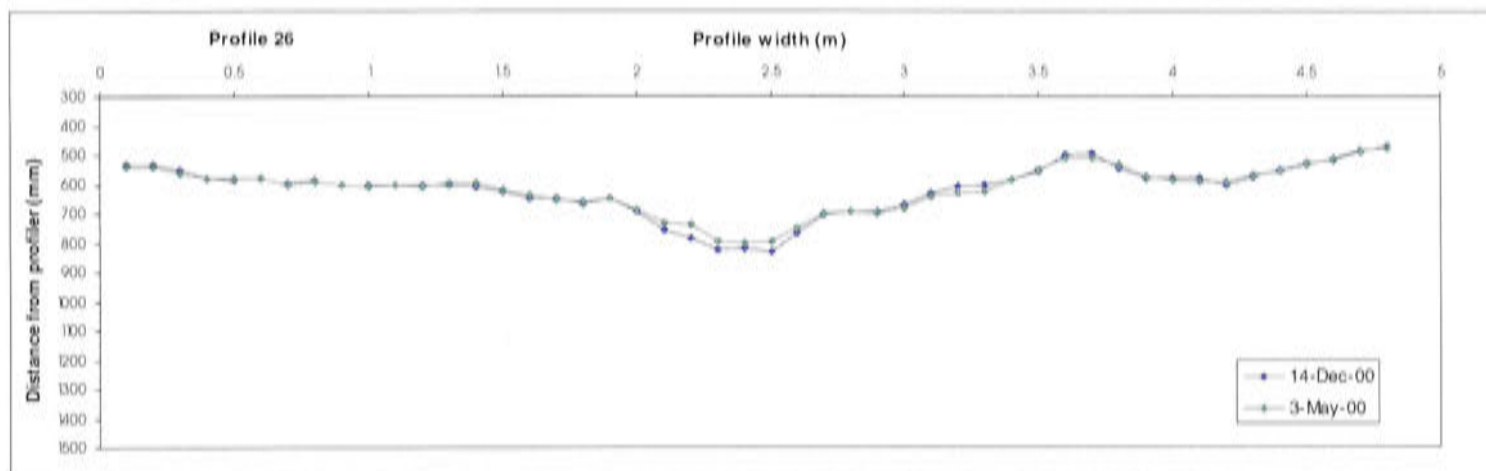
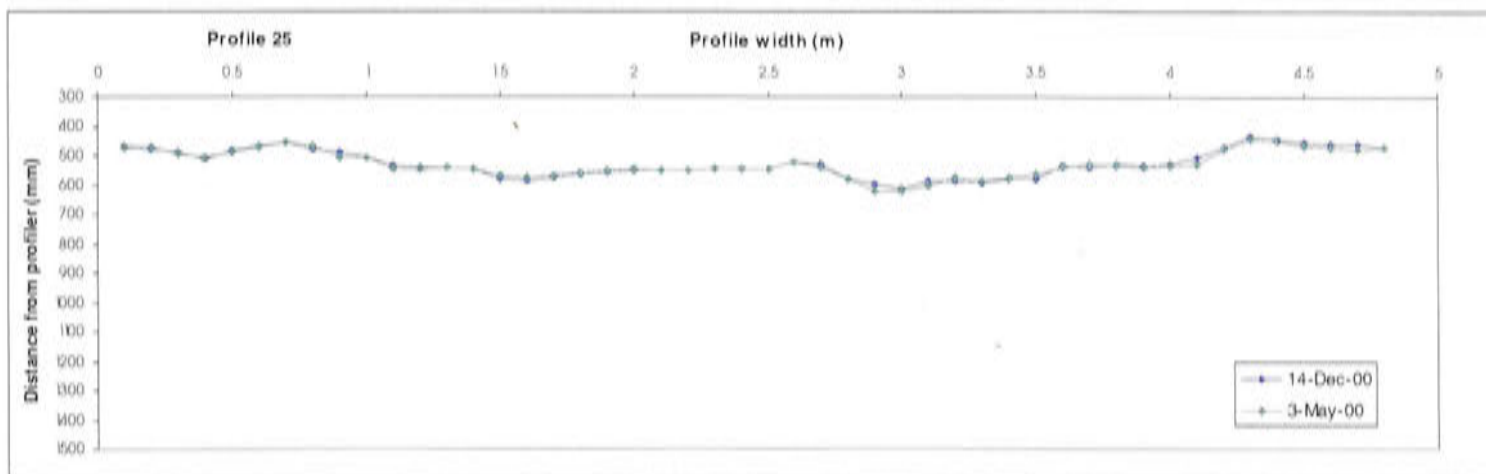




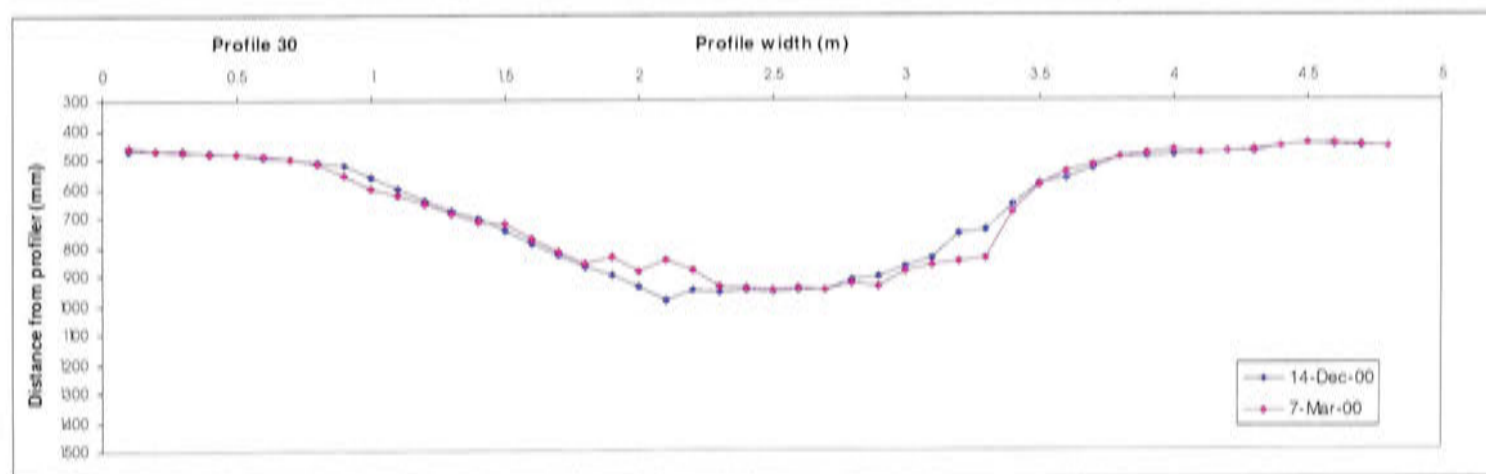


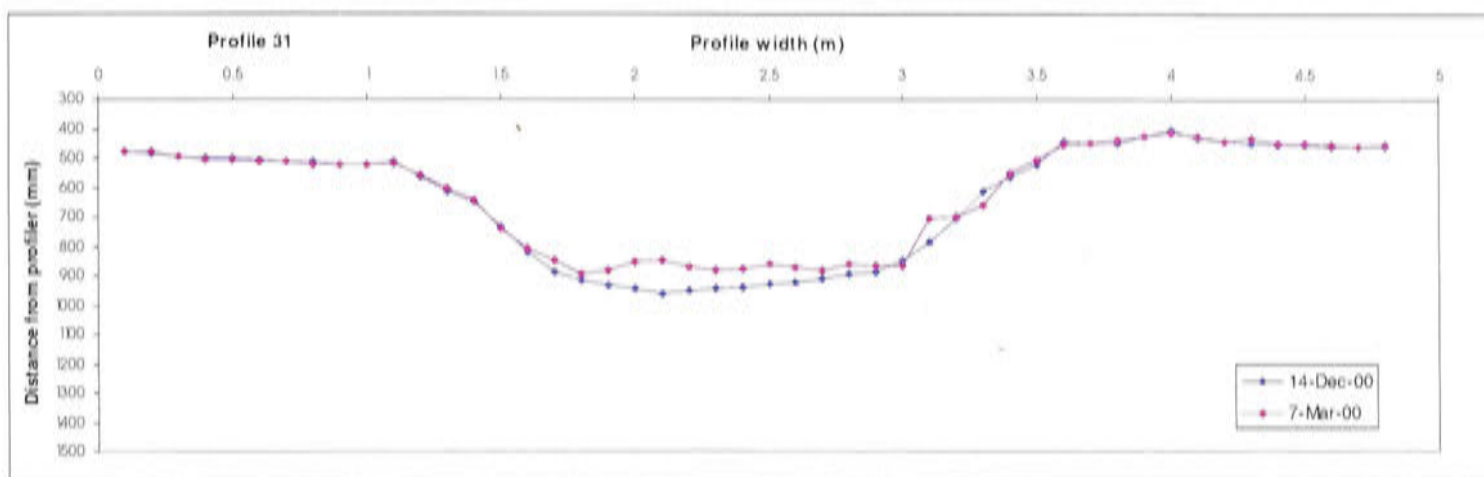
Profiles 18- 21, 25-27: Season 99-00



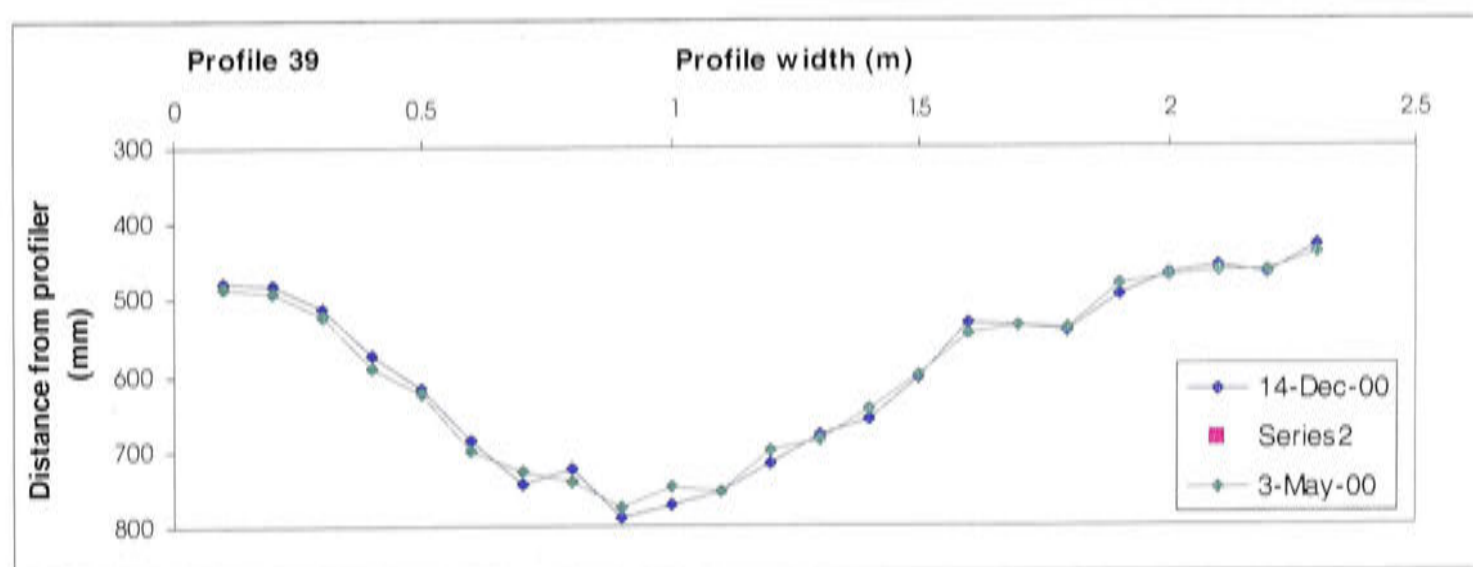
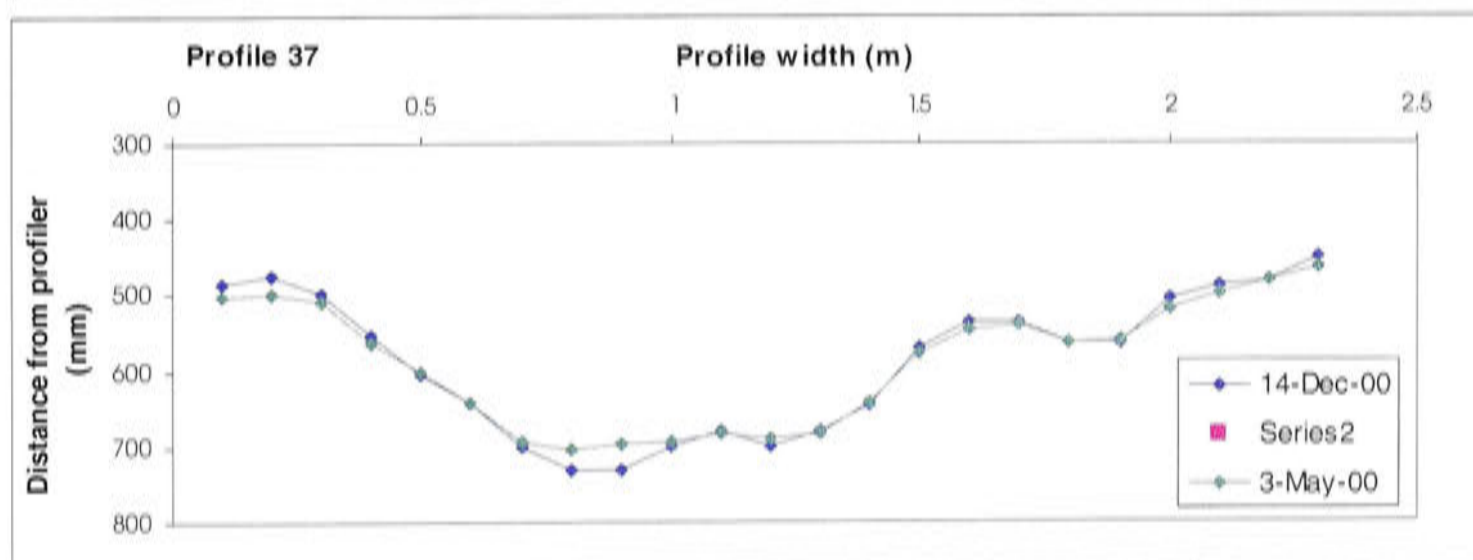
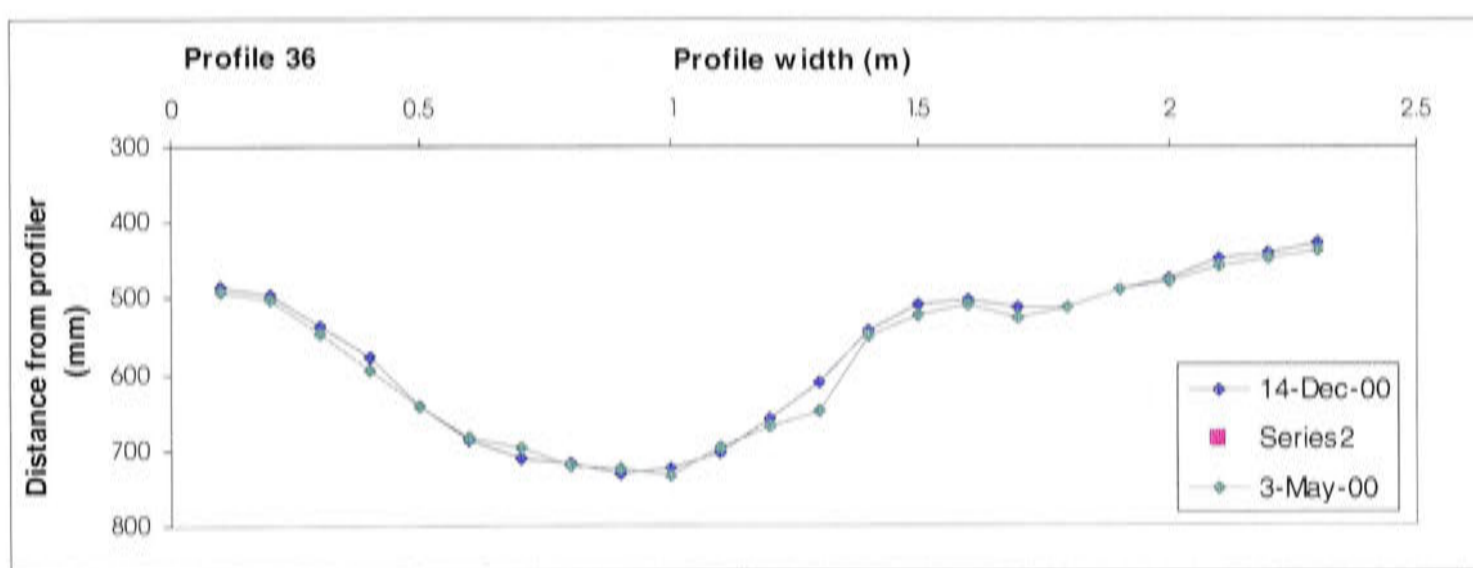


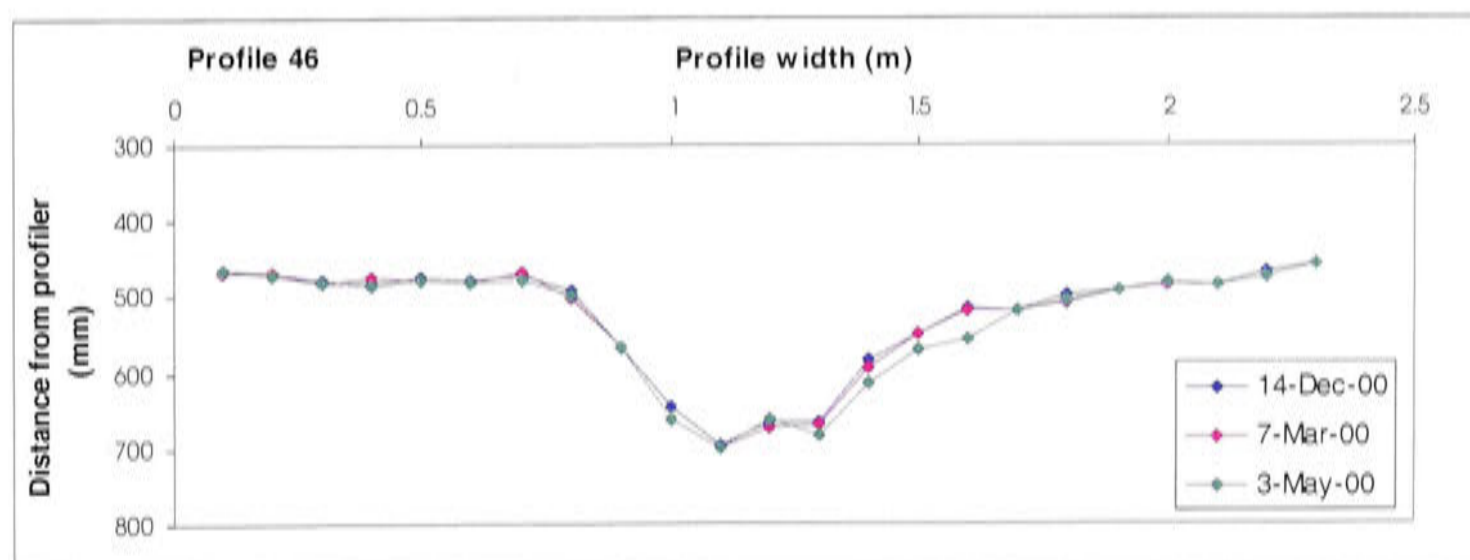
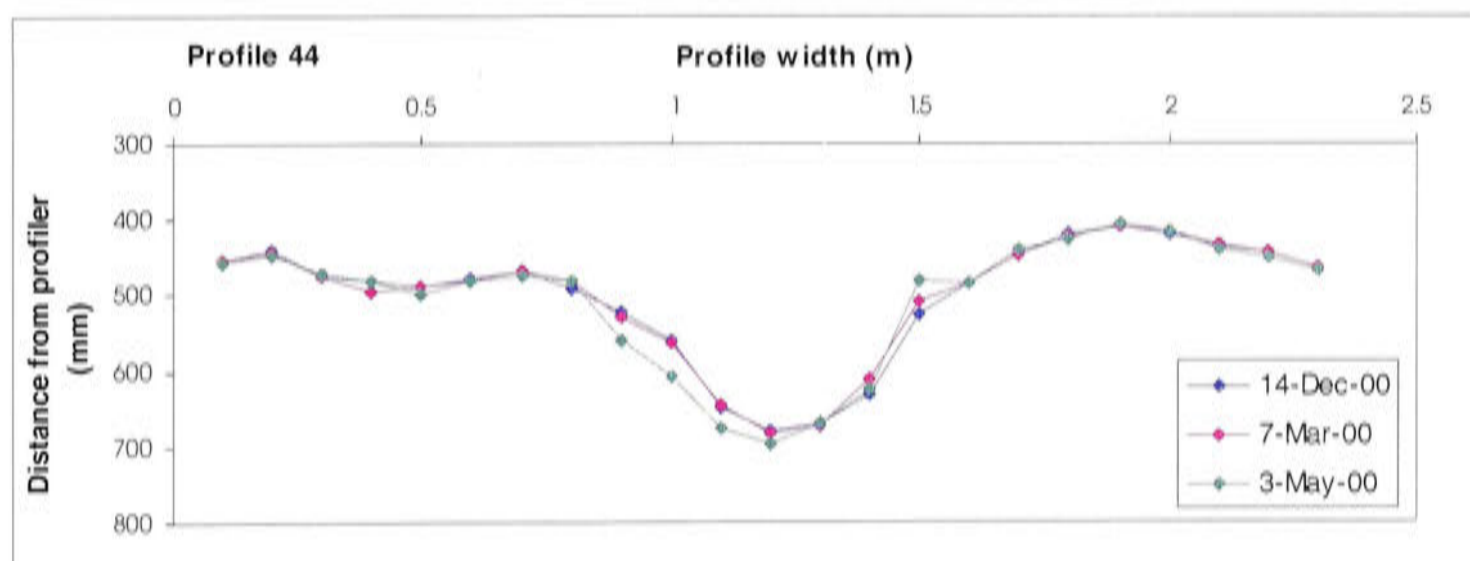
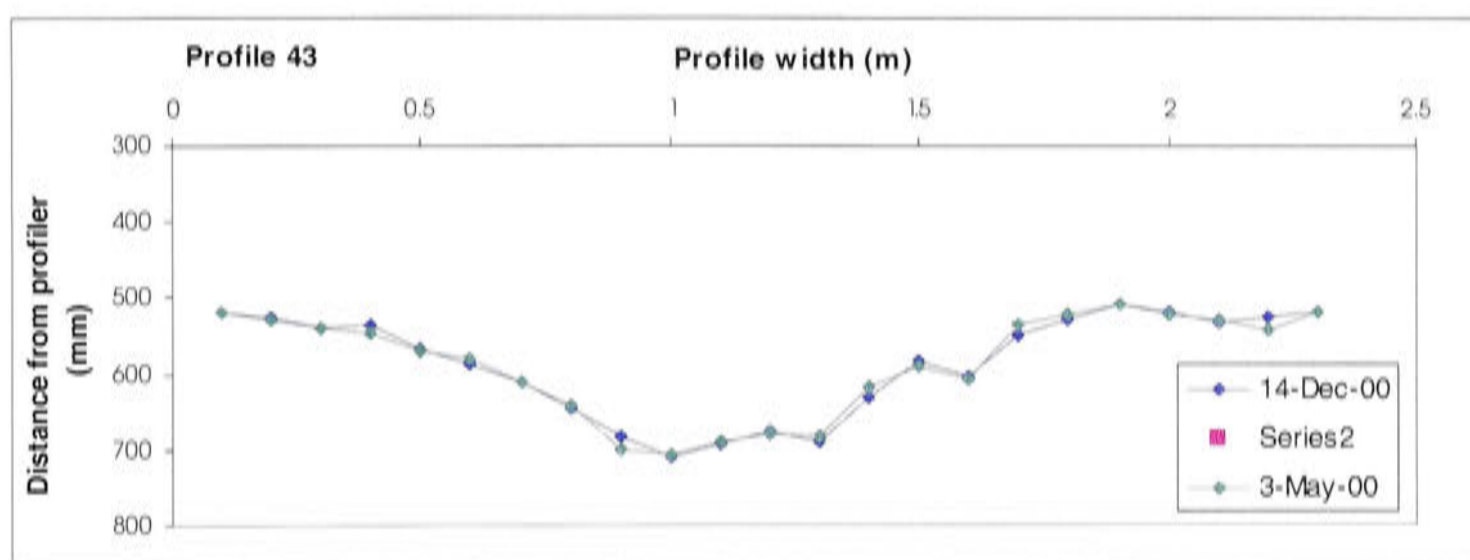
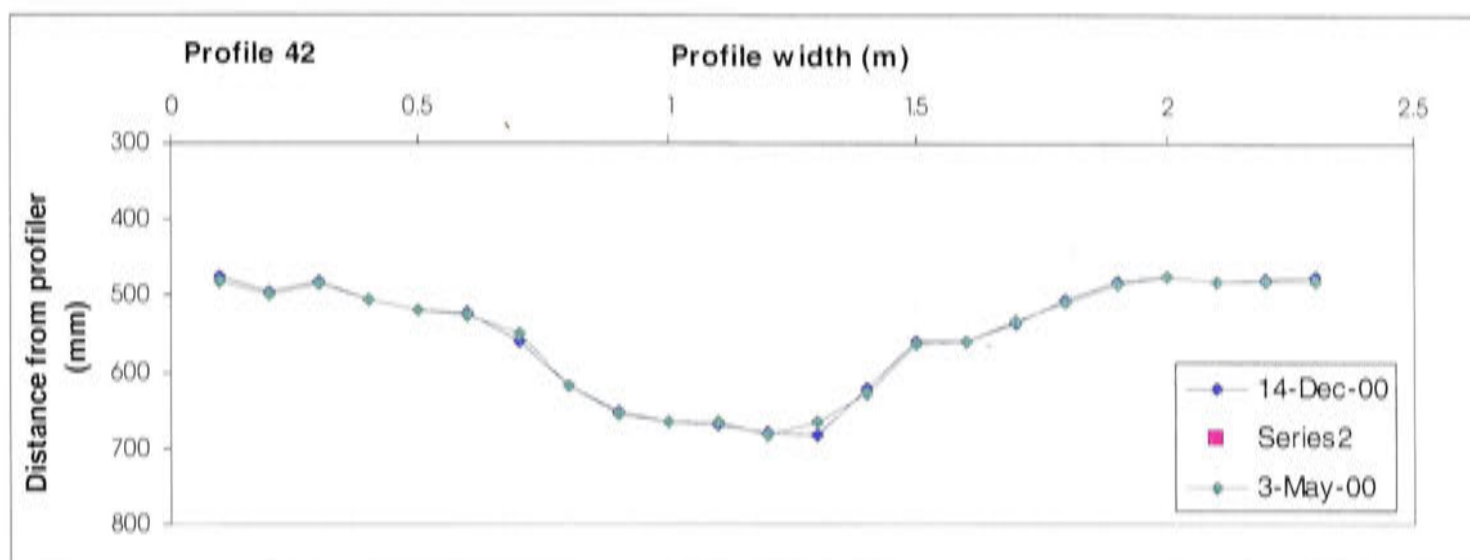
**Profiles 30,31: Season 99-00**



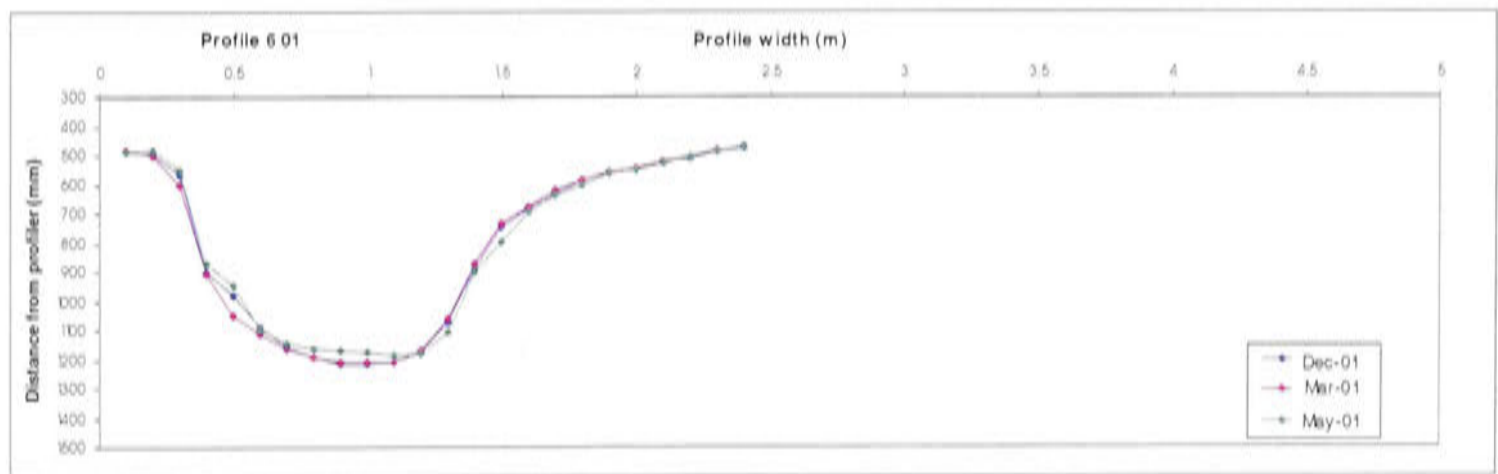
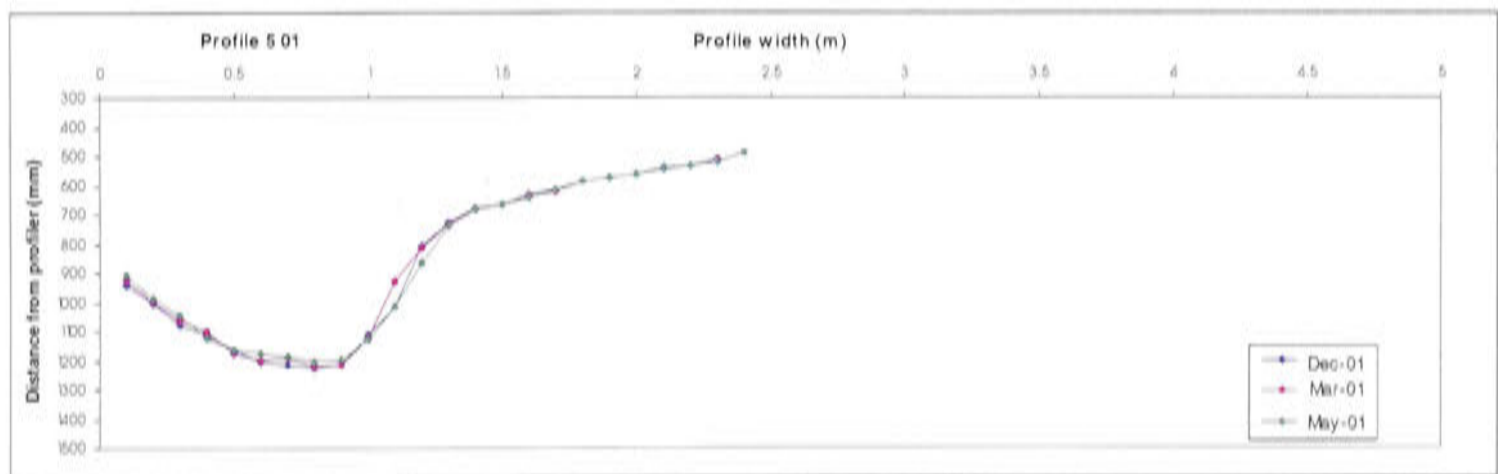
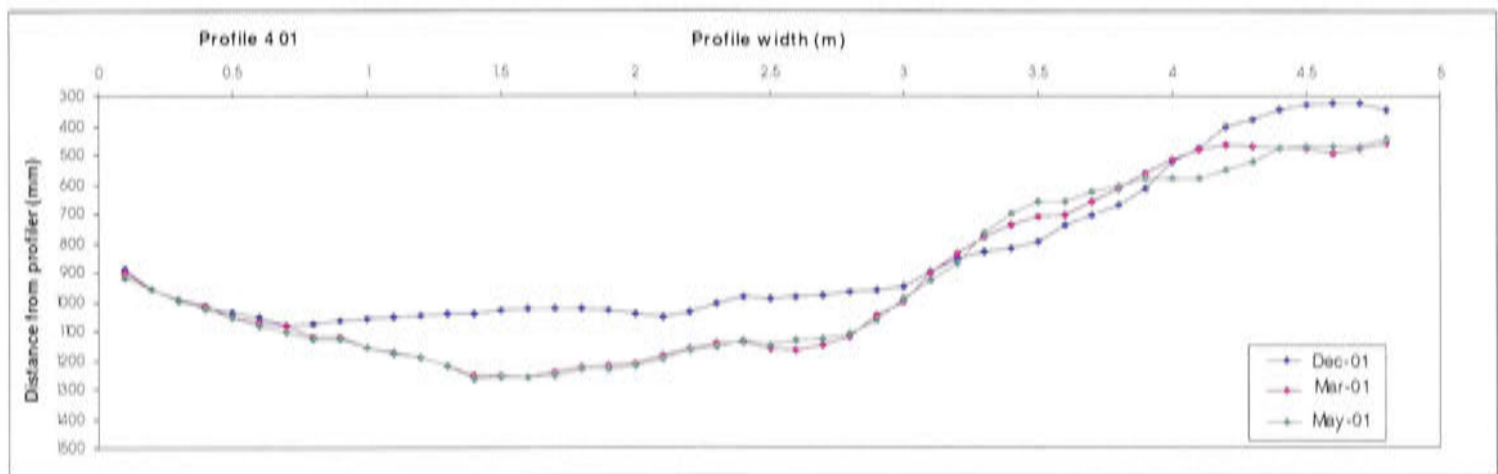
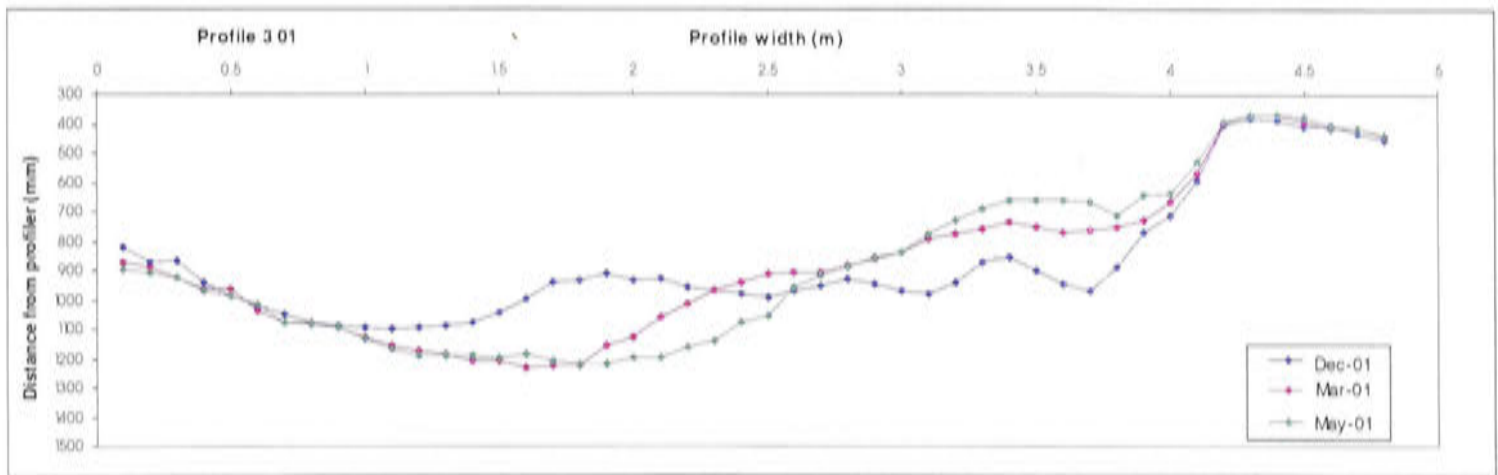


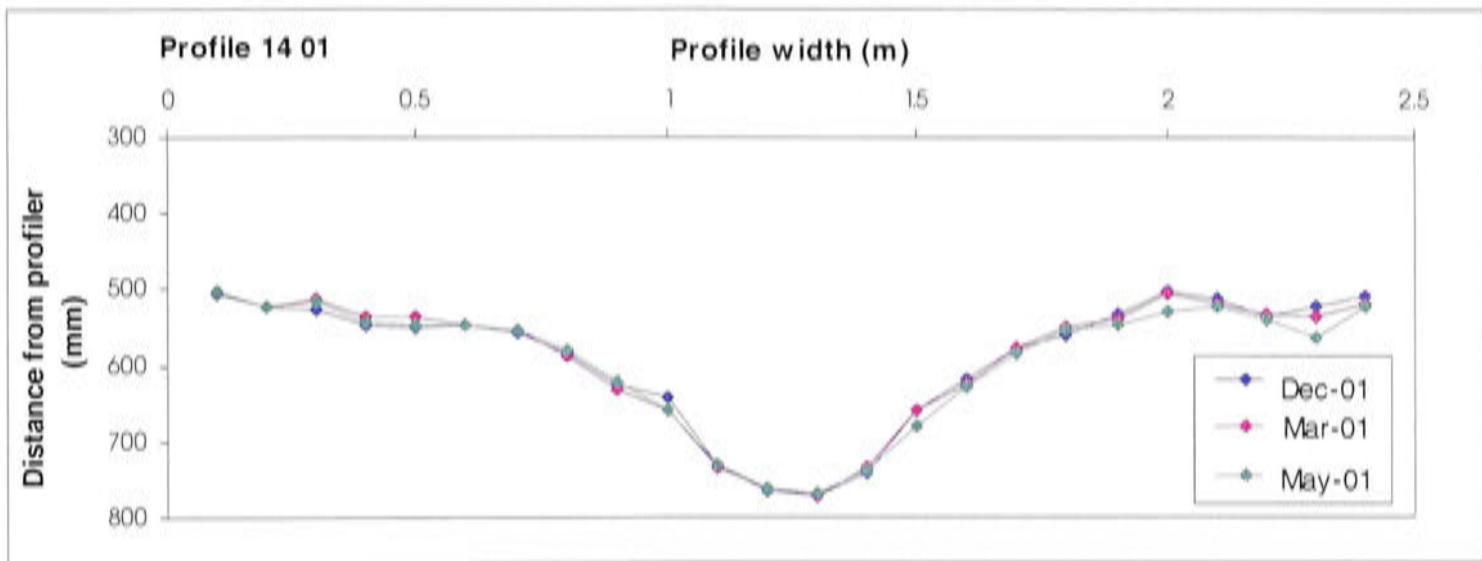
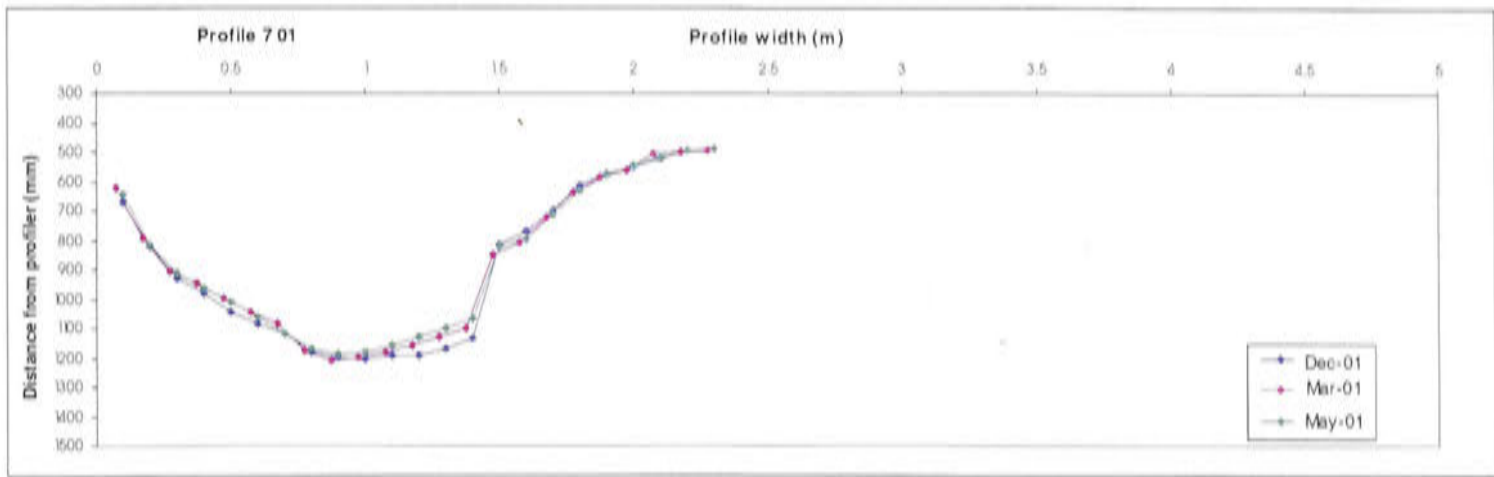
**Profiles: 36, 37, 39, 42, 43, 44, 46 Season 99-00**



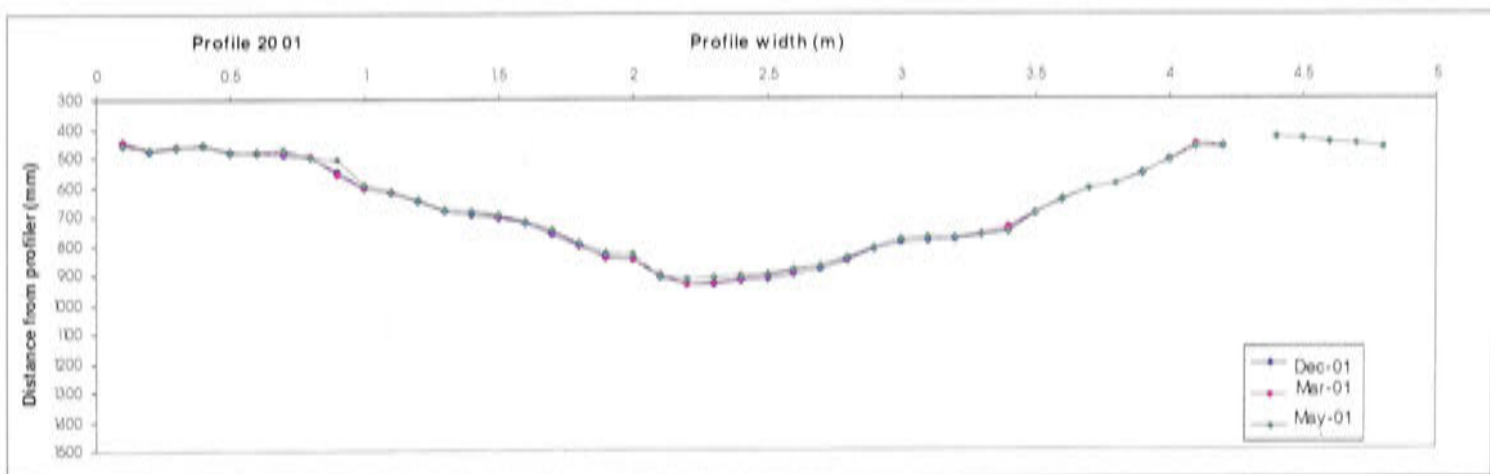
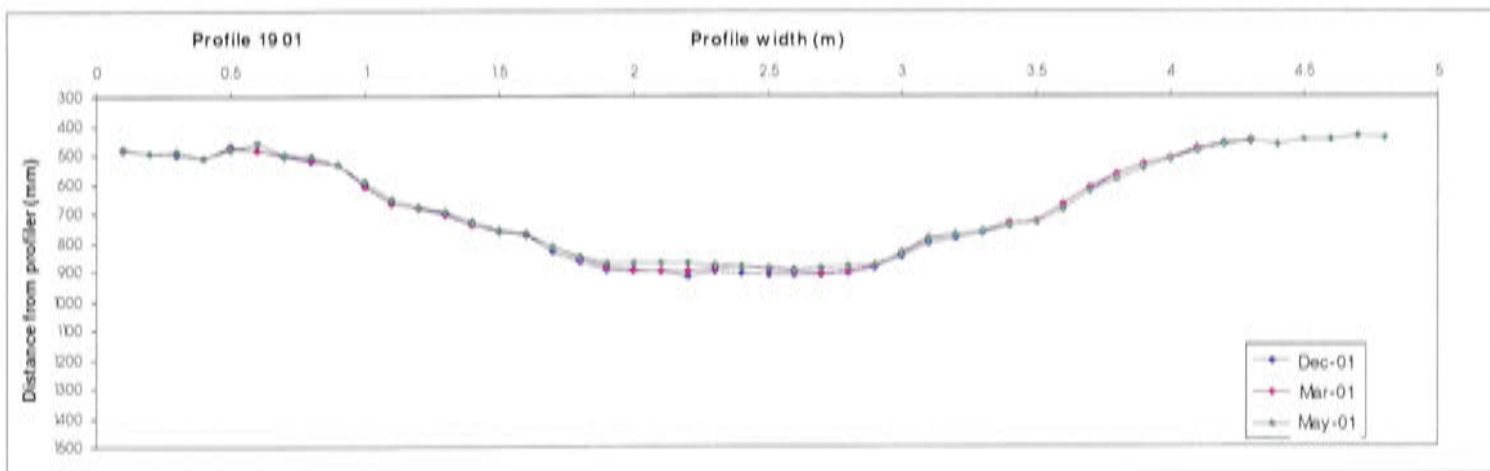


Profiles: 3-6, 14, 15 Season 00-01

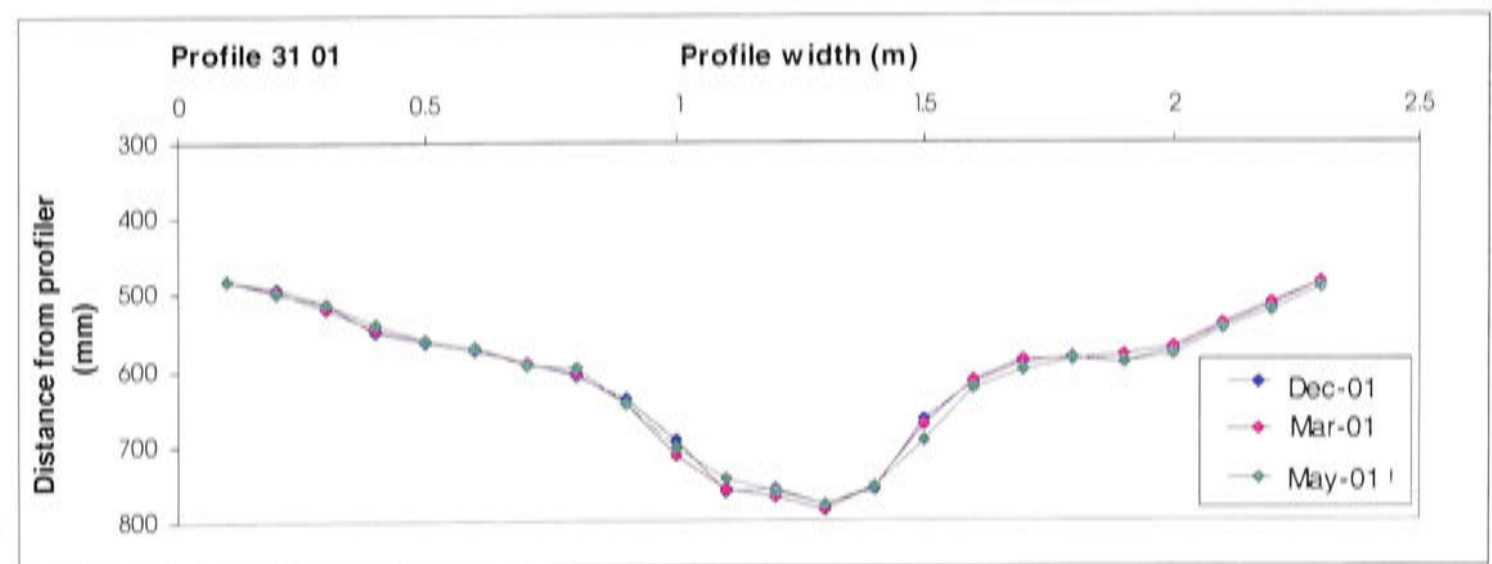
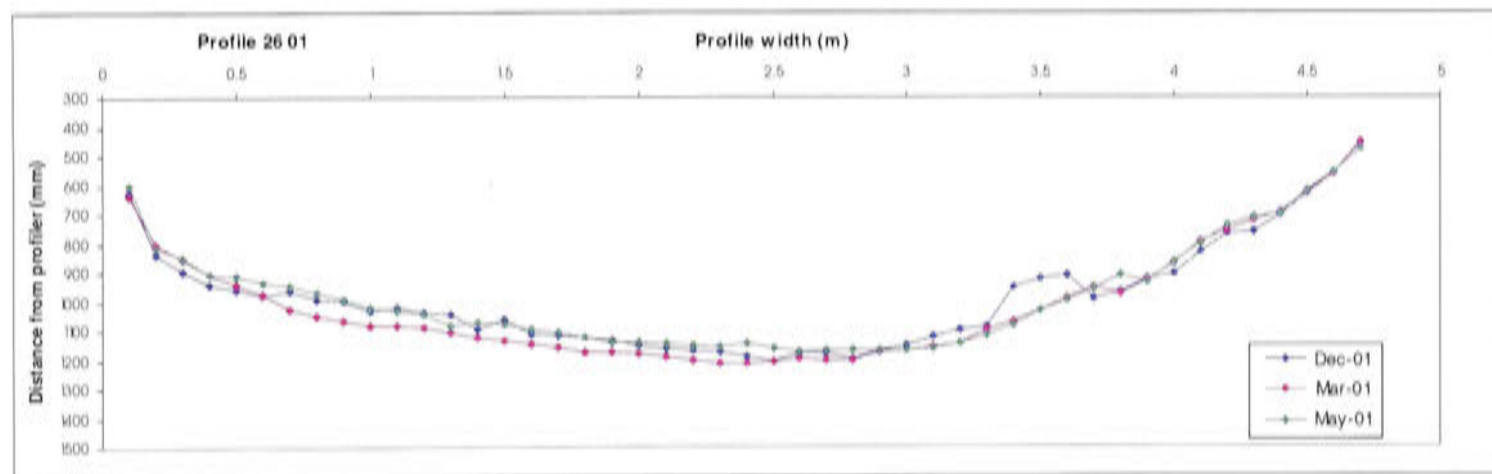
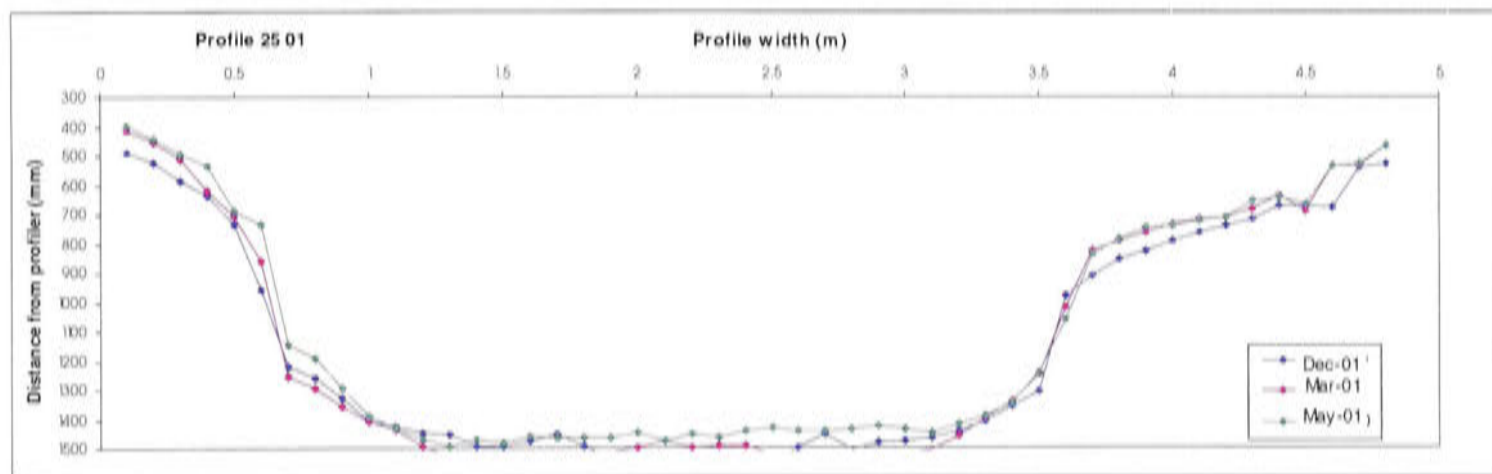
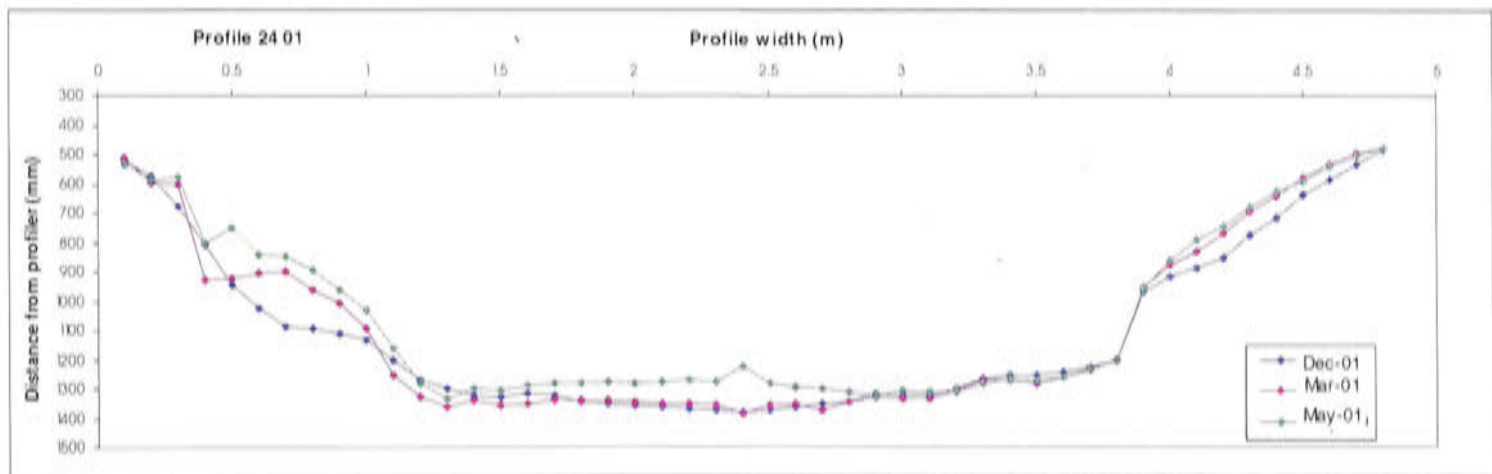




**Profiles: 19, 20 Season 00-01**



Profiles: 24-26, 31 Season 00-01

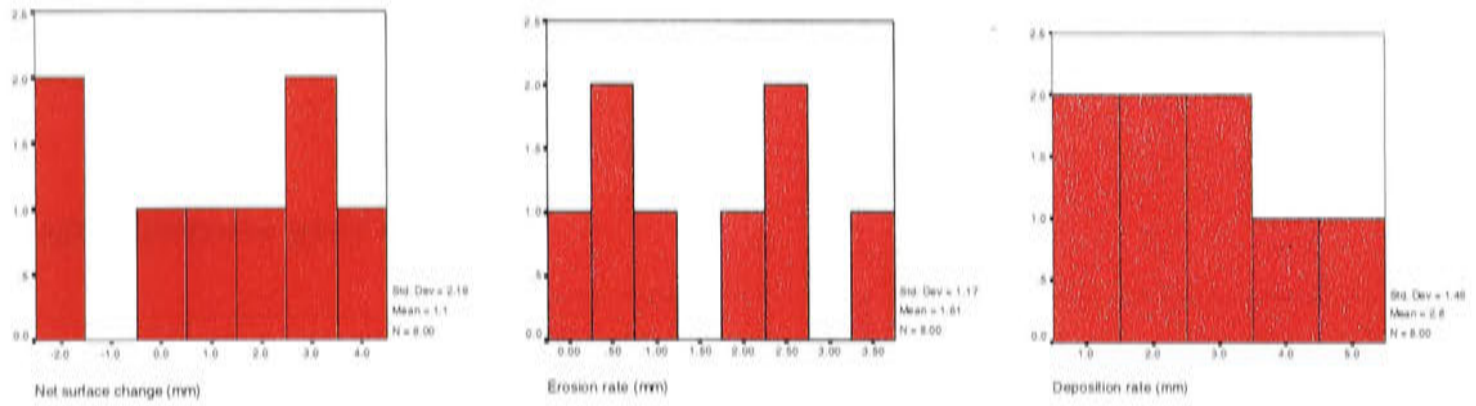




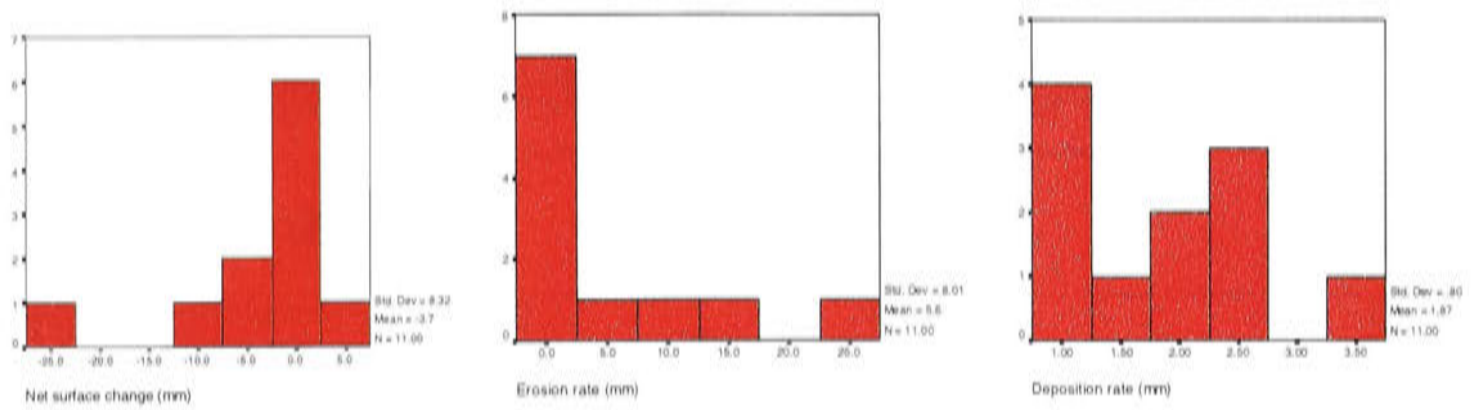
**APPENDIX J**

Histograms for surface profile data (adjusted) from the 99-00 budget season.

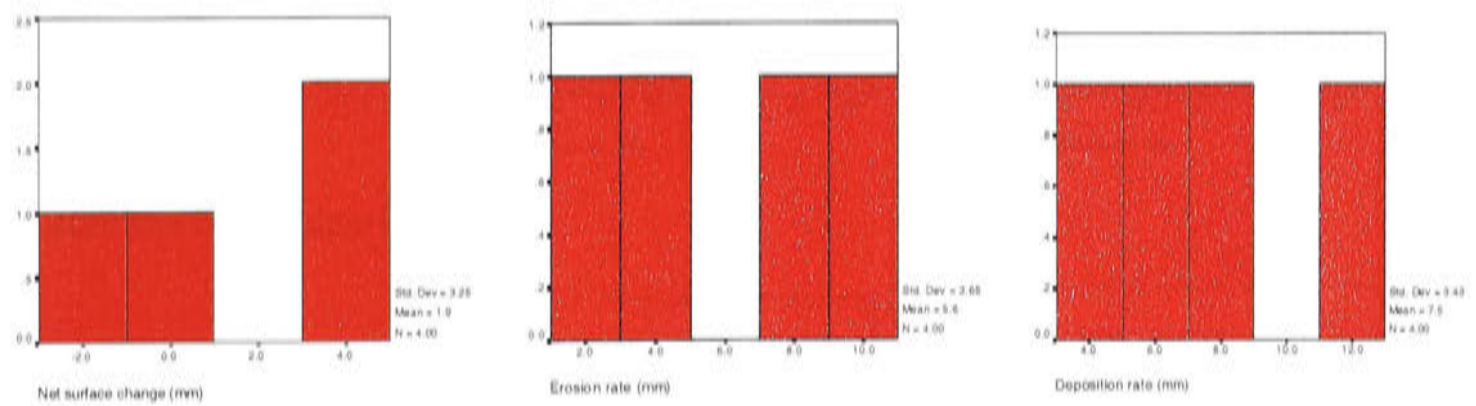
**Minor drains**



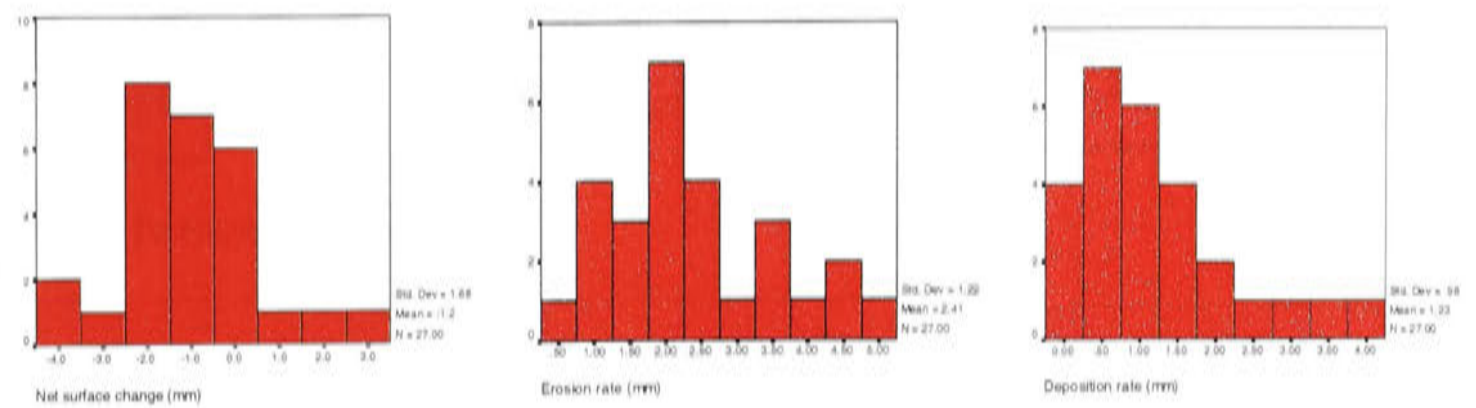
**Major drains**



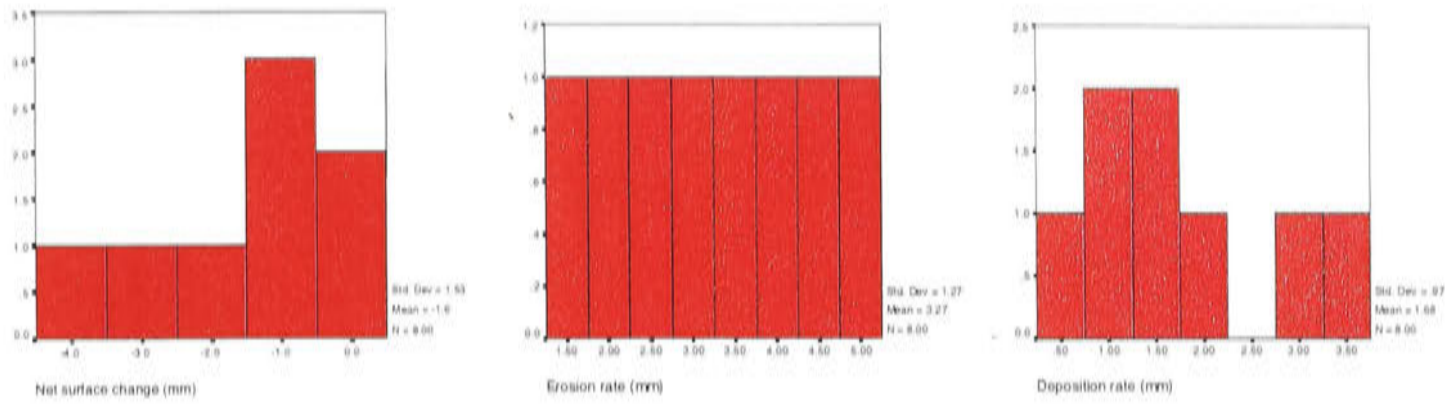
**Ripple Drain**



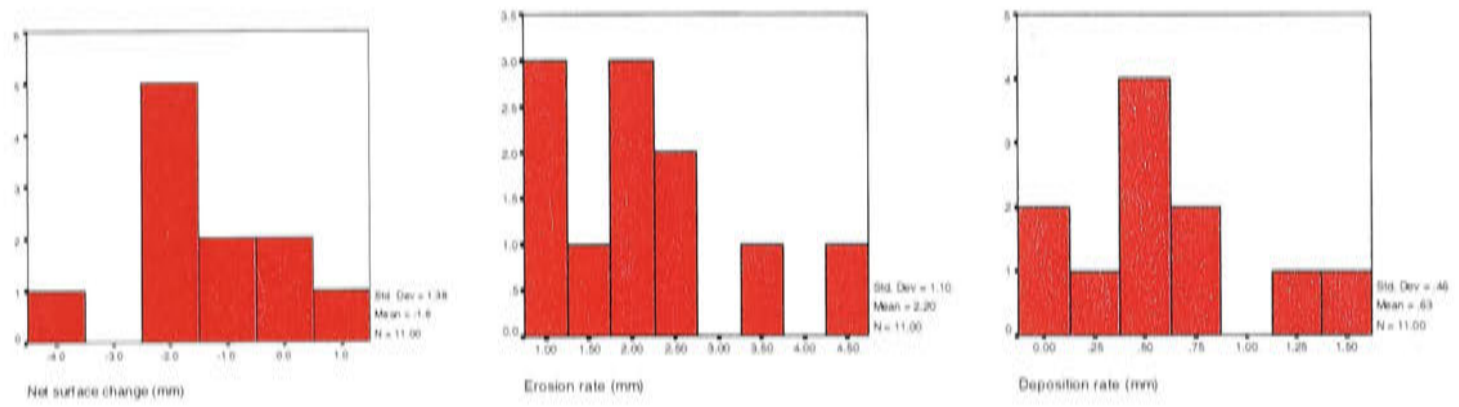
**Water furrows**



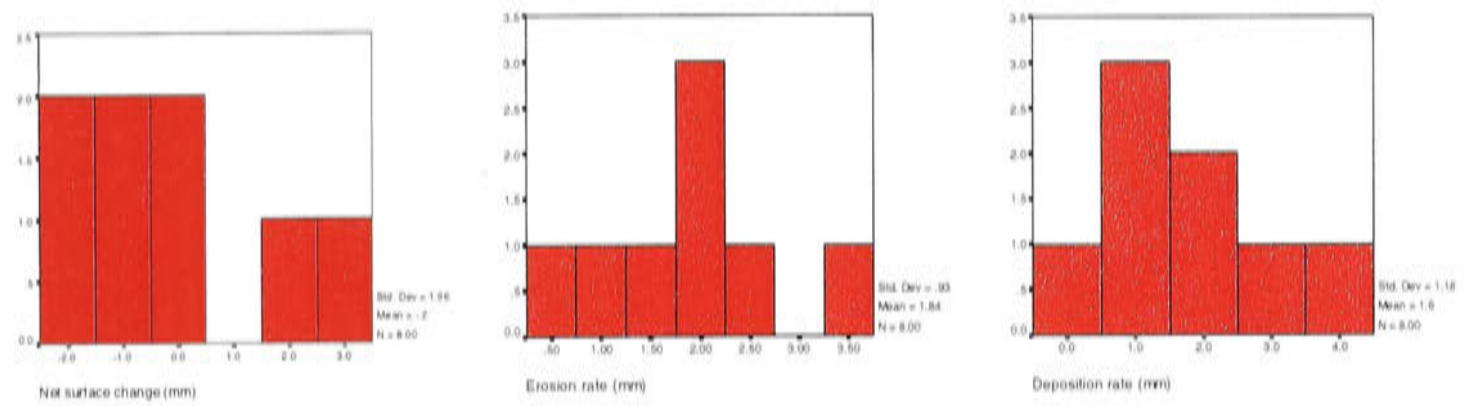
**Water furrows clay**



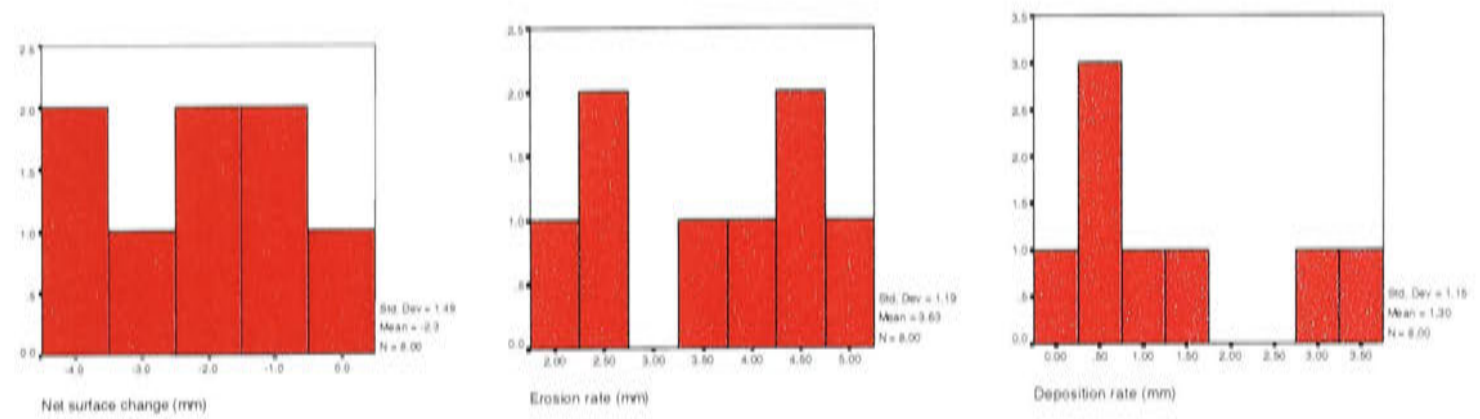
**Water furrows grey sand**



**Water furrows silty clay**



**Water furrows plant cane**



**Water furrows ratoon**

